ECONOMIC ASSESSMENT IN THE SYNTHESIS OF OPTIMISING CONTROL SCHEMES

A thesis submitted for the degree of

Doctor of Philosophy

by

Chandrasekhar Gannavarapu , M. Eng.

Department of Chemical Engineering

The University of Sydney

March 1991

ERRATA

* Positive (+) line number is referenced from the top of the page with negative numbers (-) from the bottom.
* An arrow (-->) indicates that a change is to be made in the argument on the left to the one on the right.

PAGE NUMBER	LINE NUMBER	CORRECTIONS/COMMENTS
1	-3	Chemical --> chemical
2	+10	the advanced --> advanced
2	+17	connecting --> connect
2	+18	if often --> is often
3	+10	have contributed --> has contributed
8	-14	The lighter hydrocarbons refer to C_1-C_{15}, not C_1-C_5.
17	+9	Michelson --> Michelsen
18	-13	IIR here implies 'spurious IIR'. In other words, the response of the model DOES NOT follow that of the actual process.
24,25	Equns (2.3.1) - (2.3.5)	The distillation model proposed is based essentially on the CMO assumption and is therefore applicable only about a limited range of operation.
54	+2	compartment --> compartments
54	-3	From --> from
63	(b)	applicable, while --> applicable only, while
63	-4	set of separation --> set of separation equations
65	-18	Although relative volatility also varies with composition, in high pressure columns, the pressure effects may be more significant.
66	Table 2. 5.1	Clearly the UCM model does not include flow and energy dynamics, however, is less complex and requires less computations. Several modifications proposed essentially attempt to incorporate these dynamic effects and have their own advantages and limitations.
73	-8	nature of mixture --> nature of the mixture
86	-3	applied distillation --> applied to distillation
93	-2	computational power --> computational effort
95		In the titles for Figures 2.6.7 and 2.6.8, COMPSOTION --> COMPOSITION
102	-11	three case --> three cases
115		Holdups used for the overhead condensers here actually include the reflux drum holdups also.
130		The following range of errors are considered to be typical in the data collected during plant trials. Instruments (pre-calibrated) : ± 1% Mass balance on columns : ± 1% Laboratory analyses : ± 2%
147	+5	studies was --> studies were
171	+2	SISO O --> SISO
171	+4	MIMO systems , here, also include processes with more than one SISO loops.

ERRATA (contd...)

176	Eq.(4. 2.6)	The second variable is not printed clearly and is actually ' y_2'
180		Designing decouplers was not attempted in this thesis, therefore, no mention was made about the effects and the associated problems with time-delays, in this context.
184	-2	interaction among --> interaction amongst
186	+7	Morari et al. .'s --> Morari and co-workers
206	Eq.(4.3.56)	dig --> diag
223	-13	manipulated variable --> manipulated variables
234	+1	the operation in this case can be 'infeasible' or 'undesirable' with reference to any specific constraint, depending on the nature of the constraint.
234	-6	manipulated --> manipulated variables
237	-11	cancel-off --> cancel out
251	-3	from in --> in
257	+10	feed disturbances --> feed disturbance
257	-14	a with --> with a
258	+6	The choice of the second largest open loop back-off is certainly arbitrary here. Further work along these lines is currently on the way.
269	(b)	is when --> are when
294	Ref : Eq. (6. 2. 5)	The back-off required was taken as 5.0 because, even the second largest back-off estimated was still greater than what is actually feasible !!
294	+20	Table 6.3.3 --> 6.2.3
296	+15	that each --> each
297	-10	reduces --> reduce
306	+3	remain same --> remain the same
311	-18	The examiner's comment may not actually be true. Will there then be a separate tuning for each type of disturbance ?
311	-8	Figures 6.6.22 - 6.6.28 --> Figures 6.5.22-6.5.28
311	-2	Figures 6.6.29 - 6.6.35 --> Figures 6.5.29-6.5.35
312	+3	Figures 6.6.29 - 6.6.35 --> Figures 6.5.29-6.5.35
312	+17	Figures 6.6.22 - 6.6.35 --> Figures 6.5.22-6.5.35
312	-8	likelyhood --> likelihood
315-334		In all the Figures (6.5.1-6.5.35), the physical units of the variable HOLDUP are actually KG-MOLES, but not KG-MOLES/HR as mentioned. Similarly, temperature has the units of DEG C.
335	+15	have to be --> has to be

PREFACE

The conditions of Candidature for the Degree of Doctor of Philosophy in the University of Sydney require that "the candidate must state generally in the preface and specifically in the notes the sources from which his information is derived, the extent to which he has availed himself of the work of others, and the portions of work he claims as original ".

The new reduced-order dynamic model for distillation columns presented (Chapter 2) is original. All the SPEEDUP models and Fortran programmes used are original unless stated otherwise. The design details for the distillation columns used in this thesis are supplied by Shell. However to maintain confidentiality, design details and the SPEEDUP and Fortran programmes relevant to the entire case-study, are not enclosed in this thesis, but are available on request from the author or his supervisor. The approach used for assessing initial inverse response in compartmental models is new (Section 2. 4). The ideas presented on modelling condensers and reboilers, and estimation of vapour-liquid equilibrium mixture temperatures are also original (Appendices A4 , Appendix A5 and Section 2. 5).

The methodology proposed in Section 5. 3 for the synthesis of optimising control systems for continuous processes is original. The economic issues addressed through this approach are original. However, the open-loop indicators used for assessing process controllability and screening of alternative control systems are not new. Except the design calculations, all the other calculations used in the case-study of this thesis are worked out by the author.

The following are the research publications derived entirely from the work contained in this thesis:

(1) Gannavarapu, C., Barton, G.W. and J. D. Perkins, "Simulation , Optimisation, and Control System Design for an Industrial Process " , I.Chem.E. Symposium Series No., 114, Leeds, England , pp. 141 - 156, 1989.

(2) Perkins, J.D. , Barton, G.W. and C. Gannavarapu, "Choosing Control Structures based on Economics", Symposium on 'Control for Profit', New Castle , England, 1989.

(3) Barton,G.W., Gannavarapu, C., Lear, J.B. and J. D. Perkins, "Choice of Control Structure for Continuous Processes Based on Economics", American Control Conference, San Diego, California, USA, 1990.

(4) Gannavarapu, C., Barton, G.W., Perkins, J. D. and J. B. Lear, "Economic Choice of Control Structures for Continuous Processes", The Fourth Conference on Control Engineering Gold Coast, Australia, 1990.

ACKNOWLEDGEMENTS

I wish to express my deepest thanks to Dr. Geoff Barton for his constant encouragement and inspiring supervision. His assistance in clarifying concepts and aiming for the highest presentation standards has been invaluable. I would also like to thank my co-supervisor Prof. John Perkins of Imperial College, London , who was instrumental in laying the foundations in the early phase of this work . His vision, and constructive criticism have been extremely useful throughout this project.

I thank Mr. Ron Van Wijk of Shell Australia Pty. Ltd. for co-ordinating this industrial project. I appreciate all the help I received at various times of the project from Ms. Rhonda Keene, Mr. Arie Van Doorne and Mr. Richard Bergin of the Technology group at Shell's Clyde refinery, Australia. The financial support from both the Chemical Engineering Foundation and the University of Sydney in the form of post-graduate research award, is very much acknowledged. I thank Prof. R. G. H. Prince, the Head of the department of Chemical Engineering for his support and encouragement.

My sincere thanks to Mr. John Delich, Ms. Sheila Krishnan, Mr. John Lear, Mr. Mark Padley and Mr. Sandy Legovich of the Systems Group at the Chemical Engineering department, for all the help and discussions we had all through these years. The generous help of our computer staff in the department - Mr. John Czerniecki, Mrs. Syrindar Woo , Mr. Warren Simon and Dr. Tim Pearce - is greatly appreciated. I also appreciate all the help I received from Dr. Costos Pantelides, Mr. Lakis Liberis and Mr. Larry Narraway of Imperial College, and Dr. Ian Cameron of University of Queensland.

I am grateful to Anantha and Rekha Vanamalis for their affection, concern and friendship. I thank Sreenath and Sujatha Charys for generously allowing me to use their residence for the preparation of this thesis. My special thanks to Mr. Ashish Agar for his comments and suggestions in formatting this thesis . The timely assistance from Mr. Karthy Subendranathan and Ms. Rajinder Pal Kaur is very much appreciated.

Lastly, but not least, I thank my parents and family for their love, continuous support and encouragement , that have always been a great inspiration to me.

To my parents

SUMMARY

The desire for the development of more efficient process designs - with lower unit costs and a greater ease of operation - has been responsible for recent progress in control system synthesis for chemical plants. A range of open-loop indicators have been developed which seek to provide means of assessing controllability of alternative processes. The major drawback with all the available measures is that they do not yet provide a consistent basis for screening alternative processes based on both economic and controllability grounds together. It is therefore possible that processes that offer significant economic benefits may not possess good controllability characteristics, and vice versa. Several case-studies reported in the literature (e.g. Chan et al. [1986]) confirm the seriousness of this problem. Therefore what is required is a common basis for both identifying the potential economic benefits of "good" control on a process, and a reliable means of determining how to achieve such benefits. It was the aim of this thesis to develop and test such an approach to control system synthesis.

A two-stage approach for the synthesis of optimising control structures is presented in this thesis that seeks to provide the required consistent basis between economic and controllability criteria for process operability. Process conditions at an economic optimum, along with the set of active constraints and the associated Lagrange multipliers, are determined in the first stage of the new approach. The action of external disturbances on a process would be to perturb its operation away from the optimum. To avoid operating in an infeasible region during the transient stage, one simple approach is to make a deliberate back-off in the operating point from the optimum. In practice this can be achieved by moving away from certain process constraints that are *active* at the selected optimum. Information about the key disturbances normally influencing process operation can be used to estimate both the necessary back-off from each of the active constraints at the optimum and the economic penalty associated with it. A linear analysis, using the process transfer function relating the disturbances to the active constraints, is used to provide the estimate of the economic penalty. An open-loop penalty for back-off from the optimum with "no control " can thus be defined, and provides an upper bound on the economic loss in the potential benefits from employing an optimising control scheme on the process. On the other hand, if "perfect control" can be implemented on the process, then no back-off from the optimum operating conditions is necessary, and hence there is no economic penalty. Thus the latter case provides a lower bound on the economic penalty for back-off from the optimum, while the difference between these two bounds gives the maximum potential benefit a control system can offer on such a process. The larger this difference is, the greater is the incentive for installing a control system. Thus, at the end of the first stage of

the new methodology, the control engineer has available to him quantitative information on the economic importance of the control system.

In the second-stage of this approach, the major process characteristics preventing perfect control being achieved are examined. Open-loop indicators such as the minimum condition number are used to assess and screen alternative control schemes to find those that can regulate the process close to the selected optimum. The concept of *the maximum percentage recovery* (MPR) is introduced here. This provides a measure of the anticipated degree of closeness to perfect control. Processes with a small minimum condition number over the entire frequency range of interest should not experience large fluctuations in the process variables during regulatory control transients. Thus one can make a smaller back-off from the optimum value (i.e. a smaller closed-loop back-off) and still avoid constraint violations during normal process operation. Processes with a large MPR value hence should be able to provide good closed-loop regulatory performance for all the disturbances considered. A systematic methodology for such an assessment is provided in this thesis.

The proposed optimising control system synthesis methodology was applied to an industrial case-study in the form of the CDU gas-tail at Shell's Clyde refinery in Sydney, Australia. A new compartmental approach to distillation column modelling , called the Universal Compartmental Model (UCM), was proposed and used for modelling the three columns of the gas-tail. The UCM approach was tested on various distillation columns reported in the literature involving both binary and multicomponent separations. Good agreement with more rigorous column models was observed for both steady-state and dynamic simulation results in all cases . Steady-state validation of the gas-tail model based on the UCM approach was achieved using both steady-state plant trial data and simulations carried out on a more rigorous gas-tail model. The same UCM based gas-tail model was used to identify the optimum operating conditions under a variety of operating conditions. Large economic benefits were identified for installing an optimising control scheme on the gas-tail. Several alternative control configurations were examined and a new optimising control scheme developed that should provide both significant economic benefits (relative to the existing control scheme) and good closed-loop performance. The simulated closed-loop performance of the gas-tail columns for various set-point and disturbance changes were consistent with the predictions of the proposed methodology.

The primary reason for developing the UCM approach was so that the modelling , simulation, optimisation and control system design could all be performed in a single environment (here the SPEEDUP flowsheeting package was used). This study demonstrated the benefits and flexibility of employing such a single environment approach.

TABLE OF CONTENTS

LIST OF FIGURES

LIST OF TABLES

CHAPTER 1

INTRODUCTION

1.1 OBJECTIVES OF PROCESS CONTROL

Set-point tracking and regulation are still today the major tasks of process control. However, in view of recent changes in the growth in complexity of chemical processes , more advanced control policies, therefore, have been sought to assist process operation. Buckley [1964] has been one of the major pioneers in the chemical industry in addressing the question of a more fundamental and practical approach to process control. He pointed out that the two major requirements of process control so as to achieve the required operational objectives are :

(a) The maintenance of a material balance. This is to do with the maintenance of inventories between their minimum and maximum levels. It also ensures that the product rates can always meet the demand.

(b) The production of materials that satisfy prescribed specifications.

Although both these objectives are inter-related, Buckley treated them independently. Material balance control deals primarily with the slow, or low frequency changes in such things as the feed stocks. Product quality control aims to reduce the impact of relatively fast, or high frequency disturbances. Both these control policies work together but in a largely decoupled fashion. Thus, one of the major implications of this approach is that two different types of controllers can be assigned to different tasks. The product quality control loops which deal with high frequency disturbances can be separated from the material balance control loops, that deal with the low frequency changes. As a result of this two-level approach , the attention of process control shifted from the control of individual units to the control of entire processes.

In the decades since the pioneering work of Buckley, it has become increasingly apparent that a clear understanding of process behaviour, and the dynamic interactions is crucial before designing a control system for that process (Zakrzewski [1983], Stephanopoulos [1983]). Indeed, Foss [1973], argued that the lack of good understanding of process dynamics has probably been the main reason preventing chemical engineers from developing a suitable control theory for process control. However, Chemical processes are often complex and are inherently nonlinear in nature. Interactions can exist both within a single unit and among the various units that form a process flowsheet. A sound

understanding of both these interactions is necessary in characterising the dynamics of the entire process flowsheet. The nonlinear nature of the processes introduces additional complexities into such an understanding. One way of identifying the process behaviour and estimating the process interactions is through plant trials. Such an approach , however, has limited application and often is impractical , especially when the process is large. A validated simulation model, on the other hand, can provide a good process description over a wide range of operating conditions. These process simulation models vary both in complexity and rigour. Many modern control algorithms (Lee and Sullivan [1988]) use a model of the process to determine the regulation necessary to account for disturbances or changes in the required operating conditions. One of the key issues of the advanced process control, therefore, is how best to obtain a good process model.

1.2 CONTROL SYSTEM SYNTHESIS

Until the early 1960's, control system design had essentially been at the single process unit level. However, a chemical process generally consists of several processing units put together in a flowsheet, so as to convert certain raw materials into products in the most economic way. The drive over the last two decades, therefore, has been to find methodologies to design control systems for a complete flowsheet rather than designing control systems for individual units and then somehow "connecting" all such unit control schemes together. Such an integrated approach to control system design if often referred to as "control system synthesis ".

Control performance is linked with the dynamics of the process, which is often determined largely by the process design. Therefore, process design is one of the key issues in process control. Traditionally, process design has been carried out using steady-state economic considerations alone. Little consideration was given to the process dynamics at the design stage. After the entire process had been designed and the control objectives and the manipulated variables decided upon, using plant experience and simple heuristics, control system was designed for the existing process design.

Little consideration was given to the control performance likely to be achieved , as the control engineer was mainly concerned with the safe regulation of the process in the face of disturbances influencing the process operation. However, it has gradually been realised that unsatisfactory control performance is often due to a poor understanding of the basic process dynamics and the ad-hoc design of control systems. Foss [1973] pointed out in his classic paper that "it is not uncommon that process dynamics is greatly enhanced by a clever modification of the process itself ". Enhancements to both the process and control

system performances can also be achieved by perceptive changes in the process design (Anderson [1966], Shinskey [1983]). It seems, therefore, to be sensible to incorporate control aspects at the process design stage itself.

Process synthesis techniques have, recently received considerable attention (Stephanopoulos [1980] , Nishida et al. [1981]). Heat exchanger network synthesis, in particular, has been shown to offer substantial improvements over previous modes of operation (Linhoff and Turner [1980]). While significant economic improvements have been reported in such cases, they still suffer from the same deficiency of not considering the process dynamics at the process design stage.

A variety of pressures have contributed significantly to an increased emphasis on control system synthesis for chemical processes over the last two decades. Changing feed stocks, the increase in the importance of environmental issues and the growing need for reliability and safety has led, in general , to integrated process designs. The major consequence of such an approach is that units in a process flowsheet are now coupled in more intricate ways, which may lead to severe process interactions among the units. All such process interactions tend to limit the level of achievable control performance for a process. Other important issues for such highly integrated processes are :

(a) The flexibility of the process (can it accommodate changes in market demand).
(b) The selection of control objectives and manipulated variables as the process operating conditions change.
(c) The prediction of process behaviour given both process and parametric uncertainties.

To accomplish all the above tasks, the traditional hierarchical structure for plant design and operation (see Figure 1. 2. 1) must be modified so that each level interacts with the various other levels.

One common feature of any overall design technique is that often there are multiple designs that can provide the required performance. In a traditional approach , the choice of the most suitable design was generally based on steady-state economic factors and finalised fairly early on. It would be more appropriate , however, to consider the process dynamics in such decision making. Dynamic simulations on various alternative process designs can provide useful information that can be used in screening alternative process designs. However, there are a variety reasons why an approach based on dynamic simulations is not desirable :

Figure 1. 2. 1
Traditional design of a control system on a process plant

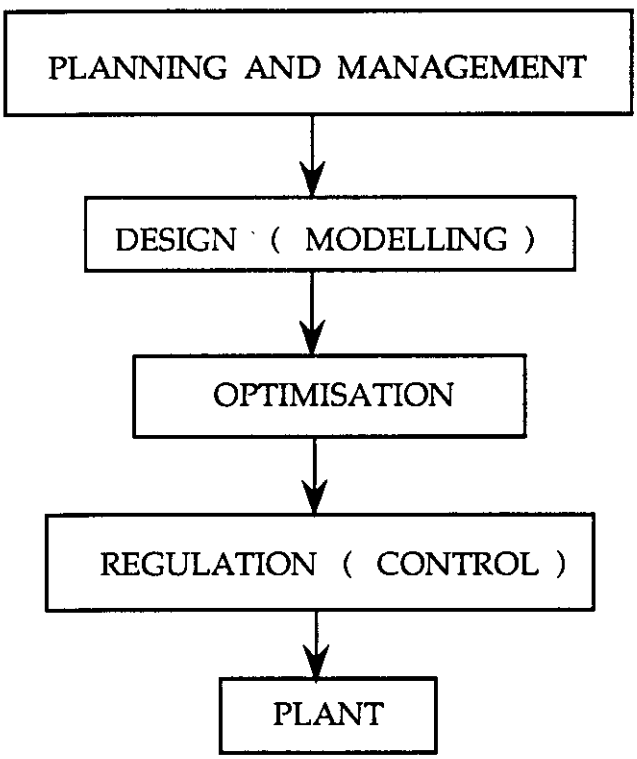

(a) It requires considerable computational power and reliable dynamic models. Thus, it is often a very time consuming process and may be impractical for large number processes.

(b) Poor control performance may be due either to poor design of the controller or to the poor design of the process itself. Dynamic simulations may assist in identifying likely poor performance. However, the dynamic simulation information will not generally provide any further insights into the cause behind such poor performance or how to rectify it.

These limitations, prompted the search for faster and more reliable means of dynamic assessment.

The controllability of a system may be defined as the degree of difficulty associated with the control of that system. The controllability of a process has been shown to be a very promising concept (Rosenbrock [1962a], Wong [1984], Perkins and Wong [1985], Johnston and Barton [1985a, b], Lau and Jensen [1985]) , as it seeks to provide substantial information about the dynamic characteristics of the process itself. Thus, controllability can be considered as one of the crucial stages of overall control system synthesis.

Several attempts have been made over the last decade (Morari et al. [1980], Douglas [1980, 1981], Govind and Powers [1982], Morari [1982, 1983], Perkins and Wong [1985], Lau and Jensen [1985] , Johnston and Barton [1985a, b]), to provide a systematic basis and consistent methodology that can be applied to the control system synthesis of chemical processes. The major criticism of all such approaches is that the emphasis has mainly been on the design and selection of control configurations rather than on the entire control synthesis problem. What is ideally required is an integrated approach between process design, process control and process economics, at the whole plant level.

The incorporation of economic considerations is a key point. Control system synthesis techniques available to date tend to place particular emphasis on process controllability. The proposed indicators provide a good picture of the inherent dynamic characteristics of a process. However, they fail to address the impact of process economics on their dynamic estimations. It is quite possible that a process design with good steady-state economic benefits may have poor operability characteristics. A design engineer may, therefore, need to consider a compromise between such a design and an alternative design with not quite so good economic benefits, but with good operability characteristics. At present, there is no rational and consistent basis on which to compare these estimations, one related to process economics and one related to operability.

Indeed, as pointed out by Perkins [1989], the tools currently available for the assessment of process operability are not ideal, for two major reasons.

(1) Being based on linear theory, all the available open-loop indicators do not guarantee that their results are reliable when implemented on nonlinear processes. However, use of these open-loop indicators for several industrial applications has shown that the closed-loop performance in each case was consistent with the indicator predictions (Morari and Skogestad [1985], Perkins and Wong [1985], Lau and Jensen [1985], Barton and Perkins [1987], Chan et al. [1986]).

(2) The proposed criteria for operability assessment do not relate directly to plant economics , so any trade-off between dynamic and steady-state economic performance is often difficult to make.

1.3 THESIS AIMS AND ORGANISATION

In this thesis, an attempt is made to provide a systematic methodology for control system synthesis of continuous processes that incorporate economics considerations. An industrial process of reasonable size (i.e. a gas-tail section of Shell's Clyde refinery) was chosen as a case-study, to test the applicability of the proposed methodology. The thesis is organised in the following manner.

The gas-tail consists of three distillation columns in series. Therefore, the dynamics associated with the gas-tail system depend essentially on the dynamics of individual columns along with the interactions existing among them. A good dynamic model for simulating distillation columns , therefore, is essential. Chapter 2 reviews the current status of dynamic distillation column modelling. A new compartmental modelling approach for predicting the dynamics of distillation columns is also proposed in this chapter.

Any simulation model should be validated thoroughly before being used. Chapter 3 deals with model development and verification for the gas-tail. Comparison of the various steady-state gas-tail model simulations with plant trial data will be made in this chapter. Optimum operating conditions, that provide potentially large improvements over the current operation of the gas-tail will also be presented in this chapter. These two chapters together provide the information necessary for the development of an optimising control scheme.

Necessary control theory background and the current status of control system synthesis will be reviewed in Chapter 4. Different approaches used for control system synthesis along with their major limitations will be examined here.

One of the major contributions of this thesis involves a new economics based control system synthesis approach. The rationale and theory behind such an approach will be introduced in Chapter 5. A two-stage method that seeks to provide a consistent basis for assessing process operability and plant economics is proposed in this chapter. Application of the proposed approach to a single column example will be presented.

Extension of the proposed methodology to the gas-tail case-study will be discussed in Chapter 6. The selection and screening of various alternative control systems will be addressed in this chapter. Major limitations of the control scheme currently in operation on the gas-tail will be identified and a new control scheme that potentially offers improved closed-loop performance will be discussed here. Both the open-loop indicators and the closed-loop simulation results obtained will be presented in this chapter.

Chapter 7 presents the conclusions from this study together with recommendations for future work.

CHAPTER 2

A NEW APPROACH TO REDUCED-ORDER DYNAMIC DISTILLATION MODELS

2.1 INTRODUCTION

2.1.1 INTRODUCTION TO THE CASE - STUDY

The major case-study used in the current work is a part of Shell's Clyde refinery in Sydney, Australia, called the gas-tail (see Figure 2. 1. 1). The crude distillation unit (CDU) at this refinery is designed to separate out various fractions of the crude oil such as the light hydrocarbons, kerosene, gas-oil, heavy oil etc.,. Light hydrocarbons (C_1 - C_5) are present in the distillate product stream from the CDU, coming both from the crude feedstock and also from some unavoidable cracking of heavier hydrocarbons during the crude distillation process itself. These lighter fractions must be removed in order that the final motor gasoline products meet stringent vapour pressure requirements. Thus the light hydrocarbons are collected as a distillate stream from the CDU stabiliser column (see Figure 2. 1. 2) which is then separated into individual fractions in the gas-tail system. Some of these products are sold directly and some of them are sent to other refinery plants for use in further processes. In the absence of any separation of the light hydrocarbons in this manner through the gas-tail system, they would have been simply burnt as fuel gas , thus eliminating a potential source of profit.

The feed to the gas-tail actually comes from a number of sources, as shown in Figure 2. 1. 2. Crude oil is distilled into various hydrocarbon fractions in the main CDU column. The tops from this column contain light hydrocarbons (C_1 - C_{15}) which are further treated in the CDU stabiliser to remove very light hydrocarbons (C_1 - C_6) as distillate. Kerosene and naphtha present in the bottoms of the CDU stabiliser are separated into their respective fractions in the distillate splitter. Light hydrocarbons from both this column and the platformer stabiliser, together with additional light hydrocarbons produced due to cracking, are all sent as additional sources of feed to the gas-tail. Therefore the lighter fractions of the crude oil, coming from various sections of the CDU and the upstream stabilisers, form a single feed stream to the gas-tail. Hence the feed to the gas-tail depends heavily on the type of crude being distilled in the CDU, and the operating conditions of the upstream units. Feed to the gas-tail, therefore, fluctuates widely both in flowrate as well as in composition. Ethane, propane and i-butane are separated sequentially as distillates from the three gas-tail columns , while n-butane is taken as a side stream product from the last column (see Figure 2. 1. 1). The de-ethaniser which has been designed to separate out the lighter components (such as ethane and the accompanying

Figure 2.1.1

GAS - TAIL FLOWSHEET

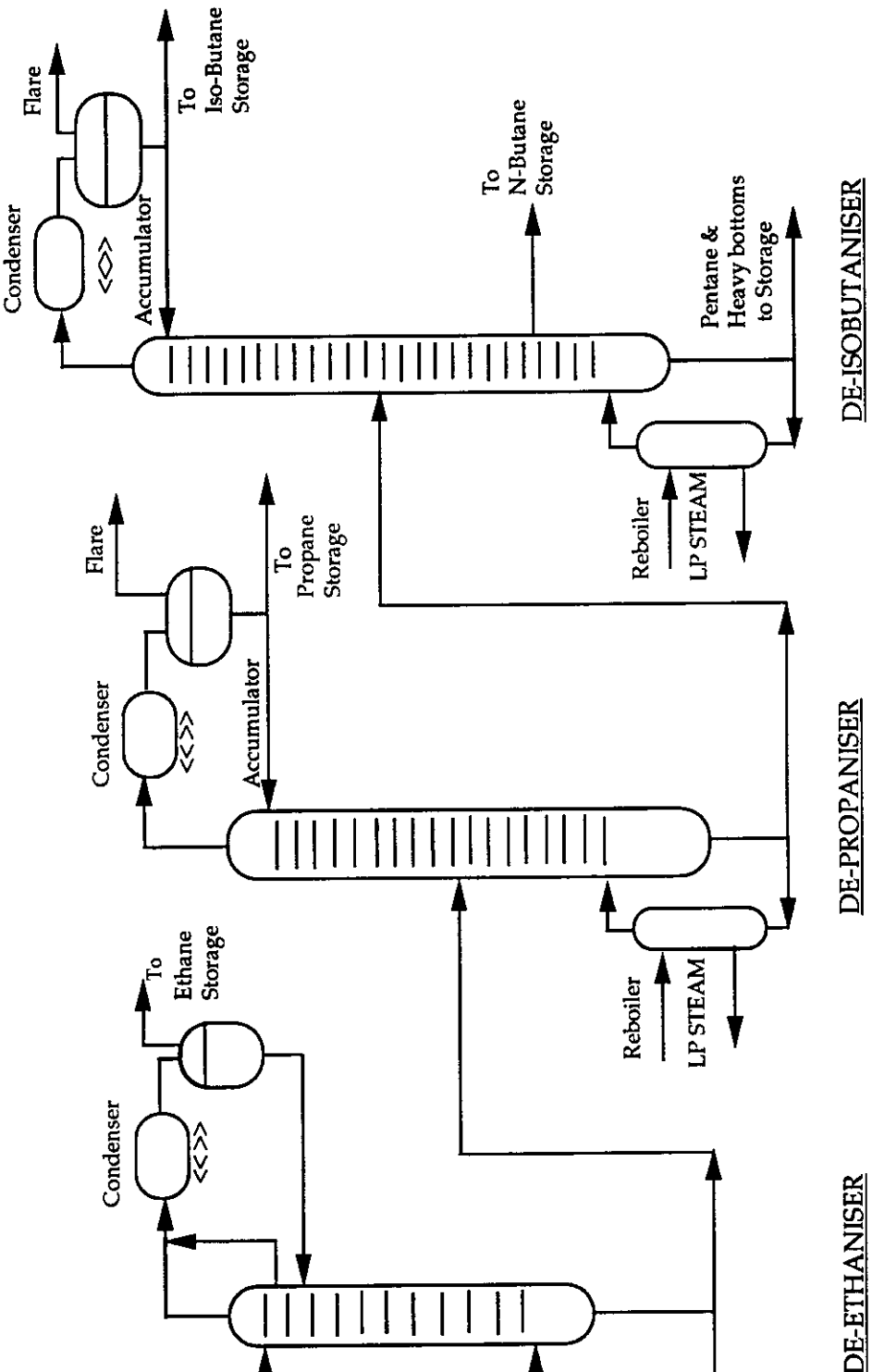

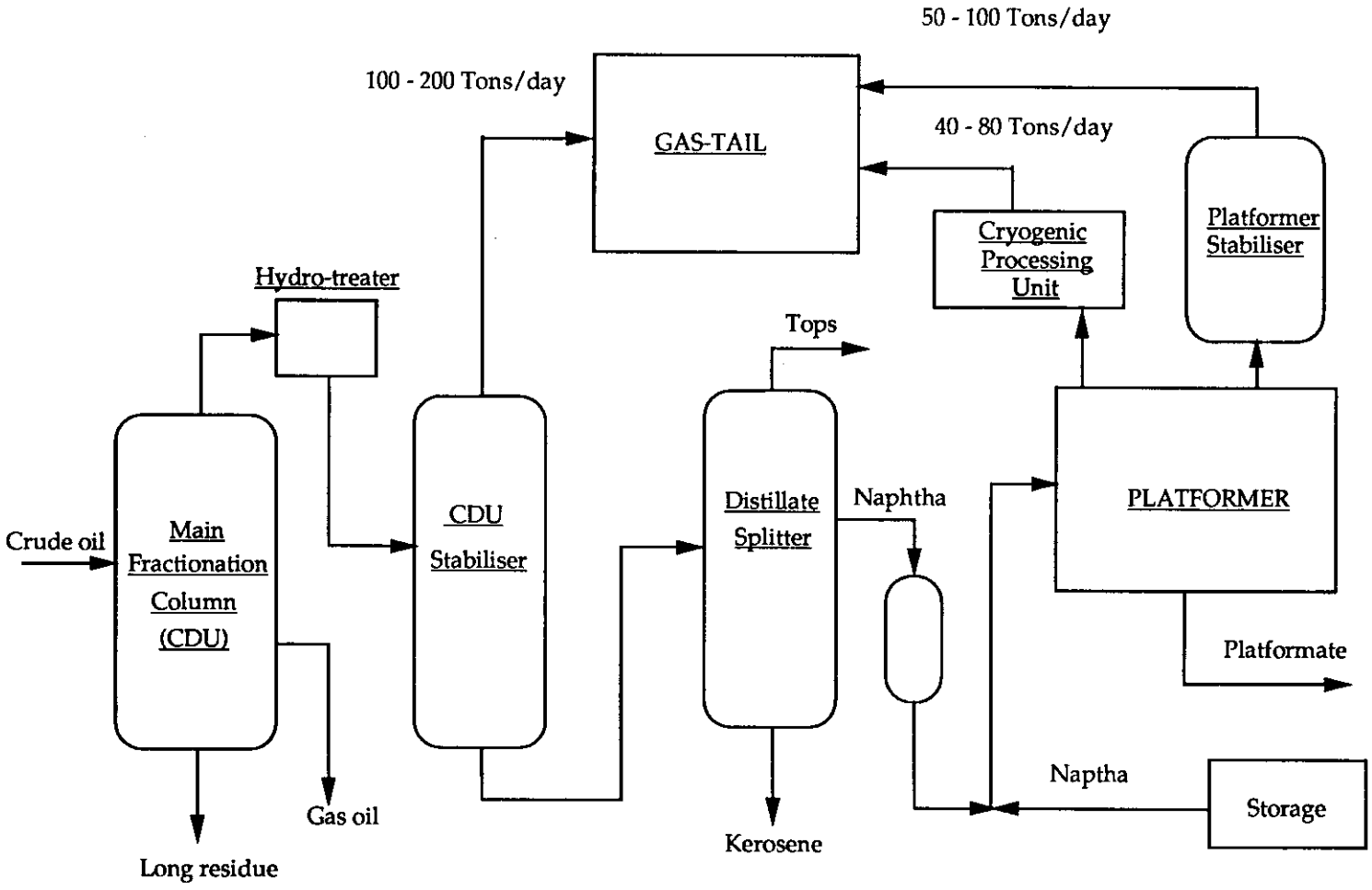

Figure 2. 1. 2
Sources of feed to the gas-tail

traces of methane) has 15 trays , all of them being of the sieve tray type. The column has been designed to operate at a pressure range of 27 - 30 bar so that most of the ethane or any other lighter components are separated from the feed. The column was designed such that the feed tray is in fact the top most tray of the column. Vapour from the feed tray combined with liquid product from the tray below are sent to a partial condenser (see Figure 2. 1. 1). The distillate product is collected as a fuel gas. Cooling for the condenser is supplied through a fin-fan air cooler. Air flowrates can be varied by adjusting the pitch of the fin-fans. Low pressure (LP) steam is supplied as the heating medium in the reboiler, which is of the thermosyphon type. However traces of ethane (3 - 5 mole %), via the de-ethaniser bottoms, are allowed through to the de-propaniser column - where the distillate product is collected as liquid petroleum gas (LPG , whose the major component is propane). These traces of ethane and other lighter components increase the vapour pressure and help provide a better separation of propane from the heavier components. However, large amounts of ethane (> 6 %) in the LPG are undesirable not only due to quality control restrictions on the LPG, but also to prevent unwanted pressure fluctuations in the de-propaniser column. These pressure fluctuations are partly due to the way the existing control system has been designed whereby the column pressure is controlled through the steam input rate to the reboiler and the distillate composition through adjustment of the reflux rate. When a high percentage of light components (> 6 %) enters the de-propaniser, a sudden decrease in de-propaniser top temperature (and hence the column pressure) takes place. The inherent interactions between the pressure and composition control loops severely affect the internal operating conditions of the column. Low temperatures at the top of the column are undesirable due to the limited capacity of the condensers which are currently operated at close to their maximum capacities.

The de-propaniser column is a 35 sieve tray column which has been designed to operate over a pressure range of 17 - 20 bar. Feed to this column comes from the bottom of the de-ethaniser reboiler. Due to the large pressure difference (10 -12 bar) in the operating pressures between the de-ethaniser and the de-propaniser, the liquid feed undergoes flashing and the resultant vapour-liquid equilibrium mixture enters at the 13^{th} tray of the de-propaniser. Pressure on tray 3 is measured and controlled through the steam input rate in the reboiler. Fin-fan air coolers supply the cooling medium for the overhead condenser. Fine tuning of the pressure , however, may also be done by adjusting manually the condenser air flowrate or the flowrate of the flare gases, generated in the condenser due to partial condensation. LP steam supplies the necessary heat duty in the thermosyphon reboiler.

The final distillation column of the gas-tail, the de-isobutaniser, produces an i-butane distillate which is then "sold" to the alkylation plant. N-butane which is used as "tops" in fuel oil is collected as a side-stream (from tray 6 , trays are counted from the

bottom of the column) in the bottom section of the column. Again, due to quality control restrictions, only a very low quantity of propane (< 5 %) is allowed in the feed to this column, which contains 50 trays of the sieve type. The bottoms from the de-propaniser enters this column at tray 22. Any traces of ethane reaching this column due to poor operation of the two upstream columns cause considerable control problems and result in poor separation of the i-butane. Low amounts of propane and i-butane in the n-butane product are necessary due to vapour pressure requirements.

2.1.2 LIMITATIONS OF THE GAS-TAIL

The gas-tail was originally designed to handle a feed rate up to a maximum of 320 tons/day and containing up to 20 mole % pentanes (or higher hydrocarbons). The gas-tail has had a history of poor performance dating back at least a decade with off-grade products often being produced. The gas-tail performance has been found to be satisfactory when the feed rate is low with a low pentanes content, as this requires low reboiler and condenser duties which are adequately met by the existing heat-exchangers. Major problems encountered with the operation of the gas-tail have been attributed to the following :

(a) Feed rates to the gas-tail depend heavily on the operating conditions of the upstream units and over a very short period of time can vary from 150-360 tons/day.

(b) The types of crudes processed in the CDU change considerably over a period of time and can contain very high amounts of pentanes. Thus, the feed to the gas-tail can contain up to 35 mole % pentanes, which is much higher than what the gas-tail has been designed to handle.

(c) Most of the time, all the condensers and reboilers in the gas-tail operate at or close to their maximum capacities, giving little scope for tight control of the gas-tail.

(d) The present gas-tail control scheme seems to be very interactive as the stability of all the columns is affected when any one of the columns is affected by a disturbance.

(e) Many of the level controllers used in the reflux accumulators and reboilers of the gas-tail are of the proportional type and have large proportional gains, resulting in significant movement in the corresponding manipulated variables.

(f) There is only poor knowledge of the internal operating conditions of the columns. For instance, the de-propaniser operates with internal flows that are typically in the range 360 - 400 tons/day , whilst the recommended levels are in the range 430 - 470 tons/day. The column's sieve trays were designed such that weeping occurs below 400 tons/day. Hence, large amounts of entrainment are expected in this column leading to poor separation.

2.1.3 OBJECTIVES OF THE CURRENT WORK

Apart from the limitations affecting the smooth operation of the gas-tail outlined above, other reasons for the poor performance can be associated with a poor understanding of process operations and the existing control system's performance. All the information available to date on the operation and process conditions of the gas-tail has been limited to steady-state simulation studies and plant trials. However, this is inadequate as due to continuous feed fluctuations and process disturbances the gas-tail seldom operates under steady-state conditions. A dynamic model would provide the transient response of the gas-tail in the range of operating conditions of interest and is, therefore, essential to the understanding of the operation and performance of the current control system. It would also be necessary in the selection and screening of alternative control systems that might improve the performance of the gas-tail. The objectives of the current work , therefore, are as follows:

(a) Perform plant trials to assess the current performance of the gas-tail.

(b) Develop a steady-state model for the gas-tail and validate it against both the plant trial data and a rigorous steady-state model.

(c) Extend the steady-state model to include dynamics and verify the predicted response against other dynamic models.

(d) Optimise the steady-state gas-tail model to identify the most profitable operating conditions and the major process constraints limiting the gas-tail performance.

(e) Determine alternative control schemes for optimising control of the gas-tail and assess their economic impact.

2.2 DISTILLATION COLUMN MODELLING

2.2.1 INTRODUCTION TO DISTILLATION COLUMN MODELLING

Distillation is both a complex and widely used separation process. The related questions of how to accurately model the dynamics of distillation columns and how to design good regulatory control schemes continue to attract considerable attention both from industrial and academic researchers. Considerable work has been done (Holland [1975]) on the steady-state modelling and simulation of distillation columns ranging from simple binary distillation to complex multicomponent distillation with non-ideal separations. Most of the work reported has been based on treating each separation stage/tray as being at equilibrium during separation. Consequently, control of distillation columns has been largely based on information available from steady-state models, extensive plant experimentation and heuristics (Holland [1975] , Browne et al. [1977], Kisakurek [1983]). However, this approach is very limiting and is often not practicable as the size and complexity of the column increases. An alternative approach is to design the control system based on information about the column dynamics obtained through simulations. Such an approach requires a dynamic model that captures the essential dynamic characteristics of the column.

There has been a steady development of dynamic models for distillation columns (Gani et al. [1986]), the complexity of which varies according to the needs and requirements. Doherty and Perkins [1982] made an excellent survey on the available distillation models for plate columns and systematically categorised them according to their degree of complexity. The dynamics of a multicomponent separation in a multistage distillation column can be represented by a system of coupled nonlinear ordinary differential equations. Doherty and Perkins identified five such models.

(i) The tray dynamics of composition, holdup and energy are each taken into account. The model thus obtained is called a Composition (C), Holdup (H) and Energy (E) or CHE model and represents the most rigorous form of distillation modelling.

(ii) Only changes in the tray composition and holdup dynamics are taken into account (i.e. enthalpy changes are assumed to occur instantaneously). This is called a Composition (C) and Holdup (H) or CH model.

(iii) Only changes in the tray composition and enthalpy dynamics are taken into account (i.e. it is assumed that the column has very fast holdup dynamics). This is called a Composition (C) and Energy (E) or CE model.

(iv) Only changes in the tray composition dynamics are taken into account. This is called a Composition or C model.

(v) Only tray composition dynamics are considered but with changes in the internal flows taking place instantaneously over a column section. This is the simplest and most used form of all dynamic distillation models and is called the Constant Molar Overflow or CMO model.

Finally, Doherty and Perkins emphasised the need to direct more theoretical and experimental work towards understanding CMO models for multicomponent distillation. Based on their recommendation, and keeping in mind their extensive use in distillation control studies, modelling work in this project has been directed towards developing simple dynamic distillation models on the lines of existing CMO models.

2. 2. 2 SIMPLIFIED DYNAMIC DISTILLATION MODELS - NEEDS AND CHARACTERISTICS

The literature on modelling staged distillation systems is extensive. Several packages (for example, PROCESS , SPEEDUP ; see Appendix A8 for more details) have efficient models to simulate their behaviour. Though the rigorous models thus developed can be very accurate, their extension to include dynamics can be computationally very expensive. Thus, there is a need to develop alternative, simplified dynamic models to simulate staged distillation systems. This is achieved by considering only the dominant characteristics of the system. The models thus obtained are called " low-order " or " reduced-order " models. In general, reduced-order models are needed for the following reasons.

(a) The large number of differential equations encountered in rigorous dynamic models , their non-linearities and the stiffness often associated with them pose considerable problems in numerical integration.

(b) Simple models are often quite adequate in decision making, optimisation, economic evaluation and screening of alternative control schemes.

(c) On - line optimisation and model-based control design are becoming increasingly important in the operation of chemical plants, and require process models that are both accurate and need an acceptable computational effort. Simple models are very useful in all such cases.

(d) For general purpose flowsheeting packages , where there are a large number of columns linked together in a process flowsheet with recycle streams and/or heat integration , simple models are useful.

2.2.3 REVIEW OF LOW - ORDER DYNAMIC MODELLING METHODS

Benallou et al. [1986] have made a good review of this topic. The classification they used was based on the extent of any linearity i.e. models were classified as linear , bi-linear models and nonlinear. Under the first category (i.e. linear models), model reduction and the use of transfer functions have been the most commonly used methods. The transfer function approach is based on performing frequency or Laplace domain analysis on the linearised model. This approach has the distinct advantage of relating the model parameters to physical properties of the actual process. Extensive work on the physical interpretation of the parameters used in this type of model has resulted in a number of empirical and theoretical relationships between the model parameters and process characteristics (Wahl and Harriott [1970], Celebi and Chimowitz [1985], Benallou et al. [1986], Skogestad and Morari [1988b]). Different versions of these models have been used in both column simulations and control system design (Skogestad and Morari [1988b], Skogestad et al. [1989]). However , this approach has been best suited to predicting the dynamic behaviour of the outputs (e.g. the distillate and bottoms products compositions) of the column but not the transient responses at the intermediate stages. Celibi and Chimowitz [1985] proposed an analytical model reduction technique based on modal analysis of the linearised dynamic equations of the complete column model. Their approach was based on sound physical reasoning and was found to provide results that were in good agreement with a range of more rigorous models including complex models with non-ideal separations. The major criticism of linear models in general has been their limited operational range. Some of the nonlinear effects exhibited by real columns such as asymmetric dynamics (Stathaki et al. [1985]) cannot be captured through these models. Low order nonlinear models can overcome some of the above deficiencies. The work reported in the literature on these models falls into two categories:

(i) Distributed parameter models
(ii) Lumped parameter models

In the former category, composition is assumed to vary as a continuous function of distance along the column, leading to a distributed parameter model described by partial differential equations (PDE's). Discretisation is then carried out using a net mass transfer coefficient for a column section (Osborne and Maddox [1965]) or through orthognal collocation techniques (Wong and Luss [1980]) to arrive at the solution. However, both

these methods are limited to linear models or linearised form of nonlinear models. In an alternative approach, Cho and Joseph [1983] developed a method which uses model reduction by direct transition to a polynomial representation of the composition and flow profiles in the column, and then using orthogonal collocation to find a solution. This general approach has been found to give excellent agreement with more rigorous models. The accuracy achieved can be increased by the choice of PDE approximation, the type of polynomial used or the number of collocation points used. All these methods select the collocation points based on methods developed for continuous systems (Villadsen and Michelson [1978]). Stewart et al. [1981, 1983] developed a column model based on stage-wise operation where profiles of each of the state variables were approximated by polynomials in distance, fitted to the process model at various collocation points (i.e. along the column) that were designed to give a good approximation to the full set of stages. The results obtained indicated that the model can predict the dynamic behaviour of a column very well. In all the collocation based models , mathematical complications do seem to arise. Also, they yield a set of fictitious state variables and generally the collocation points do not correspond to the actual tray locations.

In the latter category (i.e. in the lumped parameter modelling approach), the state variables vary only as a function of time. Thus the dynamic behaviour of a distillation column can be described by a set of non-linear ordinary differential equations corresponding to mass and energy balances. It was Rosenbrock [1962c] who first hinted that distillation models could be reduced by lumping several stages together. Osborne and Maddox [1965] were the first to model distillation columns based on this lumped section approach. Subsequently, all the work done based on this approach has been referred to as lumped section or compartmental models. If the column can be reasonably described by such a lumped parameter approach , the dynamic response can be expressed a set of nonlinear, first-order ordinary differential equations in time (Levy et al. [1969]). Overall dynamics of the column is governed by several time constants, each of which corresponds to a differential or state variable. The dynamic response resulting from each of these time constants is associated with a specific direction known as a 'mode'. The overall response of the column is influenced by all these modes. The results of Levy et al. [1969] suggested that only two or three modes of a distillation column were sufficiently slow to affect the response and, thus, in theory only two or three state variables corresponding to the slowest modes would be needed to model a column. They also observed that modes corresponding to compositions were the slowest and thus have the major influence on the dynamic behaviour of the column. This general approach has both sound mathematical and physical bases. The dynamic model development for distillation columns given in the following section has therefore been based on a lumped section approach.

2.2.4 DYNAMIC COMPARTMENTAL MODELS

The compartmental model for a binary distillation column developed by Osborne and Maddox [1965] was the first of its kind. However it suffered from the drawback of being treated like a 'black box' with just inputs and outputs. Dalhquist [1980] proposed a new approach for lumping the trays of a column together. He defined the regions where external streams meet the column as 'nodes' and used a liquid holdup, for such nodes, of one tray. The trays in between the 'nodes' were lumped into 'sections'. Adjacent nodes were thus interconnected through sections that absorbed the remaining holdup of the column. Each section was modelled based on the constant molar over flow (CMO) assumption with constant 'K ' (separation or equilibrium constant) values. Benallou et al. [1986] proposed a model based on the above approach, but which used more elaborate techniques to divide the column into different 'compartments'. Several trays lumped together were called a 'compartment' that was associated with a differential equation corresponding to the 'most sensitive stage' of the compartment, but having a holdup equal to the total holdup of all trays within the compartment. This single equation represented the total composition dynamics of the compartment. Physically, the most 'sensitive stage' was defined as the stage or location in a compartment where disturbances enter the system and thereby affected its dynamics. Separation associated with the rest of the trays was treated as a steady-state process. Though the results obtained through this approach were quite encouraging, the number of compartments required to model a column were decided on arbitrarily. Such a division of a column into an arbitrary number of compartments leads to a structure that is not unique. One consequence of this is that there may always be a compartmental structure that has better 'performance' than the one that is chosen. Also, the reasons for the initial inverse response (IIR) , observed to occur in this approach, have not been explained.

Howell [1984] proposed a model based on Dalhquist's [1980] approach known as the node-section model. Here, a distillation column was represented by a series of 'nodes' and 'sections'. The points where feed or product streams join the column were called 'nodes', with adjacent nodes being linked by 'sections' that transfer material and energy between the nodes. The sensitive stage was split between adjacent nodes , using a specific holdup distribution policy , and the resulting model was shown to avoid IIR. This model can be considered as a special case of Benallou et al. [1986] 's approach , where the sensitive stage was always taken as the bottom-most tray of a compartment. The conditions in each (Howell) section were obtained by solving all the steady-state separation equations simultaneously. A simple distillation column was thus represented by three nodes and two sections ; a column with one side stream by four nodes and three sections and so on. In a

simple one feed, two product column, the holdup of all trays in the rectifying section and the condenser was distributed between the top and middle nodes. Similarly the holdup of the stripping section trays and reboiler was distributed between the middle and bottom nodes. The eigenvalues of a physical system (see Section 4. 1. 4) provide a measure of the time-constants that influence the dynamics of the system. It was shown for several examples that the eigenvalues predicted for the node-section model were very similar to the smallest eigenvalues of a more rigorous model. Thus, the predicted dynamic response was also very good. However, the policy adopted in distributing the holdups amongst adjacent nodes was still very arbitrary. In addition, no explanation was offered for assigning the node composition to that of the bottom-most tray of a compartment.

Gannavarapu et al. [1989] proposed a new model based on some of the above ideas and called it the 'average node section (ANS) ' or 'average node composition ' model (see Figure 2. 2. 1a). The concept of 'nodes' and 'sections' was carried over from previous models but with the arithmetic average composition of all the trays within the compartment being taken as the node composition.

Consider, for example, a compartment (Figure 2. 2. 1b) of trays , where a binary mixture is being separated. The separation taking place on each tray can be represented by the following set of differential equations:

$$M_1 \frac{dX_1}{dt} = V(Y_2 - Y_1) + L(X_0 - X_1) \qquad (2.2.1)$$

$$M_2 \frac{dX_2}{dt} = V(Y_3 - Y_2) + L(X_1 - X_2) \qquad (2.2.2)$$

$$\vdots$$

$$M_N \frac{dX_N}{dt} = V(Y_0 - Y_N) + L(X_{N-1} - X_N) \qquad (2.2.3)$$

These equations along with the phase equilibrium relationships for the vapour and liquid phases on each tray will completely specify a staged separation system. The ANS approach assumes that the total dynamics of a set of trays can be lumped into a 'node', a fictitious envelope superimposed over a 'section' encompassing all the trays representing steady-state separation. Mathematically, this can be represented by a single differential equation accounting for the overall composition dynamics on the set of trays obtained by adding equations (2. 2. 1) - (2. 2. 3).

$$M_1 \frac{dX_1}{dt} + M_2 \frac{dX_2}{dt} + \ldots\ldots + M_N \frac{dX_N}{dt} = V(Y_0 - Y_1) + L(X_0 - X_N) \qquad (2.2.4)$$

Figure 2. 2. 1

(a) Compartmental representation of a distillation column

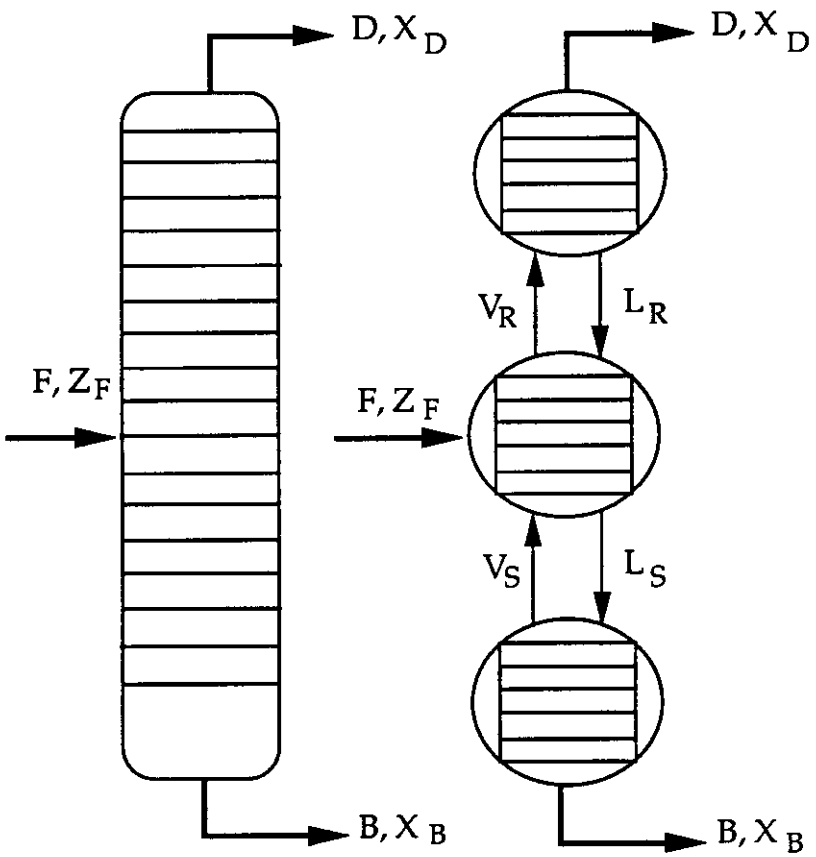

(b) Component balance in a typical compartment

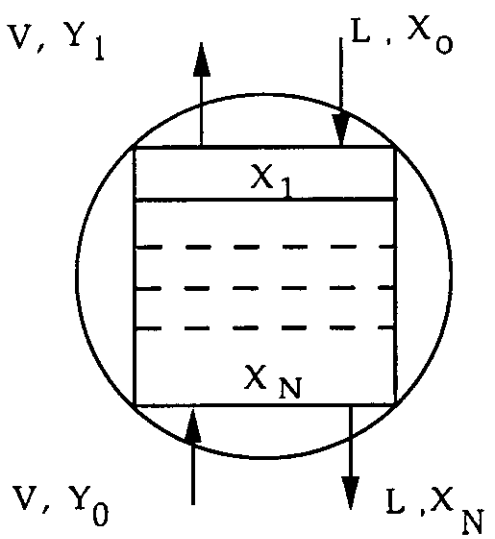

To satisfy the degrees of freedom , we need an additional (N -1) equations, each representing the steady-state separation over a single tray. For all but the bottom-most tray, these are :

$$0 = V(Y_2 - Y_1) + L(X_0 - X_1) \qquad (2.2.5)$$

$$0 = V(Y_3 - Y_2) + L(X_1 - X_2) \qquad (2.2.6)$$

$$\vdots$$

$$0 = V(Y_N - Y_{N-1}) + L(X_{N-2} - X_{N-1}) \qquad (2.2.7)$$

If the holdup on each tray is constant and equal i.e.

$$M_1 = M_2 = \cdots = M_N = M$$

then Equation (2. 2. 4) can be further simplified to give ,

$$M\left(\frac{dX_1}{dt} + \frac{dX_2}{dt} + \ldots\ldots + \frac{dX_N}{dt} \right) = V(Y_0 - Y_1) + L(X_0 - X_N) \qquad (2.2.8)$$

Equation (2. 2. 8) can also be written as,

$$\frac{(N*M)\left\{ \frac{dX_1}{dt} + \frac{dX_2}{dt} + \ldots\ldots + \frac{dX_N}{dt} \right\}}{N} = V(Y_0 - Y_1) + L(X_0 - X_N) \qquad (2.2.9)$$

or,

$$M_T \frac{dX_{avg}}{dt} = V(Y_0 - Y_1) + L(X_0 - X_N) \qquad (2.2.10)$$

where,

$N*M = M_T$, the total holdup on all N trays

and $$X_{avg} = \frac{(X_1 + X_2 + \ldots\ldots + X_N)}{N} \qquad (2.2.11)$$

Mathematically, the node composition is the arithmetic average of the compositions on all the trays. Though the node composition is a fictitious variable that cannot physically be assigned to any single tray of a section , it still has significance in that it represents a 'mixed cup concentration' over the whole set of trays. This concept of averaging the compositions over a set of trays is not new and has frequently been used (Wahl and Harriott [1970] , Espana and Landau [1978]) in the distillation modelling

literature. The ANS modelling approach thus had a strong physical and mathematical basis , however it still suffers from the drawback of IIR in its outputs.

A further new model based on the compartmental approach is proposed in the next section and called the universal compartmental model (UCM). This model will be shown to have good dynamic characteristics with no spurious IIR in its outputs. Model development and comparison with various other compartmental models is made in the following sections.

2.3 UNIVERSAL COMPARTMENTAL MODEL (UCM)

2.3.1 MODEL DESCRIPTION

The nomenclature adopted in this section with respect to a tray, a node, a section and a compartment is as follows :

(i) A tray represents a physical stage over which the separation of a binary or a multicomponent mixture is being carried out.

(ii) A node is an envelope over a section of trays that absorbs all the dynamics of the trays enclosed.

(iii) A section encompasses a set of trays carrying out a steady-state separation.

(i v) A compartment is formed from a node and a section.

In this section, the UCM based model development and its application to binary mixtures will be discussed. In the later part of this chapter, extension of the UCM to multicomponent mixtures will be examined.

Consider a compartment containing N trays in which the separation of a binary mixture is taking place (see Figure 2. 2. 1b). The separation carried out on each tray can be represented by unsteady-state mass and energy balance equations combined with equilibrium relationships. Levy et al's., [1969] work has indicated that in a distillation column, thermal and hydraulic modes decay faster than composition dynamics and hence do not usually contribute significantly to the separation dynamics. It has been shown (see Section 2. 5) that, on a range of industrial distillation columns studied , the internal flow profiles of the columns (based on rigorous steady-state models) match reasonably well with the flow profiles based on the constant molar overflow (CMO) assumption. Therefore, based on the CMO assumption, the separation dynamics of a tray are given by a single unsteady-state balance equation for the most volatile component of the mixture on the tray. Likewise, for a group of trays, a set of equations can be written for each tray. Solution of these equations would give the dynamic behaviour for this group of trays at any

instant of time. Composition of the remaining component , in each case, is obtained by solving the overall component balance equation (i.e. $X_1 + X_2 = 1.0$; the subscripts 1 and 2 represent components 1 and 2 , respectively). However, performing dynamic simulations using even this simplified model could prove computationally expensive, especially when the number of trays is very large. Further, if one makes the assumption that the separation dynamics associated with each tray are fast compared to the overall dynamics of a set of trays or 'compartment', then the above model reduces to an unsteady-state balance equation for each component over the whole compartment. The dynamics of the column are, thus, reduced to the separation dynamics associated with a set of 'nodes'. Each compartment in the column model may thus be thought of as made up of two parts:

(i) A "section" in which the stage by stage (equilibrium) separation at steady-state is performed.

(ii) A dynamic "node" which approximates the separation dynamics of the entire set of trays within the compartment.

This approach is quite attractive in that,

(a) Solving a system of steady - state equations is generally much easier than solving the corresponding set of dynamic equations.

(b) It captures the slow composition dynamic modes which are the important ones from the composition control point of view.

In the UCM approach, there is no limit on the number of compartments that may be used (see Figure 2. 2. 1a). Computational time, however, increases as the size of the compartment used decreases and , in the limit, approaches that of a tray by tray model when the compartment size is unity. None of the previous workers have investigated what the "optimum" size of a compartment should be. Based on our experience over a range of industrial columns (see Section 2. 5) , a compartment size of five trays provides a good compromise between speed and accuracy and has been used throughout this study.

Since the compositions of a binary mixture are not independent (i.e. $X_{1,J} + X_{2,J} = 1.0$ for all $j = 1,..., N$; the first subscripts 1 and 2 indicate component 1 and 2 , respectively, while the second subscript shows the tray number), only one of the components (in this case, the more volatile component) will be used throughout the following analysis. Thus, composition of the more volatile component is denoted by X , while the subscript indicates the tray number. The model equations representing a compartment for a binary system, therefore, are:

$$M_T \frac{dX_{node}}{dt} = L(X_0 - X_N) + V(Y_0 - Y_1) \qquad (2.3.1)$$

$$L(X_0 - X_1) + V(K_2X_2 - K_1X_1) = 0 \qquad (2.3.2)$$

$$L(X_1 - X_2) + V(K_3X_3 - K_2X_2) = 0 \qquad (2.3.3)$$

$$\vdots$$

$$L(X_{N-2} - X_{N-1}) + V(K_NX_N - K_{N-1}X_{N-1}) = 0 \qquad (2.3.4)$$

$$Yj = f(\alpha_1, Xj) \qquad (j = 1, ..., N) \qquad (2.3.5)$$

where α_1 is the relative volatility of the more volatile component in the binary mixture.

Equation (2. 3. 1) describes the node composition dynamics while Equations (2. 3. 2) - (2. 3. 4) are the steady-state tray component balances for (N - 1) trays of the compartment, with vapour-liquid equilibrium given by Equation (2. 3. 5). Consequently, steady-state component balances can be written for all but one of the trays in a compartment, the final mass balance equation being provided by the node equation. The UCM approach differs from other compartmental modelling approaches with respect to the definition of the node composition. The node composition in this model is equated to that of the lowest tray of a compartment.

$$X_{node} = X_N \qquad (2.3.6)$$

The mathematical rationale behind this will be explained in detail later.

The liquid holdup attributed to a node is taken to be the total holdup of all trays within the compartment and is assumed to be constant.

$$M_T = \sum_{j=1}^{N} M_j \qquad (2.3.7)$$

Tray holdups are calculated for a given column and tray specifications, using standard design procedures provided in the literature (Gani et al. [1986]).

The UCM approach requires relative volatilities for each of the components throughout the column. These relative volatilities depend strongly on the tray pressures and compositions. Therefore, methods used to estimate relative volatilities from equilibrium constant (K) charts available in the literature (for example, the Engineering Data Book [1980]) are usually subject to large errors. However, rigorous steady-state simulation data, if available over a range of operating conditions, can be used to estimate relative

volatilities with a reasonable accuracy. Therefore, the first step in building any simple dynamic model is to perform steady-state simulations for the desired operating conditions on a rigorous steady-state model for the column of interest, using any of the available simulation packages (for example, SPEEDUP, PROCESS). These steady-state simulation results are needed for the following two reasons :

(i) To estimate the relative volatilities for each of the components throughout the column using the equilibrium constant (K) data generated.

(ii) The CMO assumption used for the internal flows in the simple dynamic model can be validated against the flow profiles from the more rigorous model. This establishes bounds on the range of operating conditions over which the CMO assumption is valid.

If the relative volatilities do not vary significantly over the entire column or over a section of a column , then a constant relative volatility (for example, an arithmetic average over the whole column or column section) can be used. However, if they vary significantly over the whole column, a reasonable compromise would be to use constant relative volatilities for each compartment, values being averaged over all the trays contained in the compartment.

One of the major advantages of the UCM approach is that it preserves commonly observed nonlinear characteristics of distillation columns such as 'asymmetric dynamics'. The following case-study on a 20-tray distillation column of Stewart et al. [1981] demonstrates this feature. The responses of the distillate and bottoms compositions of the tray-by-tray model (Stewart et al. [1981]) to a 40% increase and decrease in feed rate, have been plotted in Figures (2. 3. 1) and (2. 3. 2). The response curves are not symmetric with respect to the steady-state under consideration. In other words, the column's response is found to depend both on the magnitude and the direction of the change made which is a characteristic of nonlinear processes. The UCM approach simulates these nonlinear effects accurately.

2. 3. 2 COMPARISION OF UNIVERSAL COMPARTMENTAL MODEL WITH OTHER COMPARTMENTAL MODELS

The responses of various compartmental models are studied through the following case-study of a 20-tray distillation column of Stewart et al. [1981], which represents the separation of a binary mixture of constant relative volatility (α = 1.6). Constant molar overflow (CMO) has been assumed for all the models used in the case-study. Stewart

TABLE 2.3.1

20 TRAY BINARY DISTILLATION COLUMN EXAMPLE

Process details	
Type of column	1 Feed and 2 Products
Type of mixture	Binary
Number of trays	20
Reflux rate (Kg -moles/hr)	4000
Vapour rate (Kg- moles/hr)	5000
Feed rate (Kg -moles/hr)	2000
Distillate rate (Kg- moles/hr)	1000
Bottoms rate (Kg- moles/hr)	1000
Tray holdup (Kg- moles)	100
Condenser holdup (Kg- moles)	300
Reboiler holdup (Kg- moles)	200
Feed composition Components (1) and (2) (Saturated liquid)	0.5 and 0.5
Relative volatility	1.6
Distillate composition Component (1)	0.933
Bottoms composition Component (1)	6.73E-2
Types of step changes made	(a) +40 % in feed flowrate (b) +40 % in feed composition (c) -10 % in reboiler vapour rate (d) +10 % in reflux rate

Figure 2.3.1
ASYMMETRIC DYNAMICS OF UNIVERSAL COMPARTMENTAL MODEL(UCM)
RESPONSE OF DISTILLATE COMPOSITION
FOR A 40% STEP CHANGE IN THE FEEDRATE

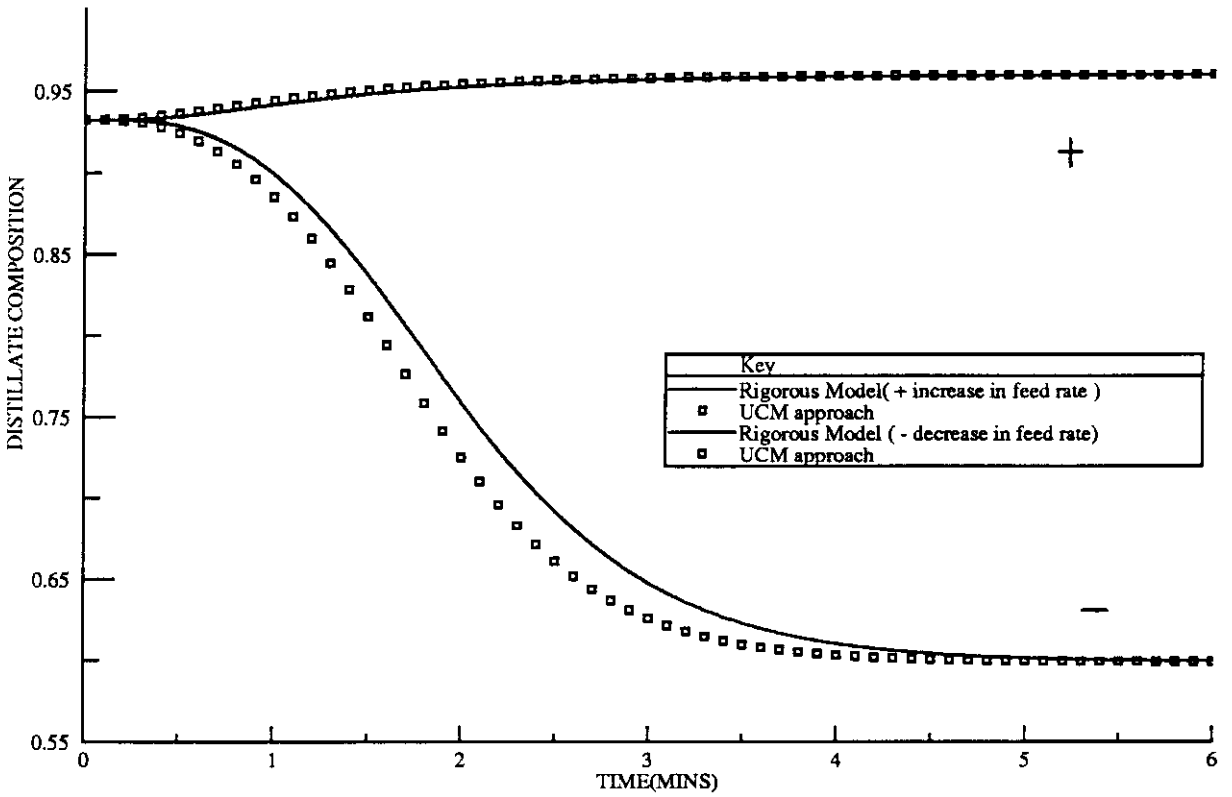

Figure 2.3.2
ASYMMETRIC DYNAMICS OF UNIVERSAL COMPARTMENTAL MODEL (UCM)
RESPONSE OF BOTTOMS COMPOSITION
FOR A 40 % STEP CHANGE IN THE FEEDRATE

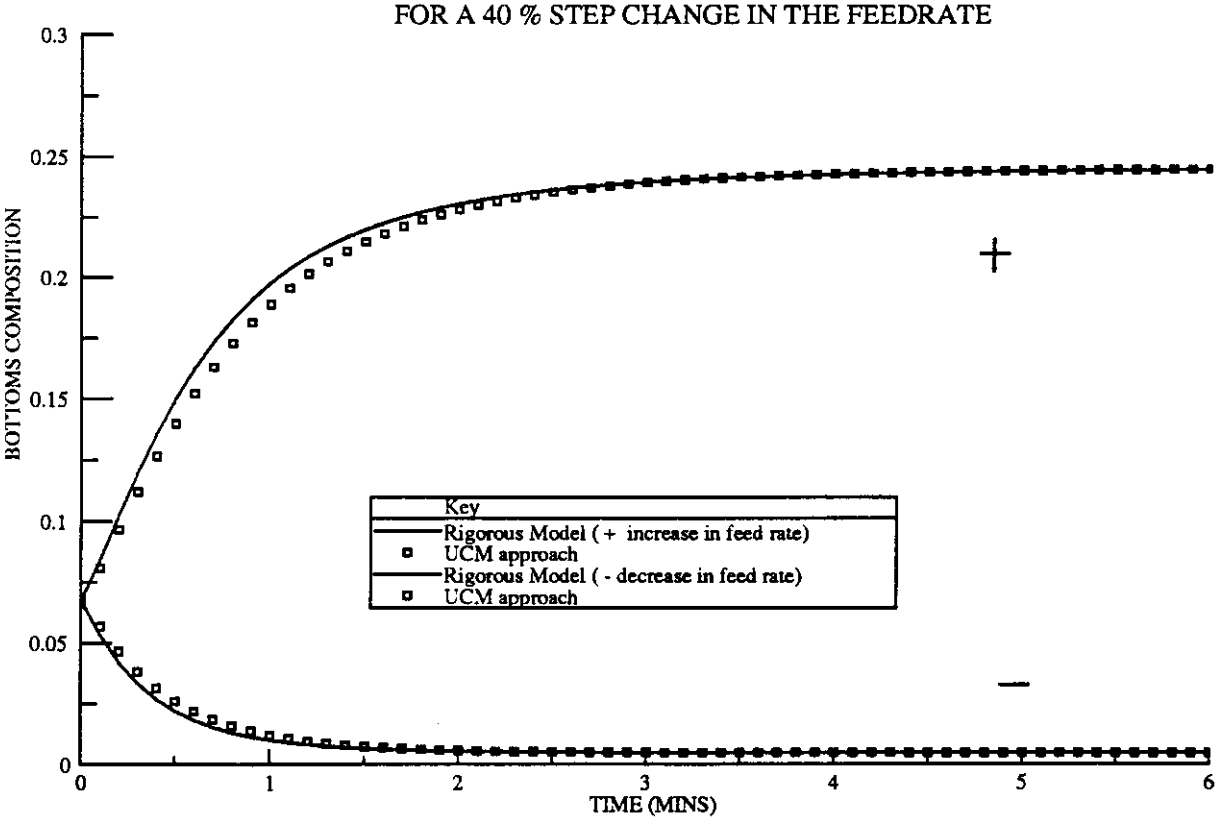

et al.'s [1981] collocation model, Benallou et al.'s [1986] compartmental model , Gannavarapu et al.'s [1989] average node section model (ANS) , Howell's [1984] node section model and the universal compartmental model (UCM) have all been compared with the rigorous tray-by-tray model (Stewart et al. [1981]) both at steady-state (see Table 2. 3. 1) and dynamic (see Figures 2. 3. 3 - 2. 3. 10) conditions. Due to the non-availability of the policy that was originally used by Howell [1984] for distributing holdups amongst the adjacent nodes, a policy in which - " the inventory in each section (plus any from the reboiler or condenser) will be distributed equally amongst the adjacent nodes (Lear et al. [1989]) " - has been used for Howell's model in the present case-study. All the assumptions used by other researchers have been used as reported.

Various characteristics observed are discussed below.

(a) Except for the collocation model , all the other models lead to the same final steady-state for each of the changes examined. The discrepancy arises (Benallou et al. [1986]) due to the fact that the collocation points used in collocation models seldom correspond to the actual tray locations and interpolation is, therefore, required to estimate the tray compositions. As shown, this can lead to steady-state inaccuracies.

(b) Overall, the UCM has superior dynamic tracking compared to the other simple dynamic models.

(c) Open-loop poles (which are the inverse of the column time constants) significantly influence the column dynamics. Comparison of the open-loop poles (see Table 2. 3. 2) shows that the UCM results in time constants that are closest to the smallest time constants of the rigourous tray-by-tray model and hence close dynamic tracking is to be expected. All the other models give time constants smaller than the tray-by-tray model, thereby giving faster response.

(d) All the models except the UCM, in some case or other seem to exhibit a spurious 'initial inverse response' (IIR) in their outputs (see Figures 2. 3. 11 and 2. 3. 12).

In other words, the other simple dynamic models all have some form of weakness or other. Benallou' et al .,'s model seems to be physically meaningful , but mathematically it is not very rigorous and it also exhibits IIR , the reason for which has not been explained clearly. The ANS model is arguably more mathematically rigorous , however , it also exhibits IIR. Howell's node-section model avoids IIR. However, it does not explain explicitly how the holdups should be distributed among adjacent nodes. Also, the physical meaning of 'splitting the sensitive stage among adjacent nodes' to avoid IIR has

TABLE 2.3. 2

COMPARISON OF TIME CONSTANTS OF VARIOUS REDUCED-ORDER MODELS WITH THE SMALLEST TIME CONSTANTS OF A RIGOROUS TRAY-BY-TRAY MODEL FOR A 20-TRAY DISTILLATION COLUMN

Rigorous model	UCM	ANS model	Benallou's model	Howell's model
- 4.108E -1	-4.308 E-1	- 4.096 E-1	-4.009 E-1	-7.206 E-1
- 1.791E+0	-1.810 E+0	-1.992 E+0	-2.065 E+0	-4.046 E+0
- 5.436E+0	-5.634 E+0	-6.776 E+0	-7.468 E+0	-1.074 E+1
- 1.018E+1	-7.004 E+0	-1.199 E+0	-1.683 E+0	-
- 1.652E+1	-1.106 E+1	-2.230 E+0	-3.299 E+1	-
- 2.584E+1	-5.710 E+1	-6.679 E+1	-7.303 E+1	-
- 3.564E+1	-	-	-	-

Figure 2.3.3
DYNAMIC RESPONSE OF 20-TRAY DISTILLATION COLUMN
RESPONSE OF DISTILLATE COMPOSITION
FOR A +40% STEP CHANGE IN FEED FLOWRATE

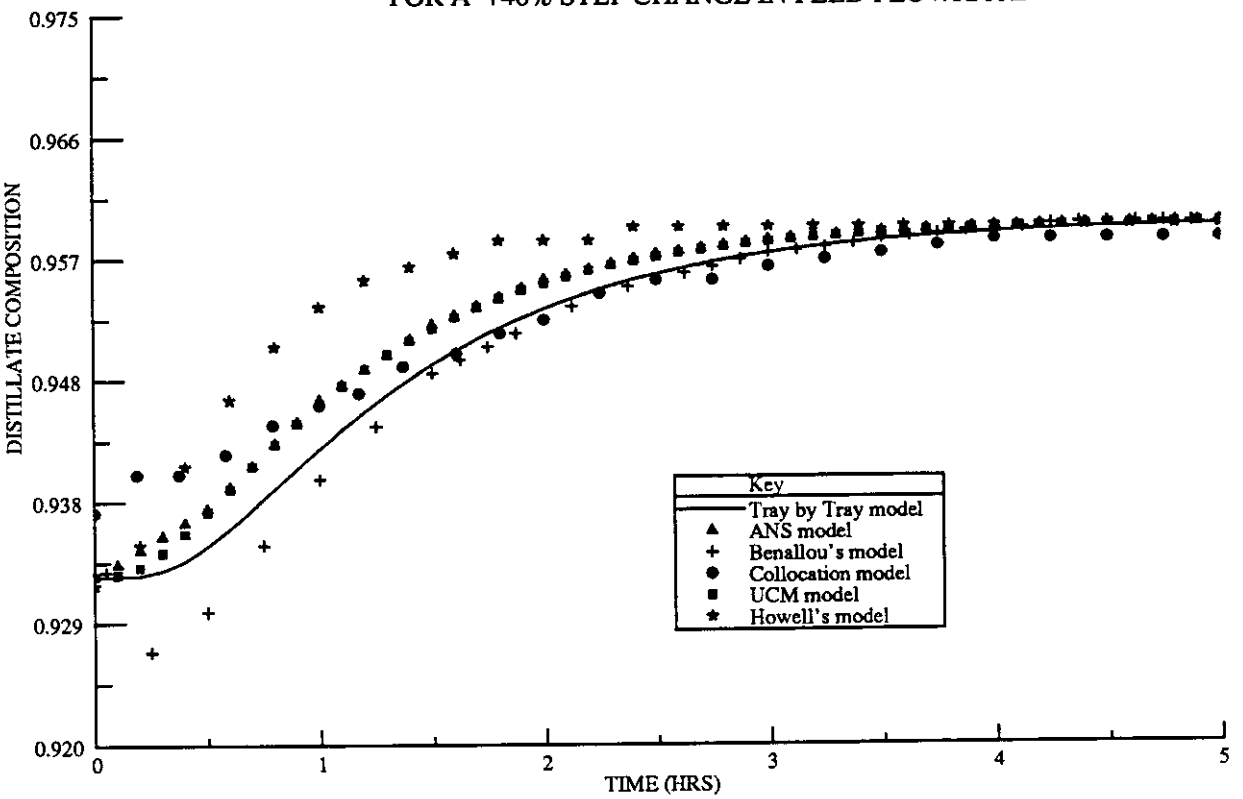

Figure 2.3.4
DYNAMIC RESPONSE OF 20-TRAY DISTILLATION COLUMN
RESPONSE OF BOTTOMS COMPOSITION
FOR A +40% STEP CHANGE IN FEED FLOWRATE

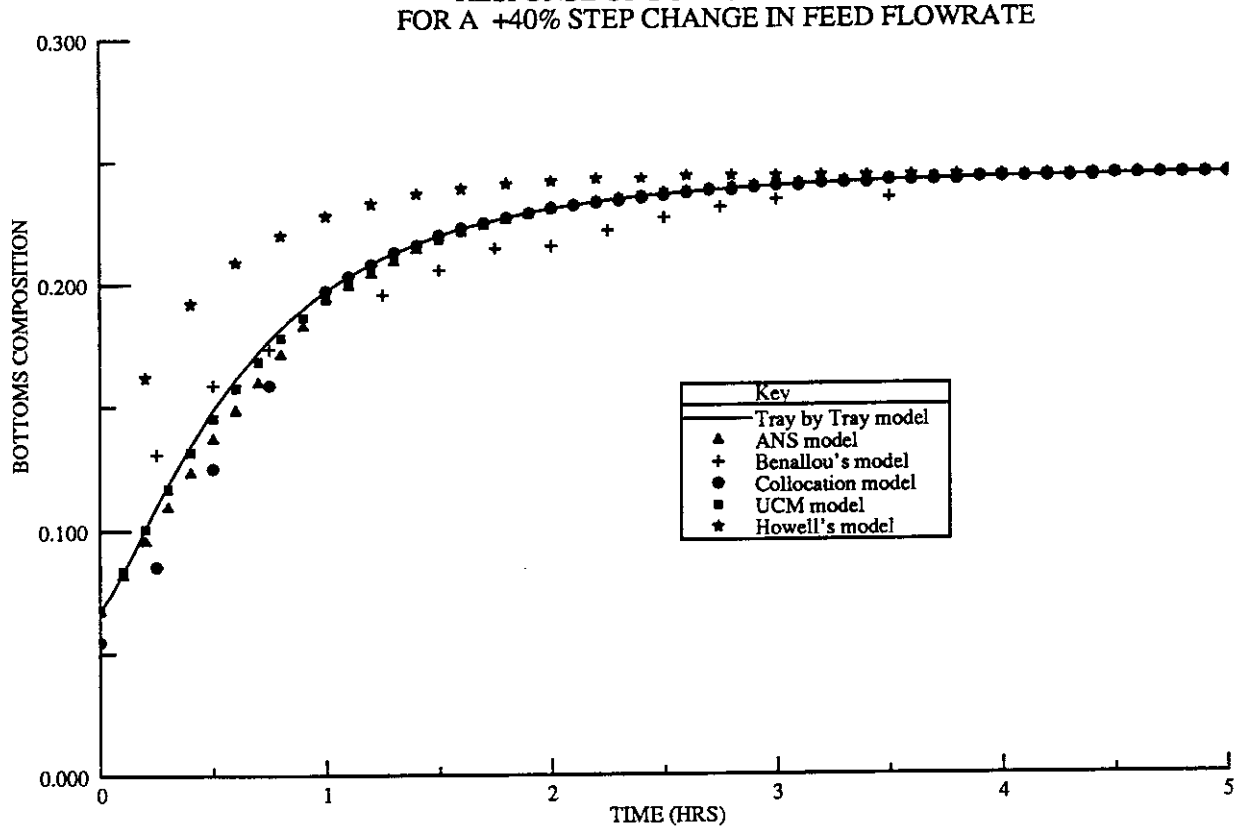

Figure 2.3.5
DYNAMIC RESPONSE OF 20-TRAY DISTILLATION COLUMN
RESPONSE OF DISTILLATE COMPOSITION
FOR A +40% STEP CHANGE IN FEED COMPOSITION

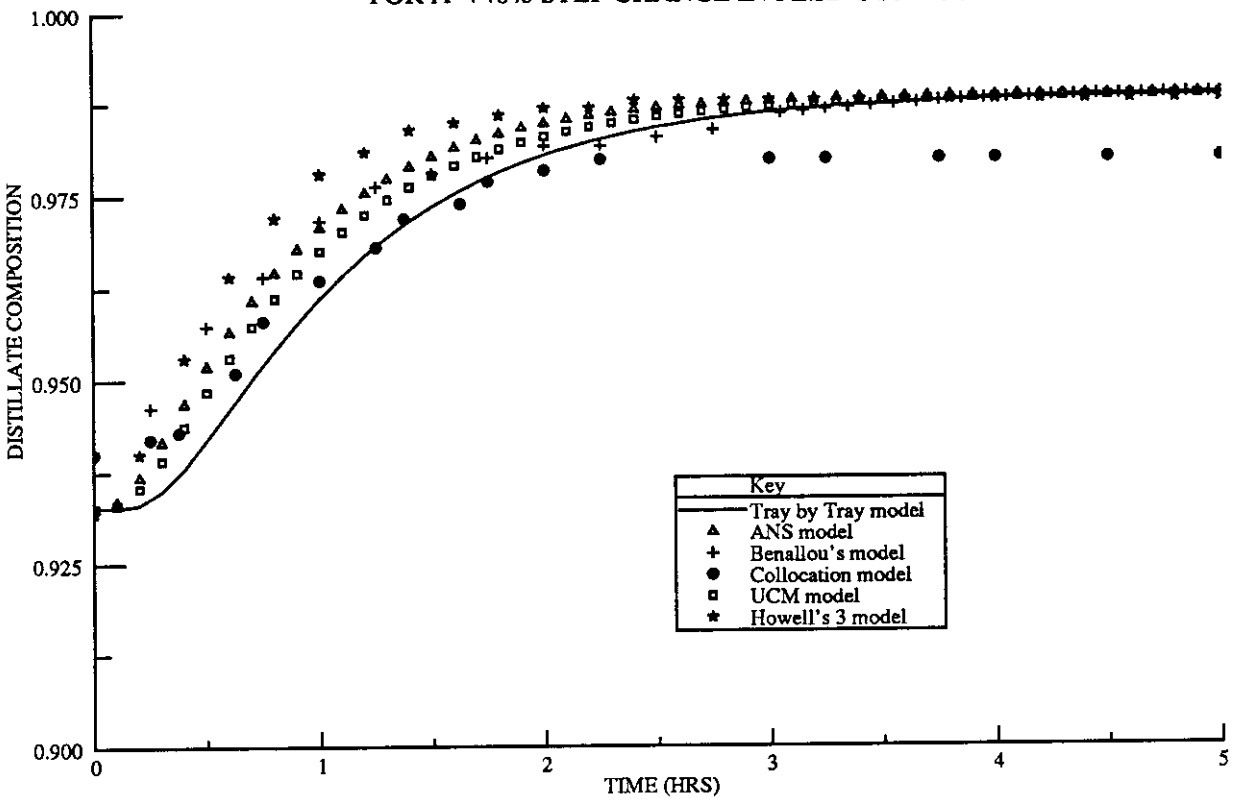

Figure 2.3.6
DYNAMIC RESPONSE OF 20-TRAY DISTILLATION COLUMN
RESPONSE OF BOTTOMS COMPOSITION
FOR A +40% STEP CHANGE IN FEED COMPOSITION

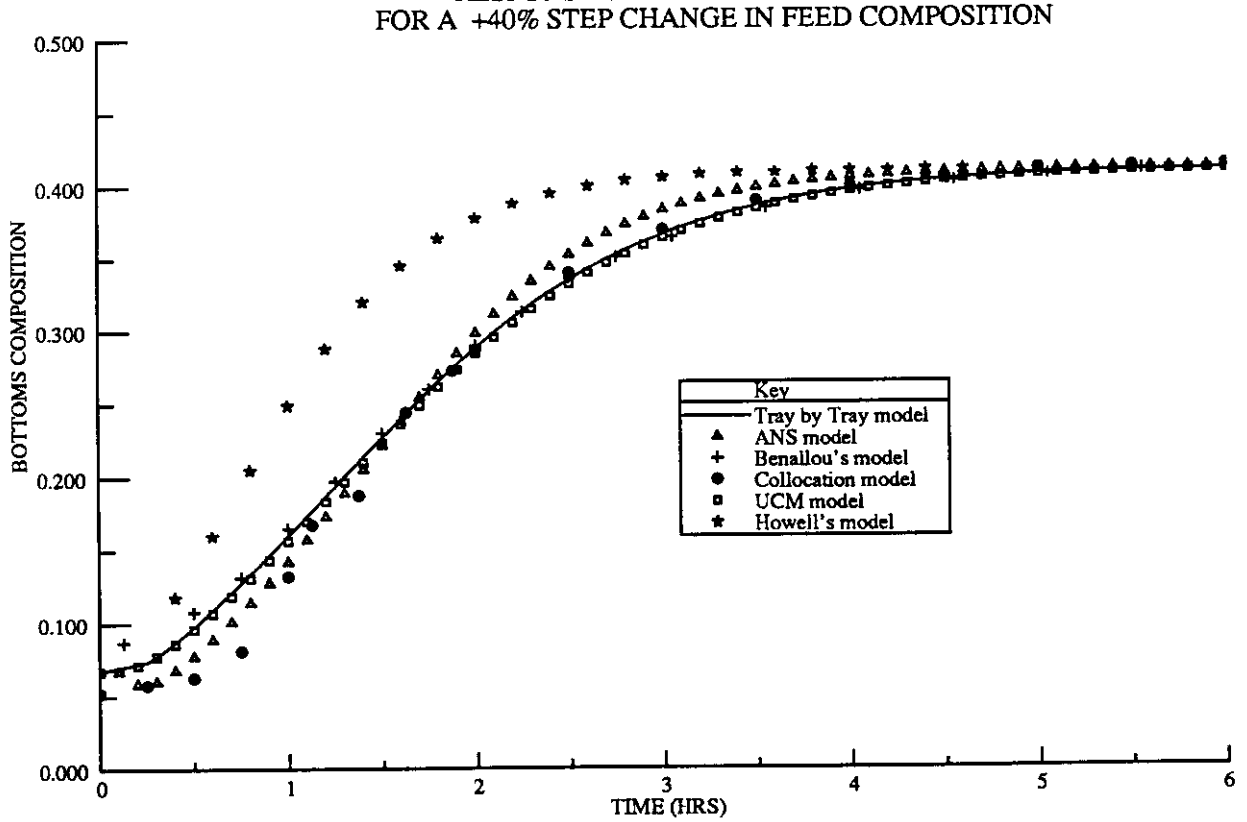

Figure 2.3.7
DYNAMIC RESPONSE OF 20-TRAY DISTILLATION COLUMN
RESPONSE OF DISTILLATE COMPOSITION
FOR A -10% STEP CHANGE IN REBOILER VAPOUR RATE

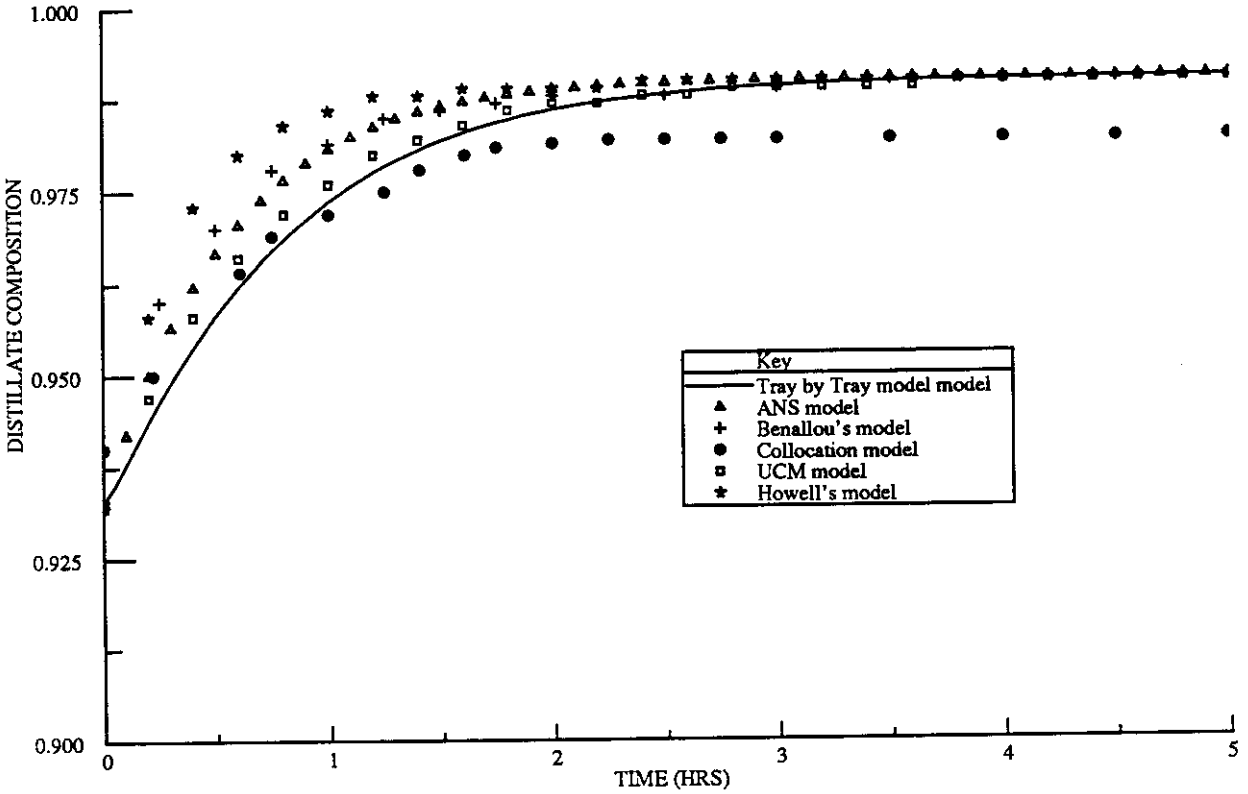

Figure 2.3.8
DYNAMIC RESPONSE OF 20-TRAY DISTILLATION COLUMN
RESPONSE OF BOTTOMS COMPOSITION
FOR A -10% STEP CHANGE IN REBOILER VAPOUR RATE

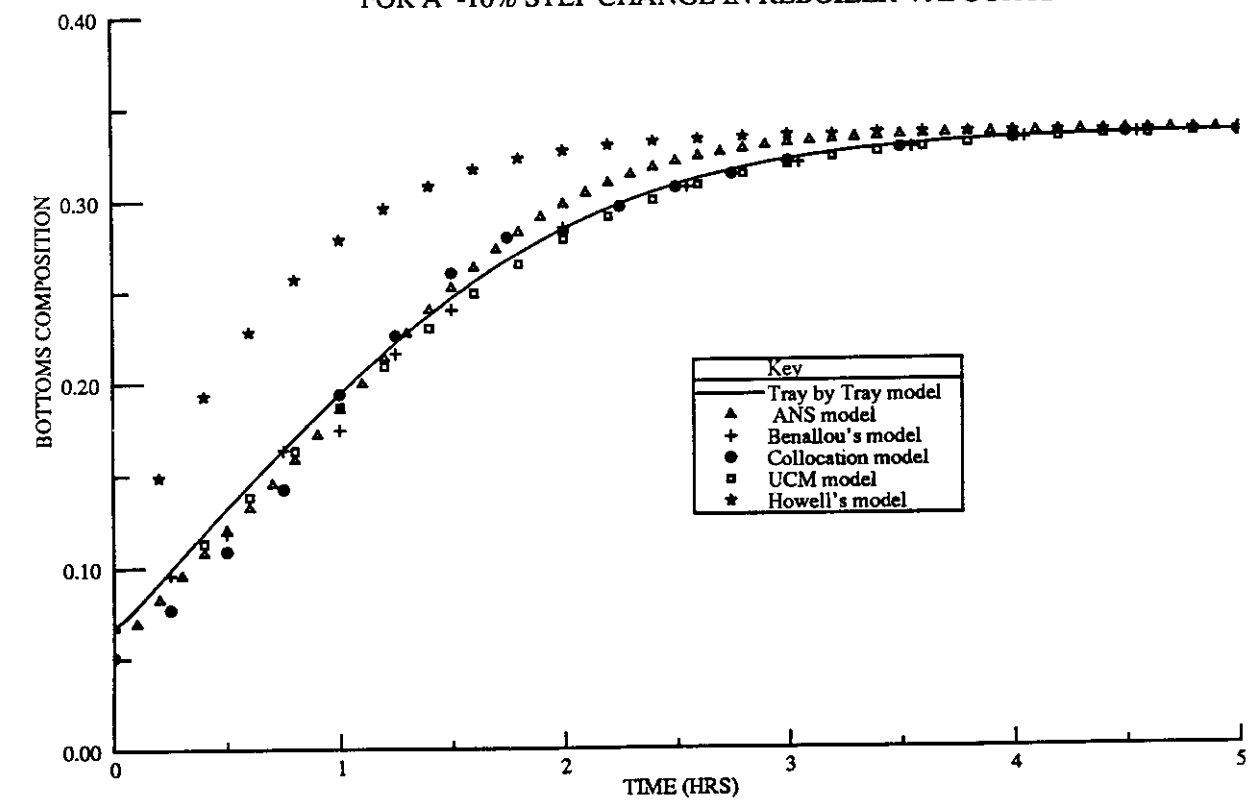

Figure 2.3.9
DYNAMIC RESPONSE OF 20-TRAY DISTILLATION COLUMN
RESPONSE OF DISTILLATE COMPOSITION
FOR A +10% STEP CHANGE IN REFLUX RATE

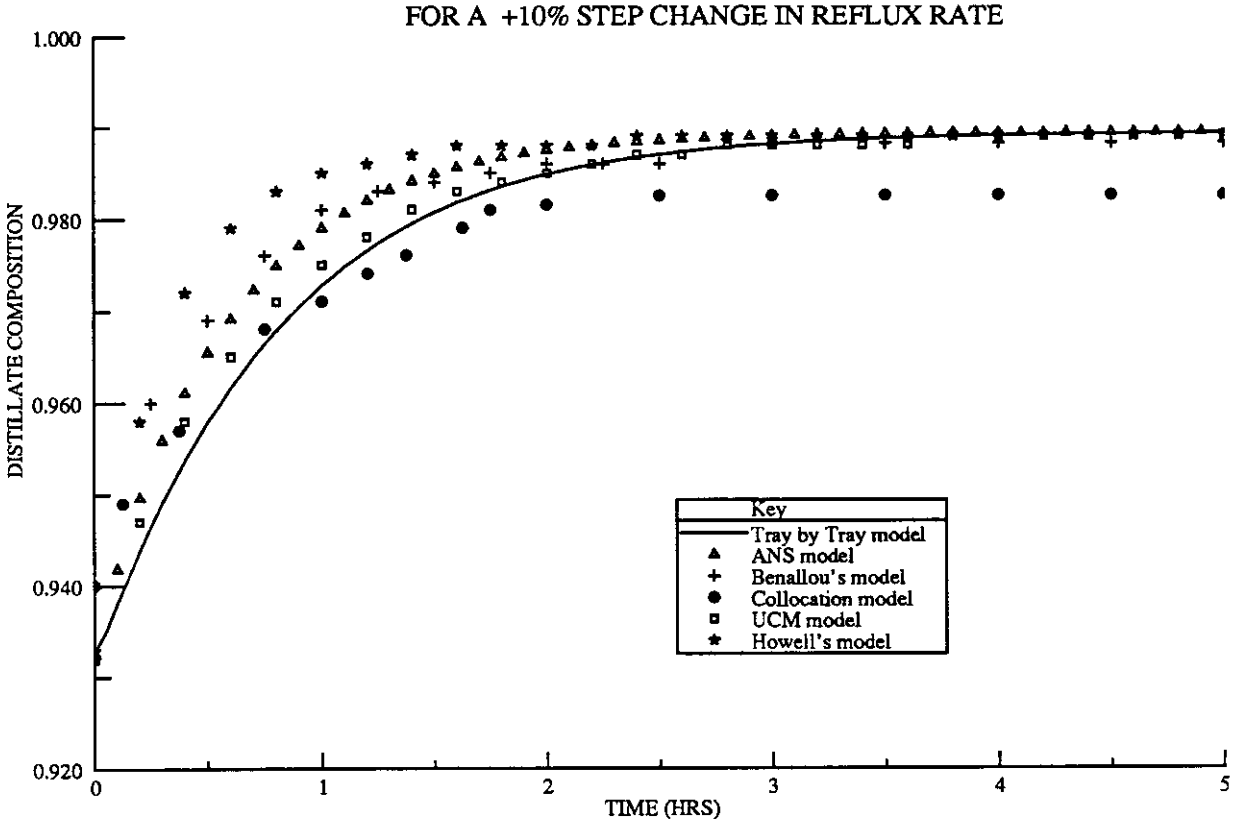

Figure 2.3.10
DYNAMIC RESPONSE OF 20-TRAY DISTILLATION COLUMN
RESPONSE OF BOTTOMS COMPOSITION
FOR A +10% STEP CHANGE IN REFLUX RATE

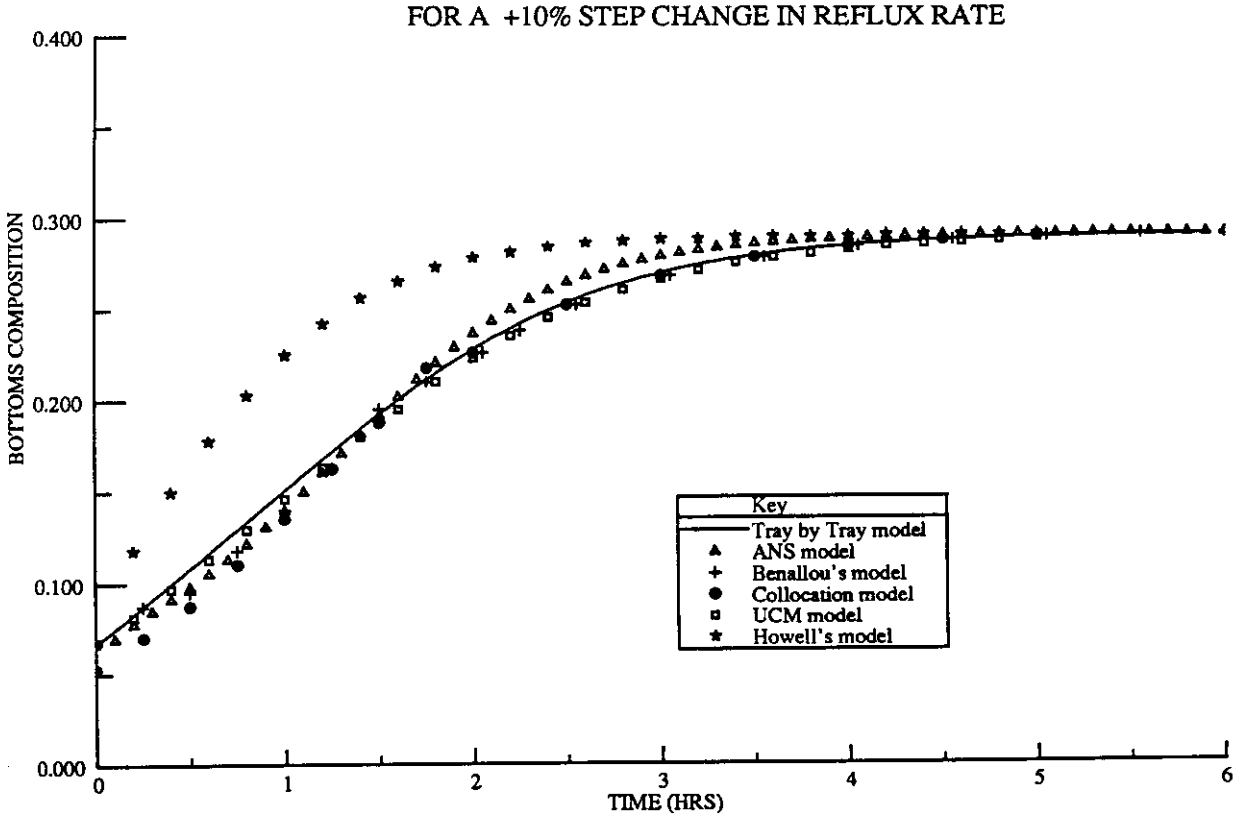

Figure 2.3.11
INITIAL INVERSE RESPONSE IN COMPARTMENTAL MODELS FOR A 20-TRAY DISTILLATION COLUMN - RESPONSE OF DISTILLATE COMPOSITION FOR A +40% STEP CHANGE IN FEED FLOWRATE

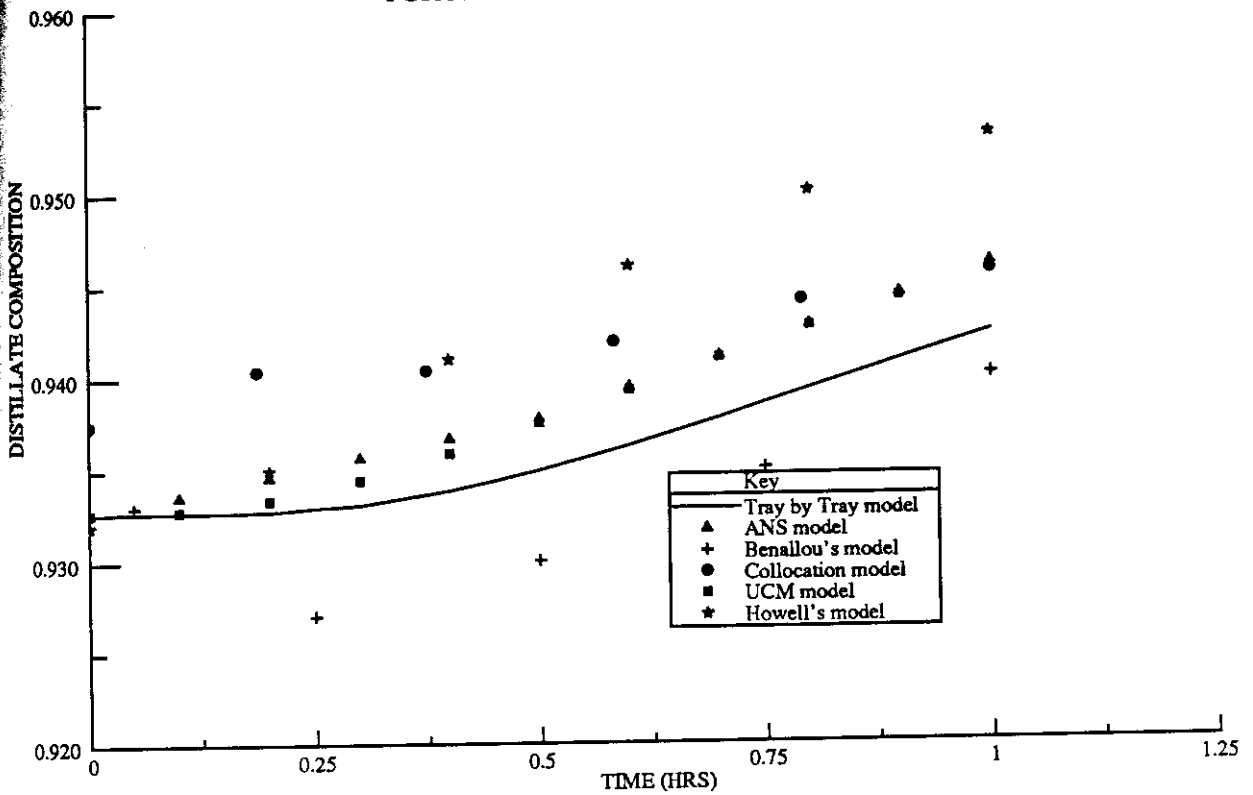

Figure 2.3.12
INITIAL INVERSE RESPONSE IN COMPARTMENTAL MODELS FOR A 20-TRAY DISTILLATION COLUMN - RESPONSE OF BOTTOMS COMPOSITION FOR A +40% STEP CHANGE IN FEED FLOWRATE

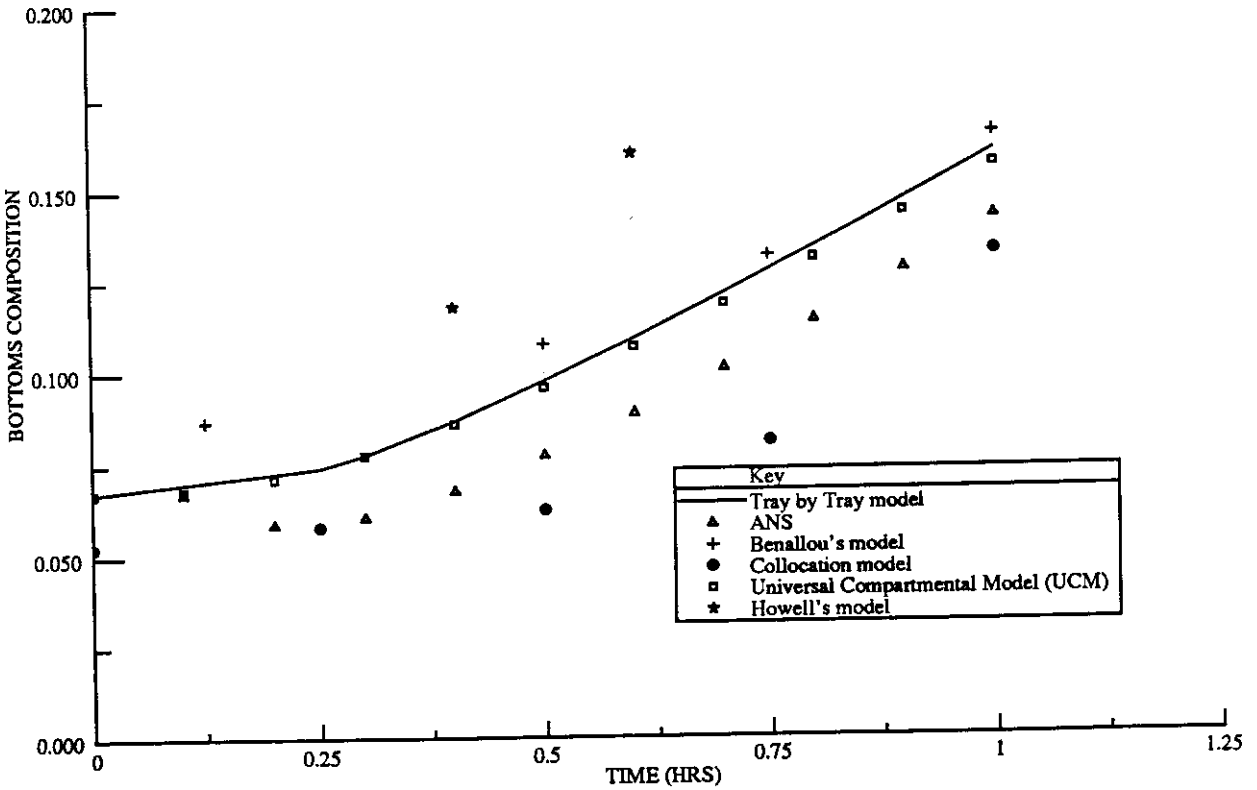

not been clearly explained. The UCM on the other hand provides excellent dynamic tracking and also avoids any spurious IIR . Thus, this new approach seems better than the other models in various aspects and forms a viable alternative to the existing compartmental models.

To explore the reasons why IIR is present in the other compartmental models - but not in the UCM - it is necessary to first examine the mathematical basis for IIR itself.

2.4 INVESTIGATION OF INVERSE RESPONSE IN DISTILLATION MODELLING

2.4.1 WHAT IS INITIAL INVERSE RESPONSE ?

Physical systems sometimes exhibit a property called initial inverse response in their outputs. For a step change in one of their inputs, the initial response is in the opposite direction to where it eventually ends up. Since the initial response is in the opposite direction from the final steady-state, it seems logical that such systems would present control difficulties. The following example refers to one of the commonly encountered chemical processes with inverse response characteristics.

Example 2.4.1

Consider a simple drum boiler as shown in Figure 2. 4. 1 (Stephanopoulos [1984]). If the flowrate of the cold feed water is suddenly increased, then the volume of the boiling water and consequently the liquid level will be decreased initially but then starts rising after a while , as shown in Figure 2. 4. 2. Such behaviour is the net result of two opposing effects , as explained below :

(1) Initially, the cold feedwater causes a temperature drop which decreases the volume of the entrained vapour bubbles leading to a decrease in the liquid level of the boiling water. Such a response follows a first-order type behaviour with a transfer function $[-K_1 / (\tau_1 s + 1)]$ (see Figure 2. 4. 3b; curve 1).

(2) After some time, due to a constant heat supply and steam production rate remaining the same, the additional feed water starts accumulating in the boiler, resulting in a rise in liquid level. Such a rise in the liquid level follows a pure capacitive response with a transfer function , $[K_2 / s]$ (see Figure 2. 4. 3 b, curve 2).

Thus, the overall response is a consequence of two effects acting in opposite directions (see Figure 2. 4. 2).

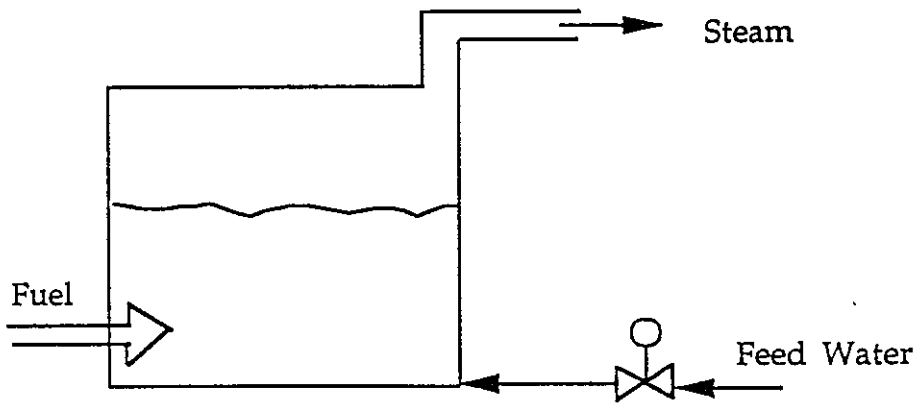

Figure 2. 4. 1
Drum Boiler

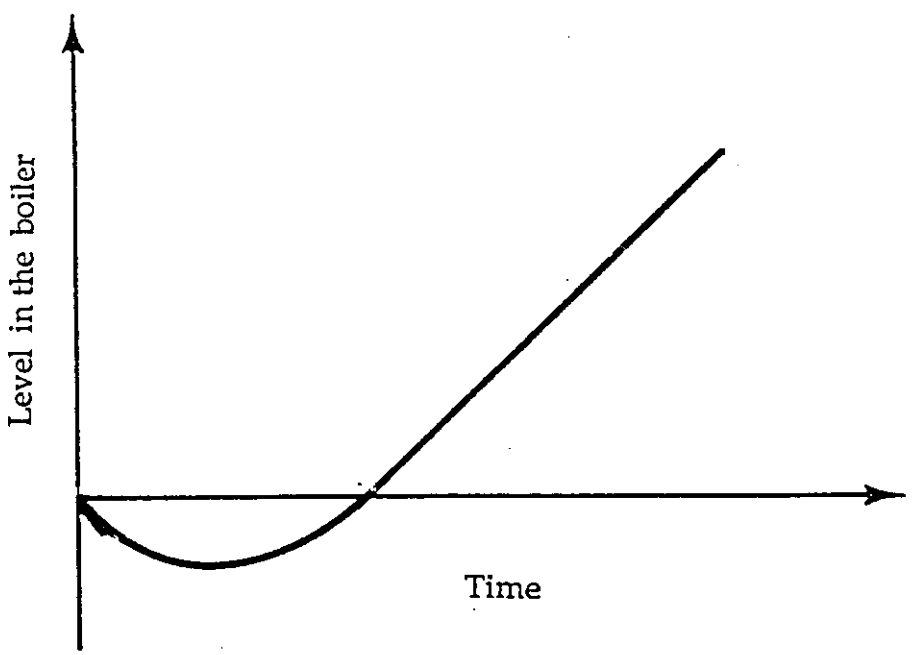

Figure 2. 4. 2
Response of boiler liquid level to a step increase
in the cold feed water

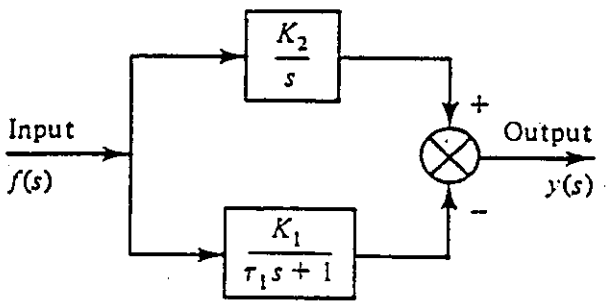

(a)

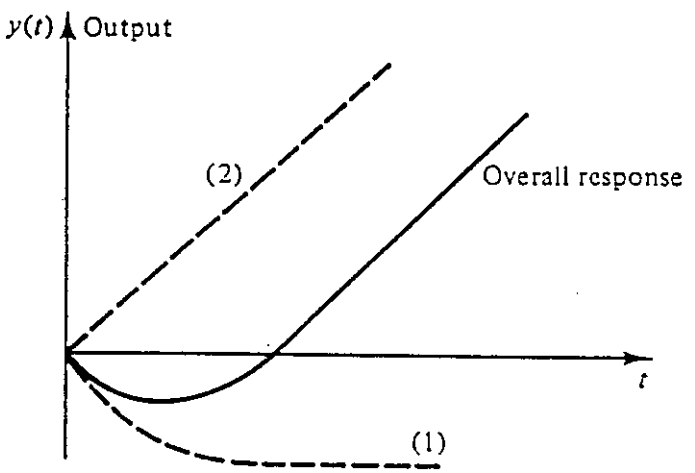

(b)

Figure 2. 4. 3

(a) Block diagram of liquid level dynamics in the reboiler system

(b) The overall inverse response

$$Y(s) = \left(\frac{K_2}{s} - \frac{K_1}{(\tau_1 s + 1)} \right) F(s) \qquad (2.4.1)$$

or,

$$Y(s) = \left(\frac{(K_2\tau_1 - K_1)s + K_2}{s(\tau_1 s + 1)} \right) F(s) \qquad (2.4.2)$$

Therefore, for ($K_2\tau_1 < K_1$) we have inverse response when the second term $[-K_1/(\tau_1 s + 1)]$ initially dominates the overall dynamics.

The above example demonstrates that inverse response may be the net result of two opposing effects. Several such opposing effects commonly observed in practice are shown in Figure 2. 4. 4 (Iinoya and Altpeter [1962]). The chief characteristic feature observed in all these cases is that, *when the system possesses an inverse response, its overall transfer function has a positive or right half plane (RHP) zero.* Thus, in general systems having RHP zeros will exhibit inverse response in their respective outputs (Iinoya and Altpeter [1962] , Waller and Nygardas [1975] , Stephanopoulos [1984]) and seem to provide considerable difficulties in their control as ;

(1) RHP zeros cannot be moved or cancelled using a controller and must be "endured" (Holt and Morari [1985]).

(2) Perfect control (see Section 4. 3. 2) is not achievable for systems with RHP zeros (Kwakernaak and Sivan [1972]).

(3) The presence of RHP zeros for a system is associated with the process design and can , therefore, only be changed by changing it's design.

The ideas presented above on inverse response are applicable only to single-input single-output (SISO) systems. In the case of multi-input multi-output (MIMO) systems, where the transfer functions are represented in a matrix form , the analogues to SISO right half plane zeros are known as right half plane transmission (RHPT) zeros (MacFarlane and Karcanias [1976], Holt and Morari [1985]). In the case of MIMO systems, there is no simple explanation or correspondence between the observed inverse response and the RHPT zeros of the system (Holt and Morari [1985]). However, if some transfer function elements of a MIMO transfer function matrix (each of which representing a SISO system) have RHP zeros , then it can be shown that under certain conditions all such RHP zeros lead to inverse response in the corresponding outputs.

Figure 2. 4. 4

Commonly observed systems with inverse response

1. Pure capacitive minus first-order response

$$G(s) = \frac{K_2}{s} - \frac{K_1}{\tau_1 s + 1} = \frac{(K_2\tau_1 - K_1)s + K_2}{s(\tau_1 s + 1)}$$

for $K_2\tau_1 < K_1$ zero $= -K_2/(K_2\tau_1 - K_1) > 0$.

2. Difference between two first-order responses

$$G(s) = \frac{K_1}{\tau_1 s + 1} - \frac{K_2}{\tau_2 s + 1} = \frac{(K_1\tau_2 - K_2\tau_1)s + (K_1 - K_2)}{(\tau_1 s + 1)(\tau_2 s + 1)}$$

for $\frac{\tau_1}{\tau_2} > \frac{K_1}{K_2} > 1$ zero $= -(K_1 - K_2)/(K_1\tau_2 - K_2\tau_1) > 0$

3. Difference between two first-order responses with dead time:

$$G(s) = \frac{K_1 e^{-t_1 s}}{\tau_1 s + 1} - \frac{K_2 e^{-t_2 s}}{\tau_2 s + 1}$$

for $K_1 > K_2$ and $t_1 > t_2 \geq 0$.

4. Second-order minus first-order response:

$$G(s) = \frac{K_1}{\tau^2 s^2 + 2\zeta\tau s + 1} - \frac{K_2}{\tau_2 s + 1}$$

for $K_1 > K_2$.

5. Difference between two second-order responses:

$$G(s) = \frac{K_1}{\tau_1^2 s^2 + 2\zeta_1\tau_1 s + 1} - \frac{K_2}{\tau_2^2 s^2 + 2\zeta_2\tau_2 s + 1}$$

for $\tau_1^2/\tau_2^2 > K_1/K_2 > 1$.

6. Difference between two second-order responses with dead time:

$$G(s) = \frac{K_1 e^{-t_1 s}}{\tau_1^2 s^2 + 2\zeta_1\tau_1 s + 1} - \frac{K_2 e^{-t_2 s}}{\tau_2^2 s^2 + 2\zeta_2\tau_2 s + 1}$$

for $K_1 > K_2$ and $t_1 > t_2 \geq 0$.

2.4.2 STATE - SPACE REPRESENTATION OF A MIMO SYSTEM

An important requirement of any control system design is a mathematical representation of the dynamics of the process to be controlled. The dynamics of many physical processes can be adequately described by a set of partial differential equations that describe the variation of process variables in time as well as in space. However, such models are very difficult to solve. Such an approach is not practical especially in the preliminary stages of process (and it's control system) design. A good compromise therefore is to lump all the space effects and express the process dynamics only in terms of time. Such a model is called a lumped parameter model and can be represented by a set of ordinary differential equations (ODE's) or by a mixed set of differential and algebraic equations (DAE system). Lumped parameter models are usually nonlinear in nature for real processes.

Many classical and modern control system design and analysis methods are based on a set of linear first-order ODE's called a state-space model. In this section, the approach used to convert a nonlinear DAE system into a state-space model, will be briefly described.

Consider a physical process , the dynamics of which are represented in a lumped parameter form by the following set of DAE's.

$$f(\dot{X}, X, U, Z) = 0 \qquad (2.4.3)$$

$$g(X, U, Z) = 0 \qquad (2.4.4)$$

where ,

f is a set of 'n' differential equations and

g is a set of 'p' algebraic equations.

Variables used in the present context have the following meaning .

(a) State variables (X) : A set of variables that represent the transients associated with the process. $\dot{X}$ in Equation (2.4.3) represents differentials of the state variables with respect to time.

(b) Input variables (U) : A set of "forcing variables" from which a subset of inputs or manipulated variables can be chosen.

(c) Output variables (Y) : A set of variables that need to be held at their set-points.

(d) Algebraic variables (Z) : A set of variables from which a subset of outputs can be chosen.

Each of these variables can be further classified as:

$$X=\begin{bmatrix} y_2 \\ r \end{bmatrix} \; ; \; U = \begin{bmatrix} m \\ v \end{bmatrix} \; ; \; Z = \begin{bmatrix} y_1 \\ w \end{bmatrix} \; ; \; Y = \begin{bmatrix} y_1 \\ y_2 \end{bmatrix} \tag{2.4.5}$$

where

- m — are the input variables specified by the user as the manipulated variables ;
- v — are the remaining inputs taken as constants or specifications ;
- y_1 — are the output variables chosen for control from the set of algebraic variables ;
- w — are the remaining algebraic variables after y_1 has been chosen;
- y_2 — are the output variables chosen for control from the set of state variables ;
- r — are the remaining state variables after y_2 has been chosen.

Since control is here concerned with holding the process close to a 'steady-state', linearising the nonlinear process around the steady-state of interest still provides a reasonably good picture of the process in the vicinity of the steady-state. Using a Taylor's expansion series, the DAE system can be linearised around the steady-state and expressed in terms of perturbation variables,

$$\frac{\partial f}{\partial \dot{X}} \delta\dot{X} + \frac{\partial f}{\partial X} \delta X + \frac{\partial f}{\partial U} \delta U + \frac{\partial f}{\partial Z} \delta Z = 0 \tag{2.4.6}$$

$$\frac{\partial g}{\partial X} \delta X + \frac{\partial g}{\partial U} \delta U + \frac{\partial g}{\partial Z} \delta Z = 0 \tag{2.4.7}$$

The partial derivatives are evaluated at the known steady-state and will subsequently be written in the following form :

$$f_{\dot{X}} = \frac{\partial f}{\partial \dot{X}} \; ; \; f_X = \frac{\partial f}{\partial X} \; ; \; f_U = \frac{\partial f}{\partial U} \; ; \; f_Z = \frac{\partial f}{\partial Z} \tag{2.4.8}$$

$$g_X = \frac{\partial g}{\partial X} \; ; g_U = \frac{\partial g}{\partial U} \; ; \; g_Z = \frac{\partial g}{\partial Z} \tag{2.4.9}$$

From Equations (2. 4. 6) and (2. 4. 7) , δZ can be eliminated such that,

$$\delta Z = -(g_Z^{-1} \, g_X) \, \delta X - (g_Z^{-1} \, g_U) \, \delta U \tag{2.4.10}$$

Substituting for δZ and thence simplifying Equation (2. 4. 6) we get ,

$$f_{\dot{X}} \, \delta\dot{X} + f_X \, \delta X + f_U \, \delta U - f_Z \left[(g_Z^{-1} \, g_X) \, \delta X + (g_Z^{-1} \, g_U) \, \delta U \right] \tag{2.4.11}$$

or,

$$\delta\dot{X} = (-f_{\dot{X}}^{-1})(f_X - f_Z \, g_Z^{-1} \, g_X) \, \delta X + (-f_{\dot{X}}^{-1})(f_U - f_Z \, g_Z^{-1} \, g_U) \, \delta U \tag{2.4.12}$$

The state-space form of a model is usually represented in the following form ,

$$\delta\dot{X} = A\,\delta X + B\,\delta U \tag{2.4.13}$$

where **A** and **B** are the state and input matrices, respectively.

Comparing Equations (2. 4. 12) and (2. 4. 13) we have

$$A = -f_{\dot{X}}^{-1}\,(f_X - f_Z\,g_Z^{-1}\,g_X) \tag{2.4.14}$$

$$B = -f_{\dot{X}}^{-1}\,(f_U - f_Z\,g_Z^{-1}\,g_U) \tag{2.4.15}$$

The outputs used for control purposes (Y) can be chosen from both the algebraic variables (Z) and the state variables (X). Therefore,

$$Y = \begin{bmatrix} y_1 \\ y_2 \end{bmatrix} = h(X, Z, U) \tag{2.4.16}$$

Equation (2. 4. 16) is obtained by rearranging Equations (2. 4. 3 - 2. 4. 4) and expressing them in terms of the selected output variables . The total derivative for the Equation (2. 4. 16) is given by

$$\delta Y = h_X\,\delta X + h_Z\,\delta Z + h_U\,\delta U \tag{2.4.17}$$

δZ in the above equation can be eliminated using Equation (2. 4. 10) and simplified to the following form,

$$\delta Y = (h_X - h_Z\,g_Z^{-1}\,g_X)\,\delta X + (h_U - h_Z\,g_Z^{-1}\,g_U)\,\delta U \tag{2.4.18}$$

or,

$$\delta Y = C\,\delta X + D\,\delta U \tag{2.4.19}$$

Equation (2. 4. 19) represents the state-space representation of the output variables. Thus, Equations (2. 4. 13) and (2. 4. 20) together form the linear state-space representation of the nonlinear model.

$$\begin{aligned} \delta\dot{X} &= A\,\delta X + B\,\delta U \\ \delta Y &= C\,\delta X + D\,\delta U \end{aligned} \tag{2.4.20}$$

The perturbation variables in Equation (2. 4. 21) represent the changes in the variables from their respective steady-state values as shown below :

$$\delta\dot{X} = \dot{X} - \dot{X}_S \tag{2.4.21}$$

$$\delta X = X - X_S \tag{2.4.22}$$

$$\delta U = U - U_S \tag{2.4.23}$$

$$\delta Y = Y - Y_S \tag{2.4.24}$$

where the subscript 'S ' means a value at a known steady-state.

2.4.3 INVERSE RESPONSE IN COMPARTMENTAL MODELS

Distillation is inherently a multi-input multi-output (MIMO) system. However, in the present context, it has been assumed that the initial inverse response frequently observed in most of the previously presented distillation compartmental models is due to the presence of right half plane (RHP) zeros in the individual transfer function elements of the transfer function matrix, each of which may be thought of as representing a single-input single-output (SISO) system. This is strictly true, only when one input variable at a time is subjected to a change and the response of each output variable to such a change is similar to a SISO response.

Each compartmental model can be represented as a system of differential and algebraic equations which may be linearised around a steady-state to obtain the transfer function matrix for the chosen inputs and outputs (see Section 2. 4. 2). Analytically it will now be shown that, for a binary separation system , except for the universal compartmental model , all the other compartmental models have right half plane zeros in at least one transfer function element , leading to spurious initial inverse responses in one or more of their outputs.

Consider a distillation compartment encompassing N trays, wherein separation of a binary mixture is taking place. Based on the assumptions used in compartmental modelling (i.e. constant molar overflow and constant relative volatility in a section) , the system can be represented by the following set of equations.

$$M_T \frac{dX_{node}}{dt} = L(X_0 - X_N) + V(Y_0 - Y_1) \qquad (2.4.25)$$

$$L(X_0 - X_1) + V(K_2X_2 - K_1X_1) = 0 \qquad (2.4.26)$$

$$L(X_1 - X_2) + V(K_3X_3 - K_2X_2) = 0 \qquad (2.4.27)$$

$$\vdots$$

$$L(X_{N-2} - X_{N-1}) + V(K_NX_N - K_{N-1}X_{N-1}) = 0 \qquad (2.4.28)$$

where,

(i) $X_{avg} = X_N$ ..... UCM approach (2.4.29)

(ii) $X_{avg} = \frac{(X_1 + X_2 + \ldots\ldots + X_N)}{N}$ ..... ANS approach (2.4.30)

(iii) $X_{avg} = X_S \qquad 1 < S < N$ ..... Benallou's approach (2.4.31)

Using the following approach, the nonlinear separation equations (2. 4. 25 - 2. 4. 31) can be linearised around a known steady-state and expressed in state-space form as explained in the previous section. Inlet liquid and vapour compositions are chosen as the 'inputs' and outlet vapour and liquid compositions as the 'outputs', to obtain a state-space representation of the compartment. The state-variables (**X**), the inputs (**U**), the outputs (**Y**) and the algebraic variables (**Z**) for the compartment section are,

$$X = X_{avg} \; ; \quad U = \begin{Bmatrix} X_0 \\ Y_0 \end{Bmatrix} \; ; \quad Y = \begin{Bmatrix} K_1 X_1 \\ X_N \end{Bmatrix} \; ; \quad Z = \begin{Bmatrix} X_1 \\ X_2 \\ X_3 \\ . \\ . \\ X_N \end{Bmatrix} \tag{2.4.32}$$

where $Y_1 = K_1 X_1$.

The state-space matrices (and subsequently the transfer function matrix) are obtained using the following ;

(i) $f_X = -1.0$ and $f_X = 0$ (2.4.33)

(ii) $$f_Z = \left\{ -\frac{K_1 V}{M_T} \quad 0 \quad 0 \quad ..... \quad -\frac{L}{M_T} \right\} \tag{2.4.34}$$

(iii) g_Z is a matrix of derivatives of each of the algebraic equations (2. 4.. 26 - 2. 4. 31) with respect to the vector **Z**. It is clear that the matrix thus obtained will be a square (N X N) with the first (N - 1) rows (i.e those due to Equations 2. 4. 26 - 2. 4. 28) being the same for all the models. The N^{th} row (i.e that one due to one of the Equations 2. 4. 29 - 2. 4. 31) is different for different compartment models. It is in fact inverse of g_Z that is needed to generate the state-space models ,

$$g_Z^{-1} = \begin{Bmatrix} C_{11} & C_{12} & . & C_{1N} \\ C_{21} & C_{22} & . & C_{2N} \\ . & . & . & . \\ . & . & . & . \\ . & . & . & . \\ C_{N1} & C_{N2} & . & C_{NN} \end{Bmatrix} \tag{2.4.35}$$

where all the constants, C_{ij}, i = 1, ..., N and j = 1, ..., N are obtained from transposing the matrix of cofactors of of g_Z. Appendices A1, A2 and A3 discuss the structure and nature of some key elements of the g_Z^{-1} matrix.

$$(iv) \quad g_X = \begin{Bmatrix} a_{X1} \\ a_{X2} \\ . \\ . \\ . \\ a_{XN} \end{Bmatrix} \tag{2.4.36}$$

where for,

(a) UCM approach : $a_{Xi} = 0 (i = 1, ..., N-1)$ and $a_{XN} = 1$ (2.4.37)

(b) ANS approach : $a_{Xi} = 0 (i = 1, ..., N-1)$ and $a_{XN} = N$ (2.4.38)

(c) Benallou's approach : $a_{Xi} = 0 (i = 1, ..., N-1)$ and $a_{XN} = 1$ (2.4.39)

$$(v) \quad f_U = \begin{Bmatrix} \frac{L}{M_T} & \frac{V}{M_T} \end{Bmatrix} \qquad (vi) \quad g_U = \begin{Bmatrix} L & 0 \\ 0 & 0 \\ . & . \\ . & . \\ 0 & 0 \end{Bmatrix} \tag{2.4.40}$$

$$(vii) \quad h_X = 0; \quad h_U = 0 \quad \text{and} \quad h_Z = \begin{Bmatrix} K_1 & 0 & . & . & 0 \\ 0 & 0 & . & . & 1.0 \end{Bmatrix} \tag{2.4.41}$$

Using the above equations, along with Equations (2.4.14), (2.4.15), (2.4.19) and (2.4.20), the state-space matrices (A, B, C, D) can be shown to have the following form :

$$A = \frac{a_{XN}}{M_T} (V K_1 C_{1N} + L C_{NN}) \tag{2.4.42}$$

$$B = \begin{Bmatrix} \frac{L}{M_T} (1 + V K_1 C_{11} + L C_{N1}) & \frac{V}{M_T} \end{Bmatrix} \tag{2.4.43}$$

$$C = -\begin{Bmatrix} a_{XN} K_1 C_{1N} \\ a_{XN} C_{NN} \end{Bmatrix} \tag{2.4.44}$$

$$D = -\begin{Bmatrix} K_1 L C_{11} & 0 \\ L C_{N1} & 0 \end{Bmatrix} \tag{2.4.45}$$

The Laplace domain transfer function matrix, relating inputs directly to outputs is given by,

$$G = C(sI-A)^{-1}B + D$$

$$= \begin{pmatrix} G_{11} & G_{12} \\ G_{21} & G_{22} \end{pmatrix} \qquad (2.4.46)$$

where,

$$G_{11}(s) = -\frac{\{(K_1 L C_{11} M_T)s + K_1 L^2 a_{XN}(C_{1N}C_{N1} - C_{11}C_{NN}) + a_{XN} K_1 L C_{1N}\}}{(M_T s - a_{XN}(V K_1 C_{1N} + L C_{NN}))} \qquad (2.4.47)$$

$$G_{21}(s) = -\frac{\{(L C_{N1} M_T)s - K_1 L V a_{XN}(C_{1N}C_{N1} - C_{11}C_{NN}) + a_{XN} L C_{NN}\}}{(M_T s - a_{XN}(V K_1 C_{1N} + L C_{NN}))} \qquad (2.4.48)$$

$$G_{12}(s) = -\frac{K_1 V C_{1N}}{(M_T s - a_{XN}(V K_1 C_{1N} + L C_{NN}))} \qquad (2.4.49)$$

$$G_{22}(s) = -\frac{V C_{NN}}{(M_T s - a_{XN}(V K_1 C_{1N} + L C_{NN}))} \qquad (2.4.50)$$

It can be seen clearly from Equations (2. 4. 47 - 50) that, only $G_{11}(s)$ and $G_{21}(s)$ can have right half plane zeros. Therefore, the presence of RHP zeros for different modelling approaches is tested below only in these two transfer function elements.

UNIVERSAL COMPARTMENTAL MODEL APPROACH

From Appendix A2, the constants used to derive the transfer function elements for the UCM approach (i.e. through Equations 2. 4. 47 - 2. 4. 50), have the following characteristics for both N odd and even;

$$C_{11} < 0$$
$$C_{1N} < 0$$
$$C_{N1} = 0$$
$$C_{NN} = -1$$

and $$C_{11}C_{NN} - C_{N1}C_{1N} > 0$$

For a physically realisable system, K_i (for all i=1, ..., N), L and V are always positive. Therefore, it can be shown that,

(a) The numerator of G_{11} (s) is of the form

$$G_{11}(s) = (q_1 s + q_2) \qquad (2.4.51)$$

where q_1 and q_2 are both less than 0 for N either even or odd ;

$$q_1 = K_1 L C_{11} M_T \qquad (2.4.52)$$

$$q_2 = K_1 L^2 a_{XN} (C_{1N} C_{N1} - C_{11} C_{NN}) + a_{XN} K_1 L C_{11} \qquad (2.4.53)$$

Hence, there is no RHP zero possible for this transfer function element.

(b) The numerator of G_{21} (s) has a form that is a constant and, hence, is independent of s .

Thus, none of the four transfer function elements for the UCM approach has a right half plane zero. Consequently, no inverse response is possible.

AVERAGE NODE SECTION MODEL APPROACH

From Appendix A2 , the constants used to derive the transfer function elements for the ANS approach, have the following characteristics for both N odd and even ;

$$C_{11} < 0$$
$$C_{1N} < 0$$
$$C_{N1} > 0$$
$$C_{NN} < 0$$

and $$C_{11} C_{NN} - C_{N1} C_{1N} > 0$$

Once again, for a physically realisable system, K_i (for all i=1, ..., N) , L and V are always positive. Therefore, it can be shown that,

(a) The numerator of G_{11} (s) is of the form

$$G_{11}(s) = (q_3 s + q_4) \qquad (2.4.54)$$

where

$$q_3 = K_1 L C_{11} M_T \qquad (2.4.55)$$

$$q_4 = K_1 L^2 a_{XN} (C_{1N} C_{N1} - C_{11} C_{NN}) + a_{XN} K_1 L C_{1N} \qquad (2.4.56)$$

Therefore, q_3 and q_4 are both less than zero for N either even or odd ;

Hence there is no RHP zero for this transfer function element.

(b) The numerator of $G_{21}(s)$ is of the form,

$$G_{21}(s) = (q_5 s + q_6 + q_7) \qquad (2.4.57)$$

where

$$q_5 = L C_{N1} M_T \qquad (2.4.58)$$

$$q_6 = K_1 L V a_{XN} (C_{1N} C_{N1} - C_{11} C_{NN}) \qquad (2.4.59)$$

$$q_7 = a_{XN} L C_{NN} \qquad (2.4.60)$$

and q_5 is always greater than zero for N either even or odd;

From Appendix A2, it can be shown that,

$$q_7 + q_6 < 0$$

This shows the presence of a RHP zero.

Thus, one of the four transfer function elements has a RHP zero, leading to an inverse response in the corresponding output.

BENALLOU 'S APPROACH

From Appendix A3, the constants used to derive the transfer function elements for Benallou's approach, have the following characteristics:

C_{11}	< 0	for N odd or even (all S)
C_{1N}	< 0	for N odd or even (all S)
C_{N1}	> 0	for N odd or even (all S)
C_{NN}	< 0	for N odd or even (all S)
and $C_{11}C_{NN} - C_{N1}C_{1N}$	> 0	for N odd or even (all S)

where 'S' represents the sensitive tray of the compartment.

Again, for a physically realisable system, K_i (for all i=1, ..., N), L and V are always positive. Therefore, it can be shown that,

(a) The numerator of $G_{11}(s)$ is of the form

$$G_{11}(s) = (q_8 s + q_9) \qquad (2.4.61)$$

where

$$q_8 = K_1 L C_{11} M_T \qquad (2.4.62)$$

$$q_9 = K_1 L^2 a_{XN} (C_{1N} C_{N1} - C_{11} C_{NN}) + a_{XN} K_1 L C_{1N} \qquad (2.4.63)$$

Therefore, q_8 and q_9 are both less than zero for N either even or odd.

Hence there is no RHP zero for this transfer function element.

(b) The numerator of $G_{21}(s)$ is of the form,

$$G_{21}(s) = (q_{10}s + q_{11} + q_{12}) \qquad (2.4.64)$$

where

$$q_{10} = LC_{N1}M_T \qquad (2.4.65)$$

$$q_{11} = -K_1 LV a_{XN}(C_{1N}C_{N1} - C_{11}C_{NN}) \qquad (2.4.66)$$

$$q_{12} = a_{XN} LC_{NN} \qquad (2.4.67)$$

Therefore, q_{10} is always greater than zero for N either even or odd.

From Appendix A3, it can be shown that

$$q_{12} + q_{11} < 0$$

for all values of L, V and K_i (for all i=1, ..., N).

This shows the existence of a RHP zero for this transfer function element.

Thus, at least one of the transfer function elements has a right half plane zero, leading to an initial inverse response in the corresponding output. This is illustrated in the following example.

Example 2.4.2

Consider a distillation compartment containing three trays (i. e. N = 3). Let the middle tray (i.e S = 2) be considered as the most sensitive tray. The constants C_{11}, C_{N1}, C_{1N} , C_{NN}, and det of Benallou's model can be determined from Appendix A3 as ,

$$C_{11} = \frac{VK_3}{\det} \;,\; C_{N1} = -\frac{L}{\det} \quad \text{and} \quad C_{1N} = \frac{V^2 K_2 K_3}{\det}$$

$$C_{NN} = \frac{L^2 + V^2 K_1 K_2 + VLK_1}{\det} \quad \text{and} \quad \det = -VK_3(L + VK_1)$$

The presence of a RHP zero for the transfer function element $G_{21}(s)$ can be tested for as follows ;

$$\therefore \; q_{10} = LM_T\left[\frac{-L}{\det}\right] > 0$$

$$\therefore \; q_{11} = LVK_1\left\{\frac{VK_3(L^2 + V^2K_1K_2 + VLK_1) + LV^2K_2K_3}{(\det)^2}\right\}$$

$$\therefore \; q_{12} = -\left\{\frac{L(L^2 + V^2K_1K_2 + VLK_1)}{(\det)}\right\}$$

$$\text{i.e.} \quad q_{12} + q_{11} = -\left\{\frac{L^4VK_3 + L^3V^2K_1K_3}{(\det)^2}\right\}$$

Hence $q_{12} + q_{11} < 0$ for all N.

$$\therefore \quad s = \frac{-(q_{11} + q_{12})}{q_{10}} > 0$$

This shows that the corresponding transfer function element has a RHP zero.

It has been shown , thus far, that for a compartment of size N trays , spurious initial inverse response in the outputs may be expected for all the compartmental models , except for the universal compartmental model (UCM) approach. This result was shown to be independent of the size of the compartment. Mathematically this can be explained by the structure of the equations. No simple physical explanation can be offered at this stage. Howell's node -section model , has an equation structure similar to that of the UCM, and hence also avoids initial inverse response.

It has been shown that with feed compositions to a compartment as the 'inputs', the possibility of inverse response in the exit composition 'outputs' can be detected by looking at the zeros of elements of the transfer function matrix. Similar arguments might be developed using flowrates to a compartment as the 'inputs'. However, an analytical proof for the latter case involves some very complex algebra and hence no simple explanation can be offered for the observed inverse response characteristics in the previous 20-tray column example.

2.4.4 PRESENCE OF INVERSE RESPONSE WHEN MULTIPLE COMPARTMENTS ARE MERGED

Using any compartmental modelling technique , a distillation column can be represented as a series of compartments interconnected as shown in Figure 2. 2. 1a. In this section , the effect of merging two or more compartments on the right half plane zeros of the combined transfer function elements will be examined.

Consider two compartments, each with a known (2 X 2) transfer function, merged together. A block diagram approach can be used to develop the overall transfer function of the combined compartment (see Figure 2. 4. 5).

From Figure 2. 4. 5 , it is clear that ,

$$Y_1(s) = G_{11}^{(1)}(s)\, X_0(s) + G_{12}^{(1)}(s)\, Y_2(s) \qquad (2.4.68)$$

$$X_1(s) = G_{21}^{(1)}(s)\, X_0(s) + G_{22}^{(1)}(s)\, Y_2(s) \qquad (2.4.69)$$

$$Y_2(s) = G_{11}^{(2)}(s)\, X_1(s) + G_{12}^{(2)}(s)\, Y_0(s) \qquad (2.4.70)$$

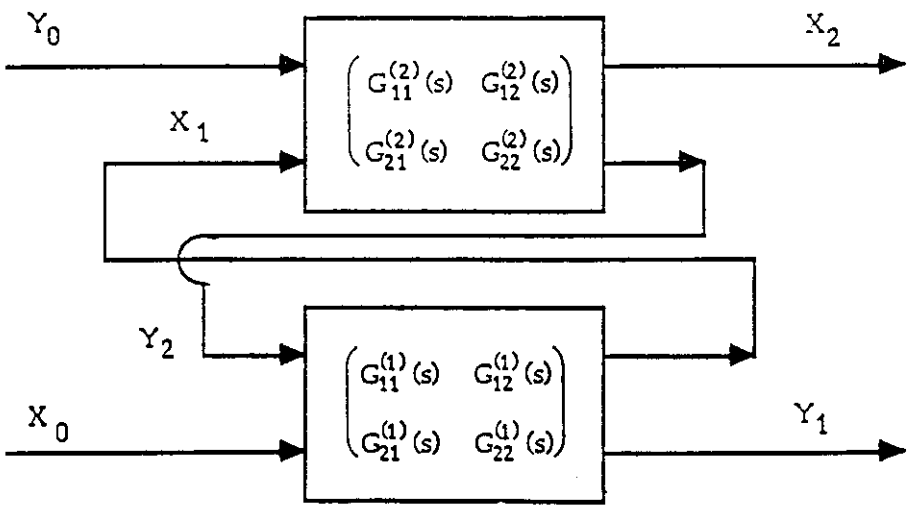

Figure 2. 4. 5
Block diagram for the
Combined transfer function matrix

$$X_2(s) = G_{21}^{(2)}(s)\, X_1(s) + G_{22}^{(2)}(s)\, Y_0(s) \qquad (2.4.71)$$

Eliminating X_1 and Y_2 using Equations (2. 4. 68) to (2. 4. 71) , we get the combined transfer function for the merged compartment as,

$$\begin{pmatrix} Y_1(s) \\ X_2(s) \end{pmatrix} = \begin{pmatrix} G_{11}^{*}(s) & G_{12}^{*}(s) \\ G_{21}^{*}(s) & G_{22}^{*}(s) \end{pmatrix} \begin{pmatrix} X_0(s) \\ Y_0(s) \end{pmatrix} \qquad (2.4.72)$$

where Y_1 and X_2 are the outputs for the merged compartment . In terms of the original two transfer function elements,

$$Y_1(s) = \frac{G_{11}^{(1)}(s) + G_{11}^{(2)}(s)\ \det^{(1)}(s)}{1 - G_{22}^{(1)}(s)\, G_{11}^{(2)}(s)}\, X_0(s) + \frac{G_{12}^{(1)}(s)\, G_{12}^{(2)}(s)}{1 - G_{22}^{(1)}(s)\, G_{11}^{(2)}(s)}\, Y_0(s) \qquad (2.4.73)$$

$$X_2(s) = \frac{G_{21}^{(1)}(s)\, G_{21}^{(2)}(s)}{1 - G_{22}^{(1)}(s)\, G_{11}^{(2)}(s)}\, X_0(s) + \frac{G_{22}^{(2)}(s) + G_{22}^{(1)}(s)\ \det^{(2)}(s)}{1 - G_{22}^{(1)}(s)\ G_{11}^{(2)}(s)}\, Y_0(s) \qquad (2.4.74)$$

where,

$$G_{11}^{*}(s) = \frac{G_{11}^{(1)}(s) + G_{11}^{(2)}(s)\ (\det^{(1)}(s))}{1 - G_{22}^{(1)}(s)\ G_{11}^{(2)}(s)} \qquad (2.4.75)$$

$$G_{12}^{*}(s) = \frac{G_{12}^{(1)}(s)\ G_{12}^{(2)}(s)}{1 - G_{22}^{(1)}(s)\ G_{11}^{(2)}(s)} \qquad (2.4.76)$$

$$G_{21}^{*}(s) = \frac{G_{21}^{(1)}(s)\ G_{21}^{(2)}(s)}{1 - G_{22}^{(1)}(s)\, G_{11}^{(2)}(s)} \qquad (2.4.77)$$

$$G_{22}^{*}(s) = \frac{G_{22}^{(1)}(s) + G_{22}^{(2)}(s)\ (\det^{(2)}(s))}{1 - G_{22}^{(1)}(s)\ G_{11}^{(2)}(s)} \qquad (2.4.78)$$

and

$$\det^{(1)}(s) = G_{21}^{(1)}(s)\ G_{12}^{(1)}(s) - G_{11}^{(1)}(s)\ G_{22}^{(1)}(s) \qquad (2.4.79)$$

$$\det^{(2)}(s) = G_{21}^{(2)}(s)\ G_{12}^{(2)}(s) - G_{11}^{(2)}(s)\ G_{22}^{(2)}(s) \qquad (2.4.80)$$

Using the expressions above, we can examine the combined transfer function for the new merged compartment in terms of the transfer function elements of the two individual compartments.

It has been shown in previous sections that except for the Universal Compartmental Model approach, all other such compartmental models have transfer function elements, at least one of which has a RHP zero. It was also observed that these characteristics are independent of the size of the compartment. When compartments are merged together, it is possible that the RHP zeros of individual compartments will be carried over and

reappear in the combined transfer function elements. In the following section , the conditions for such an occurrence will be investigated.

Consider a compartment containing N trays . The transfer function matrix elements for each of the compartmental models of interest have been shown (see Section 2. 4. 3) to have the general forms, as discussed in the previous section. Using Equations (2. 4. 73) - (2. 4. 80) , the elements of the combined transfer function matrix, when two compartments are merged , can be determined for each of these models.

In the case of the average node-section model (ANS) approach, from Equations (2. 4. 54 - 2. 4. 60) the elements of a compartment transfer function matrix relating input and output compositions are of the form ,

$$\left.\begin{aligned} G_{11}(s) &= \frac{s+Z_1}{s+P_1} \qquad G_{21}(s) = \frac{s-Z_2}{s+P_1} \\ G_{12}(s) &= \frac{b_2}{s+P_1} \qquad G_{22}(s) = \frac{c_2}{s+P_1} \end{aligned}\right\} \qquad (2.4.81)$$

where Z_1 , Z_2 are zeros and P_1 is a pole (all being positive).
b_2 and c_2 are constants.

In the case of Benallou's modelling approach, from Equations (2. 4. 61 - 2. 4. 67), the elements of a compartment transfer function matrix for the same inputs and outputs are of the form ,

$$\left.\begin{aligned} G_{11}(s) &= \frac{s+Z_3}{s+P_2} \qquad G_{21}(s) = \frac{s-Z_4}{s+P_2} \\ G_{12}(s) &= \frac{b_3}{s+P_2} \qquad G_{22}(s) = \frac{c_3}{s+P_2} \end{aligned}\right\} \qquad (2.4.82)$$

where Z_3 , Z_4 are zeros and P_2 is a pole (all being positive).
b_3 and c_3 are constants.

In both these modelling approaches, the transfer function element G_{21} (s) has a RHP zero. When two compartments having transfer function matrices of a similar form , given by Equation (2. 4. 81) or (2. 4. 82), are combined in series (see Figure 2. 4. 5), Equation (2. 4. 77) shows that the RHP zero of the G_{21} (s) element for each compartment will reappear in the corresponding transfer function element of the combined transfer function matrix (i.e. G_{21}^{*} (s)). Thus , inverse response will be observed in the combined

compartment system. The same line of argument can be extended to the case where more than two compartment are merged.

The presence or not of RHP zeros for other transfer function elements in the combined system (i.e. $G^*_{11}(s)$, $G^*_{12}(s)$ and $G^*_{22}(s)$), however, is not so obvious. Further examination of these transfer function elements , however, need not be made because the sufficient condition for the absence of any inverse response has already not been met , in that one of the elements of the combined transfer function matrix (i.e. $G^*_{21}(s)$) contains a RHP zero.

The following example illustrates this observation.

Example 2. 4. 3

Consider two compartments each containing three trays (i.e. N = 3) representing separation of a binary mixture. The relative volatility on all trays of both compartments has been taken to be constant (α = 1.3) and CMO has been assumed. Input stream compositions are chosen as 'inputs' and output stream compositions taken as the 'outputs'. Operating conditions and information about any zeros in the elements of the individual transfer functions are given in Tables 2. 4. 1 and 2. 4. 2. It must be noted here that only the composition of the more volatile component of the binary mixture is reported in Tables 2. 4. 1 and 2. 4. 2 and in the following calculations. A compartment of six trays is formed by merging the two compartments in series , i.e. the vapour product stream of compartment 1 becomes the vapour feed to compartment 2 and the liquid product stream of compartment 2 becomes the liquid feed to compartment 1. Operating conditions and any zeros in the elements of the combined transfer function matrix have been given in Table 2. 4. 3.

The RHP zeros in the combined transfer function matrix, for the case of the average node section (ANS) model, is discussed in more detail below.

Compartment 1

L = 2000 Kg-moles/ hr, V = 5000 Kg-moles/ hr , are the liquid and vapour flowrates, respectively, while K_1 = 1.1245, K_2 = 1.1266, K_3 = 1.1274, are the vapour-liquid equilibrium constants for tray 1, tray 2 and tray 3 of the compartment , respectively

Using the expressions From Appendix A2 , the constants used to determine the transfer function elements are as follows,

$$\det = -(L^2 + V^2 K_1 K_2 + V L K_1) - V K_3 (L + V K_1 + V K_2)$$

$$= 1.2164 \times 10^{8}$$

$$C_{11} = \frac{(L + VK_2 + VK_3)}{\det} = -1.0909 \times 10^{-4}$$

$$C_{NN} = \frac{(L^2 + V^2 K_1 K_2 + VLK_1)}{\det} = -0.3857$$

$$C_{N1} = -\frac{(2L + VK_2)}{\det} = 7.9194 \times 10^{-5}$$

$$C_{1N} = \frac{(V^2 K_3 K_2)}{\det} = -0.2610$$

The element G_{11} has a zero given by the numerator of Equation (2. 4. 47) ;

Zero = - 35. 43

The element G_{21} has a zero given by, numerator of Equation (2. 4. 48) ;

Zero = + 4. 15 (i.e. is a RHP zero.)

Compartment 2

In the same manner as done previously for compartment-1

$L = 2000$, $V = 5000$, $K_1 = 1.08095$, $K_2 = 1.1079$, $K_3 = 1.1196$,

$\det = 1.1829 \times 10^{8}$

$C_{11} = -1.0943 \times 10^{-4}$, $C_{NN} = -0.37829$

$C_{N1} = 8.0643 \times 10^{-5}$, $C_{1N} = -0.262147$

and , therefore,

The element G_{11} has a zero given by the numerator of Equation (2. 4. 47) ;

Zero = - 35.29

The element G_{21} has a zero given by, numerator of Equation (2. 4. 48) ;

Zero = + 4.99 (i.e. is a RHP zero.)

Compartments 1 and 2

When the two compartments are merged , any zeros for the elements of the combined transfer function matrix can be determined using Equations (2. 4. 73) - (2. 4 . 80) to be :

Zeros of G^*_{11} : - 12.88 and - 31.60

Zeros of G^*_{21} : 4. 99 and 4. 15 (both RHP zeros.)

Zeros of G^*_{12} : None

Zero of G^*_{22} : 12.42

So as shown analytically , in the case of the ANS modelling approach , RHP zeros in the transfer function element G_{21} of each compartment reappear in the $G_{21}{}^*$ element of the combined transfer function matrix.

Similar calculations were performed for the Benallou's compartment model and the results are summarised in Tables 2. 4. 1 - 2. 4. 3.

It is shown through the above illustrative example that both the ANS approach and Benallou's approach for compartmental models, would provide initial inverse response even when multiple compartments are combined. In the following section, the effect of merging compartments on the UCM approach will be examined.

2. 4. 5 EFFECT OF COMPARTMENT MERGING ON THE UCM APPROACH

As noted previously, in the case of the UCM approach, the transfer function elements G_{21} or G_{12} do not possess RHP zeros and hence, when two or more compartments are merged the corresponding transfer function elements of the combined transfer function matrix (i.e. G^*_{21} or G^*_{12}) cannot have RHP zeros. However, the presence of RHP zeros in the combined case for the other transfer function elements (i.e. G^*_{11} and G^*_{22}) is not obvious and needs to be examined.

Consider a compartment modelled on the UCM approach. The elements of the transfer function matrix can be shown to have the following form (from Equations (2. 4. 47 - 2. 4. 50) and (2. 4. 51 - 2. 4. 53)).

$$\left.\begin{aligned} G_{11}(s) &= d_1\left\{\frac{s+Z_5}{s+P_3}\right\} & G_{21}(s) &= \frac{a_1}{s+P_3} \\ G_{12}(s) &= \frac{b_1}{s+P_3} & G_{22}(s) &= \frac{c_1}{s+P_3} \end{aligned}\right\} \qquad (2.4.83)$$

where Z_5 is a zero , P_3 is a pole and a_1 , b_1 , c_1 and d_1 are constants such that Z_5 , P_3 , a_1 , b_1 , c_1 and $d_1 > 0$.

It must be realised that Z_5 , $P_3 > 0$ implies , both the zero and pole are in the left half of the complex plane.

The constants are given by the following expressions ;

$$a_1 = -\frac{\{-K_1 L V a_{XN}(C_{1N}C_{NI} - C_{11}C_{NN}) + a_{XN} L C_{NN}\}}{M_T} \qquad (2.4.84)$$

$$b_1 = -\frac{K_1 V C_{1N}}{M_T} \qquad (2.4.85)$$

$$c_1 = -\frac{V C_{NN}}{M_T} \qquad (2.4.86)$$

$$d_1 = -(K_1 L C_{11}) \qquad (2.4.87)$$

while, $$Z_5 = \frac{K_1 L^2 a_{XN}(C_{11}C_{NN} - C_{1N}C_{N1}) - a_{XN}K_1 L C_{1N}}{-(K_1 L C_{11} M_T)} \quad (2.4.88)$$

and $$P_3 = -\left(\frac{a_{XN}}{M_T}\right)(VK_1 C_{1N} + LC_{NN}) \quad (2.4.89)$$

The transfer function elements for any two arbitrary compartments will have the same form as Equation (2.4.83) and can be represented as,

$$\left.\begin{aligned} G_{11}^{(1)}(s) &= d_1^{(1)}\left\{\frac{s+Z_5^{(1)}}{s+P_3^{(1)}}\right\} \qquad G_{21}^{(1)}(s) = \frac{a_1^{(1)}}{s+P_3^{(1)}} \\ G_{12}^{(1)}(s) &= \frac{b_1^{(1)}}{s+P_3^{(1)}} \qquad G_{22}^{(1)}(s) = \frac{c_1^{(1)}}{s+P_3^{(1)}} \end{aligned}\right\} \quad (2.4.90)$$

and

$$\left.\begin{aligned} G_{11}^{(2)}(s) &= d_1^{(2)}\left\{\frac{s+Z_5^{(2)}}{s+P_3^{(1)}}\right\} \qquad G_{21}^{(2)}(s) = \frac{a_1^{(2)}}{s+P_3^{(1)}} \\ G_{12}^{(2)}(s) &= \frac{b_1^{(2)}}{s+P_3^{(2)}} \qquad G_{22}^{(2)}(s) = \frac{c_1^{(2)}}{s+P_3^{(2)}} \end{aligned}\right\} \quad (2.4.91)$$

where the superscripts (1) and (2) indicate compartments 1 and 2, respectively.
From Equations (2.4.79) and (2.4.80), we can determine expressions for $\det^{(1)}(s)$ and $\det^{(2)}(s)$ to be,

$$\det^{(1)}(s) = \left\{\frac{a_1^{(1)}b_1^{(1)} - d_1^{(1)}(s+Z_5^{(1)})c_1^{(1)}}{(s+P_3^{(1)})^2}\right\} \quad (2.4.92)$$

and

$$\det^{(2)}(s) = \left\{\frac{a_1^{(2)}b_1^{(2)} - d_1^{(2)}(s+Z_5^{(2)})c_1^{(2)}}{(s+P_3^{(2)})^2}\right\} \quad (2.4.93)$$

Finally, from Equations (2.4.73) and (2.4.78) we can determine the elements G^*_{11} and G^*_{22} of the combined transfer matrix.

(a) Transfer Function Element G^*_{11}

This element can be shown to have the following form

$$G^*_{11} = d_1^{(1)}\left\{\frac{s+Z_5^{(1)}}{s+P_3^{(1)}}\right\} + d_1^{(2)}\left\{\frac{s+Z_5^{(2)}}{s+P_3^{(2)}}\right\}\left\{\frac{a_1^{(1)}b_1^{(1)} - d_1^{(1)}(s+Z_5^{(1)})c_1^{(1)}}{(s+P_3^{(1)})^2}\right\} \quad (2.4.94)$$

In Equation (2.4.94), the numerator of G^*_{11} can be rearranged into the following form,

$$d_1^{(1)} s^3 + s^2 \left\{ d_1^{(1)} Z_5^{(1)} + d_1^{(1)} P_3^{(1)} + d_1^{(1)} P_3^{(2)} - d_1^{(1)} d_1^{(2)} c_1^{(1)} \right\}$$
$$+ s \left\{ d_1^{(1)} Z_5^{(1)} P_3^{(1)} + d_1^{(1)} Z_5^{(1)} P_3^{(2)} + d_1^{(1)} P_3^{(2)} P_3^{(1)} + \right.$$
$$\left. d_1^{(2)} a_1^{(1)} b_1^{(1)} - d_1^{(1)} d_1^{(2)} Z_5^{(1)} c_1^{(1)} - d_1^{(1)} d_1^{(2)} Z_5^{(2)} c_1^{(1)} \right\}$$
$$+ \left\{ d_1^{(1)} Z_5^{(1)} P_3^{(1)} P_3^{(2)} + d_1^{(1)} a_1^{(1)} b_1^{(1)} Z_5^{(2)} - d_1^{(1)} d_1^{(2)} Z_5^{(1)} c_1^{(1)} Z_5^{(2)} \right\} \quad (2.4.95)$$

The nature of the roots of the cubic Equation (2. 4. 95) can be determined through Routh's criteria (Stephanopoulos, [1984]). The Routh array for a cubic equation can be constructed as follows;

Row	1	$d_1^{(1)}$	B_1	(.... coefficients of s^3 and s)
Row	2	B_2	B_3	(.... coefficients of s^2 and s^0)
Row	3	B_4		

where,

$$B_1 = \left\{ d_1^{(1)} Z_5^{(1)} P_3^{(1)} + d_1^{(1)} Z_5^{(1)} P_3^{(2)} + d_1^{(1)} P_3^{(2)} P_3^{(1)} + \right.$$
$$\left. d_1^{(2)} a_1^{(1)} b_1^{(1)} - d_1^{(1)} d_1^{(2)} Z_5^{(1)} c_1^{(1)} - d_1^{(1)} d_1^{(2)} Z_5^{(2)} c_1^{(1)} \right\} \quad (2.4.96)$$

$$B_2 = \left\{ d_1^{(1)} Z_5^{(1)} + d_1^{(1)} P_3^{(1)} + d_1^{(1)} P_3^{(2)} - d_1^{(1)} d_1^{(2)} c_1^{(1)} \right\} \quad (2.4.97)$$

$$B_3 = \left\{ d_1^{(1)} Z_5^{(1)} P_3^{(1)} P_3^{(2)} + d_1^{(1)} a_1^{(1)} b_1^{(1)} Z_5^{(2)} - d_1^{(1)} d_1^{(2)} Z_5^{(1)} c_1^{(1)} Z_5^{(2)} \right\} \quad (2.4.98)$$

and $$B_4 = B_1 B_2 - d_1^{(1)} B_3 \quad (2.4.99)$$

The terms b_1 and c_1 , and all the poles and zeros , have numerical values that are an order of magnitude larger than the terms a_1 and d_1 (see Appendix A1 and Equations (2. 4. 83 - 2. 4. 87)). It can also be shown that B_2 and B_4 are both positive.

In other words, positive elements in the first column of the Routh array (i.e. $d_1^{(1)}$, B_2 and B_4) indicate that there can be no right half plane solutions for the cubic Equation (2. 4. 95) and hence no RHP zeros for this element of the combined transfer function matrix.

(b) Transfer Function Element G^*_{22}

This element can be shown to have the following form,

$$G^*_{22} = d_1^{(2)}\left\{\frac{s+Z_5^{(2)}}{s+P_3^{(2)}}\right\} + d_1^{(1)}\left\{\frac{s+Z_5^{(1)}}{s+P_3^{(1)}}\right\}\left\{\frac{a_1^{(2)}b_1^{(2)} - d_1^{(2)}(s+Z_5^{(2)})c_1^{(2)}}{(s+P_3^{(2)})^2}\right\} \quad (2.4.100)$$

The structure of Equation (2. 4. 100) is similar to that of Equation (2. 4. 94) and, consequently, similar arguments can be proposed about the absence of RHP zeros for this transfer function element.

Thus , it is clear from the above analysis that merging two or more compartments, each modelled on the UCM approach , does not give rise to RHP zeros in the resulting combined transfer function matrix elements and hence no inverse response will be observed in the corresponding outputs. The following example illustrates some of these concepts.

Example 2. 4. 4

Consider the same three tray distillation compartments as previously used in Example (2. 4. 3). The presence of RHP zeros in the elements of the combined transfer function matrix , however now modelled using the UCM approach, can now be examined as follows.

For Compartment 1 ,

$$L^{(1)} = 2000,\ V^{(1)} = 5000,\ K_1^{(1)} = 1.1245,\ K_2^{(1)} = 1.1266,\ K_3^{(1)} = 1.1274$$

where all the variables have the same meaning as previously explained in Example (2. 4. 3). Using Equations (2. 4. 51 - 2. 4. 53) and results given in Appendix A1, the pole and zero for Compartment 1 can be determined to be ;

$$P_3^{(1)} = 19.351 \text{ and } Z_5^{(1)} = 18.398$$

From Equations (2. 4. 84 - 2. 4. 89) we have,

$$a_1^{(1)} = 2.545,\ b_1^{(1)} = 12.652,\ c_1^{(1)} = 16.667 \text{ and } d_1^{(1)} = 0.3659$$

Similarly for Compartment 2,

$$L^{(2)} = 2000,\ V^{(2)} = 5000,\ K_1^{(2)} = 1.08095,\ K_2^{(2)} = 1.1079,\ K_3^{(2)} = 1.1079,$$
$$a_1^{(2)} = 2.460,\ b_1^{(2)} = 12.485,\ c_1^{(2)} = 16.667 \text{ and } d_1^{(2)} = 0.3642$$
$$P_3^{(2)} = 19.151 \text{ and } Z_5^{(2)} = 18.330$$

TABLE 2.4.1

DETAILS OF PROCESS CONDITIONS AND ZEROS FOR COMPARTMENT 1

Process details	Value (s)
Number of trays	3
Liquid feed rate (Kg- moles/hr)	2000
Liquid feed composition (mole fraction)	0.537
Vapour feed rate (Kg -moles/hr)	5000
Vapour feed composition (mole fraction)	0.574
Holdup per tray (Kg -moles)	100
Relative volatility	1.3
Vapour product rate (Kg- moles/hr)	5000
Liquid product rate (Kg-moles/hr)	2000
Vapour product composition	0.585
Liquid product composition	0.510
Zeros of the transfer function elements	
(a) UCM approach	
G_{11}	-18.39
G_{12} , G_{21}, G_{22}	none
(b) ANS approach	
G_{11}	-35.43
G_{21}	4.15 (RHPZ)
G_{12}, G_{22}	none
(c) Benallou's approach	
G_{11}	-25.66
G_{21}	6.67 (RHPZ)
G_{12}, G_{22}	none

N.B.: RHPZ - Right Half Plane Zero

TABLE 2.4.2

DETAILS OF PROCESS CONDITIONS AND ZEROS FOR COMPARTMENT 2

Process details	Value(s)
Number of trays	3
Liquid feed rate (Kg-moles/hr)	2000
Liquid feed composition (mole fraction)	0.9
Vapour feed rate (Kg-moles/hr)	5000
Vapour feed composition (mole fraction)	0.585
Holdup per tray (Kg-moles)	100
Relative volatility	1.3
Vapour product rate (Kg-moles/hr)	5000
Liquid product rate (Kg-moles/hr)	2000
Vapour product composition	0.730
Liquid product composition	0.537
Zeros of the transfer function elements	
(a) UCM approach	
G_{11}	-18.33
G_{12} , G_{21}, G_{22}	none
(b) ANS approach	
G_{11}	-35.29
G_{21}	4.99 (RHPZ)
G_{12}, G_{22}	none
(c) Benallou's approach	
G_{11}	-25.03
G_{21}	6.667 (RHPZ)
G_{12}, G_{22}	none

N.B.: RHPZ - Right Half Plane Zero

TABLE 2.4.3

DETAILS OF PROCESS CONDITIONS AND ZEROS FOR THE COMBINED COMPARTMENT

Process details	
Number of trays	6
Liquid feed rate (Kg- moles/hr)	2000
Liquid feed composition (mole fraction)	0.9
Vapour feed rate (Kg -moles/hr)	5000
Vapour feed composition (mole fraction)	0.574
Holdup per tray (Kg -moles)	100
Relative volatility	1.3
Vapour product rate (Kg-moles/hr)	5000
Liquid product rate (Kg- moles/hr)	2000
Vapour product composition	0.730
Liquid product composition	0.510
Zeros of the transfer function elements	
(a) UCM approach	
G_{11}	- 18.18 and - 10.81
G_{22}	-10.68
G_{12}], G_{21}	none
(b) ANS approach	
G_{11}	- 12.88 and - 31.60
G_{21}	4.99 and 4.15 (RHPZ)
G_{22}	-12.42
G_{12}	none
(c) Benallou's approach	
G_{11}	- 25.35 and - 12.07
G_{21}	6.667 and 6.667 (RHPZ)
G_{22}	-11.67
G_{12}	none

N.B.: RHPZ - Right Half Plane Zero

Hence, the elements of the Routh array are,

$$B_1 = 324.97,\ B_2 = 18.59,\ B_3 = 1962.24 \text{ and } B_4 = 5325.81$$

Therefore as $d_1^{(1)}$, B_2 and B_4 are all positive , there are no RHP zeros for this transfer function element, as expected. The results of this example are summarised in Tables 2. 4. 1 - 2. 4. 3.

In conclusion then, it has been shown analytically that, a distillation compartment representing a binary mixture, will not exhibit spurious inverse response behaviour in its outputs when the UCM approach is used. The same result was shown to be true when multiple compartments are merged to form a complete distillation column.

It must be realised that the following are the noted limitations of this analytical approach on the initial inverse response in the compartmental models ;

(a) applicable only for binary mixtures ;
(b) applicable , while compositions are chosen as inputs and outputs.

2. 5. EXTENSION OF THE UNIVERSAL COMPARTMENTAL APPROACH TO MULTICOMPONENT DISTILLATION

2. 5. 1 MODEL DEVELOPMENT

Extension of the UCM approach to multicomponent distillation will be examined in this section. The same approach as used for a binary system i.e. model development followed by several illustrative examples will be used here also. Consider a compartment containing N trays in which the separation of a n component mixture is taking place (see Figure 2. 2. 1b). Once again, the separation taking place in a compartment can be represented by an unsteady component balance equation for the node , followed by (N-1) steady-state component balance equations for any (N-1) trays. However, such a set of separation are now required for any (n-1) components of the separation mixture. Composition of the remaining component is obtained by solving the overall composition balance equation for each of the trays (i.e $\sum X_i = 1.0$ for all i = 1, 2.., n).

$$\frac{dX_{i,Node}}{dt} = \frac{L}{M_T}(X_{i,0} - X_{i,N}) + \frac{V}{M_T}(Y_{i,0} - Y_{i,1}) \qquad (2.5.1)$$

$$L(X_{i,0} - X_{i,1}) + V(Y_{i,2} - Y_{i,1}) = 0 \qquad (2.5.2)$$

$$L(X_{i,1} - X_{i,2}) + V(Y_{i,3} - Y_{i,2}) = 0 \qquad (2.5.3)$$

. .

$$L(X_{i,N-2} - X_{i,N-1}) + V(Y_{i,N} - Y_{i,N-1}) = 0 \qquad (2.5.4)$$

$$Y_{i,j} = f\{\alpha_i, X_{i,j}\} \qquad i = 1,...,n$$

$$j = 1,.....N \qquad (2.5.5)$$

where α_i is the relative volatility of component 'i' of the separation mixture.

It must be realised that a binary system is a special case of a multicomponent system with the number of components equal to two (i.e. n = 2).

Again, the node composition in the UCM approach is equated to that of the lowest tray of a compartment. Thus, for an n component mixture ;

$$X_{i,Node} = X_{i,N} \quad \text{for} \quad i = 1,2,...,n\text{-}1 \qquad (2.5.6)$$

Composition of the n^{th} component is , once again obtained from the overall composition balance equation. Here also, the liquid holdup attributed to a node is taken to be the total holdup of all trays within the compartment and is assumed to be constant (see Equation 2. 3. 7).

2.5.2 APPLICATION OF THE UCM APPROACH

Applicability of the UCM approach to multicomponent distillation has been tested on a number of industrial distillation columns. The results obtained, as well as the limitations and possible extensions of this approach with respect to design and simulation problems will be addressed in this section.

The UCM approach introduced in the previous sections has many desirable characteristics, such as good dynamic tracking , physically meaningful state variables and an absence of any spurious inverse response and , hence , forms a viable alternative for modelling distillation columns. However, the assumptions used in this approach (in particular , constant molar over-flow and constant relative volatility within a set of trays) may become inadequate in the case of complex separations, especially if flow and energy dynamics become significant. Case studies performed on six industrial multicomponent columns revealed that some modifications to the basic UCM , as described previously, are required in some cases to achieve reasonable estimates of steady-state operating conditions. The six industrial columns studied were ,

(1) HCl column (Vinyl Chloride Monomer plant, ICI, Sydney, Australia)
(2) Product de-butaniser (Crude Stabilisation Plant, ESSO, Longford, Australia)
(3) C3- splitter (Olefins plant , ICI, Sydney , Australia)
(4) De-ethaniser (Gas-tail, Shell Refinery, Sydney, Australia)

(5) De-propaniser (Gas-tail, Shell Refinery, Sydney, Australia)

(6) De-isobutaniser (Gas-tail, Shell Refinery, Sydney, Australia)

Further information about the operating conditions and columns studied are given in Tables (2. 5. 1) and (2. 5. 2).

Modifications required to the basic UCM for application to industrial multicomponent columns fall into several categories :

(i) Relative volatility.

(ii) Internal flows.

(iii) Pressure drop.

(iv) Bubble and Dew point temperatures.

(v) Condenser and Reboiler sections.

(vi) Estimation of vapour-liquid equilibrium temperatures.

Each of these will be discussed in more detail below.

RELATIVE VOLATILITY

Relative volatility is a function of the operating pressure and can vary significantly as the column pressure changes. This is particularly true for the mixtures with large differences in the vapour-liquid equilibrium constants. For example, in the case of the C3 - splitter (Column 3 of the case-studies), the change in pressure from the top of the column to the bottom is about 5 % and this is equivalent to a change of the relative volatility of propane of about 2 %. For all such systems, the constant block relative volatility (i.e. relative volatility constant in a section of trays) assumption should be modified to express relative volatilities as a function of the pressure in the column. Within a compartment, each relative volatility is constant , but it now depends on the operating pressure of the compartment. This modification was found to be required in the case of the HCl column and the C3- splitter. In the case of the other columns, the assumption of constant relative volatilities throughout within a compartment was found to be quite adequate.

Normally, the key component for defining the relative volatilities is chosen to be the heaviest component in the mixture. However, it should be realised that no restriction is imposed in the UCM approach on the key component used. In other words, we can chose any component to be the key component and the relative volatilities are then calculated using the following equation :

Table 2. 5. 1

APPLICATION OF THE UCM APPROACH TO MULTICOMPONENT DISTILLATION COLUMNS

Column Details	Column -1	Column-2	Column-3
Type of process plant	Vinyl Chloride Monomer (VCM) Plant	Crude Stabilisation Plant	Olefins plant
Type of column	HCL column	Product de-butaniser	C3 Splitter
Number of trays in the column			
Theoretical	73	40	130
Actual	38	22	117
Number of components in the separation mixture	3	8	5
Type of components in the separation mixture	Chloro Carbons and HCl	Lighter hydrocarbons	Light hydrocarbons
Number of compartments used in the dynamic model	6	5	23

(contd.....)

Steady-state validation	Steady-state validation was performed against RADFRAC. Accuracy of +/-8% in the key component of the distillate product.	Steady-state results validated against PROCESS. Accuracy of model predictions were within 2-8 % for the key component both in the distillate and the bottoms products.	Steady-state results verified against FLOWPACK. Accuracy of model predictions were within 5% for the key components both in the distillate and bottoms products.
Modifications required to the basic UCM	(1) Constant relative volatility changed to relative volatility as a function of pressure.	(1) Constant molar overflow changed to include an estimate of internal flows.	(1) Constant relative volatility changed to relative volatility as a function of pressure.
	(2) Constant molar overflow changed to include an estimate of internal flows.		(2) Constant molar overflow changed to include an estimate of internal flows.

Table 2. 5. 2

APPLICATION OF THE UCM APPROACH TO MULTICOMPONENT DISTILLATION COLUMNS

Column Details	Column 4	Column 5	Column-6
Type of process plant	Gas-tail	Gas-tail	Gas-tail
Type of column	De-ethaniser	De-propaniser	De-isobutaniser
Number of trays in the column			
Theoretical	15	35	50
Actual	13	30	44
Number of components in the separation mixture	8	8	8
Type of components in the separation mixture	Light hydrocarbons	Light hydrocarbons	Light hydrocarbons
Number of compartments used in the dynamic model	3	6	8
Steady-state validation	Steady-state validation performed against SMBP*. Accuracy of ± 2 % in the ethane mole fraction of the distillate product.	Steady-state validation performed against SMBP*. Accuracy of ± 4 % in the propane mole fraction in the distillate product.	Steady-state validation was performed against SMBP*. Accuracy of ± 4 % in the i-butane mole fraction in the distillate product.

SMBP* - Shell Model Building Package (see Section 3. 1. 3).

$$\alpha_i = \frac{K_i}{K_m} \qquad \text{for all } i = 1, \ldots, m-1 \qquad (2.5.7)$$

where ' m ' is the key component.

INTERNAL FLOWS

If the flow profiles change very rapidly within the column, then the constant molar overflow assumption is inadequate. However, correction factors for the internal flows may be defined to still obtain reasonable accuracy from the UCM approach. This is an indirect way of incorporating the effects of energy balances into the UCM approach. Correlations for these correction factors can be determined from the steady-state simulation results of a rigorous (tray-by-tray) model. This was found to be essential in the case of the HCl column and Esso's product de-butaniser. When the internal liquid and vapour flows were plotted against the tray number , it was found that there were sections within these columns with flat flow profiles but with relatively sharp changes between adjacent sections. For example, the HCl column results are shown in Figure 2. 5. 1. The CMO assumption in the rectifying and stripping sections with the UCM approach results in an incorrect steady-state. The accuracy could be improved by using a more rigorous model that accounts for changes in the internal flows. Incorporating these internal flow changes for each compartment, however, would require a significant amount of computation. A good compromise, therefore, is to use simple correlations to estimate the internal flows as they leave a compartment. This can be achieved in one of the following two ways.

(a) Vapour and liquid flows leaving a compartment are estimated using simple flow correlations such as,

$$V^{out} = k_1 V^{in} \qquad (2.5.8)$$

$$L^{out} = k_2 L^{in} \qquad (2.5.9)$$

where ,

$$k_1 = f_1(P,T) \text{ and } k_2 = f_2(P,T) \qquad (2.5.10)$$

k_1 and k_2 are compartment specific and have to be estimated for the particular column of interest using rigorous steady-state results. Such correlations were estimated and used for both the HCl column and Esso's product de-butaniser and gave steady-state results that were significantly better.

Figure 2. 5. 1
Internal flow profiles within the HCl column

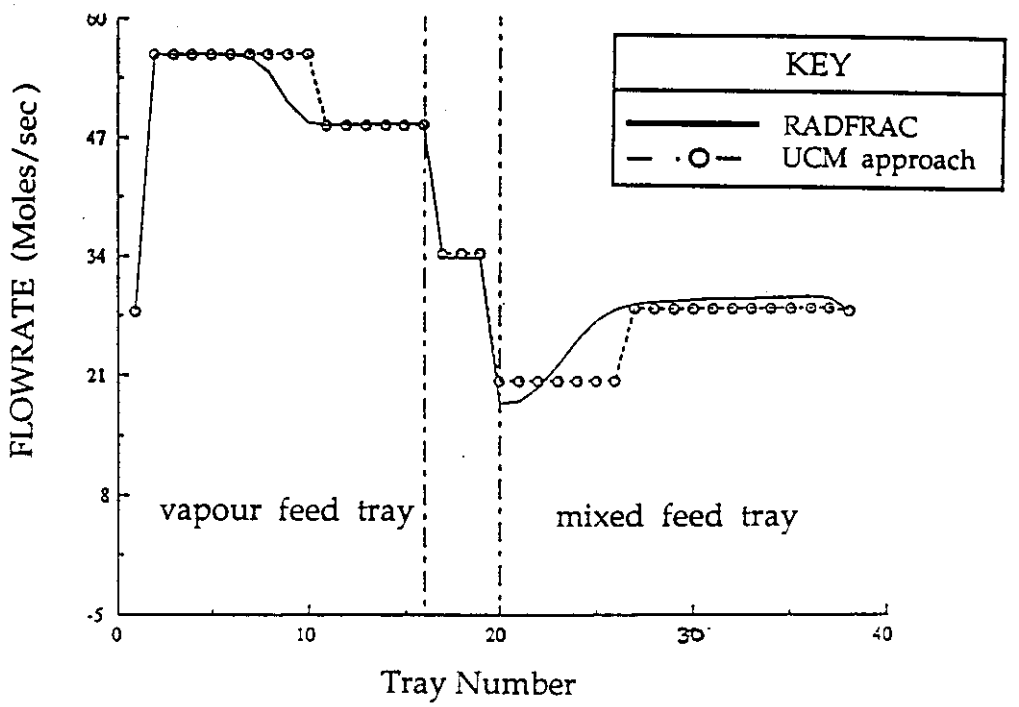

(a) Vapour flow profile in HCL column

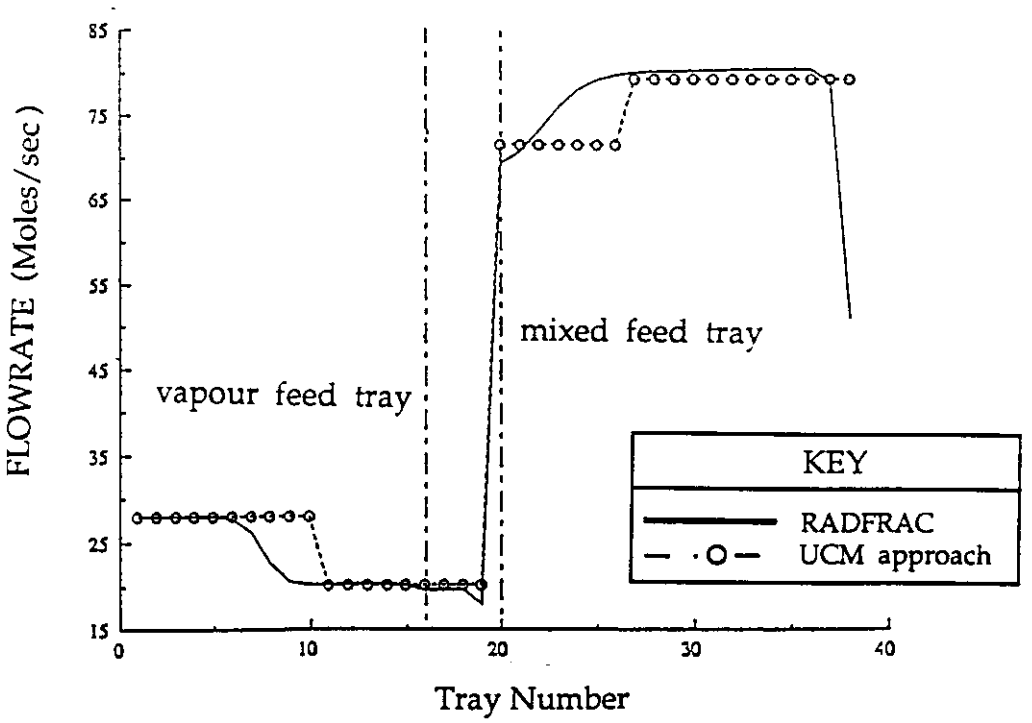

(b) Liquid flow profile in HCL column

Example 2. 5.1

Esso's product de-butaniser column was modelled using 22 theoretical stages (i.e. an average tray efficiency of 50 %). The column was designed to separate n-butane and i-pentane from a mixture of eight light hydrocarbon components. The UCM for simulating this column used five compartments along with a condenser and a reboiler. The following changes in the internal flows were necessary to obtain acceptable accuracies in the simulation results. The liquid leaving any compartment (L^{out}) was related to the liquid entering the compartment (L^{in}) by ,

$$L^{out} = k\, L^{in}$$

while the vapour flow leaving the compartment (V^{out}) was related to the other internal flows by ,

$$V^{out} = V^{in} + (L^{in} - L^{out})$$

where V^{in} is the vapour flow entering the compartment.

The correlation constant (k) was obtained for each of the compartments separately using the results of more rigorous steady-state simulations run over a range of operating conditions.

Compartment type		k - value
Compartment 1	(rectifying section)	0.97
Vapour feed compartment	(rectifying section)	0.94
Liquid feed compartment	(stripping section)	1.00
Compartment 2	(stripping section)	1.00
Compartment 3	(stripping section)	1.00

(b) Vapour and liquid flows leaving a compartment can also be estimated through a steady-state energy balance equation. Enthalpies of the streams entering or leaving a section are estimated based on equilibrium assumptions and simple enthalpy correlations. These enthalpy correlations can be developed for any specific separation mixture using physical property data tables (Furzer [1989]) or obtained through a series of case-studies on a rigorous steady-state model with an appropriate physical property package. Correlations for enthalpies were used to estimate internal flows in the case of the C3- splitter (Lear et al. [1989]).

Both these approaches require a number of steady-state simulations over the range of operating conditions of interest. In general, internal flow correction is required if either of the following conditions are encountered:

(1) The steady-state simulation results (obtained from a more rigorous simulation model) indicate that the internal liquid/vapour profiles vary significantly (i.e. flows in the design conditions are not in line with the CMO assumption).

(2) If (1) is not satisfied , check if the steady-states determined by the CMO based UCM model for different set of conditions (i.e. different from the original design conditions) are close to those determined from the more rigorous model. If not, internal flow corrections are necessary.

PRESSURE DROP

If the internal flow profiles are not very steep in a column, then a fixed pressure drop can be assumed per tray (or per compartment). Otherwise, pressure drop in the compartment section should be estimated using calculated internal flows and standard orifice equations (Coulson and Richardson, [1983]). A constant pressure drop for each tray or compartment was found to be reasonable for all the columns studied.

ESTIMATION OF BUBBLE AND DEW POINT TEMPERATURES

The vapour and liquid phases on a tray, in a condenser or in a reboiler at any instant have been assumed to be at equilibrium. The temperature of such an equilibrium mixture can be related to the relative volatilities of the components and estimated as follows.

Consider a mixture of ' n ' components. For an ideal mixture at equilibrium, vapour and liquid compositions are related by,

$$Y_i = K_i X_i \qquad (i = 1,\ldots,n) \tag{2.5.11}$$

$$K_i = \left(\frac{P_i^{sat}}{P^{total}} \right) \tag{2.5.12}$$

where

Y_i is the vapour composition of the 'i' th component

X_i is the liquid composition of the 'i' th component

P_i^{sat} is the saturated vapour pressure of the 'i' th component

and P^{total} is the total pressure.

The relative volatility (α_{ik}) for the 'i ' th component with respect to the key component (k) is defined as,

$$\alpha_{ik} = \frac{K_i}{K_k} \qquad (i = 1,\ldots, n) \tag{2.5.13}$$

From Equations (2. 5. 12) and (2. 5. 13) we have,

$$P_i^{sat} = P^{total} (K_k \alpha_{ik}) \quad (i = 1,..., n) \tag{2.5.14}$$

which can be written as,

$$P_i^{sat} = P_k^{sat} \alpha_{ik} \quad (i = 1,...., n) \tag{2.5.15}$$

Finally, from Equations (2. 5. 11) and (2. 5. 15) we obtain,

$$Y_i = \left(\frac{P_i^{sat}}{P^{total}} \right) (\alpha_{ik} X_i) \quad (i = 1,...., n) \tag{2.5.16}$$

Bubble point is the liquid temperature at which the first drop of vapour is formed. For the vapour thus formed,

$$\sum_{i=1}^{n} Y_i = 1.0 \tag{2.5.17}$$

From Equations (2. 5. 16) and (2. 5. 17) , the bubble point temperature can be estimated by taking a summation of vapour compositions for all components of the mixture.

$$\sum_{i=1}^{n} Y_i = \left(\frac{P_k^{sat}}{P^{total}} \right) \sum_{i=1}^{n} (\alpha_{ik} X_i) = 1.0 \tag{2.5.18}$$

noting that $\alpha_{kk} = 1.0$.

Equation (2. 5. 18) can be rearranged as ,

$$P_k^{sat} = \left(\frac{P^{total}}{\sum_{i=1}^{n} (\alpha_{ik} X_i)} \right) \tag{2.5.19}$$

However, Equation (2. 5. 19) does not take into account the non-ideal nature of mixture. An overall non-ideality coefficient (γ_{bub}) can be introduced to account for any such effects,

$$P_k^{sat} = \gamma_{bub} \left(\frac{P^{total}}{\sum_{i=1}^{n} (\alpha_{ik} X_i)} \right) \tag{2.5.20}$$

This coefficient (γ_{bub}) will in general, depend on the nature of the mixture components , the pressure and the temperature. Appendix A6 explains the method used here for estimating γ_{bub} .

From the Antoine equation (Smith and Van Ness [1975]) the saturated vapour pressure of the key component is related to the bubble point temperature (T_{bub}) by,

$$\ln(P_k^{sat}) = A + \frac{B}{T_{bub} + C} \qquad (2.5.21)$$

where **A , B** and **C** are the Antoine constants for the key component.

Solution of Equations (2. 5. 20) and (2. 5. 21) gives the bubble point temperature. An illustrative example is given below.

Example - 2. 5. 2

Consider a six component mixture of hydrocarbons with the following composition.

Propane	0.00692
i-butane	0.238
n-butane	0.503
i-pentane	0.09575
n-pentane	0.07268
n-hexane	0.08365

n-pentane is chosen to be the key component. The Antoine constants for n-pentane, valid over the pressure range of consideration , are (Chilton and Perry [1985])

$$A = 9.31 , \quad B = -2510.78 \quad \text{and} \quad C = 39.47$$

At a pressure of 17.0 Bar , the bubble point of this mixture can be estimated from a solution of Equations (2. 5. 20 - 2. 5. 21) as,

$$T_{bub} = 111.47 \text{ deg C} \quad \text{where} \quad \gamma_{bub} = 0.78 \text{ (see Appendix A6).}$$

Using PROCESS , the bubble point temperature at the same pressure was found to be,

$$T_{bub} = 111.69 \text{ deg C}$$

The error in the estimation of the bubble point temperature using the simplified approach outlined above , therefore, is approximately - 0. 2 %.

Dew point is the temperature at which the first drop of the liquid is formed when vapour is being cooled. For the liquid drop thus formed,

$$\sum_{i=1}^{n} X_i = 1.0 \qquad (2.5.22)$$

Using Equations (2. 5. 11 - 2. 5. 16) and (2. 5. 22), we have,

$$\sum_{i=1}^{n} X_i = P^{total} \frac{\sum_{i=1}^{v} \left(\frac{Y_i}{\alpha_{ik}} \right)}{P_k^{sat}} = 1.0 \qquad (2.5.23)$$

noting again that $\alpha_{kk} = 1.0$.

Equation (2. 5. 23) can be rearranged as ,

$$P_k^{sat} = P^{total}\left(\sum_{i=1}^{n-1} \left(\frac{Y_i}{\alpha_{ik}} \right) \right) \qquad (2.5.24)$$

Once again, Equation (2. 5. 24) does not take into account the non-ideal nature of mixture. An overall non-ideality coefficient (γ_{dew}) can be introduced to account for all such effects ;

$$P_k^{sat} = \gamma_{dew}\, P^{total}\left(\sum_{i=1}^{n-1} \left(\frac{Y_i}{\alpha_{ik}} \right) \right) \qquad (2.5.25)$$

This coefficient (γ_{dew}) also depends on the nature of the mixture components , the pressure and the temperature. Appendix A7 explains the method used here for estimating γ_{dew}. Using the Antoine Equation (2. 5. 21) for vapour pressure, we can estimate this time the dew point temperature (T_{dew}) by solving simultaneously Equations (2. 5. 21) and (2. 5. 25). An illustrative example is given below.

Example - 2. 5. 3

Consider a four component mixture of hydrocarbons with the following composition.

Ethane	0.0187
Propane	0.911
i-butane	0.0616
n-butane	0.00897

n-pentane is taken as the key component and so that the Antoine constants are ,

A = 9.31, B = - 2510.78 and C = 39.47

At a pressure of 19.1 Bar , the dew point of this mixture can be estimated from the solution of Equations (2. 5. 21 and 2. 5. 25) as,

T_{dew} = 57. 16 deg C where γ_{dew} = 0.52 (see Appendix A7).

Using PROCESS , the dew point temperature at the same pressure and vapour composition was found to be,

T_{dew} = 57. 98 deg C

The error in the estimation of the dew point temperature using the simplified approach outlined above , therefore, is approximately - 1. 4 % .

This method of estimating bubble and dew points was used throughout the gas-tail case-study. γ_{bub} and γ_{dew} values used in the gas-tail case-study are given in Table (3. 1. 3 - 3. 1. 8).

CONDENSERS AND REBOILERS

In the UCM approach, both condensers and reboilers were modelled as heat exchangers, where mass and energy transfer between the phases takes place. Enthalpy correlations and bubble/dew point calculations (as defined in the previous sections) were used to model these sections. The following assumptions were made in both the condenser and reboiler models.

(a) Vapour and liquid phase changes take place at constant pressure.

(b) Enthalpy changes equilibrate significantly faster than composition changes and hence only the composition dynamics need to be modelled.

(c) Pressure dynamics in the column are driven by the pressure dynamics occuring in the condenser.

(d) The temperature difference between process stream and steam (i.e the heat source) in the reboiler, provides the necessary driving force for heat transfer , while the heat actually transferred comes entirely from the latent heat of vaporisation of steam.

Further details on the design equation used are given in Appendices A4 and A5.

ESTIMATION OF VAPOUR - LIQUID EQUILIBRIUM TEMPERATURE

In the case of a separation tray , a partial condenser or a reboiler of the thermosyphon type, the temperature of the vapour and liquid phases at equilibrium is neither the bubble nor the dew point temperature, but has a value somewhere in between these temperatures. This equilibrium temperature can be estimated as explained below.

Consider a flash unit with vapour and liquid phases of a binary mixture at equilibrium (see Figure 2. 5. 2). At constant pressure , the T - X -Y diagram gives the the bubble and dew points as a function of composition (see Figure 2. 5. 3). Consider a liquid mixture of composition X_1 at it's bubble point (T_{bub}), i.e. at point A as shown in Figure 2. 5. 3. Tie-lines (such as AB) indicate that the vapour of composition (b) and the liquid of composition (X_1) are in equilibrium. With a change in the amount of liquid present in the flash at any time, mixtures of various vapour/liquid ratios are formed. The temperatures and compositions in each case being given by the tie-lines CD, EF etc., (see Figure 2. 5. 3). When all of the liquid has just been vaporized , the vapour thus formed

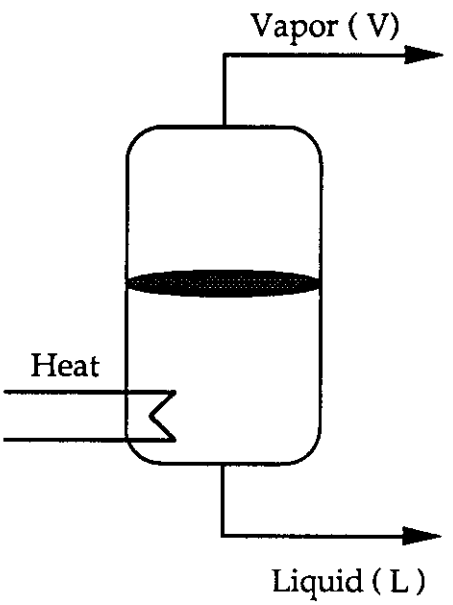

Figure 2. 5. 2 Flash drum

Figure 2. 5. 3
T - X - Y diagram for a binary mixture

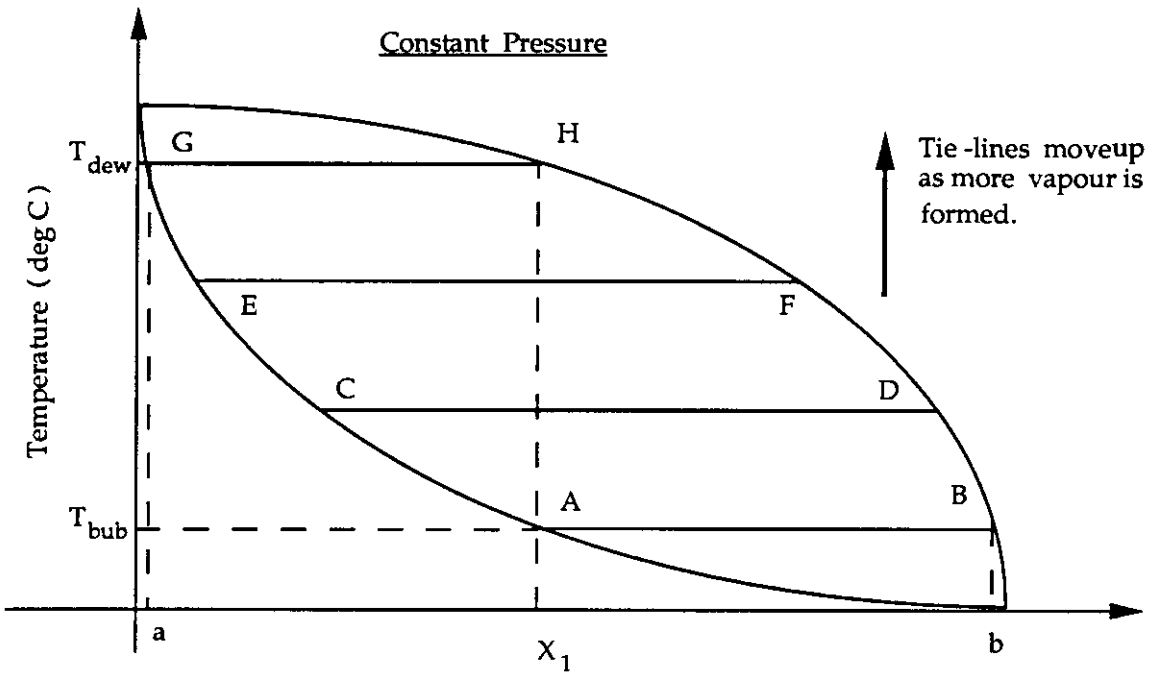

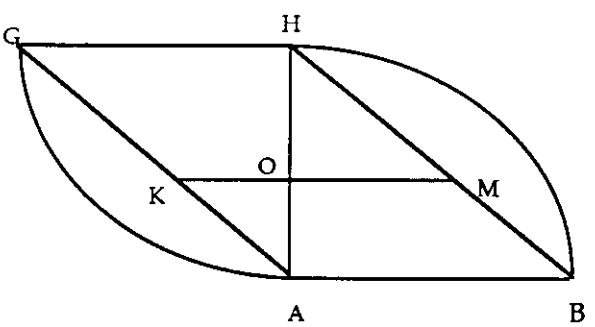

Figure 2. 5. 4
Estimation of Vapour-Liquid
Equilibrium Mixture Temperature

will be at it's dew point T_{dew} , where the liquid and vapour compositions are given by the tie-line **GH**. Over a composition range of interest, if we make the assumption that the curves **GA** and **HB** are straight lines then **ABGH** forms a parallelogram (see Figure 2. 5. 4) , the following expressions can be derived.

At the bubble point , the mixture is completely liquid (i.e. 0 % vapour , with the equilibrium compositions of the vapour and liquid are given by the tie-line **AB**). At the dew-point it is completely vapour (i.e. 100 % vapour , with the vapour and liquid equilibrium compositions are given by the tie-line **GH**). At any intermediate stage , for instance that given by the tie-line **KM** , the amount of vapour in the vapour-liquid equilibrium mixture is proportional to the length **KO** (see Figure 2. 5. 4). From the similarity of triangles we have,

$$\frac{AO}{KO} = \frac{HO}{MO} \qquad (2.5.26)$$

or alternatively

$$\frac{AO}{HO} = \frac{KO}{MO} \qquad (2.5.27)$$

This can be modified to give,

$$\frac{AO}{HO + AO} = \frac{KO}{MO + KO} \qquad (2.5.28)$$

$$\left(\text{since } \frac{a}{b} = \frac{c}{d} \Rightarrow \frac{a}{a+b} = \frac{c}{c+d} \right)$$

Now

$$KO \ \alpha \ V \ (= \text{amount of vapour present})$$

$$MO \ \alpha \ L \ (= \text{amount of liquid present})$$

$$AO = (T_{KM} - T_{bub})$$

and

$$HO = (T_{dew} - T_{KM})$$

and, thus,

$$\therefore \quad \frac{T_{KM} - T_{bub}}{T_{dew} - T_{bub}} = \frac{V}{V + L} \qquad (2.5.29)$$

which after rearrangement becomes,

$$T_{KM} = T_{bub} + \frac{V}{V + L} (T_{dew} - T_{bub}) \qquad (2.5.30)$$

Equation (2. 5. 30) , thus has a structure similar to an 'inverse lever arm law' and relates the vapour -liquid equilibrium mixture temperature to the fraction of the mixture vaporised.

This useful technique for the estimation of the temperature for a vapour-liquid mixture in equilibrium is illustrated using several examples and was found to give good estimates for both binary and multicomponent mixtures.

Example - 2. 5. 4

Consider a binary mixture of acetone and acetonitrile (see Figure 2. 5. 5). Using the simulation package PROCESS , the data required to construct a T -X -Y diagram were generated at a pressure of 0.552 atm . Table (2. 5. 3) shows the actual temperatures (calculated using PROCESS) and those calculated using Equation (2. 5. 30) over a range of mixture compositions and vapour-liquid ratios. Excellent agreement between the two mixture temperatures (a maximum error of 0.8%) can be seen, as shown in Figure 2. 5. 6. Points on the 45 degree line indicate that the estimated and actual temperatures are the same.

Example - 2. 5. 5

Consider now a binary mixture of ethanol and toluene which forms an azeotrope at a pressure of 1 atm at a composition of 88% ethanol (see Figure 2. 5. 7). Similar temperature calculations to those carried out in the previous example indicate that good agreement between the estimated and the actual (as generated from PROCESS) values of the mixture temperature are again obtained over a range of compositions and vapour-liquid ratios. As vapour and liquid compositions become indistinguishable at the azeotropic temperature, the mixture temperature at this point is equal to the dew point / bubble point temperature. The comparative results are shown in Table (2. 5. 4) and Figure 2. 5. 8. Again, points on the 45 degrees line indicate that the estimated and actual temperatures are the same.

It is clear from both the previous examples that estimation of the vapour-liquid mixture temperature , using the approximation suggested above (see Equation 2. 5. 30) is more than adequate over the entire range of compositions and vapour-liquid ratios for binary systems. The following example examines the applicability of above procedure for a multicomponent mixture.

Example - 2. 5. 6

Consider a seven component mixture containing the light hydrocarbons as shown below.

Component	Composition (mole %)
Ethane	0.1
Propane	21.3
i-Butane	17.2
n-Butane	37.3
i-Pentane	10.1
n-Pentane	12.0
n-Hexane	2.0

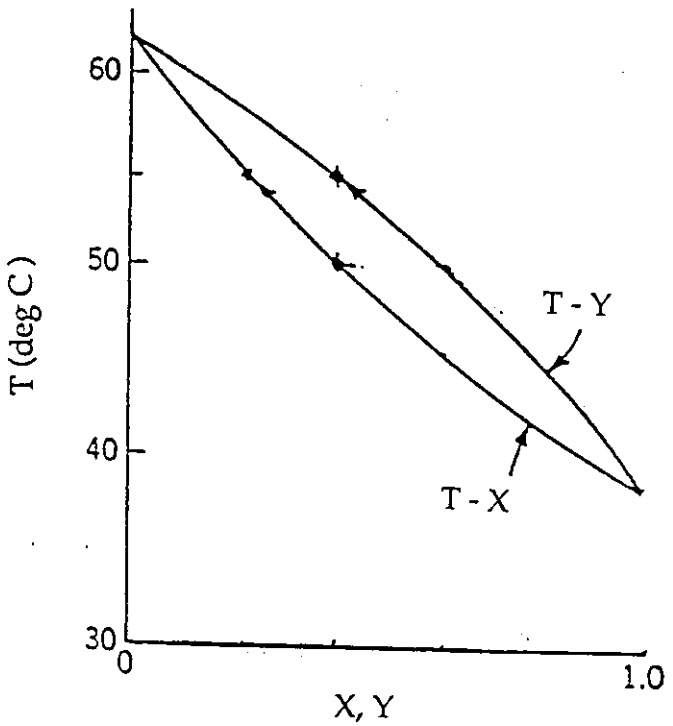

Figure 2.5.5

T-X-Y Diagram for

Acetone - Acetonitrile (binary) system

Figure 2.5.6

ESTIMATION OF VAPOUR-LIQUID EQUILIBRIUM MIXTURE TEMPERATURE FOR ACETONE-ACETONITRILE SYSTEM

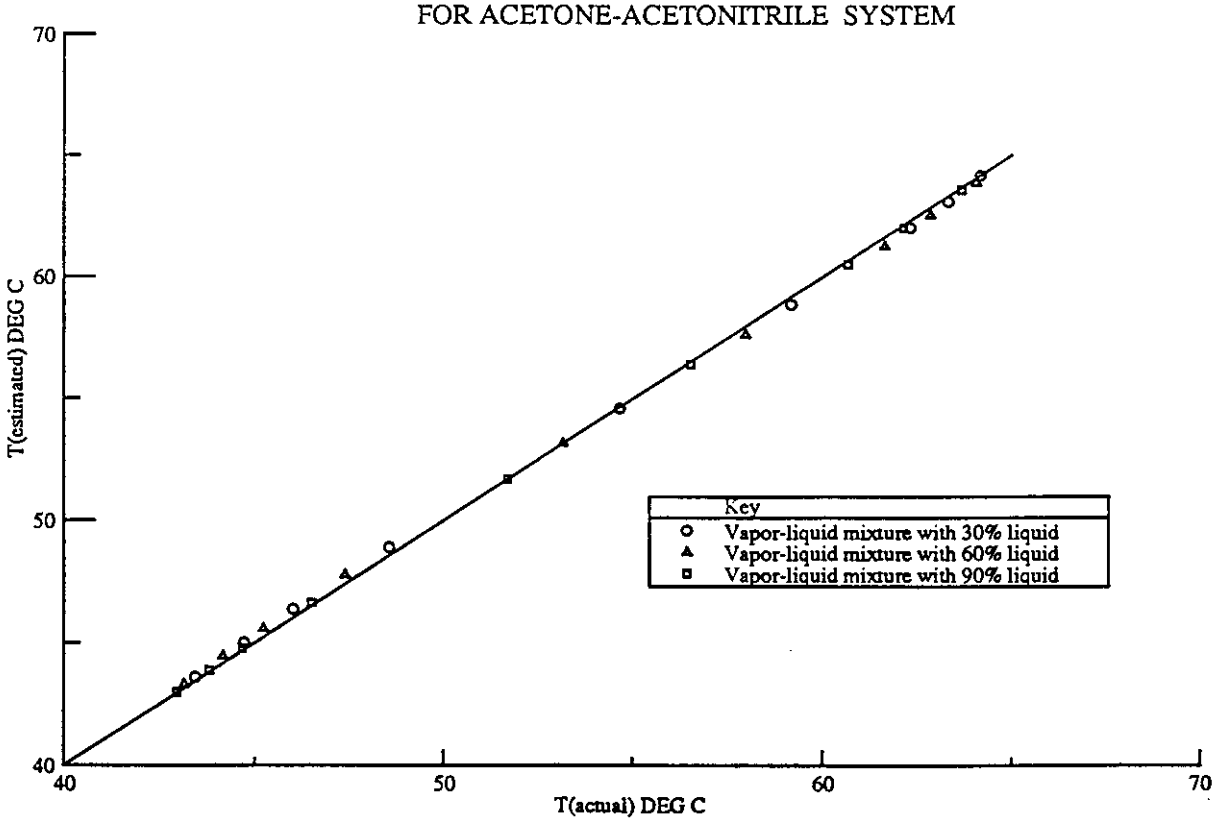

Table 2. 5. 3
ESTIMATION OF VAPOUR-LIQUID EQUILIBRIUM MIXTURE
TEMPERATURE FOR ACETONE - ACETONOTRILE (BINARY) SYSTEM

X	T(Bubble)	T(Dew)	Mixture Temperature					
			30% Liquid		60% Liquid		90% Liquid	
			T (Actual)	T(Estimated)	T (Actual)	T(Estimated)	T (Actual)	T(Estimated)
0.05	106.34	109.09	108.74	108.26	108.16	107.44	107	106.62
0.10	102.88	107.77	107.06	106.3	105.93	104.83	103.89	103.36
0.15	99.87	106.39	105.35	104.43	103.71	102.48	101.04	100.52
0.30	92.87	102.05	100.02	99.29	97.26	96.53	93.97	93.79
0.50	86.57	95.6	92.66	92.88	89.68	90.18	87.23	87.47
0.75	81.5	86.4	84.08	84.93	82.62	83.46	81.72	81.99
0.85	80	82.6	81.29	81.82	80.56	81.04	80.12	80.26
0.90	79.34	80.86	80.09	80.4	79.67	79.94	79.4	79.49
0.95	78.71	79.33	79.03	79.14	78.85	79.96	79.96	78.77

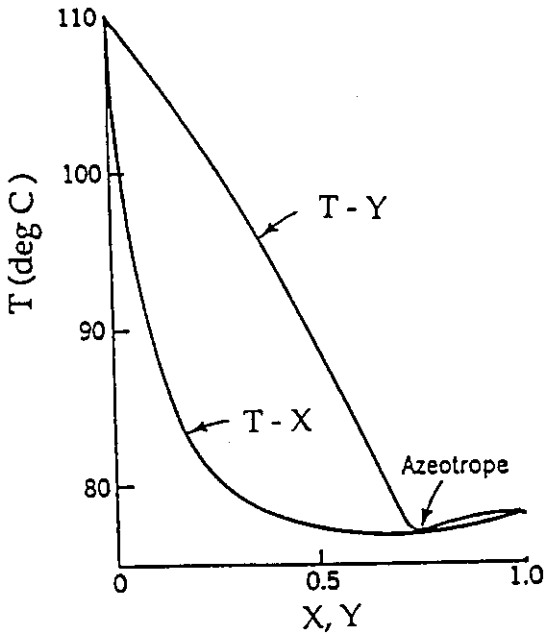

Figure 2.5.7
T-X-Y Diagram for
Etanol-Toluene (binary) system

Figure 2.5.8
ESTIMATION OF VAPOUR-LIQUID EQUILIBRIUM
MIXTURE TEMPERATURE
FOR ETHANOL-TOLUENE SYSTEM

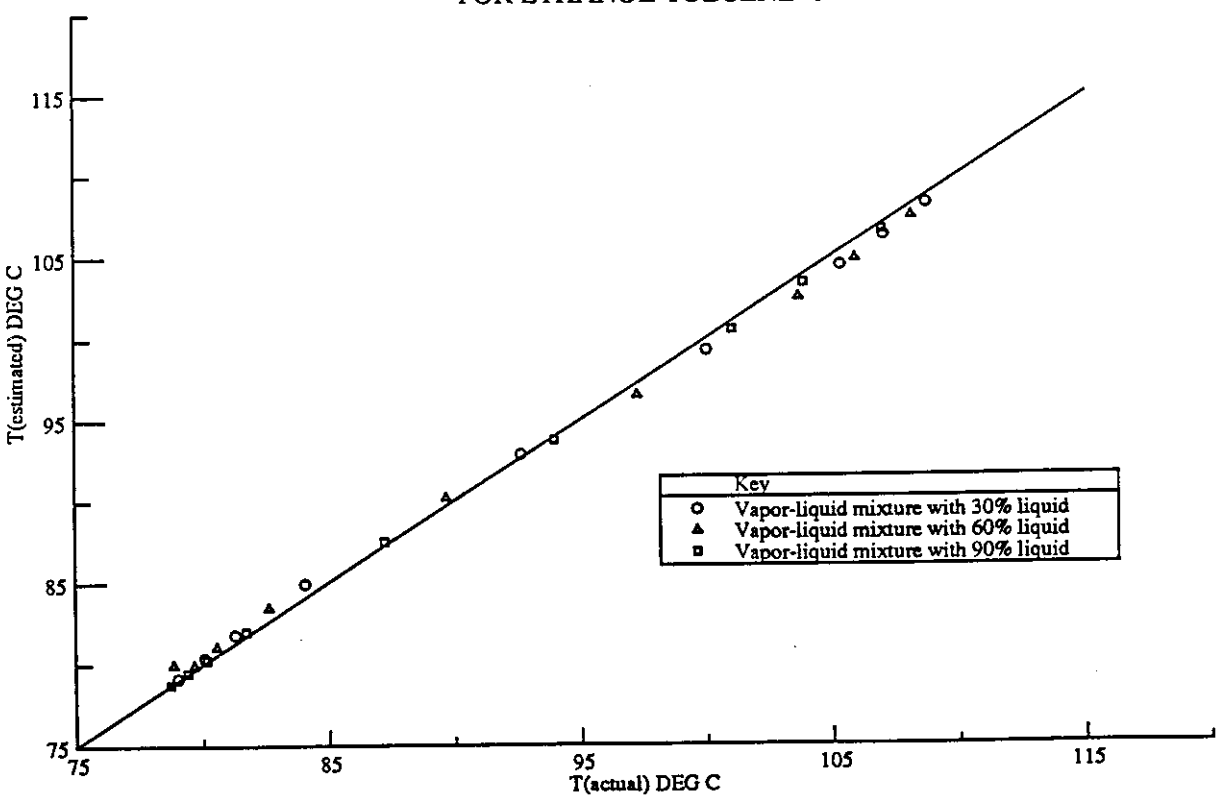

Table 2. 5. 4
ESTIMATION OF VAPOUR-LIQUID EQUILIBRIUM MIXTURE
TEMPERATURE FOR ETHANOL - TOLUENE (BINARY) SYSTEM

X	T(Bubble)	T(Dew)	Mixture Temperature					
			30% Liquid		60% Liquid		90% Liquid	
			T (Actual)	T(Estimated)	T (Actual)	T(Estimated)	T (Actual)	T(Estimated)
0.05	60.49	64.46	64.29	64.17	64.06	63.88	63.68	63.59
0.10	61.83	63.64	63.32	63.1	62.86	62.56	62.15	62.02
0.15	60.26	62.79	62.22	62.04	61.64	61.28	60.67	60.52
0.30	56.01	60.11	59.18	58.88	57.99	57.65	56.54	56.42
0.50	51.22	56.08	54.67	54.62	53.16	53.17	51.68	51.71
0.75	46.26	50.3	48.56	48.9	47.39	47.77	46.51	46.64
0.85	44.52	47.16	46.01	46.37	45.22	45.58	44.67	44.79
0.90	43.69	45.59	44.72	45.02	44.16	44.45	43.79	43.89
0.95	42.89	43.92	43.42	43.61	43.13	43.3	42.94	42.99

Using PROCESS , the following temperatures at a pressure of 17.0 bar, were estimated ;

(i)	Bubble point temperature	= 126.4 deg C
(ii)	Dew point temperature	= 138.7 deg C
(iii)	Mixture temperature (when 50 % of the liquid is vaporised)	= 133.3 deg C

Using Equation (2. 5. 30), we have an estimated value for the mixture temperature at 50 % vaporisation of,

$$T = 126.4 + 0.5\ (138.7 - 126.4) = 132.6 \text{ deg C}$$

The error in the estimated value is , thus, about 0.6 %.

Thus, the proposed method has been found to provide a good estimate of the mixture temperature for both binary (with and without an azeotropic state) and multicomponent mixture.

The following are a few extensions and observed limitations of this approach.

(1) This approximation holds good only if the bubble and dew point curves of the T-X -Y diagram are reasonably straight over the composition range of interest.

(2) The inverse lever principle should strictly be used only for 'extensive' properties like mass and energy. The assumption that lines **GA** and **HB** are parallel implies that the composition varies linearly with temperature. In fact, enthalpy is related to the composition , temperature and pressure ;

$$H = f(X, T, P)$$

At constant pressure , if the composition variation is linear with temperature,then enthalpy can be expressed as a function of temperature alone, i.e.

$$H = g(T)$$

The advantage of this expression is that, it permits the use of the inverse lever principle for an intensive property such as temperature. Equation (2. 5. 30), therefore, is justified in the light of the assumptions used.

(3) There is no simple analytical proof that this approach can be used to estimate the temperature for a multicomponent mixture. However, it is

assumed (as shown through the illustrative Example (2. 5. 6)) that the same physical interpretation holds good for multicomponent mixtures as well.

Despite all the noted limitations , the proposed approximation method seems to provide, at least, a good first estimate of the mixture temperature for both binary and multicomponent systems. The same approach was used in all the industrial columns considered in the current study.

All the changes that have been suggested for incorporation into the universal compartmental model (UCM) for its application to multicomponent distillation columns are to some extent both optional and hierarchical in nature. In other words, depending on the accuracy required, we can incorporate one or all of the features suggested. Case-studies performed on various industrial columns, along with the operating conditions and the changes incorporated in the basic UCM so as to achieve the required accuracy, are summarised in Tables (2. 5.1) and (2. 5. 2).

Apart from the performance type problems (discussed previously in this chapter), another type of problem that is frequently met in process synthesis is concerned with designing a process that can achieve a desired goal. With respect to distillation , this means that for a given separation of a feed mixture, we want to find out the number of trays the distillation column should have, the the reflux ratio to use etc.,. The UCM can be used to carryout such design problems. Its implementation within the SPEEDUP environment makes it a convenient and robust tool for solving such design problems. This has been demonstrated (Krishnan, [1990]) using an example taken from the literature (the Williams - Otto [1963] plant). The component splitter used in the original reference was replaced by a distillation column based on the UCM approach. Both, the number of trays required to achieve a given separation, and the relative volatilities of the various components were estimated, for a given feed and product compositions, with relatively little computational effort.

2. 6. A CASE STUDY OF A MULTICOMPONENT DISTILLATION COLUMN USING THE UCM APPROACH

Using the case-study of a 20-tray binary distillation column (Stewart et al. [1981]), the UCM approach was shown to provide better dynamic tracking than the available compartmental models. From the discussions in Section 2. 5 , it was clear that the UCM approach, with some modifications, can be applied distillation columns carrying out multicomponent separations. In the following case-study, an extension of the UCM based approach to a multicomponent mixture system will be investigated.

The case-study is for a 20-tray distillation column (Gani et al. [1986]) carrying out a three component separation. The column was designed to separate n-butane, as distillate, from a feed mixture of n-butane, n-pentane and benzene. Table 2. 6. 1 provides the design details and steady-state operating conditions of this column. Following are the different steps involved in extending in developing a distillation column model based on the UCM approach.

(1) A rigorous dynamic tray-by-tray simulation model was used initially to obtain data on the steady-state operating conditions of the 20 tray column. Rigorous mass and energy balances for each tray were used along with the physical property routines for the three component mixture. Hydraulics , temperature and pressure dynamics for each tray along the column were also used in this model. Vapour-liquid equilibrium coefficients for each trays, together with pressure ,temperature and column internal flow profiles were obtained (see Figures 2. 6. 1 - 2. 6. 4). Model development and simulation runs were performed using the SPEEDUP flowsheeting package. A simulation time of about 750 CPU seconds was required on Micro Vax II with VMS operating system , for the steady-state simulation of this rigorous distillation column model.

(2) A compartmental model based on the UCM approach was developed next, also using SPEEDUP. Initially the CMO assumption for the internal flows was used. Four compartments along with a reboiler and a condenser were used in this model. Benzene, the least volatile component of the three components , was chosen as the key component. The relative volatilities of the remaining two components, for each of the column trays were then calculated using the Equation 2. 5. 7. A constant value for each relative volatility (i.e. an arithmetic average over all the trays), within each compartment , was used throughout the case-study. A total of 14 trays (i.e. 3 trays for each of the 4 compartments , thus one tray each for the reboiler and the condenser, respectively) gave a good steady-state match between the rigorous and the UCM based compartmental model simulations (see Table 2. 6. 2) .

The next issue is whether to introduce internal flow correction factors to improve the UCM model fit. Based on the recommendations made in Section 2. 5. the primary check involved a comparison of the internal flow profiles for the rigorous and UCM models (see Figures 2. 6. 3 and 2. 6. 4). Clearly, the CMO assumption used in the basic UCM model appears to be inadequate and flow corrections may be necessary. The other check is to examine how closely the steady-state results are, at different operating conditions , for both rigorous and UCM models. Table 2. 6. 3 summarises the results for a new steady-state defined by an - 8 % change in the feed

Table 2. 6. 1
20 TRAY MULTICOMPONENT DISTILLATION COLUMN DESIGN DETAILS

Column details	Value(s)
Number of trays	20
Tray efficiency	100%
Number of components in the feed	3
Components (1)	n-Butane
(2)	n-Pentane
(3)	Benzene
Feed tray location	11 (top tray = 1)
Feed state	Liquid at its bubble point
Feed flow rate (Kg-moles/hr)	226.8
Feed temperature (deg C)	39.1
Feed enthalpy (Kcal / Kg-moles)	1106.9
Feed pressure (Bars)	2.27
Column pressure on tray 1 (Bars)	2.09
Condenser type	Total condenser
Reboiler	Thermosyphon type
Reflux rate (Kg-moles/hr)	429.0
Bottoms product rate (Kg-moles/hr)	138.5
Reboiler duty (Kcal/ hr)	2.76E6
Condenser duty (Kcal/ hr)	2.67E6

Table 2. 6. 2
20 TRAY MULTICOMPONENT DISTILLATION COLUMN CASE-STUDY.
STEADY-STATE MODEL RESULTS.

Column variables		Rigorous model	UCM (with CMO assumption)
Feed flow rate (Kg-moles/hr)		226.8	226.8
Reflux rate (Kg-moles/hr)		429	428.24
Bottoms product rate (Kg-moles/hr)		138.5	138.5
Distillate rate (Kg-moles/hr)		88.3	88.3
Distillate product composition	(1)	0.993	0.993
	(2)	6.77E-3	6.56E-3
	(3)	0	0
Bottoms product composition	(1)	7.96E-5	45.88E-5
	(2)	0.682	0.682
	(3)	0.318	0.318

Table 2. 6. 4
20 TRAY MULTICOMPONENT DISTILLATION COLUMN CASE-STUDY.
INTERNAL FLOW CORRECTION FACTORS.

Section	Constant (a)	Constant (b)
Compartment 1 (rectifying section)	2.359	-0.002667
Compartment 2 (feed tray section)	12.21E-3	2.08E-3
Compartment 3 (stripping section)	0.832	18.70E-5
Compartment 4 (stripping section)	1.615	- 98.46E-5

Table 2. 6. 3
20 TRAY MULTICOMPONENT DISTILLATION COLUMN CASE-STUDY.
STEADY-STATE MODEL RESULTS FOR VARIOUS MODELS.

Column variables		Steady-state (1)			Steady-state (2)		
		Rigorous model	UCM (with CMO assumption)	UCM (with internal flow corrections)	Rigorous model	UCM (with CMO assumption)	UCM (with internal flow corrections)
Feed flowrate	(Kg-moles/hr)	226.8	226.8	226.8	209	209	209
Reflux rate	(Kg-moles/hr)	429	428.24	428.24	429	428.24	428.24
Bottoms product rate	(Kg-moles/hr)	138.5	138.5	138.5	138.5	138.5	138.5
Distillate rate	(Kg-moles/hr)	88.3	88.3	88.3	70.5	70.5	70.5
Distillate product composition	(1)	0.993	0.993	0.993	0.895	0.953	0.891
	(2)	6.77E-3	6.56E-3	6.56E-3	9.95E-2	0.045	0.103
	(3)	0	0	0	5.50E-3	2.00E-3	6.00E-3
Bottoms product composition	(1)	7.96E-5	45.88E-5	45.88E-5	1.50E-3	9.00E-3	4.00E-3
	(2)	0.682	0.682	0.682	0.656	0.666	0.651
	(3)	0.318	0.318	0.318	0.343	0.325	0.345

Figure 2. 6. 1
CASE STUDY ON THE SEPARATION OF A 3-COMPONENT MIXTURE.
TEMPERATURE PROFILE ALONG THE COLUMN AT STEADY-STATE

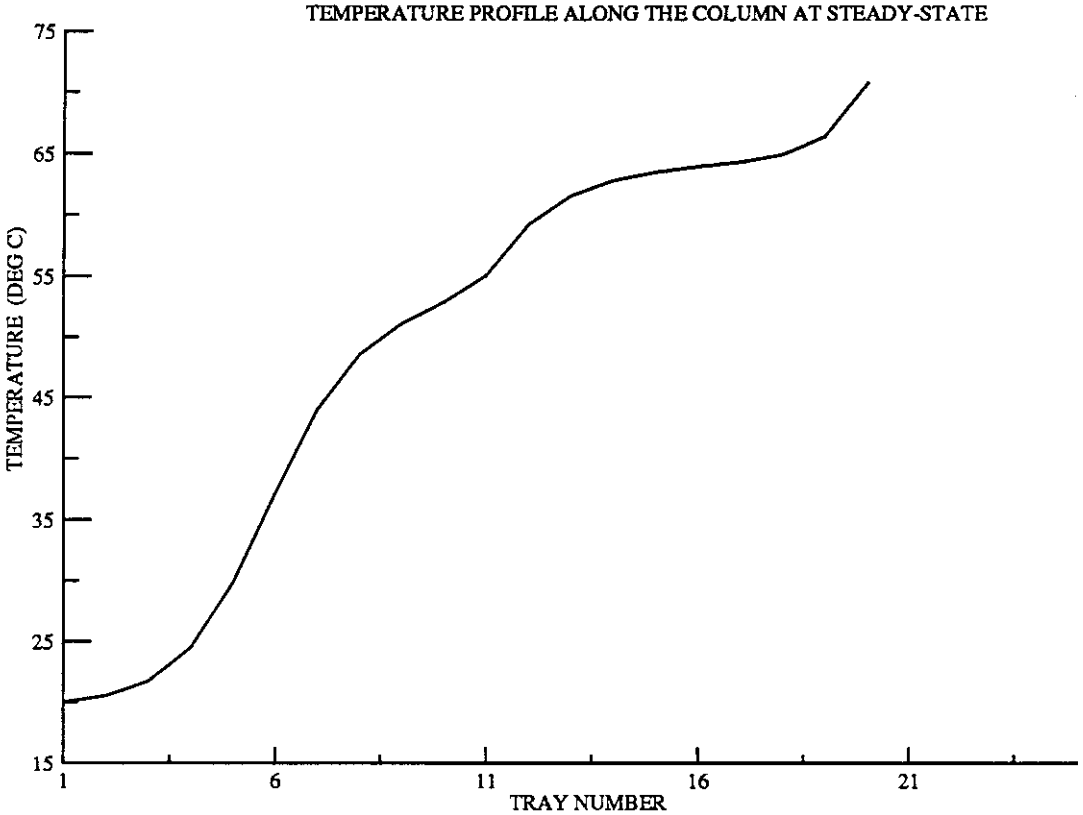

Figure 2. 6. 2
CASE STUDY ON THE SEPARATION OF A 3-COMPONENT MIXTURE.
PRESSURE PROFILE ALONG THE COLUMN AT STEADY-STATE

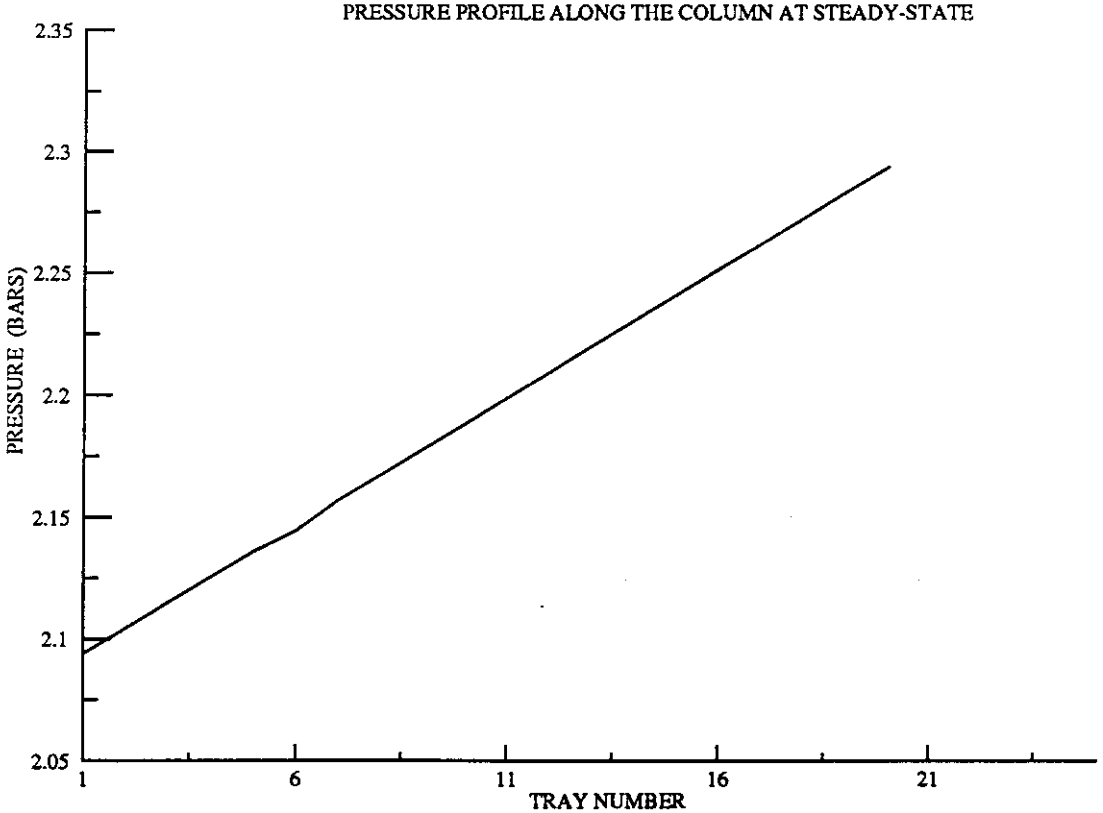

Figure 2. 6. 3
THREE COMPONENT 20-TRAY DISTILLATION COLUMN.
VAPOUR FLOWRATE ALONG THE COLUMN.

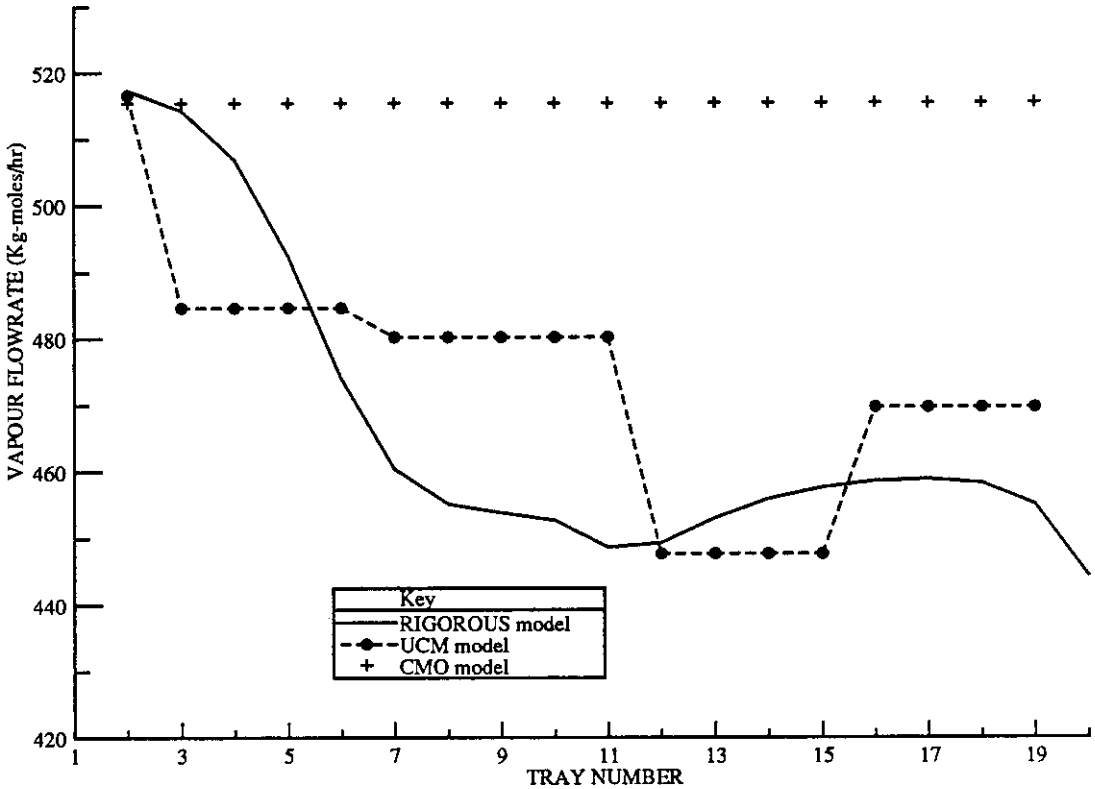

Figure 2. 6. 4
THREE COMPONENT 20-TRAY DISTILLATION COLUMN.
LIQUID FLOWRATE ALONG THE COLUMN.

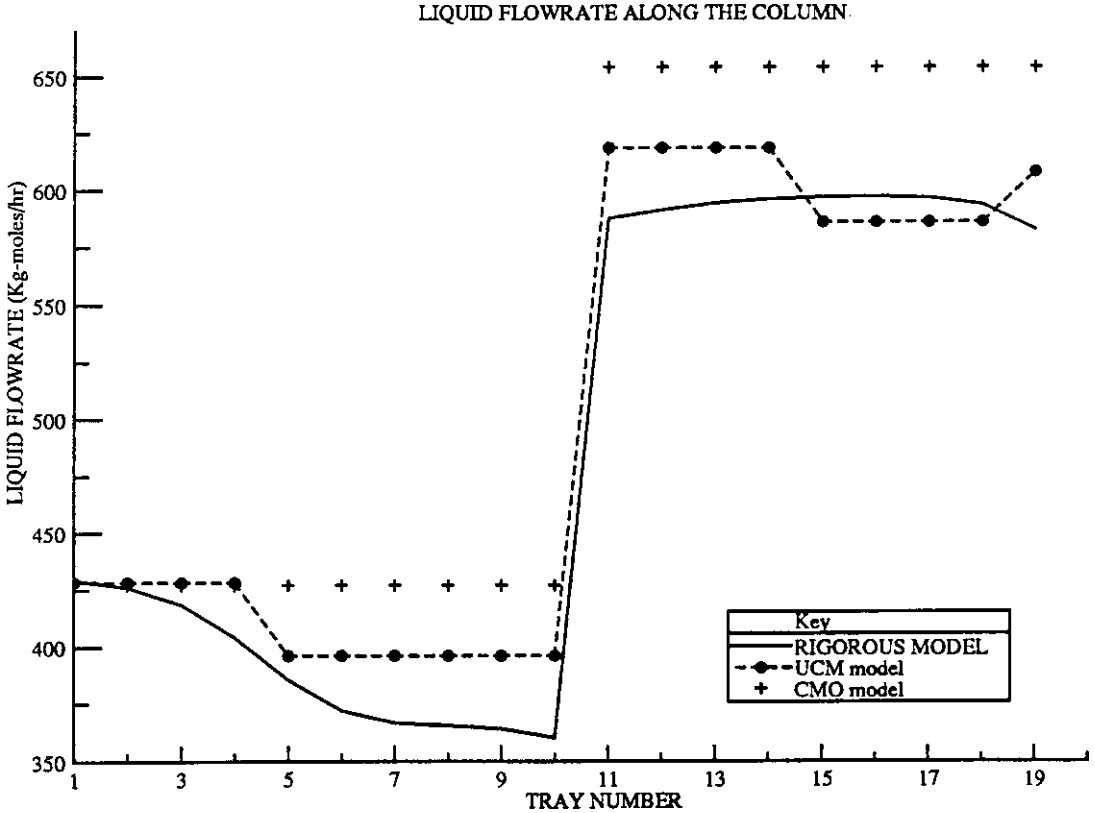

flowrate from the original steady-state value. The UCM steady-state, was significantly different (e.g. an error of about + 7 % in the n-butane composition in the distillate). Both these observations indicate that internal flow correction factors are necessary to obtain reliable UCM model results. Based on the simulation data generated from the rigorous model, correlations for the internal flow correction factors were defined. For each compartment in the UCM model, the inlet vapour and liquid flowrates were related to the exit vapour and liquid flows via ,

$$L^{out} = kL^{in}$$

where $$k = (a + bL^{in})$$

and $$V^{out} = V^{in} + (L^{in} - L^{out})$$

where k, a and b are the correlation constants.

Table (2. 6. 4) lists all the constants for the different compartments. Table (2. 6. 3) shows a significant improvement in the steady-state agreement with the inclusion of flow correction factors into the UCM model. For an 8 % change in the feed flowrate from the original steady-state value the modified UCM , errors in the steady-state estimations are of the order 0.5 % in the n-butane composition in the distillate and 0.8 % in the i-butane in the bottoms product. A simulation time of the order 80 CPU seconds on MicroVax II , was needed for a modified UCM steady-state simulation , almost a tenfold reduction compared with the rigorous model.

(3) The open-loop dynamic response of the UCM model was compared with that of the rigorous model for the following changes ;

(a) An exponential change of - 10 % (i.e. final change being 10 % lower than the initial value) in the feed rate to the column (see Figure 2. 6. 6).

(b) An exponential change of - 5% change in the reflux rate (see Figure 2. 6. 5).

Transient composition responses in both the distillate and bottoms product streams are shown in Figures (2. 6. 7 - 2. 6. 14). Reasonably good agreement is observed between the modified UCM model predictions and the rigorous model results. As expected , the predictions of the original UCM model (based on the CMO assumption) were different considerably, both in it's dynamics and in it's final steady-state.

The results of this case-study would seem to confirm the extension of the UCM approach to multicomponent separations. Thus, the UCM approach provides acceptable modelling of the dynamics of distillation columns but with significantly less computational power than required for a full tray-by-tray dynamic model.

Figure 2. 6. 5
CASE STUDY ON THE SEPARATION OF A 3-COMPONENT MIXTURE.
A - 5% EXPONENTIAL CHANGE IN THE REFLUX RATE.

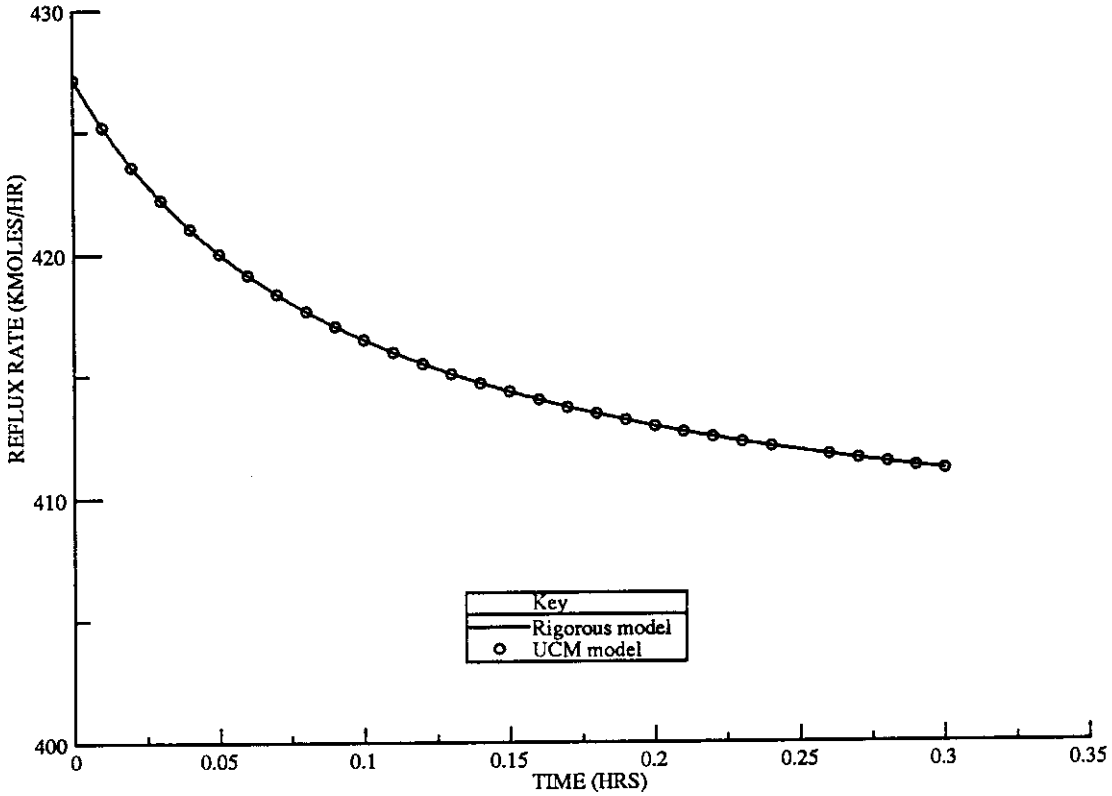

Figure 2. 6. 6
CASE STUDY ON THE SEPARATION OF A 3-COMPONENT MIXTURE.
A - 10% EXPONENTIAL CHANGE IN THE FEED FLOW RATE.

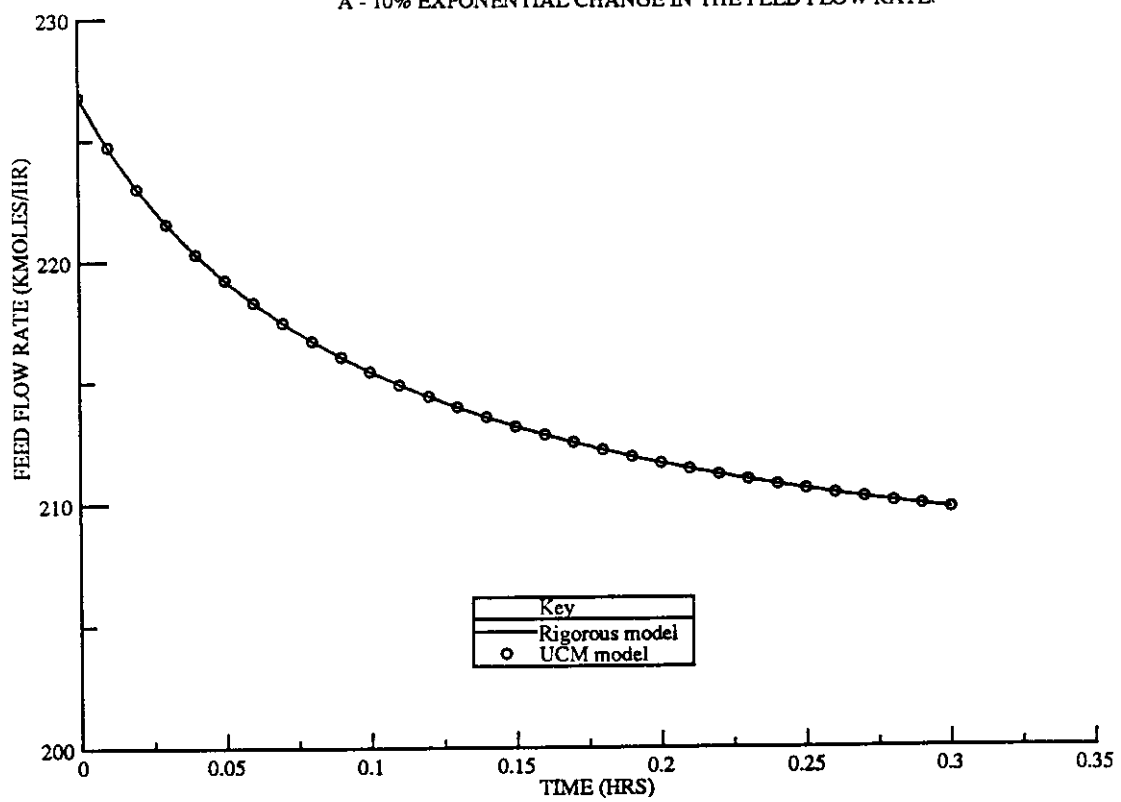

Figure 2. 6. 7
CASE STUDY ON THE SEPARATION OF A 3 COMPONENT MIXTURE.
RESPONSE OF DISTILLATE COMPSOTION
FOR A - 5% EXPONENTIAL CHANGE IN THE REFLUX RATE.

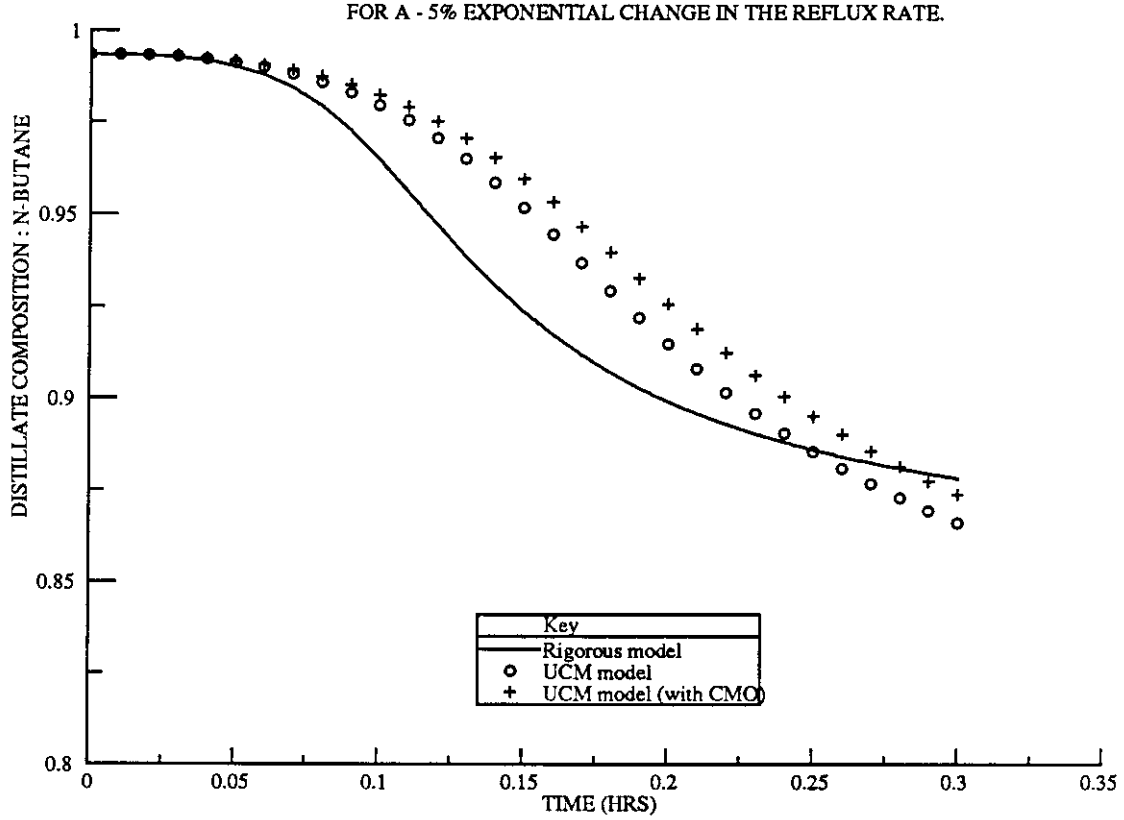

Figure 2. 6. 8
CASE STUDY ON THE SEPARATION OF A 3 COMPONENT MIXTURE.
RESPONSE OF DISTILLATE COMPSOTION
FOR A - 5% EXPONENTIAL CHANGE IN THE REFLUX RATE.

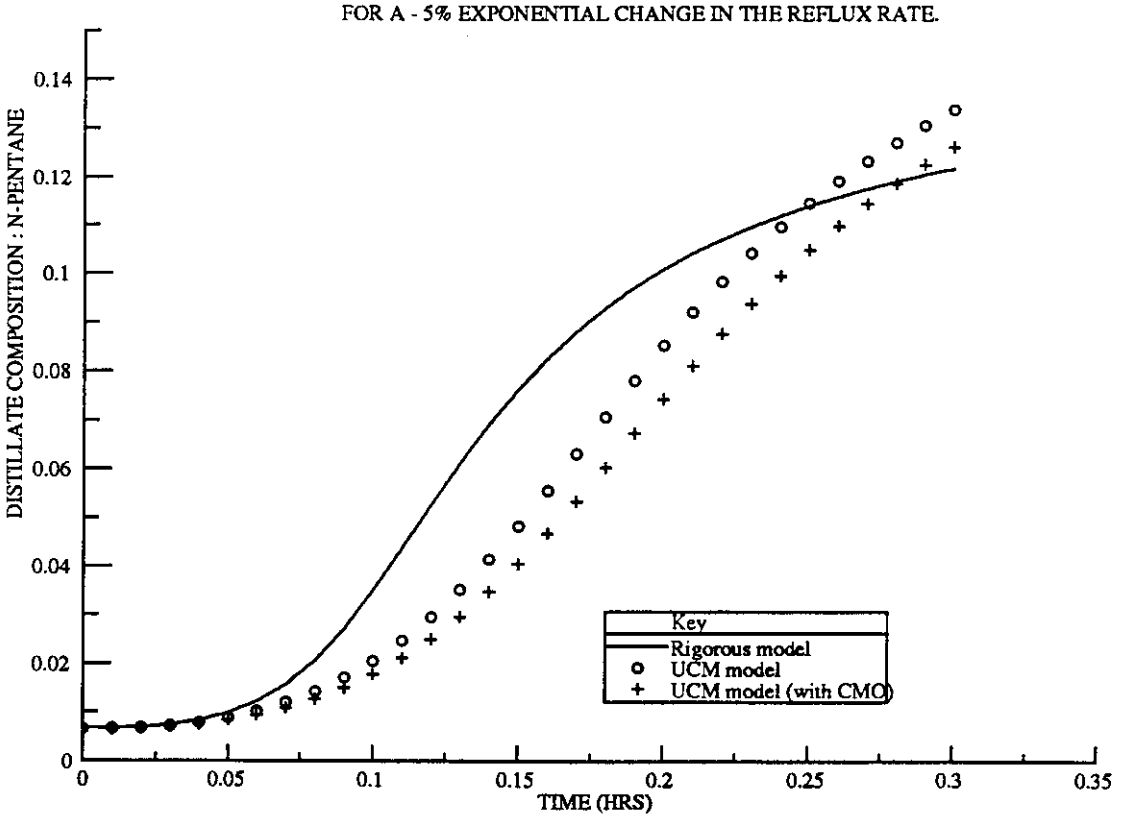

Figure 2. 6. 9
CASE STUDY ON THE SEPARATION OF A 3 COMPONENT MIXTURE.
RESPONSE OF BOTTOMS FLOW COMPOSITION
FOR A - 5% EXPONENTIAL CHANGE IN THE REFLUX RATE.

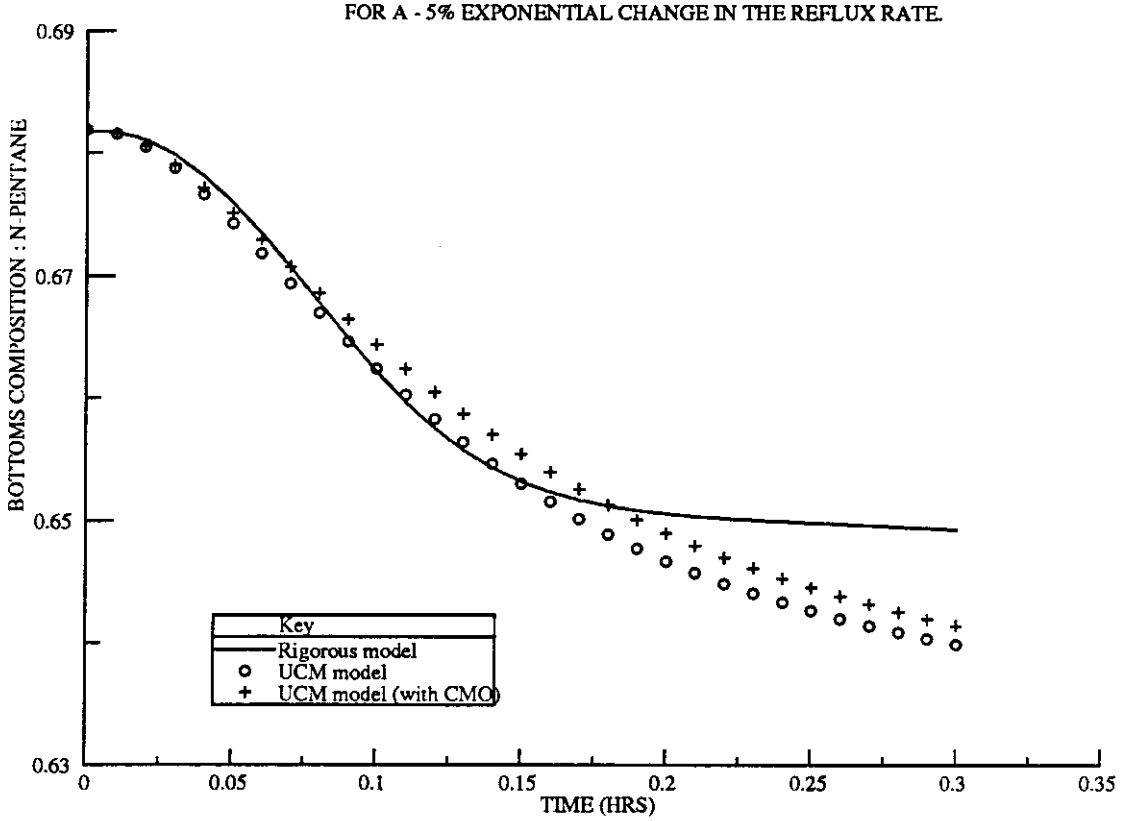

Figure 2. 6. 10
CASE STUDY ON THE SEPARATION OF A 3 COMPONENT MIXTURE.
RESPONSE OF BOTTOMS FLOW COMPOSITION
FOR A - 5% EXPONENTIAL CHANGE IN THE REFLUX RATE.

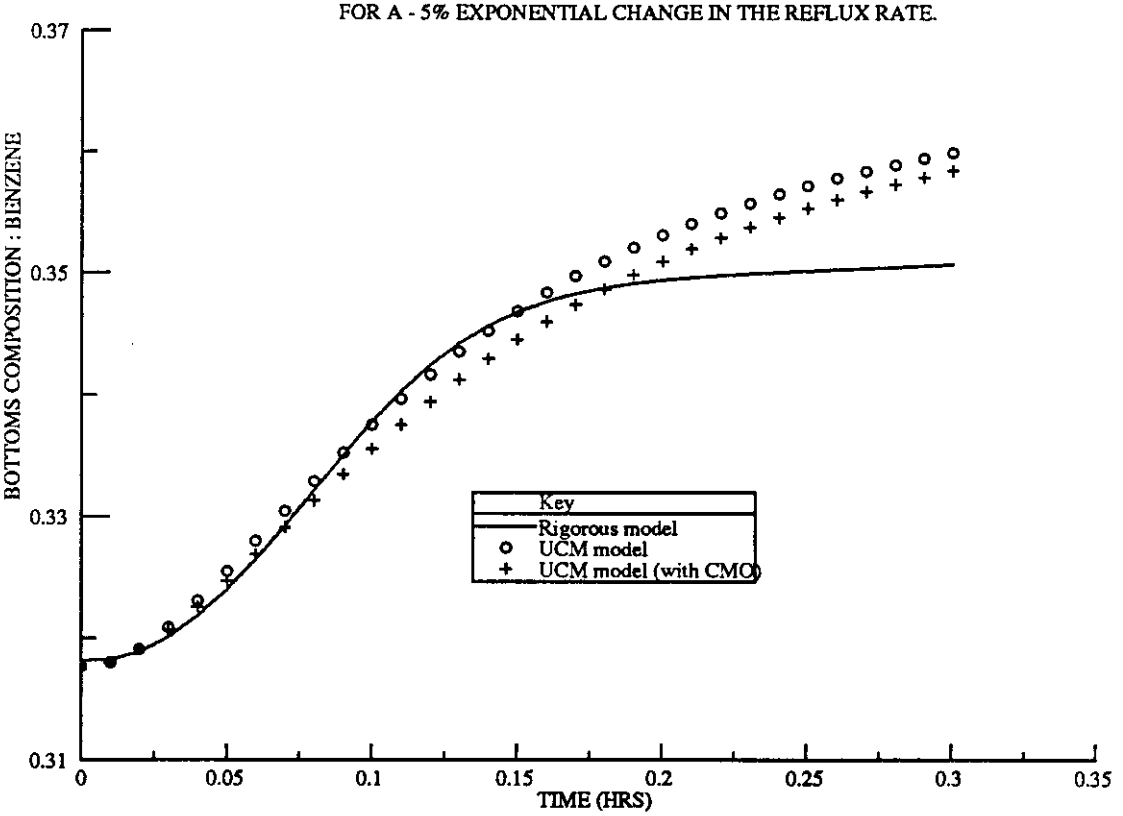

Figure 2. 6. 11
CASE STUDY ON THE SEPARATION OF A 3 COMPONENT MIXTURE.
RESPONSE OF DISTILLATE COMPOSITION
FOR A - 10% EXPONENTIAL CHANGE IN THE FEED FLOW RATE.

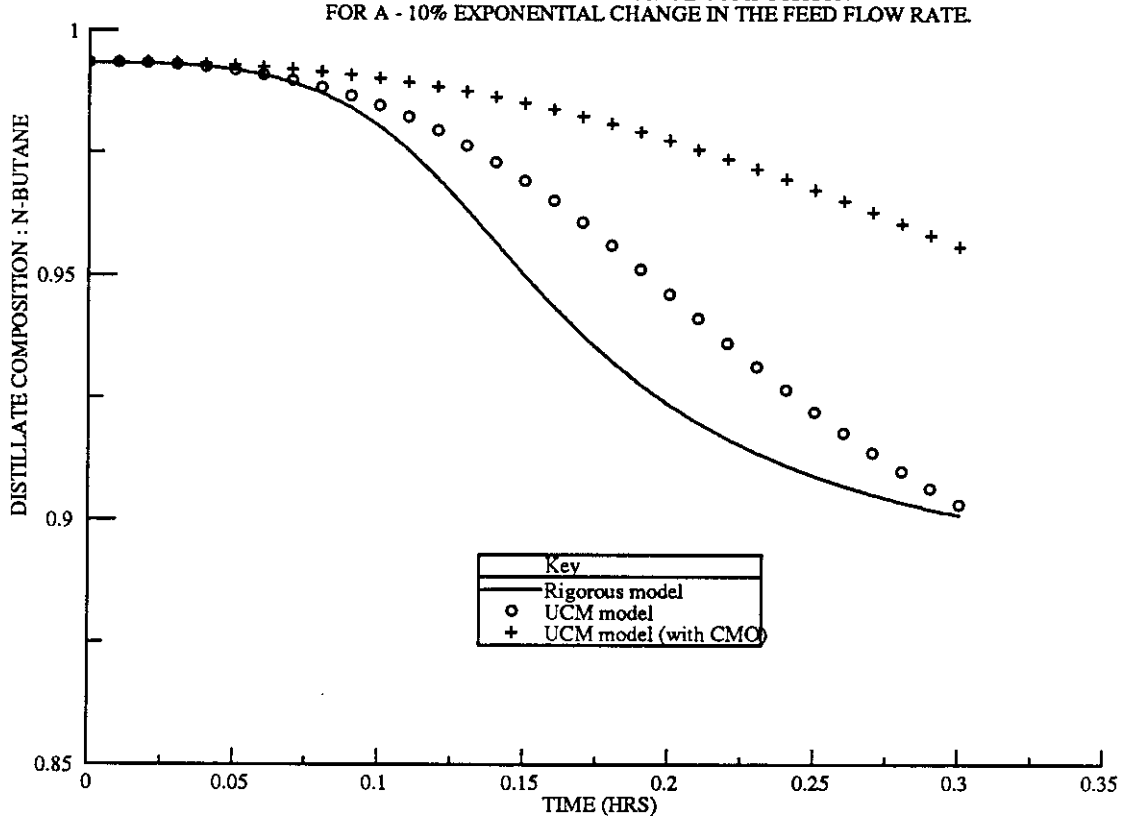

Figure 2. 6. 12
CASE STUDY ON THE SEPARATION OF A 3 COMPONENT MIXTURE.
RESPONSE OF DISTILLATE COMPOSITION
FOR A - 10% EXPONENTIAL CHANGE IN THE FEED FLOW RATE.

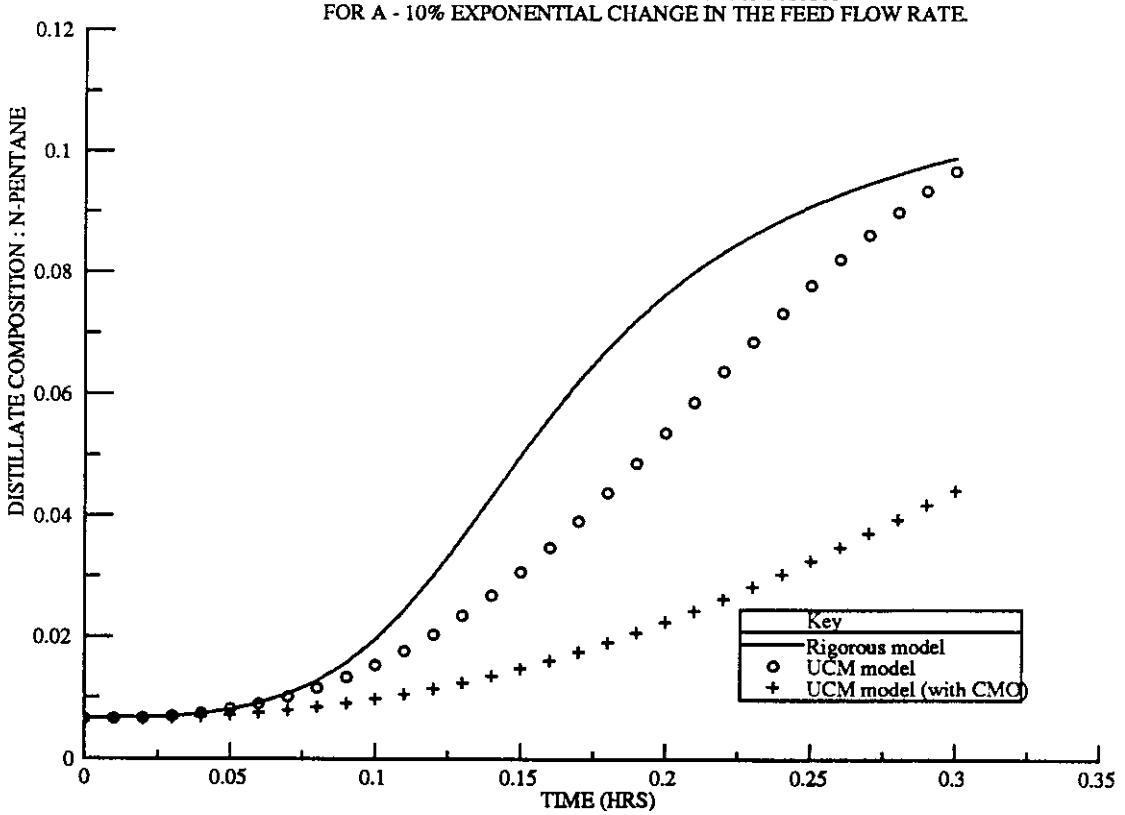

Figure 2. 6. 13
CASE STUDY ON THE SEPARATION OF A 3 COMPONENT MIXTURE.
RESPONSE OF BOTTOMS FLOW COMPOSITION
FOR A - 10% EXPONENTIAL CHANGE IN THE FEED FLOW RATE.

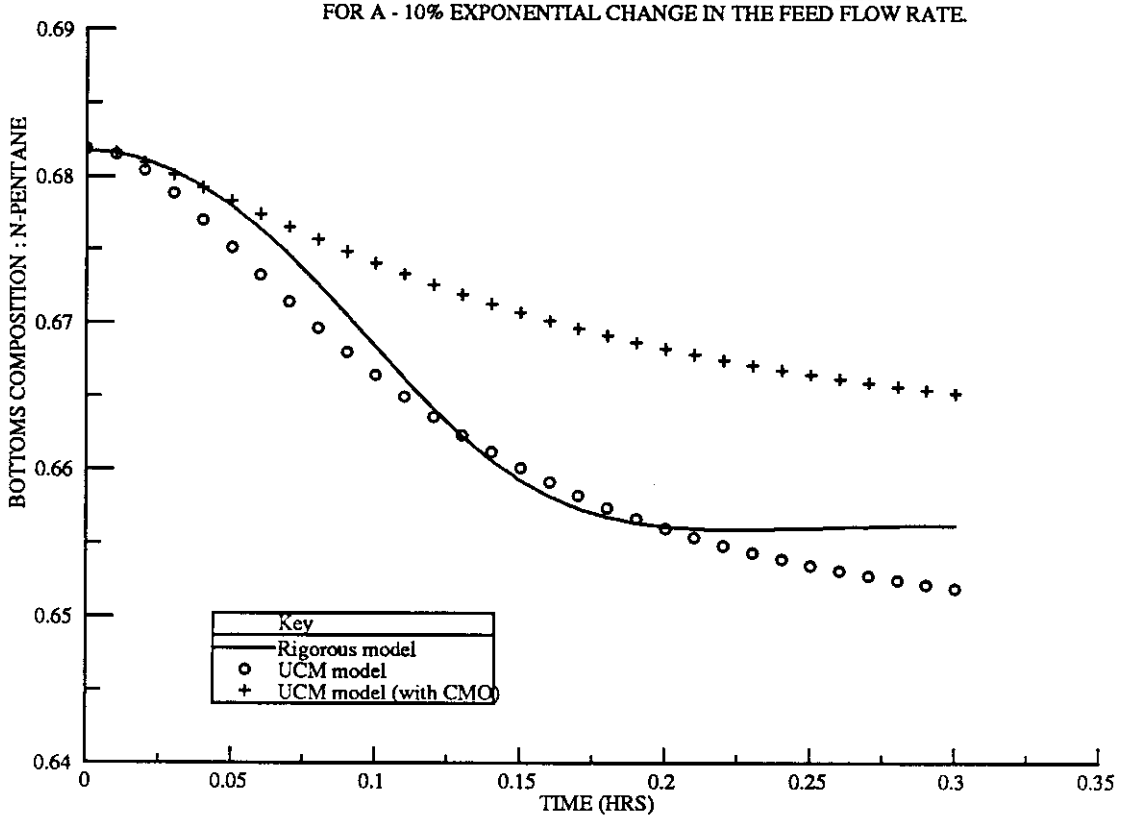

Figure 2. 6. 14
CASE STUDY ON THE SEPARATION OF A 3 COMPONENT MIXTURE.
RESPONSE OF BOTTOMS FLOW COMPOSITION
FOR A - 10% EXPONENTIAL CHANGE IN THE FEED FLOW RATE.

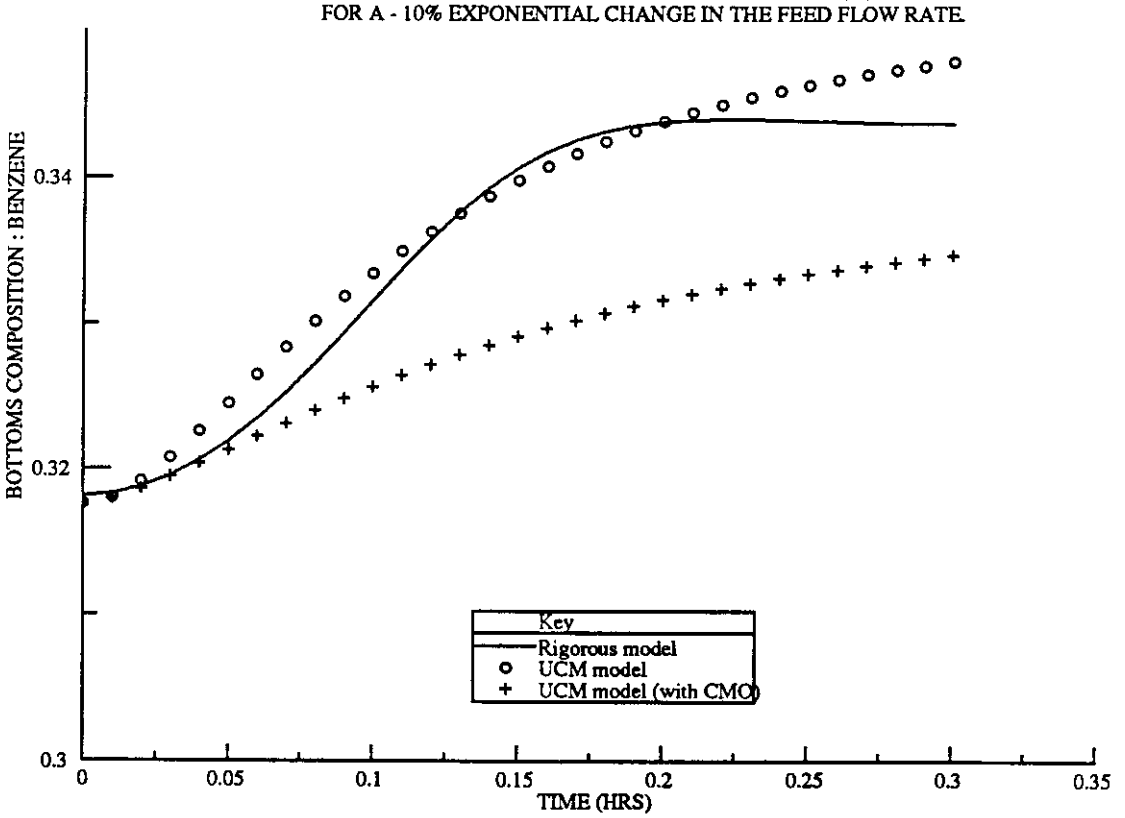

the dynamics of distillation columns but with significantly less computational power than required for a full tray-by-tray dynamic model.

2.7 SUMMARY

In summary then, a new approach to modelling staged distillation columns, called the universal compartmental model has been developed. It has been shown using a range of examples that good steady-state and dynamic behaviour, as well as an absence of any spurious inverse response can be achieved through use of this new modelling approach. The key issue highlighted in this chapter is that, modelling of distillation columns using the UCM approach within the SPEEDUP simulation package provides a consistent framework that allows us to use the same column model for steady-state simulations, optimisation studies, dynamic simulations and for control system synthesis , as will be shown in the following chapters.

CHAPTER 3

GAS-TAIL MODEL DEVELOPMENT AND OPTIMISATION

3.1. MODEL DEVELOPMENT AND VALIDATION

The UCM reduced-order dynamic distillation model introduced in the previous chapter was used to model each column in the gas-tail section of the Crude Distillation Unit. For the model developed to be useful for the proposed optimisation and control synthesis studies, it was important that it accurately matched the behaviour of the gas-tail. Steady-state plant trials were performed to verify the simulation results of the gas-tail model over a wide range of typical process conditions. Steady-state simulations based on rigorous steady-state models , available within the Shell Model Building Package (SMBP) , were also performed at all these sets of trial conditions to further check the validity of the UCM gas-tail model.

3.1.1. GAS - TAIL MODEL DEVELOPMENT

Large and uneven fluctuations in both the feed rate and composition are the major disturbances influencing smooth operation of the gas-tail (see Figures 3. 1. 1. and 3. 1. 2). To meet the product quality and operational requirements in the face of these disturbances, process conditions for each of the gas-tail columns have to be changed. Any mathematical model used for the gas-tail simulation should be flexible enough to accommodate all these changes over the complete range of operating conditions. However, to get reasonable accuracy, such a model would require a rigorous mathematical basis together with a good physical properties package interfaced to it. Such an approach would be computationally very demanding. Reduced-order models on the other hand need less computational effort, but provide acceptable accuracy only over a limited range of operating conditions. An approach based on the previously described UCM column model will be used here, such that for any given range of operating conditions the gas-tail simulation can be performed with both the required accuracy and acceptable computational speed. Physical property data required for the compartmental column models were estimated using the SMBP (the Shell Model Building Package) steady-state simulation results for the gas-tail, as will be described later in this chapter.

The major variation in the feed composition to the gas-tail is with respect to the "pentanes" content. The pentanes in this context include i-pentane, n-pentane, other pentane related compounds and any higher order hydrocarbons. The first two compounds,

Figure 3. 1. 1
FEED DISTURBANCES TO THE GAS-TAIL
OVER A PERIOD OF TWO AND A HALF MONTHS

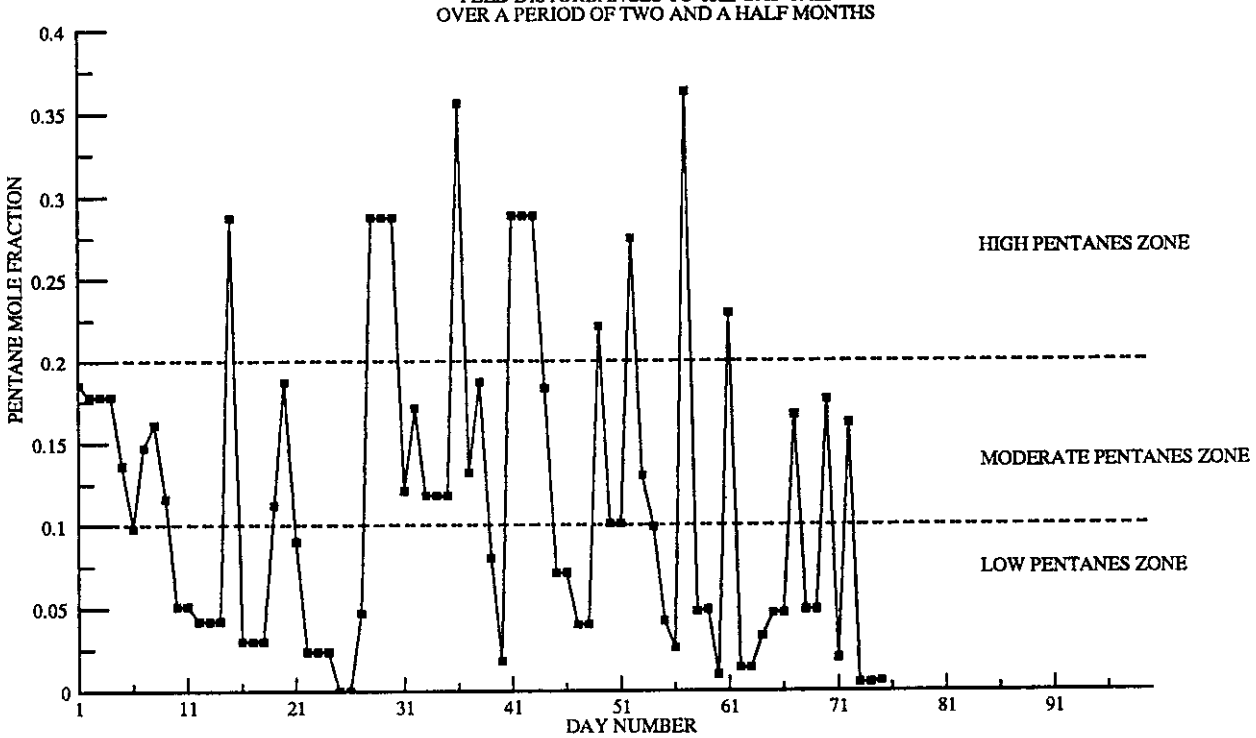

Figure 3. 1. 2
FEED DISTURBANCES TO THE GAS-TAIL
OVER A PERIOD OF TWO AND A HALF MONTHS

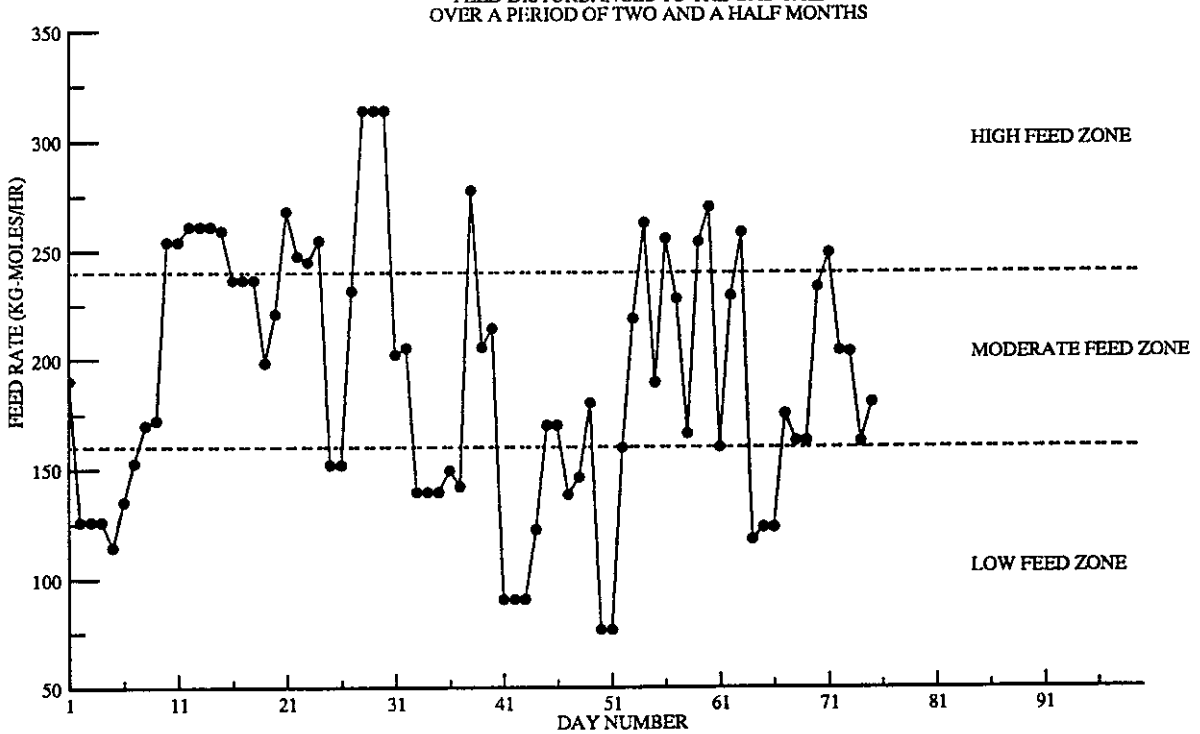

however, constitute the major percentage of the "pentanes". The gas-tail had originally been designed to handle a pentanes composition in the range 5 - 15% of the feed. However, a range of 0 - 35 % pentanes in the feed has been commonly observed in the recent times (see Figure 3. 1. 1). The other major variation is associated with the feed rate to the gas-tail (see Figure 3. 1. 2). The approach taken in this work involved developing a model for the gas-tail that is valid for a certain range of operating conditions (see (a) to (i) below). The different forms of the gas-tail model thus developed differed only in certain physical properties (such as latent heats of vaporisation/ condensation , bubble/dew point non-ideality correction factors, etc.,.). Based on Figures 3. 1. 1. and 3. 1. 2, the operating conditions for the gas-tail at any time can be assigned to one of the following categories :

(a) High feed rate (250 - 350 tons/ day) with high pentanes (20 - 35 %).
(b) High feed rate (250 - 350 tons/ day) with moderate pentanes (10 - 20 %).
(c) High feed rate (250 - 350 tons/ day) with low pentanes (< 10%).
(d) Moderate feed rate (170 - 250 tons/ day) with high pentanes (20 - 35 %).
(e) Moderate feed rate (170 - 250 tons/ day) with moderate pentanes (10 - 20 %).
(f) Moderate feed rate (170 - 250 tons/ day) with low pentanes (< 10%).
(g) Low feed rate (< 170 tons/ day) with high pentanes (20 - 35 %).
(h) Low feed rate (< 170 tons/ day) with moderate pentanes (10 - 20 %).
(i) Low feed rate (< 170 tons/ day) with low pentanes (< 10%).

Of all the above possible cases, the most commonly observed conditions from the plant data available were (a) , (f) and (h). Test runs were, thus, performed at each of these three cases (as will be discussed in the next section). The gas-tail model developed, using the UCM approach was validated against the test run data in each of the three case.

As discussed in Section 2.3, information on the relative volatilities of the components in the separation mixture is the primary requirement for the development of a distillation column model based on the UCM approach. The required data on the component relative volatilities along a column can be obtained from the simulation results of a rigorous steady-state distillation column model (see Section 2.5). To get acceptable performance both from a steady-state and a dynamic point of view, it is necessary to incorporate several modifications into the basic UCM model (see Section 2. 5). Results from the rigorous steady-state simulations are all that is needed to estimate all the necessary physical properties and the required modifications. To develop a steady-state model for the complete gas-tail based on the basic UCM approach, the following modifications were necessary.

FEED TO GAS-TAIL COLUMNS

The gas-tail consists of three distillation columns connected in series. These columns were each modelled using the UCM approach. All column models used have compartments containing (at most) five separation trays. The tray efficiencies estimated from the rigorous simulation data for all the columns were never more than 90 %, and hence the gas-tail distillation column models each had fewer trays than a real column (see Table 2. 5. 2). Due to the large pressure difference (10 - 12 bar) in the operating pressure between the de-ethaniser and the de-propaniser, the liquid feed to the latter undergoes flashing and the resultant vapour-liquid equilibrium mixture enters at the 13^{th} tray of the de-propaniser. Flashing of the liquid feed to the de-propaniser was incorporated into the gas-tail model through the inclusion of a separate flash model. In the gas-tail model thus developed, the bottoms from the de-ethaniser's reboiler first enters a flash tank and the resulting vapour-liquid equilibrium phases then enter the de-propaniser as separate feeds as shown in Figure 3. 1. 3. A similar arrangement was also used for the feed to the de-isobutaniser. The complete model of the gas-tail , therefore , contains three distillation columns in series, each modelled using the UCM approach and separated by a flash unit (see Figure 3. 1. 3).

REBOILER AND CONDENSER DESIGN DATA

Model development for the condensers and reboilers in the gas-tail was based on the model description in Appendices A4 and A5, respectively. All the condensers are modelled as cross-flow heat exchangers and all the reboilers as counter-current heat-exchangers. Calculations are based on an average mean temperature as the driving force with appropriate overall heat transfer coefficients and cross-flow correction factors for the condenser models (see Tables 3. 1. 1 and 3. 1. 2). The overall heat transfer coefficient for a heat exchanger , changes with the flowrates of the process and heating/cooling media. This effect has been incorporated into the condenser and reboiler models of the gas-tail using the following correlation.

$$UA = k\,(\text{Flowrate})^{b} \qquad (3.1.1)$$

where UA is the overall effective heat transfer coefficient , and
k , b are the correlation constants.

It should be noted that UA here represents the product of both the overall heat transfer coefficient and area available for heat exchange.

Figure 3. 1. 3

MODIFIED FLOWSHEET FOR THE GAS-TAIL
BASED ON THE UCM APPROACH

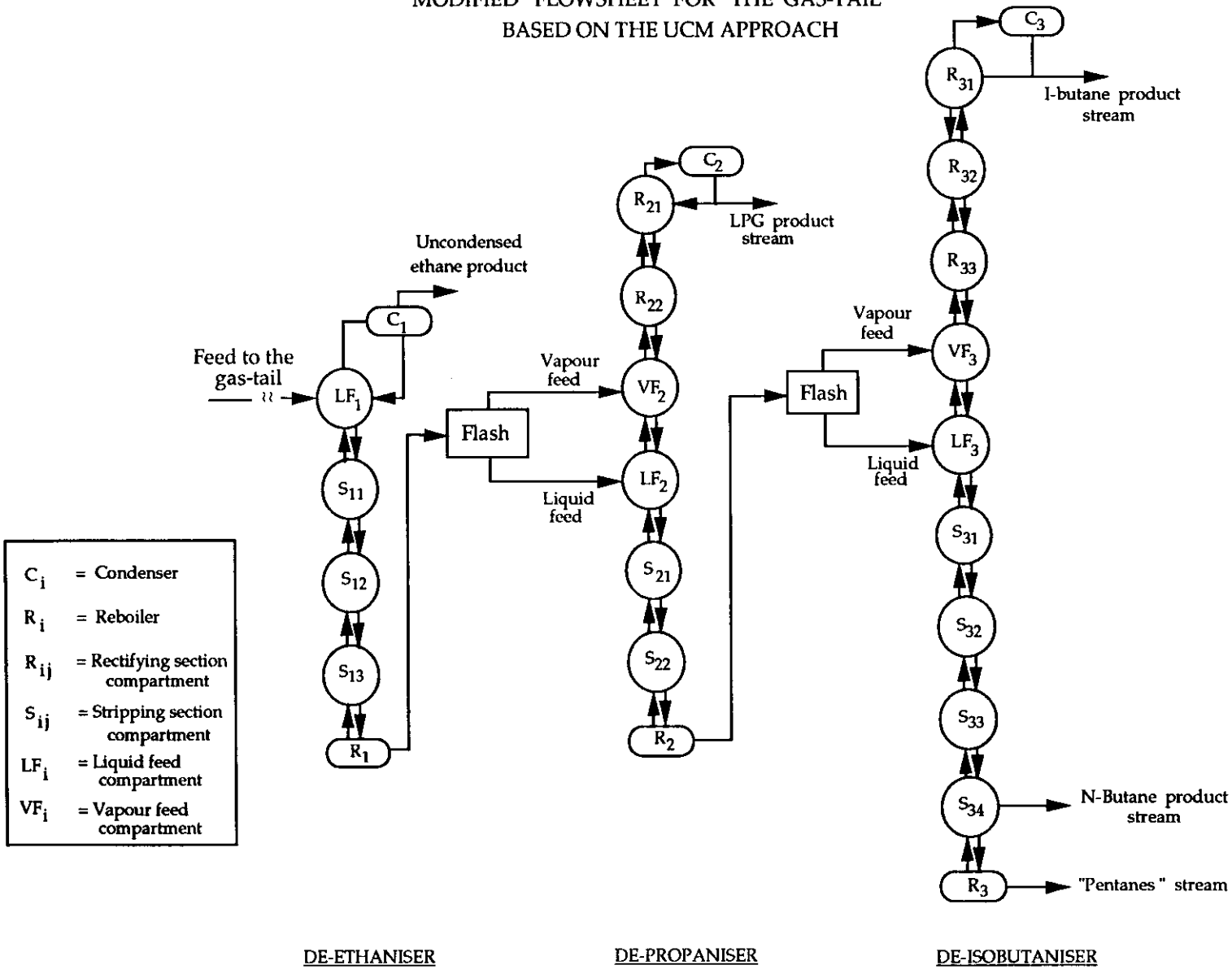

Table 3. 1. 1
Constant (k) relating the overall heat transfer coefficient
to the flowrate in the the gas-tail heat exchangers.

Unit	Constant (k)		
	High feed, high pentanes case (Case 1)	Moderate feed, low pentanes case (Case 2)	Low feed, moderate pentanes case (Case 3)
De-ethaniser overhead condenser	4.012	6.815	4.099
De-ethaniser reboiler	4.822	2.594	1.852
De-propaniser overhead condenser	8.025	6.378	6.012
De-propaniser reboiler	1.427	1.712	1.416
De-isobutaniser overhead condenser	5.715	4.281	6.117
De-isobutaniser reboiler	3.306	1.035	1.196

Table 3. 1. 2
Cross-flow factors used for log-mean temperature difference (LMTD)
correction in the gas-tail overhead condensers

Overhead condenser	Cross-flow correction factor
De-ethaniser	0.75
De-propaniser	0.55
De-isobutaniser	0.95

In the case of air-cooled fin-fan condensers, the air-side controls the overall heat transfer coefficient and hence the air flowrate is used in the above correlation. However, for thermosyphon reboilers, the process side (which is a vapour-liquid mixture at equilibrium) seems to exert the most influence on the overall heat transfer coefficient, and hence in this case the flowrate of the process fluid is used in Equation 3. 1. 1. The validity of Equation (3. 1. 1) has been tested for a range of process conditions using the rigorous heat-exchanger models in SMBP (see Section 3. 1. 3 for further details on SMBP) for each of the condensers and reboilers in the gas-tail . The constants (k and b) best satisfying Equation (3. 1. 1) were estimated for each of the gas-tail condensers and reboilers based on a rigorous SMBP steady-state model data. Figures 3. 1. 19 - 3. 1. 24 show the correlations obtained for the high feed rate , high pentanes case. The constants best fitting the data for all the other test-run cases were estimated using a similar procedure and are given in Table 3. 1. 1 . Constant values for the constant (b) have been used (i.e. **0. 6** for all the reboilers and **0. 2** for all the air-cooled condensers, respectively), in all the case-studies. A large change in the air flowrate, therefore, is required to cause a significant change in the corresponding effective heat transfer coefficient. This may be one of the reasons for the poor performance of the gas-tail's condensers. The constant (k), on the other hand, was found to vary significantly with the operating conditions of the heat exchanger. Hence, a constant value for (k), obtained specifically for each heat exchanger, has been used (see Table 3. 1. 1) in all the case-studies.

Other physical property data required for the design of the fin-fan condensers and thermosyphon reboilers in the gas-tail (such as the latent heats of vaporisation / condensation of mixtures and bubble/dew point non-ideality correction coefficients), were also obtained from the SMBP steady-state simulation results (see Tables 3. 1. 3 - 3. 1. 8 and Appendices A4 - A7 for the estimation procedures). The latent heat of vaporisation/ condensation of a mixture usually varies with the pressure and the operating conditions in a condenser/reboiler . It is often very difficult to provide a correlation for the latent heat, accounting for all such variations. A simulation method suggested in Appendices A4 and A5 offers an alternative and relatively simple means of estimating the latent heats of vaporisation/condensation in the gas-tail's condensers / reboilers. The data thus obtained were found to differ quite considerably between the high , moderate and low pentanes feed cases.

RELATIVE VOLATILITY

Changes in the pentanes content were found to have little or no effect on the relative volatilities of the various components of the separation mixture. However, the relative volatilities were found to vary with both the column pressure and tray temperature.

Table 3. 1. 3
Physical properties used
in the overhead condenser model for the de-ethaniser

Physical property	High pentanes feed	Moderate pentanes feed	Low pentanes feed
Latent heat of condensation (λ, Tcal / Kg-mole)	3.46	2.61	3.46
Bubble point correction factor (γ_{bub})	0.36	0.62	0.55
Dew point correction factor (γ_{dew})	0.31	0.33	0.38

Table 3. 1. 4
Physical properties used
in the reboiler model for the de-ethaniser

Physical property	High pentanes feed	Moderate pentanes feed	Low pentanes feed
Latent heat of vaporisation (λ, Tcal / Kg-mole)	4.37	3.59	3.43
Bubble point correction factor (γ_{bub})	0.54	0.51	0.61
Dew point correction factor (γ_{dew})	0.81	0.62	0.64

Table 3. 1. 5
Physical properties used
in the overhead condenser model for the de-propaniser

Physical property	High pentanes feed	Moderate pentanes feed	Low pentanes feed
Latent heat of condensation (λ, Tcal / Kg-mole)	3.16	2.13	3.12
Bubble point correction factor (γ_{bub})	0.49	0.49	0.49
Dew point correction factor (γ_{dew})	0.52	0.52	0.52

Table 3. 1. 6
Physical properties used
in the reboiler model for the de-propaniser

Physical property	High pentanes feed	Moderate pentanes feed	Low pentanes feed
Latent heat of condensation (λ, Tcal / Kg-mole)	3.33	2.76	3.31
Bubble point correction factor (γ_{bub})	0.78	0.72	0.71
Dew point correction factor (γ_{dew})	0.98	0.8	0.91

Table 3. 1. 7
Physical properties used
in the overhead condenser model for the de-isobutaniser

Physical property	High pentanes feed	Moderate pentanes feed	Low pentanes feed
Latent heat of condensation (λ, Tcal / Kg-mole)	3.41	3.94	2.89
Bubble point correction factor (γ_{bub})	0.76	0.75	0.76
Dew point correction factor (γ_{dew})	0.79	0.79	0.79

Table 3. 1. 8
Physical properties used
in the reboiler model for the de-isobutaniser

Physical property	High pentanes feed	Moderate pentanes feed	Low pentanes feed
Latent heat of vaporisation (λ, Tcal / Kg-mole)	4.14	4.04	4.11
Bubble point correction factor (γ_{bub})	1.25	0.98	0.83
Dew point correction factor (γ_{dew})	1.21	1.05	0.97

Relative volatilities were estimated for each of the equilibrium trays up to a pressure range up to ± 2 bars about the design pressure (see Figures 3. 1. 4 - 3. 1. 18). SMBP steady-state simulation results gave vapour-liquid equilibrium constants (K) for each of the components and were used to estimate the relative volatilities. Tray compositions seemed to have a greater effect than the column operating pressure on the component relative volatilities . Thus, constant relative volatilities for each of the components within a compartment in the UCM approach (i.e. arithmetic average values over all the trays contained in the compartment) were used in further analyses.

TRAY HOLDUPS

Tray holdups were estimated for each of the gas-tail columns using Shell tray design data and design procedures (see Figures 3. 1. 25 - 3. 1. 27 for the results calculated at the high pentane feed test run conditions). A sharp change in the liquid holdup of the de-ethaniser on tray 10 is due to the reflux rate entering the column at this tray (see Figures 3. 1. 25). In the de-isobutaniser, however, the sharp change in the liquid holdup on tray 6 is due to the recovery of the n-butane as a side-stream product (see Figure 3. 1. 27). Constant values for all tray holdups were used in the various compartments of the gas-tail model (see Table 3. 1. 9). However, the estimated holdups in the reflux drums and reboilers were quite significant (i.e. an order of magnitude larger) relative to the individual tray holdups and were known to change quite markedly with the process operating conditions . Thus, the reboiler and condenser sections of the gas-tail model were designed to account for these holdup changes.

COLUMN INTERNAL FLOW CORRECTION FACTORS

A UCM model based on the CMO assumption has flat liquid and vapour profiles throughout the column. As discussed in Section 2.5 (see Table 2. 5. 2) , such an assumption was quite adequate for all the columns in the gas-tail. No correction factors for internal flow changes , therefore, were used in this case-study. This may be due to the fact that, the latent heats for light hydrocarbons are all about the same in the desired operational range.

TEMPERATURE AND PRESSURE PROFILES ALONG THE COLUMN

The pressures in the condensers of the gas-tail model at test-run conditions were estimated using the physical property data (see Tables 3. 1. 3 , 3. 1. 5 and 3. 1. 7) and the method proposed in Appendix A4. A fixed pressure drop for each tray of a column (i.e. 0.01 bar ,

Figure 3. 1. 6
EFFECT OF PRESSURE ON COMPONENT RELATIVE VOLATILITIES.
PROPANE IN DE-ETHANISER OF THE GAS-TAIL
(WITH N-PENTANE AS THE KEY COMPONENT)

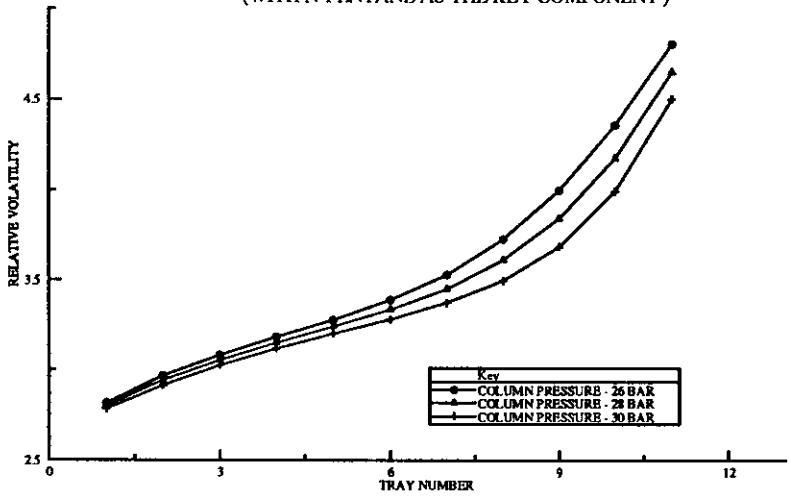

Figure 3. 1. 7
EFFECT OF PRESSURE ON COMPONENT RELATIVE VOLATILITIES.
I-BUTANE IN DE-ETHANISER OF THE GAS-TAIL
(WITH N-PENTANE AS THE KEY COMPONENT)

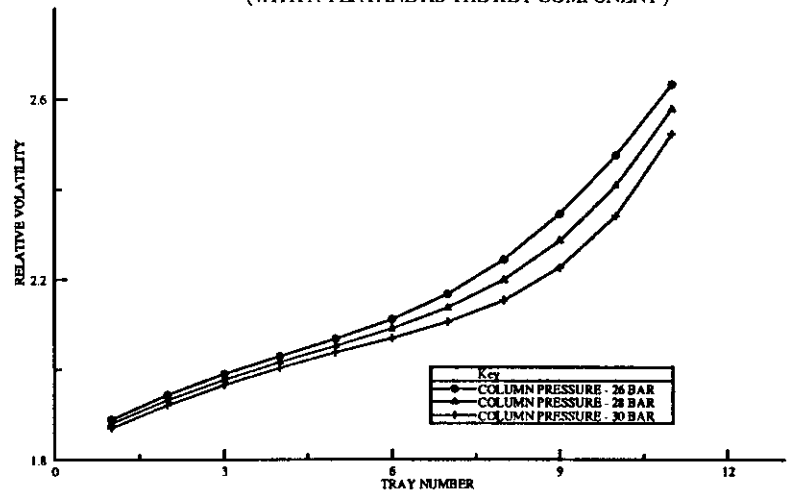

Figure 3. 1. 4
EFFECT OF PRESSURE ON COMPONENT RELATIVE VOLATILITIES.
METHANE IN DE-ETHANISER OF THE GAS-TAIL
(WITH N-PENTANE AS THE KEY COMPONENT)

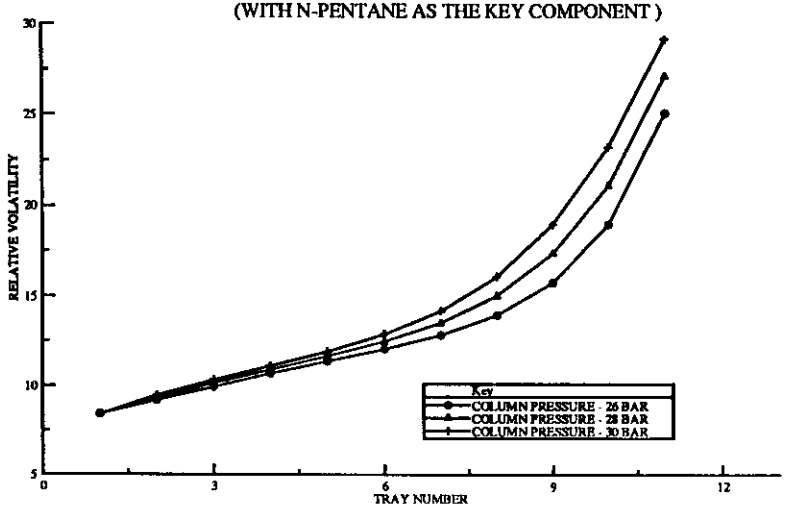

Figure 3. 1. 5
EFFECT OF PRESSURE ON COMPONENT RELATIVE VOLATILITIES
ETHANE IN DE-ETHANISER OF THE GAS-TAIL
(WITH N-PENTANE AS THE KEY COMPONENT)

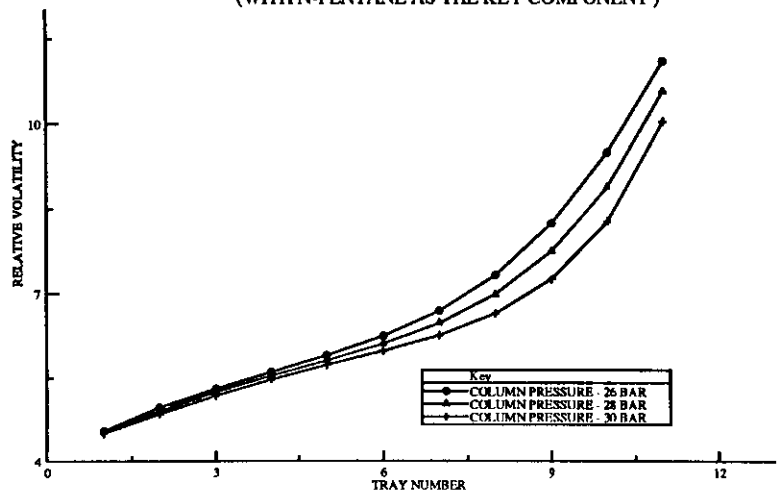

Figure 3. 1. 10
EFFECT OF PRESSURE ON COMPONENT RELATIVE VOLATILITIES.
ETHANE IN DE-PROPANISER OF THE GAS-TAIL
(WITH N-PENTANE AS THE KEY COMPONENT)

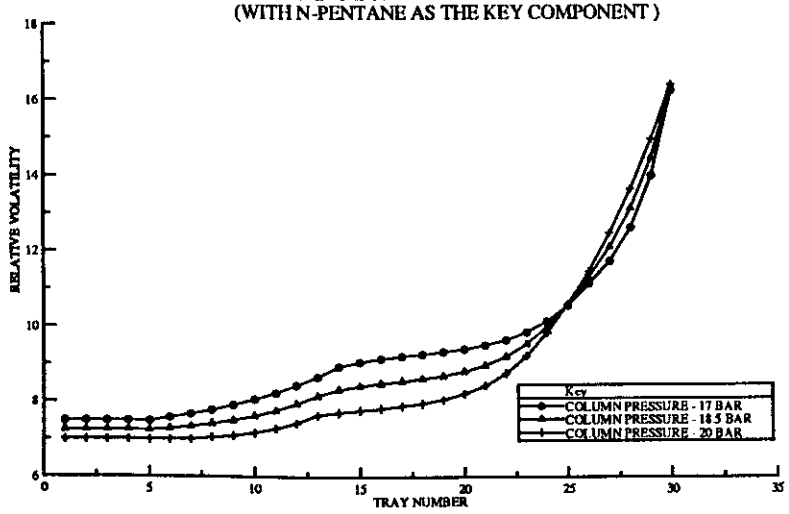

Figure 3. 1. 11
EFFECT OF PRESSURE ON COMPONENT RELATIVE VOLATILITIES.
PROPANE IN DE-PROPANISER OF THE GAS-TAIL
(WITH N-PENTANE AS THE KEY COMPONENT)

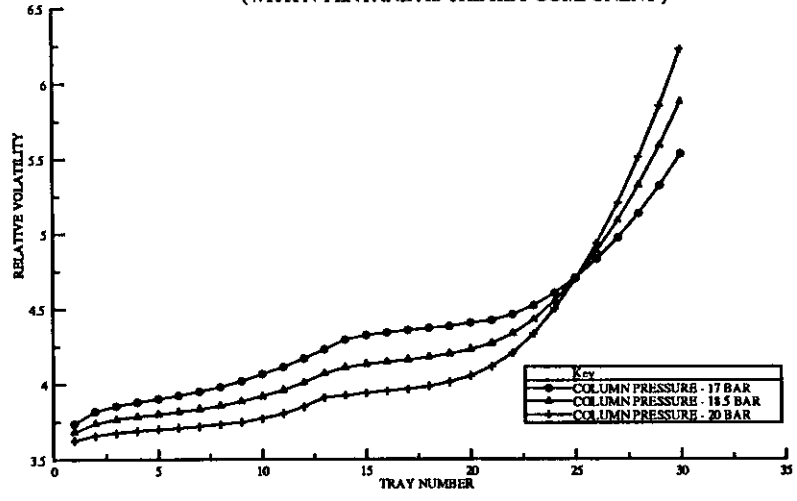

Figure 3. 1. 8
EFFECT OF PRESSURE ON COMPONENT RELATIVE VOLATILITIES.
N-BUTANE IN DE-ETHANISER OF THE GAS-TAIL
(WITH N-PENTANE AS THE KEY COMPONENT)

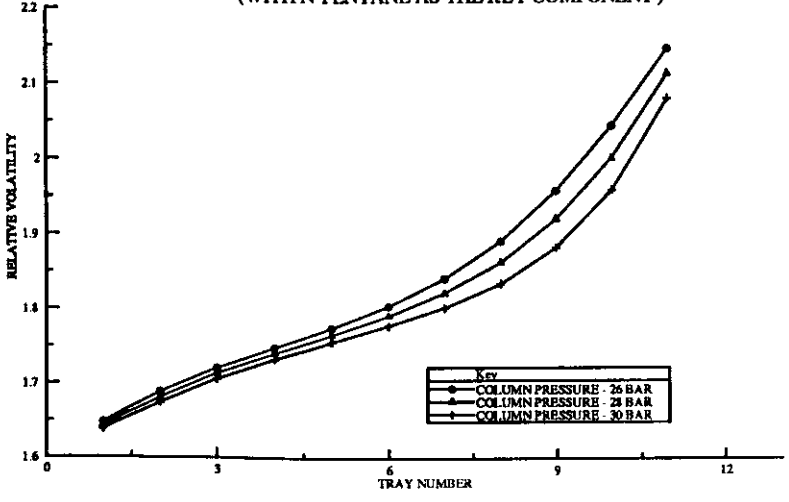

Figure 3. 1. 9
EFFECT OF PRESSURE ON COMPONENT RELATIVE VOLATILITIES.
I-PENTANE IN DE-ETHANISER OF THE GAS-TAIL
(WITH N-PENTANE AS THE KEY COMPONENT)

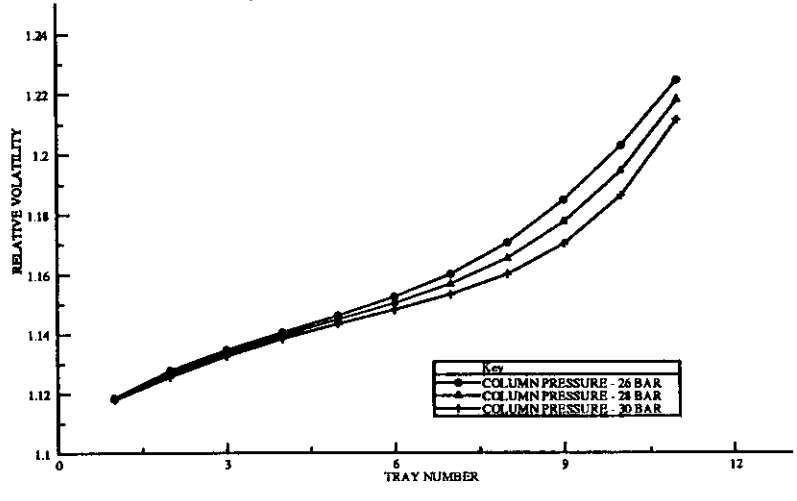

Figure 3. 1. 14
EFFECT OF PRESSURE ON COMPONENT RELATIVE VOLATILITIES
I-PENTANE IN DE-PROPANISER OF THE GAS-TAIL
(WITH N-PENTANE AS THE KEY COMPONENT)

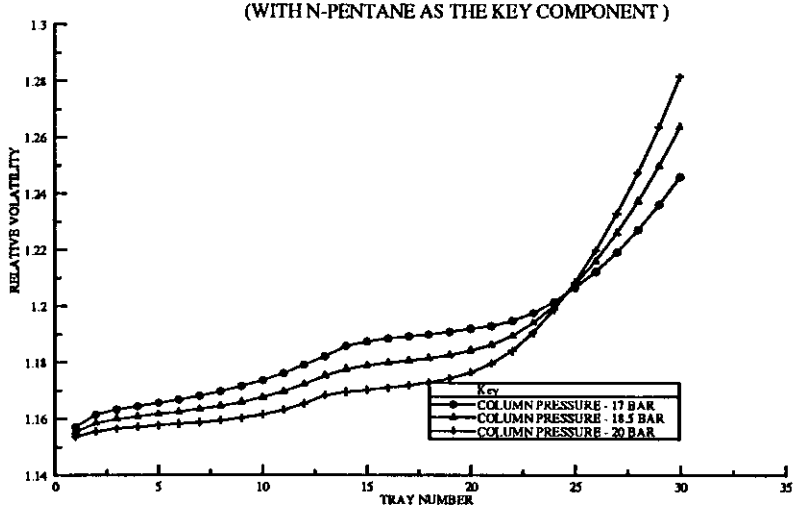

Figure 3. 1. 12
EFFECT OF PRESSURE ON COMPONENT RELATIVE VOLATILITIES
I-BUTANE IN DE-PROPANISER OF THE GAS-TAIL
(WITH N-PENTANE AS THE KEY COMPONENT)

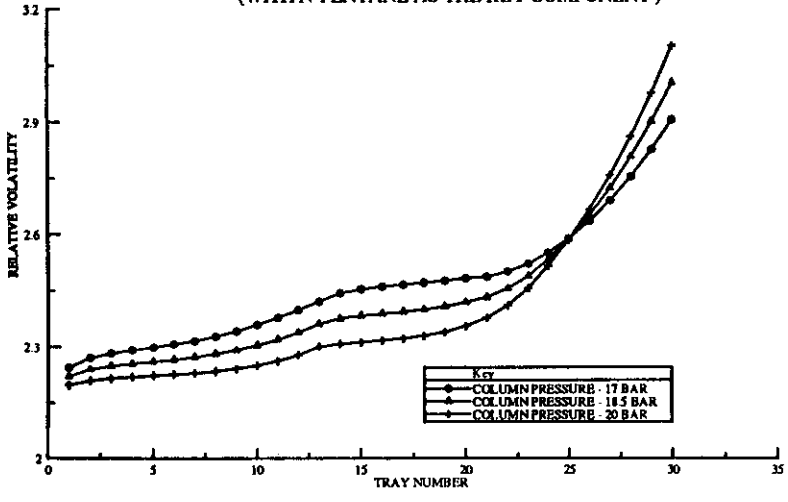

Figure 3. 1. 13
EFFECT OF PRESSURE ON COMPONENT RELATIVE VOLATILITIES
N-BUTANE IN DE-PROPANISER OF THE GAS-TAIL
(WITH N-PENTANE AS THE KEY COMPONENT)

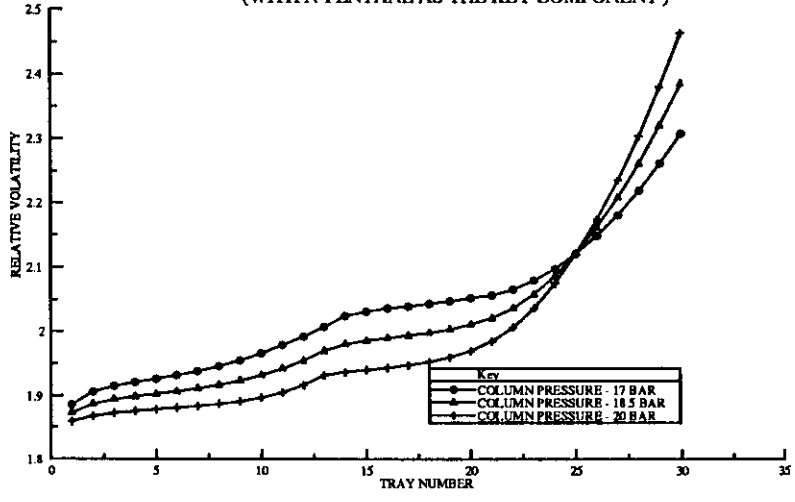

Figure 3. 1. 17
EFFECT OF PRESSURE ON COMPONENT RELATIVE VOLATILITIES.
N-BUTANE IN DE-ISOBUTANISER OF THE GAS-TAIL
(WITH N-PENTANE AS THE KEY COMPONENT)

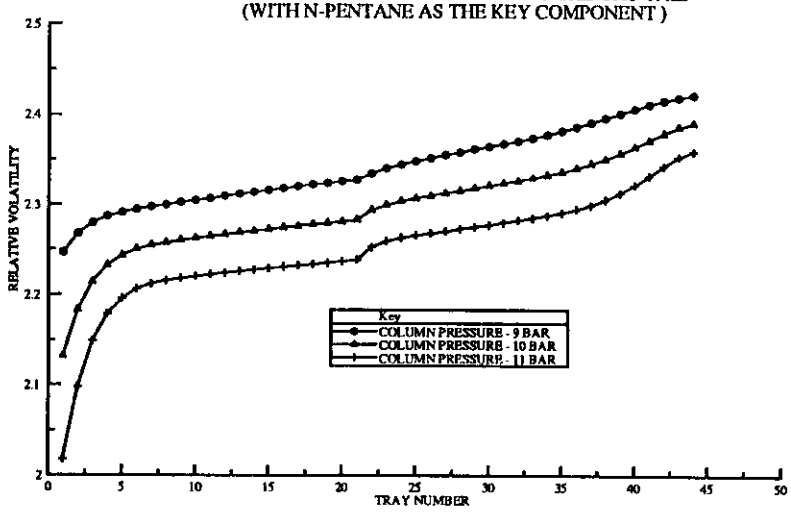

Figure 3. 1. 18
EFFECT OF PRESSURE ON COMPONENT RELATIVE VOLATILITIES.
I-PENTANE IN DE-ISOBUTANISER OF THE GAS-TAIL
(WITH N-PENTANE AS THE KEY COMPONENT)

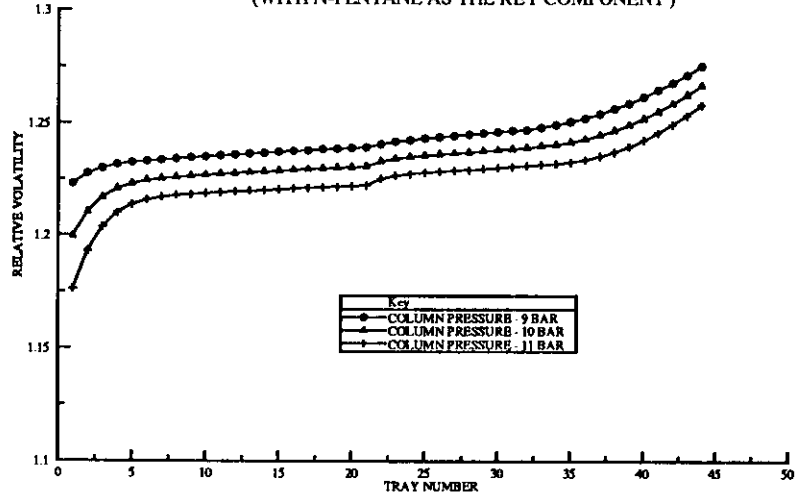

Figure 3. 1. 15
EFFECT OF PRESSURE ON COMPONENT RELATIVE VOLATILITIES.
PROPANE IN DE-ISOBUTANISER OF THE GAS-TAIL
(WITH N-PENTANE AS THE KEY COMPONENT)

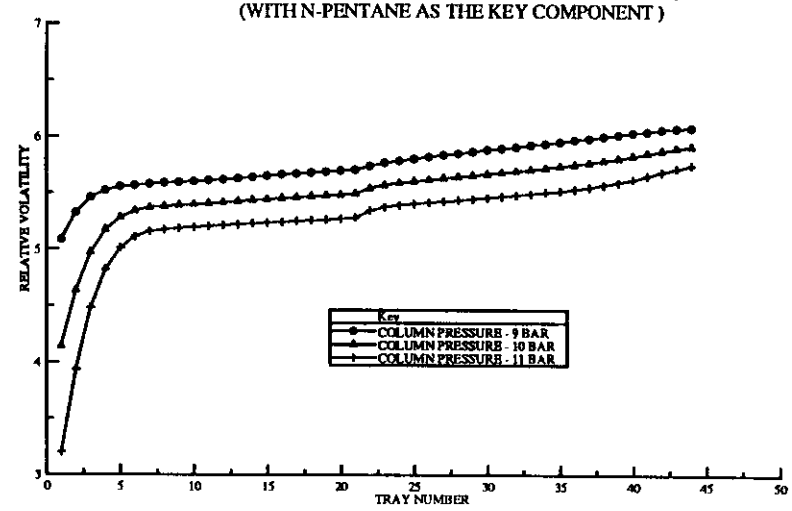

Figure 3. 1. 16
EFFECT OF PRESSURE ON COMPONENT RELATIVE VOLATILITIES.
I-BUTANE IN DE-ISOBUTANISER OF THE GAS-TAIL
(WITH N-PENTANE AS THE KEY COMPONENT)

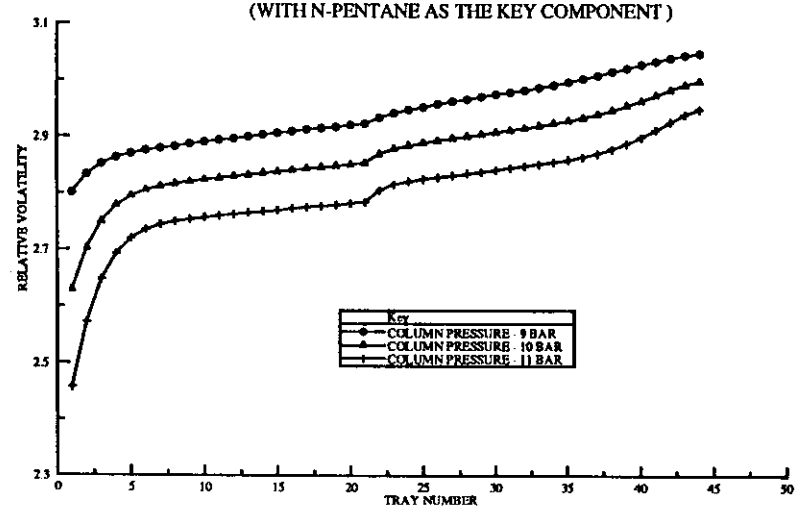

Table 3. 1. 9
Details of the compartment sections of the gas-tail model
at the high pentanes feed test-run conditions (i.e. Case 1)

Compartment	Number of trays in the compartment	Holdup in the compartment (Kg-moles)
DE-ETHANISER		
LF_1 - Liquid feed compartment	2	2.45
S_{11} - Compartment 1 of stripping section	4	4.88
S_{12} - Compartment 2 of stripping section	4	4.88
S_{13} - Compartment 3 of stripping section	2	2.45
C_1 - Overhead condenser	1	8
R_1 - Reboiler	1	5
DE-PROPANISER		
LF_2 - Liquid feed compartment	3	3.66
S_{21} - Compartment 1 of stripping section	2	2.44
S_{22} - Compartment 2 of stripping section	2	2.44
VF_2 - Vapour feed Compartment	3	3.42
R_{21} - Compartment 1 of Rectifying section	4	4.56
R_{22} - Compartment 2 of Rectifying section	4	4.56
C_2 - Overhead condenser	1	8.5
R_2 - Reboiler	1	5
DE-ISOBUTANISER		
LF_3 - Liquid feed compartment	5	9.7
S_{31} - Compartment 1 of stripping section	4	9.7
S_{32} - Compartment 2 of stripping section	4	9.7
S_{33} - Compartment 1 of stripping section	4	9.7
S_{34} - Compartment 2 of stripping section	4	9.7
VF_3 - Vapour feed Compartment	5	8.4
R_{31} - Compartment 1 of Rectifying section	5	8.4
R_{32} - Compartment 2 of Rectifying section	5	8.4
R_{33} - Compartment 3 of Rectifying section	5	8.4
C_3 -Overhead condenser	1	9.5
R_3 - Reboiler	1	5

Figure 3. 1. 19
Heat exchanger correlation for the air-cooled condenser of the de-ethaniser

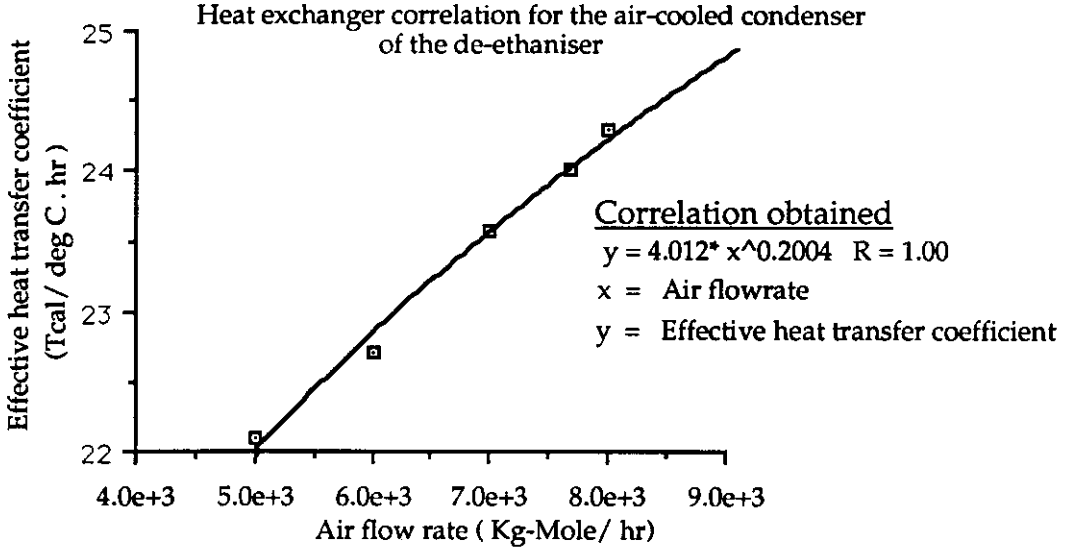

Figure 3. 1. 20
Heat exchanger correlation for the air-cooled condenser of the de-propaniser

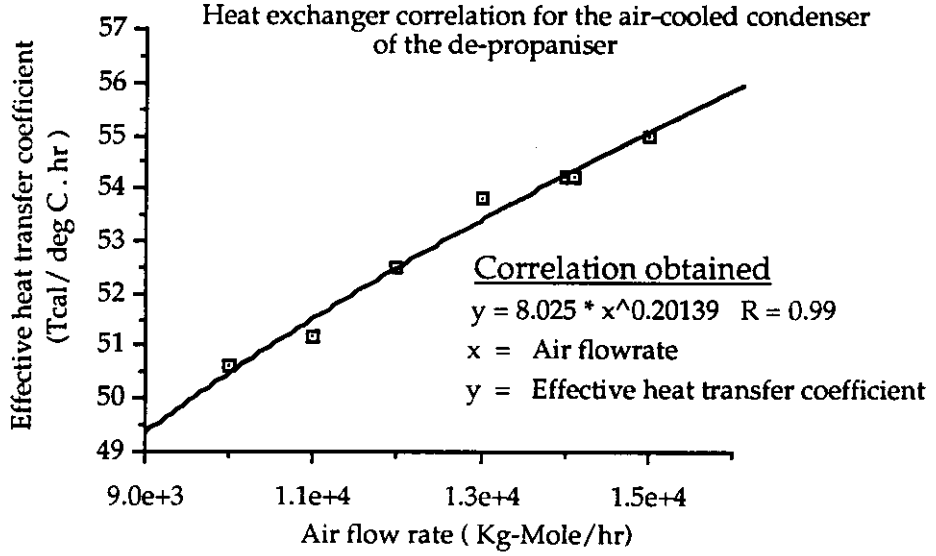

Figure 3. 1. 21
Heat exchanger correlation for the air-cooled condenser of the de-isobutaniser

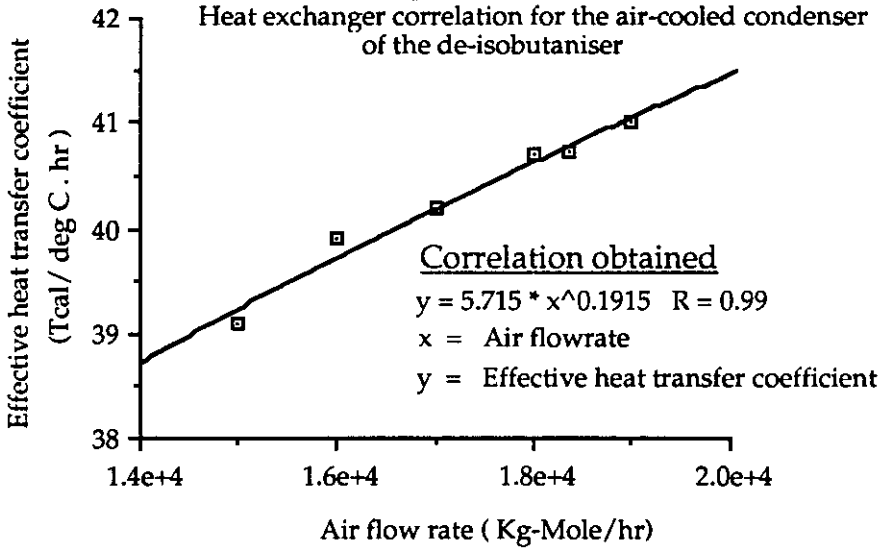

Figure 3. 1. 22
Heat exchanger correlation for the thermosyphon reboiler of the de-ethaniser

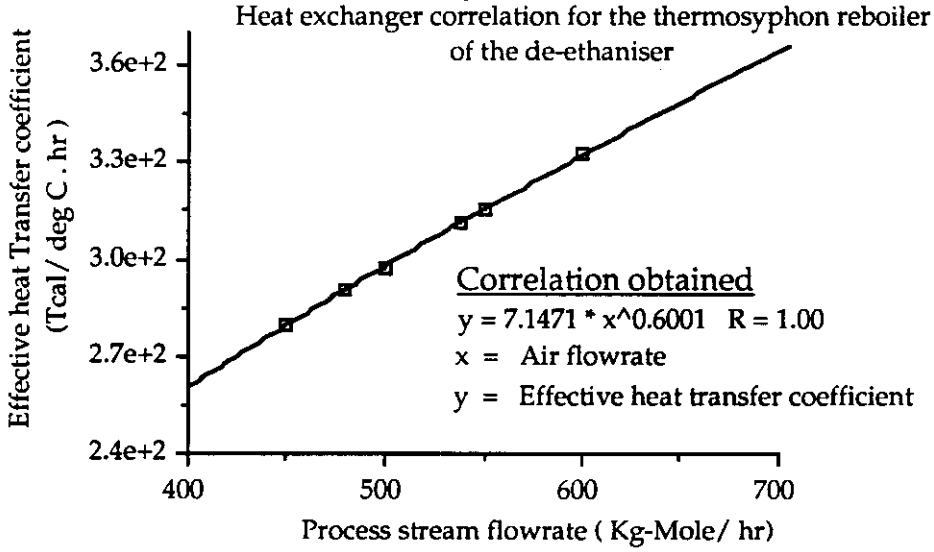

Figure 3. 1. 23
Heat exchanger correlation for the thermosyphon reboiler
of the de-propaniser

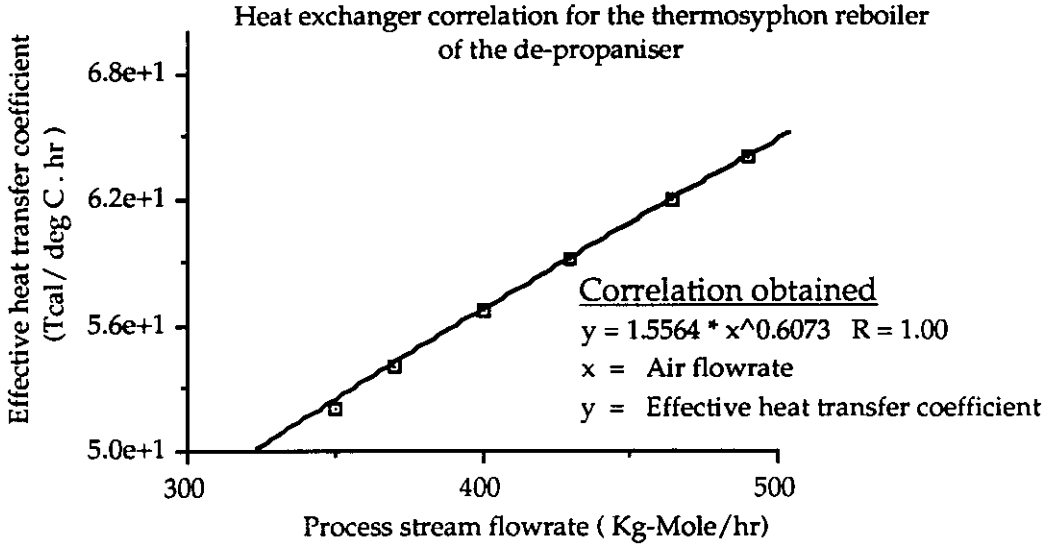

Figure 3. 1. 24
Heat exchanger correlation for the thermosyphon reboiler
of the de-isobutaniser

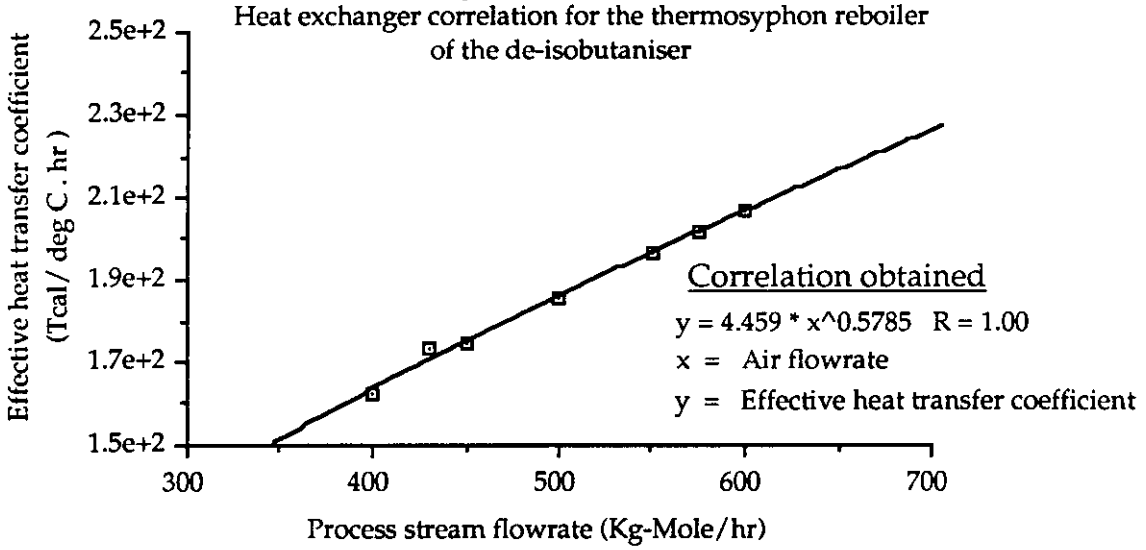

Figure 3. 1. 27
LIQUID HOLDUPS ON THE TRAYS IN THE DE-ISOBUTANISER
FOR HIGH PENTANES FEED TEST-RUN CONDITIONS

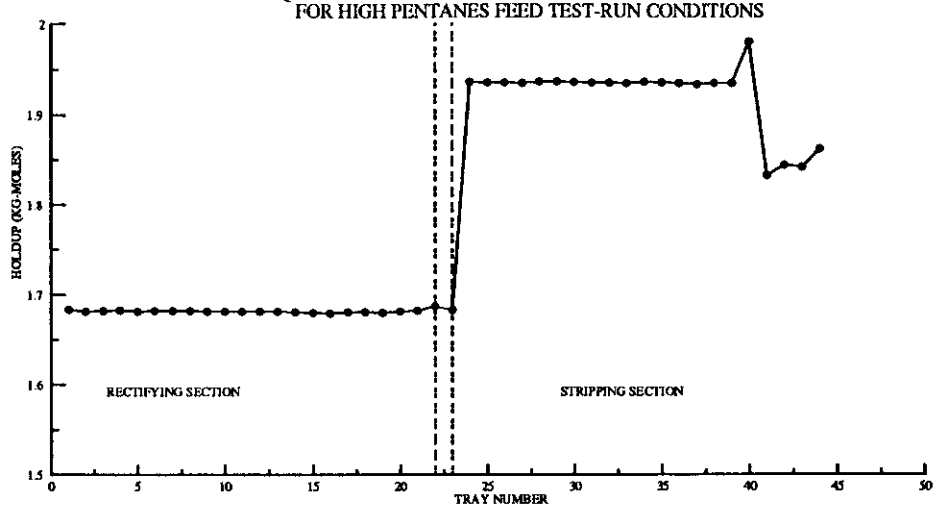

Figure 3. 1. 25
LIQUID HOLDUPS ON THE TRAYS IN THE DE-ETHANISER
FOR HIGH PENTANES FEED TEST-RUN CONDITIONS

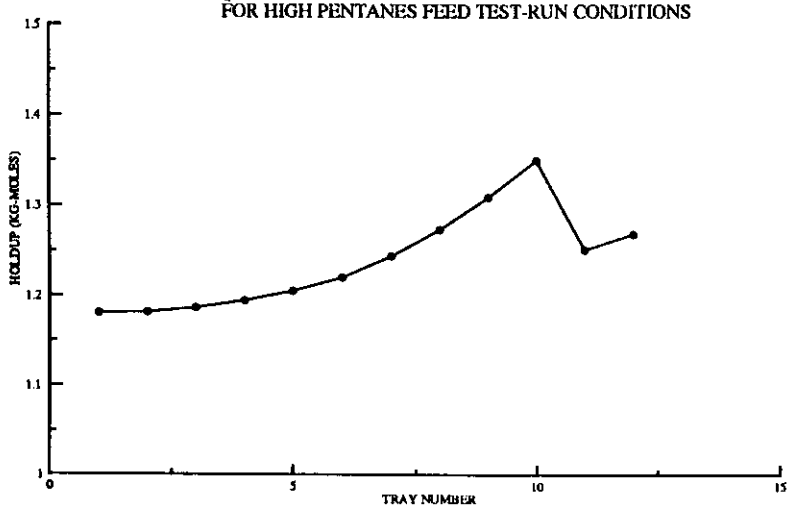

Figure 3. 1. 26
LIQUID HOLDUPS ON THE TRAYS IN THE DE-PROPANISER
FOR HIGH PENTANES FEED TEST-RUN CONDITIONS

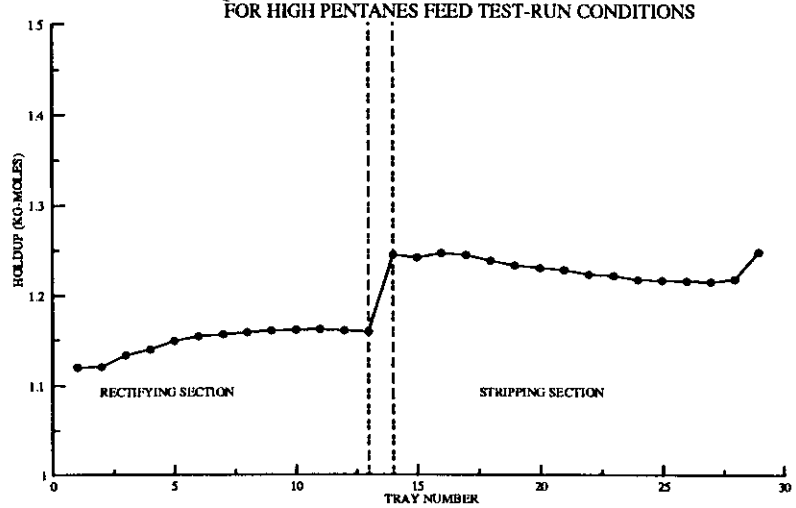

Figure 3. 1. 28
PRESSURE PROFILE ALONG THE DE-PROPANISER COLUMN
FOR HIGH PENTANES FEED TEST-RUN CONDITIONS

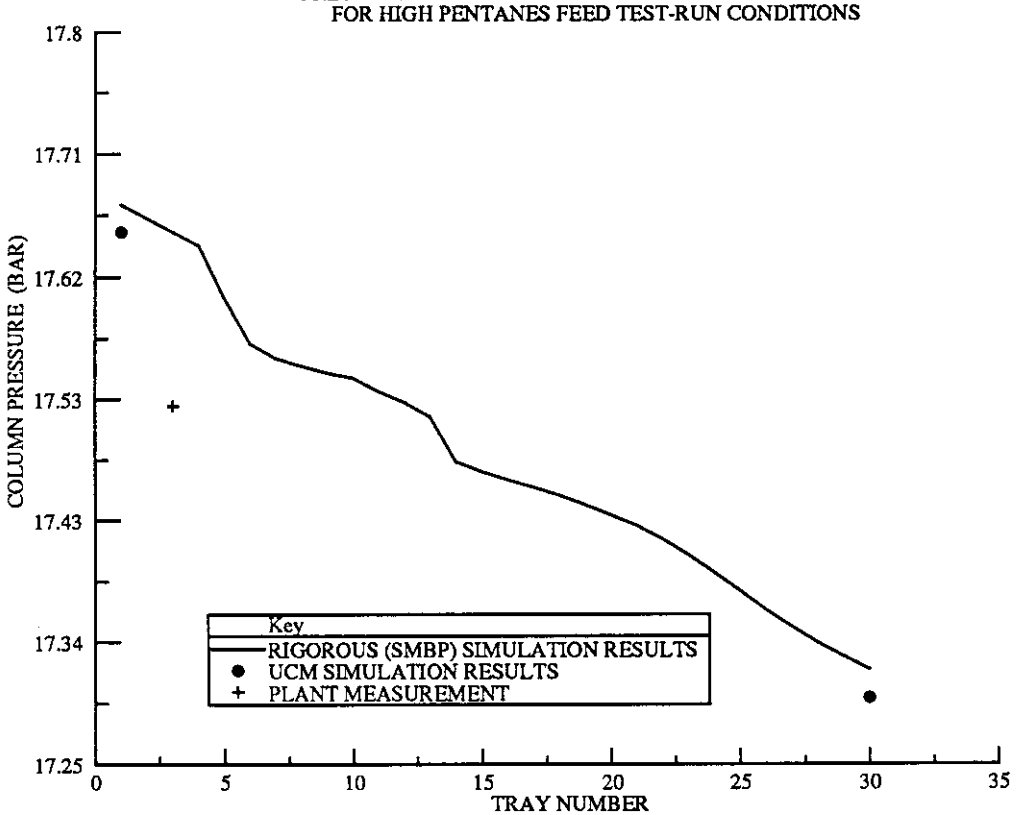

Figure 3. 1. 29
TEMPERATURE PROFILE ALONG THE DE-PROPANISER COLUMN
FOR HIGH PENTANES FEED TEST-RUN CONDITIONS

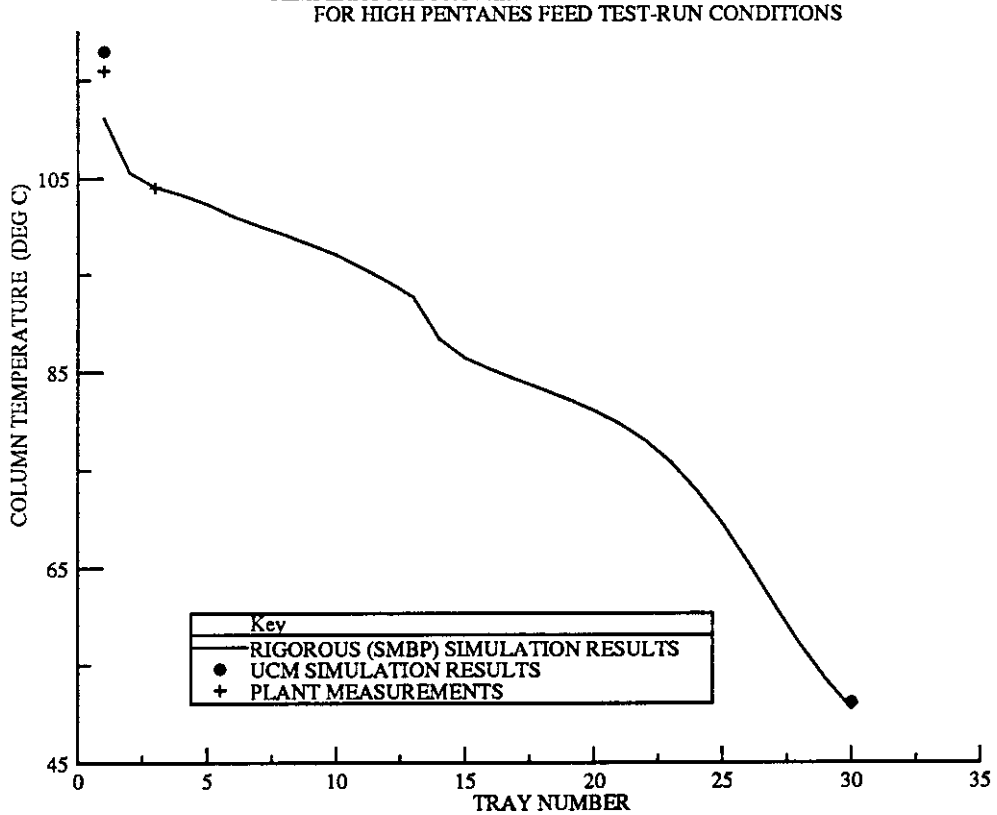

based on Shell experience), was used to estimate the pressure in the reboilers of the gas-tail columns (see Figure 3. 1. 28). The temperature on a tray in any column can be estimated using the method described in Section 2. 5. The "temperature" of a compartment in a distillation column model based on the UCM approach, however, represents an average temperature within the compartment and cannot physically be associated with any one of the trays in the column. Therefore, a meaningful temperature could only be estimated in condensers and reboilers of all the gas-tail columns (see Figure 3. 1. 29). In general , if the temperature and the pressure effects on the column separation are significant, care must be taken to incorporate all such effects in any column model used.

The gas-tail model thus obtained by incorporating all the modifications described above was fitted to various plant test run and rigorous SMBP simulation data (see Section 3. 1. 3 for details). A typical simulation time of 60 - 120 CPU seconds was needed to solve this gas-tail model using SPEEDUP on a Micro Vax II computer running under the VMS operating system.

3. 1. 2 GAS - TAIL PLANT TRIALS

Plant test runs are necessary in validating a simulation model. In reality, a continuous process operate never operates at absolutely steady conditions. "Steady-state" plant trials for a continuous process, therefore, involve performing test runs when the variation in the process conditions is at a minimum . For many industrial processes, the minimum variation in process operating conditions is taken to be about ± 2. 5 % around an average value.

Steady-state plant trials for the gas-tail were performed at the following set of feed conditions.

(i) Case 1: High feed rate (320 tons/day) with high pentanes (> 25 %).
(ii) Case 2: Moderate feed rate (240 tons/day) with low pentanes (< 5 %).
(iii) Case 3: Low feed rate (165 tons/day) with moderate pentanes (5 % - 15 %).

Plant trials on the gas-tail involved sample collection and analysis for all the distillate product streams (i.e the fuel-gas stream , the LPG stream , the i-butane and the n-butane streams). To minimise inconsistencies in the sampling data, two samples of each product stream separated by about 10 minutes were taken during each plant trial. Averaged compositions were then used. Compositions of the bottoms product for each of the columns were obtained from the steady-state mass balance equations. Operating conditions for the gas-tail (such as flow rates, column pressure and temperatures) at the time of each

plant trial were also required. Measurements of the desired process variables were made using the instruments available on the plant . All these instruments were calibrated before the plant trials to ensure as reliable data as possible. A time mean average for each of these measurements (i.e. averaged over the period of plant trial) was used (see Table 3. 1. 10 - 3. 1. 18).

3. 1. 3 STEADY - STATE MODELLING OF THE GAS - TAIL USING THE SMBP SIMULATION PACKAGE

Plant test run results usually only provide a limited amount of information about the operating conditions. Complete pressure and temperature profiles along a column , for example, cannot easily be obtained from plant trials.

Simulation results from a rigorous model of the plant at the test run conditions, on the other hand, provide a complete view of the process operating conditions. Also, rigorous model results are necessary in developing a UCM based gas-tail model applicable over a range of operating conditions. Test run data, therefore, were initially matched to simulation results from a rigorous model of the gas-tail. The SMBP simulation package employs a sequential modular approach and uses a library of process equipment models and a physical property database. The CDU's gas-tail was modelled on SMBP and simulations performed for each of the test run conditions. The following information was necessary to perform an SMBP simulation at each of the test run conditions.

(a) The number and nature of the components in the feed mixture.

(b) The feed rate and feed composition entering the de-ethaniser column of the gas-tail.

(c) The reflux rates in each of the gas-tail columns.

(d) The LP steam supply rate to each of the column reboilers.

(e) In the case of the de-ethaniser , which has a partial overhead condenser, the recovery rate of the uncondensed vapours is also required. The condensers for both the de-propaniser and the de-isobutaniser were usually operated as total condensers and consequently there was no vapour flow from these units.

(f) The pressure at the bottom most tray of each column. Based on Shell experience, an average pressure drop of 0.01 bar per tray was used to estimate the internal pressure profile.

(g) The column efficiencies estimated based on Shell experience (de-ethaniser column = 85 % ; de-propaniser column = 85 %; de-isobutaniser = 90 %), were used in all simulations. The number of theoretical trays in each gas-tail column was calculated based on this assumption (see Table 2. 5. 2).

Table 3. 1. 10
Plant measurements at the test-run conditions
for de-ethaniser column
(Case 1 : high feed , high pentane conditions)

Measurement		Instrument reading
Feed rate to the gas-tail	(tons/day)	315
Feed temperature	(deg C)	26.7
LP steam input rate to the reboiler	(tons/day)	58.9
Lp steam temperature	(deg C)	230
Overhead vapour temperature	(deg C)	57.8
Tray 3 temperature	(deg C)	102
Tray 2 pressure	(bar g)	27.84
Overhead condenser pressure	(bar g)	27.9
Reflux flow rate	(tons/day)	574
Reflux temperature	(deg C)	42
Fuel gas flow rate from the overhead condenser	(tons/day)	27.3
Reboiler bottoms product flow rate	(tons/day)	256
Bottoms product temperature	(deg C)	114
Reboiler return temperature	(deg C)	120

Table 3. 1. 11
Plant measurements at the test-run conditions
for de-propaniser column
(Case 1 : high feed , high pentane conditions)

Measurement		Instrument reading
LP steam flow rate	(tons/day)	40.8
LP steam temperature	(deg C)	230
Overhead vapour temperature	(deg C)	54.5
Tray 3 temperature	(deg C)	104
Tray 3 pressure	(bar g)	16.52
Overhead reflux flow rate	(tons/day)	374
Reflux temperature	(deg C)	51
Fuel gas flow rate from the overhead condenser	(tons/day)	0
Reboiler bottoms product flow rate	(tons/day)	182
Bottoms product temperature	(deg C)	108
Reboiler return temperature	(deg C)	116
LPG product flow rate	(tons/day)	70.3
LPG product temperature	(deg C)	33.8

Table 3. 1. 12
Plant measurements at the test-run conditions
for de-isobutaniser column
(Case 1 : high feed , high pentane conditions)

Measurement		Instrument reading
LP steam input rate to the reboiler	(tons/day)	97.4
Lp steam temperature	(deg C)	230
Overhead vapour temperature	(deg C)	68
Tray 6 temperature	(deg C)	86
Tray 50 pressure	(bar g)	9.8
Overhead reflux flow rate	(tons/day)	662
Reflux temperature	(deg C)	67.5
Fuel gas flow rate from the overhead condenser	(tons/day)	0
Reboiler bottoms product flow rate	(tons/day)	39.1
Bottoms product temperature	(deg C)	45.3
Reboiler return temperature	(deg C)	121
Isobutane product flow rate	(tons/day)	23.1
Isobutane product temperature	(deg C)	32.7
n-butane product flow rate	(tons/day)	109
n-butane product temperature	(deg C)	37

Table 3. 1. 13
Plant measurements at the test-run conditions
for de-ethaniser column
(Case 2 : moderate feed , low pentane conditions)

Measurement		Instrument reading
Feed rate to the gas-tail	(tons/day)	265
Feed temperature	(deg C)	38
LP steam input rate to the reboiler	(tons/day)	62.5
LP steam temperature	(deg C)	221
Overhead vapour temperature	(deg C)	65.3
Tray 3 temperature	(deg C)	103
Tray 2 pressure	(bar g)	29.2
Overhead condenser pressure	(bar g)	28.6
Overhead reflux flow rate	(tons/day)	500
Reflux temperature	(deg C)	51
Fuel gas flow rate from the overhead condenser	(tons/day)	36.6
Reboiler bottoms product flow rate	(tons/day)	229

Table 3. 1. 14
Plant measurements at the test-run conditions
for de-propaniser column
(Case 2 : moderate feed , low pentane conditions)

Measurement		Instrument reading
LP steam flow rate	(tons/day)	52.2
LP steam temperature	(deg C)	221
Overhead vapour temperature	(deg C)	57.2
Tray 3 temperature	(deg C)	108
Tray 3 pressure	(bar g)	18.61
Overhead reflux flow rate	(tons/day)	377
Reflux temperature	(deg C)	55.5
Fuel gas flow rate from the overhead condenser	(tons/day)	0
Reboiler bottoms product flow rate	(tons/day)	168
Bottoms product temperature	(deg C)	111
Reboiler return temperature	(deg C)	115
LPG product flow rate	(tons/day)	71.4
LPG product temperature	(deg C)	30.5

Table 3. 1. 15
Plant measurements at the test-run conditions
for de-isobutaniser column
(Case 2 : moderate feed , low pentane conditions)

Measurement		Instrument reading
LP steam input rate to the reboiler	(tons/day)	70.5
LP steam temperature	(deg C)	221
Overhead vapour temperature	(deg C)	69.5
Tray 6 temperature	(deg C)	81.5
Tray 50 pressure	(bar g)	9.6
Overhead reflux flow rate	(tons/day)	561
Reflux temperature	(deg C)	69
Fuel gas flow rate from the overhead condenser	(tons/day)	0
Reboiler bottoms product flow rate	(tons/day)	97
Bottoms product temperature	(deg C)	63.5
Reboiler return temperature	(deg C)	91.8
Isobutane product flow rate	(tons/day)	37.9
Isobutane product temperature	(deg C)	33.2
n-butane product flow rate	(tons/day)	30.8
n-butane product temperature	(deg C)	37.5

Table 3. 1. 16
Plant measurements at the test-run conditions
for de-ethaniser column
(Case 3 : low feed , moderate pentane conditions)

Measurement		Instrument reading
Feed rate to the gas-tail	(tons/day)	165.5
Feed temperature	(deg C)	35
LP steam input rate to the reboiler	(tons/day)	58.9
LP steam temperature	(deg C)	230
Overhead vapour temperature	(deg C)	64.2
Tray 3 temperature	(deg C)	100.2
Tray 2 pressure	(bar g)	28.84
Overhead condenser pressure	(bar g)	28.74
Overhead reflux flow rate	(tons/day)	511.7
Reflux temperature	(deg C)	41.2
Fuel gas flow rate from the overhead condenser	(tons/day)	20
Reboiler bottoms product flow rate	(tons/day)	145
Bottoms product temperature	(deg C)	113.5
Reboiler return temperature	(deg C)	115.7

Table 3. 1. 17
Plant measurements at the test-run conditions
for de-propaniser column
(Case 3 : low feed , moderate pentane conditions)

Measurement		Instrument reading
LP steam flow rate	(tons/day)	52.2
LP steam temperature	(deg C)	52.2
Overhead vapour temperature	(deg C)	55.3
Tray 3 temperature	(deg C)	79.6
Tray 3 pressure	(bar g)	19.54
Overhead reflux flow rate	(tons/day)	415.2
Reflux temperature	(deg C)	55.3
Fuel gas flow rate from the overhead condenser	(tons/day)	0
Reboiler bottoms product flow rate	(tons/day)	116
Bottoms product temperature	(deg C)	68
Reboiler return temperature	(deg C)	83.8
LPG product flow rate	(tons/day)	29.4
LPG product temperature	(deg C)	35.4

Table 3. 1. 18
Plant measurements at the test-run conditions
for de-isobutaniser column
(Case 3 : low feed , moderate pentane conditions)

Measurement		Instrument reading
LP steam input rate to the reboiler	(tons/day)	70.5
LP steam temperature	(deg C)	221
Overhead vapour temperature	(deg C)	64.24
Tray 6 temperature	(deg C)	77.7
Tray 50 pressure	(bar g)	10.2
Overhead reflux flow rate	(tons/day)	554.6
Reflux temperature	(deg C)	64.2
Fuel gas flow rate from the overhead condenser	(tons/day)	0
Reboiler bottoms product flow rate	(tons/day)	64.94
Bottoms product temperature	(deg C)	81.2
Reboiler return temperature	(deg C)	83.6
Isobutane product flow rate	(tons/day)	24
Isobutane product temperature	(deg C)	35.6
n-butane product flow rate	(tons/day)	27
n-butane product temperature	(deg C)	35.3

As shown in Tables (3. 1. 10) - (3. 1. 18), several measurements on the gas-tail columns were made during each test run. Information other than that required for the SMBP simulations (i.e. (a) - (g) above) was later used to check the simulation results.

The gas-tail model based on the UCM approach was next fitted to the SMBP simulation results. The following operations were performed so as to obtain good agreement between these two simulations.

(a) The relative volatilities, latent heats of vaporisation/condensation, the effective overall heat transfer coefficients were all estimated as discussed previously.

(b) The primary modification required in the UCM based model was associated with the estimation of the number of compartments and the total number of trays required for each of the gas-tail columns. The following approach was used to model each of the gas-tail columns.

(i) Initially, use the same number of trays in the UCM column model as used in the SMBP model. This provides a good first estimate. Next, calculate the number of compartments required in each column, each compartment containing four or five trays.

(ii) Perform a simulation using the resulting UCM model and compare both the distillate and bottoms product compositions with that of the SMBP simulation. If the error in the main component (e.g. LPG is the main component of the de-propaniser's distillate) is large , then repeat the UCM simulation changing the number of trays in the column. This means that the number of trays per compartment will also change. It must be realised here that no specific rules can be specified for either reducing or increasing the number of trays, relative to the number used in the SMBP simulation. Although the approach used is one of trial-and-error, convergence to the correct number of trays giving good agreement with the SMBP simulation results was achieved rapidly in all cases.

(iii) If the differences in the UCM and SMBP composition estimations are large, reducing (or increasing) only the number of trays in a fixed number of compartments may be inadequate. Therefore, repeat the UCM simulation changing the number of compartments in a column.

In the gas-tail case-study, reducing the number of trays per compartment was always found adequate to obtain good steady-state matching. Several steady-state trial simulations for the UCM based gas-tail were required to obtain a good match with the SMBP model. Such an estimation of the number of compartments

and the trays needed per column, however, was made only for the high feed rate, high pentanes test-run conditions. The same number of compartments (and the same number of trays within each of these compartments) was used for the other two plant trial conditions. Table 3. 1. 9 provides a list of the number of compartments used in each of the gas-tail columns, along with the number of trays in each of these compartments.

(c) Since the CMO assumption was found to be adequate (see Table 2. 5. 2), no correction factors for internal flow changes were used in the gas-tail case-study.

Thus, identifying the number of compartments was the only modification required to obtain good agreement between the two gas-tail models.

Comparisons are made between the simulation data and the plant trial results in Tables (3. 1. 19 - 3. 1. 27) . The main component in each product stream is underlined in these tables. A maximum error of 5 % in the estimation of the composition of the major component in a stream by the UCM model was obtained. Figures (3. 1. 28) and (3. 2. 29) show the temperature and pressure profiles along the column as calculated by the SMBP model, for the de-propaniser at the high pentanes feed test-run conditions (i.e. Case 1). Both the temperature and pressure in the condenser and reboiler of the column, were also obtained from the UCM based gas-tail simulations (see Section 3. 1. 1). Comparisons between these simulated values and the actual plant measurements are also made on these figures.

Comparisons with both the plant trial data and the rigorous SMBP simulations indicated that, the gas-tail model developed using the UCM approach combines both computational efficiency and accuracy over the entire range of test run conditions. The same gas-tail model, therefore, was used subsequent in optimisation (see Section 3. 2) and control system design studies (see Chapter 6).

Table 3. 1. 19
Comparison of steady-state simulation results and test-run data
for the de-ethaniser distillate composition
(Case 1 : high flow , high pentanes feed)

Component	Test run results	SMBP Simulation	UCM Simulation
C1	0.067	0.067	0.067
C2	0.651	0.651	0.647
C3	0.181	0.181	0.179
iC4	0.037	0.037	0.039
nC4	0.056	0.055	0.059
iC5	0.005	0.004	0.005
nC5	0.003	0.003	0.003
nC6	0.002	0.001	0.001
	Percentage error in the main component = 0.6 %		

Table 3. 1. 20
Comparison of steady-state simulation results and test-run data
for the de-propaniser distillate composition
(Case 1 : high flow , high pentanes feed)

Component	Test run results	SMBP simulation	UCM simulation
C2	0.017	0.013	0.019
C3	0.912	0.933	0.916
iC4	0.065	0.052	0.057
nC4	0.008	0.003	0.007
	Percentage error in the main component is= 1.8 %		

Table 3. 1. 21
Comparison of steady-state simulation results and test-run data
for the de-isobutaniser distillate composition
(Case 1 : high flow , high pentanes feed)

Component	Test run results	SMBP simulation	UCM simulation
C3	0.075	0.062	0.064
iC4	0.872	0.879	0.859
nC4	0.053	0.048	0.077
	Percentage error in the main component = 2.3%		

Table 3. 1. 22
Comparison of steady-state simulation results and test-run data
for the de-ethaniser distillate composition
(Case 2 : moderate flow , low pentanes feed)

Component	Test run results	SMBP simulation	Simple model simulation
C1	0.045	0.067	0.067
C2	0.640	0.621	0.618
C3	0.233	0.239	0.245
iC4	0.080	0.031	0.029
nC4	0.001	0.039	0.038
iC5	0.001	0.003	0.003
nC5	0.000	0.001	0.001
	Percentage error in the main component is 0.48 %		

Table 3. 1. 23
Comparison of steady-state simulation results and test-run data
for the de-propaniser distillate composition
(Case 2 : moderate flow , low pentanes feed)

Component	Test run results	SMBP simulation	Simple model simulation
C2	0.005	0.003	0.002
C3	0.972	0.969	0.966
iC4	0.022	0.027	0.029
nC4	0.001	0.001	0.002
	Percentage error in the main component is 0.31%		

Table 3. 1. 24
Comparison of steady-state simulation results and test-run data
for the de-isobutaniser distillate composition
(Case 2 : moderate flow , low pentanes feed)

Component	Test run results	SMBP simulation	Simple model simulation
C3	0.007	0.003	0.015
iC4	0.954	0.973	0.971
nC4	0.039	0.025	0.014
	Percentage error in the main component is 0.21 %		

Table 3. 1. 25
Comparison of steady-state simulation results and test run data
for the de-ethaniser distillate composition
(Case 3 : low flowrate , moderate pentanes feed)

Component	Test run results	SMBP simulation	UCM simulation
C1	0.035	0.035	0.035
C2	0.646	0.639	0.646
C3	0.239	0.243	0.239
iC4	0.027	0.028	0.027
nC4	0.049	0.052	0.049
iC5	0.002	0.002	0.002
nC5	0.001	0.001	0.001
nC6	0.001	0.001	0.001
	Percentage error in the main component is		-1.1 %

Table 3. 1. 26
Comparison of steady-state simulation results and test run data
for the de-propaniser distillate composition
(Case 3 : low flowrate, moderate pentanes feed)

Component	Test run results	SMBP simulation	UCM simulation
C2	0.008	0.007	0.006
C3	0.940	0.963	0.931
iC4	0.045	0.027	0.053
nC4	0.005	0.002	0.001
	Percentage error in the main component is 3.3 %		

Table 3. 1. 27
Comparison of steady-state simulation results and test run data
for the de-isobutaniser distillate composition
(Case 3 : low flowrate, moderate pentanes feed)

Component	Test run results	SMBP simulation	UCM simulation
C3	0.075	0.087	0.027
iC4	0.673	0.782	0.787
nC4	0.250	0.131	0.186
	Percentage error in the main component is - 0.64 %		

3.2 GAS - TAIL OPTIMISATION STUDIES

Improved plant performance in terms of improved product yields and more effective utilisation of available energy resources, usually provides substantial economic benefits. Optimisation involves identifying the operating conditions for a physical process that maximise an objective function for the process (such as the overall profit of the process) subject to certain physical and operational constraints.

The importance of optimisation with reference to the operation of a chemical plant can be represented through its position in a hierarchical structure (see Figure 3. 2. 1). A chemical plant can be represented by a mathematical model describing the process operation. The operating conditions maximising the profit of the process, subject to constraints, can be identified using an optimiser. "Fast" external disturbances acting on such a process may move the process operating conditions away from the optimum. A control system, therefore, is required to hold the process at the optimum conditions which are the set-points for the control system. As will be discussed later, a major issue here is which control system allows us to operate as close as possible to this optimum, despite the action of any "fast" disturbances. Thus, for a given set of "slow" disturbances, the optimiser not only identifies the operating conditions that are economically most beneficial but also provides the necessary information to the control system (i.e. the set-point) to regulate the process against the "fast" disturbances. However, such an optimiser relies heavily on the accuracy of the process models and frequent updating of this model based on plant measurements may be necessary to obtain reliable performance. Such an overall approach is usually called "optimising control" and will be investigated in detail later for the current case - study.

It should be clear from the above that any steady-state problem seeking an optimal solution should be organised to have the following :

(a) A mathematical model that is a close representation of the physical process.
(b) A suitable objective criterion to guide the decision making.
(c) A set of constraints to provide the limits or boundaries of the operation of the process.
(d) A set of freed variables to search with so as to find an optimum in the feasible operating space.

Distillation is probably the most widely used separation process in the chemical industry. Edgar and Himmelblau [1989] have made a good review of the current status of work on optimisation problems for steady-state distillation, with particular emphasis on various

Figure 3. 2. 1
Hierarchical structure for an optimising control scheme

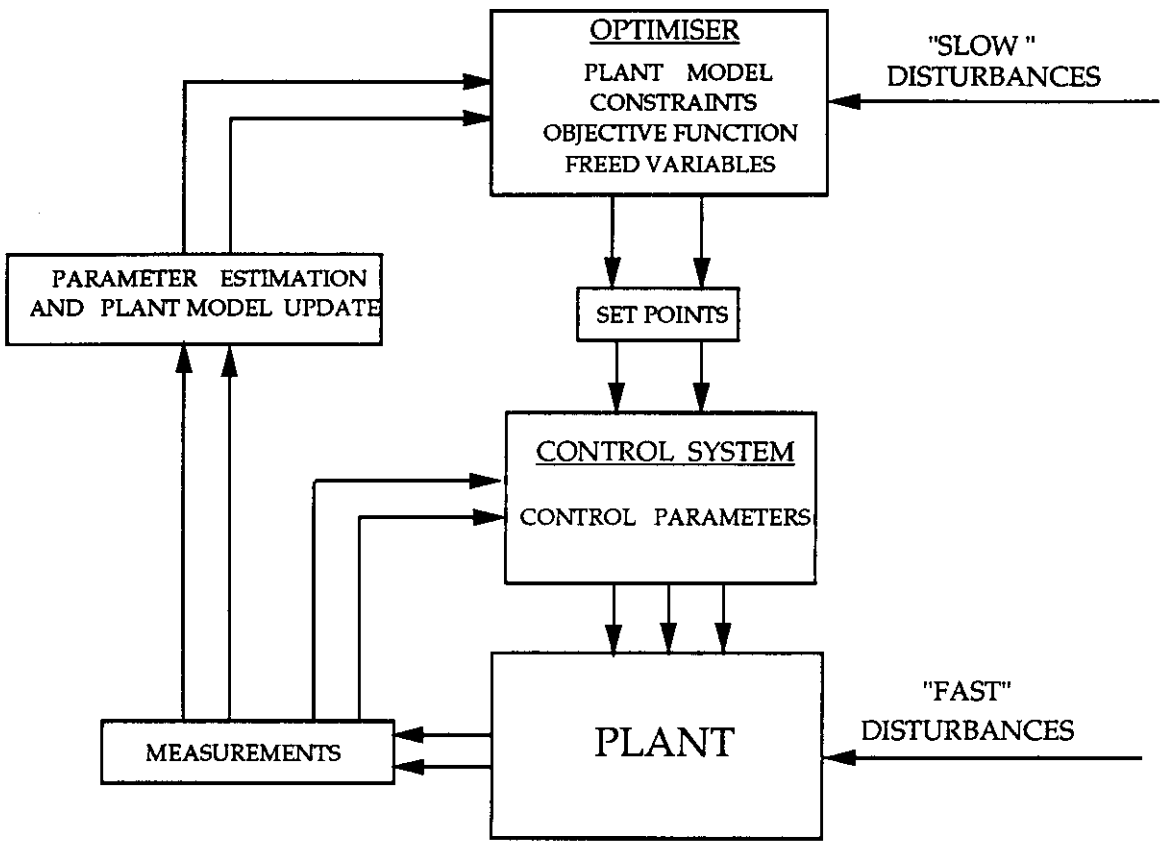

levels of complexity involved in the problem formulation. The gas-tail has three distillation columns in series and hence optimisation of the gas-tail essentially involves optimising the operating conditions of all three distillation columns together. The problem formulation involves maximising an objective function , which in the present context is the net profit obtained from the gas-tail. The product quality requirements, the operational limitations of the columns (such as flooding and weeping), reboilers and condensers together form a set of inequality constraints. The model describing the complete gas-tail represents a set of equality constraints that need to be satisfied at all operating conditions. Both the equality and inequality constraints are nonlinear in the present case. Therefore, the gas-tail optimisation is a nonlinear constrained optimisation problem and requires suitable software to obtain an optimal solution. An optimiser routine FEASOPT in SPEEDUP has been used throughout the gas-tail case-study.

At an optimum, in most cases, some of the inequality constraints become equality constraints. In other words , to be at the optimum one is required to operate the process right on some of the inequality constraints. All such inequality constraints are said to be " active " at the optimum. Active constraints play a key role both in steady-state optimisation and in the optimising control of a process. However, active constraints can change especially as the external disturbances change. The sensitivity of an optimum to changes in an active constraint is quantified by a " Lagrange multiplier ". The larger the value of a Lagrange multiplier, the greater the sensitivity of the optimum with respect to the corresponding active constraint. All constraints that are not active at the optimum (frequently known as " inactive constraints ") have zero Lagrange multipliers . Thus, the optimum is completely insensitive to inactive constraints. Further discussion on the importance of active constraints and their corresponding Lagrange multipliers in the design of an optimising control system, will be addressed in Chapter 5.

3. 2. 1 OPTIMISATION OF DISTILLATION COLUMNS

The "degrees of freedom" for a process model are the set of variables that can be varied independently, but must be specified so as to ensure that the model is soluble. Another set of variables, called the "freed variables " refers to those variables that can be allowed to vary during optimisation to search for the optimum solution. Freed variables usually form a sub-set of the degrees of freedom. Both these types of variables will be referred to throughout the following sections .

Consider a simple distillation column with one feed and two products. Maarleveld and Rijnsdorp [1970] pointed out that for a given feed rate and feed composition, the heat duty in the pre-heater and the column pressure are the most common freed variables available

for column optimisation. This assumed that the levels of both the overhead accumulator and the reboiler were being controlled using the distillate and bottoms product flows and , while the top and bottom compositions are controlled using the reflux rate and the reboiler duty, respectively. However, there is no means of preheating the feed in the case of the gas-tail columns. Also, the purpose of the current study is not merely to identify the optimum operating conditions for the gas-tail, but also to look for a control system that holds the plant as closely as possible to the desired optimum conditions. This latter stage considers a range of additional control structures that can be implemented on the gas-tail, besides the more traditional ones. Therefore , the freed variables for the gas-tail are not as simple as those employed by Maarleveld and Rijnsdorp and are obtained as follows. The following discussion on the degrees of freedom for a distillation column is made keeping in mind both the optimisation and control of the column. This is because the degrees of freedom selected will be candidates as freed variables for optimisation and as manipulated variables for control . Consider again, a simple distillation column with one feed and two products with a fixed number of trays. For a given feed rate and feed composition, the amount of separation achieved depends on the specifications used in both the reboiler and condenser. For a given reflux rate in the column, only one specification is required for the design of the reboiler , either the heat duty or the steam input rate to the reboiler. On the other hand, for a total condenser at a known overhead vapour rate and enthalpy, two specifications are required for a complete description of the condenser. These are the cooling duty or the operating pressure and either the distillate or reflux flow rate. For a partial condenser, however, an extra specification is needed besides these two (i.e. the rate at which the uncondensed vapour is removed). The cooling duty in a condenser is usually specified through the flowrate of the cooling medium. If the condenser has a sufficiently large capacity, then the operating pressure of the condenser can be varied and it's optimum value estimated (Maarleveld and Rijnsdorp [1970] , Roffel and Fontein [1979]). From the point of view of control , holding the condenser operating pressure at the selected optimum value (for instance , by manipulating the cooling duty) is not always possible because of inadequate cooling capacity. For an already existing process, the condenser may have a fixed or a limited capacity and replacing the condenser with a larger and/or more efficient one may not be economically feasible. In such cases, using the condenser operating pressure as a freed variable for optimal column performance may not be feasible and the cooling duty or more likely the cooling medium flowrate, therefore, is the proper choice as a degree of freedom . It may be noted that in this case the column pressure is allowed to "float". In summary, then, for the existing gas-tail distillation columns , the reboiler heat duty, the condenser heat duty (or the cooling medium flowrate) and the reflux (or distillate rate) , are the most appropriate choices as "freed variables " for use in optimisation studies.

To obtain a steady-state solution to a UCM column model , we are required to specify the holdups in the overhead accumulator and in the reboiler. For a dynamic solution to such a model, however, the holdups in both the overhead accumulator and the reboiler vary with time and hence cannot be specified as constants. Therefore, we have two additional degrees of freedom for a dynamic model. In this case, either the distillate or the reflux rate can be chosen as one of the degrees of freedom. Similarly, the bottoms product rate can be used as an additional degree of freedom.

All these concepts will be used in the following gas -tail case-study.

3. 2. 2 GAS - TAIL OPTIMISATION

A simple (one feed and two products) column , for a given feed rate, feed composition and a fixed number of trays (or compartments), will have three degrees of freedom. A column with a side stream, on the other hand, will have four degrees of freedom, since in the latter case the side stream product flow can be varied independently. The gas-tail with its three distillation columns (see Figure 3. 1. 3), therefore, has 10 degrees of freedom (the de-ethaniser = 3; the de-propaniser = 3; the de-isobutaniser = 4) . The freed variables used in all the optimisation runs for the gas-tail are listed below :

(1) De-ethaniser - Distillate flowrate
(2) De-ethaniser - Steam input rate to the reboiler
(3) De-ethaniser - Air flowrate in the condenser
(4) De-propaniser - Distillate flowrate
(5) De-propaniser - Steam input rate to the reboiler
(6) De-propaniser - Air flowrate in the condenser
(7) De-isobutaniser - Distillate flowrate
(8) De-isobutaniser - Steam input rate to the reboiler
(9) De-isobutaniser - Air flowrate in the condenser
(10) De-isobutaniser - Side-stream flowrate

As discussed previously (see Section 2. 1) the major role of the de-ethaniser column in the gas-tail is to remove most of the ethane and all the accompanying light hydrocarbons from the feed. The resulting bottoms product, therefore, contains primarily propane , i-butane and n-butane, which are separated in the downstream columns. Pentanes accompanying this bottoms product will eventually end up as bottoms product of the de-isobutaniser column. Some propane and other high value hydrocarbons leave the gas-tail in the low value ethane product stream and are lost. The recovery of ethane product stream , therefore, is associated with an "economic loss", due to the lost propane etc.,. Also, operation of the de-ethaniser itself incurs a normal operational cost through

steam usage. Both these costs reduce the overall profit achieved by the gas-tail. Other gas-tail product streams (i.e. distillate of the de-propaniser, distillate and side-streams of the de-isobutaniser) , on the other hand, contribute mostly towards it's profit.

The objective function is to maximise the net profit , which is given by :

$$\phi = P_{181} + P_{182} - P_{180} \qquad (3.2.1)$$

where

ϕ = Net profit from the gas-tail

P_{180} = Loss associated with the operation of the de-ethaniser

= (fuel gas rate * value of the fuel gas + net cost of the reboiler steam)

P_{181} = Profit associated with the operation of the de-propaniser

= (LPG stream recovery rate * value of the LPG - net cost of the reboiler steam)

P_{182} = Profit associated with the operation of the de-isobutaniser

= (i-butane stream recovery rate * value of the i-butane + n-butane stream recovery rate * value of the n-butane - net cost of the reboiler steam)

Equation (3. 2. 1) can be rearranged and expressed as,

ϕ = LPG stream recovery rate * value of LPG
+ i-butane stream recovery rate * value of i-butane
+ n-butane stream recovery rate * value of n-butane
- fuel gas recovery rate * value of fuel gas
- total cost of steam for all the columns together
+ total value of condensate from all the columns (3.2.2)

Representative values of all the products and the steam costs are given in Table 3. 2. 1.

As noted in Figure 3. 2. 1, disturbances acting on the gas-tail can be classified as either "slow disturbances" or "fast disturbances". "Slow disturbances" refer to those inputs that change gradually over a long period of time, such as ambient air temperature , changes in the feed composition with respect to the amount of pentanes (which depends primarily on the type of crude used in the crude distillation unit). "Fast disturbances", on the other hand, refer to those inputs, that change both quickly and frequently. Feed flow rate to the gas-tail and the pressure of the LP steam to the reboilers are typical members of this category. In optimising control, slower disturbances are usually handled by the optimiser that identifies the set-points for optimal operation. The control scheme, on the other hand, regulates the plant operation at these set-points in the face of the fast disturbances.

Table 3. 2. 1
The value/costs associated with various gas-tail streams

Stream	Value / cost associated with the stream ($/ (Kg-moles))
Fuel-gas	1
LPG	7.82
Isobutane	17.55
n-butane	8.874
LP steam - cost - value of the condensate	0.091 0.009

TYPES OF CONSTRAINTS MET IN THE OPTIMISATION OF DISTILLATION COLUMNS

Any real process is constrained to a feasible operating region that is determined through limitations imposed on various process variables , such as product quality , and operational and physical requirements. There are three major types of constraints frequently met in the optimisation of distillation columns.

(a) **Product quality specifications**

To meet the quality control requirements of the products being sold, constraints are imposed by a minimum purity required (or a maximum amount of impurities allowed) in the product streams. In the present case, all the gas-tail product streams (i.e. the LPG stream , the i-butane stream and the n-butane stream) have these types of constraints imposed. Another type of product quality constraint arises due to operational difficulties. For example, excessive amounts of ethane (or any other light hydrocarbon) present in the feed to the de-propaniser or the de-isobutaniser invariably results in poor separation as well as control problems in these columns (see Section 2. 1. 2). Thus, constraints need to be imposed on the maximum amount of ethane that can be allowed in the feed to the downstream columns.

(b) **Operational constraints**

Constraints falling under this category are concerned with operational efficiency. Three types of such constraints can be identified for the current case-study.

(i) For a given feed rate, the internal flows in a distillation column have a major effect on the separation achieved in that column with high internal flows generally increasing the efficiency of separation. At very high liquid rates or very low vapour rates , however, the separation efficiency drops off quickly (Treybal [1955]). These upper (i.e. on liquid rate) and lower (i.e. on vapour rate) limits for the internal flows in a column depend largely on the internal design specifications of the column and are termed the "flooding " and "weeping " flows, respectively. To avoid operating in these low efficiency regimes, constraints are required on the maximum and minimum values of internal flows for each column of the gas-tail.

(ii) In the reboilers and condensers, the temperature difference driving force controls the amount of heat exchanged between the hot and the cold streams. Heat exchanged between two streams varies nonlinearly with the temperature difference. For a certain temperature difference between the

streams, the efficiency of heat transfer reduces to a minimum and forms a lower bound on the quantity of heat exchanged. Therefore, a constraint on this minimum temperature difference is required for all the streams exchanging heat.

(iii) Operational pressures for distillation columns are constrained by physical limitations. This pressure range for any column is determined based on both design calculations and experience.

(c) **Physical constraints**

The maximum heat duty a reboiler or a condenser can provide depends mainly on the maximum flowrate of the heating or cooling medium. This is generally set by the physical size and construction of the control valve used in the supply line or the size of the pump or fan. Constraints to account for such physical limitations are required in the gas-tail.

The details of the various constraints necessary for the gas-tail are given in the following section and in Table 3. 2. 4.

CONSTRAINTS USED IN THE GAS - TAIL OPTIMISATION

Table (3. 2. 4) summarises the list of constraints used throughout all the gas-tail optimisation runs. These constraints were obtained based on the following considerations.

(a) Composition constraints on the minimum purity required with respect to the main component of a product stream (i.e. the propane content in the LPG stream , the i-butane content in the i-butane product stream and the n-butane content in the de-isobutaniser side-stream product) are decided by quality control requirements.

(b) The range of operable column pressures for each of the gas-tail columns was obtained based on operational experience.

(c) The temperature of the vapour stream leaving a reboiler is often referred to as the "reboiler return temperature ". A lower reboiler return temperature provides a larger temperature driving force for heat transfer in the reboiler, and thus for a given steam flow rate, a higher reboiler duty is obtained (see Appendix A5). In the case of the de-ethaniser , the reboiler return temperature is an indirect measure of the amount of ethane and other light hydrocarbons present in the reboiler. Case studies examining the variation of reboiler return temperature over a range of reboiler compositions with different amounts of ethane were

performed for the de-ethaniser at an average operating pressure of 29 bar. A rigorous approach to performing such case-studies would involve a steady-state simulation of the de-ethaniser column at various operating conditions (using SMBP), corresponding to different ethane compositions in the reboiler. An alternative and simple approach involves treating the reboiler as a flash unit. The effect of the ethane composition on the reboiler return temperature can , now, be obtained by estimating the flash temperature for various feeds, differing in their ethane content. The later approach is computationally less demanding and was used for the present case. A steady-state flash model available within SMBP, was used in this case-study. Figures 3. 2. 2 and 3. 2. 3 show the variation of bubble and dew point temperatures with ethane composition in the de-ethaniser's reboiler. A vapour-liquid mixture at equilibrium will have a temperature somewhere in between the bubble and dew point temperatures (see Section 2. 5). The higher the equilibrium mixture temperature , the smaller the amount of ethane and other light hydrocarbons passing on to the downstream columns (i.e. the de-propaniser and the de-isobutaniser). However, high equilibrium mixture temperatures lead to poor heat transfer and can limit the amount of heat exchanged. From Figure (3. 2. 2) it is clear that for a high pentanes feed , a mixture temperature above 130 deg C represents a minimum level of ethane (< 2 mole %) in the reboiler. The minimum temperature difference constraint on the reboiler (see Table 3. 2. 4) , however, requires a reboiler return temperature below 130 deg C. A constraint on the minimum reboiler return temperature of 130 deg C , therefore, satisfies both these requirements. Similarly, the constraint on the minimum reboiler return temperature for the low pentanes feeds has been taken to be 120 deg C (see Figure 3. 2. 3). In the case of the de-propaniser, the two factors influencing the reboiler return temperature are the amount of propane in the reboiler (i.e. must be below 5 mole %) and the steam temperature, these two determining the driving force for the heat transfer. Similar studies can be performed for the reboilers of the other gas-tail columns. Simulation studies on an SMBP flash unit representing the de-propaniser's reboiler indicated that constraints of 117 deg C and 110 deg C on the reboiler return temperature for the high pentanes and low pentanes feeds, respectively, provide a good compromise. Similarly, constraints of 125 deg C and 98 deg C for high pentanes and low pentanes feeds , respectively, have been used for the de-isobutaniser reboiler return temperature. In the latter case, the i-butane composition in the reboiler (i.e. must be below 5 mole %) and the minimum temperature difference for heat transfer were again the key factors influencing the reboiler return temperature.

Figure 3. 2. 2
EFFECT OF ETHANE COMPOSITION ON THE DE-ETHANISER REBOILER RETURN TEMPERATURE FOR HIGH PENTANES FEED
(AT AN AVERAGE OPERATING PRESSURE OF 29 BARS)

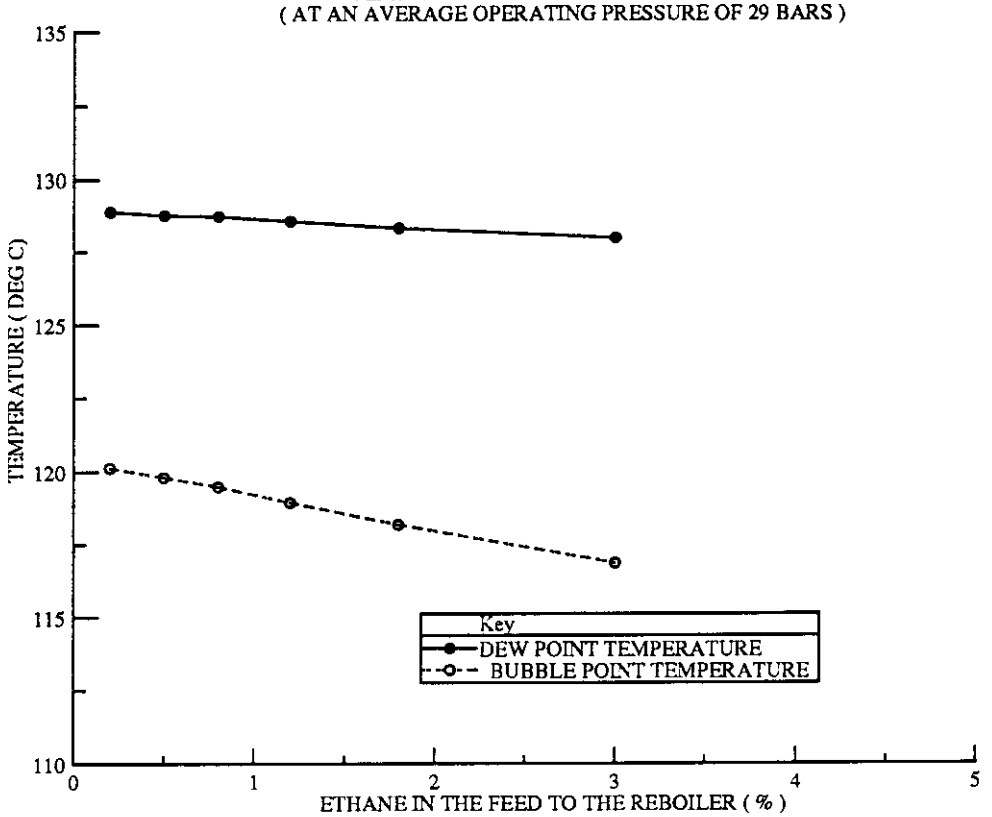

Figure 3. 2. 3
EFFECT OF ETHANE COMPOSITION ON THE DE-ETHANISER REBOILER RETURN TEMPERATURE FOR LOW PENTANES FEED
(AT AN AVERAGE OPERATING PRESSURE OF 29 BARS)

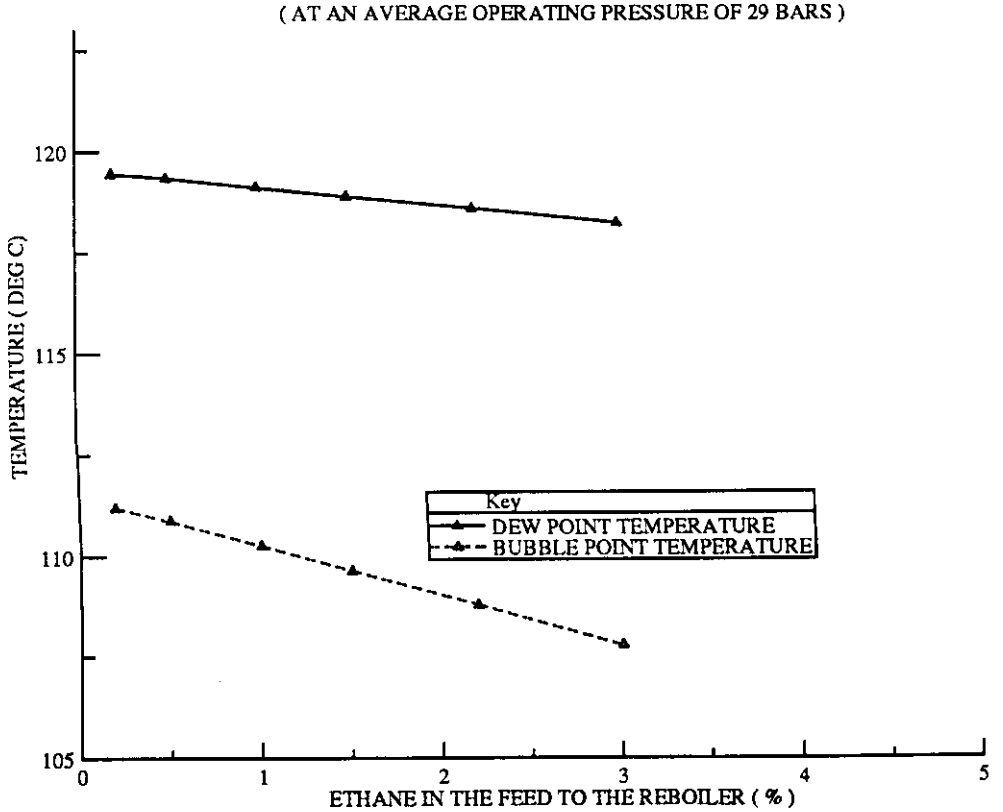

(d) Maximum flowrates of air in the gas-tail's condensers and of steam for the reboilers were obtained from the their mechanical design data.

3. 2. 3 STEADY - STATE OPTIMISATION RESULTS FOR THE GAS - TAIL

Both the active constraints and the optimum operating conditions can vary due to changes in the slow disturbances. A " constraint map " provides a description of the active constraints over a desired operational range. Gas-tail optimisation studies was performed over a range of ambient air temperatures (10 - 22 deg C) both for high pentanes and the low pentanes feeds. Constraint maps are given in Tables 3. 2. 2 and 3. 2. 3. The same model that had previously been used in the steady-state UCM model validation (see Section 3. 1. 3) was used to perform gas-tail optimisation. The optimiser used was the " Feasible Path Optimser (FEASOPT) " which is available within SPEEDUP.

Complete details on both the initial (i.e. test run) and optimum operating conditions for the gas-tail are provided in Tables (3. 2. 5 and 3. 2. 6), for the case of a high flow, high pentanes feed (i. e. for Case -1 of Section 3. 1. 2) and an ambient air temperature of 20 deg C.

The major results obtained from the gas-tail optimisation study are given below.

(1) In all cases studied, the number of freed variables is more than the number of active constraints. Hence a " constraint control " approach (see Section 5.2) cannot directly be used to maintain the process at its optimum conditions.

(2) Product composition constraints are active at the optimum in all cases and have the largest Lagrange multipliers (see Tables 3. 2. 2. - 3. 2. 3).

(3) For a low pentanes feed , it is necessary to always operate the de-ethaniser column at its maximum internal liquid flowrate (see Table 3. 2. 3). The maximum liquid flow rate occurs in the stripping section, where a significant amount of the total column separation is achieved.

(4) Reboilers reach their limiting heat transfer capacities with high pentanes feed while condensers become limiting at high ambient air temperatures (see Tables 3. 2. 2 - 3. 2. 3).

(5) In the majority of cases, all the gas-tail condensers are required to be operated at their maximum air flowrates (i. e. with the control valves fully open) at the

Table 3. 2. 2
List of active constraints and their Lagrange multipliers at various ambient air temperatures.
(Case 1 : for the high flow, high pentanes feed)

Active constraint	Ambient temperature (10 deg C)	Ambient temperature (20 deg C)	Ambient temperature (22 deg C)
DE-ETHANISER			
Reboiler return temperature	X(0.397)	X(0.68)	X(0.733)
Condenser air flowrate	At a maximum	At a maximum	At a maximum
DE-PROPANISER			
Reboiler return temperature	X(1.33)	X(7.98)	X(9.33)
Condenser air flowrate	At a maximum	At a maximum	At a maximum
Propane mole fraction in the LPG stream	X(725.47)	X(370.96)	X(415.30)
DE-ISOBUTANISER			
Reboiler return temperature	-	X(7.05)	X(7.57)
Condenser air flowrate	At a maximum	At a maximum	At a maximum
Isobutane mole fraction in the distillate product stream	X(1378.40)	X(2583.24)	X(2845.2)
n-butane mole fraction in the side-stream product	X(3148.99)	X(2830.30)	X(1900.12)
Maximum reboiler duty	X(0.174)	-	-

X Indicates that the constraint is active.
\- Indicates that the constraint is not active.
( ) Indicates the Lagrange multiplier associated with the active constraints

Table 3. 2. 3
List of active constraints and their Lagrange multipliers at various ambient air temperatures.
(Case 2 : for the moderate flow, low pentanes feed)

Active constraint	Ambient temperature (10 deg C)	Ambient temperature (20 deg C)	Ambient temperature (22 deg C)
DE-ETHANISER			
Reboiler return temperature	X(0.57)	X(8.59)	X(8.51)
Internal liquid flow at a maximum	X(0.75)	X(0.03)	X(0.02)
Condenser - temperature driving force at a minimum	X(6.54)	-	-
DE-PROPANISER			
Reboiler return temperature	X(3.63)	X(15.99)	X(17.38)
Condenser Air flowrate	At a maximum	At a maximum	At a maximum
Propane mole fraction in the LPG stream	X(692.83)	X(691.91)	X(812.86)
DE-ISOBUTANISER			
Condenser Air flowrate	At a maximum	At a maximum	At a maximum
Isobutane mole fraction in the distillate product stream	X(2032.82)	X(4832.62)	X(5130.88)
n-butane mole fraction in the side-stream product	X(72.87)	X(1059.49)	X(1311.75)

X	Indicates that the constraint is active.
-	Indicates that the constraint is not active.
( )	Indicates the Lagrange multiplier associated with the active constraints

Table 3. 2. 4
Gas-tail constraints used in the optimisation studies

Constraint type		Constraint value	
DE-ETHANISER			
Reboiler return temperature	≥	130	(deg C)
Volumetric airflowrate	≤	247322	(m3/ hr)
Liquid flowrate in the stripping section	≥	408.5	(Kg-Moles/hr)
Liquid flowrate in the stripping section	≤	673.0	(Kg-Moles/hr)
Reboiler duty	≤	1661	(Tcal/hr)
Condenser pressure	≥	27	(Bar)
Condenser pressure	≤	31	(Bar)
Temperature difference for heat transfer - condenser	≥	5	(deg C)
- reboiler	≥	5	(deg C)
DE-PROPANISER			
Reboiler return temperature	≤	117	(deg C)
Volumetric airflowrate	≥	452508	(m3/ hr)
Liquid flowrate in the stripping section	≥	278.92	(Kg-Moles/hr)
Liquid flowrate in the stripping section	≤	582.23	(Kg-Moles/hr)
Reboiler duty	≤	1659.1	(Tcal/hr)
Condenser pressure	≥	16	(Bar)
Condenser pressure	≤	20	(Bar)
Mole fraction of C3 in the LPG product stream	≥	0.9	
Temperature difference for heat transfer - condenser	≥	5	(deg C)
- reboiler	≥	5	(deg C)
DE-ISOBUTANISER			
Reboiler return temperature	≤	125	(deg C)
Volumetric airflowrate	≥	624606	(m3/ hr)
Liquid flowrate in the stripping section	≥	307	(Kg-Moles/hr)
Liquid flowrate in the stripping section	≤	750	(Kg-Moles/hr)
Reboiler duty	≤	2436	(Tcal/hr)
Condenser pressure	≥	9	(Bar)
Condenser pressure	≤	12	(Bar)
Mole fraction of iC4 in the distillate	≥	0.88	
Mole fraction of nC4 in the side-stream	≥	0.810 for high pentanes	feed
	≥	0.850 for low pentanes	feed
Temperature difference for heat transfer - condenser	≥	5	(deg C)
- reboiler	≥	5	(deg C)

Table 3. 2. 5
Free variable values for high pentanes feed conditions (Case 1)
at an ambient air temperature of 20 deg C

Freed variable	Operating conditions at the test run	Operating conditions at the optimum
DE- ETHANISER		
Distillate rate (Kg-moles/ hr)	42.64	38.43
Condenser air flow rate (Kg-moles/ hr)	7682	9219
Reboiler steam rate (Kg-moles/ hr)	151.56	153.74
DE-PROPANISER		
Distillate rate (Kg-moles/ hr)	52.54	56.26
Condenser air flow rate (Kg-moles/ hr)	14103	16985
Reboiler steam rate (Kg-moles/ hr)	110.0	108.13
DE-ISOBUTANISER		
Distillate rate (Kg-moles/ hr)	33.42	33.17
Condenser air flow rate (Kg-moles/ hr)	18360	22037
Reboiler steam rate (Kg-moles/ hr)	220.0	233.72
Side-stream product rate (Kg-moles/ hr)	78.98	78.75

Table 3. 2. 6
Major non-freed variable values for high pentanes
feed (Case 1) conditions at an ambient air temperature of 20 deg C

Variable	Operating conditions at the test run	Operating conditions at the optimum
DE-ETHANISER		
Reflux rate (Kg-moles/ hr)	538.39	545.74
Condenser top temperature (deg C)	52.19	52.17
Condenser pressure (Bar)	28.5	29.73
Condenser duty (Tcal/ (Kg-mole . hr))	573.99	600
Condenser distillate composition (Ethane)	0.649	0.685
Reboiler bottoms product rate (Kg-moles/ hr)	151.56	208.55
Reboiler duty (Tcal/ (Kg-mole . hr))	1460.47	1474.17
Reboiler return temperature (deg C)	128.5	130
Mole fraction of ethane in the reboiler	0.025	0.012
DE-PROPANISER		
Reflux rate (Kg-moles/ hr)	345.35	347.16
Condenser top temperature (deg C)	51.09	49.92
Condenser pressure (Bar)	17.1	16.65
Condenser duty (Tcal/ (Kg-mole . hr))	1256.54	1273.99
Condenser distillate composition (Propane)	0.926	0.900
Reboiler bottoms product rate (Kg-moles/ hr)	151.56	152.29
Reboiler duty (Tcal/ (Kg-mole . hr))	1042.68	1031.12
Reboiler return temperature (deg C)	118.5	117.0
DE-ISOBUTANISER		
Reflux rate (Kg-moles/ hr)	474.75	503.25
Condenser top temperature (deg C)	70.63	70.56
Condenser pressure (Bar)	10.80	10.82
Condenser duty (Tcal/ (Kg-mole . hr))	1727.76	1823.81
Condenser distillate composition (i-butane)	0.873	0.880
Reboiler bottoms product rate (Kg-moles/ hr)	42.42	40.373
Reboiler duty (Tcal/ (Kg-mole . hr))	2102.79	2219.68
Reboiler return temperature (deg C)	123.21	125.0
Side-stream composition (n-butane)	0.808	0.810

Note : 1 Tcal = 10^3 Kcal

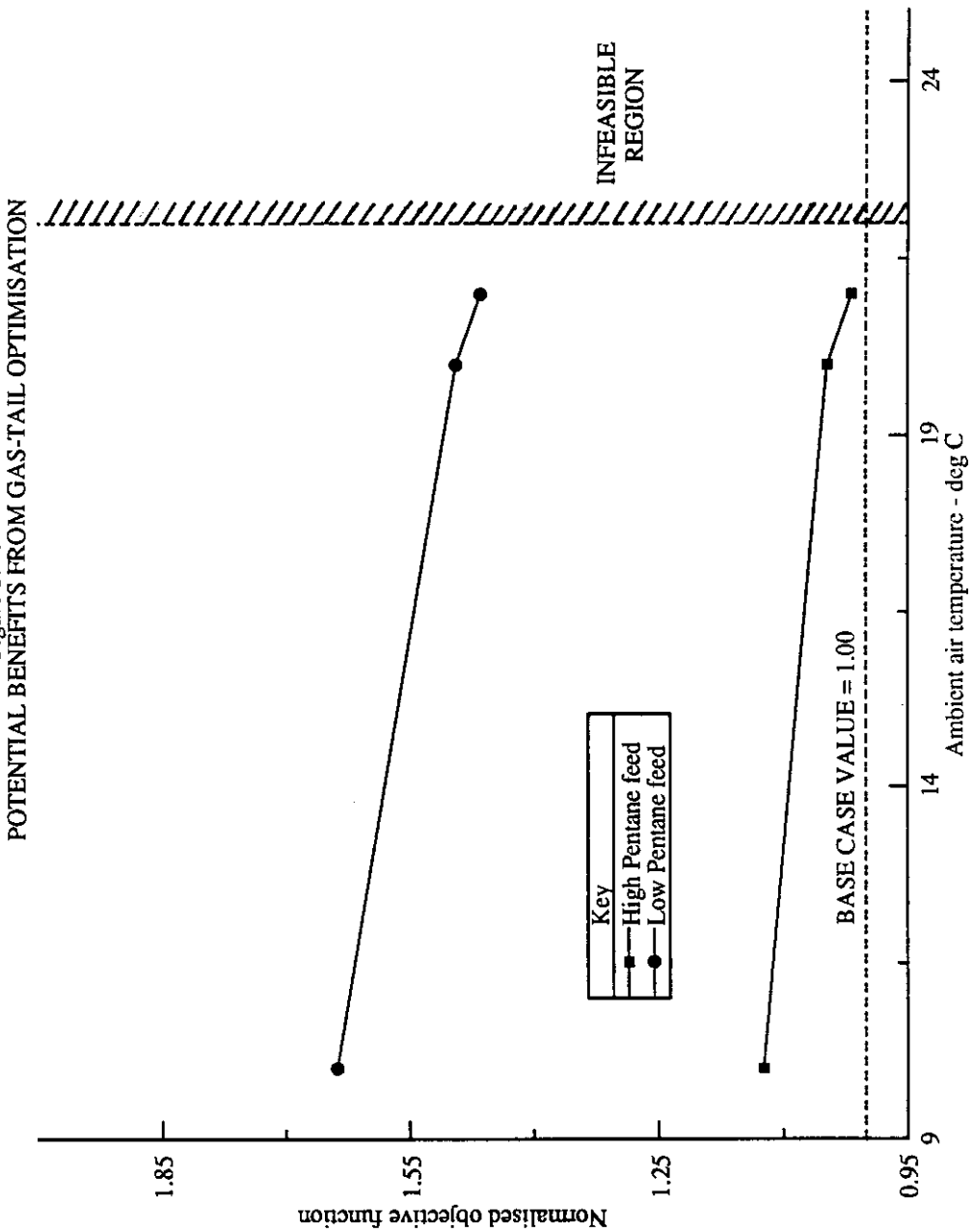

Figure 3. 2. 4
POTENTIAL BENEFITS FROM GAS-TAIL OPTIMISATION

optimum . The Lagrange multipliers associated with these active constraints have been found to be very small (less than 0.001 in many cases) indicating that the profit obtained on the gas-tail is relatively insensitive to changes in the air flowrate. This is partly associated with the poor overall heat transfer coefficients in the air-cooled condensers. The other reason for this is probably due to the nature of relationship between the effective overall heat transfer coefficient and the air flowrate (see Equation 3. 1. 1). Installation of additional fins-fans for all the gas-tail condensers alone, therefore, may not improve the profit achieved. Other factors must be examined, to improve both the economic and operational performance of the gas-tail.

(6) Ambient air temperature has a significant impact on the optimal operating conditions for the gas-tail.

(7) The optimisation results indicate that large increases in profit over the current operation can be achieved by operating the gas-tail at the optimal operating conditions. Figure (3. 2. 4) shows the objective function at optimal conditions normalised against the objective function at the corresponding test-run conditions. These potential economic benefits from gas-tail optimisation are substantially greater for low pentanes feed (up to 64 % improvement) than for high pentanes feed (up to 12 % improvement).

(8) With both high and low pentanes feeds, there is no optimum satisfying all the constraints listed in Table (3. 2. 4) above an ambient temperature of 22 deg C. This does not mean that there is no feasible operating region at all above this temperature. The fact that in practice the gas-tail still operates at ambient temperatures above 22 deg C means that some of the constraints (see Table 3. 2. 4) must be violated during actual operation. The reasons behind this observation may be explained as follows.

At low ambient air temperatures, there is a high temperature difference in the condensers. Thus, for a given air flowrate in the de-ethaniser condenser, large amounts of vapour can be condensed (including all the heavier hydrocarbons) and returned to the column as reflux. All these high value heavy hydrocarbons (i.e. propane, i-butane and n-butane) are, therefore, recovered and subsequently collected as product streams from the downstream columns. Hence, the profit from the gas-tail is large. However, at high ambient air temperatures, the temperature driving force for heat transfer in the condenser will be small. When the required duty for condensation in the de-ethaniser is more than is available (as occurs at high ambient air temperatures with the air flowrate at its

maximum possible value) some of the high value heavy hydrocarbons are lost, through being uncondensed, in the low value ethane product stream. Therefore, the feeds to the de-propaniser and the de-isobutaniser contain smaller amounts of propane and i-butane, respectively. To meet the product quality requirements, the flowrates of the LPG and i-butane product streams have to be lowered. This may also require a change in the internal operating conditions , the reflux flow rates and the bottoms flows in the downstream columns. All these effects reduce the overall profit from the gas-tail. At ambient temperatures over a limiting value (in this case, 22 deg C), no operating conditions exist (and hence no optimum is possible) that would satisfy all the constraints imposed (see Table 3. 2. 4).

Based on the optimisation results, the following two operational recommendations can be made.

(1) With low pentane feeds, the profitability of the gas-tail can be substantially improved by shutting off the side-stream from the de-isobutaniser and collecting the product from the column bottoms as the n-butanes product. This would not violate any constraints. As the pentanes content of the feed increases, the maximum flow should be withdrawn through the side-stream as n-butane product, keeping the bottoms flow at a minimum.

(2) Figures (3. 2. 5 - 3. 2. 7) show the impact of the overall heat transfer coefficient in the gas-tail condensers on the profit or cost from the three individual columns. The plots were obtained from the results of optimisation studies on the gas-tail model with a range of overall heat transfer coefficient values in each of the three columns. The profit and loss functions for each of the gas-tail columns (i. e. P_{181}, P_{182} and P_{180}) are then estimated from Equation (3. 2. 1). The net profits provided by both the de-propaniser and the de-isobutaniser to the overall objective function (i.e. P_{181} and P_{182}) increase essentially linearly with the overall heat transfer coefficient in the respective condensers (see Figures 3. 2. 6 - 3. 2. 7). Thus, any improvement in condenser effective heat transfer coefficients (for instance, by increasing the fin-fan capacities, by increasing the effective areas for heat transfer or using water-cooled instead of air-cooled condensers) for either of these columns should improve the gas-tail profit substantially. It should be pointed out , however, that this increased gas-tail profitability would eventually be limited by other constraints such as the maximum liquid flows within a column, or the maximum duty that the reboiler can deliver. Figure (3. 2. 5) shows that the net loss in the gas-tail profit due to operation of the de-ethaniser (i.e. P_{180}) goes through a minimum with the overall heat transfer coefficient. Thus,

Figure 3. 2. 5
EFFECT OF OVERHEAD CONDENSER HEAT TRANSFER COEFFICIENT
ON THE DE-ETHANISER OPERATING COST

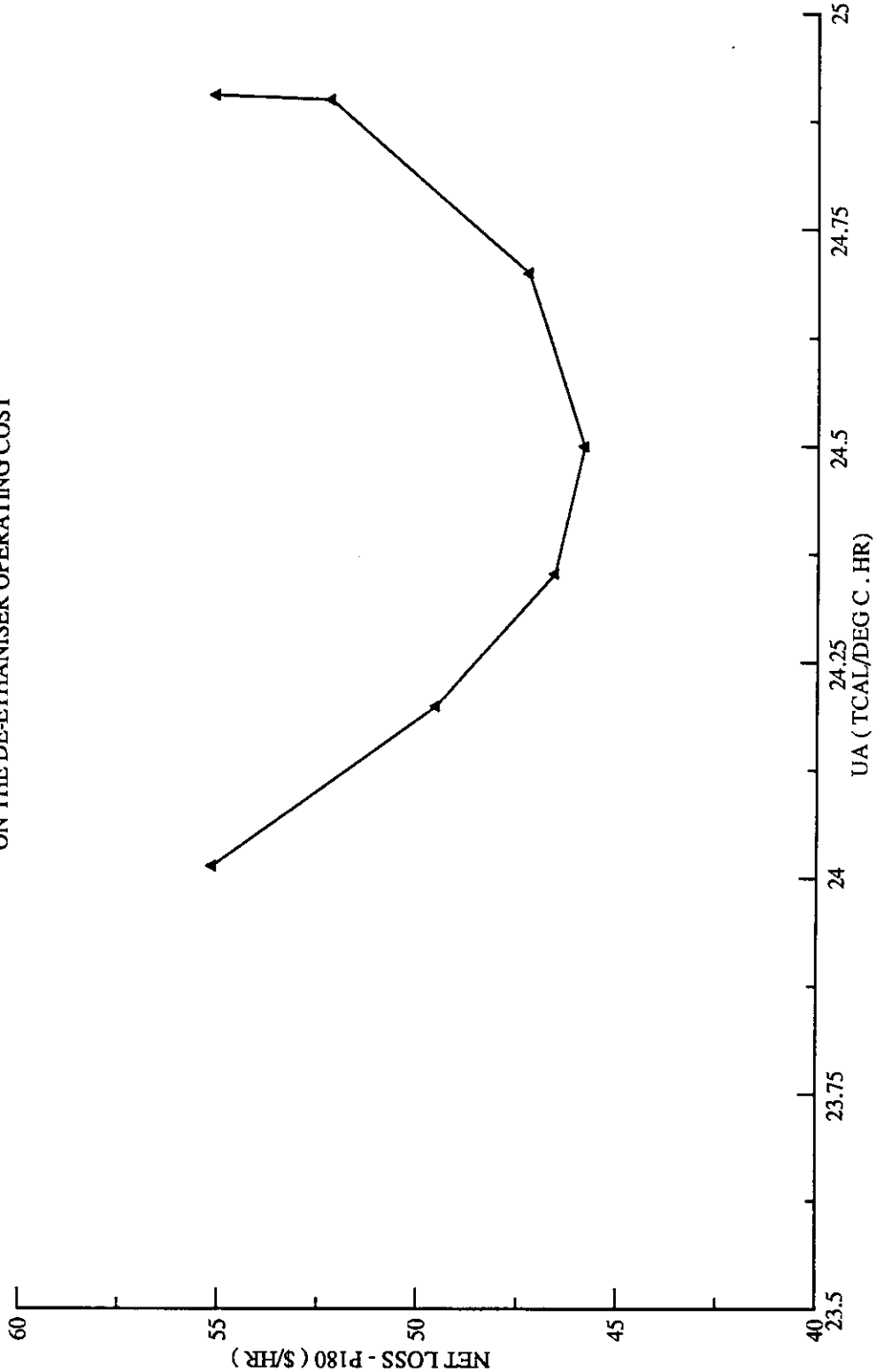

Figure 3. 2. 6
EFFECT OF OVERHEAD CONDENSER HEAT TRASNFER COEFFICIENT
ON THE DE-PROPANISER PROFIT

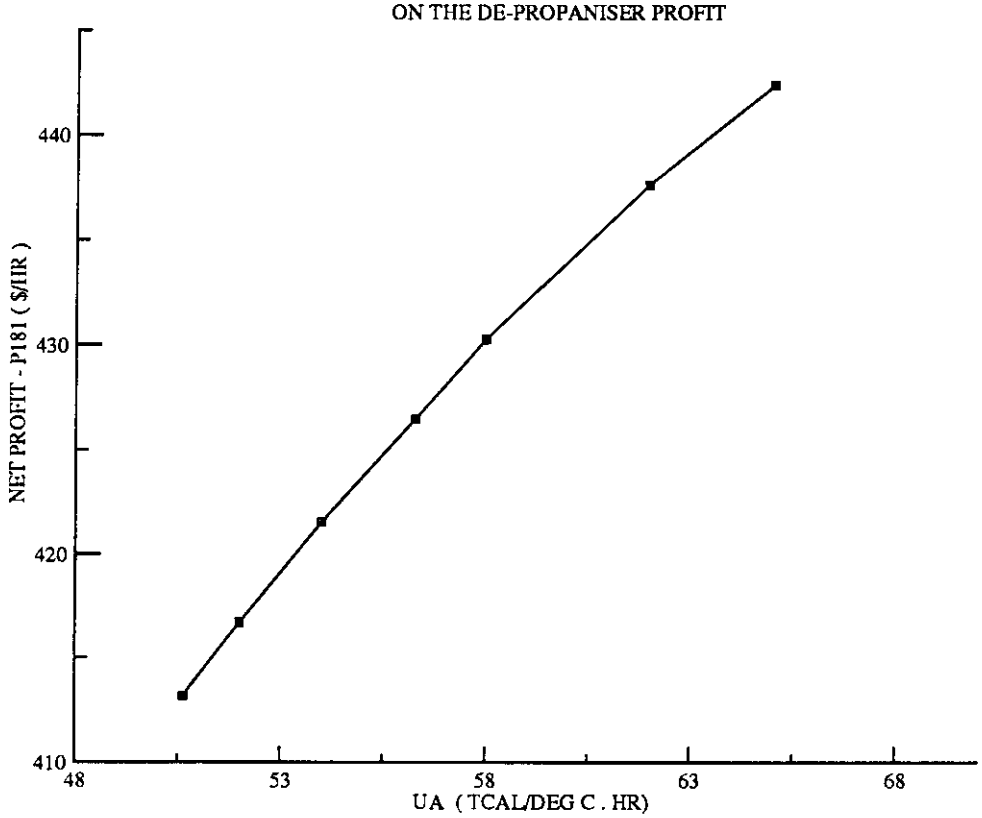

Figure 3. 2. 7
EFFECT OF OVERHEAD CONDENSER HEAT TRASNFER COEFFICIENT
ON THE DE-ISOBUTANISER PROFIT

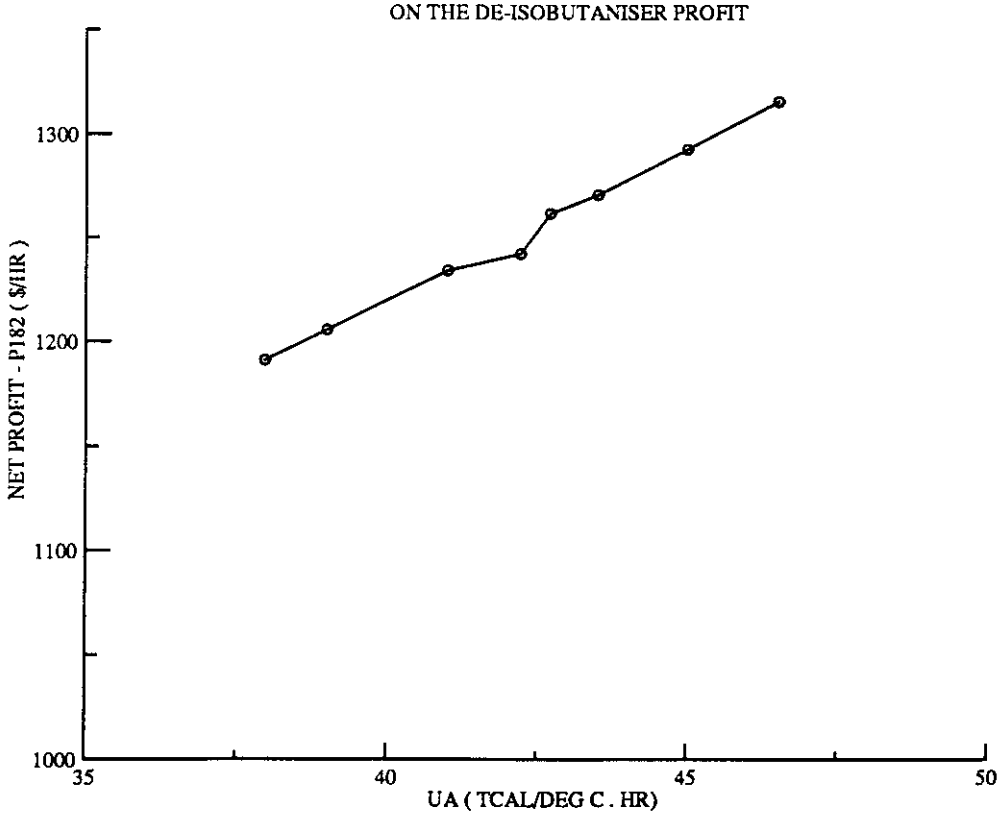

improvements in the overall heat transfer coefficient for this column do not necessarily increase the gas-tail profit. Further that, the range of profits in both the de-propaniser and the de-isobutaniser for a unit increase in the effective heat transfer coefficients are larger by orders of magnitude than the de-ethaniser. Therefore, following recommendation can be made :

" It is more beneficial to make design modifications to the overhead condensers of the de-propaniser and de-isobutaniser that would improve the effective heat transfer coefficients than it is in modifying the de-ethaniser ".

3.3 SUMMARY

Steady-state verification of the UCM based gas-tail model by comparisons with plant test-runs and rigorous SMBP simulations indicated that this approach can provide a reliable and computationally efficient steady-state model for multicomponent distillation columns. Optimisation studies were performed for the gas-tail using the UCM based model with significantly less computational effort than would be the case if rigorous column models were used. These studies revealed the optimal process conditions for the gas-tail and the potential benefits associated with such optimal operation. Constraint maps constructed using the optimisation results provided a good view of the limitations on the gas-tail performance over a wide range of operating conditions.

In the following chapters, a methodology for selecting a control scheme that would hold the gas-tail at the calculated optimum conditions will be presented. The dynamic version of the gas-tail model developed in this chapter will be used in these control studies.

CHAPTER 4

CONTROL SYSTEM SYNTHESIS

4.0 INTRODUCTION

Control system synthesis for chemical processes has become an important area of interest to both academics and industrialists in recent years. The issue of "control system synthesis " is a different one from "control system design ", as it involves developing an integrated and systematic framework for efficient control of a system of units. Although such an approach is necessary in meeting current demands on a control system, it is far from trivial and requires a good understanding of the process and its limitations. In this chapter, various issues associated with control system synthesis will be introduced.

4.1 BASIC CONCEPTS OF PROCESS CONTROL SYSTEMS

A chemical plant can be considered as an arrangement of units (such as reactors, distillation columns, pumps etc.,) whose purpose is to convert certain raw materials into desired products. The overall objective usually is to achieve a certain operational performance in the most economical way. To achieve this, a good understanding of the process and its behaviour is essential.

Many processes can be adequately described by a set of mathematical equations. Such a representation is usually called a mathematical model of the process. Any given process can usually be described by a range of models, varying both in complexity and in degree of accuracy achieved. The central role of modelling in control system synthesis will be addressed in later sections of this chapter. The following sub-sections deal with the terminology and basic concepts used in control system synthesis .

4.1.1 CLASSIFICATION OF VARIABLES IN A CHEMICAL PROCESS

The variables associated with the control of any process can be classified into two groups (Stephanopoulos, [1984]) :

(1) *Input variables* : Variables which have an effect on the process.

(2) *Output variables* : Variables which denote the response of the process.

The input variables can be further classified into the following categories:

(a) *Manipulated variables* : Variables which can be varied or adjusted freely by a human operator or a control system mechanism , so as to assist in the operation of the process.

(b) *Disturbances* : Variables that influence the process operation but are not under the control of an operator or a control mechanism.

Similarly, the output variables can also be classified into two categories :

(a) *Measured variables* : Variables that are known directly by their measurement on the process.

(b) *Unmeasured variables* : Variables that cannot be measured directly.

The following example illustrates all these types of variable associated with a chemical process.

Example 4. 1

Consider a simple distillation column with one feed and two product streams (see Figure 4. 1. 1). The major inputs influencing the process operation are the feed rate (F), the feed composition (X_F), the reboiler steam rate (S) , the condenser coolant flowrate (C) , the distillate product rate (D) and the bottoms product rate (B). . The effect of changes in these *inputs* is observed through changes in certain output variables such as the distillate composition (X_D), the bottoms composition (X_B), the column operating pressure (P) , the temperature on any tray etc.,. If the feed to the column (F) comes from upstream units , then it cannot be adjusted to meet the requirements of an operator or a control system and , therefore, forms a source of *disturbance* to the column. The same argument holds good for the feed composition (X_F). However, some of the input variables (such as the distillate product rate) can be adjusted (i.e. by opening or closing a control valve) according to our needs, and thus form a set of *manipulated* or *adjustable* variables for the column. Some of the output variables (such as the column pressure or the tray temperatures) can be measured directly and hence form a set of *measured* outputs. However, some output variables, especially those associated with compositions are frequently not measured because the instrumentation required (such as gas chromatography) is both expensive and often less than completely reliable. Therefore, all such output variables form a set of *unmeasured* outputs for the column.

Figure 4. 1. 2 summarises all these classes of variable associated with any given process. All these variables play a role in both the steady-state and the dynamic behaviour of the process. Identification of these variables, therefore, is one of the key issues in both process operation and control system synthesis.

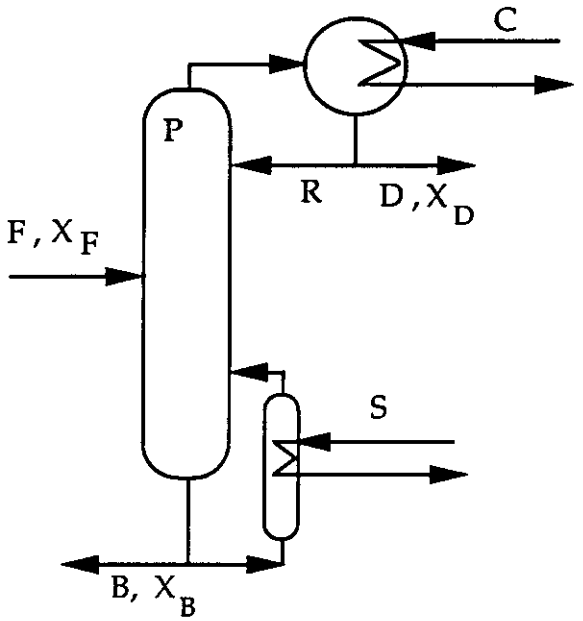

Figure 4. 1. 1
Schematic diagram of a distillation column

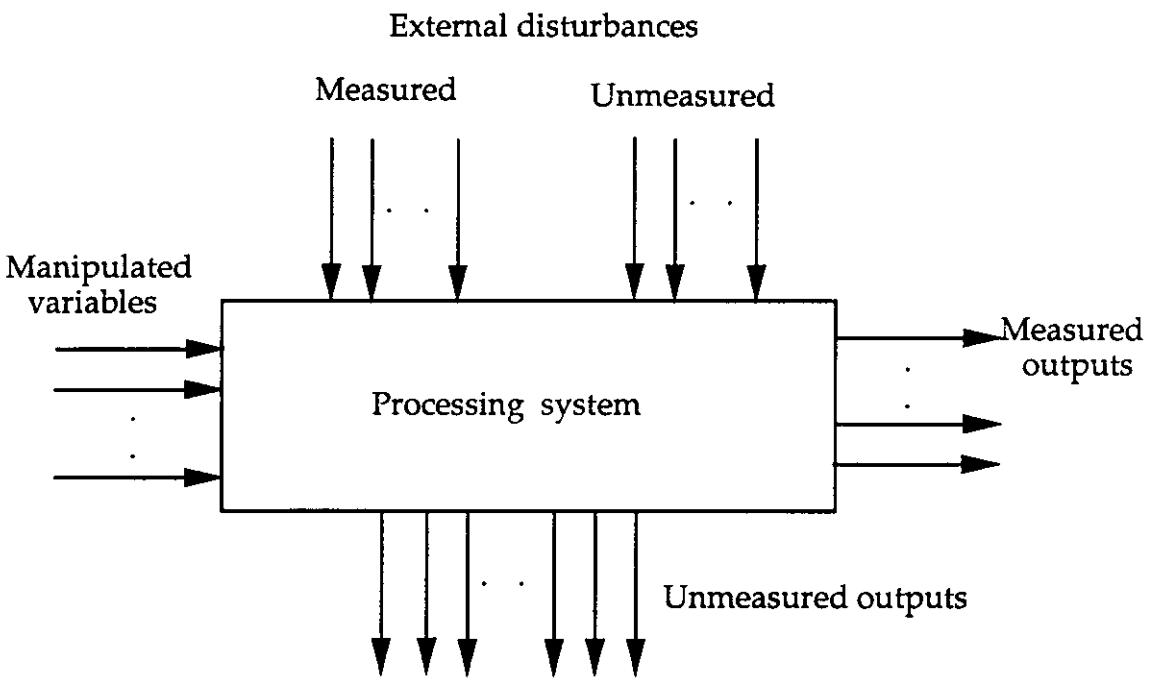

Figure 4. 1. 2
Types of variable associated with process operation
(Stephanopoulos [1984])

4.1.2 OBJECTIVES OF A CONTROL SYSTEM

A control system is necessary to meet some or all of the following general requirements associated with any plant and its operation.

(1) Safety
(2) Product quality specifications
(3) Environmental regulations
(4) Operational constraints
(5) Economics

Due to changes in these requirements and the continuous influence of external disturbances on the plant, the process operation changes with time. Thus, a control system should provide the potential for achieving the following objectives.

(1) To hold the plant at an economic optimum while providing good regulatory control at this operating point.

(2) To allow rapid (minimum cost) movement to a new optimum once such a new set of operating conditions have been identified.

(3) To suppress the influence of any external disturbances on the process, whatever the operating point.

(4) To ensure the stability of the process , whatever the operating point.

(5) To ensure safe operation in the face of a wide range of failures - both within the process and within the control scheme.

(6) To handle automatically a wide range of abnormal situations such as start-up and shut-down (both normal and emergency).

Ideally a control system should meet all the objectives stated above. The aim of control engineers , therefore, is to develop an approach to the design of control systems that provides the best performance with reference to these objectives.

4.1.3 TYPES OF CONTROL CONFIGURATIONS

The basic aim of a control system , at least in a conventional sense, is to hold various process variables at pre-determined set-points, provided by the user. Thus, such a control system consists of measurements , set-points and manipulated variables (see Figure 4. 1. 3). The information structure formed by connecting the various components of the control system is usually termed " a control configuration" or " a control structure".

Depending on the number of controlled outputs and manipulated inputs there are in the process, the control configuration can be differentiated into *single-input single-output* (SISO) and *multiple-input multiple-output* (MIMO) control systems. For example, if the objective in any one of the tanks (see Figure 4. 1. 4) is only to regulate the tank level using the outlet flow from the tank , then we have a SISO system. In a distillation column (see Figure 4. 1. 1) , on the other hand , if our objective is not only to regulate the distillate composition (X_D), but also to simultaneously control the bottoms product composition (X_B), as well as the liquid levels in both the condenser accumulator and the reboiler, then we have a MIMO system.

In the chemical industry most of the processes are MIMO systems. However, much of the control theory available in the literature was originally developed for SISO systems and then extended to MIMO systems (Ray [1981]), though such an extension has often not always been straightforward. This has happened because the concepts related to controller design are relatively simple to understand and easy to implement in the case of SISO systems.

Two different control configurations are common in process control. They differ, primarily, in the arrangement of the various components that form the control system. The objective in both configurations, however, is common, i.e. to keep the controlled variables at the desired set-points when the process is subjected to external disturbances.

(1) Feedback control configuration :

In this configuration , the measurements of the output controlled variables is directly used to adjust the values of the manipulated variables (see Figure 4. 1. 5). For example, control of both the tank levels (see Figure 4. 1. 4) using the product flowrates is a feedback control policy, as each liquid level is measured directly and any deviation from the set-point is used to adjust the product flowrate.

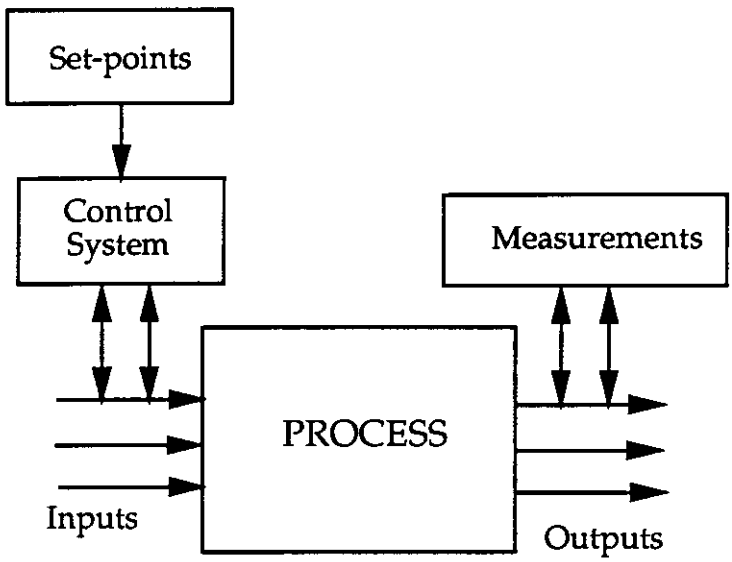

Figure 4. 1. 3
Components of a control system

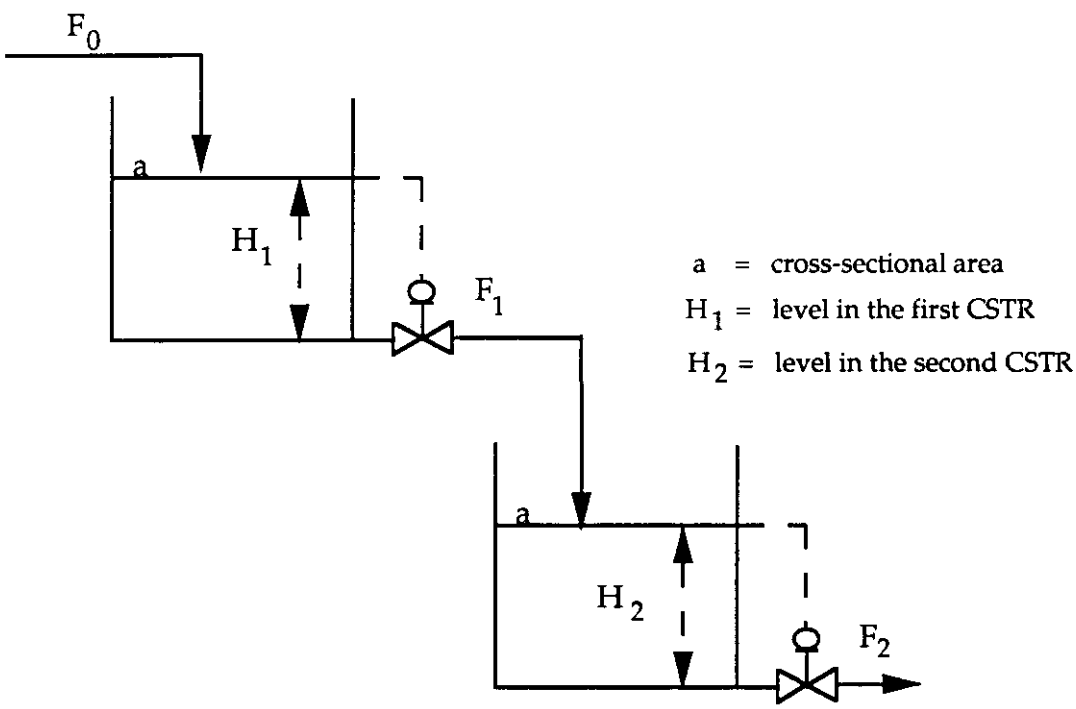

Figure 4. 1. 4
Schematic diagram of level control in two tanks in series

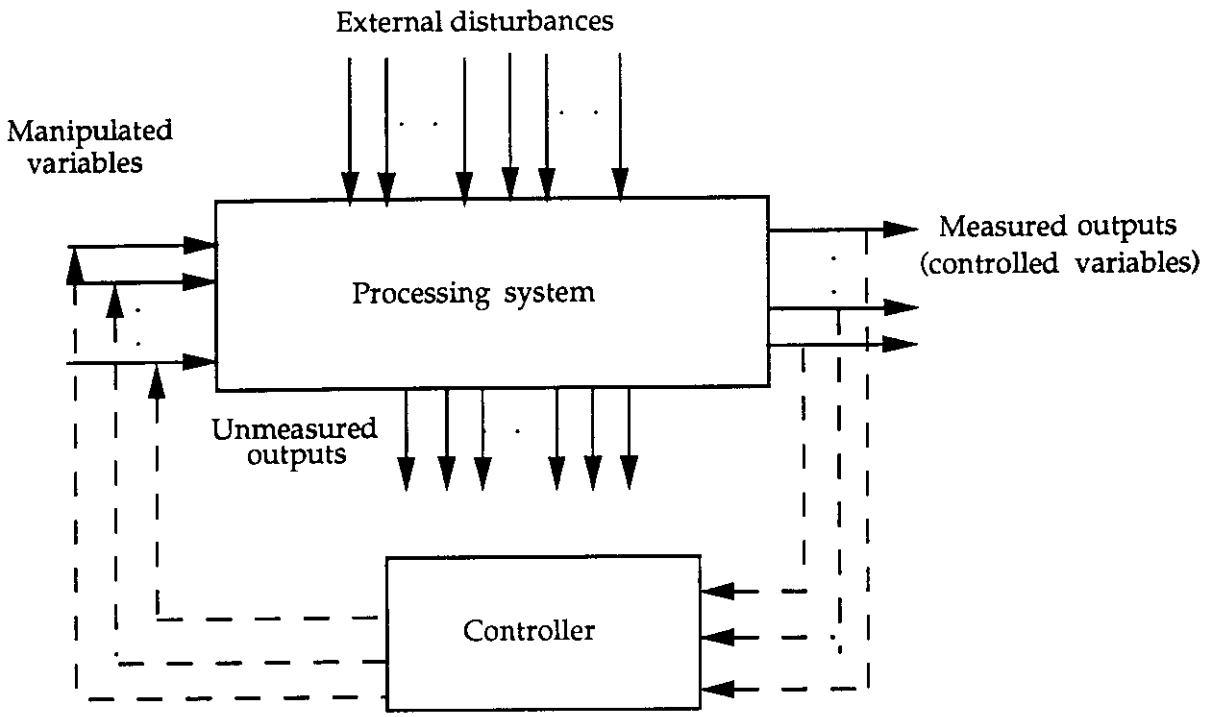

Figure 4.1.5
General structure of a feedback control configuration
(Stephanopoulos [1984])

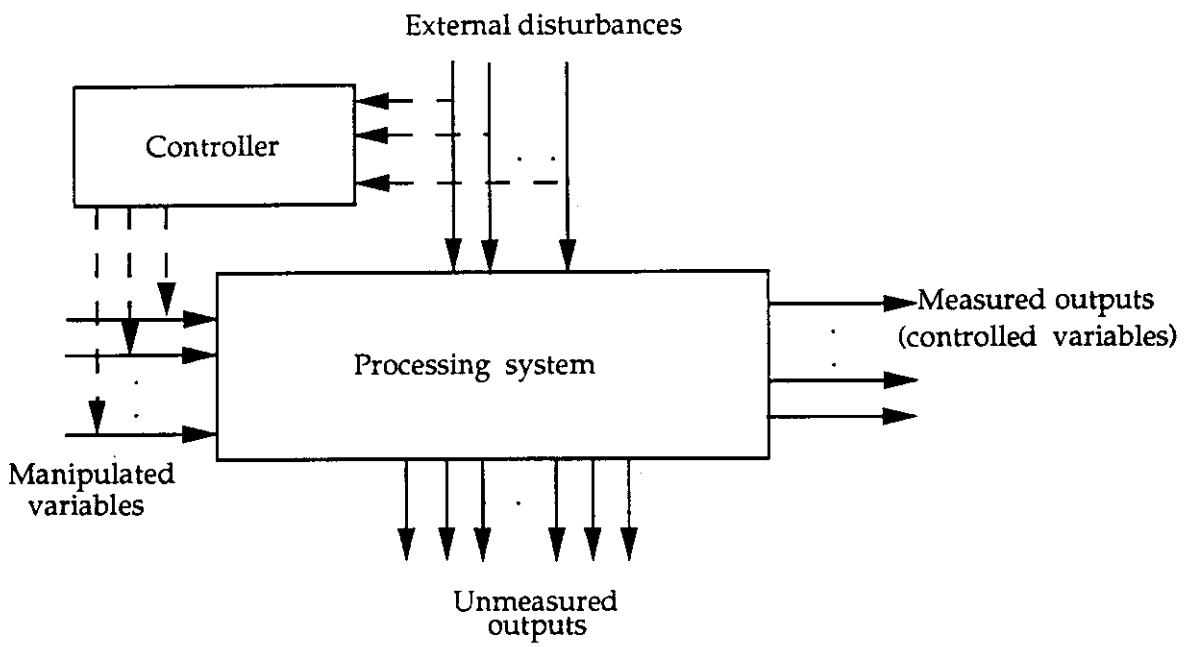

Figure 4.1.6
General structure of a feedforward control configuration
(Stephanopoulos [1984])

(2) Feedforward control configuration :

This approach uses direct measurement of some disturbances to adjust the values of the manipulated variables (see Figure 4. 1. 6). For example, this approach can be used to hold the distillate composition constant in a distillation column (see Figure 4. 1. 1). The disturbance measurement (say of the feed rate **F**) is used in estimating the extent of deviation it would have caused in the distillate composition if it was not corrected for, and then the distillate product rate is adjusted accordingly. This is done before the disturbance effect is actually felt in the distillate composition.

Note that in feedback control configurations, the control action is taken after the effects of the disturbances have been felt. However, in feedforward control configurations , control action is taken even before the disturbance enters the process. Both of these control configurations have certain advantages and disadvantages . A fuller discussion of both configurations is given elsewhere (see Stephanopoulos [1984], Shinskey [1988]). Feedback control configurations will be used in the case-study.

4. 1. 4 TRANSFER FUNCTIONS

An important tool in the study of dynamic systems represented by linear differential equations is the Laplace transform. For a continuous function **f (t)** , the Laplace transform is defined as follows:

$$F(s) = \int_0^\infty e^{-st} f(t)\, dt \qquad (4.1.1)$$

where **s** is a complex variable,

F (s) is called the Laplace transform of **f (t).**

The primary advantage of Laplace transforms is that differential equations in the time domain can be converted into algebraic equations in the Laplace domain, the manipulation of which is straightforward.

A relationship between an input and output in the Laplace domain is called a "transfer function ". The complex variable "s " can be related to the frequency induced changes in the dynamic system if the following substitution is used(Stephanopoulos [1984], Luyben [1990]):

$$s = j\,\omega \qquad (4.1.2)$$

where " j " is the square root of minus one and "ω" is the frequency.

Transfer functions generally represent a set of linear relationships between the inputs and the outputs of a nonlinear process model. The transfer function representation , therefore, is strictly valid only in the neighbourhood of the steady-state about which the linearisation was performed. In the case of MIMO systems, this set of relationships between various inputs and outputs can be represented through a matrix , called the transfer function matrix. The concept of transfer functions is an important tool in the control synthesis/design of both SISO and MIMO control systems.

The following example illustrates the transfer function relationships for a (2 X 2) control system i.e. a control system with two inputs and two outputs.

Example - 4.2

Consider the CSTR shown in Figure 4. 1. 7. The reactor temperature is using through the coolant flowrate in the jacket while the effluent concentration is controlled by manipulating the inlet flowrate. A nonlinear process model for such a CSTR can be obtained through an overall energy balance and a component mass balance (Stephanopoulos [1984]). The (linear) transfer function matrix relating both the controlled variables to both the manipulated variables is given below ;

$$\begin{bmatrix} y_1 \\ y_2 \end{bmatrix} = \begin{bmatrix} \dfrac{K_{11}}{(\tau_{11} s + 1)} & \dfrac{K_{12}}{(\tau_{12} s + 1)} \\ \dfrac{K_{21}}{(\tau_{21} s + 1)} & \dfrac{K_{22}}{(\tau_{22} s + 1)} \end{bmatrix} \begin{bmatrix} m_1 \\ m_2 \end{bmatrix}$$

where

y_i = is the i^{th} controlled variable for all i = 1, 2.

m_i = is the i^{th} manipulated variable for all i = 1, 2.

K_{ij} = is the steady-state gain between the i^{th} controlled variable and the j^{th} manipulated variables

τ_{ij} = is the first-order time constant for the transfer function relating the i^{th} controlled variable and the j^{th} manipulated variables.

Each element of the transfer function matrix represents the dynamics between a controlled and a manipulated variable.

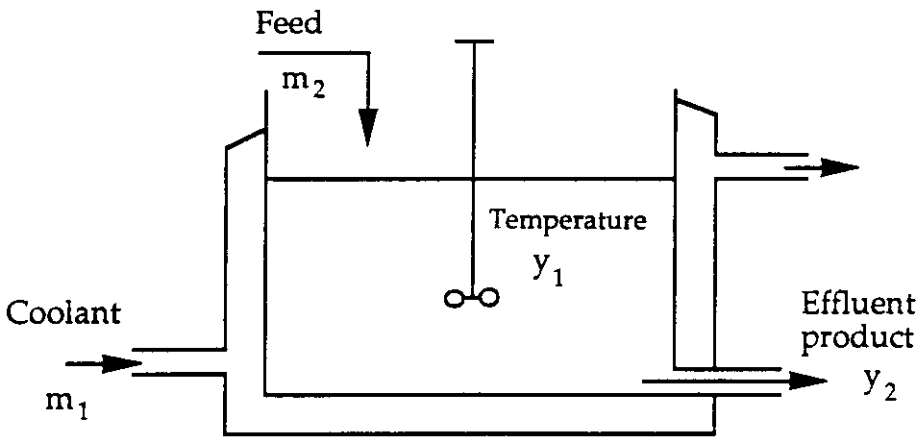

Figure 4. 1. 7
CSTR with a cooling jacket

POLES AND ZEROS OF A SYSTEM

The nonlinear dynamics exhibited by a system is often very difficult to comprehend. For linear systems, however, the dynamics can be associated with certain properties of the system. Of all such properties, the "poles" and "zeros" of the transfer function are the most important.

Frequently , the transfer function G (s) will be in the form of a ratio of two polynomials.

$$G(s) = \frac{Q(s)}{P(s)} \qquad (4.1.3)$$

The roots of the polynomial in the denominator (**P (s)**) are called the "poles" of the system , while the roots of the polynomial in the numerator (Q (s)) are called the "zeros" of the system. MacFarlane and Karcanias [1976] have made an excellent survey on the various definitions adopted in the literature and the various physical interpretations used for both poles and zeros. Their survey covered both SISO definitions for poles and zeros with extensions to MIMO systems. The literature on the role of poles and zeros in both system dynamics and control system design is extensive (see MacFarlane and Karcanias [1976] for additional references). The following simple example illustrates some of these concepts.

Example 4. 3 :

Consider the following transfer function ,

$$G(s) = \frac{(s+2)}{(s+3)} \qquad (4.1.4)$$

Both the numerator and the denominator are first-order polynomials . The roots of each polynomial(when put equal to zero) can be obtained as;

Denominator	:	$s + 3 = 0$	$s = -3$ represents the pole of the system.
Numerator	:	$s + 2 = 0$	$s = -2$ represents the zero of the system.

The transfer function can be interpreted as the way in which information is propagated through the system. Since " s " represents a complex variable, both the zero and the pole can be thought of as mappings of this variable in the complex plane. As we see here, the transfer function goes to infinity as when complex variable takes on a numerical value equal to - 3 (i.e. at the pole of the system). In other words, a pole represents " the frequency at which the system resonates with infinite amplitude ". Similarly, when "s " takes on a numerical value of for a frequency of - 2 , the transfer function of the system is zero. This can be interpreted as corresponding to a " frequency for which the information flow through the system is blocked ".

Both poles and zeros have been variously interpreted and used extensively throughout the control literature (Holt and Morari [1985]). Some of the major properties and results associated with these interpretations are listed below ;

(1) The order of the polynomial in the denominator indicates the order of the system. For physically realizable systems, the polynomial of the numerator **Q (s)** will always be of lower order than the polynomial of the denominator **P (s)** .

(2) In the case of SISO systems , poles can be interpreted in the time domain as the time constants of the dynamic system (Levy et al. [1969]). Poles in the case of MIMO systems have a similar physical interpretation. For any systems modelled by a state-space equation (see Section 2. 4. 2), the poles of the system are given by the eigenvalues of the state matrix (i.e the matrix **A**).

(3) Stable systems have all their poles lying in the left half of the complex plane. Poles lying in the right half of the complex plane lead to instability in the system behaviour. The location of the zeros in the complex plane have no such interpretation. However, they do affect the dynamics of the system, but in a more complex way. Zeros of the system lying in the right half of the complex plane (called RHP zeros), result in an inverse dynamic response and can provide considerable difficulties when a control system is implemented (see Section 2. 4).

(4) The closed-loop poles (i.e poles of the system and a controller, together) of a system can be moved around in the complex plane using a suitable controller and hence, even systems that are open-loop unstable can be made closed-loop stable using a suitably designed controller. Zeros, on the other hand, are inherent to the nature of the system and cannot be shifted or moved around using a controller (Holt and Morari [1985]). They can only be changed by changing the system itself.

(5) Closed-loop poles determine the speed of the transient response of the controlled system.

Most of the properties discussed above for poles and zeros hold good for both SISO and MIMO systems.

4.2 TRADITIONAL APPROACH TO THE SYNTHESIS OF CONTROL SYSTEMS

It was discussed in the previous section that control systems, in general, can be categorised as either SISO O or MIMO . The obvious difference is that, in the latter case, more than one output of the system needs to be controlled with more than one manipulated variable. MIMO systems are more common in the chemical industry. Control system synthesis for MIMO systems is usually determined by the general character of the control system. Following are the two commonly encountered types of system :

(a) *Multiloop system* , where the control system is essentially a network of SISO loops, with each loop controlling one of the control objective.

(b) *Multivariable system* , where all the available inputs are used simultaneously to control all the control objectives. Usually such an approach uses a model-based controller, i.e. the controller relies on a process model to help calculate the necessary corrective action .

Each of these types of MIMO control systems will be discussed in greater detail after the following section.

4.2.1 SISO CONTROLLER SYNTHESIS

As noted above, multiloop systems are essentially a collection of SISO controllers. The control literature (for example, Stephanopoulos [1983]) is filled with various approaches that can be used for the synthesis of SISO systems. Many of these approaches are based on frequency analysis of the process transfer function. Feedback control is the most common mode of control for SISO systems. The "traditional " synthesis approach can be summarised into the following sequence of stages (Stephanopoulos [1984], Luyben [1990]);

(1) Identify the input and output variables and obtain the transfer function relating the selected inputs and outputs.

(2) Choose the type of controller to be used. A proportional -integral (PI) controller is generally adequate for most SISO systems.

(3) Tune the controller (i.e. obtain the various controller parameters) to ensure both stability and performance. Various tuning methods are available (Stephanopoulos [1984], Luyben [1990] ; Ziegler-Nichols , for example) .

Although feedback control is simple and is the type most commonly encountered in the chemical industry, there exist situations where feedback control alone is inadequate to produce the desired control of a given process (Stephanopoulos [1984]). More advanced SISO controllers can be adopted in all such cases, such as dead-time compensatory control (Smith[1957], Shinskey [1988]), feedforward control (Stephanopoulos [1984], Luyben [1990]) , adaptive control (Narendra and Monopoli [1980], Landau [1979]) , inferential control (Shinskey [1978]) and cascade control (Shinskey [1988]).

In summary, all these techniques provide a fairly systematic methodology for controller design in the case of SISO systems. However, design of a control system in a SISO case is made relatively simple by the fact that there is (generally) only one input and one output.

4. 2. 2 MIMO CONTROLLER DESIGN

The design of MIMO control systems is considerably complicated by the fact that there is now more than one input and output and consequently a variety of possible control configurations. Some of the more general issues that complicate MIMO controller design are (Stephanopoulos [1984]) ;

(a) *What are the control objectives ?* Which of the (possibly many) process variables need to be held constant during operation.

(b) *Which outputs should be measured ?* Which of the possible primary and secondary (i.e inferred or estimated) variable measurements are necessary and/or adequate for implementation of good control.

(c) *Which manipulated variables should be used ?* How to identify the major inputs that can be used as manipulated variables so as to achieve good control performance.

(d) *Is multiloop control adequate ?*

(e) *Which control configuration is required for multiloop control ?* This requires a means of deciding which of the control objectives should be controlled by which of the manipulated variables.

MULTILOOP CONTROLLERS

Multiloop controllers are one form of MIMO control systems. There are two major characteristics that are specific to such multiloop control systems and which are of interest to us;

(a) Such a control system is composed of several interacting SISO systems.

(b) The number of feasible , alternative control configurations (i.e input-output pairings) , is usually large.

Thus, the major questions that need to be answered so that we can effectively design multiloop control systems are :

(1) *What policy do we use for pairing the controlled and manipulated variables , such that the resulting control loops co-exist with as little or no interaction amongst themselves as possible ?*

(2) *If harmful interactions amongst the control loops cannot be avoided, then how do we counteract these effects ?*

The first question is to do with interaction analysis and the selection of a multiloop structure that minimises the loop interactions. This topic has been of great interest to both industrialists and academics over several decades. Bristol [1966] introduced an index, called the relative gain array (RGA) to develop qualitative arguments about the interactions between the control loops. RGA will be discussed in more detail in the following section. The estimation of this index was initially based on steady-state gain information between the various inputs and outputs. Despite its limitations, this index has been the most widely used measure of interaction in control loops, particularly in industry. Other measures of interaction that are useful, but have found only a limited use, are interaction coefficients (Rijnsdorp [1965]), the average dynamic array (Gagnepain and Seborg [1979]), and a dynamic extension of the RGA called a relative dynamic gain array (Witcher and McAvoy [1977], Bristol [1978] , Tung and Edgar [1981]). Jensen et a., [1986] give a more complete review of the status of interaction measures. Chang and Davison [1986,1987] have also developed a more generic set of steady-state interaction indices based only on steady-state process information.

Bristol's [1966] relative gain array is by far the most frequently quoted interaction measure, hence its rationale and the limitations will now be explained.

RELATIVE GAIN ARRAY

Consider a two input two output system. Figure 4. 2. 1 and Figure 4. 2. 2 show the input - output relationships for such a system with and without controllers, respectively. The following terminology is used to describe both these systems :

y_i	are the outputs/controlled variables.
m_i	are the inputs/manipulated variables.
H_{ij}	are the process transfer functions relating the inputs and outputs.
G_d	for $i = 1, 2$ are the controller transfer functions.

The mathematical form of the input-output relationships is given by ;

$$y_1(s) = H_{11}(s)\, m_1(s) + H_{12}(s)\, m_2(s) \qquad (4.2.1)$$

$$y_2(s) = H_{21}(s)\, m_1(s) + H_{22}(s)\, m_2(s) \qquad (4.2.2)$$

One of the major issues in a multiloop feedback control policy is concerned with, *which of the inputs should be paired with which of the outputs, so as to have the minimum interaction between the various control loops.* Bristol [1966] suggested that the inherent interactions between various control loops are reflected through the changes in the values of the gains between inputs and outputs with and without the loops being closed (see Figure 4. 2. 2). A dimensionless number known as the *relative gain* (usually denoted by λ), which is a ratio of two open-loop gains, was introduced.

Each of these relatives gain elements can be interpreted as a measure of the interaction between the loops (Stephanopoulos [1984], Luyben [1990]). A matrix containing all such gains, called the relative gain array (RGA), can be constructed as shown below for the 2 X 2 case :

$$\Lambda = \begin{array}{c} \begin{matrix} m_1 & m_2 \end{matrix} \\ \begin{bmatrix} \lambda_{11} & \lambda_{12} \\ \lambda_{21} & \lambda_{22} \end{bmatrix} \end{array} \begin{matrix} y_1 \\ y_2 \end{matrix} \qquad (4.2.3)$$

One important feature of the RGA is that

The sum of the relative gains in a row or a column can be shown to be unity, i.e.

$$\lambda_{1i} + \lambda_{2i} = 1.0 \qquad (\text{for all } i = 1, 2) \qquad (4.2.4)$$

$$\lambda_{i1} + \lambda_{i2} = 1.0 \qquad (\text{for all } i = 1, 2) \qquad (4.2.5)$$

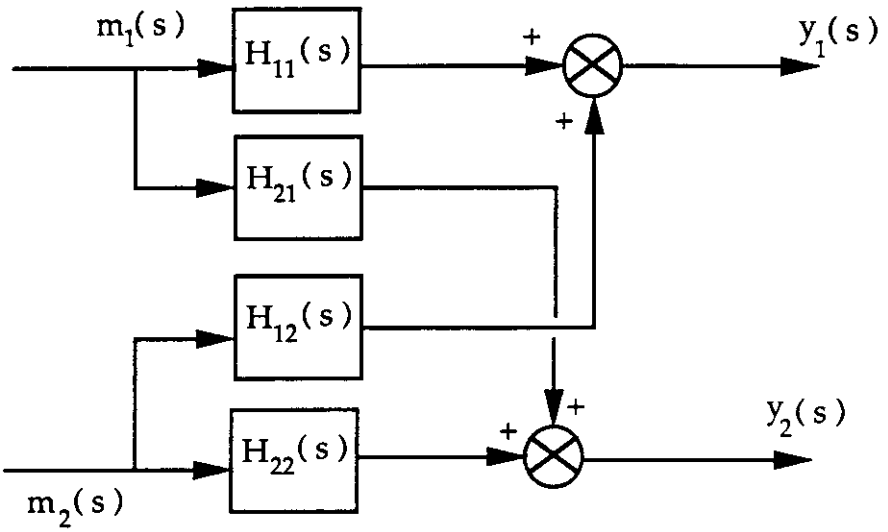

Figure 4. 2. 1
Block diagram representation of a (2 X 2) control system
(Stephanopoulos [1984])

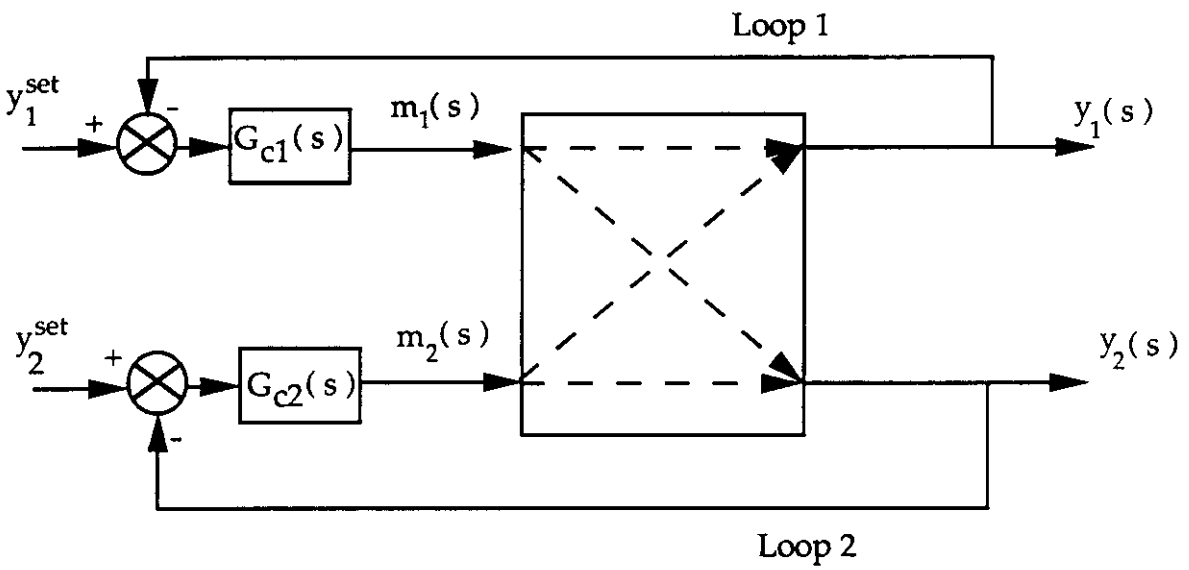

Figure 4. 2. 2
Block diagram representation of interactions in a
(2 X 2) control system (Stephanopoulos [1984])

In a system with two control loops (see Figure 4. 2. 2) , a relative gain element value of unity implies that the corresponding control loop does not interact with the remaining control loop (Bristol [1966]). Therefore,

Always choose a pairing that has a relative gain element as close to unity as possible.

Thus for a (2 X 2) case , it is sufficient to know one of the relative gains ,as the rest of them can be determined using Equations (4. 2. 4) and (4. 2. 5). This can be clearly seen through the following illustrative example.

Example 4. 4.

Consider a (2 X 2) system where the RGA has the following form ;

$$\Lambda = \begin{array}{c} \begin{matrix} m_1 & m_2 \end{matrix} \\ \begin{bmatrix} 0.9 & 0.1 \\ 0.1 & 0.9 \end{bmatrix} \end{array} \begin{matrix} y_1 \\ y_2 \end{matrix} \qquad (4.\ 2.\ 6)$$

From the above rule, it is clear that pairing m_1 with y_1 and m_2 with y_2 should result in the minimum interaction between the loops.

The following are some of the proposed extensions and noted limitations of the RGA.

(1) The original RGA was claimed to provide a measure of interaction amongst control loops, but is based only on steady-state information. No information about the " dynamic interactions " can be obtained. Tung and Edgar [1981] developed an interaction index that essentially is a dynamic extension to the original RGA.

(2) RGA is applicable only to square systems i.e where there are equal numbers of manipulated and controlled variables.

(3) Each of the elements of the RGA represents a ratio of two steady-state gains and hence is a dimensionless number. RGA elements , therefore, are insensitive to scaling (Grosdidier et al. [1985]) or independent of the physical units used for both inputs and outputs.

(4) RGA is a linear interaction measure and is often obtained by linearising a nonlinear model about a known steady-state. Being linear based, the RGA will be affected by nonlinearities and large movements away from the original operating conditions.

(5) The application of RGA is not just limited to (2 X 2) systems but can be extended to systems of higher order (Shinskey [1988], Grosdidier et al. [1985]). The extension to higher order systems is very simple and can be summarised as follows;

$$\Lambda = \begin{bmatrix} \lambda_{11} & \lambda_{12} & . & \lambda_{N1} \\ \lambda_{21} & \lambda_{22} & . & \lambda_{N2} \\ . & . & . & . \\ . & . & . & . \\ \lambda_{N1} & \lambda_{N2} & . & \lambda_{NN} \end{bmatrix} \qquad (4.2.7)$$

where λ_{ij} is the relative gain array element between the ith output (y_i) and the jth input (m_j) given by ,

$$\lambda_{ij} = \frac{(\partial y_i / \partial m_j)_m}{(\partial y_j / \partial m_j)_y}$$

where, once again the sum of any row or column is unity.

However, there is no rigorous mathematical proof that supports the applicability of RGA as a measure of interaction to systems of order other than two.

(5) For completely decoupled systems the RGA is an identity matrix (Grosdidier et al. [1985]).

(6) In a multiloop control system , even though the performance of individual control loops after tuning may be quite satisfactory, the overall system can sometimes go unstable when all loops are operated together. The interacting controllers create conditions which can destabilise an otherwise stable system Grosdidier et al. [1985], (Shinskey [1988]). Using semi-quantitative arguments, Shinskey [1977, 1988] showed that the RGA can be used as a measure of system stability as well as a measure of system interaction. Grosdidier et al. [1985] provided a more rigorous relationship between the RGA and system stability.

(7) Grosdidier et al. [1985] also established a mathematical relationship between the RGA and the minimum condition number , the latter being a measure of system sensitivity to plant- model mismatch,

$$\gamma^* = \|\Lambda\|_1 + \sqrt{(\|\Lambda\|_1^2 - 1} \qquad (4.2.8)$$

where γ^* is the minimum condition number

Λ is the relative gain array matrix ; the subscript "1 " shows that an l_1 - norm of has been taken (see Section 4. 3. 5).

$\gamma^* = 1.0$ if $\lambda_{ij} = 1$

$\gamma^* = 2(\Lambda)$ if $\lambda_{ij} = \infty$

Such a relationship was originally developed for 2 X 2 systems. The analysis was extended to higher order systems , but only on the basis of a large number of numerical experiments and no analytical expression was developed for such higher order systems. All their results are in full agreement with the results of Shinskey [1977, 1988] . The conclusion was that 'large elements in the RGA are indicators of "practically uncontrollable" systems ' . A more complete analysis of the RGA as a measure of a system's controllability (see Section 4. 3. 2 for definitions of controllability) with respect to model and controller uncertainty, has been provided by Skogestad and Morari [1986].

It conclusion, it has been shown that the RGA can be used as a measure of the interaction between control loops , a measure of a system's stability and also as a measure of the likely control system performance , at least in a qualitative sense. Despite criticism, the RGA has found widespread use and acceptance in industry.

DECOUPLING

In some instances, interaction is still significant amongst the " best choice " of control loops. It may then be necessary to employ a means of reducing these interactions. The essence of decoupling is the provision of a controller which will essentially cancel out the interactions, permitting "independent" single-loop control [(Shinskey [1988]). Though the rationale behind decoupling looks promising in a theoretical sense, its practical implementation has it's own limitations (Shinskey [1988]).

Decoupling can be better understood through the following discussion. Consider a 2 X 2 system (see Figure 4. 2. 3) with both the inputs influencing both the outputs. The effect of the second input (m_2) on the first input (y_1) is given by the transfer function H_{12} (see Equation 4. 2. 1). In order to keep y_1 constant, despite changes in m_2 , we need to take additional corrective action in m_1 such that it cancels out the effect due to m_2. The amount of corrective action needed is given by ,

$$m_1(s) = \frac{H_{12}(s)}{H_{11}(s)} m_2(s) = D_1(s) \qquad (4.2.9)$$

$D_1(s)$ in the above expression represents transfer function of the decoupler.

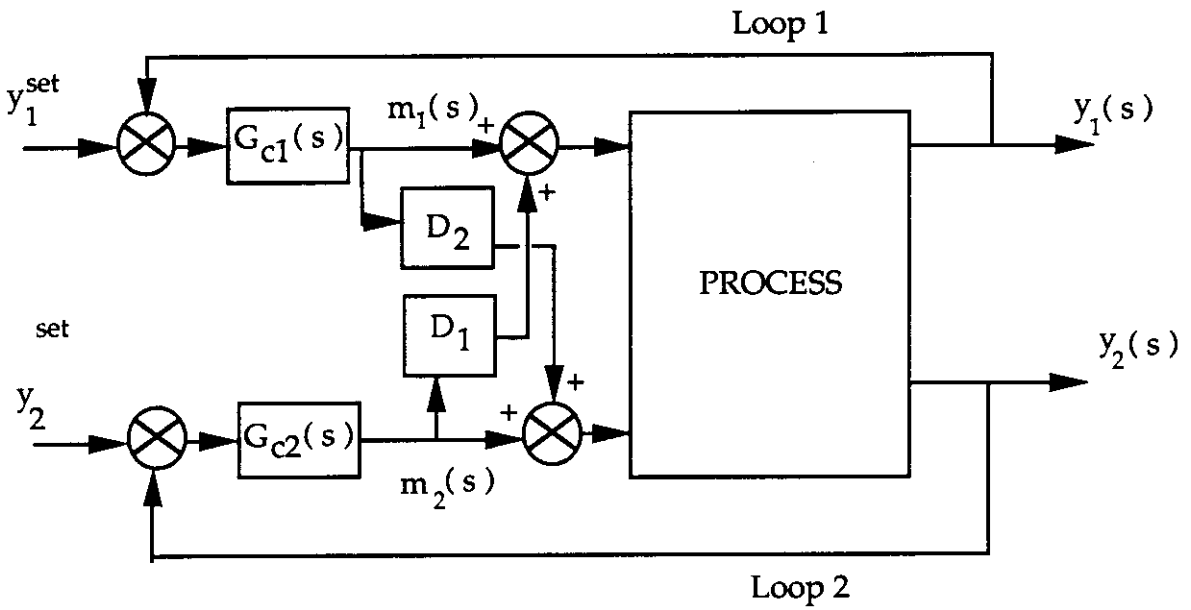

Figure 4. 2. 3
Block diagram representation of a 2 input 2 output control system with two decouplers (Stephanopoulos [1984])

Similarly, we can introduce another decoupler for the second loop, so that the influence of changes in m_1 on y_2 are nullified (see Figure 4. 2. 3). The following are some of the properties of decouplers :

(1) Decouplers are essentially feedforward control elements.

(2) Since the design of a decoupler requires a good (linear) process model (see Equation 4. 2. 9) both in normal and inverted forms (see Section 4. 3. 3 for a related discussion on Internal Model Control) , it can become susceptible to plant-model mismatch. Therefore, only partial decoupling is generally possible in practice, leaving weak interactions amongst the various loops.

(3) If the decouplers are designed using steady-state process models then they are known as *steady-state* or *static decouplers* . They are termed *dynamic decouplers* if dynamic process models are used. It has been observed that for severely interacting loops, even static decoupling is better than no decoupling at all (Stephanopoulos [1984]).

MULTIVARIABLE CONTROLLERS

Alternatively, with MIMO systems, we can take the necessary control action using all the input variables together. Such an approach is usually known as a *multivariable control policy* and generally requires detailed information about the process in the form of a mathematical model, or the relationships between the inputs and outputs. This approach is relatively difficult to implement compared to a multiloop control system. However, multivariable control should not have any problems with respect to loop interactions, since the interactions are implicitly taken care of by the control system . Implementation of model-based multivariable controllers usually requires considerable computational power and was not really possible until quite recently. High performance multivariable controllers are now becoming reasonably common in industry.

Model-based (linear) multivariable controllers that have been implemented, to date, include :

(a) Internal Model Control (Garcia and Morari [1982]).
(b) IDCOM (Shinskey [1988]).
(c) Dynamic Matrix Control (Cutler and Ramaker [1979]).
(d) Model Algorithmic Control (Rouhani and Mehra [1982]).

All of these controllers employ a linear model to represent the process and have demonstrated superior performance over the traditional (i.e. multiloop control and its enhancements) techniques for control on a variety of chemical processes. Several attempts have been made to extend these linear approaches to nonlinear processes by suitable modifications (McDonald [1987]). One model-based multivariable controller that has shown considerable potential for application to nonlinear processes is due to Lee and Sullivan [1988] , and is called Generic Model Control (GMC). Many of these model-based approaches use reduced-order dynamic models for use in the control of a process.

Model-based control is used only for the economically important , but hard to control process units. In general, all these model-based multivariable controllers are expensive (frequently in development and implementation time), and must operate in conjunction with multiloop controllers to provide a complete control system for large plants.

4.3 CONTROL SYSTEM SYNTHESIS

In the previous sections , the general methodology of control system design for single process units has been discussed. As pointed out in Section 1. 1 , the emphasis over the last two decades has been to design control systems for a complete process flowsheet. In the following sections a brief review of the methods available , to date, for such a " synthesis " approach will be given along with some of the major issues that still need to be addressed.

4. 3. 1 METHODS FOR CONTROL SYSTEM SYNTHESIS

Various researchers have attempted to develop a systematic methodology for control system synthesis. Buckley [1964] pioneered this work. He considered the decomposition of the control objectives for each processing unit into two categories (see Figure 1. 2. 1):

(a) Material balance control.
(b) Quality control.

Through this decomposition of control objectives, he showed that the design of an overall process control system for each type of control objective can be considered separately. Material balance control is concerned chiefly with low frequency (i.e slow) disturbance control, while quality control is concerned primarily with the high frequency (i.e. fast) disturbances. The value of this approach has been that it is both simple to understand and easy to implement.

Different approaches used more recently for control system synthesis include (Russell [1987]) :

(1) A Hierarchical approach (Umeda et al. [1978]).

(2) An approach based on simple models and economic evaluation (Douglas [1980]).

(3) The use of cause-and-effect graphs (Govind and Powers [1982]).

(4) A " unified approach" for control system synthesis (Morari et al. [1980]).

(5) The use of structural methods (Johnston and Barton [1985a,b]).

Each of these approaches will be discussed briefly here .

HIERARCHICAL APPROACH

A two level hierarchical approach was proposed by Umeda et al. [1978] using the principle of system decomposition (Mesarovic et al. [1970]). Here, one is concerned with the regulation of individual units (or a group of units with a common objective) in the lower level of the decomposition. The set-points for these controllers are , however, decided on at a higher level which interacts with the lower level from time to time. Due to the possibility of control conflicts between the decomposed units, an iterative approach is required. Umeda et al. suggested a structural (i.e. non-numerical) approach to eliminate unfavourable alternatives obtained from the decomposition, along with numerical methods and heuristics (based on operational experience) to decide on the final control system design. The approach considered both steady-state and dynamic aspects, and an extensive survey was made in each case to arrive at appropriate heuristics. Thus, after Buckley [1964]) their approach was the first of its kind that provided a consistent approach to control system synthesis. However, the following are some of the major criticisms of this approach (Stephanopoulos [1983) :

(a) The higher level task is not well defined.

(b) The decomposition is arbitrary or relies on heuristics.

(c) Due to it's strong dependence on heuristics, such an approach is not really suitable for inclusion in a computer-based procedure for control system synthesis.

APPROACH BASED ON SIMPLE MODELS AND ECONOMIC EVALUATION

A hierarchical economics based approach was proposed by Douglas [1980,1981] which uses process models of varying complexity at different levels of the design procedure. The key disturbances and control variables are identified using an order of magnitude steady-state analysis and an estimate of the economic optimum is obtained using a simple process model. Given satisfactory results on the potential economic benefits , dynamic modelling and controller design are then considered. Simplifying assumptions and reduced-order

dynamic models that provide a reasonably accurate description of the process performance over the range of operation of interest are used at all levels.

The procedure described by Douglas would be appropriate at the early process design stage, and is unique in its inclusion of economic issues in control system synthesis. Some of the concepts of this approach were adopted in a more systematic and unified approach to control system synthesis (Morari et al. [1980]). The major drawback of this approach is that it does not address the issue of process control explicitly at the various levels in the process design. Instead, the emphasis is on identifying the manipulated variables that could be used to regulate the control objectives. Also , there is no systematic method for selecting the control objectives at the various levels of the design procedure. It must also be realised that the emphasis in this approach really is on process design rather than control system design.

CAUSE - AND - EFFECT GRAPHS

Govind and Powers [1982] proposed an approach for control system synthesis based on three major ideas :

(a) The generation of candidate control structures using cause-and-effect diagrams.
(b) The evaluation of alternative control structures based on their feasibility, ease of measuring the controlled variables involved and both steady-state and dynamic heuristics.
(c) The use of simple models relating the process variables.

The control synthesis procedure is divided into three major control sub-tasks, dealing with the issues (i) the identification of possible ways of measuring any constraint variable (which are related to the control objectives), (ii) identifying possible ways of influencing the constraint variables using the available manipulated variables, (iii) the generation of a set of alternative control schemes based on structural (i.e. non-numerical) considerations. A structural cause-and-effect diagram is used as a basis for the generation of alternative control schemes. Screening of these alternatives can take place at various levels of complexity. In the primary stage of screening, heuristics such as known physical limitations and operational experience can be used to reduce the number of alternatives. The remaining possibilities are then further screened using simple process characteristics such as the steady-state gains, time delays and dominant time constants between the measurements and manipulated variables.

The major concepts introduced by this approach include the systematic use of structural information and the use of numerical information to reduce the number of control structure

alternatives at an early stage. Despite some deficiencies , the approach of Govind and Powers provided a significant advancement in the perception of the problem of control system synthesis. However, there are still some of the major weakness in this approach (Stephanopoulos [1983]) are :

(a) Its inability to identify a lack of structural controllability (see Section 4. 3. 2, for definition) introduced by process integrators such as a holdup in a tank.

(b) It does not allow for a multivariable control structure being oriented towards multiloop control schemes.

(c) The possibility of any systematic decomposition to reduce the magnitude of the problem was not addressed explicitly.

(d) It relies to a great extent on heuristics.

A " UNIFIED APPROACH " FOR CONTROL SYSTEM SYNTHESIS

An integrated approach to whole plant control with specific attention to control system synthesis was proposed by Morari and co-workers (Morari et al. [1980], Morari and Stephanopoulos [1980]). This approach was claimed to provide a general methodology that incorporates the niceties of all the previous approaches, such as the use of appropriate model complexity, hierarchical control, rigorous structural relationships, economic optimisation and systematic process decomposition. The proposed method addresses the following key issues :

(a) The definition of the process objectives.
(b) The selection of measured variables.
(c) The selection of manipulated variables.
(d) The design of the control structure connecting the measured variables to the manipulated variables.

Their overall methodology involves two major levels of decomposition, i.e.

(i) Process decomposition with respect to steady-state control issues (i.e. optimising control).
(ii) Process decomposition with respect to regulatory (dynamic) control issues.

Morari et al. [1980] derived analytical expressions for steady-state process decomposition with the objective being to minimise the economic interaction among the various decomposed process segments. This is achieved by considering the Lagrange multipliers of

the constrained optimising function for each sub-system with respect to the interconnections to the rest of the plant. The aim is to obtain a minimum degradation in control due to decomposition , compared to the ideal of perfect feedforward control.

At the second level, their approach is concerned with the generation of feasible regulatory control structures. Unlike the approach of Govind and Powers [1982] , a more detailed decomposition was made here, to meet most of the control objectives for each of the sub-systems from the steady-state decomposition.

STRUCTURAL METHODS

An approach addressing similar issues to those considered by Morari and co-workers in their second phase, such as a systematic procedure for generating and choosing between alternative control structures for various types of control (i.e. feedforward, feedback , cascade etc.,.), was proposed by Johnston and Barton [1985a , b]. Their structural approach is an extension and an improvement on the approach of Morari and co-workers (Morari et al. [1980], Morari and Stephanopoulos [1980]), but unlike other structural approaches is not heuristics based. This approach, however, does not explicitly address the issue of a selection criteria for ranking or rejecting alternative control structures that are all structurally feasible.

All the methods discussed above do not completely solve the problem of "control system synthesis", because all of them propose a control stategy for a flowsheet that has already been designed. In other words , at least the basic design of the flowsheet is assumed as a starting point. Improvements over the current design , driven by control issues may follow, but it is not really an integral part of this approach. A lot of emphasis is laid on the process design rather than on the process control in some of these approaches (e.g. Douglas's economics based approach [1980, 1981]). What is ideally required is a systematic approach that addresses the twin issues of design and control for a process, from the very beginning. Further discussion on this will be made in Section 5. 3.

4. 3. 2 DEFINITION AND TYPES OF CONTROLLABILITY

Controllability , which may loosely be defined as a measure of the degree of difficulty of controlling a process, has lately been recognised an as integral part of control system synthesis (Morari et al. [1980], Morari and Stephanopoulos [1980]) , Stephanopoulos [1983], Lau and Jensen [1985], Johnston and Barton [1985a,b]). Since a general definition provides only a qualitative measure , several more rigorous definitions for controllability have been developed, each dealing with a specific control objective. Controllability plays a vital role in the second phase of Morari et al. .'s unified approach which deals with the selection and screening of control structures that are relatively more difficult to control. The following sections of this chapter discusses the key issue of controllability in some detail.

STATE CONTROLLABILITY

Kalman [1960] was the first to introduce and use the concept of state controllability along with its dual , observability. These concepts were originally defined for linear dynamic systems represented by a state-space equation (see Section 2. 4. 2). Rosenbrock 's [1970] *pointwise state controllability* is the most commonly accepted form of the various state controllability definitions that followed. It is defined as :

Definition

Any system of size (n X n) represented in a state-space form (4. 3. 1) will be called pointwise state controllable if, given any two states x_1 and x_2, there exist a time $t_1 > 0$ and an input u_1 defined on the time interval $[0, t_1]$ such that the state of the system (x) is carried from x_1 to x_2 at time $t = t_1$.

$$\dot{x} = Ax + Bu \qquad (4.3.1)$$

A system described by Equation (4. 3. 1) is *pointwise* or *completely state controllable* , if and only if any one of the following conditions is true (Wong [1984]) :

(a) The rank of the matrix

$$[\, B \mid AB \mid A^2B \mid \ldots\ldots \mid A^{n-1}B \,] \qquad (4.3.2)$$

is ' n '.

(b) The rows of the matrix [exp (- At)] B are linearly independent for all $t \geq 0$.

(c) The symmetric matrix :

$$W(t_0, t_1) = \int_{t_0}^{t_1} [\exp(-A\tau)]\, B\, B^T [\exp(-A^T\tau)]\, d\tau \qquad (4.3.3)$$

is nonsingular for all $t_1 > t_0$.

All these tests have a theoretical basis and a physical significance , however, these will not be discussed here.

Example 4.5

Consider the state-space of a system having a form given by

$$\begin{pmatrix} \dot{x}_1 \\ \dot{x}_2 \end{pmatrix} = \begin{pmatrix} 1 & 0 \\ 0 & 1 \end{pmatrix} \begin{pmatrix} x_1 \\ x_2 \end{pmatrix} + \begin{pmatrix} 1 \\ 0 \end{pmatrix} u \qquad (4.\ 3.\ 4)$$

$$\therefore \quad A = \begin{pmatrix} 1 & 0 \\ 0 & 1 \end{pmatrix} \quad \text{and} \quad B = \begin{pmatrix} 1 \\ 0 \end{pmatrix} \qquad (4.\ 3.\ 5)$$

For state controllability the rank of the matrix given by Equation (4. 3. 2) should be two (i.e. it should be equal to the rank of **A** , in this case **2**).

The rank of the matrix [B AB] = $\begin{pmatrix} 1 & 1 \\ 0 & 0 \end{pmatrix}$ is unity, therefore, the given process is not state controllable.

Example 4.6

Consider the state-space equation of Example 4. 5 , but in the modified form ,

$$\begin{pmatrix} \dot{x}_1 \\ \dot{x}_2 \end{pmatrix} = \begin{pmatrix} 1 & 0 \\ 1 & 1 \end{pmatrix} \begin{pmatrix} x_1 \\ x_2 \end{pmatrix} + \begin{pmatrix} 1 \\ 0 \end{pmatrix} u \qquad (4.\ 3.\ 6)$$

$$\therefore \quad A = \begin{pmatrix} 1 & 0 \\ 1 & 1 \end{pmatrix} \quad \text{and} \quad B = \begin{pmatrix} 1 \\ 0 \end{pmatrix} \qquad (4.\ 3.\ 7)$$

For state controllability, the rank of the matrix given by Equation (4. 3. 2) should again be two.

The rank of the matrix [B AB] = $\begin{pmatrix} 1 & 1 \\ 1 & 0 \end{pmatrix}$ is now two. Therefore the process is state controllable.

State controllability assures us that the state variables can be moved from some initial values to some final values within a finite interval of time. Although the control action required for the switching is given, from which the final values of the state and output variables can be computed by solving the state-space equations, no information about the

path that the output variables will follow after they have reached their final values is available (Wong [1984]). In other words, the state of the system except at time $t = 0$ and at time $t = t_1$ is not known.

In some cases, state controllability is too strong a condition, i.e. it may not be necessary to control all states for a stable process. For this reason, alternative forms of controllability have been defined.

MODAL CONTROLLABILITY

The concept of modal controllability was first proposed by Rosenbrock [1962a, b]. The rationale behind this approach was to decide on the performance desired from a system and then determine a control system to achieve this desired performance. This is possible because the poles of the closed-loop system (i.e. the eigenvalues of the closed-loop state matrix) which have the greatest influence on the dynamics of the system (see Section 4. 1. 4) can be shifted to any desired location to achieve the desired stability and performance, using a feedback controller. In other words, the 'poles' (see Section 4. 1. 4) of the system are used as the basis on which to base the stability and performance characteristics of the closed-loop system. The ability to assign arbitrary values to the closed-loop poles of a system is quite attractive. Systems with large and negative closed-loop poles have good disturbance rejection properties, and return to their steady-states very quickly after any disturbance. However, it may not always be necessary to move all the poles , since only a few of them, in general, have a major effect on the dynamics. Also , some of the closed-loop poles of the system may be cancelled by equivalent input decoupling zeros (MacFarlane and Karcanias [1976]), and are not accessible for control. Such a system is not completely modal controllable. Therefore, a system is said to be modal controllable only if all the closed-loop poles are available and can be assigned arbitrary values in the complex plane using feedback action. Wonham [1967] showed that if a linear, time invariant system is completely state controllable, then the eigenvalues of the closed-loop state matrix (i.e. the closed-loop poles) may be assigned arbitrary values in the complex plane. Thus, complete state controllability implies modal controllability. Simon and Mitter [1968] showed that the converse is true, i.e. a system is completely state controllable if and only if it is modally controllable. Rosenbrock [1970] finally showed that the necessary and sufficient conditions for complete state controllability and modal controllability are the same.

Modal control does not address the issue of what dynamic characteristics of a system prevent good control from being realised (see Section 4. 3. 3).

STRUCTURAL CONTROLLABILITY

One of the deficiencies of state controllability is its inability to identify systems where large inaccuracies or uncertainties in the process model can lead to numerically singular systems , even though the nominal system is state controllable. The converse is also possible, i.e. a system may not be nominally state controllable, however, model inaccuracies could make the system satisfy the properties of state controllability under some circumstances. To avoid problems with numerical estimation and accuracies, Lin [1974] introduced a new concept called structural controllability which seeks to expose those systems in which uncontrollability is caused not by numerical characteristics but by the inherent structural characteristics of the system.

Definition [Lin 1970]

> The set formed by the matrices **A** and **B** of the state-space Equation (4. 3. 1) of a system is referred to as the pair **(A, B)**. This is said to be structurally controllable if and only if there exists another pair (A_0, B_0) of the same structure which is completely state controllable.

Lin(1974) employed a technique based on graph theory to illustrate his ideas. Shields and Pearson [1976] used the concept of *generic rank* (i.e the maximum possible rank a matrix can have whatever the numerical value of its elements) and extended the concept of Lin's structural controllability to MIMO state-space systems . Many other researchers (Glover and Silverman [1976], Morari et al. [1980], Morari and Stephanopoulos [1980] , Johnston et al. [1983]) have used the concept of generic rank , and extended the concepts of structural controllability into the control system synthesis area. A good review of structural controllability and its use in multiloop control system synthesis is given by Russell [1987].

On the whole, the introduction of structural controllability has brought about significant developments in the techniques available for control system synthesis (Wong [1984], Johnston and Barton [1985a, b], Morari et al. [1980]).

FUNCTIONAL CONTROLLABILITY

All the previous work on controllability has to do with the controllability of several states of the system. In practice, this may not always be feasible or it may not even be necessary to control all the states to achieve the desired performance from a process. A more useful approach, therefore, would be to test if the process follows a certain performance path as a function of time. In other words, " can the process outputs **y(t)** be steered to follow a certain trajectory in space as desired by the user ". This seems to be a

more realistic controllability requirement, and turns out to be the basis for functional controllability.

The definition of functional controllability for multivariable systems was first proposed by Brockett and Mesarovic [1965].

Definition - 1 :

Consider the state-space form of a dynamic system given by,

$$\dot{x} = Ax + Bu \qquad (4.3.8)$$

$$y = Cx + Du \qquad (4.3.9)$$

Both the equations are (generally) obtained by linearising a nonlinear model around a known steady-state.

Such a system will be called functionally controllable, if given $y(t)$ for all $0 \leq t \leq t_1$, there is an input vector $u(t)$ for all $0 \leq t \leq t_1$, which produces $y(t)$ starting from the initial condition $x(0) = 0$.

A more useful criterion can be derived using the transfer function matrix $G(s)$ of a system,

where $$G(s) = [\, C(sI - A)^{-1} B + D \,] \qquad (4.3.10)$$

The system is said to be functionally controllable if and only if we can always find an input vector, $u(s)$, that provides a given trajectory for the output vector, $y(s)$. This input vector is given by the following equation :

$$u(s) = [G^{-1}(s)]\, y(s) \qquad (4.3.11)$$

Hence, $G(s)$ should be nonsingular to satisfy the above requirement of functional controllability.

This latter definition can be better understood through the following illustrative example.

Example 4. 7

Consider two tanks in series with one feed stream as shown in Figure 4. 1. 4. The unsteady-state overall mass balance equations can be written as ,

$$a\frac{dH_1}{dt} = F_o - F_1 \qquad (4.3.12)$$

$$a\frac{dH_2}{dt} = F_1 - F_2 \qquad (4.3.13)$$

Assume that our objective is to regulate the liquid levels in both the tanks. The levels in both the tanks in this case are also state variables. With product flowrates from each tank chosen as the available manipulated variables, the state-space representation of this process model (see Section 2. 4. 2) can be written in the following form :

$$A=\begin{pmatrix}0 & 0\\ 0 & 0\end{pmatrix},\ B=\begin{pmatrix}-1 & 0\\ 1 & -1\end{pmatrix},\ C=\begin{pmatrix}1 & 0\\ 0 & 1\end{pmatrix} \text{ and } D=\begin{pmatrix}0 & 0\\ 0 & 0\end{pmatrix} \qquad (4.3.14)$$

$$\text{with } x=\begin{pmatrix}H_1\\ H_2\end{pmatrix},\ u=\begin{pmatrix}F_1\\ F_2\end{pmatrix} \text{ and } y=\begin{pmatrix}H_1\\ H_2\end{pmatrix} \qquad (4.3.15)$$

G (s) can be calculated from Equation (4. 3. 10) as,

$$\begin{aligned} G(s) &= [\, C(sI-A)^{-1}B + D \,] \\ &= \begin{pmatrix}1 & 0\\ 0 & 1\end{pmatrix}\begin{pmatrix}\frac{1}{s} & 0\\ 0 & \frac{1}{s}\end{pmatrix}\begin{pmatrix}-1 & 0\\ 1 & -1\end{pmatrix}+\begin{pmatrix}0 & 0\\ 0 & 0\end{pmatrix} \\ &= \begin{pmatrix}\frac{-1}{s} & 0\\ \frac{1}{s} & \frac{-1}{s}\end{pmatrix} \end{aligned} \qquad (4.3.16)$$

Clearly, G (s) is nonsingular for frequencies (note that $s = j\omega$) larger than zero, and thus the system is functionally controllable. From Equation 4. 3. 1, the rank of the matrix [B AB] is given by ;

$$\text{Rank of } [\, B \;\; AB \,] \;=\; \text{Rank of } \begin{pmatrix}-1 & 0 & 0 & 0\\ 1 & -1 & 0 & 0\end{pmatrix} \;= 2 \qquad (4.3.17)$$

Clearly this rank is not equal to the rank of A (i.e zero) and hence the system is not state controllable.

It must be realised that the failure of the state controllability condition implies that controlling both states together is not feasible. However, functional controllability is feasible when the same state variables are chosen as outputs. This difference arises because the definition of state controllability requires the existence of steady-states (i.e. in this case two steady-states ; see the definition of state controllability). Equation (4. 3. 12 - 4. 3. 13) represent a pure capacitive system (Stephanopoulos [1984]) , hence there are no open-loop steady-states. State controllability, therefore, is not feasible .

A more general and complete definition for functional controllability was later proposed by Rosenbrock [1970] as follows:

Definition - 2

A linear time invariant system is functionally controllable if and only if one of the following conditions is true :

(a) The system matrix **P** (s) is nonsingular.

$$\text{where } P(s) = \begin{pmatrix} sI - A & B \\ -C & D \end{pmatrix}$$

(b) The transfer function matrix **G** (s) is nonsingular.

It was shown in Example 4. 7 that this system is functionally controllable as it satisfies the second condition of the above definition. For the same system, we can test the applicability of the first condition, given by Equation (4. 3. 18) as follows :

Example 4. 8:

Consider the same tanks in series as used in the previous example. Using the state-space matrices (i.e. A, B , C and D) from Equation 4. 3. 14 , we can construct the system matrix **P** (s) as,

$$P(s) = \begin{pmatrix} sI - A & B \\ -C & D \end{pmatrix}$$

$$= \begin{pmatrix} s & 0 & -1 & 0 \\ 0 & s & 1 & -1 \\ 1 & 0 & 0 & 0 \\ 0 & 1 & 0 & 0 \end{pmatrix} \qquad (4.3.18)$$

The determinant of **P** (s) = 1. As **P** (s) is nonsingular, the system is functionally controllable. Therefore, the two conditions used for functional controllability are equivalent.

Functional controllability, therefore, seems to be a more appropriate definition for controllability. It was shown by example that state controllability is not a necessary condition for functional controllability. Unlike state controllability , the definition of functional controllability imposes conditions on bounded inputs throughout the output trajectory, (i.e. it checks for the bounds on the available inputs at every stage of its trajectory), and hence is a more appropriate form of system controllability. It will be used extensively throughout this work.

PERFECT CONTROL

The different forms of controllability defined thus far , are useful only in the sense that we can check if a system is controllable or not. None of these definitions is useful in ranking different systems with respect to controllability. Though functional controllability has been shown to be a useful means of rejecting candidate control structures, it still does not provide a basis for ranking control structures, all of which may be functionally controllable (Russell [1987]).

Davison and Chow [1974 ,1977] introduced a useful concept called perfect control, that could be used as a basis for quantitatively assessing controllability. It can be defined as follows :

Definition

A linear time invariant system, subject to disturbances , is said to be perfectly controllable if a controller can be found such that the dynamic performance index J (see Equation 4. 3. 19) can be made arbitrarily small :

$$J \equiv \int_0^\infty (\delta y^T Q \, \delta y) \; dt \qquad (4.\ 3.\ 19)$$

where Q is a positive definite weighting matrix

$\delta y = y - y_s$ are the perturbations from the reference points (y_s) of the output variables (y).

The quadratic dynamic performance index (J) can be interpreted physically as the approach possible to error-free set-point tracking and complete disturbance rejection (Russell [1987]). Thus, perfect control sets up a lower bound (in the limit $J = 0$) on the optimal performance that can be achieved from a process. This concept is potentially useful , since processes could be ranked based on how close to perfect control they can operate. In the following section, some of the major issues relating to the use of this perfect control concept will be discussed in more detail.

4. 3. 3 ASSESSING CONTROLLABILITY

In the previous section, it was shown that perfect control is a very useful and promising concept in assessing the controllability of alternative control systems. One approach that gives more insight from this concept is based on identifying the process characteristics preventing the achievement of perfect control . The motivation behind this approach is a fundamental result obtained by Davison and Chow [1974, 1977] in defining perfect control. This was the "Control Inequality Principle ", in which it is stated that :

(a) If the system to be controlled has more input variables than output variables , then it is almost always possible to achieve perfect control.

(b) If the system to be controlled has an equal number of inputs and outputs , then the ability to achieve perfect control depends on the characteristics of the system and , in particular, on whether the system is non-minimum phase or not.

(c) If the system to be controlled has more outputs than inputs, then it is never possible to achieve perfect control.

This principle makes sense physically. For any chemical process, if we have more valves for manipulation (all of which are independent) than the number of control objectives , then we would expect good control if we could adjust all the valves at once. If the number of valves is less than the number of control objectives, then it is impossible to maintain all the control variables at their desired set-points at all times. Finally, if the number of valves is the same as the number of control objectives , then good control is usually possible subject to certain limitations.

A more explicit explanation of these fundamental process limitations and various criteria for assessing controllability were proposed through the framework of Internal Model Control (IMC) by Garcia and Morari [1982]. Their approach provides a greater insight into this issue and will be discussed briefly .

Consider a typical feedback controller (see Figure 4. 3. 1) acting on a process with a transfer function matrix given by G (s). The outputs can be derived from the inputs as

$$y(s) = G(s)\, u(s) \qquad (4.3.20)$$

Ideally we require both perfect regulatory and perfect servo behaviour. For perfect regulatory control,

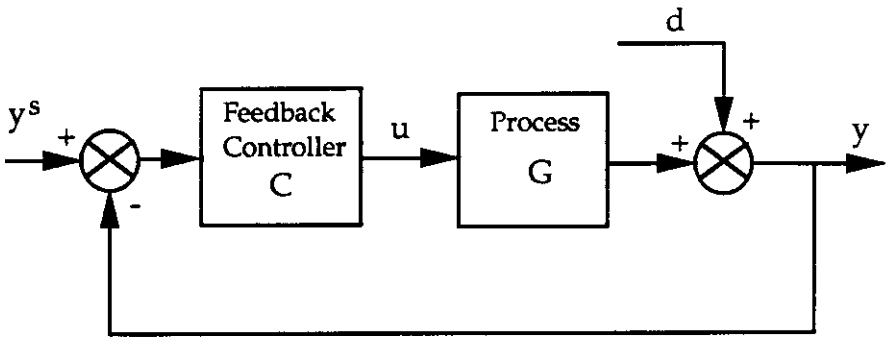

Figure 4. 3. 1
Feedback control configuration

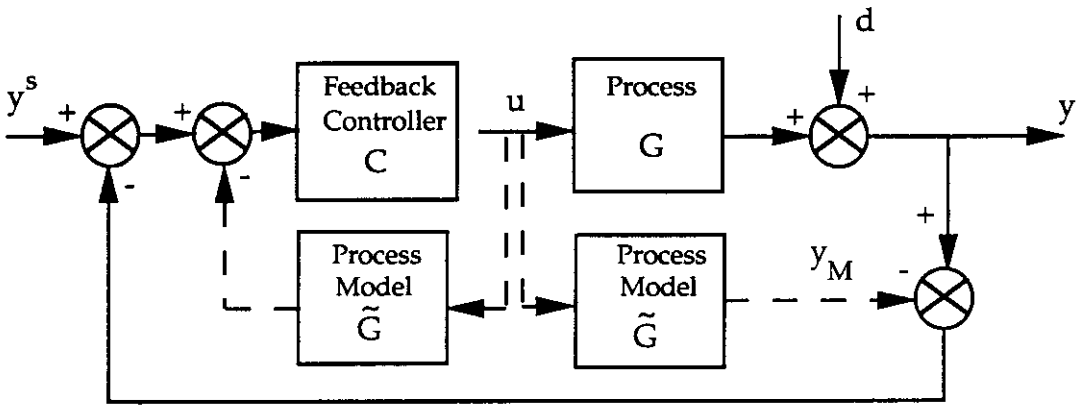

Figure 4. 3. 2
Modification of feedback configuration
to obtain Internal Model Control (IMC) structure

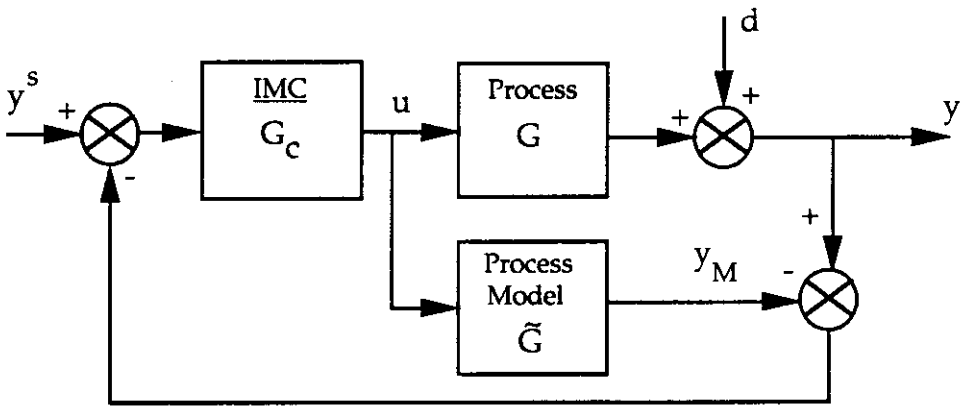

Figure 4. 3. 3
Internal Model Control (IMC) structure

$$y(s) = y_s(s) \tag{4.3.21}$$

which requires

$$u(s) = G^{-1}(s)\, y(s) \tag{4.3.22}$$

For perfect servo control,

$$y'(s) = y_s(s) - d(s) \tag{4.3.23}$$

which requires

$$u(s) = G^{-1}(s)[\, y_s(s) - d(s)\,] \tag{4.3.24}$$

As we see from Equations (4. 3. 22) and (4. 3. 24) , both ideals require the existence of $G^{-1}(s)$ which is the *right inverse* of the system transfer function matrix. The name *right inverse* is derived from the following definition.

Definition

G (s) is said to have a right inverse if and only if $G(s)\, G^{-1}(s) = I$, such that I is the identity matrix.

The following are a few consequences (Morari [1983]) of the above definition :

(1) Perfect control is possible only if G (s) has a right inverse.

(2) G (s) has a right inverse if and only if it has full rank for all values of the complex variable s. This implies that for perfect control we require the number of manipulated variables to be at least equal to the number of outputs (i.e. $m \geq n$).

These were essentially the results obtained by Davison and Chow (1974) but both were interpreted somewhat differently and extended by Morari and co-workers (Morari [1982], Garcia and Morari [1982], Morari [1983]) .

The basic structure of IMC is given in Figure 4. 3. 3. The basic motivation for IMC is that the system itself (G (s)) is never known accurately and hence only an approximate model ($\tilde{G}(s)$) is available. If the approximate process model is both added and subtracted to the feedback structure of Figure 4. 3. 1 , as shown in Figure 4. 3. 2 , there is no net change. The advantage of this manipulation is that the feedback controller and the process model can be combined to give what is called an Internal Model Controller i.e. $G_c(s)$ such that,

$$G_c(s) = C\tilde{G}(s)\,[I + C\tilde{G}(s)\,]^{-1} \tag{4.3.25}$$

or equivalently,

$$C(s) = G_c(s)\,[I - G_c(s)\tilde{G}(s)\,]^{-1} \tag{4.3.26}$$

This approach is quite different from the normal feedback control policy, as Garcia and Morari [1982] claim that ;

(a) It is easier to design $G_c(s)$ than $C(s)$.

(b) The IMC structure allows us to include controller robustness as a design objective in a very explicit manner. This is partly due to the type of feedback signal used in this structure ($\tilde{b}(s)$).

$$\tilde{b}(s) = [I + (G(s) - G_c(s))\,\tilde{G}(s)]^{-1} \qquad (4.3.27)$$

If there are no discrepancies between the actual plant and the approximate model (i.e we have a perfect model, $G(s) = \tilde{G}(s)$) then the feedback signal is unity, indicating a normal feedback controller. However, if discrepancies between the actual plant and the model do exist, then the feedback signal is modified by the extent of the model discrepancy and such information can be used as a basis for characterising controller robustness.

The closed-loop transfer function for the complete system shown in Figure 4. 3. 3 is (Garcia and Morari [1982]) given by the following equation,

$$y(s) = G G_c [I + (G(s) - \tilde{G}(s)) G_c]^{-1} [\, y_s(s) - d(s) \,] + d(s) \qquad (4.3.28)$$

where the control action is given by,

$$m(s) = G_c [I + (G(s) - \tilde{G}(s)) G_c]^{-1} [\, y_s(s) - d(s) \,] \qquad (4.3.29)$$

If there is no mismatch between the actual plant and the process model (i.e. $G(s) = \tilde{G}(s)$), then Equations (4. 3. 28) and (4. 3. 29) become,

$$y(s) = G G_c \, [\, y_s(s) - d(s) \,] + d(s) \qquad (4.3.30)$$

and

$$m(s) = G_c \, [\, y_s(s) - d(s) \,] \qquad (4.3.31)$$

If the controller is chosen to be the right inverse of the plant i.e. $G_c(s) = G^{-1}(s)$, then the closed-loop transfer function equation becomes,

$$y(s) = [\, y_s(s) - d(s) \,] + d(s) = y_s(s) \qquad (4.3.32)$$

This indicates that there is both perfect set-point tracking and complete disturbance rejection at all times , which means *perfect control.* A few important implications of the above analysis can be made as follows.

(1) If there is no plant model mismatch (i.e. $G(s) = \tilde{G}(s)$), then the system is closed-loop stable if the plant and the controller are both stable. This implies that for an open-loop stable system , as long as we choose a controller $G_c(s)$ that is stable, then the system will be closed-loop stable. This property is quite different from a typical feedback controller in that , here the major difficulty is to choose a feedback controller C in such a way as to ensure closed-loop stability (even for an open loop stable system !). This is what was claimed as ease of design of $G_c(s)$ for IMC compared to the design of C for normal feedback control.

(2) Perfect control can be obtained by choosing an IMC controller that is the right inverse of the plant model.

(3) In the usual feedback structure, one has to vary a set of control parameters that simultaneously achieve a complex compromise between stability, quality of response and modelling sensitivity. Using IMC on the other hand, one starts with the ideal of perfect control and back-off from this ideal in a well defined two step procedure, as will be shown later (Morari [1983]). Thus, IMC provides both optimal controller structure and optimal "parameters" at the same time.

The above discussion on the design of IMC not only provides insight into the concept of perfect control but also raises the issue of the fundamental limitation preventing perfect control - which cannot be achieved if the inverse of the plant cannot be calculated and implemented.

Thus, in the context of both functional controllability and perfect control, the major requirement is a design for the controller that is the inverse of the plant - a requirement which is not always feasible. Since this general approach appears to be a promising means of analysing and ranking alternative control schemes, a more detailed examination of the properties of a plant preventing the implementation of a process inverse based controller will be made in the following section.

4. 3. 4. FUNDAMENTAL LIMITATIONS TO PERFECT CONTROL

An obvious necessary condition for perfect control is that the determinant of the process transfer function matrix (G (s)) should not be identically zero for all values of ' s ', which is also the necessary and sufficient condition for functional controllability (Rosenbrock [1970], Russell [1987]). Both Bristol [1978] and Morari [1983] examined the feasibility of using the inverse of the process model as the controller and identified the critical role of non-minimum phase elements. The two stage procedure adopted by Morari and co-workers (Morari [1982], Garcia and Morari [1982], Morari [1983]) involves ;

(a) First taking care of all the fundamental limitations preventing the implementation of the plant inverse, such as the presence of non-minimum phase elements in the transfer function matrix.

(b) Then addressing the issue of system sensitivity which can lead to poor control .

Each of these stages are of great importance in control system synthesis, and hence will be discussed briefly in the following section.

NON - MINIMUM PHASE ELEMENTS

RIGHT HALF PLANE (RHP) ZEROS

It was noted in Section 2. 4. 1 that for SISO systems , the presence of RHP zeros in the transfer function may result in an inverse response, where the response of the system is initially in the opposite direction to where it finally ends up. Such systems can provide considerable control difficulties. For example, consider a SISO system with a transfer function given by,

$$G(s) = \left(\frac{s-3}{s+5} \right) \qquad (4.\ 3.\ 33)$$

The transfer function G (s) has a RHP zero at

$$s = 3 \qquad (4.3.34)$$

For the implementation of perfect control on such a system , the requirement is that G (s) is nonsingular, which is satisfied in this case. However, the inverse model controller $G_c(s)$ has a transfer function given by,

$$G_C(s) = 1 / G(s) \qquad (4.3.35)$$

i.e. $$G_c(s) = \left(\frac{s+5}{s-3} \right) \qquad (4.3.36)$$

Clearly, this shows that the zero of the process transfer function has become the pole of the controller. Such a controller is not recommended as it has a pole in the right of the complex plane and hence is unstable. The deterioration in system stability and performance was quantified for SISO systems by Holt and Morari [1985]. They have shown that the deterioration in the quality of control is inversely proportional to the distance of the RHP zero from the origin.

In the case of MIMO systems, a similar effect can be experienced. The equivalent of RHP zeros in the case of MIMO systems are RHP transmission zeros or RHPT zeros (MacFarlane and Karcanias [1976], Holt and Morari [1985]). RHPT zeros are usually a property of the matrix, not of any matrix element in particular . RHPT zeros create problems for the implementation of perfect control due to the following features (Kwakernaak and Sivan [1972], Holt and Morari [1985], Russell [1987]) :

(i) They exhibit a transmission blocking property , whereby for certain complex values of "s " equal to the RHPT zeros, the information transmission through the transfer function matrix is blocked. Equivalently, transfer function matrix inversion is not possible at these complex values of " s ".

(ii) They are invariant under feedback control. They can only be influenced by changes in the design of the process itself.

(iii) They become the poles of the system inverse , introducing instabilities into the controller.

In the presence of RHPT zeros , perfect control cannot be achieved. However, Holt and Morari [1985] suggested that close to perfect control can be achieved by suitably decomposing the transfer function matrix. Based on their results, Holt and Morari proposed some qualitative arguments regarding the likely deterioration in the control performance due to RHPT zeros in the case of MIMO systems. For some limiting cases, such as completely decoupled systems, the deterioration was shown to be inversely proportional to the distance of the RHPT zeros from the origin.

The loss of control performance due to the existence of RHPT zeros in a system may be interpreted as a limit on the feedback gain a closed-loop system can employ without incurring instability. Therefore, a natural measure of this degeneration or controllability is the value of the gain parameter at which the closed-loop system becomes unstable (Wong [1984]). Though Wong's approach seems to have a few advantages over Holt and

Morari's approach , the gain parameter is not scale invariant and should be treated with care when used to compare alternative control structures.

TIME DELAYS

Time delays or transportation lags are of particular importance in the chemical process industry because they are often the direct result of the transportation of mass and energy physically , from one location to another. They may also be characteristic of the process itself or arise due to control signal transmission or sampling and composition analysis. Russell [1987] made an extensive survey on various issues relating to time delays and the role they play in preventing the achievement of perfect control.

In a SISO system, the effect can be well understood through frequency domain analysis. Consider the following transfer function for a pure time delay process

$$G(s) = Ke^{-t_d s} \qquad (4.3.37)$$

where K is the steady-state gain
t_d is the time delay or transportation lag.

A perfect controller $G_c(s)$ for the above process can be constructed using the inverse of the process transfer function , such that $G_c(s)$ will have a form given by,

Once again,

$$G_C(s) = 1 / G(s) \qquad (4.3.38)$$

i.e.
$$G_c(s) = K' e^{t_d s} \qquad (4.3.39)$$

such that
$$K' = 1/K \qquad (4.3.40)$$

where K' is the controller steady-state gain.

The above analysis has two major implications for the process itself :

(1) A transfer function with a time delay element has an increased phase-shift in the complex plane but the same gain (or magnitude ratio) as the equivalent transfer function without a time delay. This puts a bound on the magnitude of the feedback controller gain one can use and retain a stable system, and hence forms a measure of the degeneration in the control performance brought about by the presence of a time delay.

(2) The requirement of a plant inverse for perfect control means that a predictive type of controller is required (needs the knowledge of the system behaviour in the future , to take corrective action at the current time). This is physically not realisable, .

Russell [1987] pointed out the major difficulties associated with the current methodologies for control system synthesis for systems with time-delays and proposed a general approach for time-delayed systems represented by mixed differential and algebraic equations (DAEs). Holt and Morari [1985] had previously proposed a method within the framework of IMC which involves the decomposition of the transfer function matrix with time delays into two parts, one invertible part and a non-invertible part that contains the time-delays. Wong [1984] in his investigation of functional controllability , proposed a scalar measure for the effect of time-delays on controllability based entirely on the time-delay properties of the plant (Perkins and Wong [1985]). The rationale behind this latter approach comes from the fact that the presence of time delays may require the original requirement of functional controllability (i.e the outputs should follow desired trajectories from time $t = 0$) be relaxed so that some non-zero time must elapse before such output trajectories can be defined. This minimum time which must elapse before the outputs can be independently specified was defined as the *minimum necessary delay* and is a property of the time delay structure of the system itself. Wong [1984] proposed its use as one measure of the inherent controllability of a system. From a practical point of view, the longer this delay , the less controllable the system is, since a greater restriction is placed on the desired outputs (Perkins et al. 1986]). Russell [1987] showed that both the methods proposed by Holt and Morari [1985] and Perkins and Wong [1985] were useful for small systems only, but that a more general algorithm was required to handle larger systems. Using concepts from both structural controllability and Wong's [1984] minimum necessary delay, Russell [1987] proposed such a general algorithm to handle large DAE systems.

SYSTEM SENSITIVITY

All the methods proposed above form only the first phase of perfect controller design. They are all based on the assumption that there is no plant - model mismatch (i.e. $G(s) = \bar{G}(s)$). Arkun [1986] stated that the success of these controllers in a real environment is limited by the accuracy of the models used in the analyses. Inaccuracies in the process models comes about for some of the following reasons :

(a) A poor understanding of the process itself.
(b) The assumptions used in deriving the model and a lack of complete knowledge of the limitations imposed on its validity.
(c) The linearisation of a nonlinear model.
(d) Neglecting higher order dynamics.
(d) Inaccuracies involved in the estimation of process parameters.

Depending on how sensitive the system is to these inaccuracies , the controller and the closed-loop system performance may be significantly affected. The implication of this is

that the departure from the functional controllability for any process may be due to inadequate description of the process model itself. Traditionally, feedback is used to control a plant with model uncertainty. However, intuitively it is obvious that there must be a limit to the extent that uncertainty of any type can be tolerated before the system must be detuned, thereby sacrificing the overall performance. Thus, uncertainty imposes a restriction on the achievable performance (Morari [1987]). The term *robustness* (Garcia and Morari [1982]) is often used and refers to the performance obtained from a system when system uncertainties are present. The need for providing a general framework that allows us to systematically identify these process uncertainties and then a design methodology that provides robust performance in the presence of these uncertainties has been emphasized (Grossman and Morari [1983], Arkun [1986]) over the last decade.

Doyle and Stein [1981] were the first to extend various sensitivity dependent performance criteria to MIMO systems followed. Skogestad and Morari [1987b] later derived various performance criteria for stability and robustness for a variety of uncertainty types. For MIMO systems, the concepts of system sensitivity and performance are similar to those for SISO systems. However, they require the estimation of singular values which are analogous in a way to process gains. Singular values can provide valuable information about the inherent characteristics of the system (such as system sensitivity). The following section explores some of the potential benefits of singular value analysis with respect to control system synthesis.

4.3.5 SINGULAR VALUE DECOMPOSITION - IT'S RELEVANCE IN CONTROL SYSTEM SYNTHESIS

Singular value decomposition (SVD) provides a means of calculating the singular values of a matrix. SVD has found widespread application in numerical analysis (Stewart [1973], Forsythe et al. [1977]) in recent years. The importance of SVD in the context of control system synthesis will be explored in this section.

The following terminology and definitions will be useful :

(a) *Norm of a vector :*

A norm is a measure of the length or size of a vector. The norm of a vector is usually defined as ;

$$\|x\|_p = \left(\sum_{i=1}^{n} |x_i|^p \right)^{1/p} \qquad (4.3.41)$$

where x_i is the i^{th} element of the vector x.

Three types of norm are commonly used depending on the value of ' p '. When **p =1** it is called the l_1- norm ; when **p = 2** it is called the l_2 - norm and when $p = \infty$ it is called the l_∞ - norm. The l_2 - norm is also more commonly known as the Euclidean norm. It can be shown that the l_∞ - norm is given by the absolute value of the largest element of the vector **x** and is represented as follows;

$$\| x \|_\infty = \max | x_i | \quad \text{for all} \quad i = 1, ..., n \qquad (4.3.42)$$

(b) *Norm of a matrix :*

The norm of a matrix **A** may be defined subordinate to the corresponding vector norm as;

$$\| A \|_p = \max \left(\frac{\| Ax \|_p}{\| x \|_p} \right)_{x \neq 0} \qquad (4.3.43)$$

The vector **x** when projected using the matrix **A**, gives another vector which is either enlarged or reduced in size depending on the nature of the matrix. The ratio of the norm of the resulting vector to that of the original vector is an indication of the amount of magnification or reduction obtained. The maximum of all these possible changes (for a given **p**) is usually defined as the norm of the matrix **A**. This definition provides an upper bound on the amplifying effect of the matrix **A** because of the following inequality ;

$$\| Ax \|_p \leq \| A \|_p \| x \|_p \qquad (4.3.44)$$

For the l_1, l_2 and l_∞ matrix norms, we have

$$\| A \|_1 = \max_j \left(\sum_i | a_{ij} | \right) \qquad (4.3.45)$$

$$\| A \|_\infty = \max_i \left(\sum_j | a_{ij} | \right) \qquad (4.3.46)$$

$$\| A \|_2 = \max_i \{ \lambda_i^{1/2} (A^H A) \} \qquad (4.3.47)$$

where

A^H is the complex conjugate transpose of matrix **A** ,

λ_i (for $i = 1, ..., n$) are the eigenvalues of the matrix ($A^H A$).

The square roots of the eigenvalues of $A^H A$ are known as the "singular values " of the matrix **A** (Klema and Laub [1980] , Stewart [1973]).

Singular value decomposition is a technique to decompose a complex square matrix (of size n X n) into two unitary matrices (U and V) and a set of singular values such that,

$$A = U \Sigma V^{H} \qquad (4.3.48)$$

where Σ is a diagonal matrix with real non-negative entries

$$\Sigma = \text{diag}\{\sigma_j\} \quad (\text{for } j = 1, 2, ..., n) \qquad (4.3.49)$$

All three matrices **U** , **V** and Σ are of size (n X n). The superscript **H** once again denotes the complex conjugate transpose of a matrix. The set $\{\sigma_j\}$ are the singular values of the matrix **A** such that,

$$\sigma_1 \geq \sigma_2 \geq ..... \geq \sigma_n \geq 0 \qquad (4.3.50)$$

Singular values are always real and positive (Stewart [1973]) and the number of non-zero singular values is equal to the rank of the matrix A. This implies that if **A** is nonsingular , then all the singular values are greater than zero. The smallest ($\sigma_n = \sigma_{min}$) and the largest ($\sigma_1 = \sigma_{max}$) singular values are of particular importance in control system synthesis.

The unitary matrices **U** and **V** are made up of the left and right singular vectors, (i.e. u_j and v_j), respectively. They are called unitary because of the following property ;

$$\|u_j\|_2 = 1 \quad \text{and} \quad \|v_j\|_2 = 1 \qquad (\text{for } j = 1, 2, ..., n) \qquad (4.3.51)$$

The largest amplification obtained in the form of output vector (u_j^{max}) when the input vector (v_j^{max}) is projected using the matrix **A** is given by (σ_{max}) and similarly, (σ_{min}) corresponds to the smallest amplification obtained in the input vector (v_j^{min}). The direction of all the output vectors (u_j) are given by the following equality conditions,

$$A v_j = \sigma_j (A)\, u_j \qquad (4.3.52)$$

and in particular the directions for the maximum and minimum output vectors are given by the following equations,

$$A v_{max} = \sigma_{max} (A)\, u_{max} \qquad (4.3.53)$$

$$A v_{min} = \sigma_{min} (A)\, u_{min} \qquad (4.3.54)$$

The following example should help to explain SVD.

Example 4.3.8

Consider the (2 X 2) transfer function matrix for a one feed , two product distillation column given by Skogestad and Morari [1988a]. The top and the bottoms composition were controlled by the reflux rate and the bottoms reboiler vapour rate , respectively.

The transfer function matrix was estimated to be ;

$$G(s) = \begin{pmatrix} 0.878 & -0.864 \\ 1.082 & -1.096 \end{pmatrix} \qquad (4.\ 3.\ 55)$$

From a SVD on the transfer function matrix for the selected inputs and outputs, we get ,

$$\Sigma = \mathrm{diag}\{\sigma_{max}, \sigma_{min}\} = \mathrm{diag}\{\ 1.972, 0.0139\ \} \qquad (4.\ 3.\ 56)$$

$$V = (v_{max}, v_{min}) = \begin{pmatrix} 0.707 & 0.708 \\ -0.708 & 0.707 \end{pmatrix} \qquad (4.\ 3.\ 57)$$

$$U = (u_{max}, u_{min}) = \begin{pmatrix} 0.625 & 0.781 \\ 0.781 & -0.625 \end{pmatrix} \qquad (4.\ 3.\ 58)$$

The largest plant gain is obtained when the inputs are in the direction given by,

$$v_{max} = \begin{pmatrix} 0.707 \\ -0.708 \end{pmatrix} \qquad (4.\ 3.\ 59)$$

The corresponding output vector will have a direction given by ,

$$u_{max} = \begin{pmatrix} 0.625 \\ 0.781 \end{pmatrix} \qquad (4.\ 3.\ 60)$$

This is verified using Equation (4. 3. 53) as follows ;

$$u_{max} = \left(\frac{1}{1.972} \right) \begin{pmatrix} 0.878 & -0.864 \\ 1.082 & -1.096 \end{pmatrix} \begin{pmatrix} 0.707 \\ -0.708 \end{pmatrix} = \begin{pmatrix} 0.625 \\ 0.781 \end{pmatrix} \qquad (4.\ 3.\ 61)$$

Similarly, using Equation (4. 3. 54) output vector corresponding to the lowest plant gain (i.e. minimum singular value) will have the direction given by ,

$$u_{min} = \left(\frac{1}{0.0139} \right) \begin{pmatrix} 0.878 & -0.864 \\ 1.082 & -1.096 \end{pmatrix} \begin{pmatrix} 0.708 \\ 0.707 \end{pmatrix} = \begin{pmatrix} 0.781 \\ -0.625 \end{pmatrix} \qquad (4.\ 3.\ 62)$$

CONDITION NUMBERS

It is possible to define an inverse for a square matrix **A** such that ,

$$A^{-1} = V \Sigma^{-1} U^{H} \qquad (4.\ 3.\ 63)$$

Useful properties of **A** and A^{-1} then include (Stewart [1973], Skogestad and Morari [1987c]) :

$$\sigma_{max}(A^{-1}) = \frac{1}{\sigma_{min}(A)} \qquad (4.\ 3.\ 64)$$

$$u_{max}(A^{-1}) = v_{min}(A) \qquad (4.3.65)$$

$$u_{min}(A^{-1}) = v_{max}(A) \qquad (4.3.66)$$

From Equations (4. 3.52) , (4. 3.53) and (4. 3. 64), an index called the *condition number* of a matrix **A** can be defined as follows :

$$Cond(A) = \frac{\sigma_{max}}{\sigma_{min}} = \| A \| \, . \, \| A^{-1} \| \qquad (4.3.67)$$

The condition number based on l_2 - norm is often denoted by γ. It is also possible to define condition numbers based on the l_1 - norm and l_∞ - norms.

The condition number provides a measure of the difference in the possible magnification of a vector projected using a matrix **A** . Large values indicate that the largest and smallest amplifications possible are very different. In other words, the output of the system is very sensitive to the direction of the input vector. On the other hand, values closer to unity (the minimum possible value for a condition number) indicate that the system is not very sensitive to input vector direction. This interpretation of condition numbers can alternatively as follows:

Consider a set of linear equations where the coefficients of the unknowns (x) are represented by the matrix **A** and **b** is a vector of constants.

$$Ax = b \qquad (4.3.68)$$

If this set of linear equations represents a process , the coefficients **A** will be subject to errors or uncertainties due to the various reasons discussed previously (see Section 4. 3). Let these errors be of the multiplicative type (i.e. $\Delta A_{ij} = A_{ij} \, . \, \delta A_{ij}$). The solution of the linear equations is , therefore, also subject to errors . The following terminology is applicable here ;

ΔA_{ij}	represents the magnitude of the error associated with the element in the i^{th} row and j^{th} column of the coefficient matrix **A** .
δA_{ij}	is the ratio of the magnitude of error to its normal value corresponding to the element in the i^{th} row and j^{th} column of the coefficient matrix **A** .
Δx_i	represents the magnitude of the error associated with the i^{th} element of the vector **x** .

The sensitivity of the solution (Δx) to this error can be derived as follows ;

$$(A + \Delta A)(x + \Delta x) = b \qquad (4.3.69)$$

i.e.

$$(x + \Delta x) = (A + \Delta A)^{-1} b \qquad (4.3.70)$$

From two Equations (4.3. 64) and (4. 3.65) we have that ,

$$\Delta x = [(A + \Delta A)^{-1} - A^{-1}] \; b \qquad (4.3.71)$$

Setting $(A + \Delta A) = B$, and using the following relationship,

$$B^{-1} - A^{-1} = A^{-1}(A - B) B^{-1} \qquad (4.3.72)$$

Equation (4. 3. 66) can be written as follows ,

$$\Delta x = -A^{-1} [(A + \Delta A) - A](A + \Delta A)^{-1} \; b \qquad (4.3.73)$$

i.e. $$\Delta x = A^{-1} (\Delta A) (A + \Delta A)^{-1} \; b \qquad (4.3.74)$$

Taking norms of both sides of Equation (4. 3. 74) and using the triangle inequality (Forsythe and Moler [1967]) , the following can be obtained ;

$$\frac{\| \Delta x \|}{\|x+\Delta x\|} \leq \| A \| . \| A^{-1} \| \left(\frac{\| \Delta A \|}{\| A \|} \right) \qquad (4. 3. 75)$$

Thus, from the definition of the condition number (see Equation 4. 3 68) we have,

$$\frac{\| \Delta x \|}{\|x+\Delta x\|} \leq Cond(A) . \left(\frac{\| \Delta A \|}{\| A \|} \right) \qquad (4. 3. 76)$$

This clearly shows that the larger the value of the condition number , the larger is the possible error in the solution of the linear equations . Similarly, we can estimate the sensitivity of the solution to changes (or uncertainties) in the elements of the vector ' b ' (Forsythe et al. [1977]) as follows ;

$$\frac{\| \Delta x \|}{\| x \|} \leq Cond(A) . \left(\frac{\| \Delta b \|}{\| b \|} \right) \qquad (4. 3. 77)$$

An illustrative example, for the latter case, is given below.

Example 4. 8 :

Consider the following set of linear equations (Forsythe et al. [1977]).

$$4.1 x_1 + 2.8 x_2 = 4.1$$
$$9.7 x_1 + 6.6 x_2 = 9.7$$

This system of equations can be expressed in the form of Equation (4. 3. 68) such that,

$$A = \begin{pmatrix} 4.1 & 2.8 \\ 9.7 & 6.6 \end{pmatrix} \text{ and } b = \begin{pmatrix} 4.1 \\ 9.7 \end{pmatrix}$$

The solution is given by,

$$x = \begin{pmatrix} x_1 \\ x_2 \end{pmatrix} = \begin{pmatrix} 1 \\ 0 \end{pmatrix}$$

However, if the vector b is subject to error such that the resultant vector b' is given by,

$$b' = b + \Delta b = \begin{pmatrix} 4.11 \\ 9.70 \end{pmatrix}$$

i.e. an error of 0.01 in the first element of the vector, then, the solution of the same set of equation, but with the modified vector b ' is given by,

$$x' = x + \Delta x = \begin{pmatrix} 0.34 \\ 0.97 \end{pmatrix}$$

Using the l_1 - norm, the norms of the following sensitivity functions can be calculated as,

$$\frac{\| b - b' \|}{\| b \|} = 0.0007246 \quad \text{and} \quad \frac{\| x - x' \|}{\| x \|} = 1.63$$

The condition number is given from Equation (4. 3. 77), by the ratio of these fractional changes, i.e.

$$\text{cond}(A) \geq \frac{1.63}{0.0007246} = 2249.4$$

The large value of the condition number shows that the system solution is very sensitive to errors which can be seen from the given solutions x and x ' for a relatively small change in the vector b.

The above discussion shows the importance of the condition number in describing the sensitivity of a system. Though condition numbers have been extensively used in numerical analysis (Forsythe and Moler [1967]) for some time, Doyle and Stein [1981] were the first to introduce and extend the concept of condition number in the context of control system synthesis, where it can be applied to the assessment of the sensitivity of control to modelling errors. The condition numbers of several candidate processes can be computed over a range of operating frequencies, and these condition number curves may be used by the designer as a basis for selecting those with smaller condition numbers for further considerations (Wong [1984]).

The potential application of the condition number in this flowsheet comparison role was demonstrated by Chan et al. [1986] through their flotation circuit case-study. A set of 11

mineral flotation circuits designed to separate a water/crushed ore slurry into valuable mineral and a worthless gangue were compared (see Figure 4. 3. 4). Table (4. 3. 1) gives the results steady-state optimisation studies and steady-state open-loop controllability analysis. It may be noted that the arrangement through Flowsheet 5 (not shown in Figure 4. 3. 4) could not meet the imposed product quality specification. Note also that even though flowsheets 8 and 4 have a larger mineral recovery (**R**) compared to flowsheets 1 and 2 , the minimum condition numbers for the former flowsheets (i.e 8 and 4) are significantly larger compared to the latter flowsheets (i.e 1 and 2). The significant difference in the value of the condition numbers suggested that flowsheets 8 and 4 would be relatively difficult to control compared to flowsheets 1 and 2. These predictions were confirmed by both closed-loop dynamic simulations.

There are, however, a few problems with using the condition number in such a way :

(1) Condition number provides only semi-quantitative information about the sensitivity of the process. For example, a system with a condition number of 12 may not be any less controllable than a system with a condition number of 10. However, if there are alternative processes with condition numbers that are different by an order of magnitude , then poor closed-loop performance can be expected of high condition number processes.

(2) For a given norm, the condition number is sensitive to input and output variable scaling . This is a serious problem and will be discussed further below.

(3) The condition number is a very conservative estimate about the sensitivity of a process, as it assumes *unstructured uncertainty* (Doyle and Stein [1981], Skogestad and Morari [1987b]). Newer sensitivity measure based on structured singular value (Doyle and Stein [1981]) provide a less conservative index than the condition number and appear to be very promising in estimating system sensitivity to modelling errors. However, the computations associated with the latter are demanding and were not carried out in this study.

SCALING IN CONDITION NUMBER CALCULATIONS

Though the condition number of a system has been shown to be useful as a sensitivity measure , it's applicability in control system synthesis has been questioned because of its scale dependency. In other words, the value of a condition number (for a given norm) depends on the type of physical units used, and hence a system that has a relatively large condition number with one set of units can have a smaller condition number with a change of physical units.

Figure 4. 3. 4
Eleven feasible flotation circuits
(Chan et al. [1986])

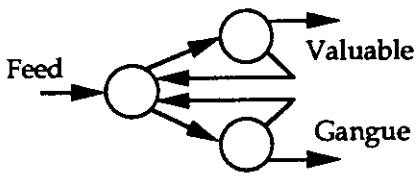

Flowsheet 1: R = 93.3%

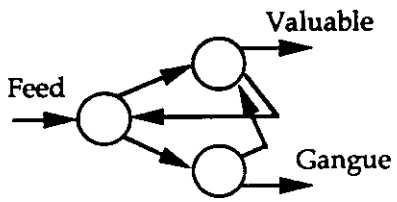

Flowsheet 2: R = 93.6%

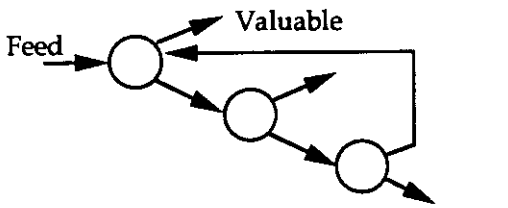

Flowsheet 3: R = 90.4%

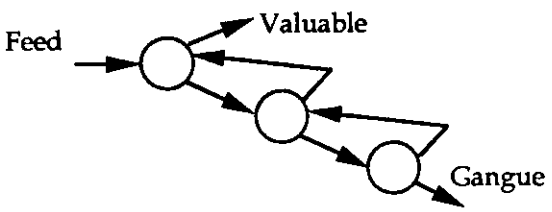

Flowsheet 4: R = 94.4%

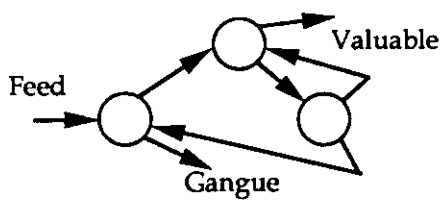

Flowsheet 6: R = 86.3%

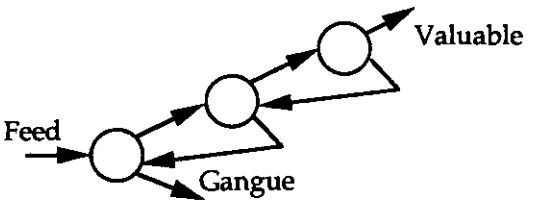

Flowsheet 7: R = 83.4%

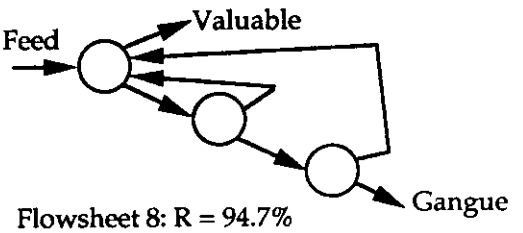

Flowsheet 8: R = 94.7%

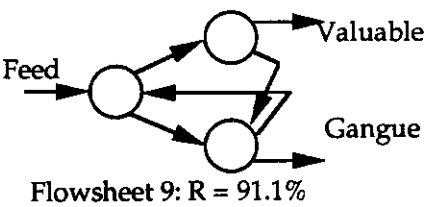

Flowsheet 9: R = 91.1%

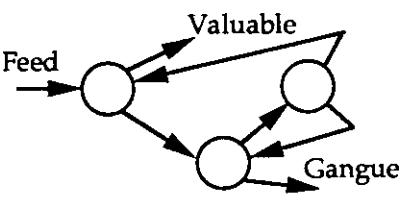

Flowsheet 10: R = 85.0%

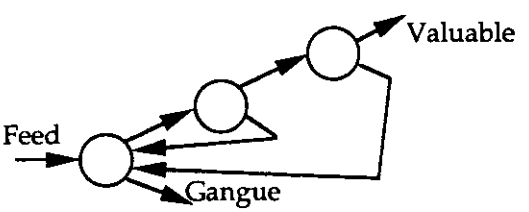

Flowsheet 11: R = 83.2%

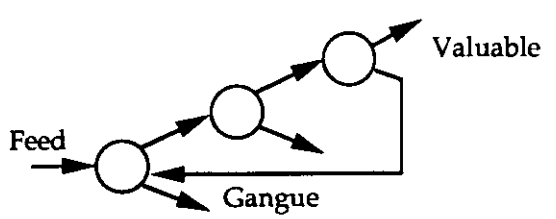

Flowsheet 12: R = 76.4%

Table 4. 3. 1
Comparision of alternative flotation circuits
(Chan et al., [1986])

Flowsheet number	Percentage recovery (R)	Minimum condition number (κ)	Relative gain array (element - λ_{12})
8	94.7	20.6	5.73
4	94.4	60.0	16.37
2	93.6	1.62	0.89
1	93.3	1.65	0.88
9	91.1	1.69	0.86
3	90.4	20.3	5.60
6	86.3	1.72	0.85
10	85.0	17.2	4.80
7	83.4	1.78	0.81
11	83.2	1.78	0.81
12	76.4	1.76	0.83

Two types of scaling have been reported in the literature (Wong [1984]). If the scaling is applied by both pre-multiplying and post-multiplying the original matrix, it is called two-sided scaling. Physically this means scaling both the inputs and outputs of a system. If, on the other hand, it is either pre-multiplied or post-multiplied only , it is called one-sided scaling. Two-sided scaling has been the more usual approach described and will be used in the present work.

One approach to the problem is to employ a two-sided scaling that minimises the condition number of a system. Mathematically this can be written as ,

$$\kappa_p = \min \{ \text{cond}(D_1 A D_2) \} \, |_{D_1, D_2} \qquad (4.3.78)$$

where,

κ_p	is the minimum condition number subordinate to the l_p- norm	
p	is the type of norm used (p = 1, 2, infinity)	
D_1	=	diag (d_{1i}) (i = 1, ..., n)
D_2	=	diag (d_{2i}) (i =1,....., n)

D_1 and D_2 are called the pre and post scaling matrices, respectively. Wong [1984] carried out an extensive survey of the various approaches to optimal scaling reported in the literature. Of all the work reported, Bauer's [1963] work on optimal scaling was the most useful. He determined the scaling matrices which minimise the condition number for the l_1 and l_∞ - norms. Businger [1968] also reported results associated with the optimal scaling of matrices. These are an extension of Bauer's [1963] work and are once again limited to the l_1 and l_∞ - norms.

None of the previous authors produced any analytical results for optimal scaling , using the l_2 - norm . Golub and Varah [1974] showed that a matrix A is optimally scaled, subordinate to the l_2 - norm and two-sided scaling , if the first and last columns of the singular vector matrices U and V (obtained from a SVD; $A = U \Sigma V^H$) have components of equal magnitude, i.e.

$$| u_{il} | = | u_{im} | \text{ and } | v_{il} | = | v_{im} | \quad \text{where } i = 1,..., m \qquad (4.3.79)$$

Apart from the limited optimal scaling methods proposed above, various other non-optimal methods of scaling have been employed. However, the results obtained in this case are dependent upon the order in which the matrix is scaled, that is , if the rows are scaled before scaling the columns or vice-versa. Johnston [1985] suggested a policy scaling for the l_2 - norm based on normalising each of the variables about it's value at a known

steady-state. Lau and Jensen (1985) also suggested scaling using a similar idea. Nguyen et al. [1988] have developed a simple , iterative means of scaling (for the l_2 - norm case) that gives results very close to the minimum condition number (as tested for using Golub and Varah's [1974] result, stated previously). This sub-optimal policy was termed as G - balancing.

Wong [1984] showed that in the absence of an analytical methodology for obtaining optimal condition numbers based on the l_2 - norm, other forms of norm (i.e. l_1 or l_∞ - norm) can be used as a good measure of system sensitivity . Through a series of case-studies , he showed that the minimum condition number based on the l_∞ - norm can be used as a reliable controllability measure.

In the current work, this minimum condition number will be used as a functional controllability measure, and alternative control schemes will be compared based on their minimum condition number values over the entire frequency range of interest.

4.3.6 USE OF SINGULAR VALUE ANALYSIS IN CONTROLLABILITY STUDIES

As discussed in Chapter 1 , SVA provides one route for assessing the controllability of continuous processes. Closed-loop SVA differs from the more familiar rigorous dynamic simulation in that it is both simple to formulate and needs relatively little computation. It has a qualitative correspondence with dynamic simulations (Johnston [1985]) and much more information is obtained from a single closed-loop SVA of a process than is contained in one dynamic simulation. Closed-loop SVA, however, is still dependent on the controller design as well as the process characteristics, making it a less attractive approach than open-loop SVA, which only requires a dynamic model of the process (Chan [1987]) . Also, the latter approach is preferred because of its potential use in the earlier stages of process design, when knowledge of the process and hence the required controller is poor.

Grossmann and Morari [1983] showed that the process condition number was a measure of performance and stability sensitivity to model uncertainty. The minimum singular value was also shown to be a measure of the amount of control action required (further discussion on this follows , later). The minimum condition number based on l_∞ - norm was shown to be a good qualitative measure of the optimal closed-loop dynamic performance of a process in a range of case-studies (Perkins and Wong [1984]). Thus, a number of SVA indicators are now available that provide useful information about a system's sensitivity, controllability characteristics, etc.,.

As discussed previously in Section 3. 2 (see Figure 3. 2. 1) , optimising control of any continuous process essentially consists of two major steps given by,

(a) *Identifying the optimum operating conditions* - this is primarily concerned with steady-state process design. This step provides information about the active constraints that should not be violated during any transient closed-loop response.

(b) *Process regulation about the optimum set-point* - this is primarily associated with the dynamics of the process and external disturbances. This stage involves the selection of a control structure that provides the necessary closed-loop performance for operating close to the optimum.

Violation of any active constraints during process transients could result in a significant loss in the objective function. The key issue in minimising such a loss is concerned with identifying and controlling those process variables that have a direct influence on the process constraints. In other words, it is important to have identified all such controlled process variables and all available manipulated variables , by the end of the first stage of the optimising control design. Further discussion of this issue will be addressed in Section 5.3. Having identified the controlled and manipulated variables the issue is then the selection of a control system that provides good (i.e close to the optimum) closed-loop performance. This also means no constraint violation during any process transient. The open-loop indicators discussed previously (e.g. RGA , condition number, etc.,) offer a means of screening candidate control optimising structures. In the current study, the minimum condition number of a dynamic process (Wong [1984]) will be extensively used as a measure of controllability to screen alternative optimising control systems.

It is clear from the above discussion that both stages are important in realising optimising control on a continuous processes. A more detailed discussion on the issues concerned with the first stage, will be made in the following chapter.

4.4 SUMMARY

For any multivariable process, several multiloop control structures are generally feasible. A major issue is how to rank these control structures with respect to their likely expected closed-loop performance. Results of dynamic simulations on each of these structures could be used but such an approach is both time consuming and needs extensive computational effort. Open-loop indicators, on the other hand , provide, all the necessary information, but require significantly less computational effort. A range of such open-loop indicators are available to screen out the poor candidates. The following are the more important open-loop indicators ;

(a) Relative gain array.

(b) Right-half-plane transmission zeros .

(c) Condition number.

(d) Minimum singular value.

A key role for such open-loop indicators in the context of developing an optimising control scheme has been noted. Control structures with good controllability characteristics should allow us to operate close to the optimum operating conditions, and hence maximise the economic benefits.

CHAPTER 5

THE ECONOMIC BASIS FOR THE SELECTION OF CONTROL SYSTEMS

5.1 INTRODUCTION

The theory and ideas presented in the previous chapter indicate that a number of indicators are available that may be used to assess the controllability of a given process design or to help design alternative processes. However the tools available to date are not ideal for two major reasons (Perkins [1989])

(a) Being based on linear theory, there is no guarantee that the results obtained will be meaningful for chemical processes -the great majority of which are nonlinear in nature.

(b) The criteria do not relate directly to plant economics, so any trade-off between dynamic operability and steady-state economic performance will be difficult to carry out.

Several authors have presented case studies (Morari and Skogestad [1985], Perkins and Wong [1985], Barton and Perkins [1987], Chan et al. [1986]) dealing with the application of linear theory to real nonlinear processes. The approach used in most of these case-studies involved using nonlinear models to estimate the steady-state operating conditions for a process, then linearising the process model around the selected operating point and using linear controllability analysis for assessing alternative process flowsheets. A control system is then designed independently based on the nonlinear model, and its closed-loop behaviour is assessed. It should be noticed that linearisation is only used at one stage in the overall control system synthesis, albeit a crucial one. Finally a comparison of the closed-loop simulation results and the linear theory predictions is performed, to assess the accuracy and reliability of both the linear theory approach and the tools associated with it. As noted above, such studies have been carried out on a variety of systems. In each of these cases it was reported that the linear theory predictions were confirmed by simulation results. Besides this, the results from several of the case-studies suggested that implementation of adequate control systems for plants predicted to have poor controllability characteristics was significantly more difficult than for those with good characteristics (Perkins [1989]). In other words, in all these cases the open-loop indicators regarding process controllability were in agreement with the closed-loop

simulation results. The main emphasis in all of these case-studies was the validation of these open-loop indications as reliable predictors of eventual closed-loop behaviour.

All these results address only the first difficulty mentioned above. What is lacking is a systematic approach that provides a common basis (such as economic value) on which to compare steady-state and dynamic considerations. This becomes more clear through the following discussion. For many processes there will be a few variables for which any deviation from the required operating point is undesirable. The desired operating point is usually provided by an economic optimum. The major difficulty to date has been estimating the economic impact of disturbances impinging on the process when it is in the vicinity of this optimum operating point. For example, the variables associated with product quality control usually fall into this category. This is because any deviations from the required quality will result in off-specification products. However for some other variables, deviations may be tolerated- provided the economic penalties associated are acceptable. An indicator in monetary terms, if developed, could be used to asses the economic penalties associated with different variables. A two-stage approach addressing this general issue will be developed in the following sections.

5.2 OPTIMISING CONTROL

Optimising control may be defined as the maintenance of a process at its optimum operating conditions , despite the action of disturbances. As discussed in Section 3. 2 optimising control offers a means of implementing on-line optimisation. The two-stage policy of Morari et al. [1983] for disturbance handling is quite attractive in the context of optimising control in the sense that the steady-state optimiser deals only with the "slow" disturbances. The "fast" disturbances are handled by the regulatory control scheme. Implementation of on-line optimisation requires that the operating condition for a process be found (using a process model) so as to maximise an objective function - usually the profit for the process. The feasible operating conditions , however, are limited by certain constraints that include safety, environmental regulations, quality control specifications and mechanical limitations. A brief introduction to optimisation theory and, in particular, the importance of constraints in nonlinear constrained optimisation will be made in the following section. The methodology for the development of an optimising control scheme and related issues will be addressed in the subsequent sections of this chapter. Application of such a methodology will be examined for the gas-tail de-propaniser as an example (see Section 5. 4).

5. 2. 1 PROCESS OPTIMISATION

The primary requirement for an optimising control scheme is determining the optimum operating point. This requires a process model and the formulation of an objective function that should be optimised (minimised or maximised), subject to certain process and operational constraints. The problem formulation can be written mathematically as :

$$\text{Maximise } \phi(x, y, z) \tag{5.2.1}$$

subject to

$$g(x, z) - y = 0 \tag{5.2.2}$$

$$h(x, z) \leq 0 \tag{5.2.3}$$

where
- ϕ is the objective function.
- x are the process variables
- g are the set of nonlinear equations forming the process model.
- h are the set of inequality constraints defining the feasible operating conditions.
- y are the set of equality constraints.
- z are the process variables that are allowed to vary during the optimisation (i.e. the freed variables).

The above is the formulation of a *nonlinear constrained optimisation problem* . If all the constraints are linear , then the problem becomes a *linear constrained optimisation problem* . The equality and inequality constraints define the feasible operating space for the process. All constraints are satisfied in this feasible space. A problem is said not to have a feasible solution if no solution space exists satisfying all the constraints.

Let ' x ' be defined as a feasible point and $P(x, \delta x)$ as a set of related feasible points in the space defined by the inequality and equality constraints. A point x^* is said to be a *local maximum* if there exists a small change 'δx ' such that

$\phi(x^*)$ belongs to $P(x, \delta x)$ and

$\phi(x^*) > \phi(v)$ for all v belonging to $P(x, \delta x)$ and $v \neq x^*$.

x^* is said to be a *global maximum* if $\phi(x^*)$ has the largest value in the entire feasible region. For a linear constrained optimisation problem x^* is always the global maximum if the above condition is satisfied (i.e. $\phi(x^*) > \phi(v)$ for all $v \neq x^*$).

Edgar and Himmelblau [1988] discuss various methods for solving equality constrained optimisation problems. One approach to finding a solution is by eliminating all the

constraint variables, thereby converting a constrained optimisation problem into a simpler one to solve unconstrained optimisation problem. This approach , though direct, is often very tedious.

Another approach is the classical method of eliminating the equality constraints (given by Equation 5. 2. 2) using Lagrange functions. This approach was originally defined only for equality constraints (Adby and Dempster [1974]) and was based on the following analysis.

$$\frac{\partial \phi}{\partial x} = \frac{\partial \phi}{\partial y} \cdot \frac{\partial y}{\partial x} \qquad (5.\ 2.\ 4)$$

As both ' x ' and ' y ' are vectors, the above equation and can also be written as

$$\frac{\partial \phi}{\partial x} = \sum_{i=1}^{m} \frac{\partial \phi}{\partial y_i} \cdot \frac{\partial y_i}{\partial x_i} \qquad (5.\ 2.\ 5)$$

where ' m ' is the size of the vector y .

The first term on the right hand side of Equation 5. 2. 5 (i. e. $\partial\phi / \partial y_i$) is the rate of change of the objective function (ϕ) for any variation in the corresponding constraint (y_i) and is denoted by 'λ_i'. Integrating both sides of Equation (5. 2. 5) with respect to x , we get

$$\phi(x, y, z, \lambda) = \phi(x^*, y^*, z^*) - \sum_{i=1}^{m} \lambda_i . g(x, z) \qquad (5.\ 2.\ 6)$$

where

λ is a vector of λ_i (for $i = 1,\ldots, m$).

An " * " as superscript indicates the optimum.

The expression on the right hand side of Equation (5. 2. 6) is called an *extended form of the objective function* or the *Lagrangian* . All the λ_i (for $i = 1,\ldots, m$) are termed *Lagrange multipliers*. The solution for such an optimisation problem is provided by the *stationary point* of the Lagrangian. For a solution to exist ;

(i) All the problem functions {i.e. $\phi(x)$, $g(x, z)$ and y } must be continuously differentiable and,

(ii) The necessary condition for x^* to be a local maximum is that

$$\nabla \phi(x^*) - \sum_{i=1}^{m} \lambda_i \nabla g_i(x^*, z^*) = 0 \qquad (5.\ 2.\ 7)$$

where the operator ∇ is used to denote the gradient of a function. The gradient in this case is defined with respect to x , and ∇ is given by ;

$$\nabla = \frac{\partial}{\partial x} \qquad (5.\ 2.\ 8)$$

An analogous result concerning the stationarity of the Lagrangian function for inequality constraints was first provided by Kuhn and Tucker [1951]. Using slack variables, they converted all the inequality constraints (i.e $h(x, z) \leq 0$) into equality constraints and defined a new Lagrangian and a new set of necessary conditions to define the optimum (Adby and Dempster [1974]). The new Lagrangian is given by

$$L(x, y, z, \lambda, \mu) = \phi(x) - \sum_{i=1}^{m} \lambda_i . g(x, z) + \sum_{j=1}^{l} \mu_j . h(g, z) \qquad (5.\ 2.\ 9)$$

where

λ_i are the Lagrange multipliers for all the equality constraints.

μ_j are the Lagrange multipliers for all the active inequality constraints.

If all the functions (i. e. including the 'l ' inequality constraints that are active at the optimum) are differentiable, then the necessary conditions for x^* to be a local maximum are given by

$$\nabla \phi(x^*) - \sum_{i=1}^{m} \lambda_i . \nabla g(x^*, z^*) + \sum_{j=1}^{l} \mu_j . \nabla h(g^*, z^*) = 0 \qquad (5.\ 2.\ 10)$$

$$\mu_j . h(x^*, z^*) = 0 \quad \text{for all } j = 1, \ldots, l \qquad (5.\ 2.\ 11)$$

$$\mu_j \geq 0 \quad \text{for all } j = 1, \ldots, l \qquad (5.\ 2.\ 12)$$

Equations (5. 2. 10) - (5. 2. 12) are called the *Kuhn -Tucker optimality* conditions. The relations given by Equation (5. 2. 11) are called the *complementary slackness* conditions since together with Equation (5. 2. 12) they imply that at an optimum, a positive Lagrange multiplier corresponds to an inequality constraint *binding* or being an *active constraint*, while a non-binding constraint corresponds to a zero multiplier. Kuhn-Tucker's first-order conditions (i.e. Equations (5. 2. 10) - (5. 2. 12)) may be regarded as a modification of the vanishing of the gradient of a function at a local unconstrained maximum, to take account of local constrained optima on the constraint boundaries. However these first-order conditions provide only the necessary conditions for the existence of an extremum. An expression similar to the second-order conditions for unconstrained optimum can be developed for the constrained case along similar lines. This is obtained from the second-order term of the Taylor's series expansion of the Lagrangian function about the extremum point (x^*, z^*). Therefore if all the functions are twice continuously differentiable, then the necessary condition for a local maximum is given by ,

$$x^T \left[\nabla^2 \phi(x^*, z^*) - \sum_{i=1}^{m} \lambda_i . \nabla^2 g(x^*, z^*) + \sum_{j=1}^{l} \mu_j . \nabla^2 h(x^*, z^*) \right] x \leq 0 \quad (5.2.13)$$

where the superscript T shows the transpose of vector x (see Appendix A10). In this case, where all the gradients are defined with respect to x, ∇^2 is given by;

$$\nabla^2 = \frac{\partial^2}{\partial x^2} \quad (5.2.14)$$

The sufficient conditions for (a local maximum) can be stated as follows :

If for any x,

$$\nabla h_j(x^*, z^*) . x = 0 \quad \text{when } \mu_j > 0 \quad (5.2.15)$$

$$\nabla h_j(x^*, z^*) . x \geq 0 \quad \text{when } \mu_j = 0, \text{ but } h_j(x^*, z^*) = 0 \quad (5.2.16)$$

$$\nabla g_i(x^*, z^*) . x = 0 \quad \text{for all } i = 1,...., m \quad (5.2.17)$$

then x^* is a local maximum.

Satisfying the second-order conditions ensures that the solution is a local maximum. Edgar and Himmelblau [1988] discuss a number of methods available to obtain the solution of an inequality constrained optimisation problem based on these ideas. Two different options are available in SPEEDUP for solving nonlinear constrained optimisation problems. **FEASOPT** is a feasible path optimisation routine that is based on Powell's [1978] algorithm. **FEASOPT** was used throughout the present study. **MINOS** is an infeasible path optimiser that has been interfaced with SPEEDUP. It is recommended for large, highly nonlinear problems but was not used in the current study.

ISSUES IN DETERMINING AN OPTIMISING CONTROL SCHEME

As noted previously, optimising control is a generic term for regulating a process at it's optimum operating conditions, despite the action of disturbances and uncertainties. Optimising control is an essential requirement for the implementation of an on-line optimisation scheme. The optimal operating point for a well designed plant usually lies at the intersection of several operational constraints (Rijnsdorp [1967], Maarleveld and Rijnsdorp [1970], Lee and Weekman [1976], Ishida [1975]). The situation is complicated by any sensitivity of this operating point to the slow disturbances. In other words the optimal operating point may switch from the intersection of one set of constraints to another set of constraints as the slow process disturbances change with time. The available literature on the regulatory behaviour of optimising control schemes indicates that this issue of changing constraints has not been completely solved (Rijnsdorp [1967], Maarleveld and Rijnsdorp [1970], Arkun and Stephanopoulos [1980]).

Several examples in the literature (Rijnsdorp [1967], Maarleveld and Rijnsdorp [1970], Lee and Weekman [1976], Arkun [1979]) indicate that in some cases, the optimum is completely defined by the active inequality process constraints. Hence, ensuring that these process constraints are met ensures optimality. Maarleveld and Rijnsdorp [1970] introduced a control policy called *constraint control* which essentially involves choosing the active constraints as the control objectives and designing a regulatory control system to hold them at the required values. Several applications along these lines have been reported to date (Roffel and Fontein [1979, Arkun and Stephanopoulos [1980], Prett and Gillette [1979]), some with a modified version of the constraint control policy. In summary, constraint control implicitly guarantees both optimality and feasibility. Also , it takes account of two of the major issues of control system synthesis, i.e. the selection of the control objectives and the manipulated variables. The necessary requirement for the implementation of constraint control is that the optimum always lies at the intersection of a set of operational constraints equal in number to the freed variables. The available freed variables can then be chosen as the manipulated variables and the active constraints taken as the control objectives.

Quite often, however, we come across processes (such as the gas-tail, described in the next chapter) where the number of active constraints is less than the number of freed variables at the calculated optimum. There is no unique way of achieving an optimising control scheme in this situation. Arkun and Stephanopoulos [1980,1981] suggested that in cases where there are more freed variables than active constraints, all the active constraints should be selected as control objectives, together with an equivalent number of freed variables as manipulated variable. Then one of the following approaches should be used to complete the control system.

(a) Select additional control objectives to make use of the freed variables that have not been used, based on the approach put forward by Morari et al. [1978].

(b) Use the additional freed variables in a feedforward fashion (i.e set at the values obtained from the steady-state optimisation).

Based on these ideas, Arkun and Stephanopoulos proposed an elaborate policy for achieving constraint control. Their procedure makes use of information about the slow disturbances influencing the process to estimate a new optimal operating point , and then identifying the feasible paths to reach the new optimum without violating any constraints in the transition. Engineering judgement along with functional controllability measures (discussed in the previous chapter) could be used to minimise the number of alternative transition routes and possible control schemes. Though such an approach is superficially

very attractive, computationally it is very demanding and no case where it has actually been implemented is known.

The optimising control scheme proposed by Arkun and Stephanopoulos should shift the process from the current optimum to the new optimum without violating any constraints in the transition. The shift in the optimum operating point is implemented through a series of small set-point changes, with the regulatory control scheme taking care of the process operation at each intermediate point. Poor regulatory control could lead to additional problems such as an excessive loss in economic performance or even infeasibility. Thus selecting a good regulatory control scheme is crucial in the successful implementation of an optimising control strategy. A new approach, seeking to provide a consistent economic basis for the selection of a good regulatory control scheme within an overall optimising control scheme, will be developed in the following sections.

5. 2. 2 SELECTION OF CONTROL SYSTEMS FOR DISTILLATION COLUMNS

The major case-study of this thesis, the Shell CDU gas-tail, consists of three distillation columns. One of the initial objectives of this work was to develop an optimising control policy that improves on the current operational performance. Such an investigation requires a good understanding of the control of distillation columns. In this section, therefore, a brief review of the issues related to distillation control will be made , with an emphasis on identifying the various control schemes possible (both traditional and more unconventional).

Consider a simple distillation column with one feed and two product streams together with a total condenser (see Figure 5. 2. 1). It is well known that there are five major control objectives likely in such a case (Rijnsdorp [1967], Maarleveld and Rijnsdorp [1970], Shinskey [1988]). They are the top and bottoms compositions, the levels in both the overhead accumulator and the reboiler , and the column pressure. Regulating these five objectives is possible using the five available manipulated variables (i.e. the distillate rate, the reflux rate, the cooling water flowrate, the steam rate to the reboiler and the bottoms product rate), and this type of control scheme is widely used in industry. It is assumed in this case that the steam supplies the heat duty necessary in the reboiler, while the cooling water provides the necessary cooling action in the condenser.

In many cases distillation control can be thought of as consisting of two types of control objectives , i.e. primary and secondary. Control objectives such as the liquid holdups in the overhead accumulator and the reboiler only have to be maintained within certain

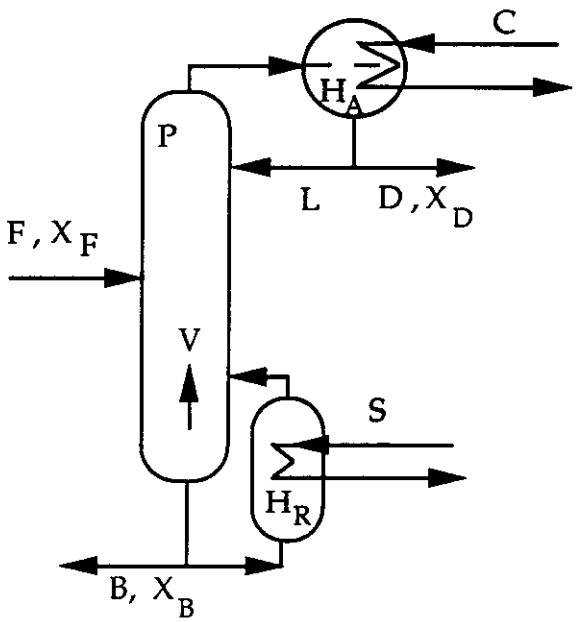

Figure 5. 2. 1
Schematic diagram of a distillation column
with one feed stream , two product streams and a total condenser.

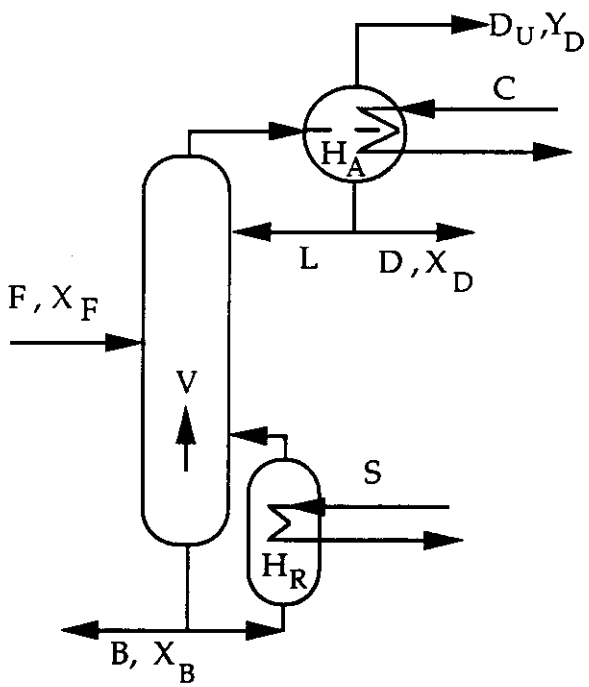

Figure 5. 2. 2
Schematic diagram of a distillation column
with one feed stream , two product streams and a partial condenser.

levels (tight control is not necessary) to ensure safe and continuous operation of the column. These can be classified as *secondary objectives* . Objectives such as the top and bottoms compositions , on the other hand, may require tight control , though generally they do not endanger process operation. Frequently these variables are linked to the product specifications and, therefore, tight control on these variables is necessary. Such variables may be classified as *primary objectives* . Column pressure , as distinct from the rest of the possible controlled variables, can fall into either of these categories and varies from column to column. Considerable plant experience and various theoretical studies (Shinskey [1988], Finco et al. [1989]) suggest that the design of a control system for the primary control objectives can be made essentially independently of the control system design for the secondary objectives. The usual approach followed is to design the controllers for the secondary objectives first (as these usually have a relatively fast dynamic response compared to the primary objectives) followed by controller design for the primary objectives.

From the point of view of control, a simple distillation column can be viewed as a 5 X 5 system. Though this could provide as many as 120 different multiloop control schemes , engineering judgement and plant experience has shown that fewer than 10 of these control schemes are in fact practicable. The following discussion briefly introduces one or two newer control schemes besides the ones that have been used traditionally.

(1) *LV control scheme (energy balance or indirect material balance control)*

This control scheme derives its name from the fact that the top and bottoms compositions (i.e. X_D and X_B respectively) are controlled by the reflux rate (**L**) and the vapour boilup rate (**V**). The distillate product rate (**D**) is used to control the overhead accumulator holdup (H_A), the bottoms product rate (**B**) is used to control the reboiler holdup (H_R), and the pressure (**P**) is controlled by the cooling water flowrate.

(2) *DV control scheme (material balance control)*

Here the top and bottom compositions are controlled by **D** and **V** respectively. The major difference from LV control is that the liquid holdup in the overhead accumulator now is regulated by the reflux rate.

(3) *DB control scheme*

Here the top and the bottom compositions are controlled by **D** and **B** respectively. Liquid holdups at the top and the bottom are regulated using **L** and **V** respectively, while cooling water flowrate regulates the column pressure.

(4) *(L/D) (V/B) control scheme (double ratio control)*

Here the top and the bottom compositions are controlled by the internal reflux ratio at the top (i.e. L /D) and the vapour boilup ratio at the bottom (i.e. V/B) respectively . Perfect control on the liquid holdups both in the condenser and reboiler is assumed, while pressure is regulated through the cooling water flowrate.

(5) *(L/D) V control scheme (Ryskamp' s scheme [1980])*

Here the top and the bottom compositions are controlled by the internal reflux ratio at the top (i.e. L /D) and V respectively. The same assumptions are used here as in (L/D) (V/B) control scheme for regulating column pressure and the liquid holdups at both the top and bottom of the column.

These control schemes represent the most commonly used dual composition (i.e. top and bottom compositions are both controlled) control schemes in the chemical industry. Such control is often possible for process flowsheets with a single distillation column . For process flowsheets containing several distillation columns in either series or parallel , however, dual composition control may not always be possible. In such cases one-point control , where only one of the two product compositions is controlled, is often employed. The three distillation columns of the gas-tail case-study each presently employ a one-point control scheme. For example, the de-propaniser column currently has the following control scheme.

(6) *Top composition and pressure control*

Here the top composition and the column pressure are chosen as the primary control objectives with the reflux rate and the vapour boilup rate providing the respective manipulated variables for regulatory control action. This is similar to the LV type of control scheme , except that the control objectives are different in the two cases. The liquid holdups at the top and bottom of the column are controlled with the distillate product rate and the bottoms product rate respectively. The air flowrate to the fin-fan condensers is not used to specifically control anything but is periodically adjusted by the operators to ensure good overall column control.

By comparison, the de-ethaniser column in the gas-tail currently uses a different form of one-point composition control.

(7) *Bottoms composition and pressure control*

Here the bottoms composition and the column pressure are the primary control objectives with the uncondensed distillate product rate (D_U) and the vapour boilup rate as the respective manipulated variables (see Figure 5. 2. 2). This scheme is similar to the **DV** type of control scheme , except that the control objectives are different. The liquid holdups at the top and bottom of the column are regulated with the reflux rate and the bottoms product rate respectively. Air flowrate to the fin-fans forms the (initial) part of a split-range controller used to regulate the column pressure.

The latter two scheme types represent fairly commonly used one-point composition control policies employed in the chemical industry. The basis for selecting these latter types of scheme is generally heuristics and plant experience. There have been few studies to date providing a systematic analysis of why such traditional choices are preferable to dual composition control, much less to a comparison with constraint control.

Some important features of the various dual-composition control schemes presented above will be discussed here.

(1) The **LV** control configuration is the most common type used in industry even though the performance reported has often been poor (Shimizu and Matsubara [1985], Shinskey [1988]).

(2) For columns having high reflux ratios, **DV** control is preferred to **LV** control (Shinskey [1988]). This is because for high reflux ratios (i.e. $D << L$) the small distillate flowrate is capable of regulating the top composition as accurately as the larger reflux flow rate. In general this is a widely accepted policy in industry for reflux ratios of the order five or more.

(3) The **DB** configuration has an infinite RGA, which was the basis used in rejecting this choice as "impossible " by earlier workers (Shinskey [1984]). However, Finco et al. [1989] reported that while such a configuration has an infinite steady-state condition number, it falls off very rapidly and can become very close to unity at high frequencies. Therefore, a **DB** type control scheme represents a potentially viable alternative to more traditional control schemes (Skogestad et al. [1989], Gannavarapu et al. [1990]). Control tuning for a **DB** type configuration , however, is not easy. Finco et al. [1989] used an on-line tuning approach to tune a **DB** type control configuration in their case-studies.

(4) The following is the " best " order for control configurations as given by Skogestad et al. [1989]. The best choice for all modes of operation is provided by the (L/D) (V/B) type scheme. The major drawback with this approach is that it requires the measurement of four flow rates , with the failure of any one of these measurements resulting in poor performance. The DV type control scheme is the next best configuration , being well suited to columns with large reflux ratios and high purity bottoms product. Failure of the top composition loop , however, seems to result in poor performance of the bottoms composition loop. DB control competes with DV control in quite a few aspects. Both of them seem to provide very similar performance. The main disadvantage of the DB control configuration is that it results in poor control scheme integrity i.e. failure of one of the control loops can result in column instability. The LV control scheme probably provides the worst performance with the (L /D) V type providing a performance level somewhere between the (L/D) (V/B) type and the LV type configurations.

Several of the control schemes reported above were investigated for the distillation columns forming the gas-tail (see Section 6. 4).

5. 3 AN ECONOMICS BASED APPROACH TO CONTROL SYSTEM SYNTHESIS

5. 3. 1 INTRODUCTION

It should now be clear (after the discussion on controllability in the previous chapter) that control system synthesis leading to perfect control has lately become a major goal for control engineers. The approach used (Morari [1983], Perkins and Wong [1985]) has been based on setting a perfect control target (i.e. perfect set-point tracking and disturbance rejection) and then finding process characteristics that prevent the target being achieved. Based on the results of case-studies reported to date, it can reasonably be said that a reliable set of techniques now exist which can be used to assess the controllability of alternatives during the process design stage. To illustrate the application of these techniques results from a case -study involving flotation circuit design (Chan et al. [1986]) will be discussed. The objective was to design a plant to separate valuable mineral from worthless gangue using froth flotation. Figure 5. 3. 1 shows three (from a total of twelve considered) alternative flowsheets for this process. Under steady-state conditions each of these plants processes the same amount of raw material and produces a concentrated valuable stream of the same quality. However, they differ in the maximum amount of valuable material which is recovered from the feed (i.e R is the valuable recovery). Figure (5. 3. 1) shows the percentage of valuable material in the feed which appears in the concentrated product stream. On the basis of steady-state analysis of these

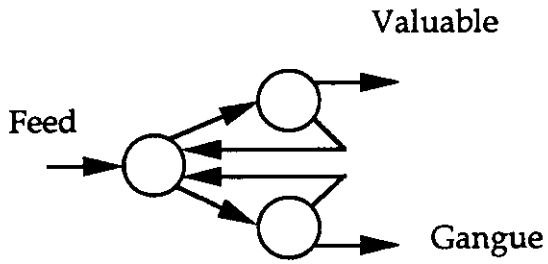

Flowsheet 1: R = 93.3%

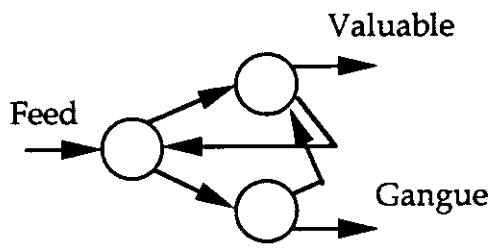

Flowsheet 2: R = 93.6%

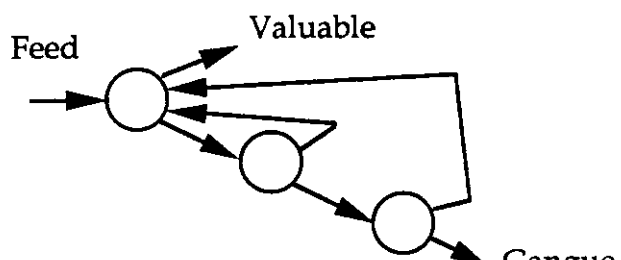

Flowsheet 8: R = 94.7%

Figure 5. 3. 1
Alternative flotation circuits

alternatives, therefore, we would probably select Flowsheet 8 since it has the highest recovery.

When the controllability of these flowsheets is assessed using the techniques outlined previously (see Section 4. 3) a different picture emerges. Chan et al. [1986] used the process condition number (along with various other open-loop indicators) to rank the alternatives for controllability. The condition number indicates the effect of plant/model mismatch and also gives some information on the likely importance of manipulated variable constraints. The condition number for Flowsheet 8 was found to be an order of magnitude higher than those for Flowsheets 1 and 2. This significant difference in the absolute value of the condition number for Flowsheet 8 suggested that indeed the plant would be difficult to control. These predictions were confirmed by designing multiloop controllers for the three alternatives, and observing their closed-loop behaviour. Not only was the dynamic performance of Flowsheet 8 significantly worse than that for Flowsheets 1 and 2 , but the control effort required to obtain reasonable performance for the worst flowsheet was also significantly greater.

It may well be that a process designer would be discouraged from proceeding with Flowsheet 8 on the basis of these results. Further, this view would be reinforced by the finding that structures like Flowsheet 8 are regarded as unconventional by the mineral processing industry. In return for the "qualitative" control benefits, the designer has given up Flowsheet 8 which in turn incurs a loss of about 1% recovery. Bearing in mind the large throughputs typical of these plants and the value of the recovered material, the loss in recovery for not choosing Flowsheet 8 can represent a significant economic penalty. Now, of course, it is well known that this steady-state performance prediction will not actually be achieved if the plant were built, but the argument would have been more convincing if both predictions (i.e. both steady-state and dynamic) could be made on the same grounds *viz* economics. Therefore, what is ideally required is a common basis for identifying the potential economic benefits and the likelihood of achieving these benefits based on some operability measure. In the following section we seek to develop a two-stage method of predicting the economic penalties associated with disturbances, and the potential of control systems to reduce these penalties.

5. 3. 2 ASSESSING THE ECONOMIC POTENTIAL OF CONTROL DURING PROCESS DESIGN

In Section 4. 3. 4 some of the major limitations associated with the existing controllability measures were identified. In addition to these, it has not been clear to date, what the economic impact of the various dynamic characteristics of a process on its operation are. What we require are indicators for assessing the impact of the dynamics of the process translated into economic terms.

The proposed approach is based on first establishing an economic context for regulatory performance. In the context of optimising control, the choice of operating point is decided by the optimiser. The whole concept of optimising control is based on the relative time scales of typical disturbances in comparison to the response time of the plant (Morari [1983]). A two-level decomposition (see Figure 3. 2. 1) for the optimal operation of a continuous plant is suggested by a classification of disturbances into "slow" and "fast" categories (Morari [1983]). The slow disturbances are handled by an optimiser which considers modification of the desired steady-state operating point of the plant. The fast disturbances are handled by a regulation system whose aim is to hold the plant at the desired (optimum) steady-state.

It was pointed out in Section 5. 2. 1 that the role of constraints is crucial in the optimisation of chemical processes. It is often the case that the best operating point for a plant is partly determined by active constraints, representing physical and other limitations. The simplest situation is the optimisation of a plant with two freed variables, as illustrated in Figure 5. 3. 2 . In this case, the shape of the objective function contours and constraints are such that the optimum operating point is completely determined by the two constraints C_1 and C_2. This situation is quite common in the process industries (Arkun and Stephanopoulos [1981] , Maarleveld and Rijnsdorp [1970]). The other common situation is where there are fewer active constraints than there are freed variables (see Figure 5. 3. 3 where there is only one active constraint). Further discussion on the latter case will be made later in this section.

The effect of disturbances at the regulation level is to perturb the plant from the desired steady-state. Thus, the point in operating space representing the designed steady-state is surrounded by a region within which the plant will operate as disturbances perturb it. One effect of this region may be to require a move in the operating point away from that determined by the optimisation level (see Figures 5. 3. 2 and 5. 3. 3). This is because, requiring the steady-state to be precisely on an active constraint will sometimes result in

Figure 5. 3. 2
Steady-state optimisation (fully constrained)

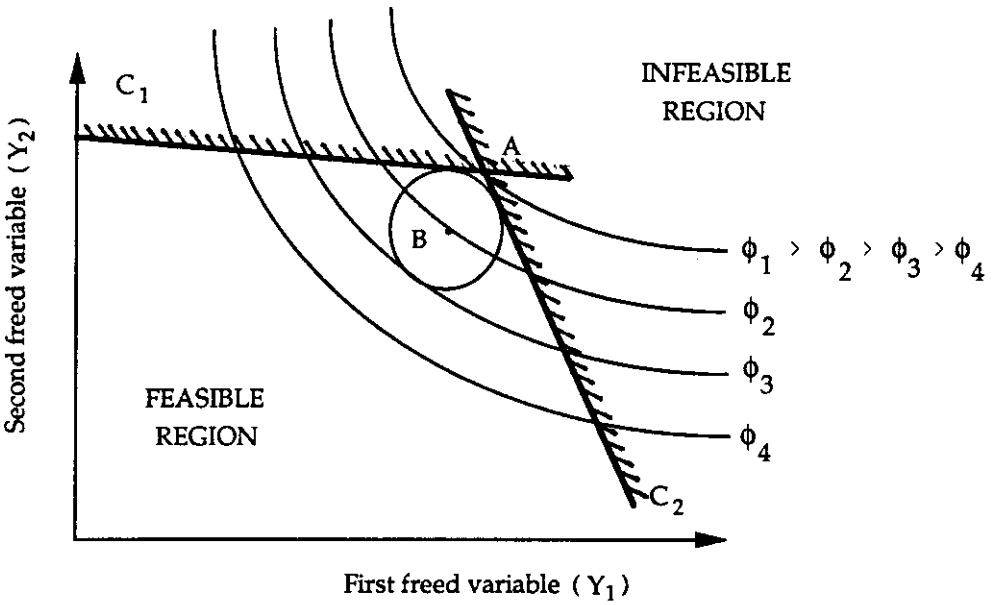

Figure 5. 3. 3
Steady-state optimisation (partially constrained)

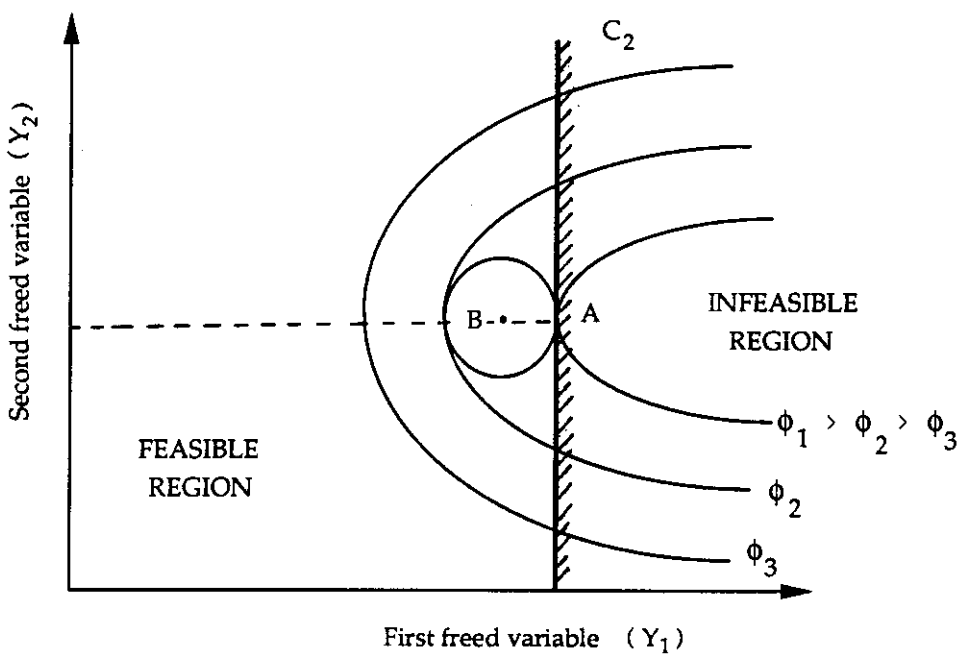

infeasible operation when a disturbance perturbs the system. To avoid this, set-points should be chosen so as to retain feasibility despite the disturbances. Note that such a move may not be necessary for all the set-points - only for those associated with active constraints. In Figure 5. 3. 2, point **A** represents the optimum operating point lying at the intersection of two constraints. Point **B** , on the other hand, represents an operation point that guarantees feasibility despite the action of disturbances. The region surrounding point **B** (shown as a circle, here) indicates the region of movement of the operating point due to the action of disturbances. If back-offs made in each of the active constraints are not equal, then such a region will not be circular.

The necessary movement away from the optimum that one has to make to avoid ever operating in the infeasible region is partly a characteristic of the process itself (the nature of the disturbances is the other factor) and usually is nonlinear in nature. One way to estimate this move is by performing dynamic simulations on the process model over the whole range of likely disturbances. Though this approach provides an accurate estimate of the necessary move, computationally it can be very demanding.

An alternative and much simpler approach to estimating the size of the necessary move is through a first-order estimate based on the linearised model of the process. A first-order estimate of the economic penalty arising from such a move may be obtained if the size of the perturbed region can be determined. The sensitivity of the optimum to a move in a direction orthogonal to a given active constraint is given by the optimal Lagrange multiplier for that constraint (see Section 5. 2 ; also Fiacco [1976]). This value may be combined with an estimate of the region size to give the economic giveaway associated with a given regulatory performance for a given constraint.

A first-order estimate of the size of the region in the absence of control may readily be determined, as will now be shown. Consider (linear) transfer function relating manipulated (**u**) and disturbances (**d**) to the chosen output variables (**y**) :

$$y(s) = G(s).\,u(s) + G_d(s).\,d(s) \qquad (5.3.1)$$

It must be realised that, throughout the current study, active constraints obtained from the steady-state optimisation will be potential choices as the output variables while the inputs are typically the freed variables used in the steady-state optimisation .

In the absence of control,

$$u(s) = 0 \qquad (5.3.2)$$

and by taking l_2 - norms of both sides of the resultant equation, we get ;

Figure 5. 3. 4
Economics of controllability

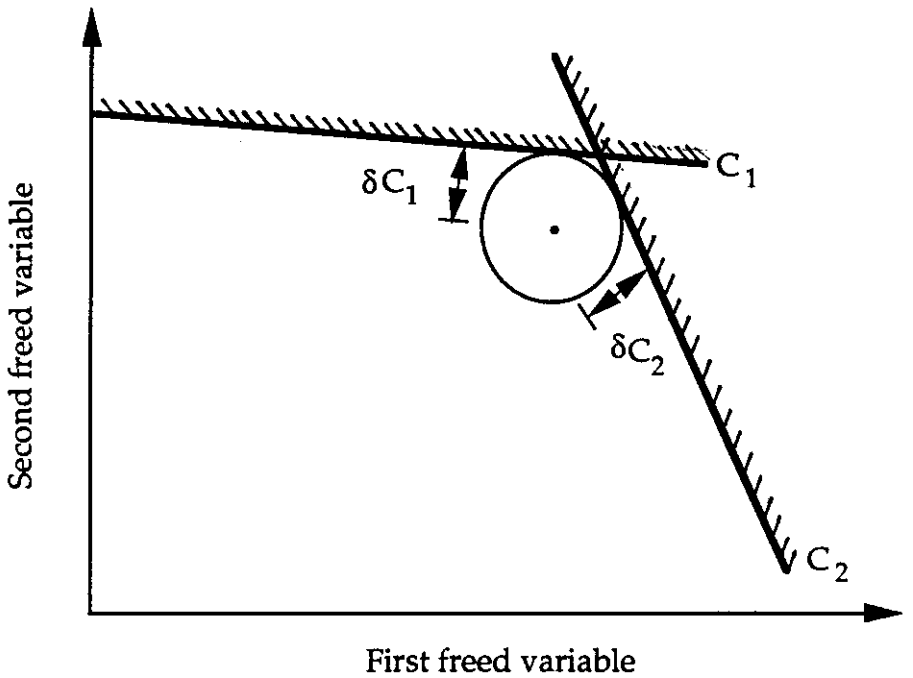

Figure 5. 3. 5
Penalty associated with a back-off from the optimum

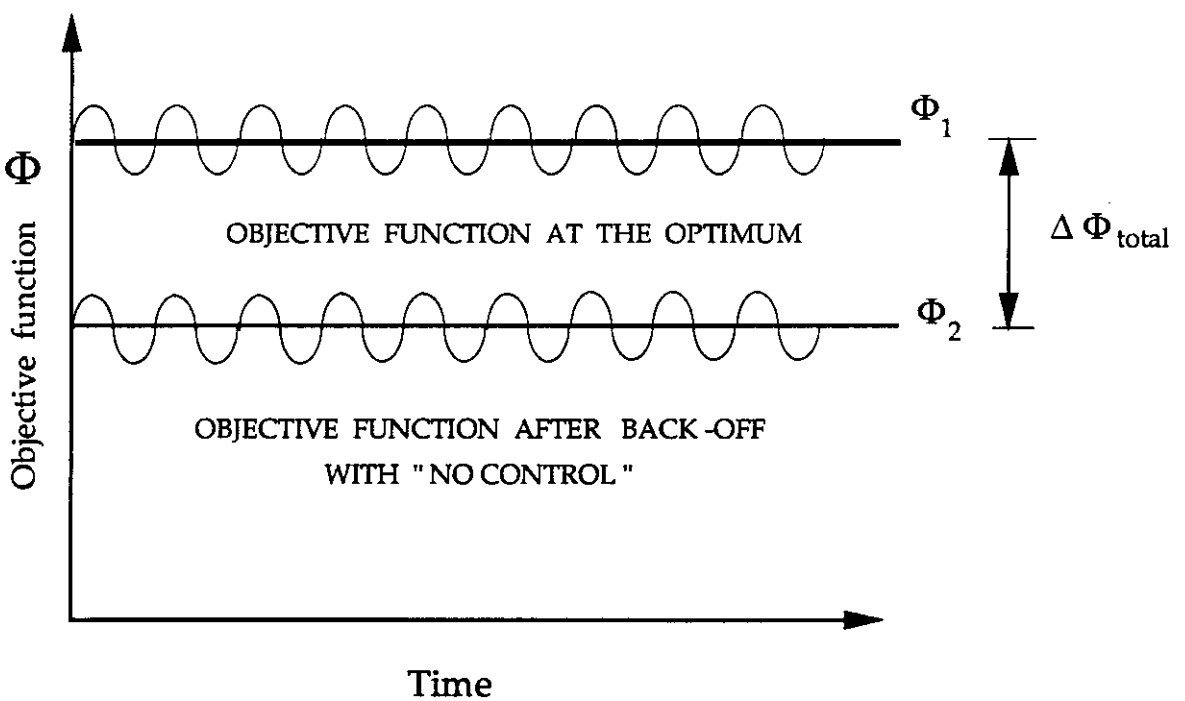

$$\| y(s) \| \leq \| G_d(s) \| . \| d(s) \| \qquad (5.3.3)$$

In principle, therefore, an estimate of the perturbed region size in the absence of any control is given by the product of the maximum singular value of the disturbance transfer function matrix and the Euclidean norm of the disturbance vector.

$$\| y(s) \| \leq \sigma_{max}(G_d) . \| d(s) \| \qquad (5. 3. 4)$$

However, such an estimate is a conservative upper limit and provides only a single measure in which all the disturbance effects are lumped together. It provides only the size of the maximum move away from the optimum required at any time if there were no control. It would undoubtedly be true that for some cases the largest move necessary would be much smaller than the largest move estimated using Equation (5. 3. 4). Another major drawback of this simple measure is scaling. The size of the move thus estimated (i.e. using Equation 5. 3. 4) will depend on the physical units used for the various process variables. Thus, it is not very clear what size of "back-off" from the optimum is required in each of the process variables. However, the concept of estimating the size of move necessary and backing-off correspondingly from the optimum operating point is quite promising as it has economic implications for the process operation. This importance can be seen through the following analysis. Consider a process with its optimum determined by two constraints (i.e C_1 and C_2 in Figure 5. 3. 4). Let δC_1 and δC_2 be the estimated back-offs required from each of these constraints, respectively. Therefore, the new operating point is at the centre of the a region obtained by backing-off from each of the constraints by the relevant amount. As discussed previously, such a region may not always be circular if the relevant moves necessary away from each of the active constraints, are not equal. In economic terms , the new operating point represents a new objective function (ϕ_2) for the process (see Figure 5. 3. 5). Figure 5. 3. 5 shows variation of the objective function with time while ϕ_1 and ϕ_2 represent the objective functions at different conditions that are averaged over the entire time scale. It may also be noted that the fluctuations shown here in the objective functions (see Figure 5. 3. 5) , may not always be symmetric. The difference in the objective function at these two operating points represents the economic penalty paid (i.e $\Delta \phi_{total} = \phi_1 - \phi_2$) due to back-off from the active constraints C_1 and C_2.

The issue that still needs to be addressed is how to estimate the back-off required from each of the active constraints. To avoid the conservativeness introduced through the use of Equation (5. 3. 4) , an alternative approach can be employed which involves the direct estimation of the actual size of the move in each output due to each disturbance of known

size. These moves can be estimated for each of the control objectives (i.e. active constraints) Equation (5. 3. 1) but with no control (i.e. $\mathbf{u} = 0$), as shown below :

$$\begin{bmatrix} \Delta y_1(s) \\ \Delta y_2(s) \\ . \\ . \\ \Delta y_n(s) \end{bmatrix} = \begin{bmatrix} G_{11}(s) & G_{12}(s) & . & G_{1m}(s) \\ G_{21}(s) & G_{22}(s) & . & G_{2m}(s) \\ . & . & . & . \\ . & . & . & . \\ G_{n1}(s) & G_{n2}(s) & . & G_{nm}(s) \end{bmatrix} \begin{bmatrix} \Delta d_1(s) \\ \Delta d_2(s) \\ . \\ . \\ \Delta d_m(s) \end{bmatrix} \qquad (5.3.5)$$

where,

$\Delta y_i(s)$ is the change in the i^{th} controlled objective due to the action of all disturbances.

$G_{ij}(s)$ is the gain between i^{th} controlled objective and j^{th} disturbance.

$\Delta d_j(s)$ is the size of the j^{th} disturbance.

Since each of the control objectives (i.e. i = 1,..., n) is associated with a certain back-off due to each of the disturbances (i.e. j = 1,..., m), the total back-off required in a given objective from the optimum (i.e. $\Delta y_i(s)$), is some combination of these individual back-offs. Depending on the direction of the disturbances, it is possible that some of these estimated individual back-offs due to various disturbances, may cancel-off. For any given control objective, therefore, a simple summation of the individual back-offs due to all the disturbances would provide only a conservative estimate. An alternative method is proposed here which will be used in this case-study.

The individual back-offs in each of the control objectives due to each of the disturbances can also be written as ,

$$b_{ij} = G_{ij}(s) . d_i(s) \qquad (5.3.6)$$

where b_{ij} is the absolute change in the i^{th} controlled variable due to the action of the j^{th} disturbance (for i = 1,..., n and j = 1,...., m).

Equation (5. 3. 6) shows that the move necessary from in each output varies with frequency. The product of an estimated size of move combined with the Lagrange multiplier associated with the corresponding constraint gives a first-order estimate of the

economic penalty resulting from taking no control action to mitigate the effect of fast disturbances for that constraint ;

$$\Delta\phi_{ij} = \lambda_i \, b_{ij} \qquad (i = 1,..., n \text{ and } j = 1,...., m) \tag{5.3.7}$$

where,

$\Delta \phi_{ij}$ is the economic penalty associated with the back-off required in the i^{th} control objective due to the j^{th} disturbance, in the case where no control action is taken.

λ_i is the Lagrange multiplier associated with the i^{th} active constraint.

Since a back-off in each of the control objectives (i.e. i = 1,..., n) is associated with a certain penalty ($\Delta \phi_{ij}$) for each of the disturbances (i.e. j = 1,..., m), the total penalty for a given objective for all disturbances is some combination of these individual penalties. If all the disturbance effects are "symmetric" about their average values, then the total penalty due to back-off from the steady-state optimum can be estimated by a simple summation of the absolute values of all the individual penalties. In the absence of any information on the nature of disturbances, such an estimate provides an upper limit on the total economic penalty associated with a back-off from the optimum. It may be realised that in such a case, all the disturbances are said to align in the "worst" input directions. However, the total penalty thus estimated is still conservative, as the disturbances may not always correspond to the "worst" case. An alternative and simple approach is proposed here that provides a good first estimate of such a penalty for back-off.

For each of the control objectives, identify the disturbance that requires the largest back-off. Such a back-off in any active constraint ensures that the constraint will not be violated for any of the disturbances. The penalty now associated with the i^{th} control objective is therefore given by

$$\Delta\phi_i = \lambda_i \, . \, b_{i,max} \qquad (i = 1, ..., n) \tag{5.3.8}$$

where $b_{i,max}$ is the maximum back-off in the i^{th} active constraint and is given by

$$b_{i,max} = \max | b_{ij} | \text{ for all } j = 1,..., m$$

Another issue that needs some attention here is associated with "infeasible back-offs ". A back-off in a constraint from the optimum by the amount thus estimated (i.e. $b_{i,max}$) may some times require violation of other constraints (such as any process or physical constraints). Therefore in such a case , it may not be possible to implement a back-off of $b_{i,max}$ from the corresponding active constraint. Hence, we need to define another

back-off for all such cases which we may call the "maximum feasible open-loop back-off - $b_i^{(ol)}$ ". The $b_i^{(ol)}$ value (i.e. in all the cases where the maximum back-off estimated through Equation 5. 3. 8 is infeasible) can be estimated as follows ;

$$b_i^{(ol)} = y_i^c - y_i^{opt} \quad (\text{for } i=1,\ldots,k) \quad \text{(i.e cases with constraint violations)}$$

$$\text{and} \quad b_i^{(ol)} = b_{i,max} \quad (\text{for } i=k+1,\ldots,n) \quad \text{(i.e cases with no constraint violations)} \qquad (5.3.9)$$

where

$b_i^{(ol)}$	is the maximum feasible open-loop back-off.
$b_{i,max}$	is the maximum open-loop back-off.
y_i^c	is the constraint that is violated , when the maximum open-loop back-off is implemented on i^{th} constraint.
y_i^{opt}	is the value of the ith active constraint at the optimum.
k	is the number of active constraints where, the maximum open-loop back-off is infeasible (i.e. cannot be implemented without violating any other constraints).

A more general form of Equation 5. 3. 8 may be given by

$$\Delta\phi_i = \lambda_i \, . \, b_i^{(ol)} \quad (i = 1,\ldots,n) \qquad (5.3.10)$$

If all these give-aways ($\Delta\phi_i$ for i=1,..., n) are small there is then little economic incentive to install a control system on the plant at all. However if any giveaway is large, then one interesting question is the effect of different control systems on its size. It may be realised at this stage that each of the these give-aways ($\Delta\phi_i$ for i=1,..., n) indicate the maximum penalty associated with a back-off in the corresponding constraint from the optimum, for the "worst" disturbance case (i.e. the largest disturbance size). A simple summation of all such penalties now would provide an upper bound on the penalty associated with a back-off from the original steady-state optimum , as disturbances in such a case are not attenuated at all by a control system. In other words, all $\Delta\phi_i$ (for i=1,..., n) values can be used to estimate the largest penalty associated with a back-off from each of the active constraints by the largest feasible values (i.e. $b_i^{(ol)}$ for i=1,..., n) , as shown below (i.e. when no control exits on the system);

$$\Delta\phi_{max} = \Sigma \Delta\phi_i \quad (\text{for } i=1,\ldots,n) \qquad (5.3.11)$$

where $\Delta\phi_{max}$ is the largest penalty due to a back-off from each active constraint, when no control action is taken. The approach used here to compute $\Delta\phi_{max}$ is only a good first estimate of the maximum penalty for back-off in all the active constraints.

Before proceeding it should be pointed out that a further complication may arise from the fact that a co-ordinate system based on the steady-state degrees of freedom is often insufficient to characterise the dynamic behaviour of a plant. It is therefore more correct to consider the complete linear dynamic model, rather than the condensed system dynamics given by Equation (5. 3. 1). This linear model is given by the following set of equations,

$$\frac{dx}{dt} = Ax + Bu + Cz + Dd \qquad (5.\ 3.\ 12)$$

$$0 = Ex + Fu + Gz + Hd \qquad (5.3.13)$$

$$y = P\begin{bmatrix} x \\ u \\ z \end{bmatrix} \qquad (5.\ 3.\ 14)$$

$$\phi = \phi(x, u, z, d) \qquad (5.3.15)$$

where

x	is an n-vector of state variables
u	is an m-vector of manipulated variables
z	is a p-vector of algebraic variables
d	is a q-vector of disturbances
y	is an r-vector of control objectives
ϕ	is the objective function.

The various matrices describing the differential and algebraic equations have the following dimensions :

A: n x n ; B: nxm ; C: nxp ; D: nxq

E: p x n ; F: pxm ; G: pxp ; H: pxq

The { r x (n + m + p) } matrix P represents the choice of which variables are control objectives. Therefore, it is made up of rows which have one non-zero element , all the other entries being zero.

Equations (5. 3. 12) - (5. 3. 14) can be transformed into the Laplace domain. Then given information on the disturbances d (s) in the form of amplitude and frequency data, the Laplace transformed equations may be solved to give the variation of all variables in the absence of control :

$$\begin{bmatrix} j\omega I - A & -C \\ -E & -G \end{bmatrix} \begin{bmatrix} x \\ z \end{bmatrix} = \begin{bmatrix} D \\ H \end{bmatrix} d(j\omega) \qquad (5.3.16)$$

$$y(j\omega) = P \begin{bmatrix} x(j\omega) \\ 0 \\ z(j\omega) \end{bmatrix} \qquad (5.3.17)$$

These variations may be substituted into the objective function expression and the economic penalty resulting from the disturbances computed. It should be appreciated that while Equations (5. 3. 12) to (5. 3. 15) provide a more complete picture of the process dynamics than Equation (5. 3. 1), the former approach is computationally more extensive and may require the solution of a large set of linear equations. However, for any system, as a first-estimate of the economic penalty due to back-off from optimum such a rigorous approach may not always be necessary. For all these reasons the latter approach is not used in the current study.

There is a second class of output variable other than those defined by an active constraint, represented for example, by Y_2 in Figure 5. 3. 3. In contrast to Y_1, where the effect of disturbances may be to cause infeasible operation, disturbances do not cause Y_2 to become infeasible. The objective function contours in this case indicate that the variable Y_2 "sits on the top of a hill". Therefore any perturbation in the value of Y_2 from it's value at the optimum causes a reduction in the objective function. Disturbance induced movement thus results in a deterioration in the average performance, even though the time averaged value of Y_2 may remain unchanged at its optimum value, and such a loss should be included in the total giveaway. All variables that are unconstrained at the steady-state optimum (i.e. like Y_2) and occur in the objective function will invariably result in an economic penalty as a result of disturbances, irrespective of whether the objective is linear or nonlinear. Variables that occur in the objective function that are unconstrained at the steady-state optimum but unlike Y_2 in Figure 5. 3. 3 do not "sit on the top of a hill", will only incur an economic penalty in cases where the objective function is non-linear. Variables that have been moved away from active constraints can be grouped with this latter class of variables and may incur an additional disturbance induced economic penalty if the objective function is nonlinear. The magnitude of the penalty associated with variables that are not determined by active constraints at the selected optimum is thus a matter of some interest, but as yet no generally applicable theory is available.

Having established a method to estimate the open-loop economic penalty for the plant arising from the effect of known disturbances , it remains to seek an estimate of the potential effect of a control system on the penalty. This would provide an estimate of the economic benefit that a control system could provide. In other words, we seek to establish an estimate of the amount of the penalty that can be recovered using a controller. Since this quantity is dependent on the choice of controller, one could employ the best choice of controller (generally a multivariable, model-based controller) to recover the maximum possible from the penalty due to back-off from the optimum operating point. However, the cost of setting up such a controller is usually large relative to the marginal benefits the controller provides in return and in many cases, the major part of the back-off penalty can be recovered using a simple multiloop control structure. The latter approach , if applicable , is relatively cheap and easy to implement. But it must be realised that it is not practical to estimate the maximum recovery one can make for the complete range of controllers one can possibly use. In any case, there are a few fundamental limitations (discussed in the previous chapter) that limit the quality of control expected for any given process. Designing an advanced control scheme for a process that has poor controllability characteristics does not necessarily offer large economic benefits.

The ratio of the penalty recovered using a controller, relative to the penalty due to back-off with "no control", can be expressed as a percentage and will be referred to as the *maximum percentage recovery* (**MPR**). For a process with perfect control, no back-off is required and hence the **MPR** is 100%. Figure 5. 3. 6 shows the objective function of a process at different levels of operation. As discussed previously for Figure 5. 3. 5 , the objective function is also shown here as a function of time while the time averaged values at various levels are used in further studies. Level **A** refers to the profit at the original steady-state optimum. If all the dynamic fluctuations in the profit due to disturbances are evenly distributed around the optimum, then the average profit over a period of time is the optimum value itself. This is possible only if the influence of disturbances on the objective function is linear and there is no additional penalty for constraint violation. Level **B** refers to the profit from the process after back-off and with "no control". Levels **A** and **B** form the upper and lower bounds of the objective function associated with the process. Level **C** on the other hand refers to the objective function for the process after back-off but now with a controller. The position of **C** depends both on the process and the type of controller used. The following expression defines the **MPR** .

$$\text{MPR} = 100 * \left(\frac{\phi_C - \phi_B}{\phi_A - \phi_B} \right) \qquad (5.\ 3.\ 18)$$

5. 3. 6
Economics of control

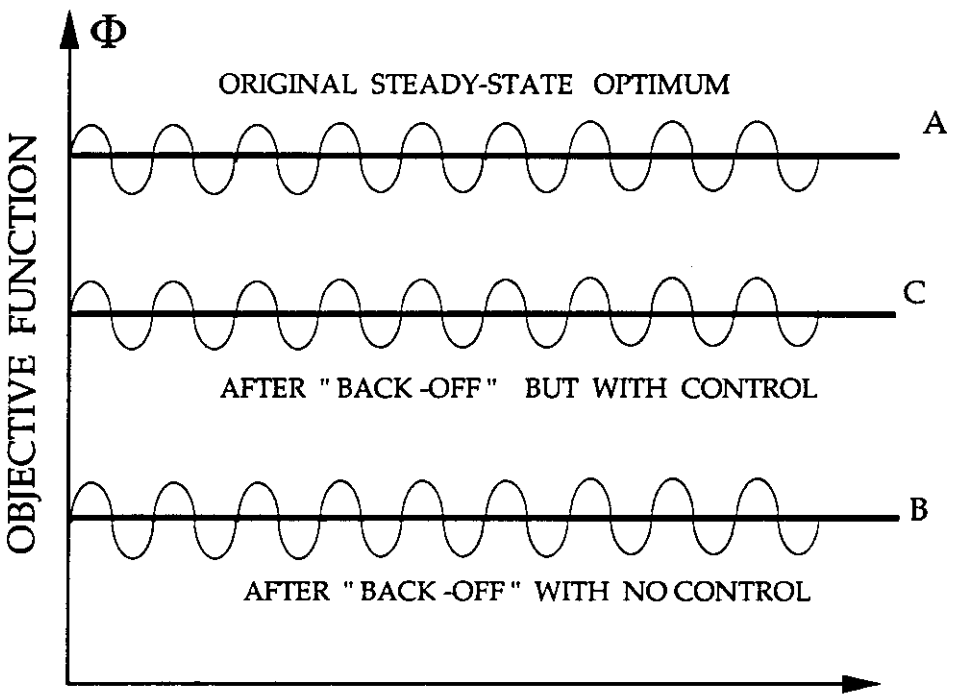

Throughout the previous chapter the discussion was about various performance indicators that provide at least a qualitative measure of how close to perfect control one can expect to get. Therefore, for a given process, we can use such indicators to determine any fundamental process limitations preventing the achievement of perfect control and hence, qualitatively, how difficult it would be to achieve a large **MPR** . Such an approach would also be useful in screening alternative processes as we would choose processes that have good controllability properties. The **MPR** is thus an economics based index that provides valuable and consistent information about the process controllability. A process with a large **MPR** should therefore have good controllability characteristics and vice versa.

The major issue is thus to identify those processes (from a set of alternative process designs) that would provide a large **MPR** or, for a given process, to estimate how large an **MPR** can be obtained using a suitable choice of controller. There are several ways of obtaining such an estimate. One common heuristic frequently used in industry (Perkins [1989]) is based on assigning a fixed percentage recovery (i.e. typically **MPR** = 50 %). This provides a very crude and often conservative estimate of the **MPR** and is independent of the type of controller actually installed. This approach has the benefit of simplicity but takes no account of any known differences in the susceptibility of plants to control. Another approach involves developing an optimal controller design to calculate the best possible closed-loop performance. This approach is rigorous but computationally demanding.

Therefore what is required is a simple way to establish bounds (with a minimum of computational effort) for the **MPR** for a system with a control system. Our previous analysis proposes a methodology for estimating the open-loop (i.e. no control) penalty, representing the maximum economic give away. To provide an upper bound for the MPR one can make use of the perfect control assumption, where it is assumed that whichever variables are chosen as control objectives they are perfectly controlled at all times. Then the system of linear Equations (5. 3. 12) - (5. 3. 14) may be solved in the Laplace domain to obtain the variation in the other system variables for a given disturbance description ;

$$\begin{bmatrix} j\omega I - A & B & C \\ -E & -F & -G \\ 0 & P & 0 \end{bmatrix} \begin{bmatrix} x \\ u \\ z \end{bmatrix} = \begin{bmatrix} D \\ H \\ 0 \end{bmatrix} d(j\omega) \qquad (5.3.19)$$

The resulting values of $x(j\omega)$, $u(j\omega)$ and $z(j\omega)$ may be substituted into the objective function expression (i.e Equation 5. 3. 15) to give an estimate of the time-average closed-loop

economic penalty resulting from the known disturbances. As with the open-loop case, obtaining such an estimate for the objective function may require solving a large set of linear equations. Depending on the form of ϕ , calculation of the closed-loop penalty may require only the solution of Equation (5. 3. 1) , with $\mathbf{y}(s) = 0$ for perfect control. In the case where the disturbances are all "symmetric " about their nominal steady-state values, and the form of ϕ is such that changes resulting from positive and negative disturbance changes cancel each other out, the closed-loop give away under perfect control will be zero. However such a situation is probably optimistic in most cases. To assess how reasonable the perfect control assumption is for a given choice of control objectives and manipulated variables , one can use the functional controllability techniques discussed in the previous chapter. Such an assessment should provide a reasonably quantitative indication of how close to perfect control one can expect to get. The advantage of this approach is that such an assessment is independent of the external controller design.

CLOSED-LOOP BACK-OFFS

The concept of MPR is very useful in estimating the amount of recovery in the open-loop economic penalty for backing-off from the optimum. However it requires identification of how close to perfect control one can operate. As discussed previously, one of the duties of a control system is to recover some of the open-loop penalty for back-off. For a given choice of control system, the back-off required in any active constraint (i.e. which is also the control objective) that ensures no constraint violations, is necessary for computing the MPR. The latter value will be referred to as a *closed-loop back-off.* Such an estimate, however, depends on both the process and the controller and is often difficult to compute.

One approach that can be used to estimate the required closed-loop back-offs is based on both the open and closed-loop transfer functions. In the absence of any set-point changes, the closed-loop transfer function relating the control objectives and the disturbances can be obtained as follows. From the block diagram of Figure 5. 3. 7, the transfer function for estimating the control objectives is given by

$$y^{(cl)}(s) = (I+G(s).K(s))^{-1} G_d(s).\, d(s) \qquad (5.3.20)$$

For an open-loop case (i.e. $u(s) = 0$; from Equation 5. 3. 1) , we have

$$y^{(ol)}(s) = G_d(s).\, d(s) \qquad (5.3.21)$$

where
- $y^{(cl)}(s)$ is a vector of control objectives in the closed-loop case
- $y^{(ol)}(s)$ is a vector of control objectives in the open-loop case
- $d(s)$ is the disturbance vector
- $G_d(s)$ is the disturbance transfer function matrix
- $G(s)$ is the process transfer function matrix

Figure 5. 3. 7
Block diagram for feedback control

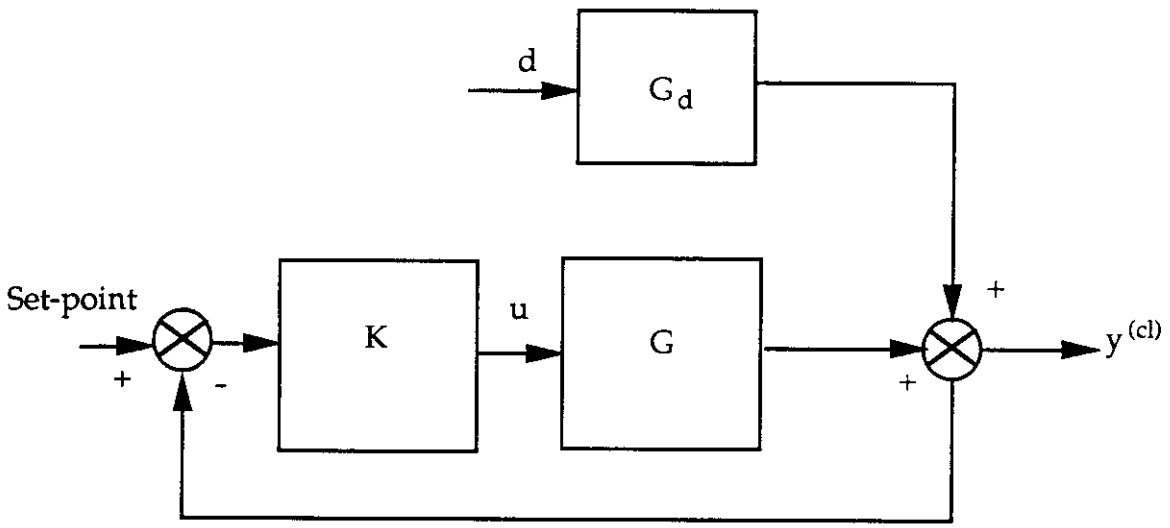

$K(s)$ is the controller transfer function.

Taking l_2 - norms of both sides of Equations 5. 3. 20 and 5. 3. 21 we get ;

$$\| y^{(d)}(s) \| \leq \| (I + G(s).K(s))^{-1} \| . \| G_d(s) \| . \| d(s) \| \qquad (5.3.22)$$

and

$$\| y^{(ol)}(s) \| \leq \| G_d(s) \| . \| d(s) \| \qquad (5.3.23)$$

From Equations 5. 3. 22 and 5. 3. 23 , the sizes of both the closed-loop and open-loop back-offs, respectively , can be estimated as follows :

$$\| y^{(d)}(s) \| \leq \sigma_{max} [(I + G(s).K(s))^{-1} . G_d(s)] . \| d(s) \| \qquad (5.3.24)$$

$$\| y^{(ol)}(s) \| \leq \sigma_{max} [G_d(s)] . \| d(s) \| \qquad (5.3.25)$$

where $\sigma_{max} [(I + G(s).K(s))^{-1} G_d(s)]$ and $\sigma_{max} [G_d(s)]$ are the maximum singular values of the matrices $[(I + G(s).K(s))^{-1} G_d(s)]$ and $G_d(s)$ respectively.

The maximum singular values of Equations (5. 3. 24) and (5. 3. 25) , both provide a measure of the largest amplification obtained in the control objectives for a given set of disturbances, in the closed and open-loop cases, respectively. The ratio of both these singular values is a dimensionless number, which is also an estimate of the fractional recovery in the open-loop back-off using a control system, and is given by

$$\frac{\| y^{(d)}(s) \|}{\| y^{(ol)}(s) \|} = \frac{\sigma_{max} [(I + G(s).K(s))^{-1} . G_d(s)]}{\sigma_{max} [G_d(s)]} \qquad (5.3.26)$$

The fractional recovery in the open-loop back-off thus estimated from Equation (5. 3. 26) is somehow related to the MPR (see Equation 5. 3. 18) , though at this stage it is not clear what the nature of relationship is . The limitations associated with such an approach are as follows :

(1) Such an estimate is a function of the controller. Computation of the required maximum singular value therefore requires selection and tuning of a control system - which is usually not known at this stage.

(2) The closed-loop back-offs estimated using Equation (5. 3. 26) provide only a conservative upper limit. It is therefore possible that for some cases the largest closed-loop back-off necessary would be much smaller than the largest back-off value estimated.

(3) Scaling of variables may pose some difficulties.

However, given suitable scaling (such as all the variables normalised against their steady-state values) and a consistent controller tuning policy (e.g. BLT tuning ; see

Appendix A9) , the approach suggested here provides a simple and easy-to-compute measure of fractional economic recovery in the open-loop back-offs.

We are now in a position to set up a two-stage procedure that seeks to provide a systematic approach for the synthesis of optimising control schemes. The proposed methodology is described below and is shown diagramatically in Figure 5. 3. 8.

STAGE 1 : ECONOMIC POTENTIAL OF A CONTROL SYSTEM

The steps in this stage are as follows.

(a) For a given set of "slow" disturbances identify all the active constraints and determine their Lagrange multipliers at the calculated optimum operating conditions.

(b) Identify the "fast" disturbances influencing the process along with a quantitative description of each one (i.e. it's maximum size and any frequency domain information available).

(c) Linearise the process model around the optimum operating conditions and obtain the transfer function relating the fast disturbances and the active constraints (i.e. G_d in Equation 5. 3. 1). The latter are taken as outputs for the control system.

(d) Estimate the back-off from each active constraint due to each of the disturbances (i.e. the b_{ij} of Equation 5. 3. 6) for the case where there is no control (i.e. open-loop case).

(e) Estimate the largest value of the necessary back-off (i.e. $b_{i,\,max}$ of Equation 5. 3. 8) for each active constraint. If the largest necessary back-off in any active constraint is infeasible (i.e. not possible to implement without violating other constraints), then estimate the largest feasible back-off from the optimum, in the corresponding active constraint (i.e. $b_i^{(ol)}$ of Equation 5. 3. 9).

(f) Using the Lagrange multipliers for each active constraint, estimate the economic penalty due to back-off from each one (i.e. $\Delta\phi_i$ of Equation 5. 3. 8).

(g) As a reasonable first estimate, the total penalty (i.e. $\Delta\phi_{total}$) associated with the back-off in all the control objectives may be taken as the simple summation of the largest back-off required for each of the active constraints.

Figure 5. 3. 8
Economics based approach to control system synthesis

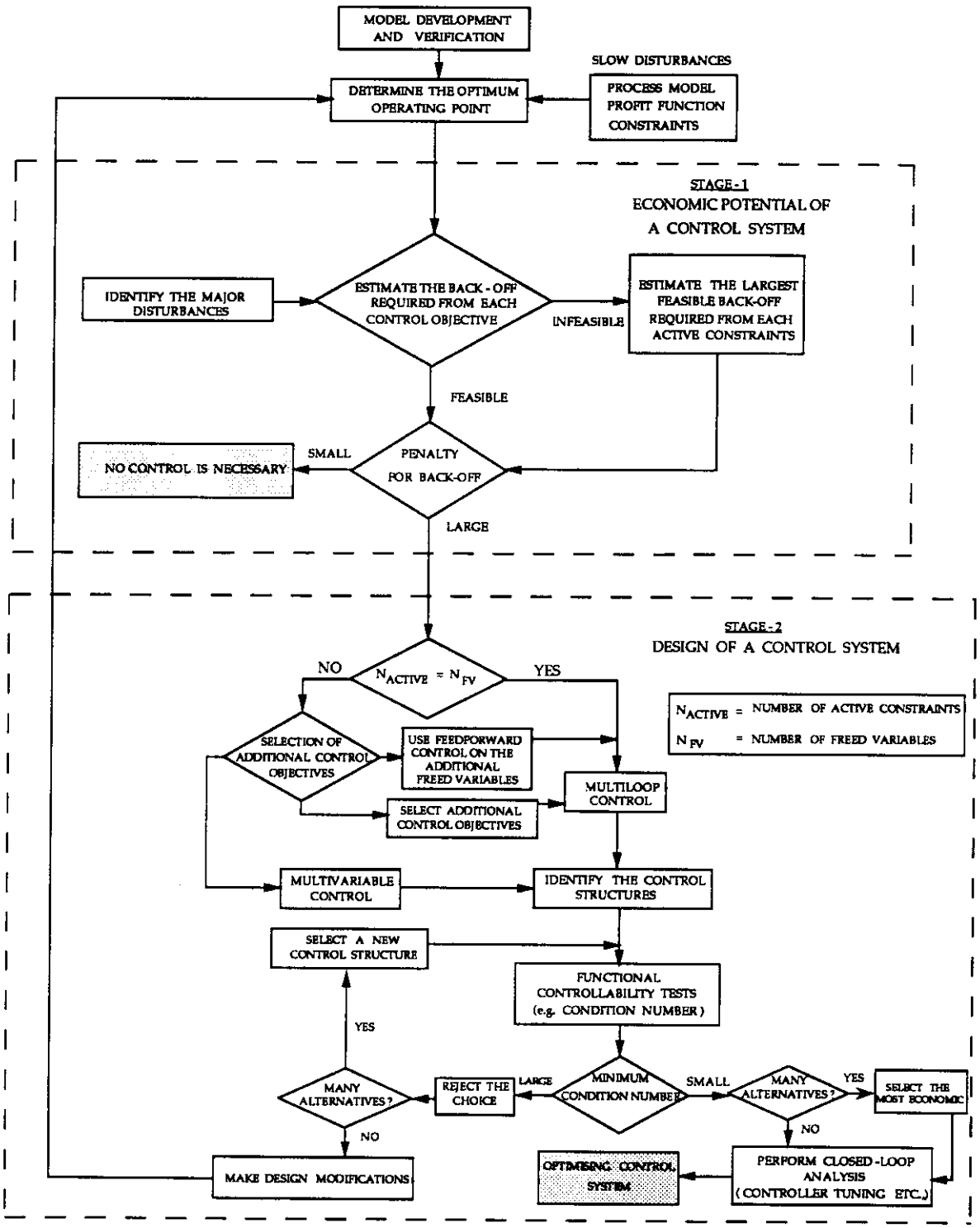

(h) If the total penalty is comparable in magnitude to the optimal value of the objective function ϕ then there is a significant benefit associated with having a control system on the process, and one can proceed with the design of a suitable control scheme (i.e. carry on to Stage 2) that would reduce this economic loss. If the total penalty on the other hand is not too large, one can back-off from the optimum by the amounts estimated and operate the process at the new operating point without a significant loss in process profitability. This latter case, without any control system, still ensures that no constraints should be violated due to the action of fast disturbances at any time during the process operation.

STAGE-2 : DESIGN OF A CONTROL SYSTEM

The steps in this stage are as follows :

(a) All the active constraints are chosen as the control objectives (or outputs) and the freed variables as the manipulated variables (or inputs) of the control system.

(b) If the number of control objectives is not equal to the number of manipulated variables then proceed to step (c). If on the other hand they are equal, then a constraint control approach can be used and we can proceed to step (d).

(c) If the number of control objectives (i.e active constraints) is not equal to the number of manipulated variables then one of the following approaches can be used :

(1) Choose a set of manipulated variables so as to be equal to the number of active constraints. The additional freed variables not selected as inputs are set at constant values obtained from the steady-state optimiser.

(2) Select additional control objectives (i.e. in addition to using all the active constraints) so as to form a square control system. Heuristics and engineering judgement could be used in this selection. However there is no unique procedure available that provides a rational and consistent basis for such a selection.

(3) Use all the freed variables as manipulated variables and all the active constraints as control objectives. This would require the development of a non-square controller policy to regulate the process at its optimum operating point. This approach would require a model-based control scheme to be implemented, and would only be employed if there was a strong economic incentive to do so.

(d) Obtain the transfer function matrix (i.e. G (s)) relating the selected choice of control objectives and manipulated variables. Note that a given process with different inputs and outputs will have different transfer function matrices. Each transfer function matrix represents the dynamic characteristics of the process.

As discussed previously, of all the available open-loop indicators the minimum condition number seems to be the best single controllability measure and is the one used in these case-studies. Estimation of the minimum condition condition number of a process based on the l_∞ - norm can be defined using the SPEECON package. Being based on the transfer function matrix of the process , such an estimation depends on the operational frequency. Therefore the minimum condition number of the transfer function matrix is estimated over the frequency range of interest. This frequency range is estimated based on the following argument.

The open-loop time constants of a process characterise its speed of response. The smallest time constant indicates the fastest response of the process. The inverse of these time constants, on the other hand, indicate the characteristic frequencies for which the system responds. The eigenvalues of the system matrix (i.e. A) for a process represented in a state-space form (see Section 2. 4. 2) can also provide such characteristic frequency information. The largest eigenvalue corresponds to the characteristic frequency of the smallest time constant of the process. Any disturbance frequency significantly larger than the largest of the system's inherent characteristic frequencies is considered too fast to have any effect on the process. Therefore only the disturbances below this frequency are of interest to us. One common heuristic, frequently used in industry to estimate this frequency range of interest, is to extend the analysis to a frequency twice the largest eigenvalue of the system matrix of a process represented in state-space form . This approacn is used throughout the study.

A large minimum condition number indicates that poor closed-loop performance can be expected from a control system. Therefore reject all those choices of inputs and outputs that give rise to large minimum condition numbers. If the minimum condition number for all remaining choices is close to unity , then the control system in each case should be able to provide similar high performance closed-loop responses. Selection of the appropriate control system would then be based primarily on other economic grounds (e.g. how much the analysers and control hardware would cost).

(e) Here, one would make a choice of whether to use a multiloop or multivariable control policy with the selected inputs and outputs. A multiloop control policy requires a rational basis for pairing the control objective and the manipulated variables. However it is relatively simple to implement. A multivariable control policy, on the other hand, is more difficult to implement and generally requires a process model to calculate the required control action. Multiloop control is often adequate for processes with small minimum condition numbers. Processes with large minimum condition numbers usually exhibit large interactions. A model-based multivariable control policy might therefore be necessary to minimise such interactions.

(f) Alternatively, if the "best" minimum condition number is large, then one could choose to modify the process design so as to obtain a smaller minimum condition number. This approach, however, would probably only be pursued when none of the control configurations available seemed likely to provide satisfactory closed-loop performance.

(g) Processes with a small minimum condition number should provide good closed-loop response, and hence one would expect to be able to operate close to the optimum. Large MPR values would be expected from such systems. A final choice between the alternatives would be based on controller design and closed-loop simulation studies.

Thus a systematic methodology for the synthesis of an optimising control scheme for a continuous process has been proposed. A control system design for the complete Shell gas-tail will be performed along these lines in Chapter 6. In the following section, however, the major advantages and limitations of this approach will be demonstrated through an illustrative example (the de-propaniser column from the gas-tail, considered on its own).

5. 4. EXAMPLE APPLICATION OF THE CONTROL SYSTEM SYNTHESIS METHODOLOGY

Application of the techniques proposed in the previous section will be demonstrated here through an example drawn from the gas-tail case study. Before applying the analysis to the entire gas-tail it was felt necessary to examine the new approach on a smaller scale problem. The gas-tail de-propaniser was therefore chosen as such an example. As described previously (see Section 2. 1) the de-propaniser was designed to separate LPG from the feed to the gas-tail, as its distillate product stream. The optimisation studies

on the gas-tail for the high feed rate, high pentane case (i.e. Case 1 ; see Section 3. 2. 2) identified the optimum operating point along with the active constraints. The optimum column conditions and the corresponding feed conditions to the de-propaniser (i.e. from the de-ethaniser), obtained from the optimisation studies on the entire gas-tail, are taken as the basis for this column. Application of the proposed economics - based control system synthesis methodology for the de-propaniser will be presented here in detail.

Optimisation studies indicate that the distillate composition ($x_D \geq 90$ % propane) and the reboiler return temperature ($T_R \leq 117$ deg C) are active constraints. The objective function at this steady-state optimum (ø) is estimated (from Equations 3. 2.1 and 3. 2. 2) as follows ;

$$
\begin{aligned}
\text{ø} &= \text{LPG stream recovery rate} * \text{value of LPG} \\
&\quad - \text{Steam flowrate} * \text{cost of steam} \\
&\quad + \text{Steam flowrate} * \text{value of condensate} \\
&= 56.26 * 7.82 - 108.13\,(0.091 - 0.009) \\
&= \$431.1 / \text{hr} \qquad (5.4.1)
\end{aligned}
$$

Tables (3. 2. 1) and (3. 2. 6) provide the necessary details at the calculated steady-state optimum.

The overhead condenser operating on the de-propaniser column is of the air-cooled type. The existing problems associated with the de-propaniser operation are largely due to the limited capacity of the overhead condenser. In all the optimisation studies, ,therefore, the overhead condensers were operated at their maximum capacities. The overhead pressure in a distillation column depends on the uncondensed vapour holdup. For a total condenser, which can be thought of as an "infinite heat sink " , any increase in the overhead vapour entering the condenser will also be condensed completely. Thus no significant change would be seen in the overhead condenser pressure. In other words, for a distillation column with a total condenser, there is no simple way to regulate the overhead pressure of the column using the condenser. With a partial condenser , on the other hand, any increase or decrease in the vapour rate to the condenser changes the vapour holdup in the condenser and causes a change in the overhead condenser pressure. If the partial condenser operates at a fixed capacity (as in the case of the de-propaniser) the column pressure "floats " around a nominal value depending on the column operating conditions and the disturbances at any particular time.

The freed variables used in the gas-tail optimisation and associated with the de-propaniser are :

(a) The distillate rate. D

(b) The LP (low pressure) steam rate to the column reboiler. S

while the air flowrate to the condenser is maintained at its maximum value, as indicated above.

One of the basic reasons for having a control scheme is that there is a significant economic incentive to provide regulatory control. The impact of various known disturbances on the control objectives when there is no control (i.e. open-loop) can be used as a basis for estimating the potential benefits a controller can provide. This calculation means identifying all the major disturbances influencing the process operation along with their likely amplitudes. The major disturbances affecting the de-propaniser column are :

(a) The feed rate to the de-propaniser.	F	(208 Kg-moles/hr	± 15 %)
(b) The pentanes composition of the feed.	X_F	(0.10	± 50 %)
(c) The ambient air temperature.	T_A	(20 deg C	± 25 %)
(d) The LP steam pressure.	P_S	(3.15 Bar	± 15 %)

The first term in the parentheses gives the values of each of the disturbances at the steady-state optimum, while their anticipated variations about their nominal steady-state values are given as the second term in a percentage form (see Table 5. 4. 1 for further details). Equation (5. 3. 1) with u (s) = 0 can be used to estimate the required move or " back-off " from each of the active constraints (taken to be control objectives) for given disturbances over the frequency range of interest. It was not necessary to use Equations (5. 3. 12) - (5. 3. 15) in this case as there was no additional economic penalty (besides that arising from the back-off from the active constraints) due to disturbance induced fluctuations, as the objective function used is linear. These predicted changes in the control objectives represent the amount of back-off from a constraint necessary to ensure that the constraint is not violated if the process is disturbed and no control action is taken. The Lagrange multipliers associated with each of the two control objectives x_D and T_R were used (see Equation 5. 4. 1) to estimate the economic penalty for each back-off over the whole frequency range of interest (see Figures 5. 4. 1 - 5. 4. 4) .

Table 5. 4. 2 summarises the necessary back-offs for the steady-state case (i.e $\omega = 0$). It is clear from this table that the feed flowrate represents the "worst" disturbance as the maximum back-off required for each of the control objectives is due to this disturbance. However for this disturbance the back-off in the case of the LPG composition is not physically realisable (i.e x_D at the new operating point after the back-off would be 0.9 + 0.282 = 1. 182 > 1). Such a move violates the physical constraint that any molefraction cannot be greater than unity. Thus the maximum back-off one can make is

Table 5. 4. 1
Disturbances affecting the gas-tail

Disturbance	Range	Frequency (/ hr)
Feed flowrate	180 - 240 Kg-moles/hr	1 - 20
Pentanes composition in the feed	5 -15 %	1- 5
Ambient air temperature	15 - 25 Deg C	1 - 5
Steam pressure	2. 7 - 3. 7 Bar	1 - 20

Table 5. 4. 2
Steady-state open-loop back-offs from the active constraints due to disturbances

Output (i.e. active constraint)	Disturbance			
	Feed flowrate	Pentanes in the feed	Ambient air temperature	Steam pressure
LPG composition in the distillate product (x_D)	0.282	8.29 e-4	1.10 e-3	2.36 e-4
Reboiler return temperature (T_R)	24.382	1.638	6.802	0.688

Figure 5.4.3
COST OF BACK-OFF FROM OPTIMUM
(EFFECT OF FEED FLOWRATE)

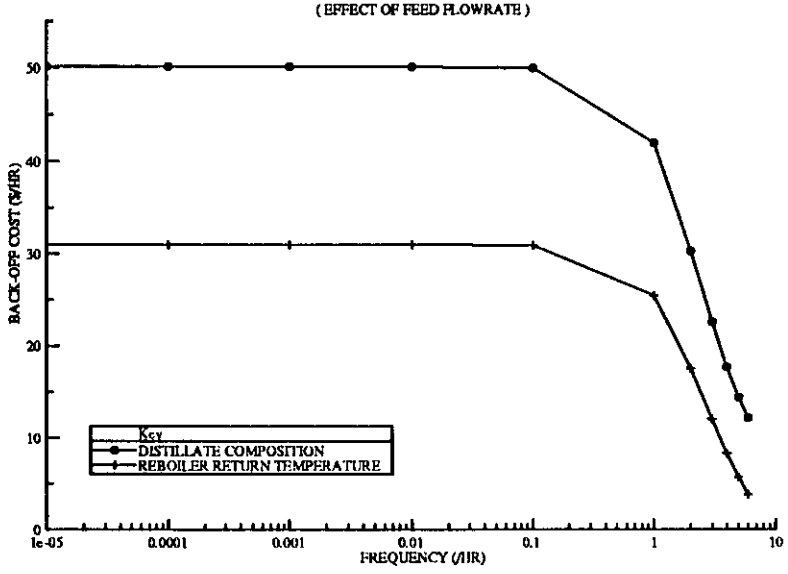

Figure 5.4.4
COST OF BACK-OFF FROM OPTIMUM
(EFFECT OF PENTANES IN THE FEED)

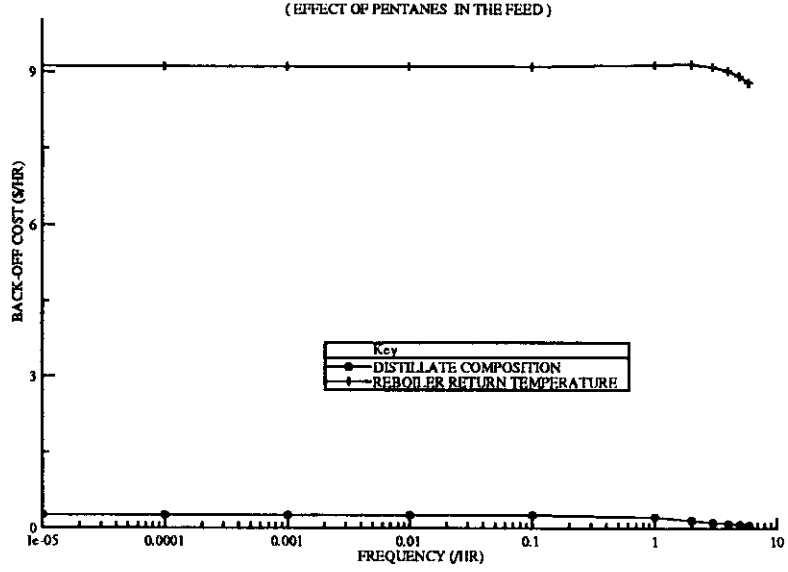

Figure 5.4.1
COST OF BACK-OFF FROM OPTIMUM
(EFFECT OF AMBIENT AIR TEMPERATURE)

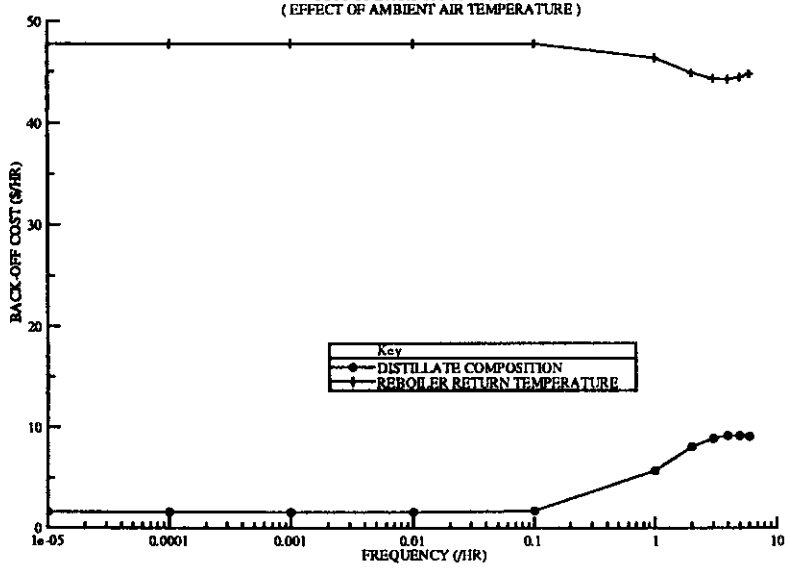

Figure 5.4.2
COST OF BACK-OFF FROM OPTIMUM
(EFFECT OF LP STEAM PRESSURE)

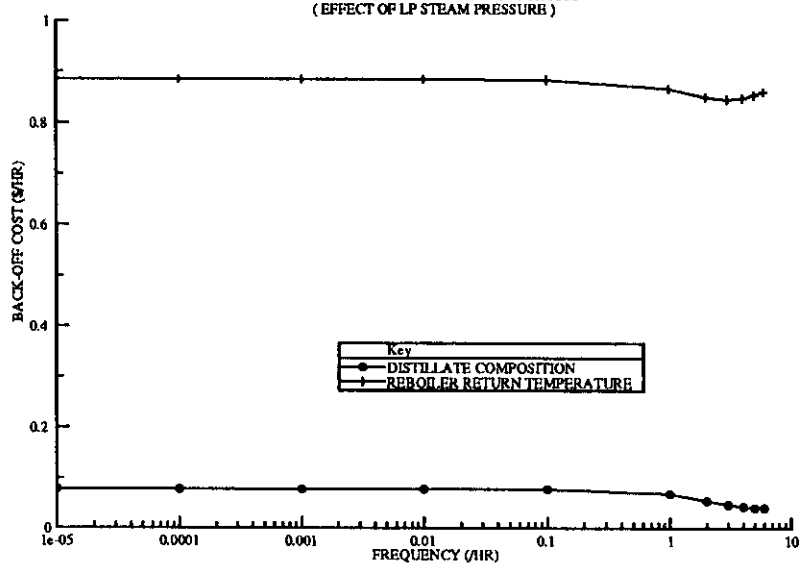

to have 100% pure LPG as the distillate product. Therefore the maximum physically realisable back-off one can make (i.e. $d_i^{(ol)}$) is $\Delta x_D = 0.1$. Similarly , the back-off required in the reboiler return temperature (T_R) for the largest feed flowrate disturbance is also too large to be realisable. T_R at the optimum is 117 deg C. The maximum back-off one can make, therefore, is $\Delta T_R = 13$ deg C (i.e. $\Delta T_R = 130 - 117$ where 130 deg C is the maximum temperature the process fluid in the reboiler can attain without violating the constraint of a minimum temperature difference between the heat exchanging streams ; see Table 3. 2. 4). One important implication of this analysis here is that for the de-propaniser column it may not be possible to get-away without any control action. In other words, for a given feed disturbances, no control action implies some of the physical constraints (discussed above) will in some circumstances be violated.

The Lagrange multipliers associated with each of these constraints are \$ 371 for x_D and \$8 for T_R (see Table 3. 2. 2) . From Equation (5. 3. 10) the penalties associated with the back-off for each of the control objectives, therefore, is given by :

$$\Delta\phi_1 = 0.1 * 371 = \$37.1 \text{ / hr} \quad (\text{for } x_D)$$
$$\Delta\phi_2 = 13 * 8 = \$104.0 \text{ / hr} \quad (\text{for } T_R)$$

Thus, from Equation (5. 3. 11),

$$\Delta\phi_{max} = \Delta\phi_1 + \Delta\phi_2$$
$$= \$141.1 \text{ / hr} \qquad (5.4.2)$$

This maximum give away, when compared to the corresponding steady-state objective function (i. e. ϕ = \$431.1 / hr ; from Equation 5. 4. 1) indicates that relatively large economic penalties are associated a with back-off from the optimum if the column has no control scheme. Clearly, there is sufficient economic incentive to install a control system on the de-propaniser column to mitigate the effect of disturbances. Note that for a new plant design there would be another option. This would involve redesigning the plant so as to reduce the variability in the feed flowrate (e. g. by installing buffer storage) and/ or reducing the sensitivity of the gas-tail to feed variations. The economic incentives thus estimated would be extremely useful in exploring such re-design options.

The back-offs estimated for each of the control objectives , however, may not be necessary. This is because the successful implementation of an effective control system would provide operation close to the current optimum (i.e. an MPR value close to 100 %). As discussed before, estimation of the MPR depends both on the nature of the process and the type of regulatory control system used. Closed-loop dynamic simulations of a process with a particular choice of control system would provide a crude means of estimating the MPR for the process. However such an approach is computationally very extensive. Apart from

closed-loop simulations there are no simple rules as to what the closed-loop back-off should be that both maximises the MPR and ensures no constraint violation. Although the method proposed in Section 5. 3 offers an alternative means of estimating the closed-loop back-offs, as discussed before all the issues associated with such an approach are yet to be resolved. Therefore in this case-study we have employed the simple heuristic of using the second largest open-loop back-off necessary in each of the control objectives. In this case, for the reboiler return temperature constraint the second largest move is due to the ambient air temperature disturbance (see Table 5. 4. 2). The back-off needed in this case (i.e. 6. 8 deg C) is both physically realisable and does not violate any other process constraint . Similarly, the second largest back-off for the other control objective (i.e. the LPG composition in the distillate product) is also due to the ambient air temperature disturbance (i.e a mole fraction change of of 0.0011). Thus the actual operating point is set by the control objectives which have been backed-off from their optimum values. If such a back-off is adequate for all the major disturbances affecting the system then the economic penalty or giveaway associated with it ($\Delta\phi_{new}$) can be estimated using the Lagrange multipliers. The MPR is calculated by estimating the economic loss for the selected amounts of back-off in each of the control objectives as follows :

$$\Delta\phi_{new} = 0.0011 * 371 + 6.8 * 8.0$$
$$= \$54.8 / hr \qquad (5.4.3)$$

$$MPR = 100 * (1 - \Delta\phi_{new} / \Delta\phi_{max})$$
$$= 61\% \qquad (5.4.4)$$

Equation (5. 4. 4) shows that about 61 % of the penalty for open-loop back-off from the optimum can be recovered by having a control system on the de-propaniser.

To summarise, the above results give an estimate of the economic giveaway due to back-off from the optimum to prevent disturbance induced active constraint violations when there is no control on the de-propaniser. The $\Delta\phi$ values for each of the active constraints indicates that there is a significant incentive to recover this economic penalty by having a control system on the de-propaniser. If perfect control could be implemented then the MPR would be 100 % and all the economic penalty could be recovered by installing a control system on the process.. On the other hand, about 60 % of the back-off penalty can be recovered by installing a realistic regulatory control system. Thus, at the end of Stage 1, we have identified the upper and lower bounds on the economic costs associated with the regulatory control of the de-propaniser.

In the second stage of the analysis it remains to see how close to perfect control we can get i.e. can we indeed expect to find a control system that provides a large MPR value. The

first step here is to identify all the possible control schemes that could be implemented on the de-propaniser. Apart from the two control objectives (x_D and T_R) that need to be maintained at their new operating points , it should be ensured that during actual operation the liquid holdups both in the overhead accumulator and the reboiler are held essentially constant. The requirement of maintaining the liquid holdup in the overhead condenser is necessary to guarantee a continuous supply of reflux at the top of the column. Similarly, enough liquid holdup in the reboiler ensures a continuous supply of vapour from the reboiler. Therefore we have two additional control objectives. Following the discussion in Section 4. 3. 3 it is therefore necessary to identify four manipulated variables. The reflux rate and the bottoms product rate from the reboiler can be used in addition to the (freed variables) distillate rate and steam flowrate. To summarise, the following are the control objectives that are required to be held constant at their set-points, and the manipulated variables that can be used to provide the necessary regulatory action :

Control objectives (outputs)

(a)	The composition of LPG in the distillate product.	x_D
(b)	The reboiler return temperature.	T_R
(c)	The overhead accumulator liquid holdup.	H_A
(d)	The reboiler liquid holdup.	H_R

Manipulated variables (inputs)

(a)	The distillate product rate.	D
(b)	The steam rate to the column reboiler.	S
(c)	The reflux rate.	L
(d)	The bottoms product rate.	B

Multiloop control is the simplest control policy and its suitability can be tested for the de-propaniser. Though there are many multiloop control schemes possible (for a 4 X 4 system the number possible is 24) , based on engineering judgement many of these schemes can be rejected , and only the following three schemes will in fact be considered (see Section 5. 2. 3).

Control scheme 1

Control objectives		Manipulated variables
x_D	paired with	D
T_R	paired with	S
H_A	paired with	L
H_R	paired with	B

Control scheme 2

Control objectives		Manipulated variables
x_D	paired with	D
T_R	paired with	B
H_A	paired with	L
H_R	paired with	S

Control scheme 3

Control objectives		Manipulated variables
x_D	paired with	L
T_R	paired with	S
H_A	paired with	D
H_R	paired with	B

The scheme currently in operation on the de-propaniser has control objectives quite different from those chosen on the basis of from the optimisation studies. The column pressure (P) instead of the reboiler return temperature (T_R) is a control objective. The following control scheme is the one currently in operation on the de-propaniser :

Control scheme 4

Control objectives		Manipulated variables
x_D	paired with	L
P	paired with	S
H_A	paired with	D
H_R	paired with	B

Figure 5. 4. 5 shows all four control schemes that form the multiloop choices for the present case-study. We need to identify which of these four possible multiloop control structures allows us to operate most closely to perfect control. Perkins [1989] has shown that the minimum (l_∞ - norm) condition number (γ_{min}) is a reliable indicator for controllability with values close to unity indicating that tight control (i.e. close to perfect control) is possible. Thus γ_{min} will be used as a basis for screening the alternative control schemes. This minimum condition number was estimated over the whole frequency range of interest for each of these four control schemes. The approach suggested in Section 5. 3 was used to estimate the frequency range of interest. The largest eigenvalue of the system matrix of the de-propaniser model, expressed in state-space form was 325. Thus only frequencies below 650 / hr (i.e twice the largest eigenvalue) are of interest to us. It should be noted that Control Systems 1, 2 and 3 have the same control objectives and manipulated variables, and differ only in the pairings. Control System 4 has different

Figure 5. 4. 5
De-propaniser control schemes

SCHEME 1

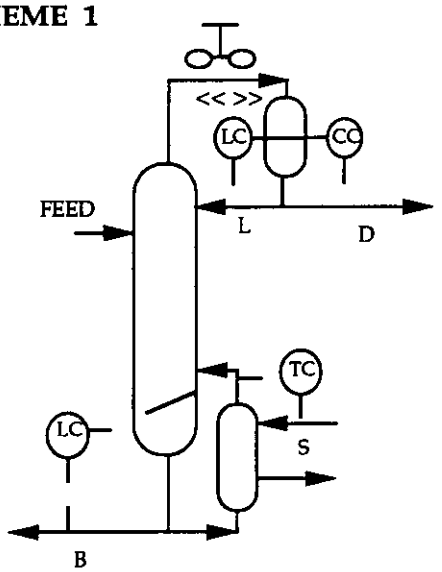

SCHEME 2

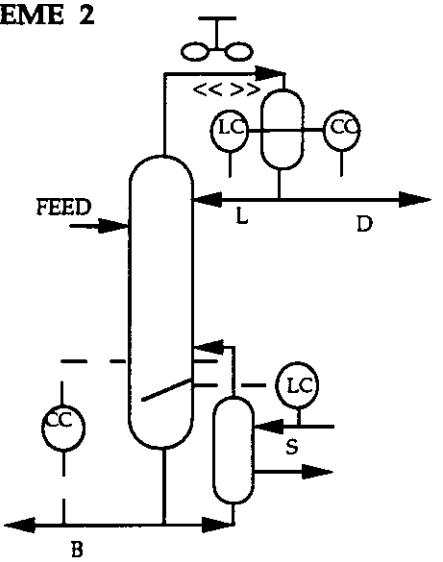

SCHEME 3

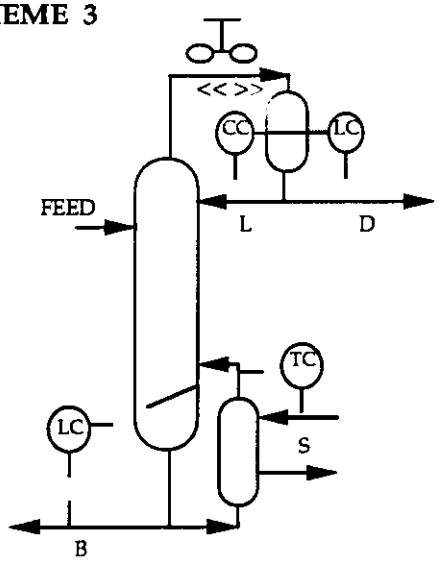

SCHEME 4

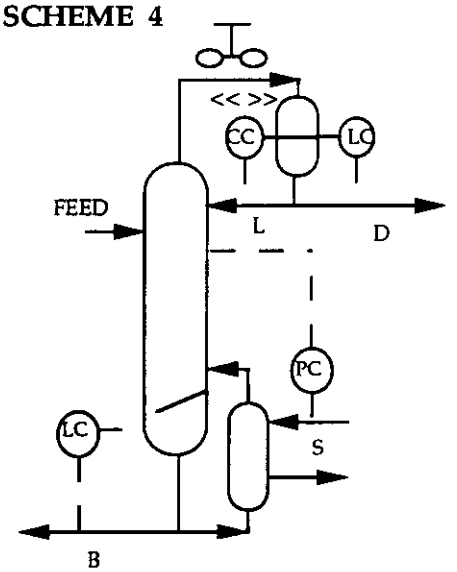

control objectives. The minimum condition number is independent of the actual pairings between the inputs and outputs and for a given choice of control objectives and manipulated variables is constant. As a first pass, therefore, we can estimate the minimum condition number for both the (4 X 4) alternatives. Figure 5. 4. 6 shows γ_{min} as a function of frequency. Although Control System 1/ 2/ 3 has a smaller condition number over most of the frequency range compared to Control System 4 , γ_{min} is relatively high in both cases.

The speed of response of the secondary control objectives (i.e. the levels in the overhead accumulator and the reboiler) is known to be an order of magnitude faster than that of the primary objectives (i.e. the LPG composition in the distillate and the reboiler return temperature). The minimum condition number , however, takes no account of the relative speed of response of any individual loops. Therefore one approach is to design controllers for the secondary objectives as a first step. The fast response of the secondary loops ensures that they do not form an additional source of disturbance to the primary control loops. If this is done, we can look at the remaining (2 X 2) control systems for the primary objectives alone. The secondary objectives were all regulated using a "square root control policy ". As the secondary control objectives in this case are all holdups, the following relationship was used to achieve the necessary regulation.

$$\text{Flowrate} = K_V \sqrt{\text{Holdup}} \qquad (5.4.5)$$

where K_V is the square root valve constant and is estimated from the steady-state results.

In many industrial applications it is often adequate to regulate the secondary control objectives within their minimum and maximum values. A square root control policy in all such cases provides a simple alternative. Another advantage of this approach is that tuning of the secondary controllers is not necessary. A square root control policy will, therefore, be used to regulate the de-propaniser reboiler/condenser holdups.

The plots of minimum condition number (see Figure 5. 4. 7) as a function of frequency clearly indicate that Control System 1 should offer the best closed-loop performance. Control System 4 (i.e. the control scheme currently in operation) has the largest minimum condition number over most of the frequency range , relative to the other three control schemes. As expected, Control System 2 has an infinite condition number (see Section 5. 2. 2) at steady-state, which then falls off rapidly at higher frequencies. The minimum condition number at steady-state for all four control schemes is also given in the Table 5. 4. 3. Another open-loop indicator, the relative gain array (RGA), provides a reliable estimate of the likely control loop interaction in a multiloop control system. Table 5. 4. 4

Figure 5. 4. 6
MINIMUM CONDITION NUMBER FOR DIFFERENT (4 X 4) CONTROL SYSTEMS
FOR THE DE-PROPANISER

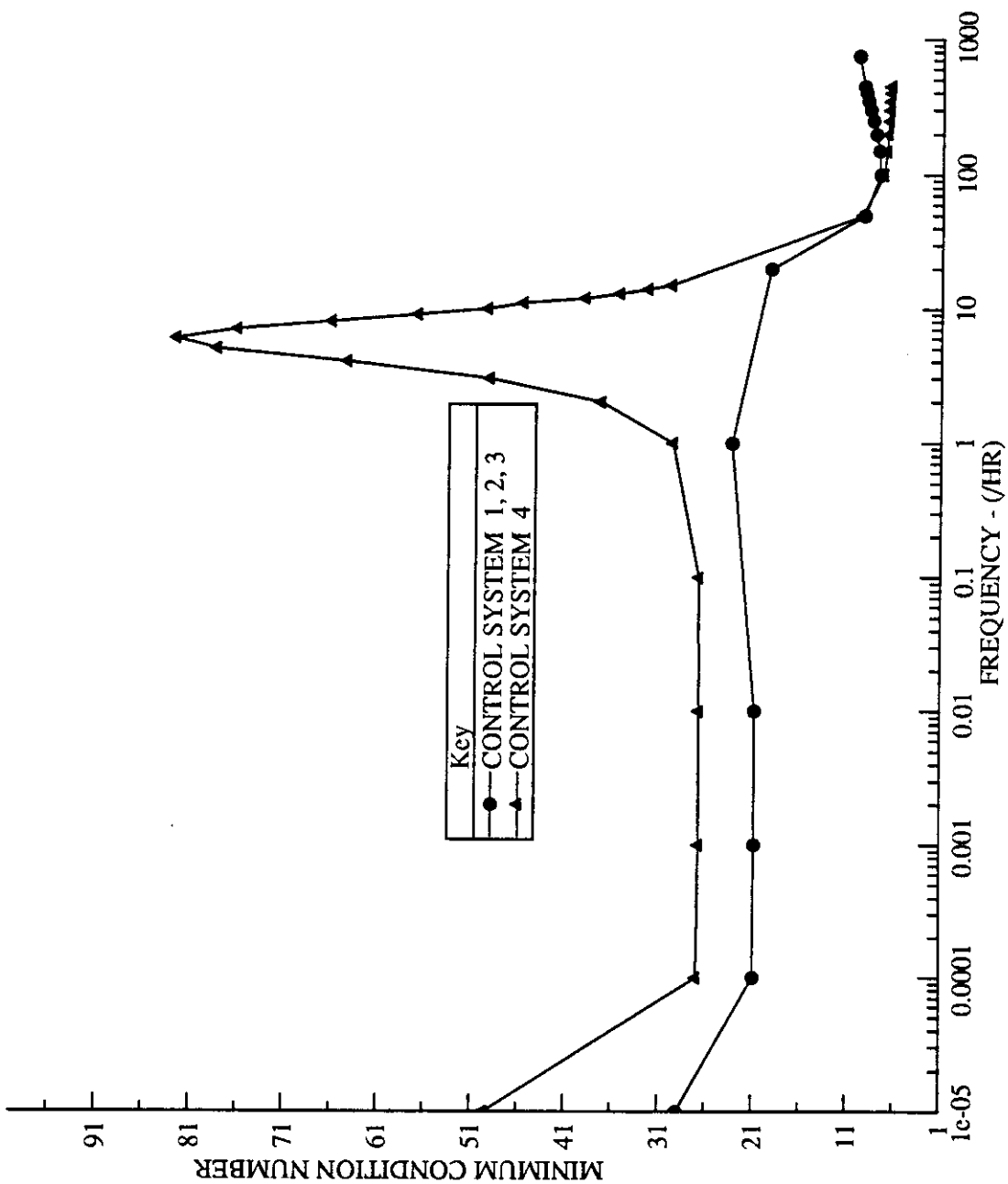

Figure 5. 4. 7
MINIMUM CONDITION NUMBER FOR DIFFERENT (2 X 2) CONTROL SYSTEMS FOR THE DE-PROPANISER

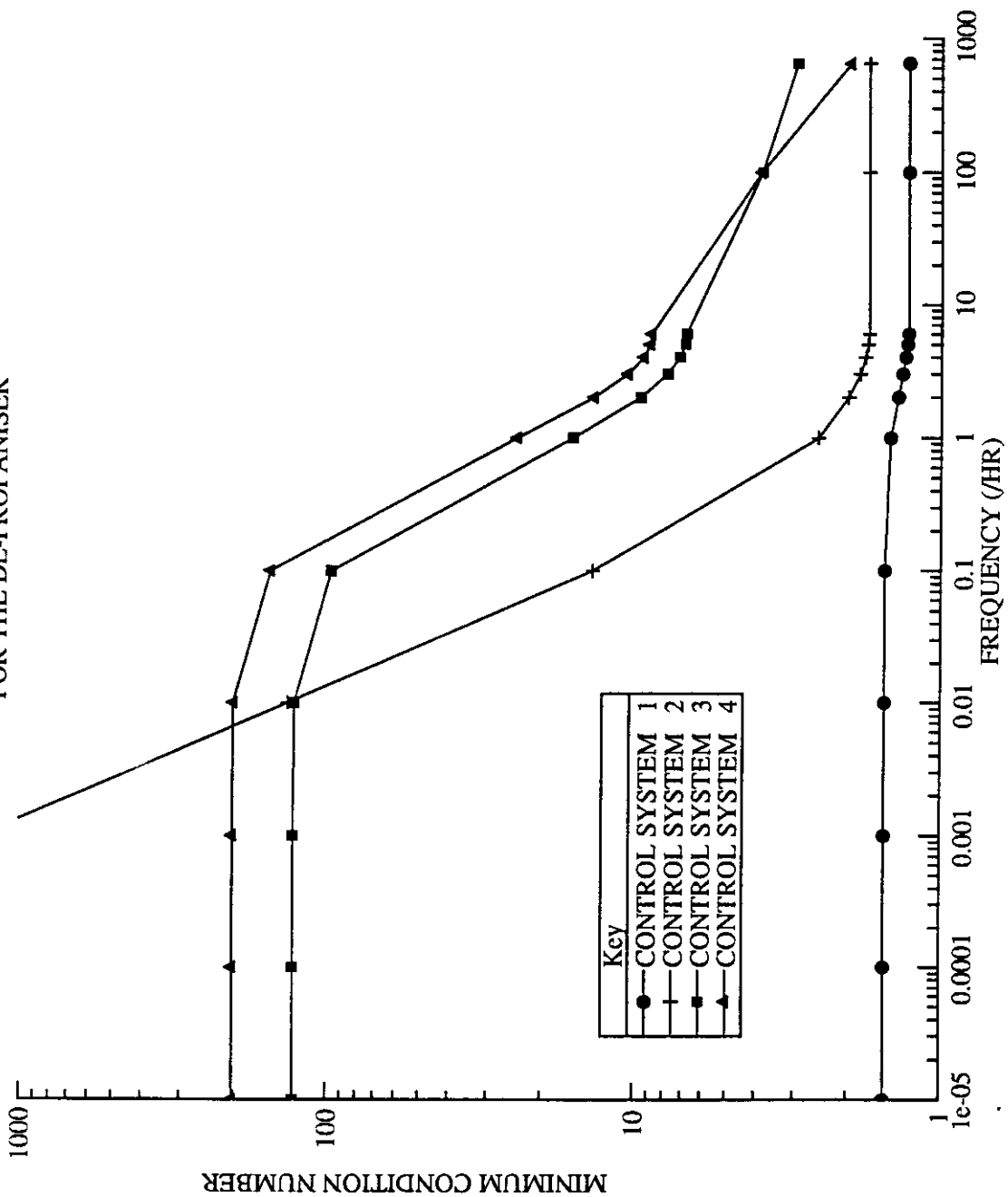

Table 5. 4. 3
Steady-state minimum condition number for
alternative (2 X 2) control schemes for
the de-propaniser

Control scheme	Minimum condition number
1	1.5
2	∞
3	128
4	203

Table 5. 4. 4
Relative gain array for alternative (2 X 2) control schemes
for the de-propaniser
(only the first diagonal element is shown)

Control scheme	Relative Gain Array (the first diagonal element) (λ_{11})
1	1.04
2	∞
3	32.10
4	50.02

shows the RGA for each of the four control schemes. The results are consistent with the minimum condition number plots , in that the ranking of the four control schemes is the same.

A physical interpretation of these open-loop results is as follows. Control Systems 1, 2 and 3 represent control at the "ends" of the column (i.e near the top and the bottom). The relatively poor controllability characteristics (i.e. RGA and minimum condition number) of Control System 3 compared to Control system 1 can be attributed to the fact that the reflux ratio in the de-propaniser is large (> 5), and in such a case top composition control through the distillate product rate is preferred to control through the reflux rate (Shinskey [1988]). Many of the de-propaniser's control problems (with the current control scheme i.e Control System 4) are known to be due to large interactions between the two primary control loops. For example, an increase in the steam rate increases the vapour rate from the reboiler. Vapour from the reboiler carries along with it some of the heavier components and these eventually end up at the top of the column. The result of this increased amount of vapour is that the column pressure increases but the composition at the top of the column, with respect to the lighter components, drops. An increase in the reflux rate is then necessary to remove the heavier components from the top of the column gives rise to a purer distillate product.

Control schemes 1 and 2 should have relatively little loop interaction and provide good closed-loop performance. The major drawback of Control scheme 2 , however, is that it requires on-line tuning and hence will not be discussed further in this example.

POTENTIAL ECONOMIC BENEFITS OF OPTIMISING CONTROL

The following question needs specific attention at this stage.

> What economic justification can we provide for switching over the de-propaniser from the current control scheme (i.e. Control scheme 4) to an optimising control scheme (i.e. Control scheme 1) ?

Figure 5. 4. 8 shows various back-offs in the active and non-active constraints for Control System 1 and Control System 4. In the case of Control System 1 , both of the active constraints (i.e. the LPG composition in the distillate product and the reboiler return temperature) are regulated while the non-active constraint (i.e. column pressure) is allowed to float about its optimum operating value. Stages A, B and C in Figure 5. 4. 8 show values for each of the de-propaniser constraints at the calculated optimum , at the open-loop back-off and at the closed-loop back-off respectively . The open-loop back-off ($b_i^{(ol)}$ for i = 1, 2) for each of the active constraints can be estimated using

Figure 5. 4. 8

Open and closed-loop back-offs for the de-propaniser column

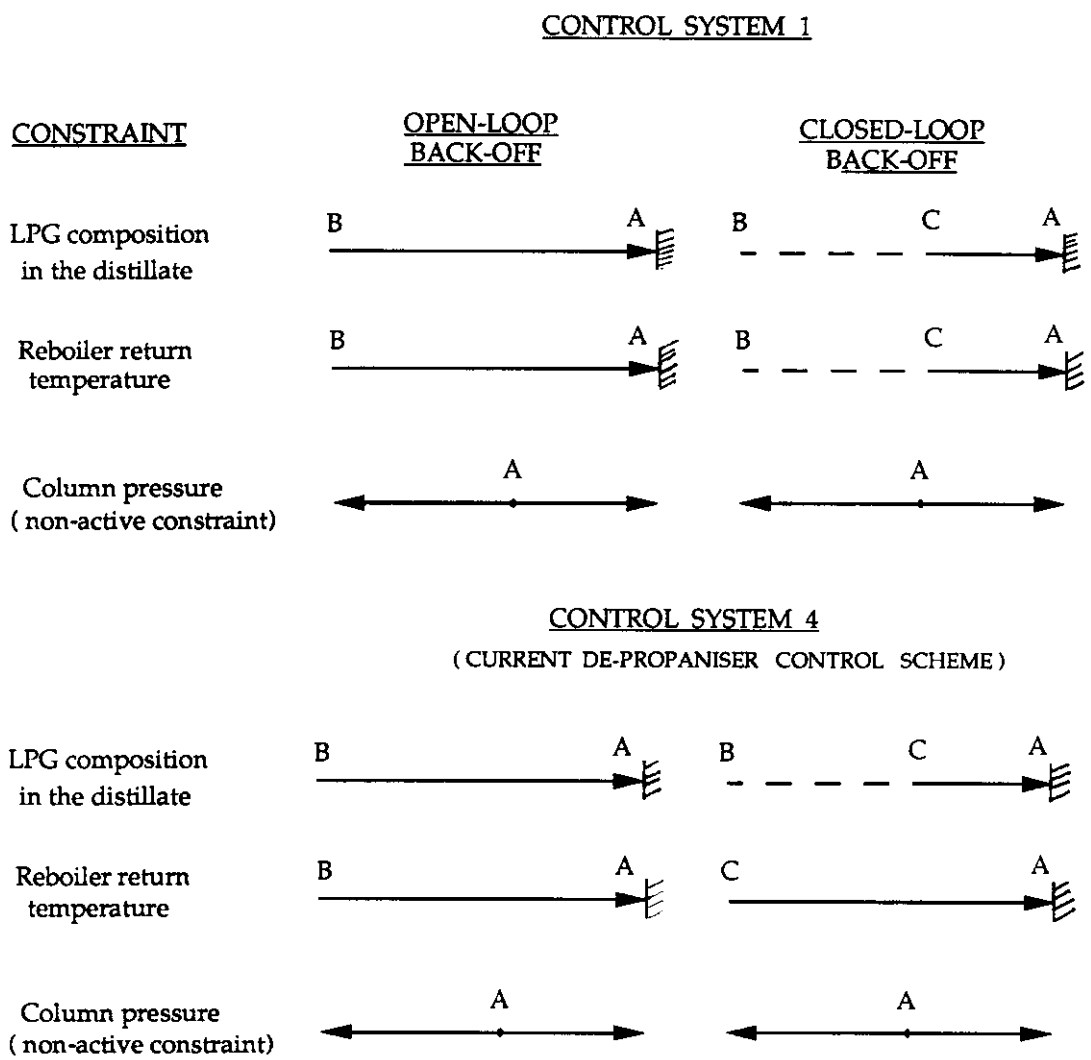

Equation 5. 3. 9. The non-active constraint (i.e the column pressure) , on the other hand, is not associated with any open-loop back-off from its optimum value. As discussed previously it is possible to recover some part of this open-loop back-off by regulating the active constraints directly using some sort of control system. The new operating point (C in Figure 5. 3. 8) that guarantees no constraint violation during any disturbance induced transient, is still associated with a back-off from the calculated optimum value. These closed-loop back-offs ($b_i^{(cl)}$ for i = 1, 2) will be smaller (in the limit point C approaches point A) the closer to perfect control we get.

Calculation of the MPR (see Equation 5. 4. 4) can be achieved as follows:

$$\Delta\phi_{max} = \lambda_1 b_1^{(ol)} + \lambda_2 b_2^{(ol)} \qquad (5.4.6)$$

and

$$\Delta\phi_{new} = \lambda_1 b_1^{(cl)} + \lambda_2 b_2^{(cl)} \qquad (5.4.7)$$

$$MPR = 100 * (1 - \Delta\phi_{new} / \Delta\phi_{max}) \qquad (5.4.8)$$

As calculated before through Equation (5. 4. 4) the MPR value for the de-propaniser column with Control System 1 is estimated to be 61 %. However in the case of Control System 4 only one of the active constraints is regulated. An open-loop back- off to point B in the non-regulated active constraint (i.e. the reboiler return temperature) is still necessary to avoid constraint violation. Since there is no regulation on this active constraint, no potential recovery of this back-off is possible. The new operating point for T_R (i.e point C) therefore remains unchanged (i.e the same as point B). The non-active constraint (i.e column pressure) regulation on the other hand does not involve any back-off from it's optimum value, and hence there is no economic penalty or recovery. An MPR estimate for Control System 4 can thus be estimated using Equations (5. 4. 6 - 5. 4. 8) and the following values:

$$\lambda_1 = 371.1 \quad \text{and} \quad \lambda_2 = 8.0$$
$$b_1^{(ol)} = 0.10 \quad \text{and} \quad b_1^{(ol)} = 13.0$$
$$b_1^{(cl)} = 0.0011 \quad \text{and} \quad b_1^{(cl)} = 13.0$$

where the subscripts 1 and 2 refer to the active constraints x_D and T_R respectively.

$$\Delta\phi_{max} = \lambda_1 b_1^{(ol)} + \lambda_2 b_2^{(ol)} \qquad (5.4.9)$$
$$= \$141.1 / hr$$
$$\Delta\phi_{new} = \lambda_1 b_1^{(cl)} + \lambda_2 b_2^{(cl)}$$
$$= \$104.4 \qquad (5.4.10)$$
$$MPR = 100 * (1 - \Delta\phi_{new} / \Delta\phi_{max})$$
$$= 26\% \qquad (5.4.11)$$

Equation (5. 4. 11) shows that with the current control system only 26 % of the back -off penalty can be recovered, while the optimising control policy of Control System 1 can recover nearly 61 % of the open-loop back-off. It is clear that the economic benefits associated with Control System 1 are significant compared to that of the current control strategy. Switching the de-propaniser column to an optimising control policy therefore has a strong economic justification.

CLOSED - LOOP DYNAMIC SIMULATIONS

It should be realised that the closed-loop simulations reported here were performed only to demonstrate the following two major issues :

(a) How good the open-loop indicator predictions are with respect to the overall control system performance.

(b) How good simple heuristics (see Section 5. 3) is when used in deciding the closed-loop back-off actually needed for each of the control objectives. The dynamic simulations should not be regarded as part of the economics based control system synthesis methodology.

Only Control System 1 (i.e. the control system with the "best " controllability properties) and Control System 4 (i.e. the control system with the " worst " controllability properties) were studied here. A consistent policy for the tuning of all the control loops was used. A consistent basis here is essential if we wish to quantitatively compare the dynamic simulation results. All the controllers used were of the PI type. For each control scheme a frequency dependent open-loop transfer function matrix for the selected choice of inputs and outputs was obtained using the SPEECON package. The operating point with the control objectives at their "backed-off values " was taken as the reference steady-state for model linearisation. Information about the frequency dependent behaviour of the various elements of the de-propaniser process transfer function matrix was used to design and tune the controllers (see Appendix A9 for details on the procedure used). See Table 5. 4 . 5 for details on the controller tuning parameters.

The closed-loop performance of both control systems was studied for the following set-point and disturbance changes :

(1) A step change of + 2. 5 % (from a value of 0.911 mole fraction) in the set-point for the first control objective, i.e. the LPG composition in the distillate product.

(2) A step change of - 3. 5 % (from a value of 123.8 deg C) in the set-point for the second control objective of Control System 1 , i.e. the reboiler return temperature.

(3) A step change of + 8 % (from a value of 16.7 Bar) in the set-point for the second control objective of Control System 2 , i.e. the pressure at the top of the column.

(4) A step change of + 10 % (from a value of 3. 14 Bar) in the disturbance input to the reboiler, i.e. the LP steam pressure.

(5) A step change of -14 % (from a value of 208 Kg-moles/hr) in the disturbance input to the de-propaniser, i.e. the feed rate to the column.

The terms in the parentheses above indicate the values of the variables at the chosen operating point (i.e. the values before any set-point or disturbance changes were made). All the dynamic simulations were performed using the SPEEDUP package. The closed-loop dynamic simulation results obtained are given in the Figures (5. 4. 9) - (5. 4. 40). From these, Control System 1 clearly provides superior closed- loop performance relative to that of Control System 4. These results are thus consistent with the predictions made using the open-loop controllability measures. Some of the major results are discussed below :

(a) Figures(5. 4. 9) - (5. 4. 12) show that the first control objective (i.e. x_D) exhibits good set-point and disturbance rejection characteristics in the case of Control System 1. The response for the same control objective in the case of Control System 4 is generally both more oscillatory and with a longer settling time. However, for a feed flowrate disturbance, the performance of Control System 1 is relatively poor compared to that of Control System 4.

(b) The second control objective in the case of Control System 1 (i.e. T_R) has good set-point and disturbance rejection performance (see Figures 5. 4. 13 - 5. 4. 16). The second control objective for Control System 4 (i.e. P) , however, never returns to it's set-point for both set-point and disturbance changes (see Figures 5. 4. 17- 5. 4. 20). These latter responses also show the highly interactive nature of the two control loops in the case of Control System 4.

(c) The severe interaction of the control loops in the case of Control System 4 also affects the two secondary control objectives i.e. the liquid holdups in the overhead accumulator and the reboiler (see Figures 5. 4. 21 - 5. 4. 28). Relatively smooth behaviour for these two control objectives can be seen in the case of Control System 1.

(d) The changes required in the manipulated variables to regulate each of the control objectives, both for set-point and disturbance changes, can be seen in Figures 5. 4. 29

- 5. 4. 40 . Clearly the manipulated variables in the case of Control System 1 do not come close to reaching "saturation " during any transient. The responses of the manipulated variables for Control System 4 are both larger and more oscillatory.

In general, violation of the constraints for each of the x_D and T_R control objectives is more significant and more common in the case of Control System 4 compared to Control System 1. Thus, for Control System 1 , the first pass estimates used for the closed-loop back-off in the control objectives (i.e. the second largest open-loop back-offs) proved to be a reasonably good choice. Frequent constraint violations in the case of Control System 4 , on the other hand, indicated that the closed-loop back-offs used and the MPR estimated (23 % from Equation 5. 4. 10) are both quite optimistic. To avoid such constraint violations during transients in the latter case, further back-offs would be necessary. This would, therefore, result in an MPR value even less than that estimated in Equation 5. 4. 10.

The off-sets in the secondary control objectives (see Figures 5. 4. 9 - 5. 4. 40) are the consequence of two major factors. Firstly, the column pressure is not controlled but allowed to "float" during the transients. Thus the process comes to a new steady-state in the neighbourhood of the original operating point. Secondly, the "controllers" used to regulate the secondary control objectives are really just open-loop relationships between the flow and the level in the vessel (see Equation 5. 3. 9). Hence they do not attempt to eliminate any off-set like a PI controller. As long as the off-sets are not too large, then this will not significantly affect the economics of the operation. As discussed before, another advantage of this control policy for regulating secondary control objectives is that it does not require tuning of controllers.

5. 5 SUMMARY

The first stage of the economics - based approach to control system synthesis provides the upper and lower bounds on the achievable economic benefits for having a regulatory control system. The larger the potential benefit, the greater is the incentive to install a control system. Having decided that a control system is economically justified , the next step is to determine how close to perfect control one can expect to get (with the proper choice of a control system). The second stage of the procedure provides this information by using various controllability indices. Screening of alternative potential control schemes is done in this stage.

This two-stage approach has been successfully demonstrated for the de-propaniser column in the Shell gas-tail. Results showed that significant economic benefits are associated with optimising strategy over the current control policy. The nonlinear closed-loop

Table 5. 4. 5
Controller tuning constants for
the "best" and "worst" (2 X 2) control schemes
for the de-propaniser column

	Controller gain K_C	Controller reset time τ_I (Hr)	Luyben detuning constants F
Control System - 1			
Distillate composition loop	-13.190	0.171	1.9
Reboiler return temperature loop	0.149	0.0418	1.9
Control System - 4			
Distillate composition loop	-289.581	0.526	2.4
Column pressure loop	0.159	0.518	2.4

Figure 5.4.11
CLOSED LOOP RESPONSE OF DE-PROPANISER CONTROL SCHEMES -
RESPONSE OF DISTILLATE COMPOSITION TO A CHANGE OF +10 %
IN THE REBOILER STEAM PRESSURE

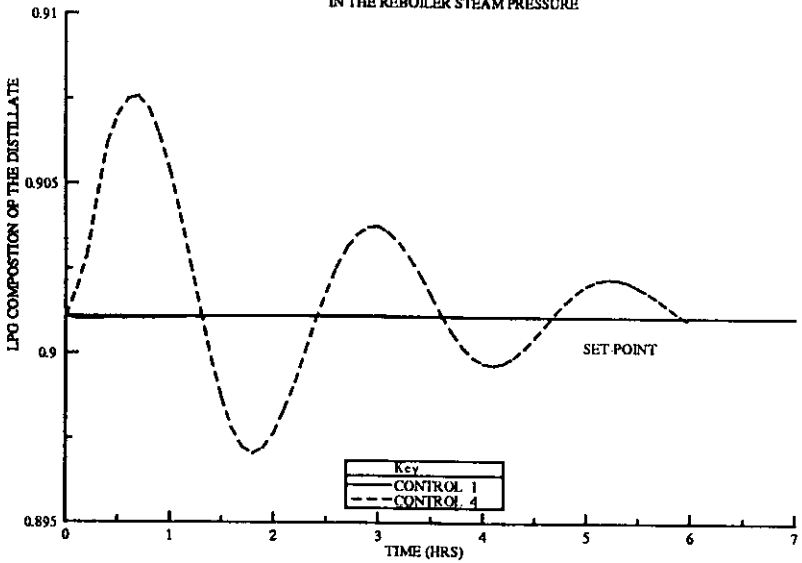

Figure 5.4.12
CLOSED LOOP RESPONSE OF DE-PROPANISER CONTROL SCHEMES -
RESPONSE OF DISTILLATE COMPOSITION TO A CHANGE OF -14 %
IN THE FEED FLOW RATE

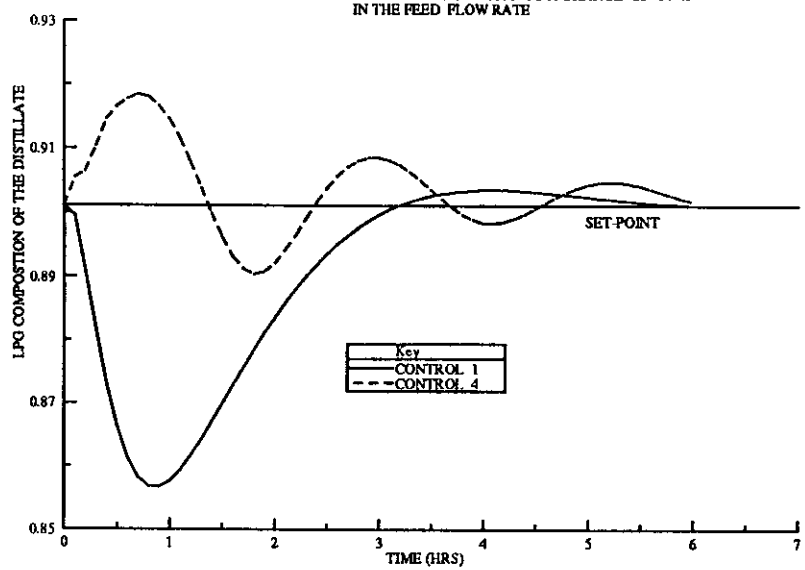

Figure 5.4.9
CLOSED LOOP RESPONSE OF DE PROPANISER CONTROL SCHEMES -
RESPONSE OF DISTILLATE COMPOSITION FOR A SETPOINT CHANGE OF +2.5 %
IN THE DISTILLATE COMPOSITION CONTROL LOOP

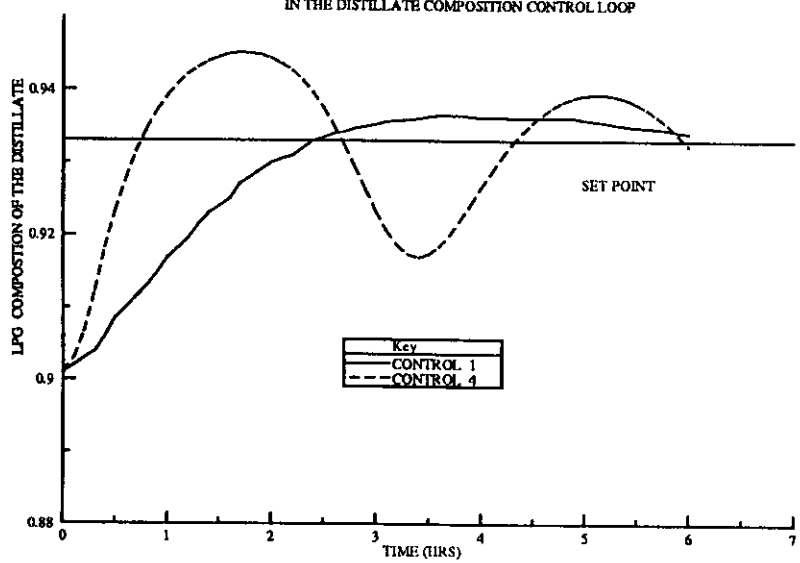

Figure 5.4.10
CLOSED LOOP RESPONSE OF DE-PROPANISER CONTROL SCHEMES -
RESPONSE OF DISTILLATE COMPOSITION FOR A SETPOINT CHANGE OF -3.5 %
IN THE REBOILER RETURN TEMPERATURE CONTROL LOOP

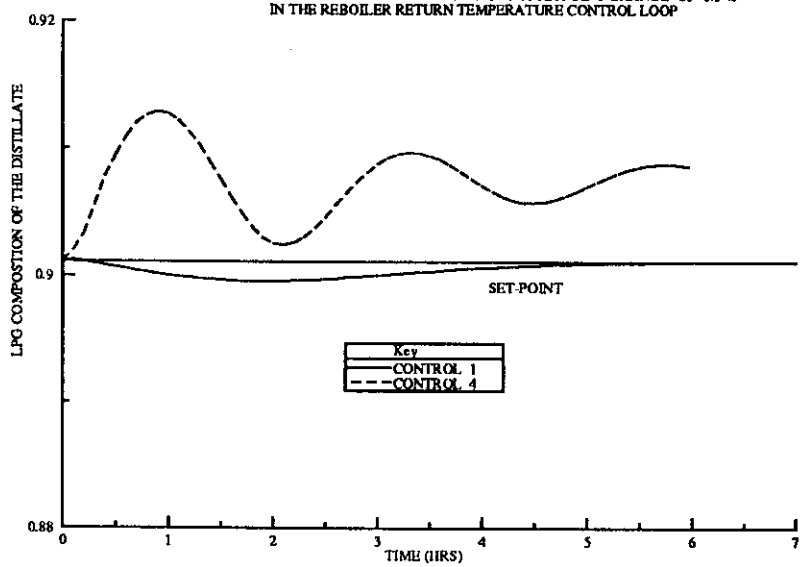

Figure 5. 4. 15
CLOSED-LOOP RESPONSE OF DE-PROPANISER CONTROL SCHEMES -
IN THE REBOILER RETURN TEMPERATURE TO A CHANGE OF +10 %
IN THE REBOILER STEAM PRESSURE

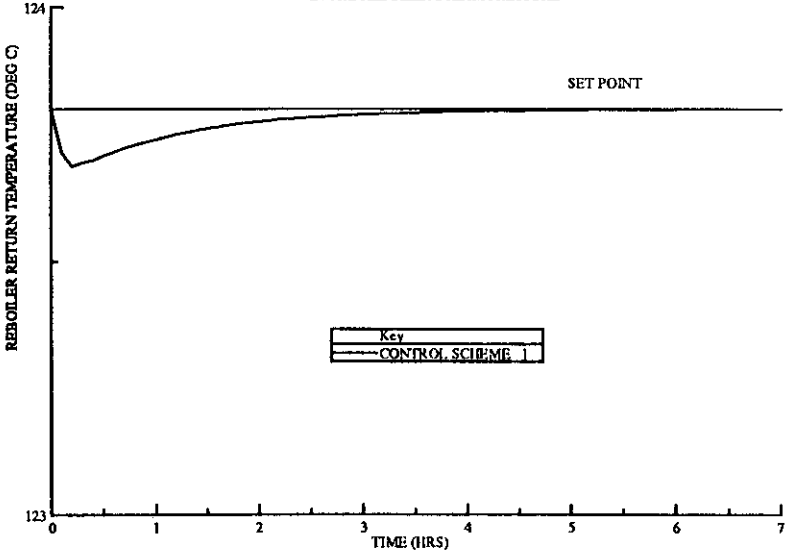

Figure 5. 4. 16
CLOSED-LOOP RESPONSE OF DE-PROPANISER CONTROL SCHEMES -
RESPONSE OF REBOILER RETURN TEMPERATURE TO A CHANGE OF -14 %
IN THE FEED FLOW RATE

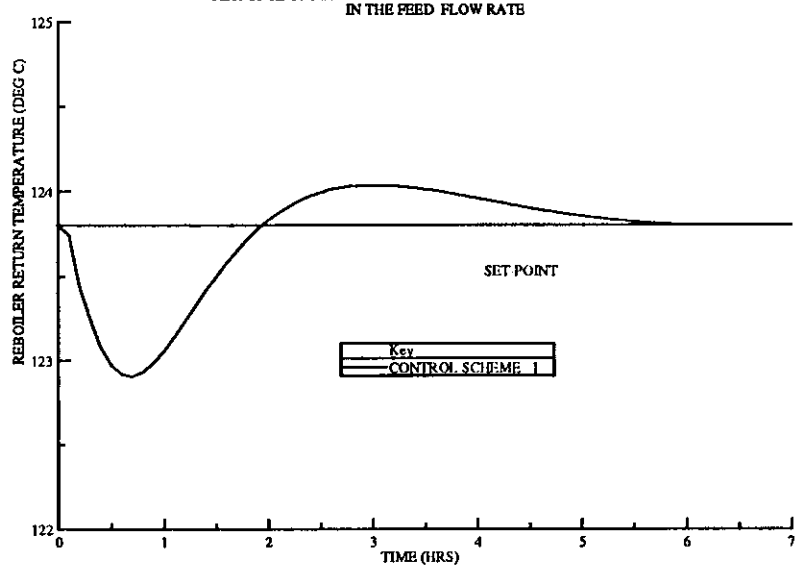

Figure 5. 4. 13
CLOSED-LOOP RESPONSE OF DE-PROPANISER CONTROL SCHEMES -
RESPONSE OF REBOILER RETURN TEMPERATURE A SETPOINT CHANGE OF +2.5 %
IN THE DISTILLATE COMPOSITION CONTROL LOOP

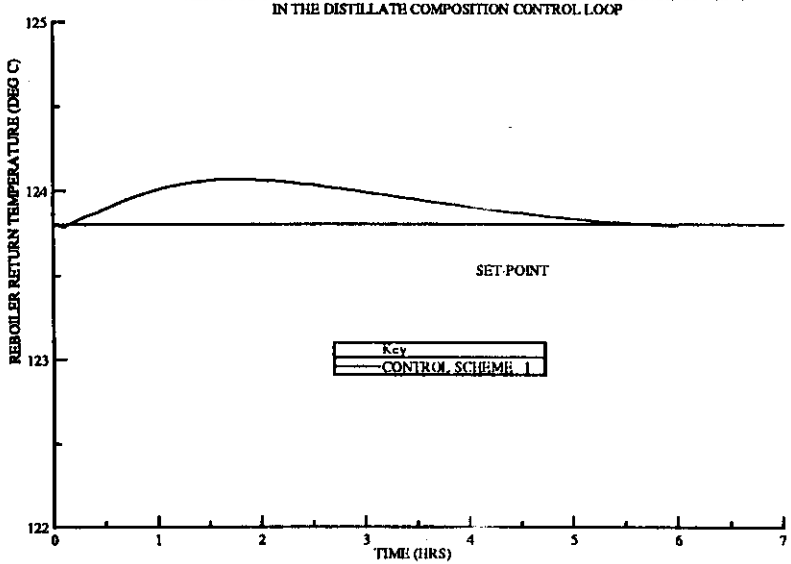

Figure 5. 4. 14
CLOSED-LOOP RESPONSE OF DE-PROPANISER CONTROL SCHEMES -
RESPONSE OF REBOILER RETURN TEMPERATURE FOR A SETPOINT CHANGE OF -3.5 %
IN THE REBOILER RETURN TEMPERATURE CONTROL LOOP

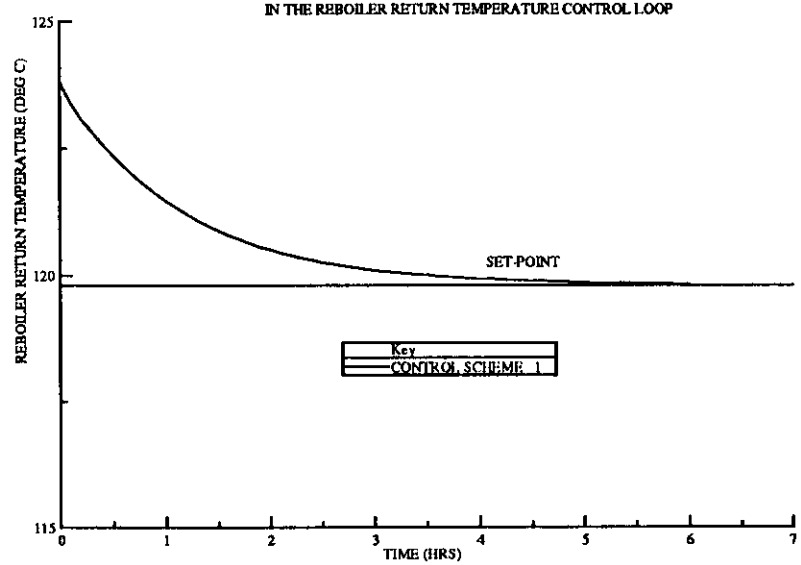

Figure 5.4.19
CLOSED-LOOP RESPONSE OF DE-PROPANISER CONTROL SCHEMES -
RESPONSE OF COLUMN PRESSURE TO A CHANGE OF +10 %
IN THE REBOILER STEAM PRESSURE

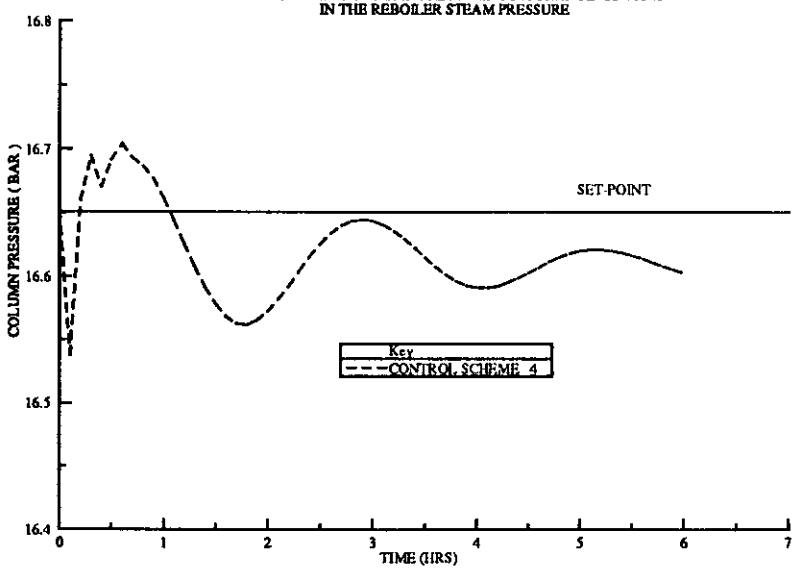

Figure 5.4.20
CLOSED-LOOP RESPONSE OF DE-PROPANISER CONTROL SCHEMES -
RESPONSE OF COLUMN PRESSURE TO A CHANGE OF -14 %
IN THE FEED FLOW RATE

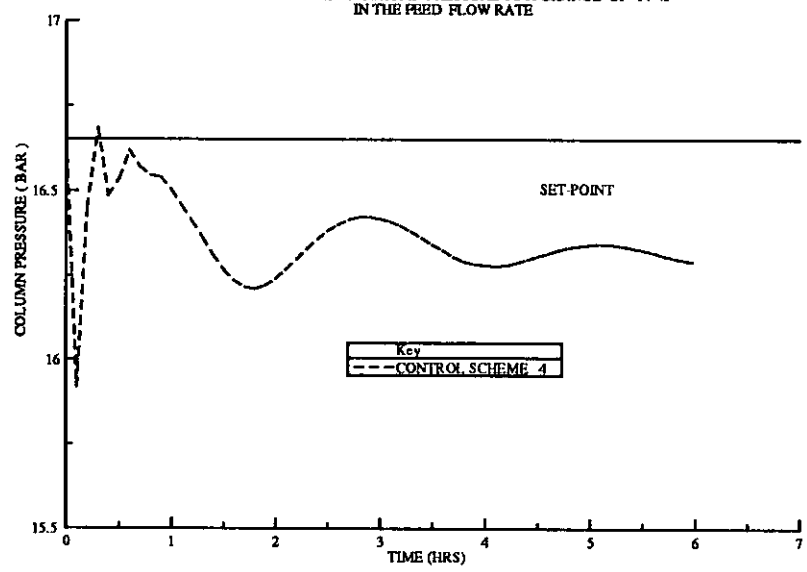

Figure 5.4.17
CLOSED-LOOP RESPONSE OF DE-PROPANISER CONTROL SCHEMES -
RESPONSE OF COLUMN PRESSURE FOR A SETPOINT CHANGE OF +2.5 %
IN THE DISTILLATE COMPOSITION CONTROL LOOP

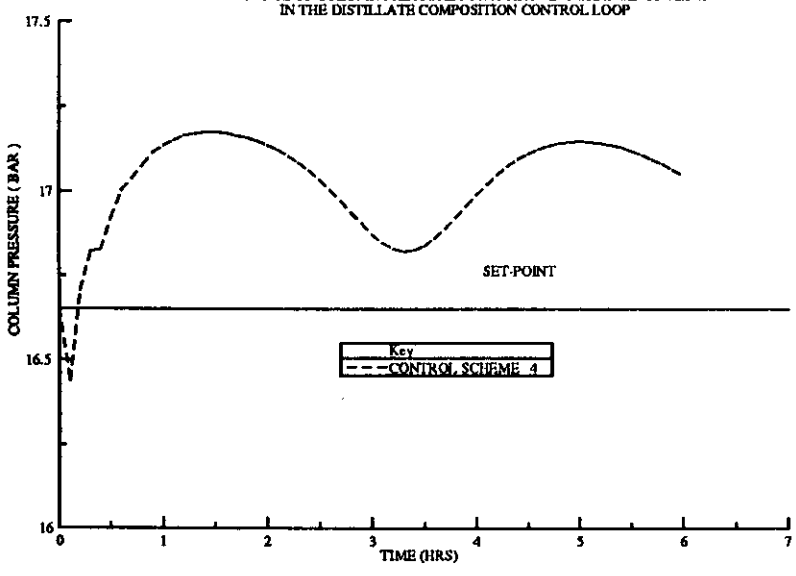

Figure 5.4.18
CLOSED-LOOP RESPONSE OF DE-PROPANISER CONTROL SCHEMES -
RESPONSE OF COLUMN PRESSURE FOR A SETPOINT CHANGE OF +8.0 %
IN THE COLUMN PRESSURE CONTROL LOOP

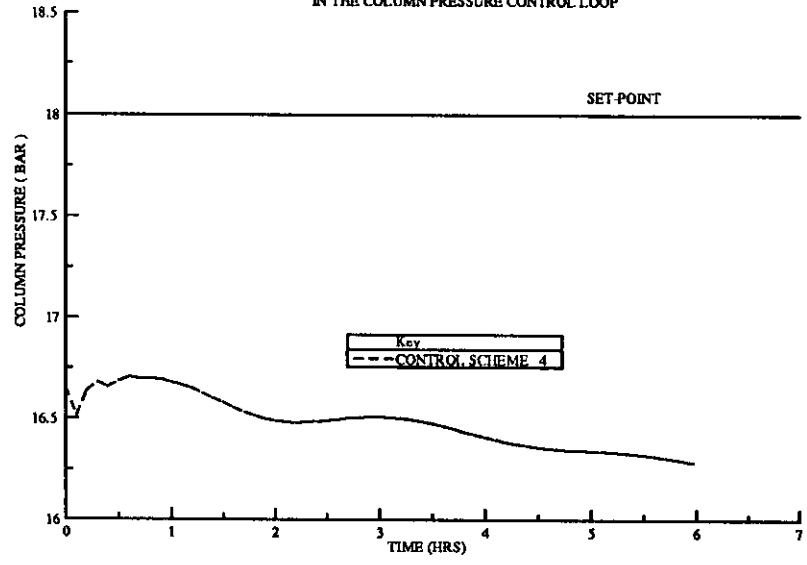

Figure 5. 4. 23
CLOSED-LOOP RESPONSE OF DE-PROPANISER CONTROL SCHEMES -
RESPONSE OF OVERHEAD ACCUMULATOR HOLDUP TO A CHANGE OF +10 %
IN THE REBOILER STEAM PRESSURE

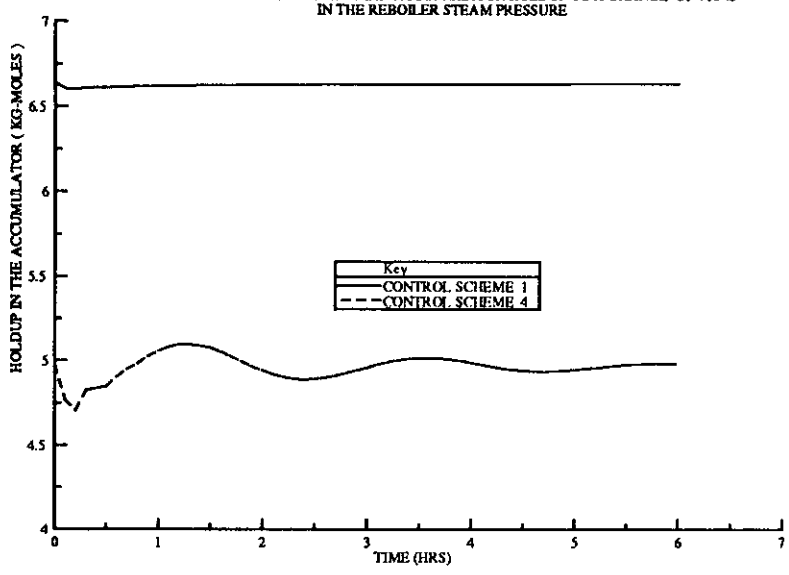

Figure 5. 4. 24
CLOSED-LOOP RESPONSE OF DE-PROPANISER CONTROL SCHEMES -
RESPONSE OF OVERHEAD ACCUMULATOR HOLDUP TO A CHANGE OF -14 %
IN THE FEED FLOW RATE

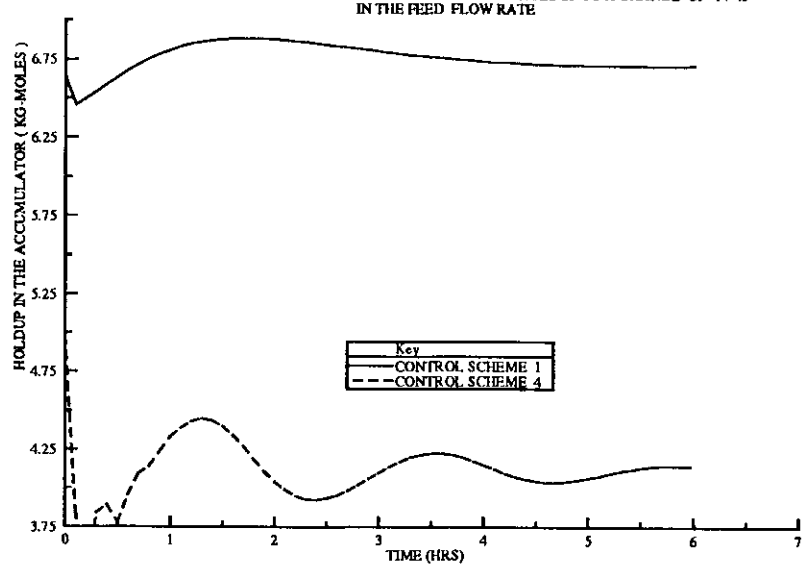

Figure 5. 4. 21
CLOSED LOOP RESPONSE OF DE-PROPANISER CONTROL SCHEMES -
RESPONSE OF OVERHEAD ACCUMULATOR HOLDUP FOR A SETPOINT CHANGE OF +2.5%
IN THE DISTILLATE COMPOSITION CONTROL LOOP

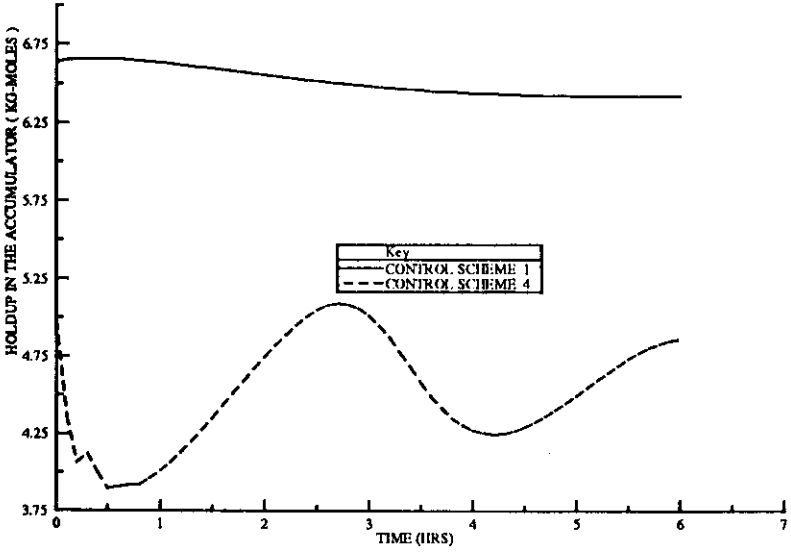

Figure 5. 4. 22
CLOSED LOOP RESPONSE OF DE-PROPANISER CONTROL SCHEMES -
RESPONSE OF OVERHEAD ACCUMULATOR HOLDUP FOR A SETPOINT CHANGE
IN THE SECOND CONTROL OBJECTIVE

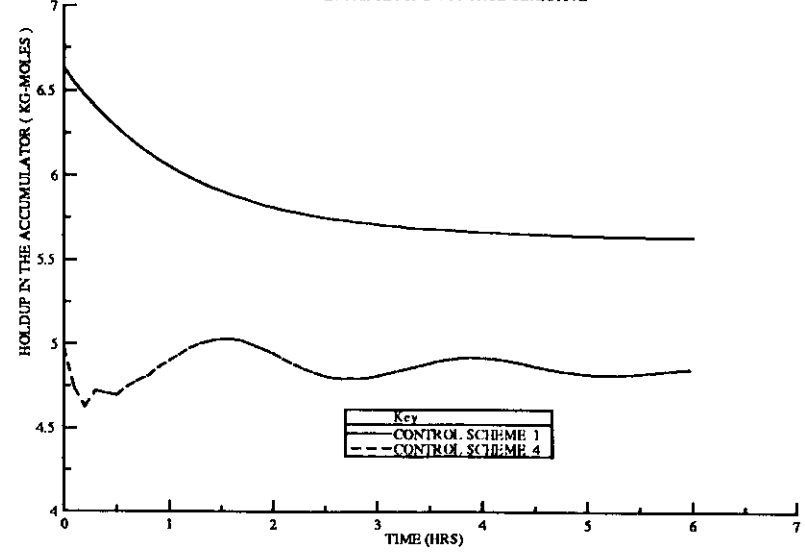

Figure 5.4.27
CLOSED-LOOP RESPONSE OF DE-PROPANISER CONTROL SCHEMES -
RESPONSE OF REBOILER HOLDUP TO A CHANGE OF +10 %
IN THE REBOILER STEAM PRESSURE

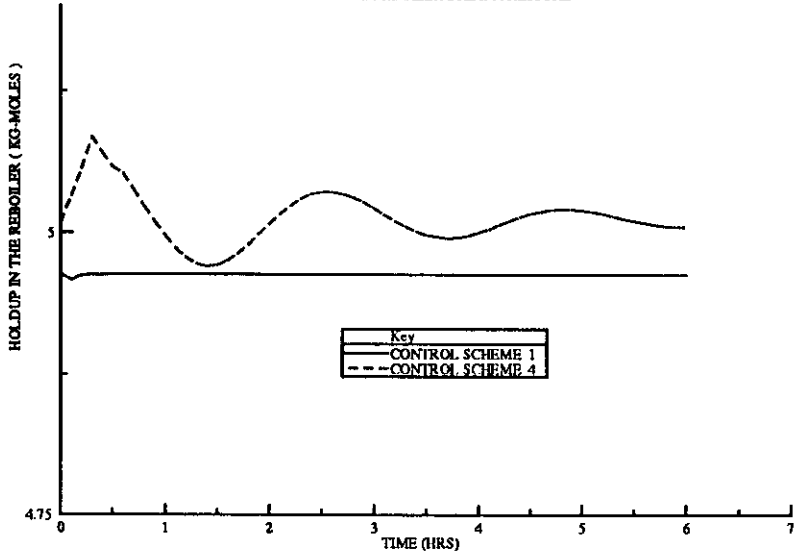

Figure 5.4.28
CLOSED-LOOP RESPONSE OF DE-PROPANISER CONTROL SCHEMES -
RESPONSE OF REBOILER HOLDUP TO A CHANGE OF -14 %
IN THE FEED FLOW RATE

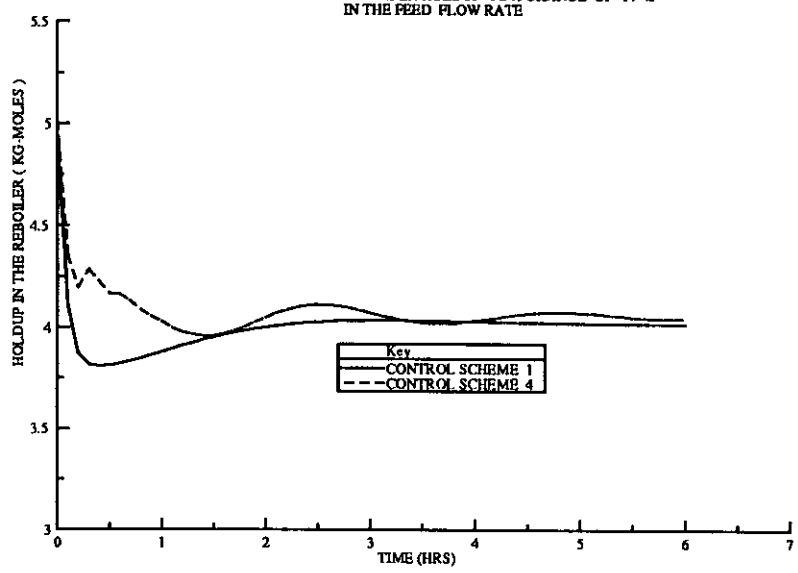

Figure 5.4.25
CLOSED-LOOP RESPONSE OF DE-PROPANISER CONTROL SCHEMES -
RESPONSE OF REBOILER HOLDUP FOR A SETPOINT CHANGE OF +2.5 %
IN THE DISTILLATE COMPOSITION CONTROL LOOP

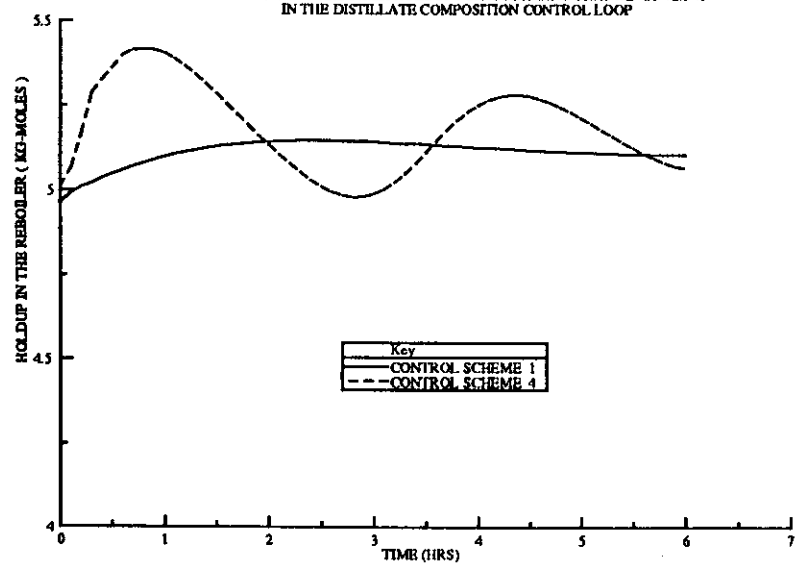

Figure 5.4.26
CLOSED-LOOP RESPONSE OF DE-PROPANISER CONTROL SCHEMES -
RESPONSE OF REBOILER HOLDUP FOR A SETPOINT CHANGE
IN THE SECOND CONTROL OBJECTIVE

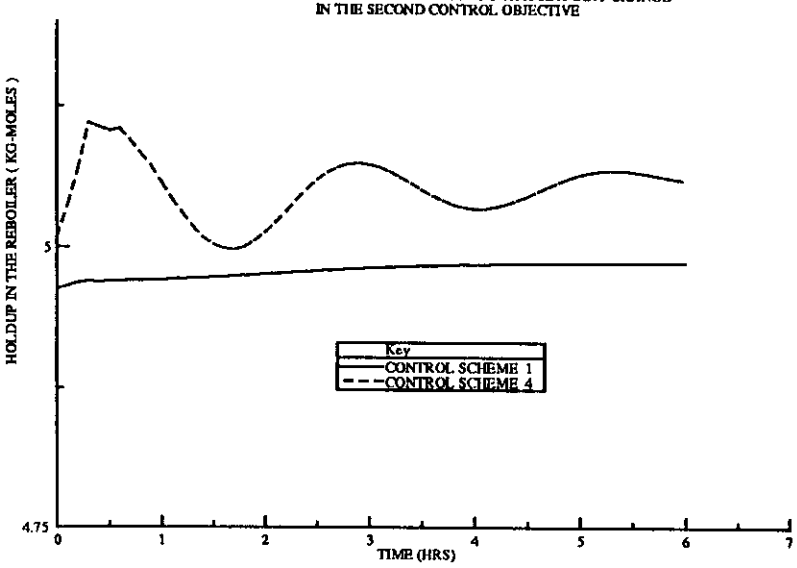

Figure 5.4.31
CLOSED-LOOP RESPONSE OF DE-PROPANISER CONTROL SCHEMES -
RESPONSE OF DISTILLATE FLOWRATE TO A CHANGE OF -10 %
IN THE REBOILER STEAM PRESSURE

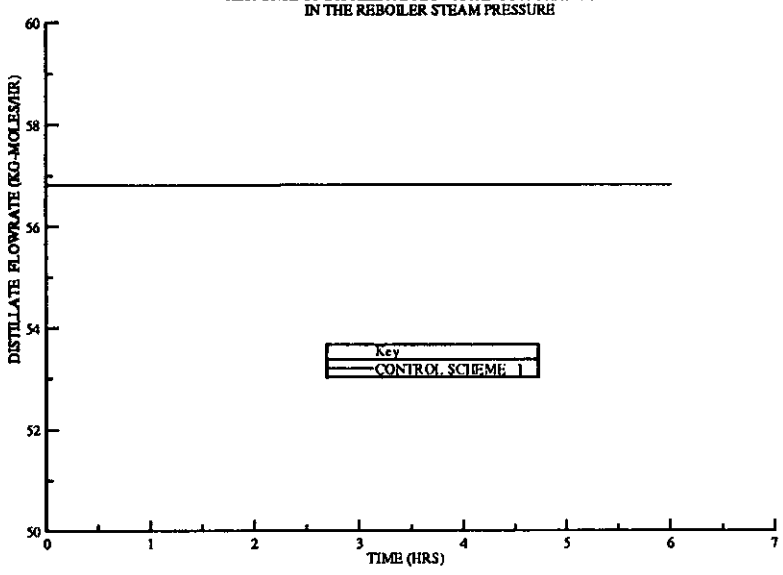

Figure 5.4.32
CLOSED-LOOP RESPONSE OF DE-PROPANISER CONTROL SCHEMES -
RESPONSE OF DISTILLATE FLOWRATE TO A CHANGE OF -14 %
IN THE FEED FLOW RATE

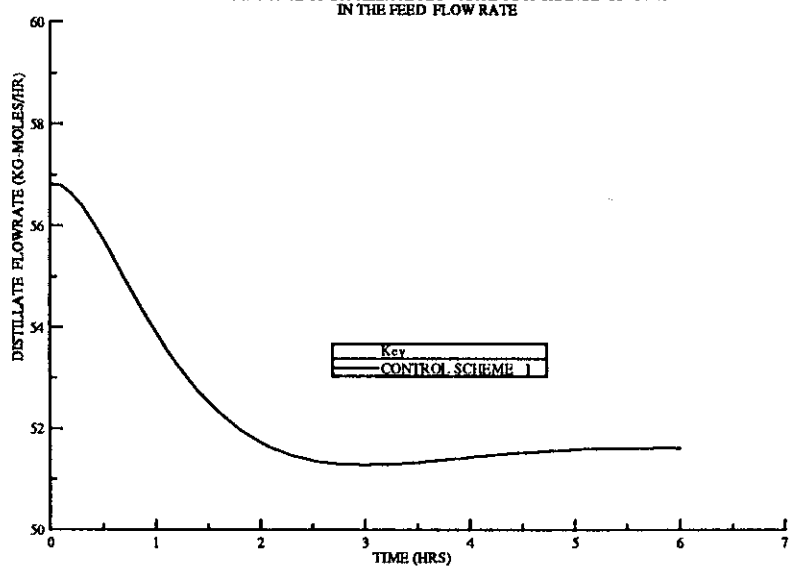

Figure 5.4.29
CLOSED-LOOP RESPONSE OF DE-PROPANISER CONTROL SCHEMES -
RESPONSE OF DISTILLATE FLOWRATE FOR A SETPOINT CHANGE OF +2.5%
IN THE DISTILLATE COMPOSITION CONTROL LOOP

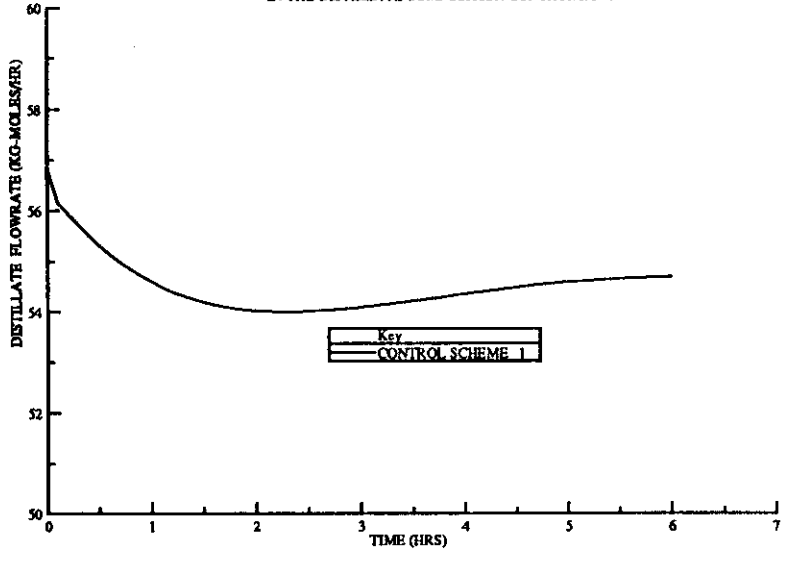

Figure 5.4.30
CLOSED-LOOP RESPONSE OF DE-PROPANISER CONTROL SCHEMES -
RESPONSE OF DISTILLATE FLOWRATE FOR A SETPOINT CHANGE OF -3.5 %
IN THE REBOILER RETURN TEMPERATURE CONTROL LOOP

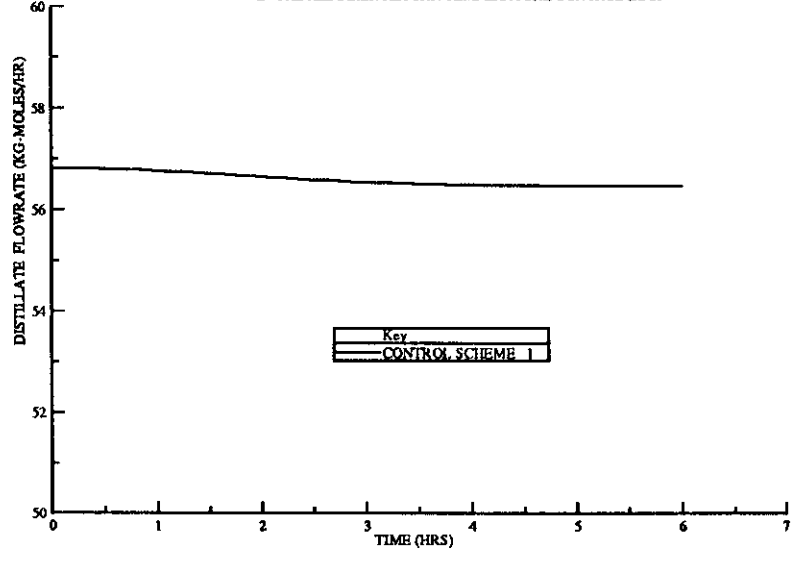

Figure 5. 4. 35
CLOSED-LOOP RESPONSE OF DE-PROPANISER CONTROL SCHEMES -
RESPONSE OF REFLUX RATE TO A CHANGE OF +10 %
IN THE REBOILER STEAM PRESSURE

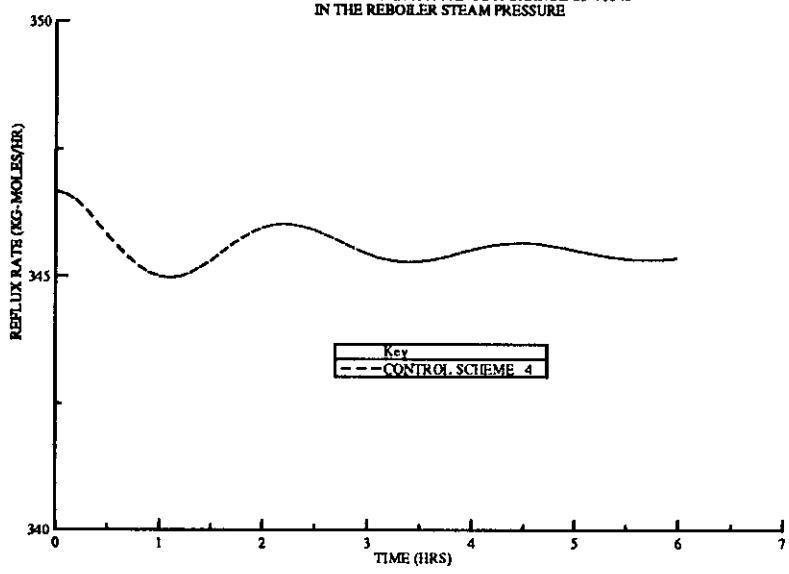

Figure 5. 4. 36
CLOSED-LOOP RESPONSE OF DE-PROPANISER CONTROL SCHEMES -
RESPONSE OF REFLUX RATE TO A CHANGE OF -14 %
IN THE FEED FLOW RATE

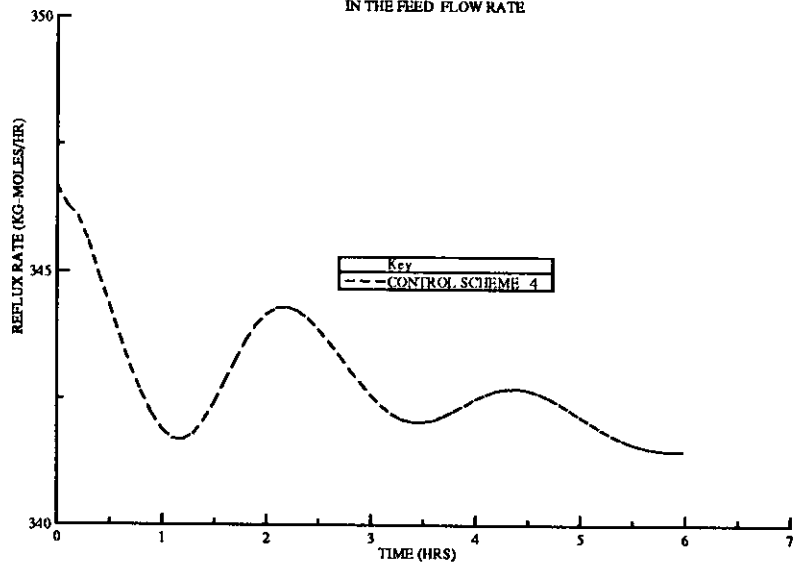

Figure 5. 4. 33
CLOSED-LOOP RESPONSE OF DE-PROPANISER CONTROL SCHEMES -
RESPONSE OF REFLUX RATE FOR A SETPOINT CHANGE OF +2.5%
IN THE DISTILLATE COMPOSITION CONTROL LOOP

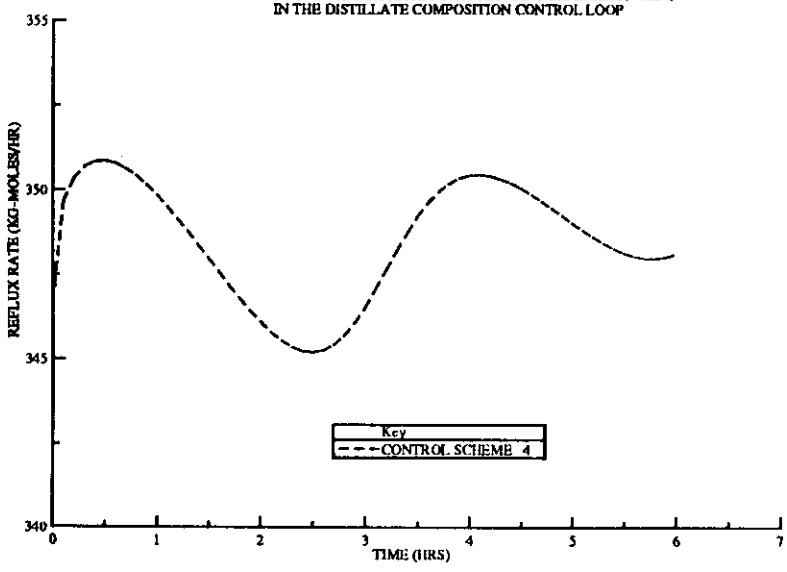

Figure 5. 4. 34
CLOSED-LOOP RESPONSE OF DE-PROPANISER CONTROL SCHEMES -
RESPONSE OF REFLUX RATE FOR A SETPOINT CHANGE OF +8.0 %
IN THE COLUMN PRESSURE CONTROL LOOP

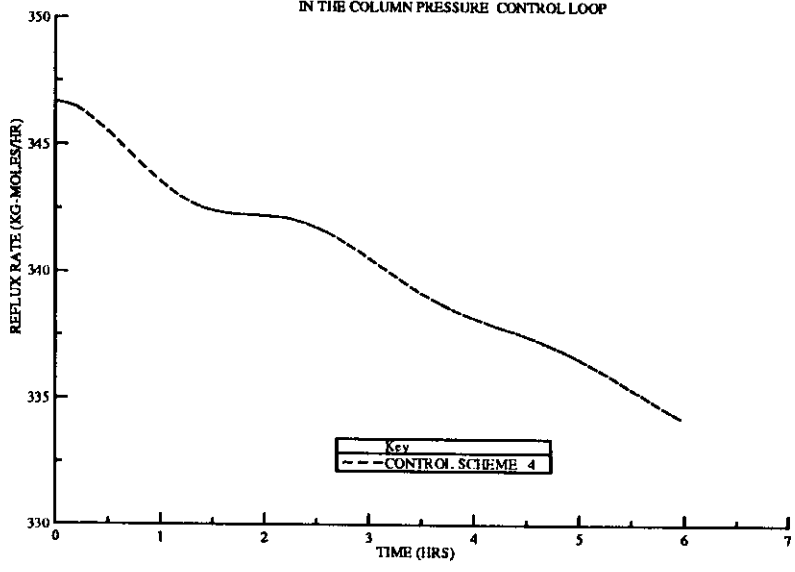

Figure 5.4.39
CLOSED-LOOP RESPONSE OF DE-PROPANISER CONTROL SCHEMES -
RESPONSE OF REBOILER STEAM FLOWRATE TO A CHANGE OF +10%
IN THE REBOILER STEAM PRESSURE

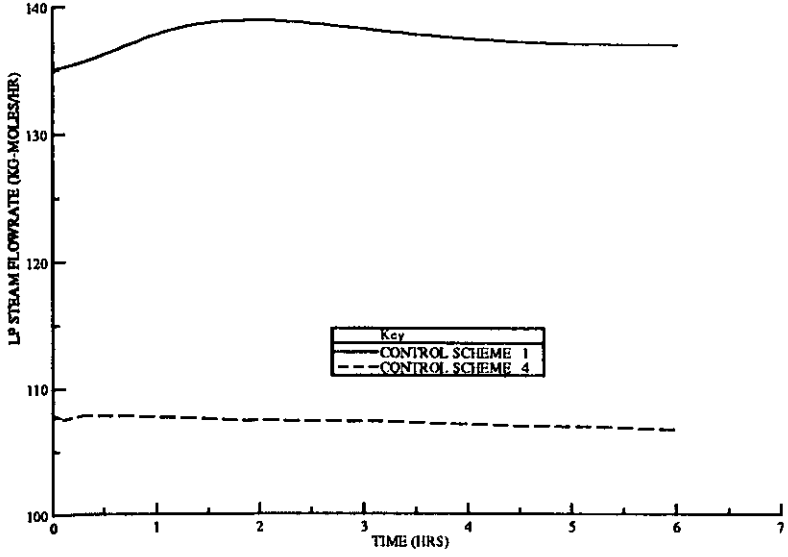

Figure 5.4.40
CLOSED-LOOP RESPONSE OF DE-PROPANISER CONTROL SCHEMES -
RESPONSE OF REBOILER STEAM FLOWRATE TO A CHANGE OF -14%
IN THE FEED FLOW RATE

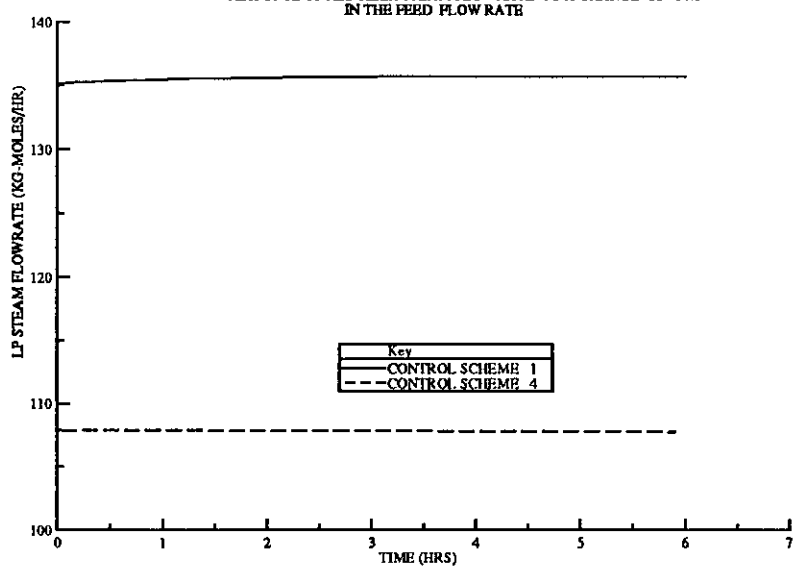

Figure 5.4.37
CLOSED-LOOP RESPONSE OF DE-PROPANISER CONTROL SCHEMES -
RESPONSE OF REBOILER STEAM FLOWRATE FOR A SETPOINT CHANGE OF +2.5%
IN THE DISTILLATE COMPOSITION CONTROL LOOP

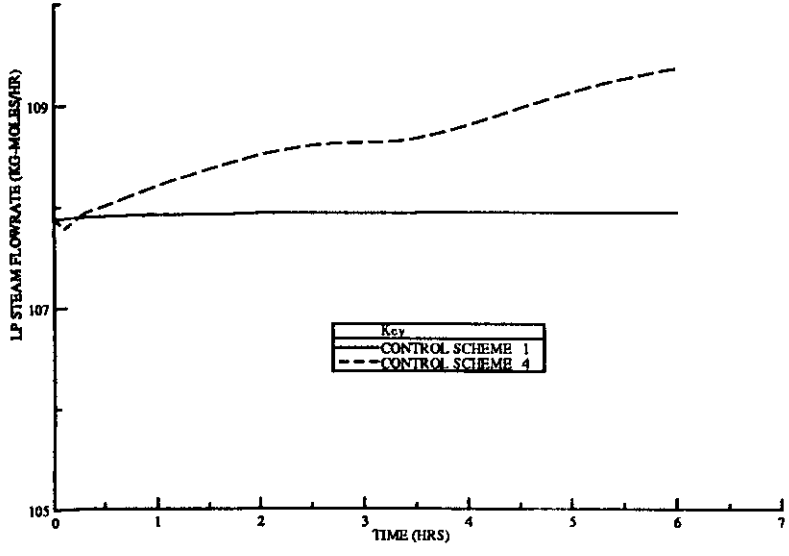

Figure 5.4.38
CLOSED-LOOP RESPONSE OF DE-PROPANISER CONTROL SCHEMES -
RESPONSE OF REBOILER STEAM FLOWRATE FOR A SETPOINT CHANGE
IN THE SECOND CONTROL OBJECTIVE

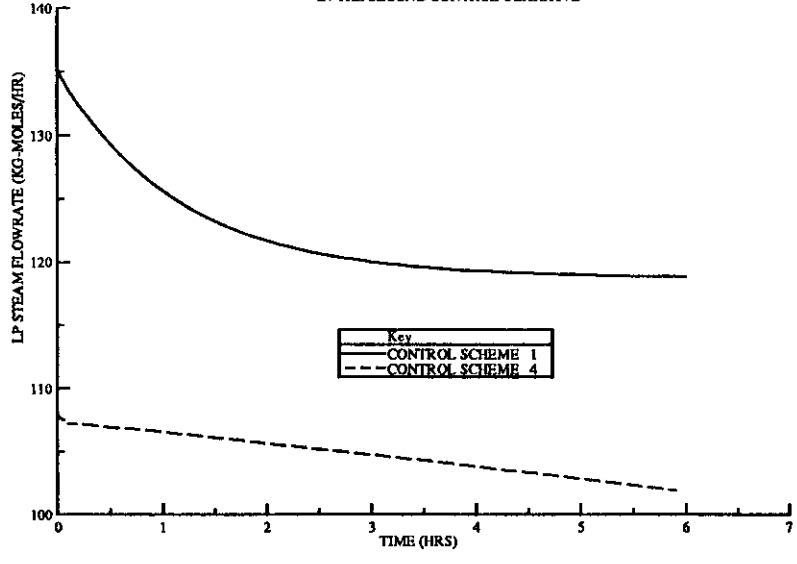

dynamic simulation results were in good agreement with the open-loop indicator predictions.

Thus the systematic methodology provided in the early portion of this chapter has been successfully applied to a realistic case-study. In the following chapter the same procedure will be extended to the synthesis of an optimising control scheme for the entire gas-tail.

CHAPTER 6

CONTROL SYSTEM SYNTHESIS FOR THE COMPLETE GAS - TAIL

6.1 INTRODUCTION

A new economics based approach was proposed in the previous chapter that seeks to provide a consistent basis for optimising control system synthesis for continuous processes. A case-study on the de-propaniser column of the gas-tail indicated the potential benefits associated with such an approach. In this chapter, this approach will be used to develop an optimising control system for the entire gas-tail. As discussed in Section 2. 1. 3, one of the primary motives behind the current work was to understand the reasons for the poor performance of the existing gas-tail control system over recent years.

The present approach requires a column simulation model. The distillation columns of the gas-tail have each been modelled using the UCM based approach (see Section 2. 3). Steady-state verification of this gas-tail model was made using both plant trial data and rigorous simulations of the gas-tail. Implementation of this gas-tail model within SPEEDUP , allowed the use of the same model for steady-state simulations , steady-state optimisation , control system design (via SPEECON) and dynamic simulation studies.

Steady-state optimisation studies on the gas-tail model demonstrated the potential economic benefits, relative to current operations, for operating at an optimum. The profit differentials are, however, found to vary with the feed type. Relatively large profit increases are possible with a low pentanes feed to the gas-tail , compared to the profit increase possible for a high pentanes feed. At the optimum, some of the process constraints become *active* . The active constraints, however, depend on both the nature of the feed and the ambient air temperature. In optimising control, identification of all such active constraints is one of the key requirements. What is essentially required is a control system that would regulate the gas-tail at its optimal operating conditions with minimum control effort. External disturbances influencing the process operation introduce additional complexity into such a controller design. The action of the disturbances on the gas-tail is to cause a variation in the process operation. Such a variation could result in active constraint violations if the process were operated near the optimum.

High feed rate with a high pentanes content is the most commonly observed feed type to the gas-tail at present. This case-study therefore investigates the economic potential

for an optimising control system for the gas-tail for such feed conditions. Application of the control system synthesis strategy to the gas-tail involves the following two steps :

(1) Estimation of the economic potential of a control system

(2) Optimising control system design.

6. 2 STEP (1) : ESTIMATION OF THE ECONOMIC POTENTIAL OF A GAS -TAIL CONTROL SYSTEM

The first requirement in this step is to identify the important disturbances (along with their magnitudes) that affect the gas-tail operation. These disturbances are given below. The disturbance "sizes" are realistic estimates based on operational experience.

Disturbance	Steady-state value	Disturbance size
(1) Feed-rate to the gas-tail.	245 Kg-moles / hr	± 25 Kg-moles/hr
(2) Pentanes in the gas-tail feed.	15.6%	± 10 %
(3) Steam pressure to all of the gas-tail reboilers.	3. 15 Bar	± 0.63 Bar
(4) Ambient air temperature	20 deg C	± 5 deg C

The objective function at this steady-state optimum (ø) is estimated (from Equation 3. 2. 2 and Tables 3. 2.1 and 3. 2.5) as follows ;

$$
\begin{aligned}
\text{ø} = \;& \text{LPG stream recovery rate} * \text{value of LPG} \\
& + \text{i-butane stream recovery rate} * \text{value of i-butane} \\
& + \text{n-butane stream recovery rate} * \text{value of n-butane} \\
& - \text{fuel gas recovery rate} * \text{value of fuel gas} \\
& - \text{total cost of steam for all the columns together} \\
& + \text{total value of condensate from all the columns} \\
= \;& 56.26 * 7.82 + 33.17 * 17.55 + 78.75 * 8.874 - 38.63 * 1 \\
& - (153.74 + 108.13 + 233.72) \; (0.091 - 0.009) \\
= \;& \$1642 / \text{hr} \qquad (6.2.1)
\end{aligned}
$$

The next step is to identify the active constraints at the optimum conditions. These constraints should not be violated for any disturbances. They are highlighted in Table 6. 2. 2 and summarised below. Values in the parentheses show the corresponding Lagrange

Table 6. 2. 1
Gas-tail freed variables at the calculated optimum operating conditions (for high flow rate , high pentanes feed)

Freed variables	Value at the optimum
DE- ETHANISER	
Distillate rate (Kmoles/hr)	38.43
Condenser air flowrate (Kmoles/hr)	9219
Reboiler steam rate (Kmoles/hr)	153.74
DE-PROPANISER	
Distillate rate (Kmoles/hr)	56.26
Condenser air flowrate (Kmoles/hr)	16985
Reboiler steam rate (Kmoles/hr)	108.13
DE-ISOBUTANISER	
Distillate rate (Kmoles/ hr)	33.17
Condenser air flowrate (Kmoles/hr)	22037
Reboiler steam rate (Kmoles/hr)	233.72
Side-stream product rate (Kmoles/hr)	78.75

Table 6. 2. 2
Gas-tail variables at the calculated optimum operating conditions (for high flow rate , high pentanes feed)

Variable		Operating conditions at the optimum
DE- ETHANISER		
Reflux rate	(Kmoles/hr)	545.74
Condenser top temperature	(deg C)	52.17
Condenser pressure	(Bar)	29.73
Condenser duty	(Tcal/ hr)	600
Distillate compostion	(Ethane)	0.685
Bottoms product rate	(Kmoles/hr)	208.55
Reboiler duty	(Tcal/hr)	1474.17
Reboiler return temperature	(deg C)	130
Molefraction of ethane in the reboiler		0.012
DE- PROPANISER		
Reflux rate	(Kmoles/hr)	347.16
Condenser top temperature	(deg C)	49.92
Condenser pressure	(Bar)	16.65
Condenser duty	(Tcal/hr)	600
Distillate compostion	(Propane)	0.9
Bottoms product rate	(Kmoles/hr)	152.29
Reboiler duty	(Tcal/hr)	1031.12
Reboiler return temperature	(deg C)	117
DE- ISOBUTANISER		
Reflux rate	(Kmoles/hr)	503.25
Condenser top temperature	(deg C)	70.56
Condenser pressure	(Bar)	10.82
Condenser duty	(Tcal/Kmole)	1823.81
Distillate compostion (isobutane)		0.88
Bottoms product rate	(Kmoles/hr)	40.373
Reboiler duty	(Tcal/hr)	2219.68
Reboiler return temperature	(deg C)	125
Side-stream composition	(n-butane)	0.81

N. B : underlined variables indicate active constraints.

multipliers at the calculated optimum operating conditions. The units of Lagrange multipliers is dollars per unit deviation from the active constraint.

Active constraints			
De-ethaniser	-	Reboiler return temperature	(0.68)
De-propaniser	-	LPG (distillate) composition	(371)
De-propaniser	-	Reboiler return temperature	(8. 0)
De-isobutaniser	-	i-Butane(distillate) composition	(2583)
De-isobutaniser	-	Reboiler return temperature	(7.0)
De-isobutaniser	-	n-Butane(side-stream) composition	(2830)

As described in Section 5. 3. 2, the next step is to linearise the process around its optimum and then obtain a frequency dependent transfer function relating the system outputs (i.e the active constraints) and the disturbances. This can be obtained from the gas-tail model at the calculated optimum operating conditions, using the SPEECON package . With the six active constraints as outputs and four disturbances (see Table 6. 2. 3 for further details on the disturbances used) , the resulting transfer function matrix (i.e. $G_d(s)$) is a (6 X 4) non-square matrix. SPEECON provides values of the elements in $G_d(s)$ both at the steady-state conditions (i.e. at zero frequency) and at various other selected frequencies. In each case, the elements of $G_d(s)$ represent a "gain" value between an input and an output variable. Given $G_d(s)$, knowing the size for each disturbance (listed above), the maximum size of the open-loop back-off needed from each of the active constraints due to each of the disturbances , when " no control " is implemented on the system, can be estimated using Equation (5. 3. 8). Table 6. 2. 3 gives such maximum back-offs needed for each of the active constraints , at the steady-state operating conditions. Figures (6. 2. 1) - (6. 2. 6) show the variation, with frequency, of the economic penalty (i.e. back-off times the Lagrange multiplier) associated with a back-off from each of the control objectives, due to each of the external disturbances. It is apparent from these results that the back-off required due to the feed flowrate fluctuations is the largest in most cases, indicating that feed flowrate represents the "worst" disturbance. Considering the necessary back-off required in each of the active composition constraints for the feed flowrate disturbance, such a move in each case violates the physical constraint that any component mole fraction cannot be greater than unity. Similarly, incorporating the back-off necessary in each of the reboil return temperature constraints (i.e. estimated for the same feed flowrate disturbance) violates the constraint of a minimum temperature difference between the heat exchanging streams (see Table 3. 2. 4) , in each of the gas-tail reboilers. The largest back-off required from each of the active constraints , therefore, cannot be achieved without violating other constraints. The maximum feasible back-offs from each of the active constraints can be estimated as follows;

Table 6. 2. 3
Open-loop back-offs required in each of the control objectives due to each of the disturbances

Active constraint	Disturbance			
	Feed flowrate	Pentanes in the feed	Ambient air temperature	Steam pressure in the reboilers
De-ethaniser - reboiler return temperature.	12.54	0.241	6.02	0.608
De-propaniser - distillate (LPG) composition.	0.262	0.000829	0.00108	0.000236
De-propaniser - reboiler return temperature.	24.38	1.64	6.8	0.688
De-isobutaniser - distillate (i-butane) composition.	0.185	0.00252	0.000369	0.0000613
De-isobutaniser - reboiler return temperature.	39.36	0.257	5.25	0.413
De-isobutaniser - side-stream (n-butane) composition.	0.2125	0.0243	0.00172	0.000484

FIGURE 6. 2. 1
ECONOMIC PENALTY OF BACK-OFF FROM THE OPTIMUM
IMPACT OF DISTURBANCES ON THE DE-ETHANISER
REBOILER RETURN TEMPERATURE CONSTRAINT

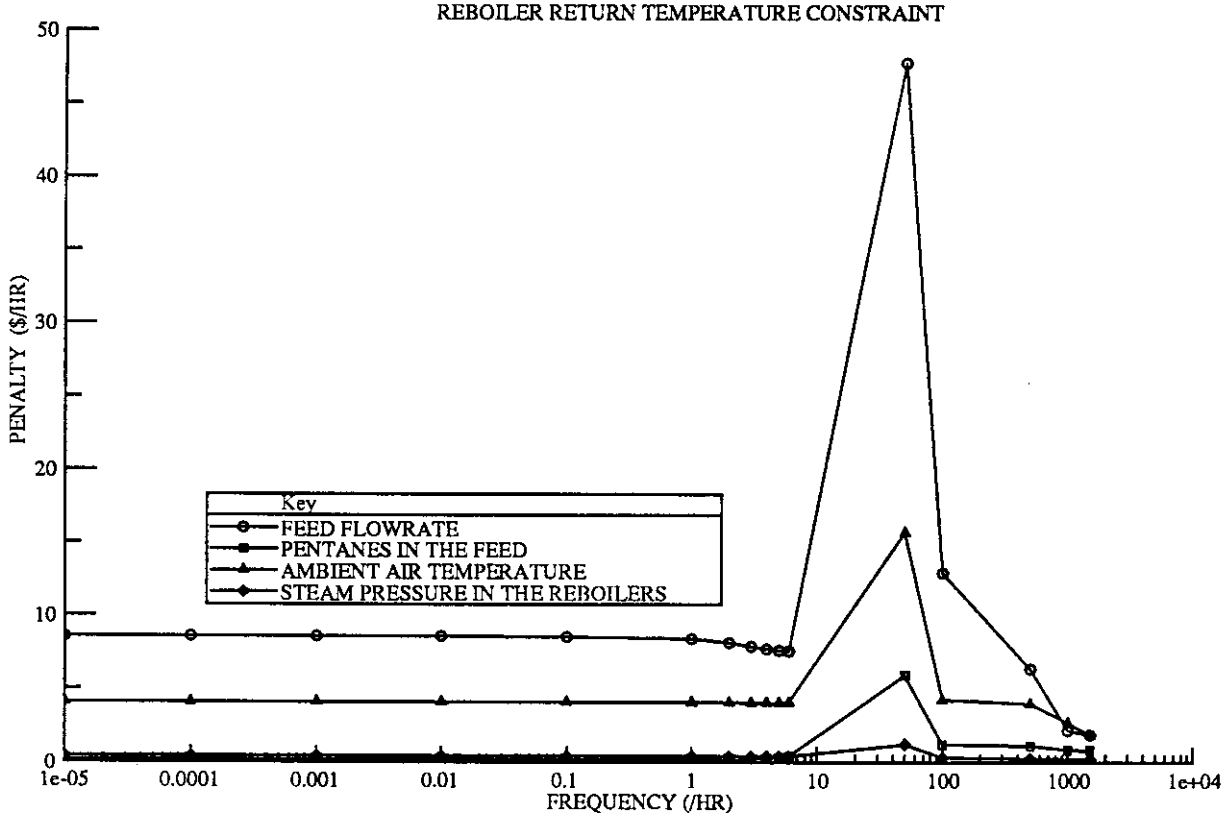

FIGURE 6. 2. 2
ECONOMIC PENALTY OF BACK-OFF FROM THE OPTIMUM
IMPACT OF DISTURBANCES ON THE DE-PROPANISER
DISTILLATE PURITY CONSTRAINT

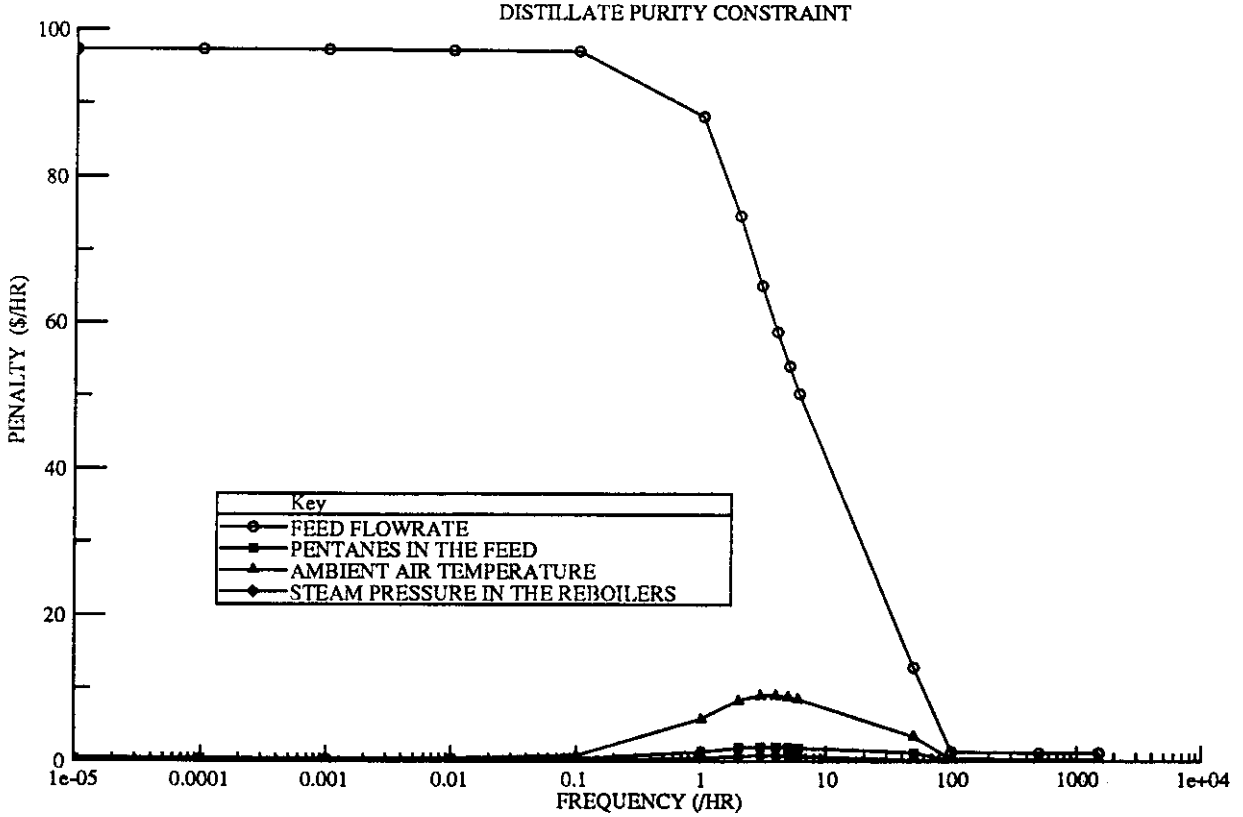

FIGURE 6. 2. 3
ECONOMIC PENALTY OF BACK-OFF FROM THE OPTIMUM
IMPACT OF DISTURBANCES ON THE DE-PROPANISER
REBOILER RETURN TEMPERATURE CONSTRAINT

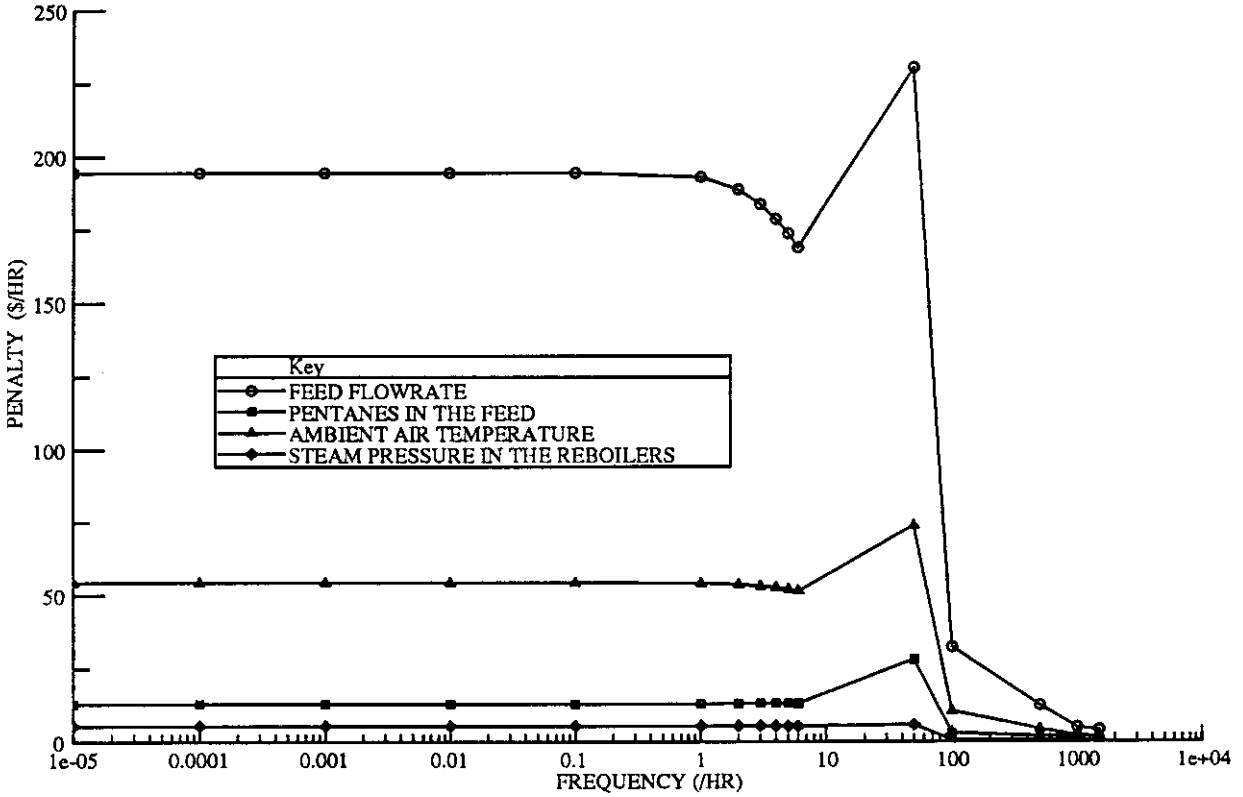

FIGURE 6. 2. 4
ECONOMIC PENALTY OF BACK-OFF FROM THE OPTIMUM
IMPACT OF DISTURBANCES ON THE DE-ISOBUTANISER
DISTILLATE PRODUCT PURITY CONSTRAINT

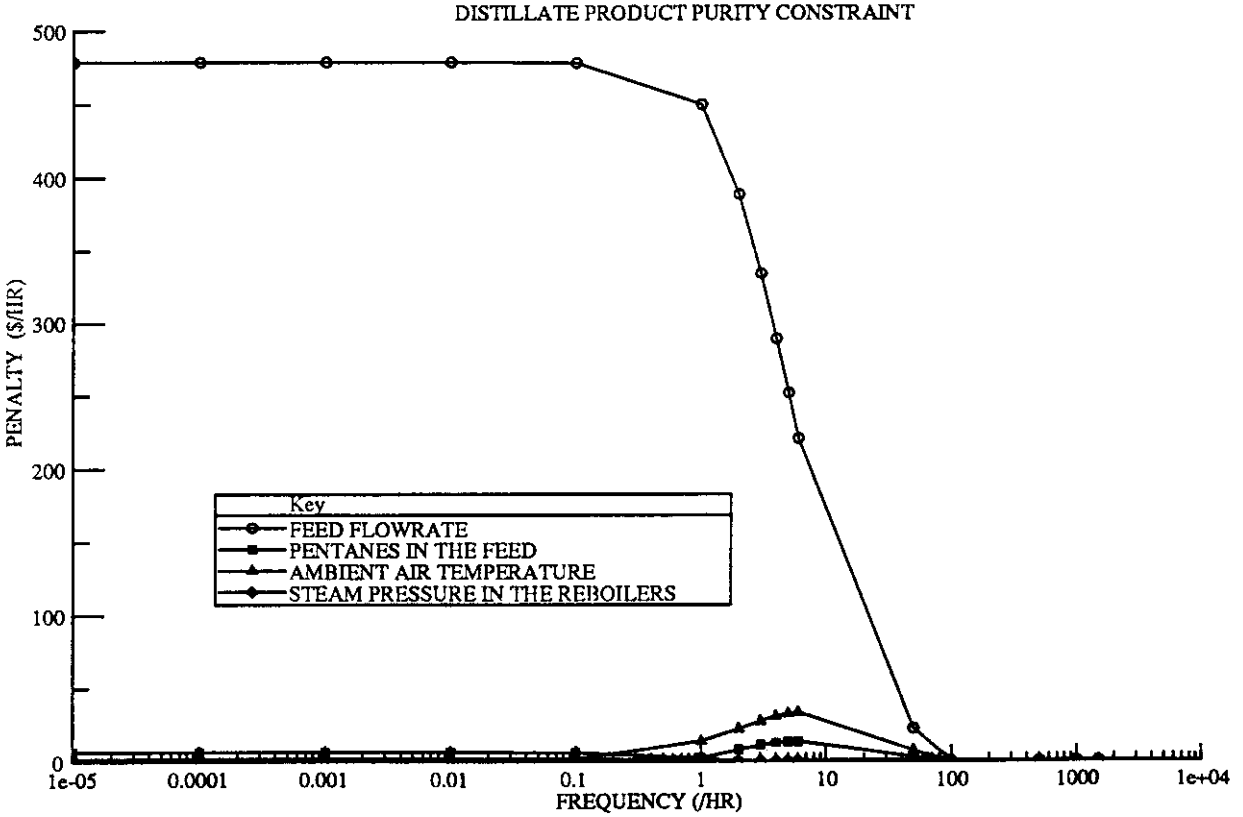

FIGURE 6. 2. 5
ECONOMIC PENALTY OF BACK-OFF FROM THE OPTIMUM
IMPACT OF DISTURBANCES ON THE DE-ISOBUTANISER
REBOILER RETURN TEMPERATURE CONSTRAINT

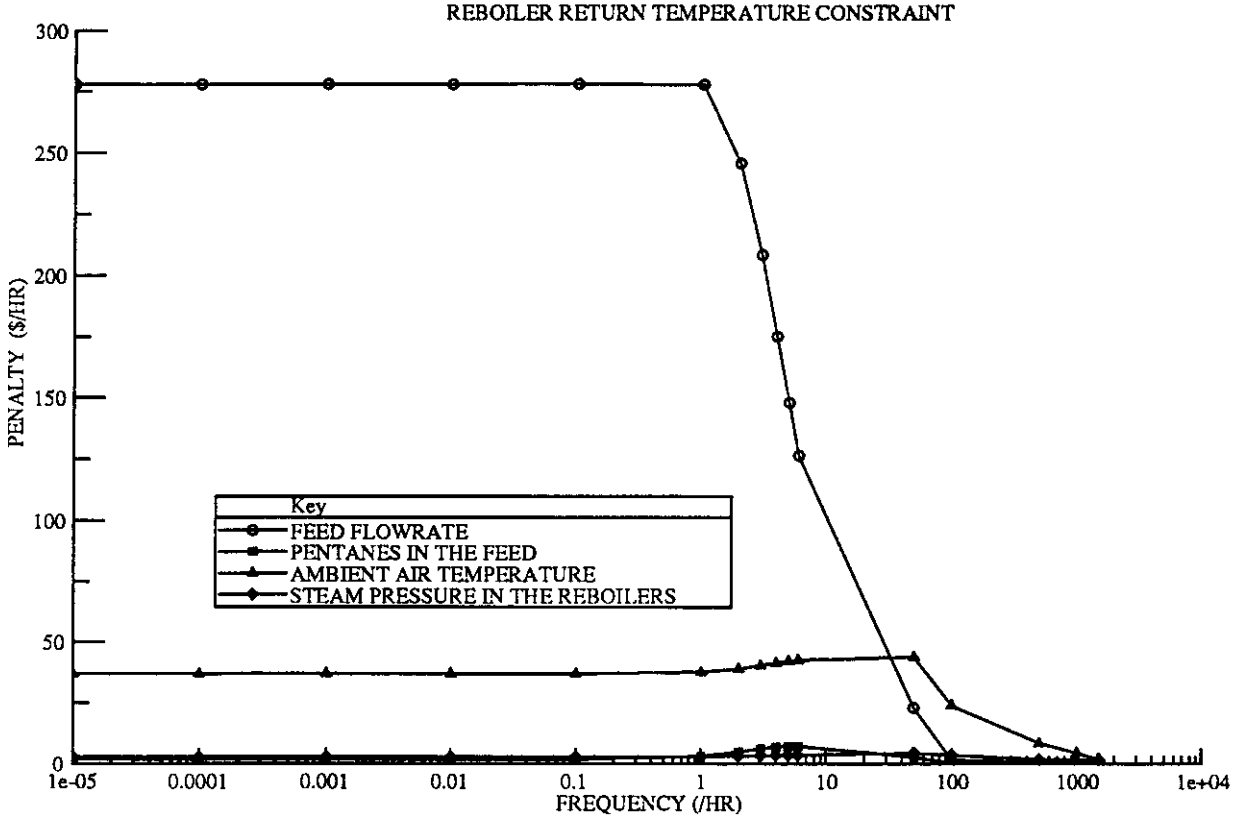

FIGURE 6. 2. 6
ECONOMIC PENALTY OF BACK-OFF FROM THE OPTIMUM
IMPACT OF DISTURBANCES ON THE DE-ISOBUTANISER
SIDE-STREAM PRODUCT PURITY CONSTRAINT

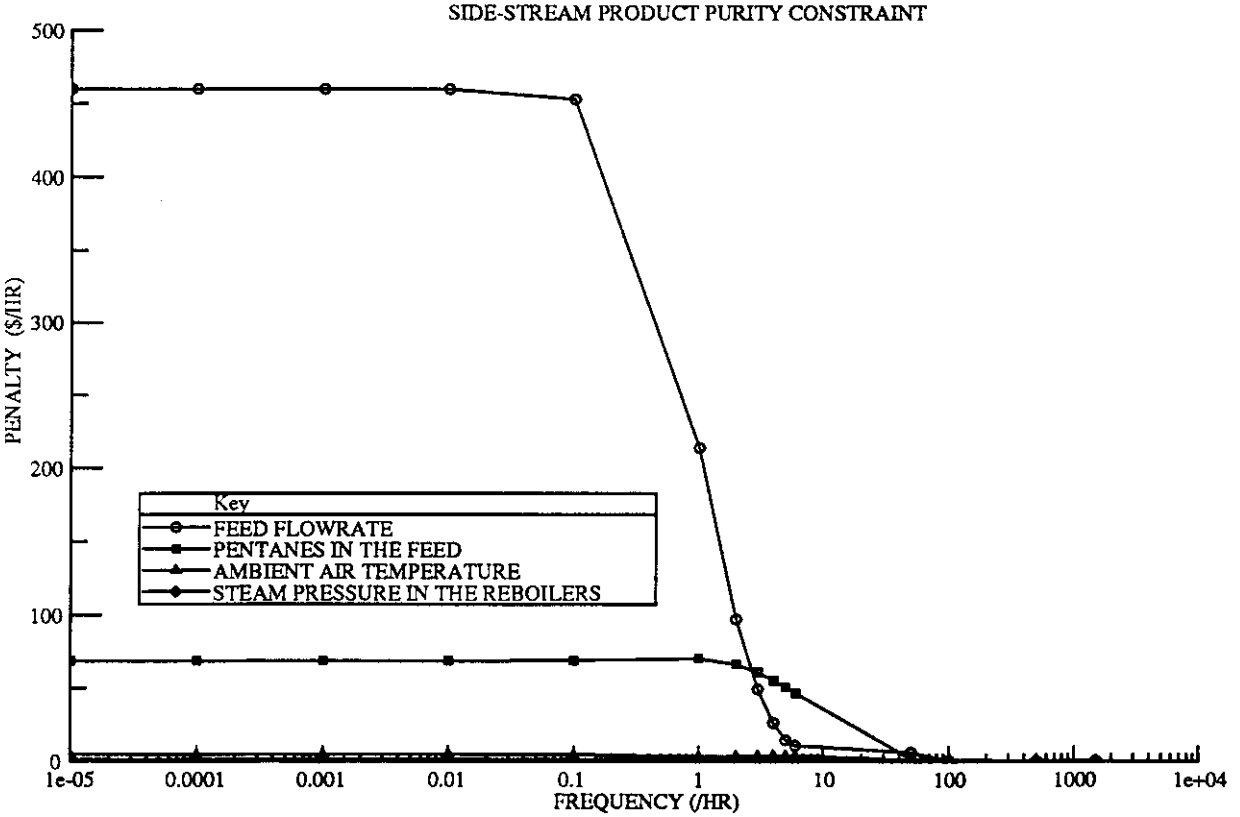

For the composition constraints :

$$\Delta X_{feas} = 1.0 - X_{opt} \qquad (6.2.2)$$

where ΔX_{feas} = the maximum feasible back-off from the corresponding composition constraint.

X_{opt} = the value of the composition constraint at the optimum operating conditions.

For the reboiler return temperature constraints :

With a temperature of the saturated steam to each of the gas-tail reboilers at 135 deg C and a minimum temperature difference of 5 deg C (see Table 3. 2. 4) required between the heat exchanging streams, the maximum temperature the reboiler vapour can attain, therefore , is 130 deg C.

$$\Delta T_{feas} = 130.0 - T_{opt} \qquad (6.2.3)$$

where ΔT_{feas} = the maximum feasible back-off from the corresponding reboiler return temperature constraint.

T_{opt} = the value of the reboiler return temperature at the optimum operating conditions.

The importance of these equations is that, at any frequency , they provide an upper bound on the back-off that is actually feasible, in any of the six active constraints. Therefore, in all those cases where the estimated maximum back-off required from any active constraint (i.e using Equation 5. 3. 8) is larger then the value estimated from Equations 6. 2. 2 or 6. 2. 3, then the latter back-off value should be used in any further analysis. Table 6. 2. 4 shows the maximum back-off actually needed (i.e. $b_{i,max}$; see Equation 5. 3. 8) and the maximum back-off that is feasible for the steady-state case (i.e. $b_i^{(ol)}$; see Equation 5. 3. 9). As discussed previously (see Section 5. 4), this analysis shows that for the disturbances given, it is not possible to operate with "no control" and expecting no constraint violations.

One important consequence of Equation (6. 2. 3) with respect to the de-ethaniser column is that the back-off feasible in the reboiler return temperature control objective (from the active constraint at 130 deg C) is zero. This is because, this temperature actually lies at the intersection of two constraints (i.e one provides an upper bound on the amount of light hydrocarbons in the reboiler, while the other forms a lower bound on the temperature difference required for heat exchange between the process and steam streams), and operation away from both these constraints is infeasible. Since perfect control of this

Table 6. 2. 4
Open-loop back-offs in each of the control objectives

Active constraint	Maximum back-off required (from linear analysis)	Maximum back-off feasible
De-ethaniser - reboiler return temperature (deg C).	12.54	0
De-propaniser - distillate (LPG) composition.	0.26	0.1
De-propaniser - reboiler return temperature (deg C).	24.38	13
De-isobutaniser - distillate (i-butane) composition	0.19	0.12
De-isobutaniser - reboiler return temperature (deg C).	39.36	5
De-isobutaniser - side-stream (n-butane) composition.	0.21	0.19

control objective is impossible to achieve in practice, we are bound to get some constraint violations at some stage during the process operation.

From Table 6. 2. 3 , it is clear that the feed flowrate disturbance requires the largest back-offs from the optimum operating point. However all such back-offs are not feasible without violating other constraints. Thus, a maximum feasible back-off possible for each of the control objectives can be defined (see Equation 6. 2. 2 and 6. 2. 3) as summarised in Table 6. 2. 4. The potential economic benefit associated with installing a control system on the gas -tail can be estimated using such maximum feasible back-offs from each of the active constraints and the Lagrange multiplier associated with it (see Equation 5. 3. 8). For the steady-state case, the maximum penalty from back-off in all the active constraints together ($\Delta\phi_{max}$) is given by,

$$\Delta\phi_{max} = 0 * 0.68 + 0.1 * 371 + 13.0 * 8.0 + 0.12 * 2583 + 5.0 * 7.0 + 0.19 * 2830$$

$$= \$\,1024 \ / \text{hr} \qquad (6.2.4)$$

As discussed in Section 5. 3, estimation of $\Delta\phi_{max}$ assumes that all the individual "worst" cases for each active constraint can be added together (linearly) to give the upper bound on the open-loop penalty for back-off. Such an approach provides a reasonable "first estimate".

Similarly, the economic penalty can be estimated over the entire frequency range of interest, although steady-state represents the "worst case". As the back-off costs are large relative to the steady-state optimum (ϕ = \$1642 / hr ; see Equation 6. 2. 1) , there are significant benefits to be realised by the installation of a control system on the gas-tail. Therefore, it is desirable to explore various control systems that could be implemented on the gas-tail. The control system that provides the maximum recovery of this back-off penalty and provides good closed-loop response should be chosen for implementation on the gas-tail.

Our aim now is to recover as much of this " no control " back-off penalty as possible using a control system. However, the actual closed-loop back-offs necessary to ensure no constraints are violated due to the action of "fast" disturbances on the process, depends both on the process and the controller. No simple approach for estimating the necessary closed-loop back-offs is available. A simple approach , however, is to choose an operating point by backing-off each of the control objectives by a definite amount. If the closed-loop simulation studies for the largest feasible size of a disturbance (or actual plant operational data) indicate that any of the control objectives would violate its corresponding active constraint during the disturbance induced transient stage, then the

closed-loop back-off chosen for that control objective is not large enough and a further back-off is required. This approach, though straightforward, may require extensive dynamic simulations. In addition, each iteration of such an approach may require controller re-tuning at the new operating point. Considering the size and nonlinearities of the gas-tail model, significant computational effort would certainly be necessary for such an approach. Estimation of closed-loop back-offs through multiple closed-loop dynamic simulations, therefore, is not a suitable alternative for the current case-study. For the reasons discussed in the de-propaniser example (see Section 5. 4) , the method proposed in Section 5. 3. was felt unsuitable here also. A simple heuristic based approach therefore was used as shown below.

As was done in the de-propaniser example (see Section 5. 4), in the current gas-tail case-study, selection of the actual operating conditions was made by selecting the "second largest feasible move " (see Table 6. 2. 3) as the necessary move away from the optimum required for each of the control objectives (see Table 6. 2. 5). As the control configuration chosen for the gas-tail should possess good controllability characteristics , a multiloop controller with this set of outputs should provide adequate closed-loop performance and no constraint violation. The second largest feasible back-off for all the gas-tail control objectives is due to either the feed composition or the ambient air temperature disturbance. Thus, the actual operating point for the gas-tail operation is obtained by backing - off all the control objectives by the respective amounts (see Table 6. 3. 3). However, in the case of the de-ethaniser reboiler return temperature (T_R) , no further back-off is feasible as this would violate minimum temperature difference constraint for heat exchanging media (see Table 3. 2. 4). Table 6. 3. 5 summarises the closed-loop back-offs thus made in each of the active constraints from their optimum values.

The **MPR** if operating at the new operating point, is given by estimating the total economic loss associated with the selected closed-loop back-offs in each of the control objectives (by multiplying with their respective Lagrange multipliers) , as shown below :

$$\Delta\phi_{new} = 0 * 0.68 + 0.0011 * 371 + 6.8 * 8.0 + 0.00252 * 2583 + 5.0 * 7.0 + 0.0243 * 2830$$

$$= \$165.09 \ / \text{hr} \qquad (6.2.5)$$

$$MPR = 100 * (1 - \Delta\phi_{new} \ / \Delta\phi_{max})$$

$$= 100 * (1 - 165.09 / 1024)$$

$$= 84\% \qquad (6.2.6)$$

Table 6. 2. 5
Closed-loop back-offs made in each of the control objectives

Active constraint	Back-off made
De-ethaniser reboiler return temperature (deg C).	0
De-propaniser distillate (LPG) composition.	0.00110
De-propaniser reboiler return temperature (deg C).	6.8
De-isobutaniser distillate (i-butane) composition.	0.00252
De-isobutaniser reboiler return temperature (deg C).	5.0
De-isobutaniser side-stream (n-butane) composition.	0.0243

An MPR of 84 % in this case indicates that 84 % of the "no-control " economic penalty can be recovered by this controller if it can hold the plant at these set-points. While it is undoubtedly true that the closed-loop back-offs are only first estimates, they do represent realistic targets for any control scheme. If the final control scheme could only get this close to the actual optimum operating conditions, then the economic figures presented above would undoubtedly justify serious consideration of an optimising control scheme.

6.3 STEP (2) : OPTIMISING CONTROL SYSTEM DESIGN FOR THE GAS-TAIL

Having shown that it is economically beneficial to have a control system on the gas-tail, our aim now is to identify realistic alternative choices of control system and select the most suitable one. At the steady-state optimum, the number of active constraints was six which was greater than the number of freed variables (i.e. ten). Implementation of a constraint control policy (see Section 5. 2) on any process requires that the number of active constraints be the same as the number of available degrees of freedom. Clearly, the present case-study does not satisfy the basic requirement for constraint control. However, it should be realised that at the optimum, the air flowrate for each of the overhead condensers is at its maximum value. Consequently, that each of these air-flowrates will not be available as a manipulated variable for regulating a control objective. This means that the number of freed (or manipulated) variables is reduced by three (i.e. one for each of the three overhead condensers). Therefore, there are in practice six active constraints and seven freed variables. This still does not satisfy the requirement for constraint control. At this stage, one could choose to develop a non-square (i.e. unequal number of manipulated and controlled variables) multivariable control system or alternatively, select an additional control objective, apart from all the active constraints, to form a square control system. Since, there is no consistent basis for the selection of such an additional control objective, the latter approach was not pursued here. The implementation of a 6 X 7 multivariable control system was felt to be impractical and was also not considered further. Constraint control, on the other hand, is relatively simple to implement and also guarantees operation at the optimum conditions. This could be achieved by regulating all six active constraints (i.e. as the control objectives) using six of the freed variables as manipulated variables. The remaining freed variable would be regulated manually or set in a feedforward fashion based on the results from the steady-state optimiser. The major issue then is how to select which of the freed variables should be excluded from the constraint control scheme. This combinatorial problem can be avoided , here , through the use of engineering judgement. A closer look at the active constraints and the freed variables indicates that in the case of the de-ethaniser there are two freed variables and only one active constraint. The obvious choice for the excluded freed variable , therefore,

would be one of those from the de-ethaniser. The freed variables and the one active constraint for the de-ethaniser are ;

Active constraint

(1) Reboiler return temperature.

Freed variables

(1) Distillate flowrate.

(2) Steam input rate to the reboiler.

Plant experience indicates that the steam input rate to the reboiler is preferred to the distillate flowrate as a means of regulating the reboiler return temperature. Thus, the distillate flowrate from the de-ethaniser is identified as the manipulated variable to be regulated manually or in a feedforward way.

The number of freed variables (i.e six), therefore, is now equal to the number of active constraints. Development of a constraint control strategy can be considered for the available choice of active constraints and freed variables. All active constraints would , therefore, be used as the control objectives and all available freed variables as manipulated variables of the potential regulatory control schemes.

In theory, for a (6 X 6) system , the number of alternative multiloop control strategies to be considered is 720 (i.e 6 !). Consideration of such a number , in practice, is impractical. The following are the two major factors considered in reducing the number of alternative choices of gas-tail control schemes.

(1) A de-centralised control policy in the case of the gas-tail involves regulating the control objectives of a distillation column (e.g the de-propaniser) with the available manipulated variables corresponding to the same column. Such an approach would considerably reduces the number of alternative multiloop control schemes for the gas-tail. This approach is extremely useful as a first pass in control system selection.

(2) It was discussed previously in Section 5. 4 that control objectives, in general, can be categorised as either primary or secondary types. The secondary control objectives are usually associated with plant operations (e.g the level in an overhead accumulator). Often , these objectives do not make a significant contribution to the process economics and can be considered independently of the primary control objectives which are typically associated with product qualities (either directly or indirectly) and thus with process economics. In the present case

study , therefore, only those control schemes dealing with the regulation of the primary control objectives will be investigated. Each of the secondary control objectives , of course, is regulated by an appropriate choice of manipulated variable.

Based on the above guide-lines and engineering judgement, the following two control configurations were felt to be the strongest candidates, in the first stage of our search for a "good" control scheme for the gas-tail.

CONTROL SCHEME 1

	Manipulated variables (Freed variables)	Primary Control objectives (Active constraints)
De-ethaniser :	Steam input rate to the reboiler	Reboiler return temperature
De-propaniser :	Distillate flowrate	Propane composition in the distillate product
De-propaniser :	Steam input rate to the reboiler	Reboiler return temperature
De-isobutaniser :	Distillate flowrate	i-Butane composition in the distillate product
De-isobutaniser :	Steam input rate to the reboiler	Reboiler return temperature
De-isobutaniser :	Side-stream flowrate	n-Butane composition in the side-stream product

For each column, the control scheme is somewhat similar to Control Scheme 1, used in the de-propaniser example in the previous chapter. To maintain continuous and safe operation of the columns the secondary control objectives should also be regulated. The following list gives the secondary control objectives and the corresponding manipulated variables used ;

	Manipulated variables		Secondary control objectives
De-ethaniser:	Reflux flowrate.	paired with	Overhead accumulator holdup.
De-ethaniser:	Bottoms product rate.	paired with	Reboiler holdup.
De-propaniser :	Reflux flow rate.	paired with	Overhead accumulator holdup.
De-propaniser:	Bottoms product rate.	paired with	Reboiler holdup.
De-isobutaniser:	Reflux flow rate.	paired with	Overhead accumulator holdup.
De-isobutaniser:	Bottoms product rate.	paired with	Reboiler holdup.

As discussed in the de-propaniser example (see Section 5. 4), a "square root control policy" (see Equation 5. 3. 9) is used here also to regulate all the secondary control objectives of Control Scheme 1.

CONTROL SCHEME 2

	Manipulated variables	Primary Control objectives (Active constraints)
De-ethaniser -	Bottoms product rate	Reboiler return temperature
De-propaniser -	Distillate flowrate	Propane composition in the distillate product
De-propaniser -	Bottoms product rate	Reboiler return temperature
De-isobutaniser -	Distillate flowrate	i-Butane composition in the distillate product
De-isobutaniser -	Bottoms product rate	Reboiler return temperature
De-isobutaniser -	Side-stream flowrate	n-Butane composition in the side-stream product

While the following are the secondary control objectives and the corresponding manipulated variables used ;

	Manipulated variables		Secondary control objectives
De-ethaniser:	Reflux flowrate.	paired with	Overhead accumulator holdup.
De-ethaniser:	Steam input rate to the reboiler.	paired with	Reboiler holdup.
De-propaniser :	Reflux flow rate.	paired with	Overhead accumulator holdup.
De-propaniser:	Steam input rate to the reboiler.	paired with	Reboiler holdup.
De-isobutaniser:	Reflux flow rate.	paired with	Overhead accumulator holdup.
De-isobutaniser:	Steam input rate to the reboiler.	paired with	Reboiler holdup.

For each of the gas-tail columns, this control scheme is somewhat similar to Control Scheme 2 (i.e. DB type control), used in the de-propaniser column example of Chapter 5. Here again, regulation of the secondary control objectives is through a square root control policy (see Equation 5. 3. 9).

These two control schemes represent different constraint control strategies. Note that in both cases, there is no direct regulation of the column pressure. The pressure in each of

the gas-tail columns, therefore, fluctuates about its nominal steady-state value during actual operation.

For comparison, the following control strategy, currently in operation on the gas-tail, was also included. The design of such a control scheme was essentially based on previous experience and not strictly on process economics.

CONTROL SCHEME 3

	Manipulated variables		Primary control objectives
De-ethaniser:	Steam input rate to the reboiler.	paired with	Reboiler return temperature.
De-ethaniser:	Distillate flowrate.	paired with	Pressure at the top of the column.
De-propaniser :	Reflux flowrate.	paired with	Propane composition in the distillate.
De-propaniser :	Steam input rate to the reboiler.	paired with	Pressure at the top of the column.
De-isobutaniser:	Reflux flowrate.	paired with	i-Butane composition in the distillate.
De-isobutaniser :	Steam input rate to the reboiler.	paired with	Pressure at the top of the column.

Listed below are the secondary control objectives and the corresponding manipulated variables used ;

	Manipulated variables		Secondary control objectives
De-ethaniser:	Reflux flowrate.	paired with	Overhead accumulator holdup.
De-ethaniser:	Bottoms product rate.	paired with	Reboiler holdup.
De-propaniser :	Distillate flowrate.	paired with	Overhead accumulator holdup.
De-propaniser:	Bottoms product rate.	paired with	Reboiler holdup.
De-isobutaniser:	Distillate flowrate.	paired with	Overhead accumulator holdup.
De-isobutaniser:	Bottoms product rate.	paired with	Reboiler holdup.

The control scheme for each of the gas-tail columns under this configuration is somewhat similar to Control Scheme 4 , used in the de-propaniser example of Chapter 5.

Having identified several feasible control configurations, our aim now is to decide which of these alternative control system choices provide both the largest MPR (maximum percentage recovery, see Section 5. 3) and good closed-loop performance. It has been pointed out that both these characteristics of a control system depend to a large extent on the inherent controllability characteristics of the process alone. The functional controllability of each of the three alternative control configurations, therefore, will be examined as the first step in the selection of a suitable control scheme for the gas-tail.

As discussed previously in Section 5. 3, perfect control provides the ideal situation with a MPR of 100%. Perfect control is impossible to achieve in practice, so we can begin by identifying the major factors preventing perfect control being achieved. In the more general case, screening of alternative control schemes could be based initially on selecting schemes that offer the least impediments to achieving perfect control. Of the available open-loop controllability indicators, the optimally scaled l_∞ - norm condition number (see Section 4. 3. 5) is felt to be the single most useful measure. It should be noted in passing that for all the alternative control configurations for the gas-tail considered above, no RHP transmission zeros (see Section 4. 3. 4) were presented. Inversion of the gas-tail process transfer function matrix (a theoretical prerequisite for achieving perfect control ; see Section 4. 3. 2 for details) , therefore, is not limited by the presence of any RHP transmission zeros.

MINIMUM CONDITION NUMBER

As discussed previously in Section 5. 4, a frequency range relevant for the gas-tail was determined based on the eigenvalues of the system matrix obtained by linearising the gas-tail model about the steady-state operating point determined in the previous section. SPEECON was used both to linearise the gas-tail model, and subsequently to determine the eigenvalues of the system matrix. The largest eigenvalue of the gas-tail system matrix was 730. Therefore a frequency range up to 1500 cycles/hr was considered appropriate for the gas-tail case-study. Figure 6. 3. 1 shows the variation of the minimum condition number (i.e. based on the l_∞ - norm) for each of the three control configurations as a function of frequency. Control System 1 has the lowest value over most of the frequency range . Such a choice should also provide the least interaction amongst the loops of a multiloop control system and hence good closed-loop response can be expected of such a system. Control System 2 , on the other hand, has an infinite condition number at steady-state (see Section 5. 2. 2) . However, at frequencies greater than zero, the minimum condition number falls off rapidly , indicating that such a system is a potential alternative to Control System 1. Up to a frequency of 1 cycle/hr, Control System 1 has a minimum condition number ($\gamma_{min} = 1.8$) that is lower than that of Control System 2 by a factor of at least

FIGURE 6. 3. 1
MINIMUM CONDITION NUMBER FOR VARIOUS CONTROL CONFIGURATIONS
FOR THE GAS-TAIL

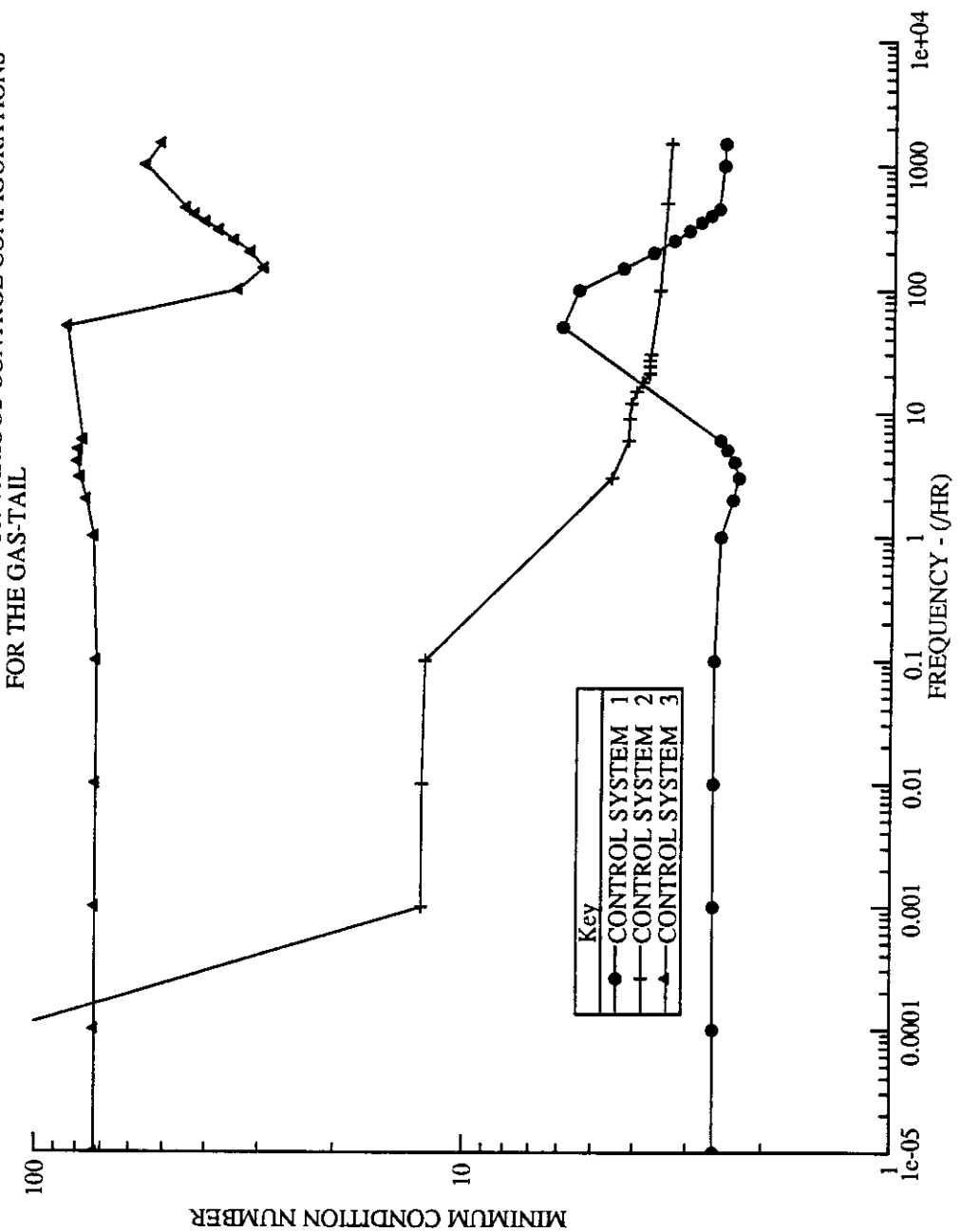

five. Wong [1984] pointed out that a factor of 2 - 5 in the minimum condition number between two systems would result in noticeably different closed-loop performance between the systems. One can therefore expect that Control System 1 gives the better closed-loop performance throughout this frequency range. However, in the case of Control System 3 (i.e. the control scheme currently in operation) the minimum condition number is large over the entire frequency range. It was shown in the example in the previous chapter (i.e Section 5. 4 , on the gas-tail de-propaniser column) that open-loop predictions using this minimum condition number were consistent with the closed-loop dynamic performance obtained from a well tuned multiloop control scheme. Therefore, poor closed-loop performance would be expected from the current control scheme on the gas-tail.

In summary, the minimum condition number indicates that we can rank the three control configurations being considered in the following order, with respect to their expected closed-loop performance :

Control System 1 (Best) > Control System 2 >> Control System 3 (Worst)

In the latter part of this chapter, these predictions are examined by carrying out closed-loop simulations on the nonlinear gas-tail model.

It must be noted that γ_{min} is an open-loop indicator that does not assume any particular control scheme (i.e either multiloop or multivariable type). Therefore, at this stage , we have to decide whether to choose a multiloop or a multivariable control policy. Multivariable controllers are preferred if the process interactions are severe, as in such cases they can provide significantly better control performance. However, such a control policy generally uses a process model and may be difficult to implement. On the other hand, if the process interactions are not too large, a multiloop control policy is quite adequate to regulate the control objectives at their set-points. A low minimum condition number ($\gamma_{min} \sim 1.0$) for Control System 1 implies low interactions amongst the control loops and hence, a multiloop control policy is probably adequate. The reasonably large minimum condition number ($\gamma_{min} \sim 10.0$ at frequencies below about 0.1 cycle per hour) in the case of Control System 2 indicates that large interactions would probably exist amongst individual control loops, and hence a multivariable control policy may be preferred to a multiloop control policy. As discussed previously, in a multivariable control policy the process model is treated as a part of the controller and hence the expected closed-loop performance is sensitive to plant-model mismatch (which is expected to increase as the minimum condition number increases). A multiloop control policy based on Control System 1 , therefore, was used for the current case-study, to achieve optimising control.

The de-ethaniser , the de-propaniser and the de-isobutaniser have one , two and three control objectives, respectively. The steam flowrate to the de-ethaniser's reboiler is chosen to regulate the reboiler return temperature (i.e. since it was decided previously that the other freed variable on this column, the distillate flowrate, should be regulated manually or in a feedforward manner). Calculation of the relative gain array (RGA) for the other two columns indicates that the following pairings are preferred (see Tables 6. 3. 1 and 6. 3. 2).

De-propaniser :

Distillate flowrate	-	Distillate (LPG) composition
Steam input rate to the reboiler	-	Reboiler return temperature

De-isobutaniser:

Distillate flowrate	-	Distillate (i-butane) composition
Steam input rate to the reboiler	-	Reboiler return temperature
Side-stream flowrate	-	Side-stream (n-butane) composition

Therefore, a "good" multiloop control scheme for the gas-tail would have the following structure :

CONTROL SCHEME 1

	Manipulated variables (Freed variables)		Primary control objectives (Active constraints)
De-ethaniser:	Steam input rate to the reboiler.	paired with	Reboiler return temperature.
De-propaniser:	Distillate flowrate.	paired with	Propane composition in the distillate.
De-propaniser :	Steam input rate to the reboiler.	paired with	Reboiler return temperature.
De-isobutaniser:	Distillate flowrate.	paired with	i-Butane composition in the distillate.
De-isobutaniser :	Steam input rate to the reboiler.	paired with	Reboiler return temperature.
De-isobutaniser :	Side-stream flowrate.	paired with	n-Butane composition in the side-stream.

The tuning of the PI controllers used for each primary control loop along with an analysis of the (simulated) closed-loop performance when Control Scheme 1 is implemented on

Table 6. 3. 1

RGA for the gas-tail distillation columns
De-propaniser - (2 X 2) control system

	Control objectives	
Manipulated variables	LPG composition in the distillate	Reboiler return temperature
Distillate product rate	1.043	-0.043
Steam rate to the reboiler	-0.043	1.043

Table 6. 3. 2

RGA for the gas-tail distillation columns
De-isobutaniser - (3 X 3) control system

	Control objectives		
Manipulated variables	I-butane composition in the distillate	Reboiler return temperature	N-butane composition in the side-stream
Distillate product rate	0.870	0.103	0.027
Steam rate to the reboiler	0.022	0.600	0.377
Side-stream product rate	0.108	0.297	0.595

the gas-tail , will be reported in Section 6. 6. As discussed previously, all the secondary control objectives (i.e holdups in both gas-tail condensers and reboilers) and their pairings, remain same and are regulated based on a square root control policy.

6.4 POTENTIAL ECONOMIC BENEFITS OF SWITCHING TO AN OPTIMISING CONTROL POLICY

The above discussion shows that Control System 1 is to be preferred over the current control policy on the gas-tail. In addition to an expected improvement in the operational performance , the economic benefits associated with the former control policy can also be estimated, as discussed in Section 5.4 for the de-propaniser example.

The rationale behind such an estimation is based on the assumption that no recovery of an open-loop back -off penalty can be achieved for an active constraint that is not regulated. In a constraint control strategy, partial recovery of the open-loop penalty for backing-off from each of the active constraints is possible. As shown in Equation (6. 2. 5), a 84% recovery (i.e an MPR of 84 %) of the open-loop penalty for back-off from the steady-state optimum is possible using the proposed constraint control strategy i.e. Control System 1.

The current control strategy, on the other hand, is not based on any constraint control policy. The recovery of the open-loop penalty for back-off from the steady-state optimum must be lower and can be estimated as follows :

Each of the active constraints at the calculated optimum is associated with an open and closed loop back-off (i.e. $b_i^{(ol)}$ and $b_i^{(cl)}$, respectively) as shown in Tables 6. 2. 4 and 6. 2. 5. Any back-off from each of the active constraints , however, is associated with a cost given by the corresponding Lagrange multiplier (see Section 5. 2). The Lagrange multipliers (i.e. corresponding to each active constraint) at the steady-state optimum for the high feed rate high pentanes (see Section 6. 2) will be used to estimate all such costs. The recovery in the open-loop penalty for the proposed optimising control for the gas-tail can be estimated in the same lines of de-propaniser example, as follows:

<u>De-ethaniser</u>

Reboiler return temperature is the only active constraint. From Tables (6. 2. 4) and (6. 3. 5) , the values of open and closed-loop back-offs for the de-ethaniser column, are

$$b_{11}^{(ol)} = 0, \quad b_{11}^{(cl)} = 0$$

From Section 6. 2, the Lagrange multiplier associated with the reboiler return temperature (i.e active constraint) is

$$\lambda_{11} = 0.68$$

The first subscript here shows the column number in the gas-tail (i.e. De-ethaniser = 1; de-propaniser = 2; de-isobutaniser = 3) while the second subscript shows the active constraint number. The superscripts i.e. (ol) , (cl) indicate open and closed-loop cases respectively. The same terminology is followed throughout this section.

It must be realised that no back-off is necessary in the other control objective (i.e the de-ethaniser column pressure) and hence it does not incur any additional penalty.

De-propaniser

In the case of the de-propaniser, two constraints are active at the steady-state optimum. The open and closed-loop back-offs associated with each of them are (from Tables 6. 2. 4 and 6. 2. 5) given below.

(1) For the LPG composition constraint in the distillate product ;

$$b_{21}^{(ol)} = 0.10 \text{ and } b_{21}^{(cl)} = 0.0011$$

The Lagrange multiplier associated with this constraint is

$$\lambda_{21} = 371.1$$

(2) Similarly, the reboiler return temperature constraint is the other active constraint (not regulated during operation). The associated open and closed-loop back-offs , and the Lagrange multiplier are given by

$$b_{22}^{(ol)} = 13.0 \text{ , } b_{22}^{(cl)} = 13.0 \text{ and } \lambda_{22} = 8.0$$

No back-off is necessary in the other control objective (i.e the de-propaniser column pressure) and hence it does not incur any additional penalty.

De-isobutaniser

In the case of the de-isobutaniser, three constraints are active at the steady-state optimum. The open and closed-loop back-offs associated with each of them are (from Tables 6. 2. 4 and 6. 2. 5) given below.

(1) For the i-butane composition constraint in the distillate product ;

$$b_{31}^{(ol)} = 0.12 \text{ and } b_{31}^{(cl)} = 0.00252$$

The Lagrange multiplier associated with this constraint is

$$\lambda_{31} = 2583.0$$

(2) For the n-butane composition constraint in the side-stream (not regulated during operation) ;

$$b_{32}^{(ol)} = 0.19 \quad \text{and} \quad b_{32}^{(cl)} = 0.19$$

The Lagrange multiplier associated with this constraint is

$$\lambda_{32} = 2830.0$$

(3) Similarly, the reboiler return temperature constraint is the other active constraint (not regulated during operation). The associated open and closed-loop back-offs , and the Lagrange multiplier are given by

$$b_{33}^{(ol)} = 5.0 \ , \ b_{33}^{(cl)} = 5.0 \text{ and } \lambda_{33} = 7.0$$

It must again be realised that here also that no back-off is necessary in the other control objective (i.e the de-isobutaniser column pressure) and hence it does not incur any additional penalty.

The maximum open-loop back-off can therefore be estimated from the following equation.

$$\begin{aligned} \Delta\phi_{max} &= \lambda_{11} b_{11}^{(ol)} \\ &+ \lambda_{21} b_{21}^{(ol)} + \lambda_{22} b_{22}^{(ol)} \\ &+ \lambda_{31} b_{31}^{(ol)} + \lambda_{32} b_{32}^{(ol)} + \lambda_{33} b_{33}^{(ol)} \\ &= \$\,1024 \,/\, hr \end{aligned} \qquad (6.4.1)$$

Similarly, the associated closed-loop back-off can be estimated as follows ;

$$\begin{aligned} \Delta\phi_{new} &= \lambda_{11} b_{11}^{(cl)} \\ &+ \lambda_{21} b_{21}^{(cl)} + \lambda_{22} b_{22}^{(cl)} \\ &+ \lambda_{31} b_{31}^{(cl)} + \lambda_{32} b_{32}^{(cl)} + \lambda_{33} b_{33}^{(cl)} \\ &= \$\,683.6 / hr \end{aligned} \qquad (6.4.2)$$

From the definition of MPR , we therefore have

$$\begin{aligned} MPR &= 100 * (1 - \Delta\phi_{new} \,/\, \Delta\phi_{max}) \\ &= 33.2\% \end{aligned} \qquad (6.4.3)$$

Thus, from Equation (6. 4. 3) , it is clear that the maximum recovery of the open-loop penalty for backing-off from the optimum operating conditions is significantly smaller (33%) for the current control scheme than that for the optimising control scheme (84%) developed using the methodology proposed in this study.

The above discussion and calculations demonstrate quite clearly that the proposed optimising control strategy on the gas-tail is associated with large operational and

economic benefits. It is , therefore, well worth considering a shift from the current control strategy to the one proposed.

6.5 CLOSED - LOOP PERFORMANCE OF THE GAS -TAIL WITH THE PROPOSED CONTROL CONFIGURATION

As discussed before in Section 5. 4 , it must be realised that the closed-loop dynamic simulations reported in this section for the gas-tail are only a demonstration of the expected closed-loop performance from the proposed Control System 1. They also show the validity of the assumptions made in estimating the proposed closed-loop back-off in this case-study. The dynamic simulations do not form part of the proposed control system synthesis methodology.

It was shown in the previous sections that Control System 1 satisfies most of the requirements for tight operation of the gas -tail. The small minimum condition number over the entire frequency range of interest indicates that implementation of such a control system on the gas -tail should ensure a large recovery in the penalties associated with the " no control " back-offs from the optimum operating point.

The new operating conditions were decided based on the "second largest feasible move" in each of the control objectives from their optimum values, as discussed previously in Section 6. 3 (see Table 6. 3. 5). Controller tunings were made at this new operating point. To provide a consistent approach, controllers were tuned based on the method given in Appendix A9. The control system for each gas-tail column was treated separately and tuning of the multiloop control systems for each column was made independently. Table (6. 5. 1) summarises the controller tuning parameters used throughout the closed-loop studies.

With a tuned Control System 1 implemented on the gas-tail, closed-loop responses for various disturbances and set-point changes were obtained (see Figures 6. 5. 1 - 6. 6. 35). Constraint lines have been included for all cases where a control objective violates its constraint value (i.e. its value at the original optimum) during the transient closed-loop behaviour. The following terminology has been used for all these plots describing the dynamic behaviour of the various columns of the gas-tail :

B	Bottoms product rate
S	Steam rate to the reboiler
T (or T_R)	Reboiler return temperature
P	Pressure at the top of a distillation column

R	Reflux rate
X_D	Distillate product composition
X_S	Side stream product composition
SS	Side stream product rate
H_A	Holdup in the overhead accumulator
H_R	Holdup in the reboiler

Below is a discussion of the quality of the closed-loop behaviour for various disturbance and set-point changes :

(1) As discussed previously in Section 3. 2. 2, with a low pentanes feed to the gas-tail, a reboiler return temperature lower then that required for the high pentanes feed, would be required at the steady-state optimum. In practise, a reduction in the set-point of the de-ethaniser's reboiler return temperature controller , therefore, is necessary while switching from a high pentanes feed to a low pentanes feed to the gas-tail. Such a set-point change in the reboiler return temperature influences the product separations within de-ethaniser as well as the downstream columns . The dynamic response of the gas-tail columns for a step change of - 4 % ($T_{(initial)}$ = 130 deg C ; $T_{(final)}$ = 125 deg C) in the de-ethaniser reboiler return temperature controller set-point is shown in Figures 6. 5. 1 - 6. 5. 7. Good closed-loop response in all the gas -tail control loops can be seen. However, Figure 6. 5. 6 shows that during the transient stage , the constraint on the LPG composition in the de-propaniser distillate is violated for a short period of time. This shows that the back-off made from the corresponding active constraint in moving away from the original optimum is not quite large enough. Similarly, the de-isobutaniser column's distillate product has a minimum purity constraint that is also violated during the transient (see Figure 6. 5. 7). No other control objective violates its constraints during the transient behaviour.

(2) Figures 6. 5. 8 - 6. 5. 14 show the dynamic response of the various gas-tail columns to a step change of + 3. 5 % ($X_{D\ (initial)}$ = 0.9011, $X_{D\ (final)}$ = 0.933) in the de-propaniser's LPG purity in the distillate product. As the flow in the gas-tail is unidirectional, changes in a column might not be expected to influence the upstream columns. However, a set-point change in the de-propaniser's distillate control loop affects this column's temperature profile which in turn affects the column pressure. Such a change would set-up a source of back pressure, which in turn propagates to the (upstream) de-ethaniser column. The temperature control loop in the de-ethaniser responds quickly to counteract this back-pressure effect. Figure 6. 5. 13 shows that the de-ethaniser reboiler return temperature violates

it's constraint (i.e. 130 deg C) in the beginning of it's regulatory response. None of the other control objectives violate their corresponding constraints during their transient behaviour.

(3) A step change of + 3 % ($X_{D\ (initial)} = 0.8825$; $X_{D\ (final)} = 0.909$) in the set-point for the controller of the de-isobutaniser's distillate product purity also changes the pressure in this column. These changes affect both upstream columns and hence influences all the gas-tail control loops. Figures 6. 5. 15 - 6. 5. 21 show the closed-loop response of all the control loops. The response of the de-ethaniser's reboiler return temperature control loop (see Figure 6. 5. 20) shows that the constraint on this temperature (i.e. 130 deg C) is violated during the transient behaviour. None of the other constraints are violated during the transient stages.

Figures 6. 5. 1 - 6. 5. 21 show that the control system proposed for the gas-tail generally provides very good closed-loop response for changes in the set-points of its major quality control loops. Violation of the constraint on the de-ethaniser's reboiler return temperature during the transient stage, however, indicates a need for design modifications in this reboiler so as to provide a larger temperature difference for heat exchange. On the other hand, violation of the constraint on the LPG purity in the de-propaniser's distillate product shows that the closed-loop back-off made from the corresponding active constraint is not quite large enough.

The above discussion is concerned with the servo behaviour of the gas-tail control system. The behaviour of the gas-tail's control system for various disturbances is considered below.

(4) The saturated LP steam to the gas-tail reboilers comes from a common source and is often subject to fluctuations in its supply pressure. Responses to a + 20 % ($P_{S\ (initial)} = 3.14$ bar: $P_{S\ (final)} = 3.77$ bar) change in the steam pressure shows that the gas-tail regulatory control system acts quickly to counteract this effect (see Figures 6. 6. 22 - 6. 6. 28). Thus, there is no significant change in any of the control objectives from their set-point values. The constraint on the de-ethaniser's reboiler return temperature and that on the constraint on the LPG purity in the de-propaniser's distillate product are the only constraints violated in the early part the transient response (Figure 6. 6. 27). None of the other control objectives violate their corresponding constraints.

(5) The other major disturbance considered is the feed flowrate. Feed to the gas-tail comes from various sources upstream and hence is subject to frequent variations in its

magnitude, depending on the operating conditions of the upstream process units. The response of the gas-tail to a step change of - 10% ($F_{(\text{initial})} = ; F_{(\text{final})} =)$ in the feed rate is shown in Figures 6. 6. 29 - 6. 6. 35. Some of the composition control objectives violate their corresponding constraints during the transient behaviour. However, all such constraint violations occur briefly in the early part of the transient behaviour. Implementing a buffer storage tank in the feed stream to the gas-tail would reduce these feed rate fluctuations and reduce the likelihood of quality constraint violations during operation. This would seem preferable to the alternative option of increasing the closed-loop back-offs and thus moving further away from the economic optimum.

Feed composition (with respect to the pentanes content) can also be a source of disturbance for the gas-tail. However, the pentanes content in the gas-tail feed usually depends on the type of crude oil being processed in the crude distillation unit and is thus better treated as a "slow" disturbance. The proposed regulatory control scheme on the gas-tail manages the "fast" disturbances (such as feed flowrate changes) , while the steady-state optimiser takes care of the "slow" disturbances.

Figures 6. 6. 22 - 6. 6. 35 show that in general good closed-loop response is obtained for the two major fast disturbances, though in some cases the control objectives violate their corresponding constraints during the early stages of the transient behaviour.

6.6 SUMMARY

The case-study used in this chapter has provided an industrial example of the systematic methodology proposed for synthesising an optimising control structure. Initially, after steady-state optimisation, the potential economic benefits of installing a control system on the gas-tail were identified. To avoid violating any constraints during the transient closed-loop response, a "back-off" from the optimum operating conditions was required. A modified constraint control strategy was then proposed for the control of the gas-tail. Open-loop controllability indicators identified likelyhood of strong interactions between the various control objectives and manipulated variables for the control scheme currently in operation. The poor closed-loop performance actually observed on the gas-tail with the current control scheme is consistent with the information provided by these controllability indicators. Using the minimum condition number as an open-loop indicator , several feasible control schemes for the gas-tail were examined. A new control scheme with good controllability characteristics was proposed. Significant economic benefits have been identified by using the proposed optimising control strategy. Both the

regulatory and servo performance of the proposed control scheme was examined via simulation studies and shown to be quite acceptable.

Table 6. 5. 1
Controller tuning constants used for
the proposed gas-tail control scheme

Control loop	Controller gain (K_c)	Controller reset time (τ_I) (Hr)	BLT detuning constant (F)
<u>De-ethaniser:</u>			
Reboiler return temperature loop	0.623	0.059	1.02
<u>De-propaniser:</u>			
Distillate composition loop	-13.19	0.171	1.9
Reboiler return temperature loop	0.149	0.042	1.9
<u>De-isobutaniser:</u>			
Distillate composition loop	416.18	1.048	1.5
Reboiler return temperature loop	1.4	0.014	1.5
Side-stream composition loop	-213.65	0.169	1.5

Figure 6. 5. 1

Dynamic response of the de-ethaniser process variables for a - 4 % step change in the de-ethaniser reboiler return temperature loop set-point

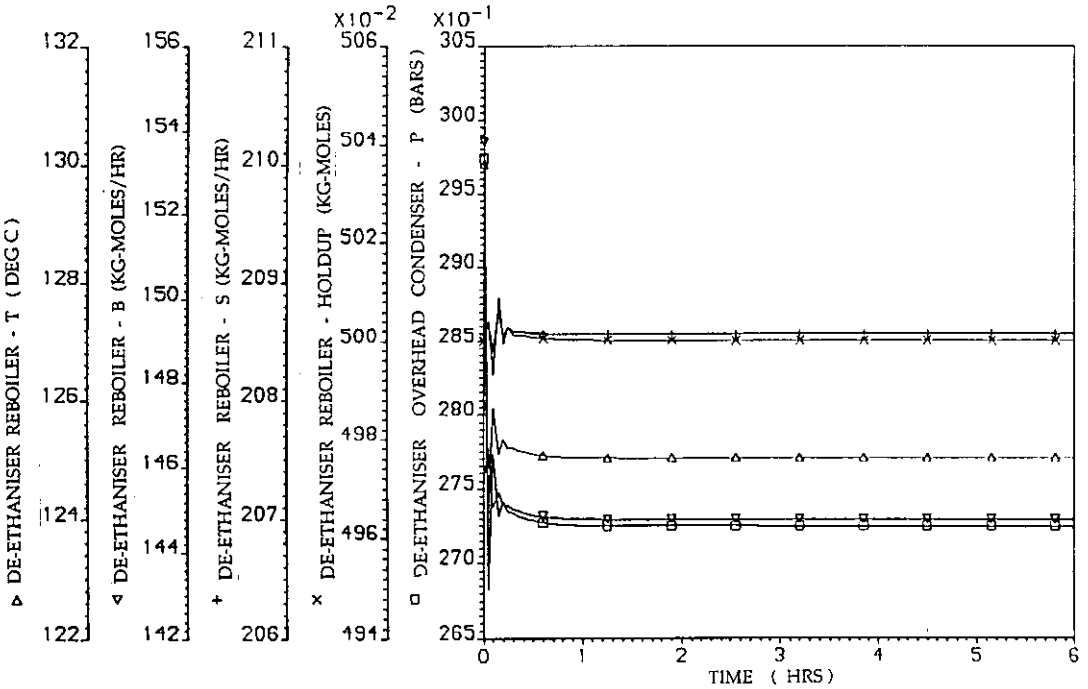

Figure 6. 5. 2

Dynamic response of the de-propaniser process variables for a - 4 % step change in the de-ethaniser reboiler return temperature loop set-point

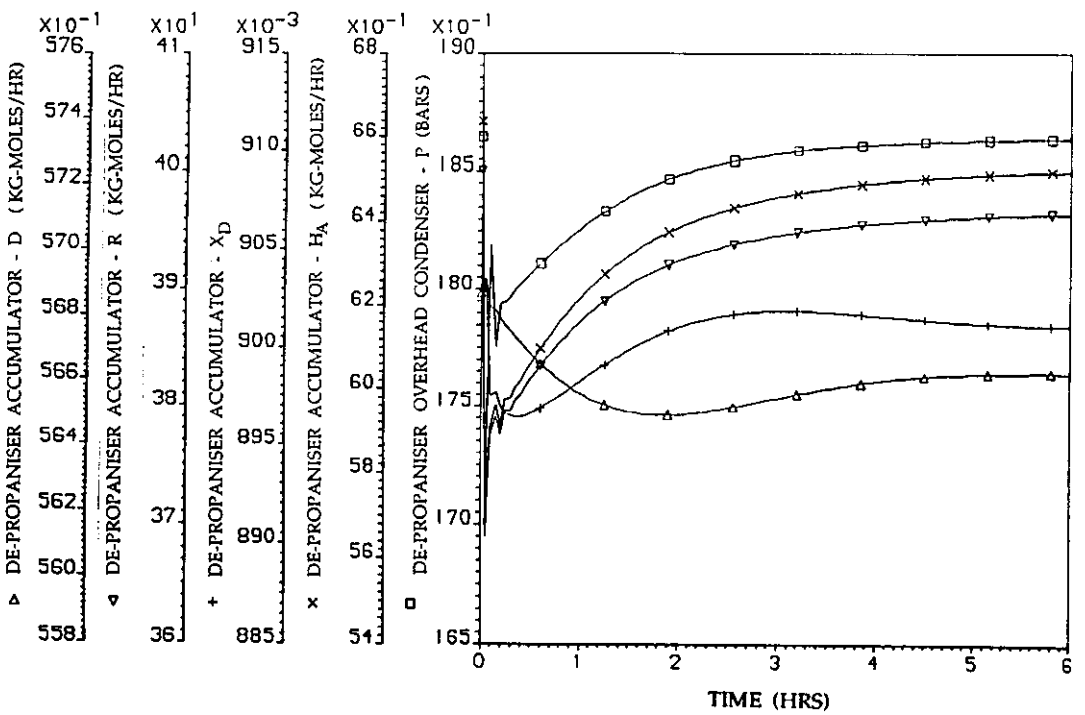

Figure 6. 5. 3

Dynamic response of the de-propaniser process variables for a - 4 % step change

in the de-ethaniser reboiler return temperature loop set-point

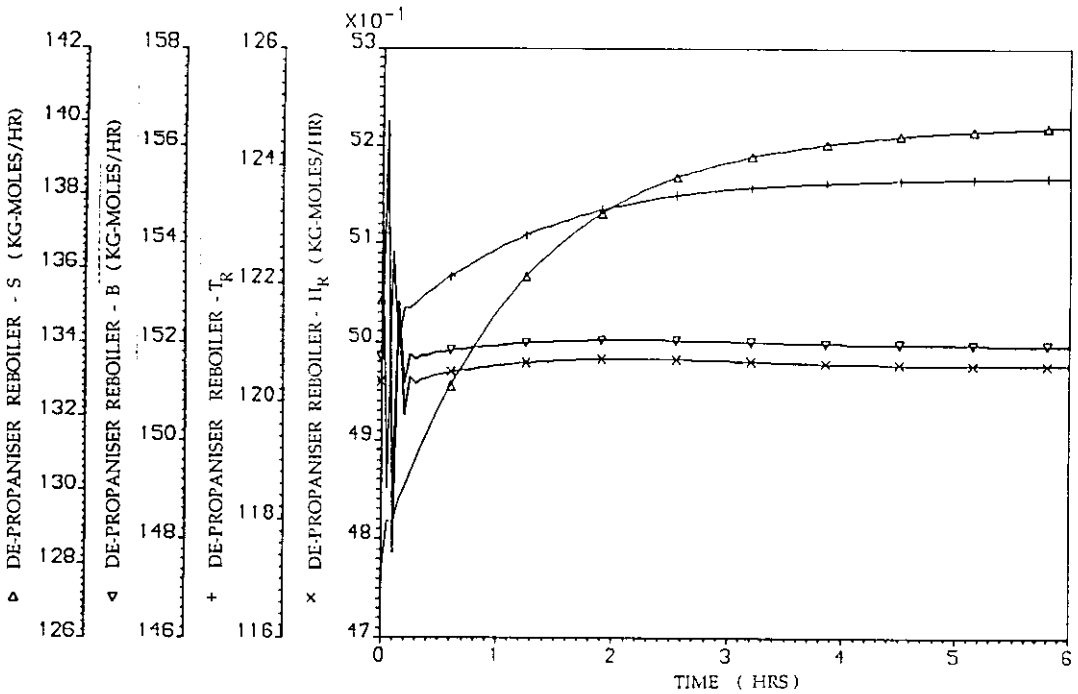

Figure 6. 5. 4

Dynamic response of the de-isobutaniser process variables for a - 4 % step change

in the de-ethaniser reboiler return temperature loop set-point

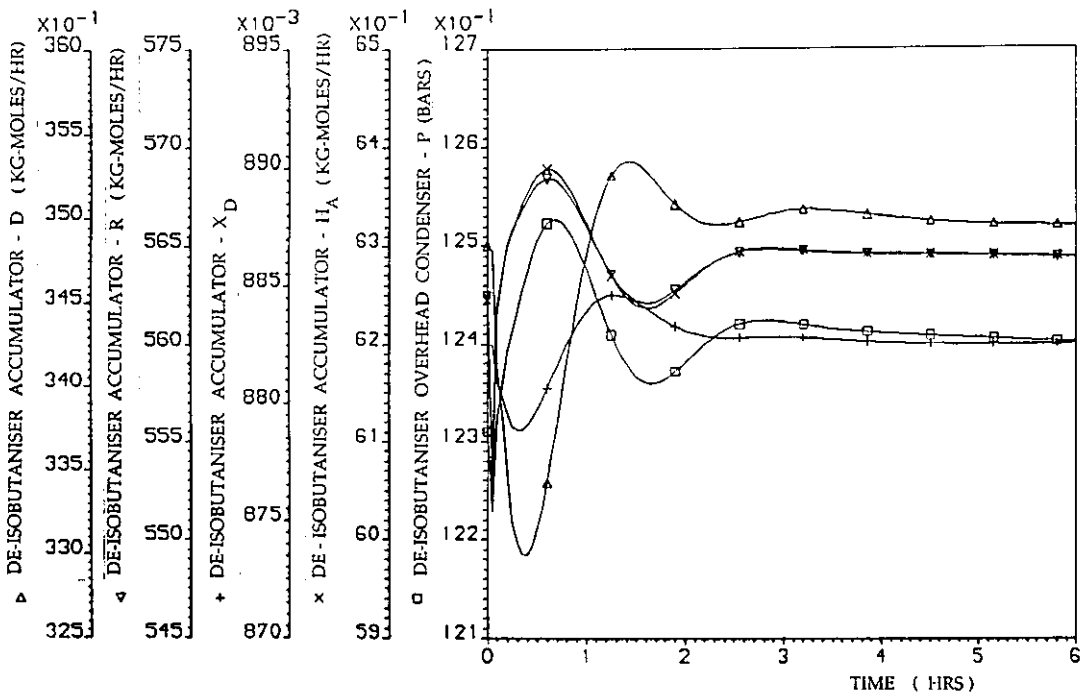

Figure 6. 5. 5

Dynamic response of the de-isobutaniser process variables for a - 4 % step change in the de-ethaniser reboiler return temperature loop set-point

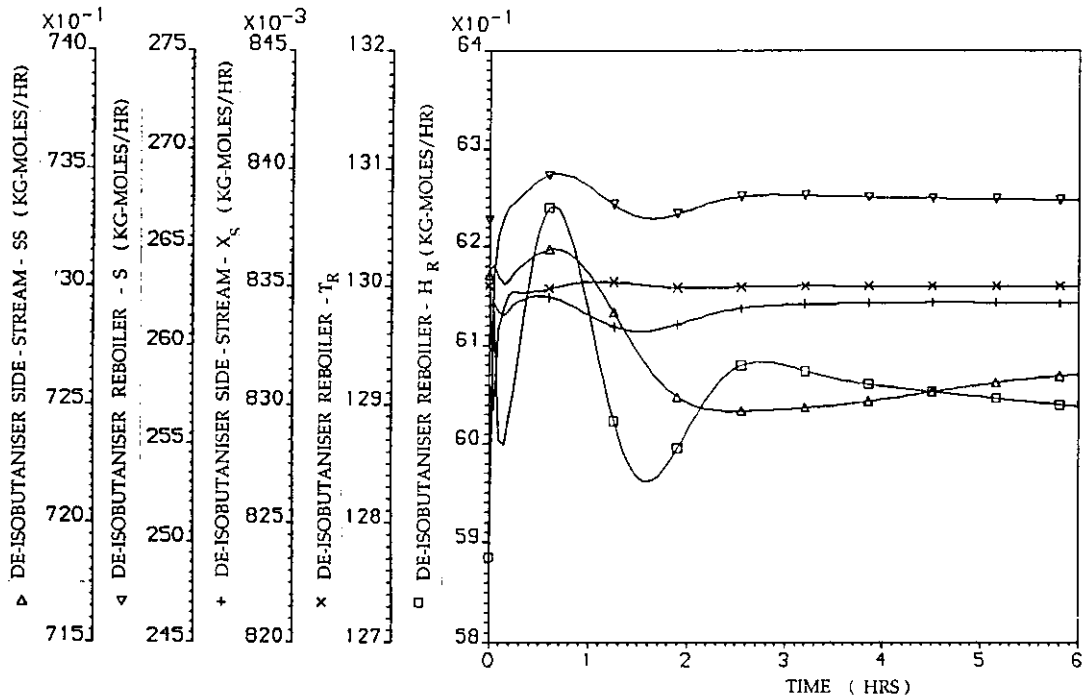

Figure 6. 5. 6

Dynamic response of the de-ethaniser and de-propaniser control objectives for a - 4 % step change in the de-ethaniser reboiler return temperature loop set-point.

(Note the constraint violation)

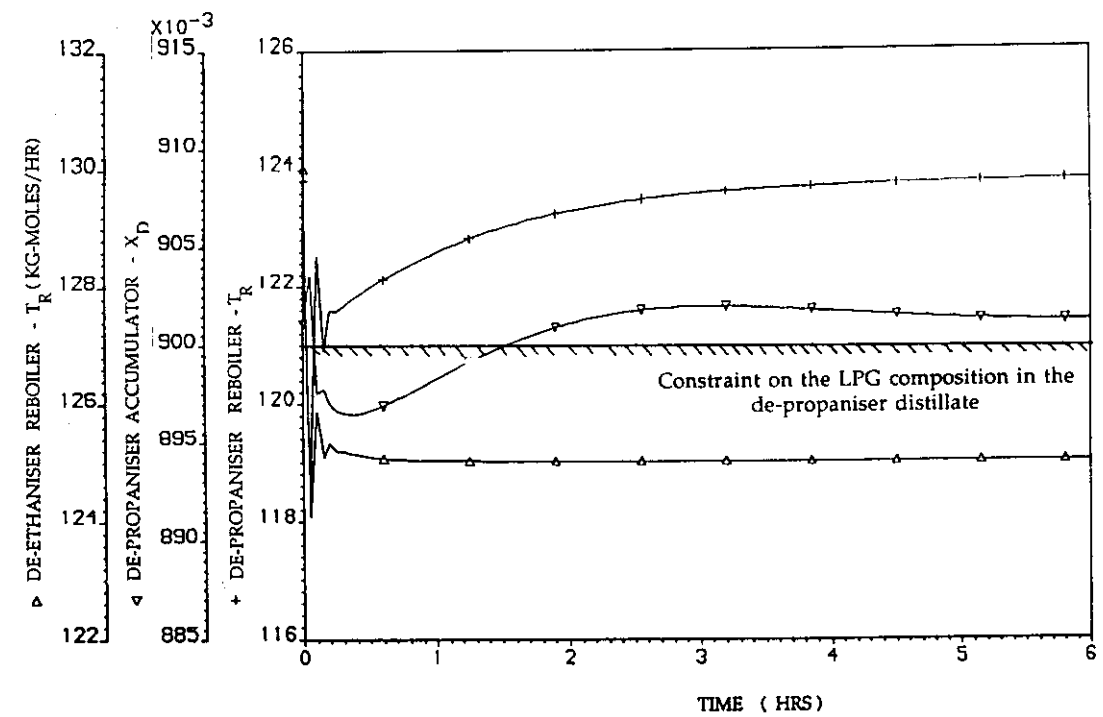

Figure 6. 5. 7

Dynamic response of the de-isobutaniser control objectives for a - 4 % step change in the de-ethaniser reboiler return temperature loop set-point.

(Note the constraint violation)

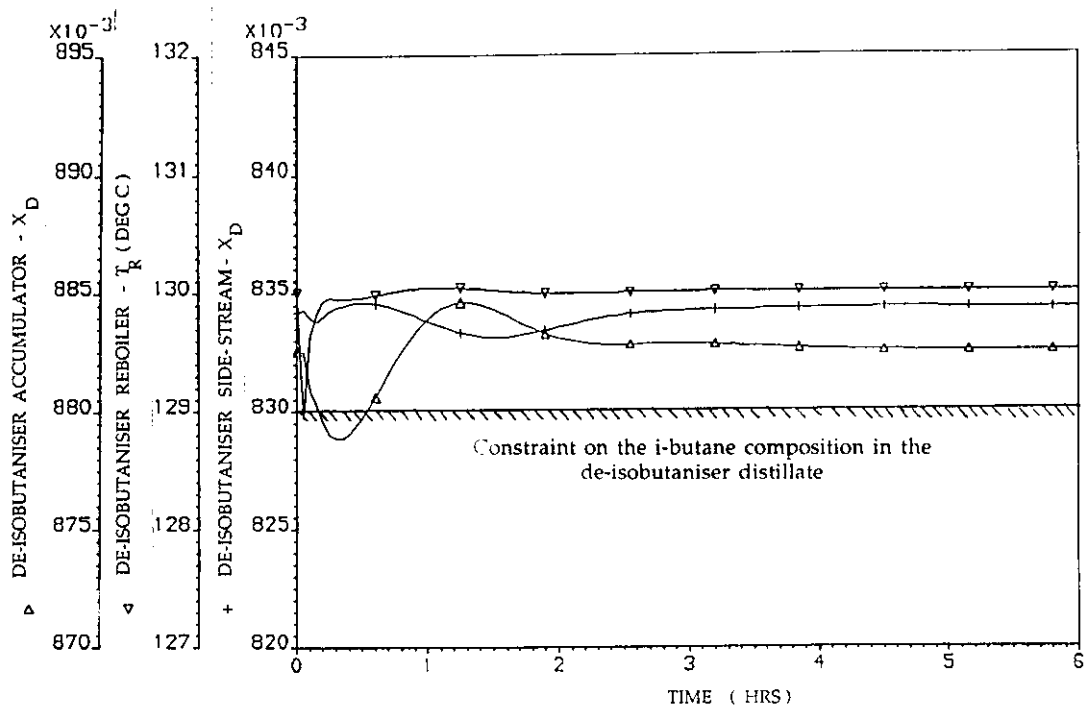

Figure 6. 5. 8

Dynamic response of the de-ethaniser process variables for a

+ 3.5 % step change in the de-propaniser distillate loop set-point

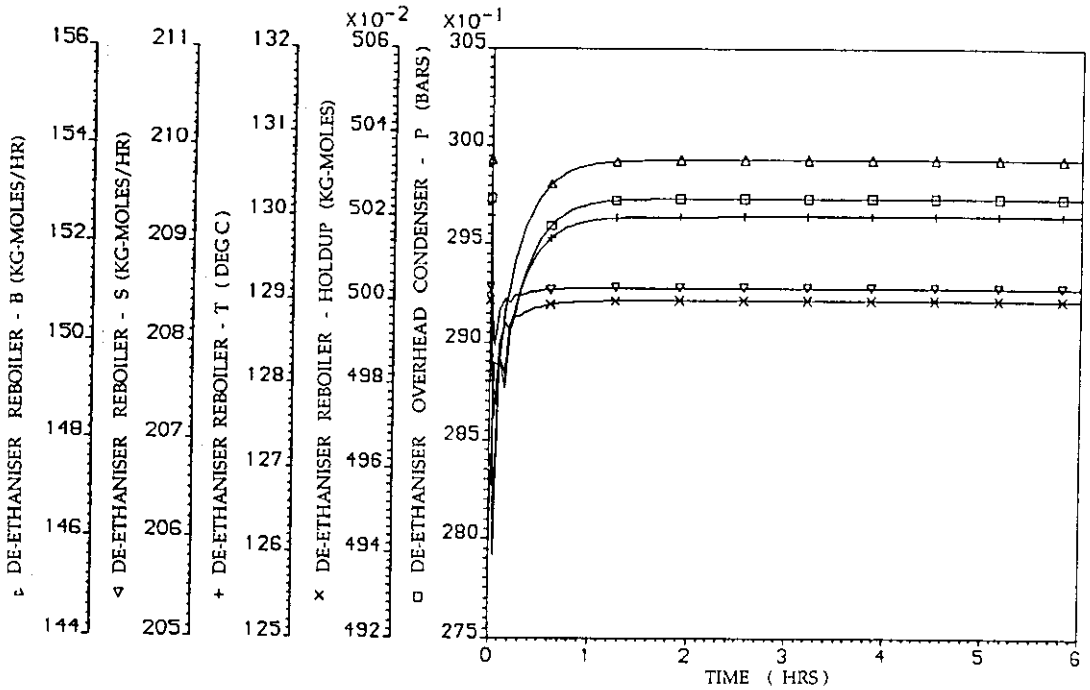

Figure 6. 5. 9

Dynamic response of the de-propaniser process variables for a

+3.5 % step change in the de-propaniser distillate loop set-point

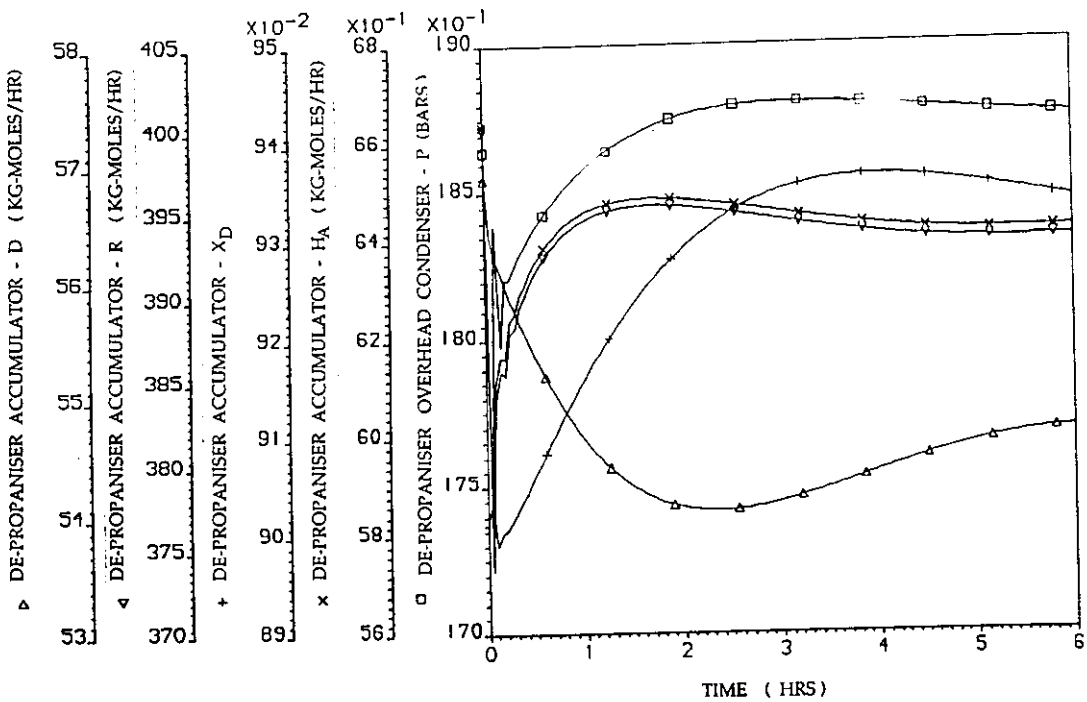

Figure 6. 5. 10

Dynamic response of the de-propaniser process variables for a

+3.5 % step change in the de-propaniser distillate loop set-point

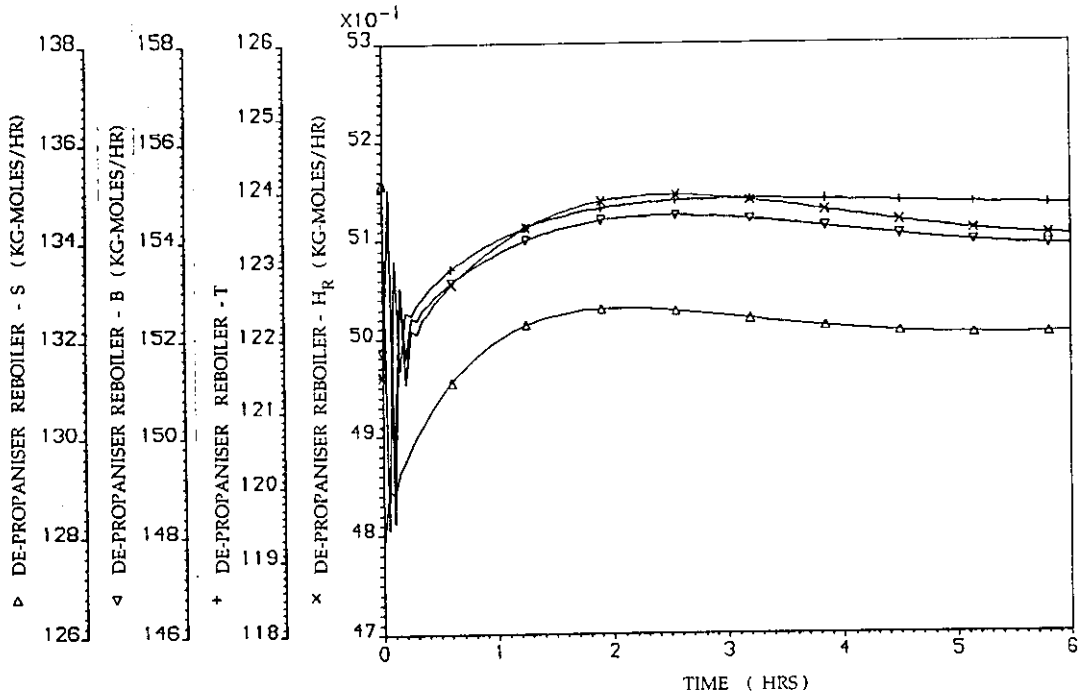

Figure 6. 5. 11

Dynamic response of the de-isobutaniser process variables for a

+3.5 % step change in the de-propaniser distillate loop set-point

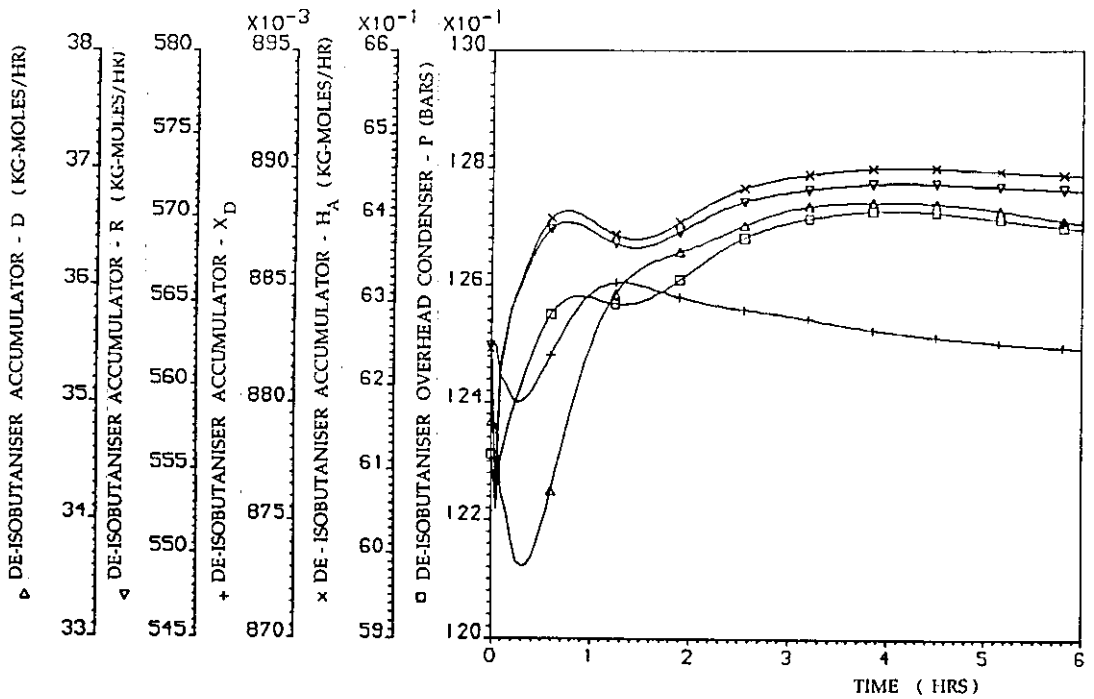

Figure 6. 5. 12

Dynamic response of the de-isobutaniser process variables for a

+3.5 % step change in the de-propaniser distillate loop set-point

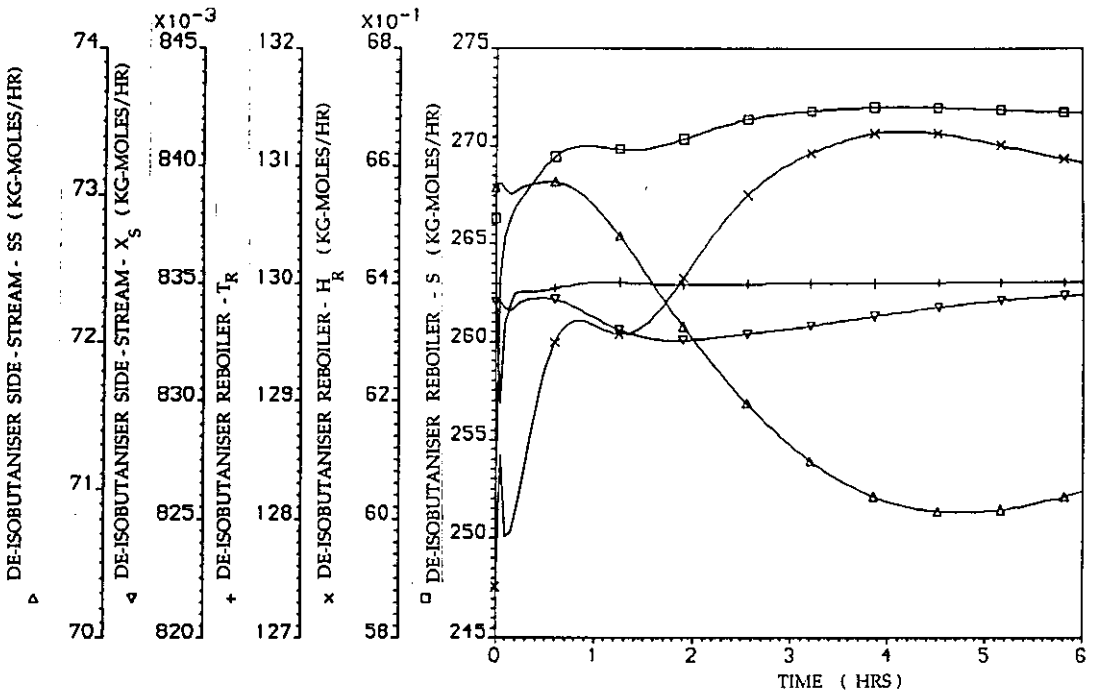

Figure 6. 5. 13

Dynamic response of the de-ethaniser and de-propaniser control objectives for a

+3.5 % step change in the de-propaniser distillate loop set-point.

(Note the constraint violation)

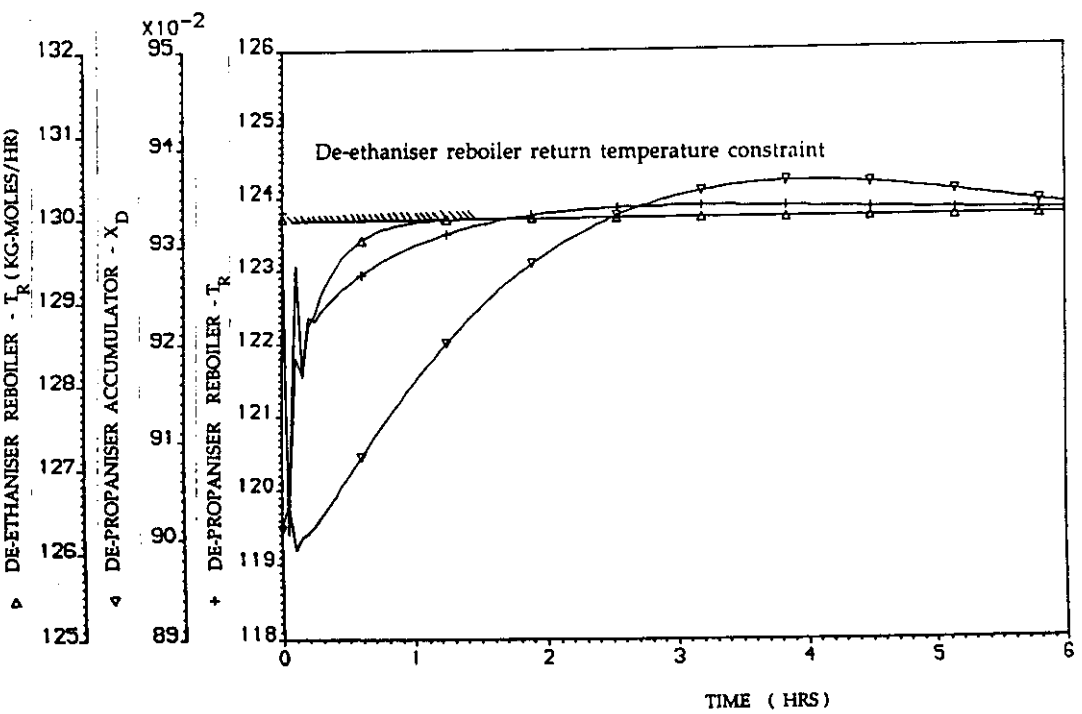

Figure 6. 5. 14

Dynamic response of the de-isobutaniser control objectives for a +3.5 % step change in the de-propaniser distillate loop set-point.

(Note the constraint violation)

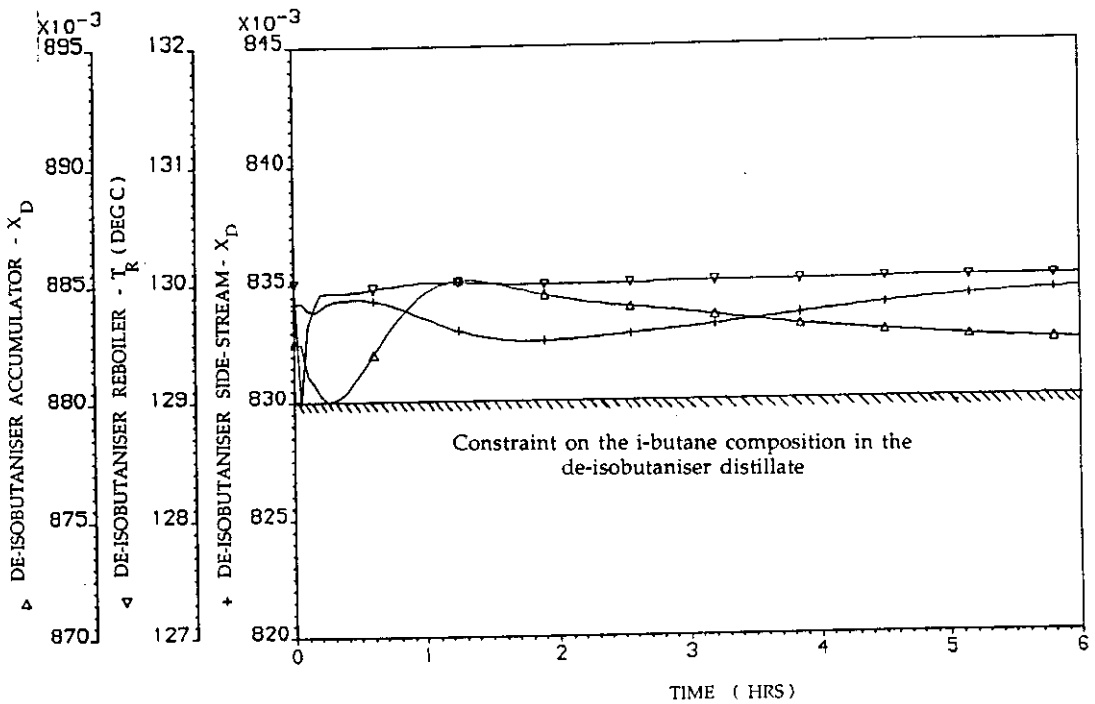

Figure 6. 5. 15

Dynamic response of the de-ethaniser process variables for a

+ 3.0 % step change in the de-isobutaniser distillate loop set-point

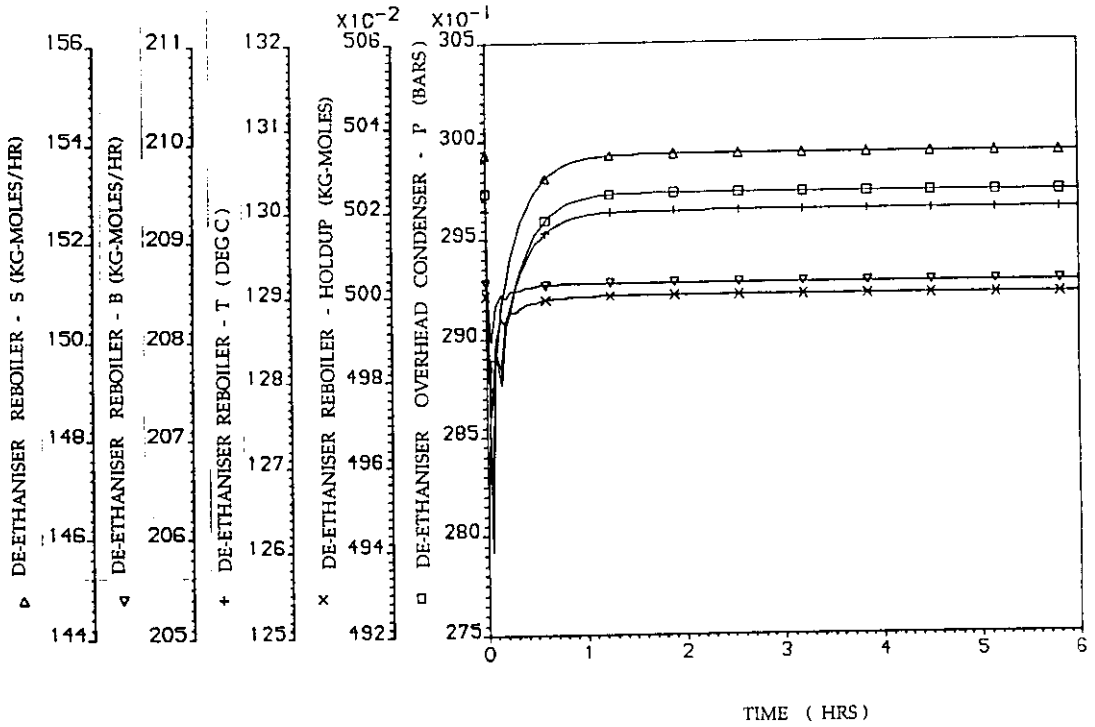

Figure 6. 5. 16

Dynamic response of the de-propaniser process variables for a

+3.0 % step change in the de-isobutaniser distillate loop set-point

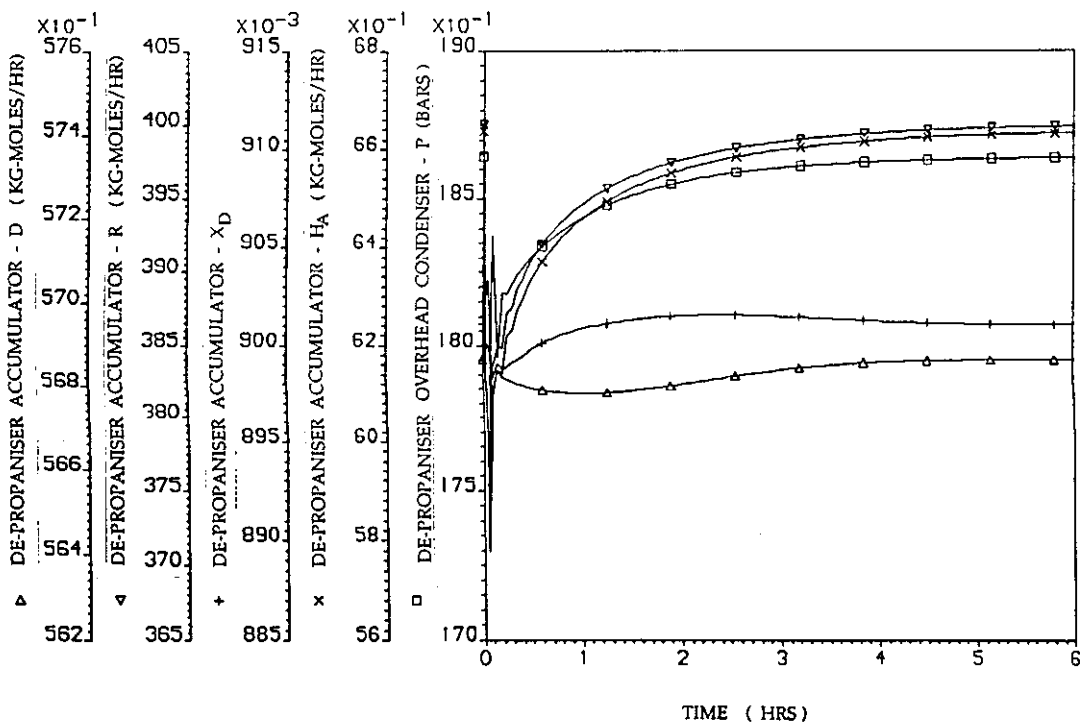

Figure 6. 5. 17

Dynamic response of the de-propaniser process variables for a

+ 3.0 % step change in the de-isobutaniser distillate loop set-point

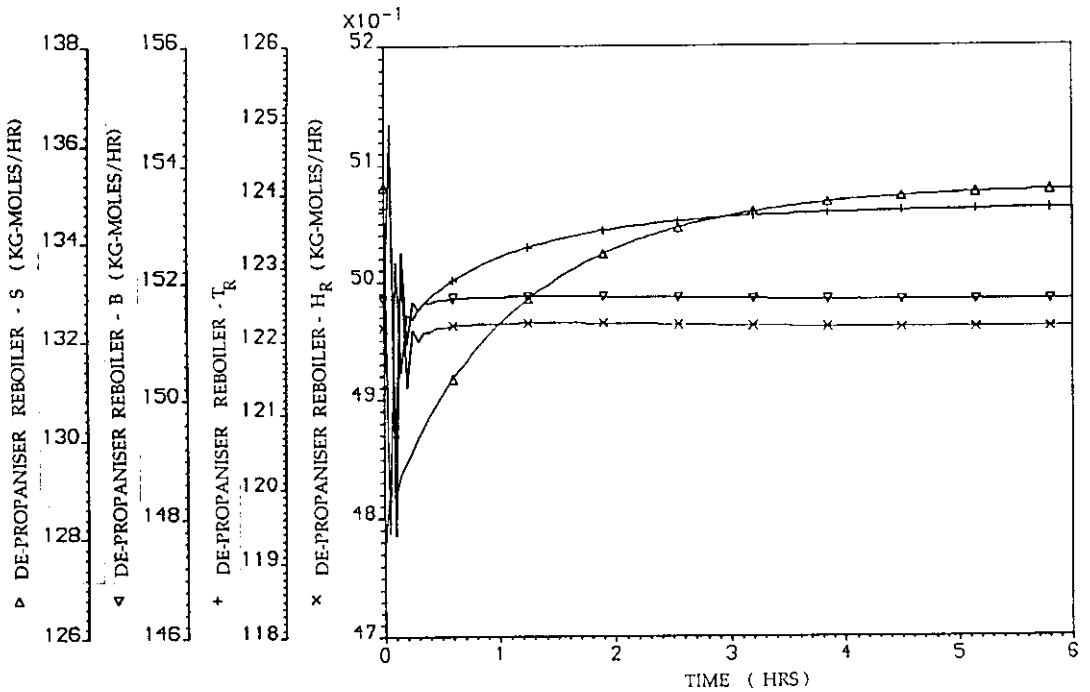

Figure 6. 5. 18

Dynamic response of the de-isobutaniser process variables for a

+ 3.0 % step change in the de-isobutaniser distillate loop set-point

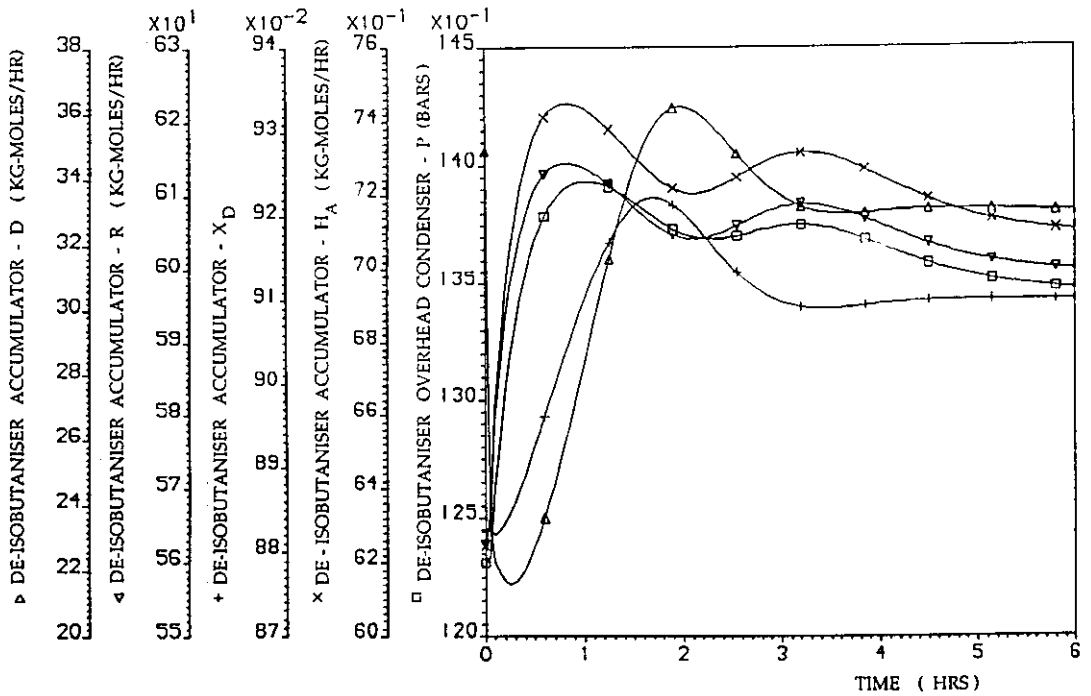

Figure 6. 5. 19

Dynamic response of the de-isobutaniser process variables for a

+ 3.0 % step change in the de-isobutaniser distillate loop set-point

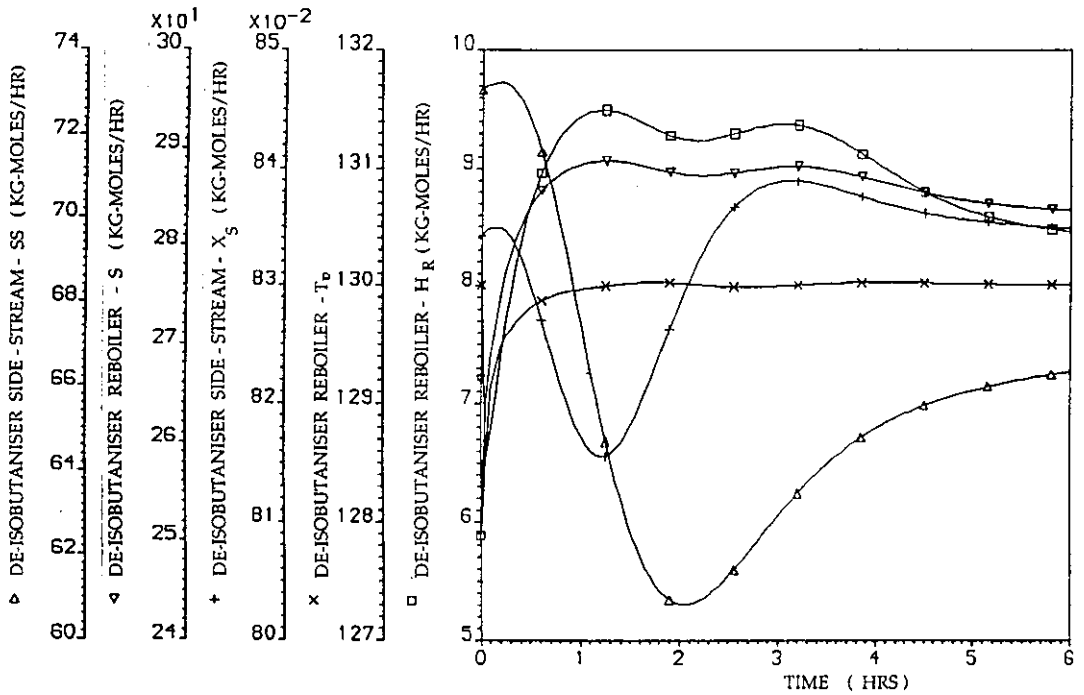

Figure 6. 5. 20

Dynamic response of the de-ethaniser and de-propaniser control objectives for a

+ 3.0 % step change in the de-isobutaniser distillate loop set-point.

(Note the constraint violation)

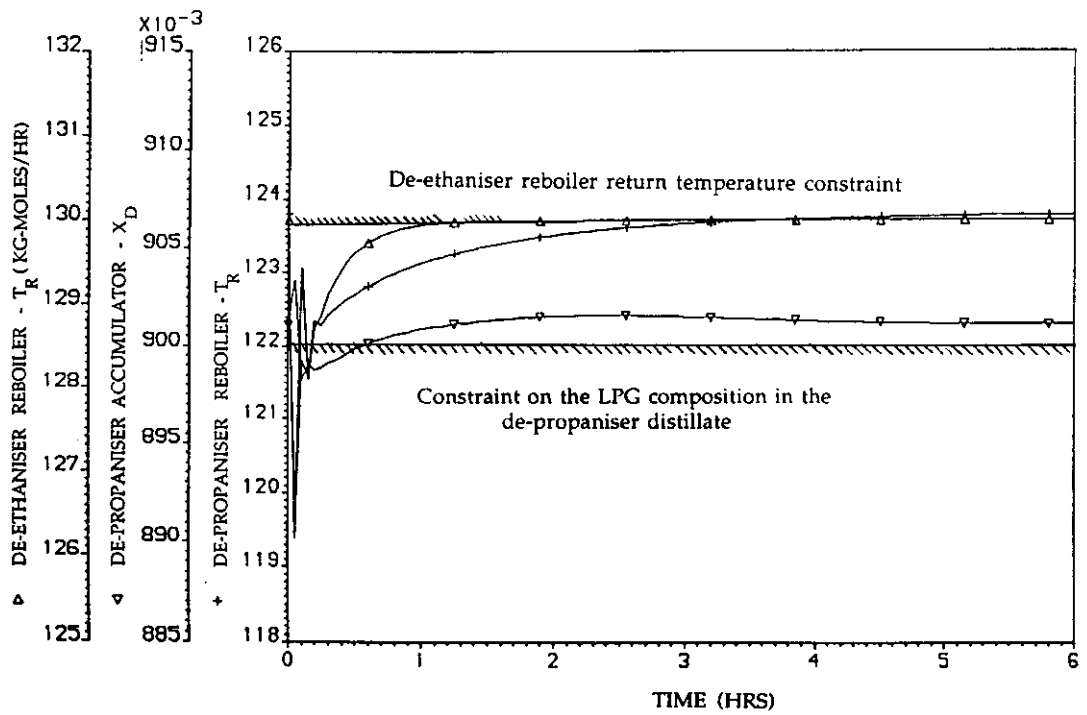

Figure 6. 5. 21

Dynamic response of the de-isobutaniser control objectives for a + 3.0 % step change in the de-isobutaniser distillate loop set-point.

(Note the constraint violation)

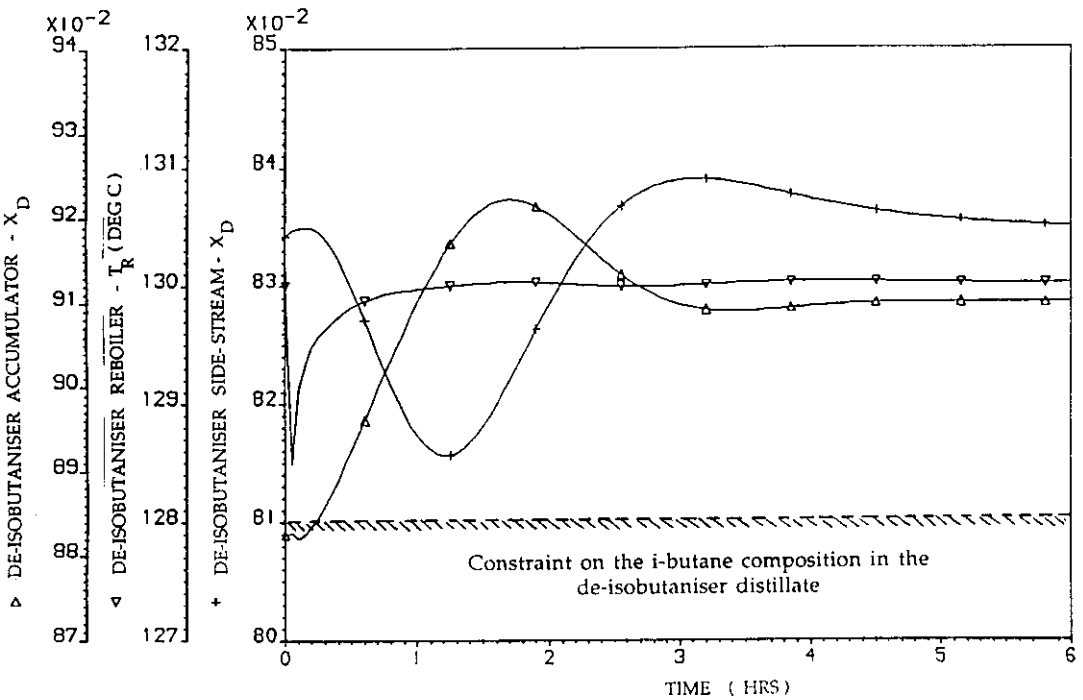

Figure 6. 5. 22

Dynamic response of the de-ethaniser process variables to a

+ 20.0 % step change in the steam pressure to the reboilers

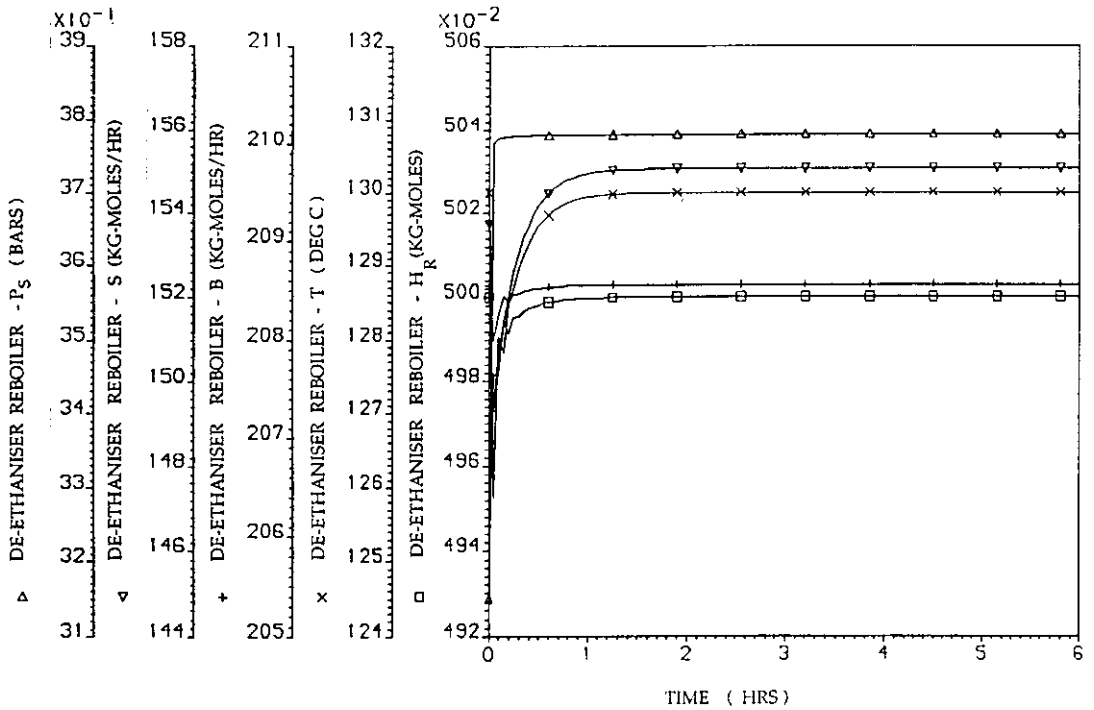

Figure 6. 5. 23

Dynamic response of the de-propaniser process variables to a

+ 20.0 % step change in the steam pressure to the reboilers

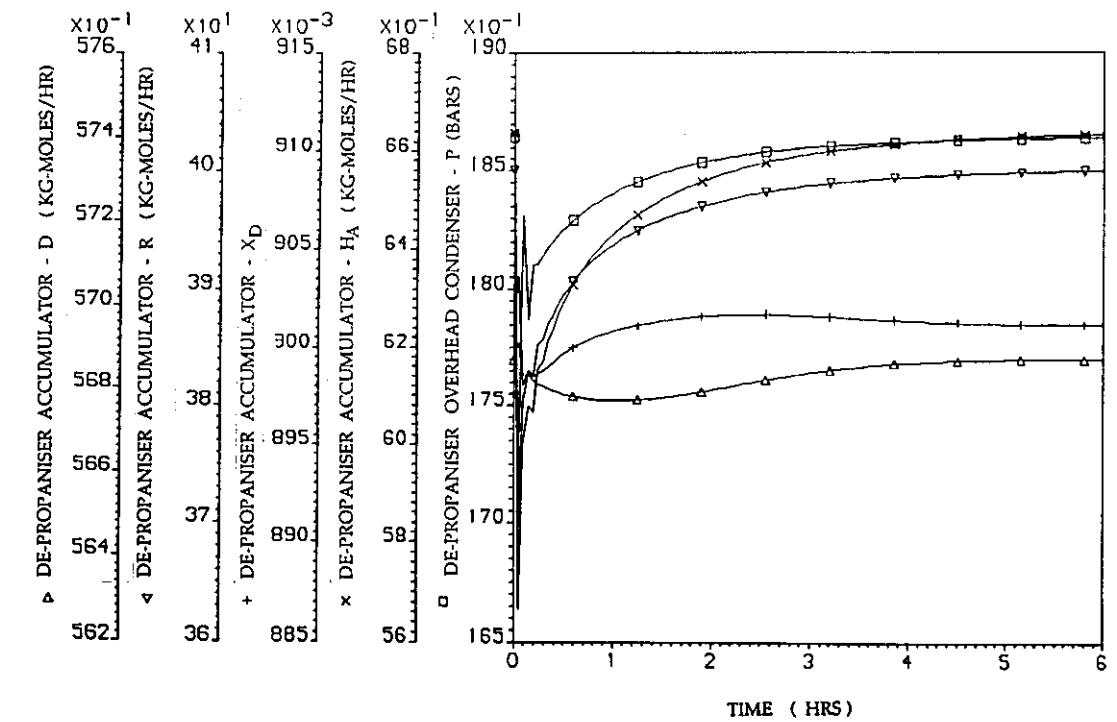

Figure 6. 5. 24

Dynamic response of the de-propaniser process variables to a

+ 20.0 % step change in the steam pressure to the reboilers

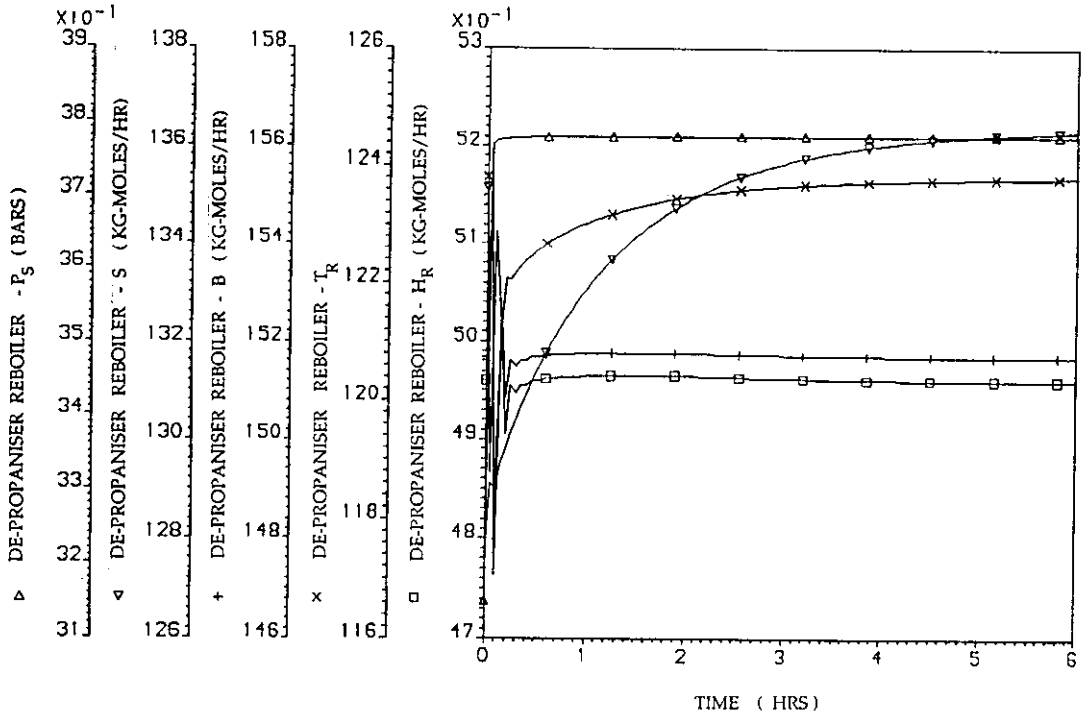

Figure 6. 5. 25

Dynamic response of the de-isobutaniser process variables to a

+ 20.0 % step change in the steam pressure to the reboilers

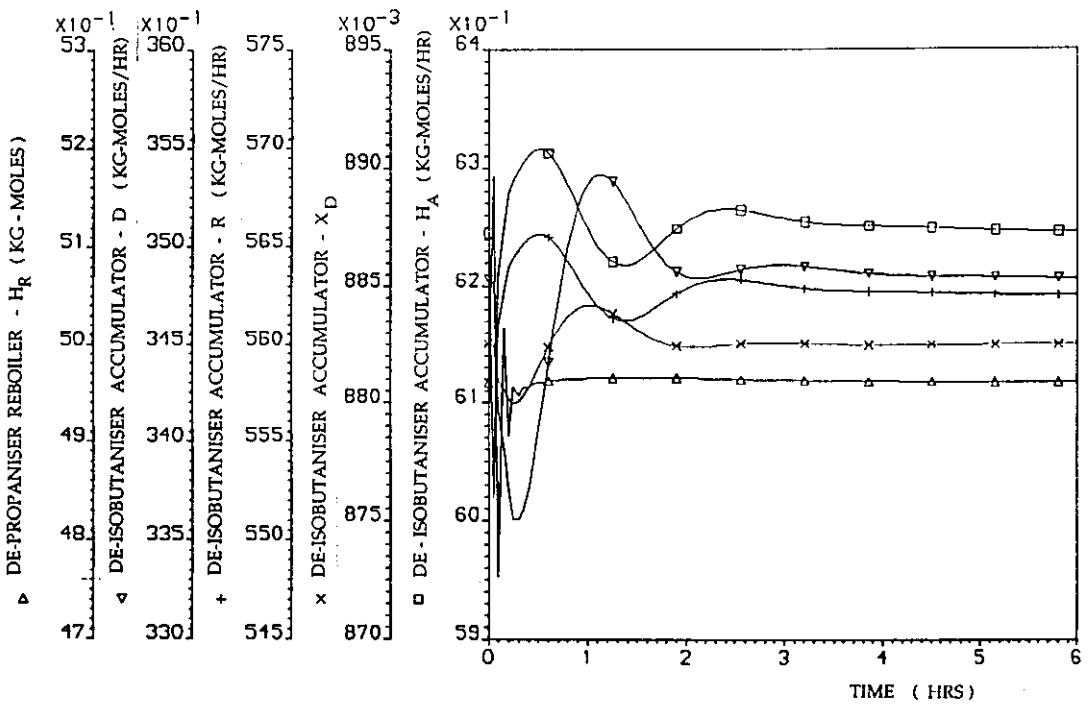

Figure 6. 5. 26

Dynamic response of the de-isobutaniser process variables to a

+ 20.0 % step change in the steam pressure to the reboilers

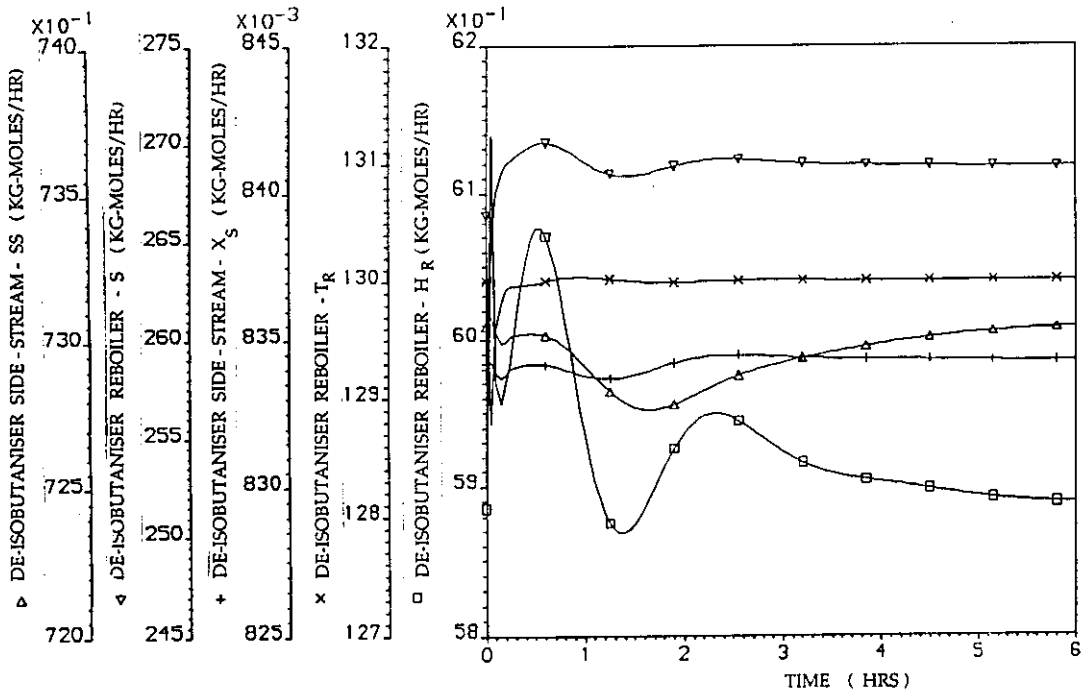

Figure 6. 5. 27

Dynamic response of the de-ethaniser and de-propaniser control objectives to a

+ 20.0 % step change in the steam pressure to the reboilers.

(Note the constraint violation)

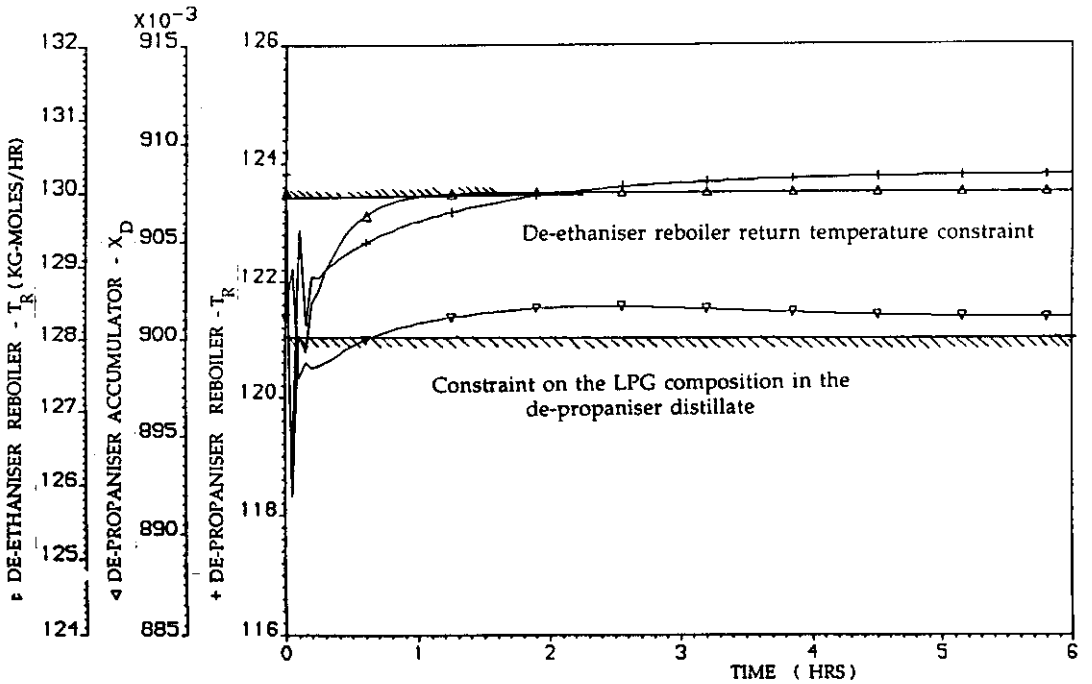

Figure 6. 5. 28

Dynamic response of the de-isobutaniser control objectives to a + 20.0 % step change in the steam pressure to the reboilers.

(Note the constraint violation)

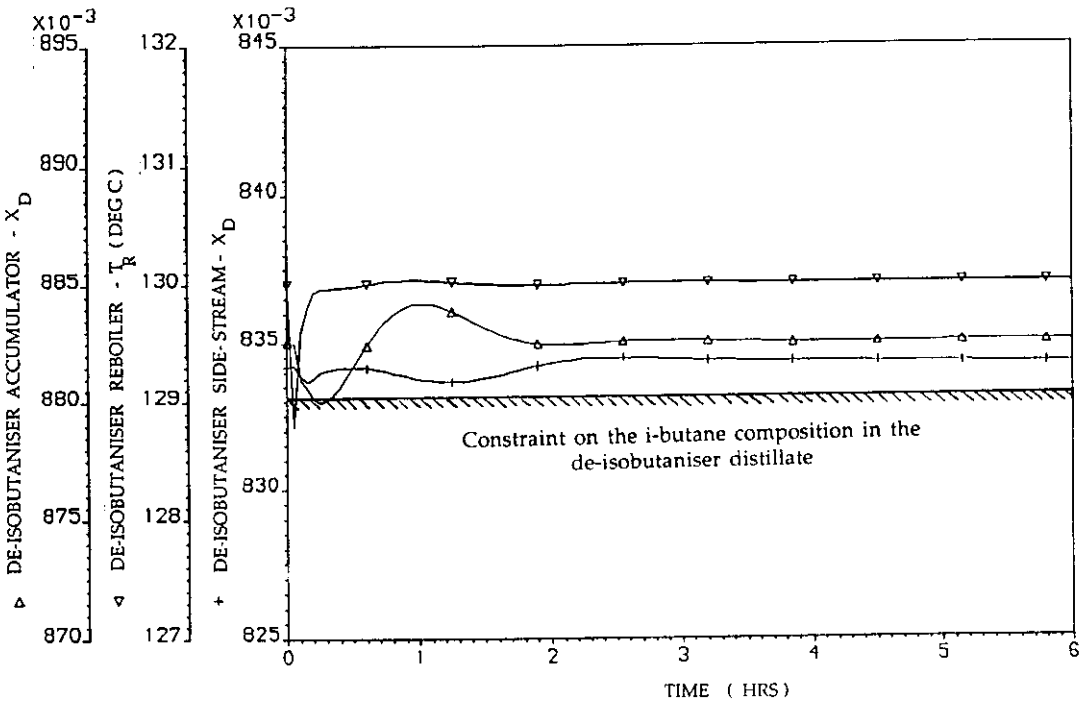

Figure 6. 5. 29

Dynamic response of the de-ethaniser process variables to a

- 10.0 % step change in the feed flowrate to the gas-tail

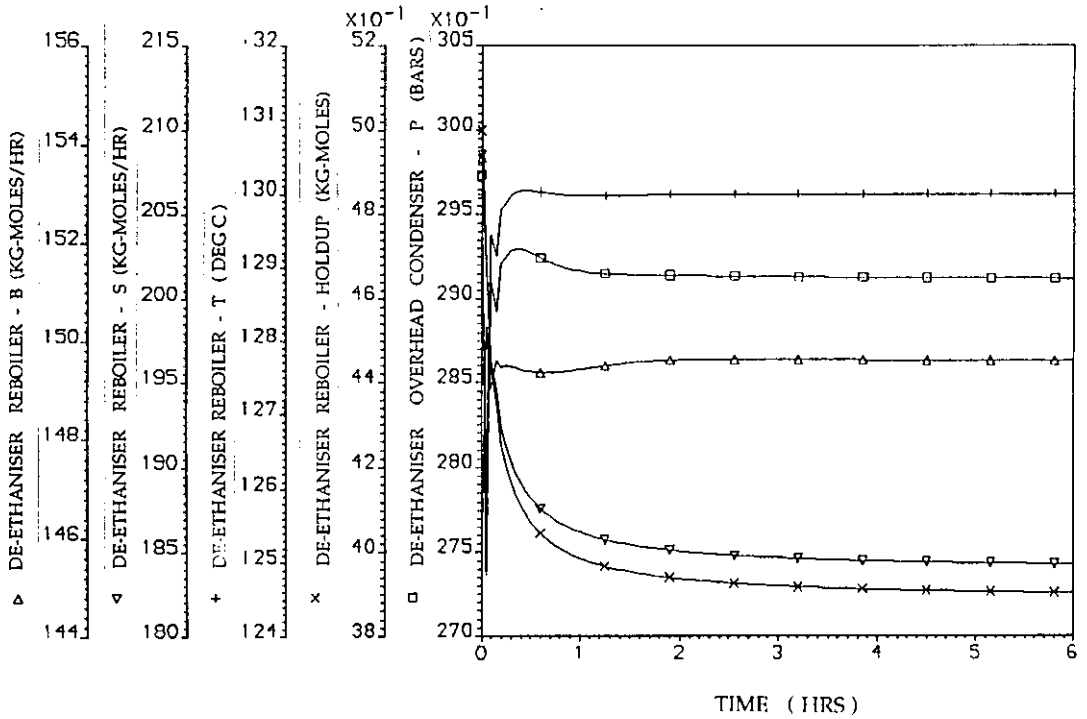

Figure 6. 5. 30

Dynamic response of the de-propaniser process variables to a

- 10.0 % step change in the feed flowrate to the gas-tail

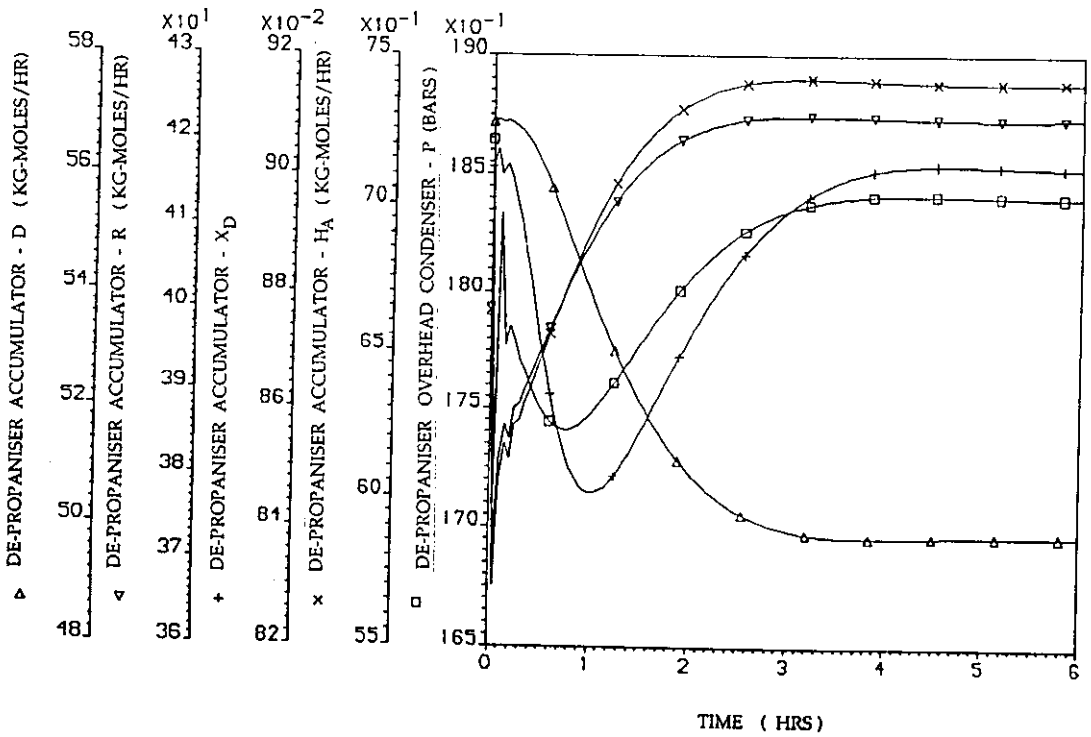

Figure 6. 5. 31

Dynamic response of the de-propaniser process variables to a

- 10.0 % step change in the feed flowrate to the gas-tail

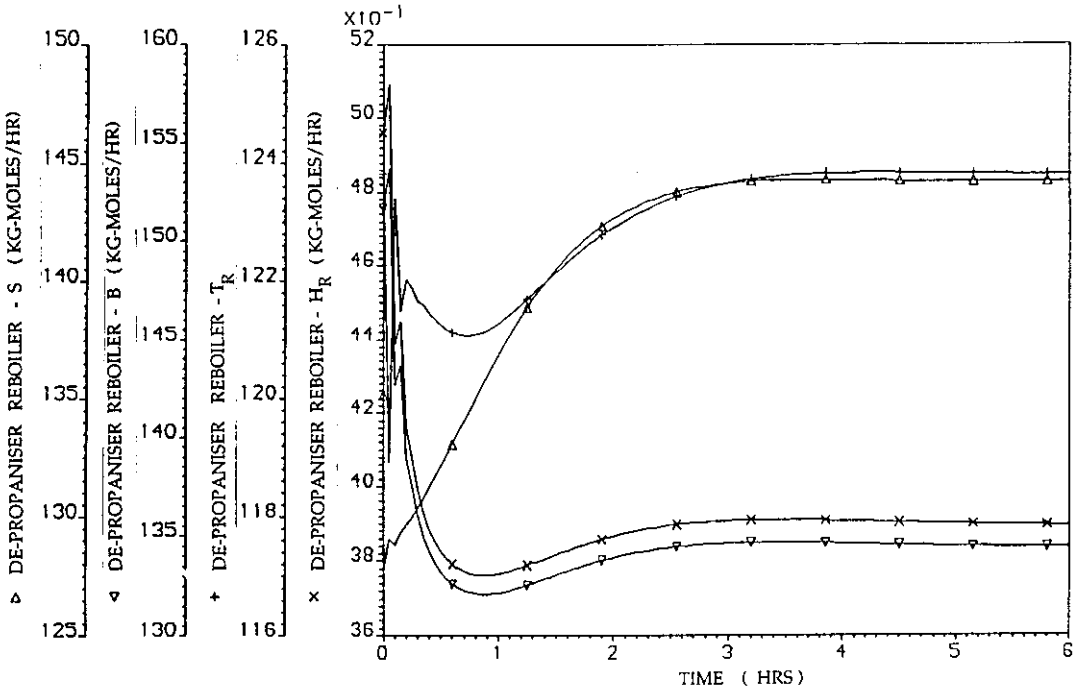

Figure 6. 5. 32

Dynamic response of the de-isobutaniser process variables to a

- 10.0 % step change in the feed flowrate to the gas-tail

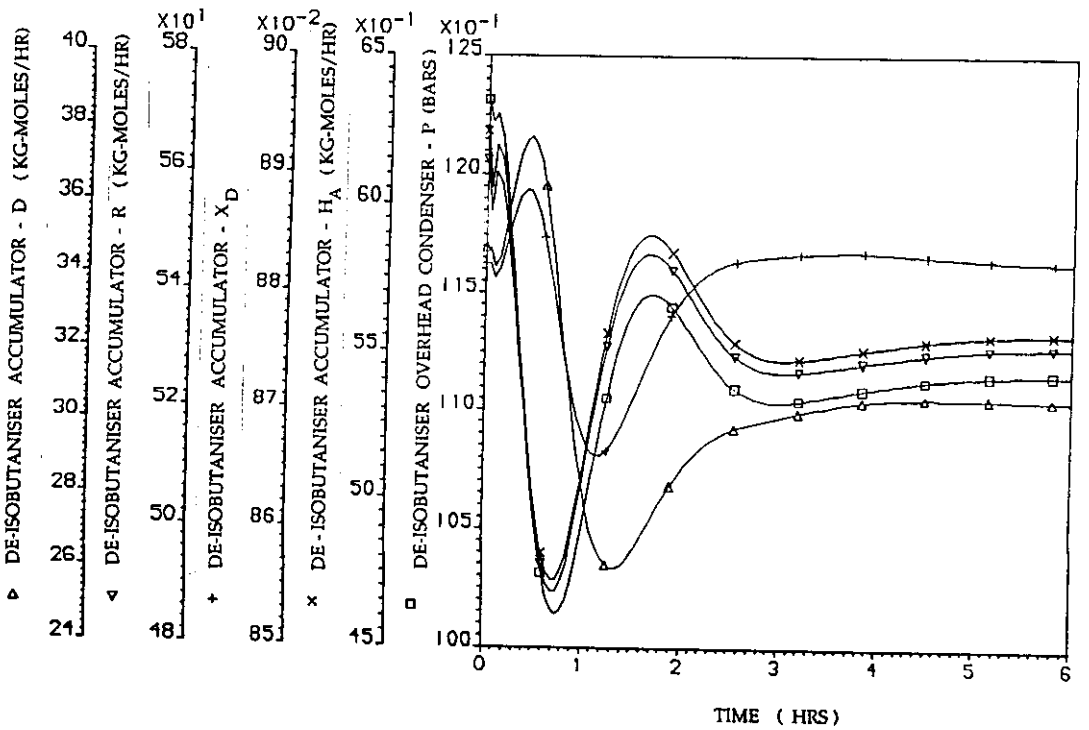

Figure 6. 5. 33

Dynamic response of the de-isobutaniser process variables to a

- 10.0 % step change in the feed flowrate to the gas-tail

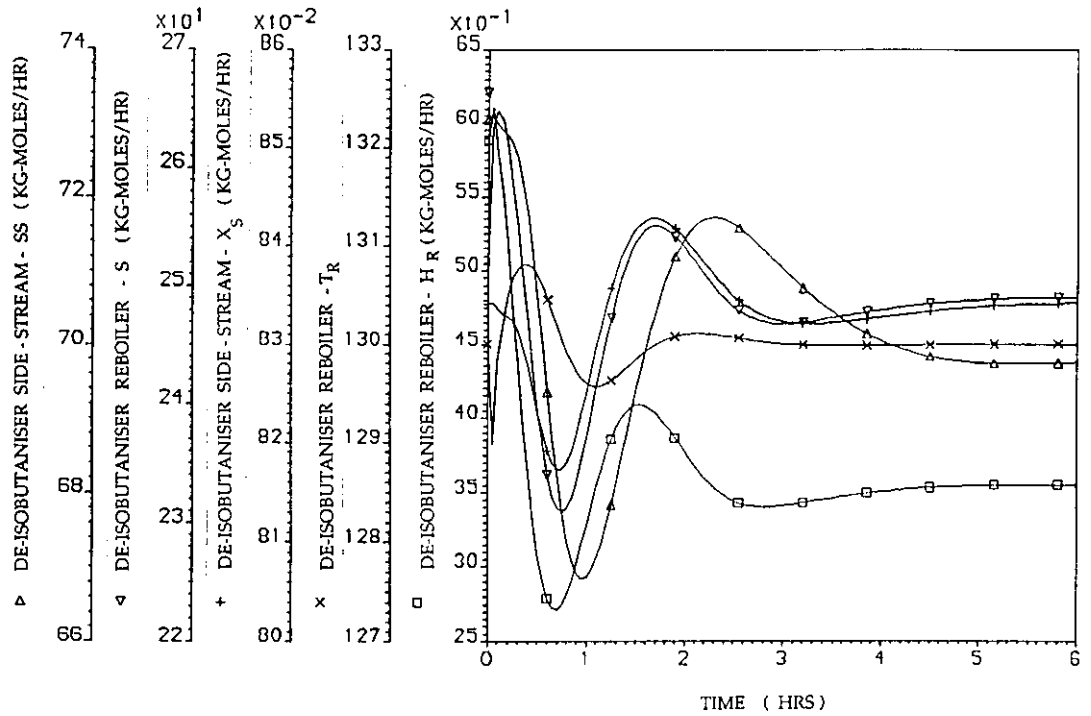

Figure 6. 5. 34

Dynamic response of the de-ethaniser and de-propaniser control objectives to a

- 10.0 % step change in the feed flowrate to the gas-tail.

(Note the constraint violation)

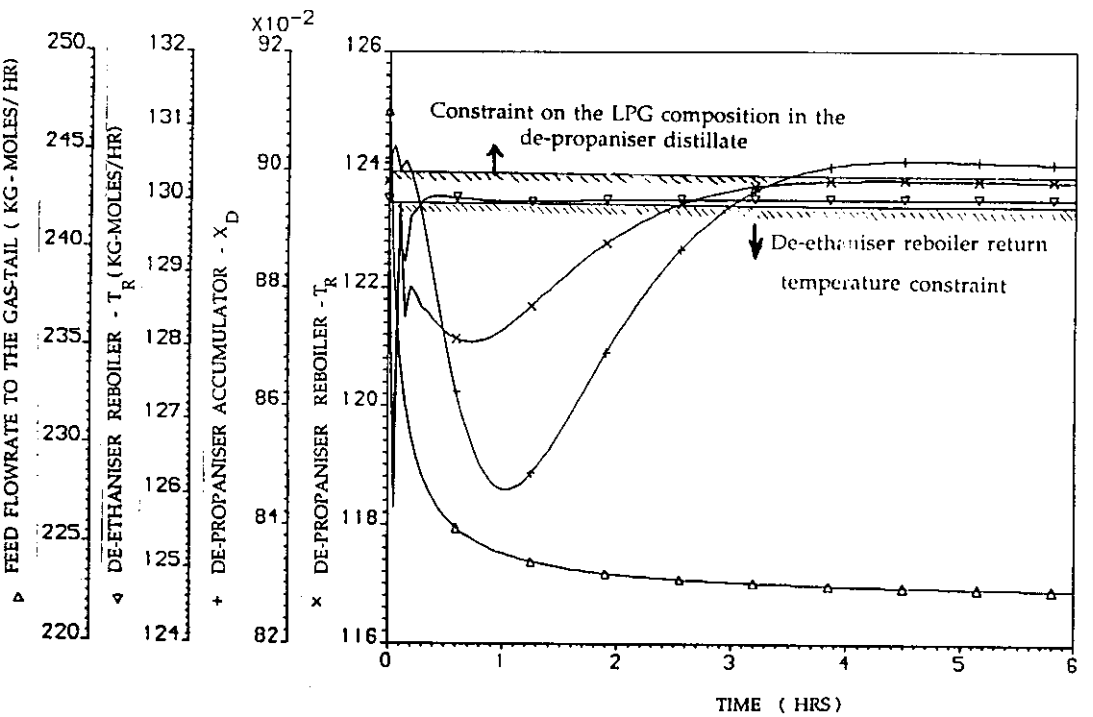

Figure 6. 5. 35

Dynamic response of the de-isobutaniser control objectives to a - 10.0 % step change in the feed flowrate to the gas-tail.

(Note the constraint violation)

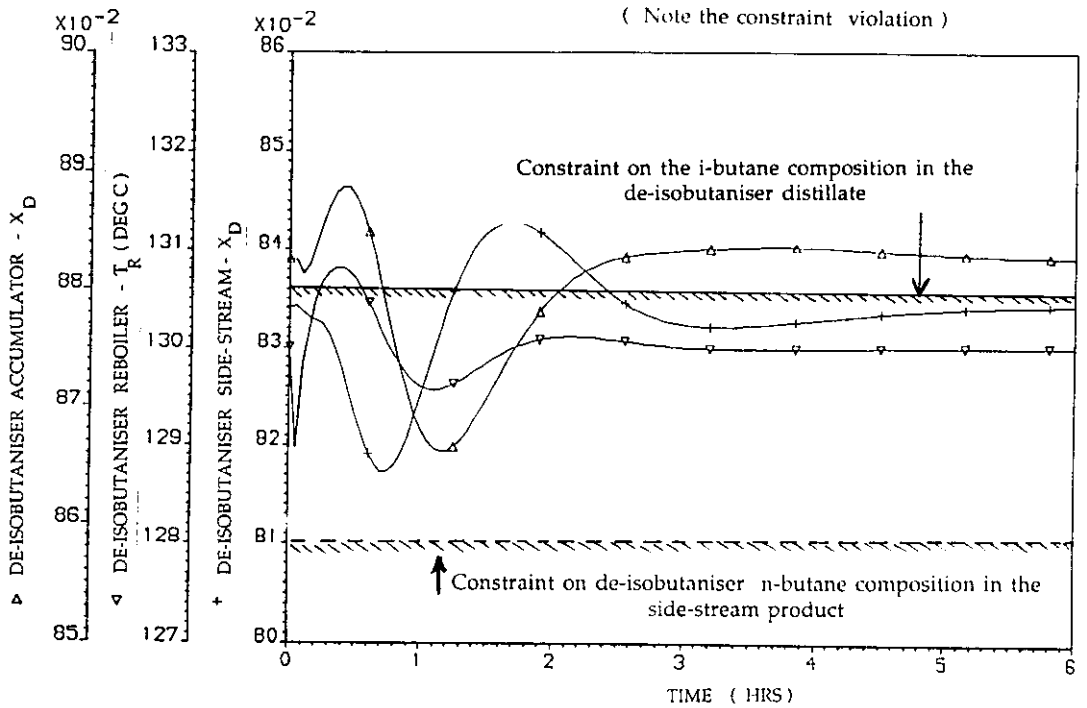

CHAPTER 7

CONCLUSIONS AND RECOMMENDATIONS

7.1 CONCLUSIONS

Control system synthesis addresses several issues related to process integration, design and control. One of the goals of control system synthesis, lately, is to develop a controller to regulate a process so as to obtain maximum possible economic benefit. The issue of optimising control, therefore, has become an important part of control system synthesis as it requires operating any process at its optimum conditions, despite any external disturbances. In developing an optimising control configuration there are two major tasks. The first task is the identification of an optimum that maximises the profit obtained from the process. The other major task is to develop a control structure that provides process regulation as close to the optimum as possible. Some of the issues related with both tasks, identification of the steady-state optimum and selection of a regulatory optimising control system, were addressed in this thesis. A two-stage approach that provides a consistent basis for the synthesis of optimising control systems was developed and applied to an industrial case-study.

In the first stage of optimising control, a good steady-state process model is required. Based on operational and design considerations, a set of constraints have to be defined that provide a feasible space for any process operation. The optimiser used then searches for a solution within this feasible space (i.e defined by the set of constraints) so as to maximise the defined objective function - in this case, net operational profit. An optimum usually lies at the intersection of several process constraints that are said to be *active* at the identified optimum conditions. The action of any external disturbances on the process is to perturb the plant operation. The key issue addressed in this thesis is that any such deviations from the active constraints either cause an infeasible operation or result in an economic loss. Our overall aim is to minimise this economic loss , whilst ensuring plant operation wholly within the feasible space. To avoid infeasible operation, one simple approach is to back-off from the optimum. This is achieved by moving away from each of the active constraints by a selected amount. The Lagrange multiplier associated with each active constraint provides a linear estimate of the penalty for any such move away from the active constraint. With some knowledge of the frequency and size of the key disturbances frequently influencing process operation , it is therefore possible to compute both the open-loop (i.e. no control) back-off required in each active constraint and the corresponding economic penalty associated with such a back-off.

Each disturbance requires a different amount of back-off from each of the active constraints. The maximum back-off for any constraint should, therefore, ensure no constraint violations during any transient stage of process behaviour arising due to the action of any single external disturbance. Thus, in the absence of a control system, constraint violations can be avoided by operating the process away from the optimum by backing-off from each active constraint by the amount computed. This provides an upper bound on the economic penalty of operating with "no control ". On the other hand, if all the active constraints are maintained by a control system throughout the entire time period, then it represents a "perfect" control system and does not require any back-off from the optimum. The economic penalty , therefore, is zero and this forms a lower bound. The difference between these bounds is the economic incentive a "control system" can offer. If such an incentive is large enough (e.g. when compared to the objective function at the calculated steady-state optimum) , then there is a strong economic justification for having a high performance regulatory control system on the process. However, it must be realised that "perfect control" is impossible to achieve in practice.

Having recognised the relative economic benefits a control system can offer, the issue that needs to be addressed in the second stage is, using a realistic controller , how much of the open-loop penalty for back-off can be recovered. The concept of MPR (i.e. a dimensionless number indicating the maximum percentage recovery) is useful here. The larger the MPR , the closer to perfect control one can get. Though design of a suitable controller followed by extensive closed-loop dynamic simulations can provide useful information regarding the likely MPR value for that controller, it is often tedious and may need significant computational times. An alternative approach is used in this thesis which involves examining the open-loop controllability characteristics of the process which are usually easy to estimate. Several studies over the last decade have confirmed that such open-loop indicators for the controllability of a process do provide useful information in assessing the dynamic characteristics of a process, and can be used to rank alternative processes in terms of their ease of control. In the present study, the l_∞ - norm minimum condition number of a process, estimated over the entire frequency range of interest , was used as the principal open-loop indicator for the process controllability assessment and in rating alternative control systems.

The main feature of this two-stage approach is that, it provides consistent economic and sensitivity information about process controllability. A control system with a large MPR, therefore, implies both a significant open-loop economic penalty recovery and good closed-loop behaviour. The reason for this is as follows. If the open-loop indicators which are fundamental characteristics are "poor", then no control system can prevent some large

fluctuations about its operating point. To avoid constraint violations during transients , despite having a control system, a larger closed-loop back-off from the original optimum may be necessary. In other words, the economic recovery is small and hence the MPR is small.

The major issue that was not satisfactorily resolved in this thesis is that of a rigorous approach for the estimation of the closed-loop back-offs that would guarantee no constraint violation during transients. Such an estimate is a function of the type of external disturbance, the process and controller characteristics , and is not straightforward to determine. A simple heuristic approach is suggested and used throughout all the case-studies.

A systematic methodology for the synthesis of an optimising control scheme for a continuous process is, thus, one of the major contributions of this thesis. To test the applicability of such a methodology, a realistic industrial case-study (i.e. the gas-tail section of Shell's Clyde refinery) was also considered in this thesis. The following are the various stages involved in this application project.

A process model for the gas-tail is essential element of the new control system synthesis approach. Rigorous dynamic models for the distillation columns of the gas-tail, however, would be difficult to develop and would require extensive column data and large simulation times. A new compartmental dynamic model for distillation columns was thus developed, called the *universal compartmental model* (UCM), and shown to provide excellent steady-state estimation and good dynamic tracking. The UCM approach was shown to avoid the spurious characteristic of *initial inverse response*, that was found to occur in other compartmental models available in the literature. The validity of the UCM modelling approach was tested for both binary and multicomponent columns reported in the literature. Good agreement was observed between the UCM and more rigorous model simulations for all the columns studied. The gas-tail of the industrial case-study was , therefore, modelled using the UCM approach and validated at steady-state against both plant trial data and rigorous model simulation results. Good agreement between the simple model, the plant trials and the rigorous simulations results were observed for all cases studied. This satisfies one of the basic requirements of our control system synthesis approach , i.e. the availability of a good process model for both steady-state and dynamic analyses.

Identifying the optimum operating conditions for the gas-tail , however, requires not only a reliable model but also an objective function and a set of constraints that define a feasible

operational space. Various process constraints were defined based on operational, quality control and column design considerations. Overall profit on the gas-tail (i.e. profit due to product sales less the operational costs) was used as the objective function. Heat duties for both the reboilers and condensers, along with the product rates from the three gas-tail columns , were used as the freed variables in the steady-state optimisation. Optimisation studies on the gas-tail model were performed for various combinations of feeds and operating conditions. All these results provided an overview of the limitations on the gas-tail operation, along with several potential design modifications that would improve operational performance.

For one set of operating conditions that are frequently observed on the gas-tail (a high feed rates and high pentanes), six constraints were active at the optimum. The proposed economics based control synthesis approach requires that all the active constraints be held constant during normal plant operation (i.e. be the outputs of the control system). The major disturbances influencing the gas-tail operation were identified along with their realistic ranges (based on plant experience). The back-off necessary from the optimum , with "no control", was first estimated. Significant potential economic benefits were, thus, estimated for installing a control system on the gas-tail. Having decided that a control system on the gas-tail was justified in recovering the large economic penalty associated with open-loop back-off, the question that remains is - which control system can provide the maximum benefit ? A modified constraint control approach, with the active constraints taken as control objectives and an equal number of freed variables as manipulated variables , while the remaining freed variables are held constant at their optimum value, was proposed. The decision of which of the freed variables should be used as manipulated variables was based on plant experience and a careful examination of the optimisation results.

Having decided on the choice of input and output variables in a multiloop control scheme, the next issues to consider are pairing and subsequent closed-loop performance. Though several control configurations are possible , based on plant experience and engineering judgement, one of the decentralised control configurations was chosen as a first pass. The small minimum condition number for the chosen control scheme over the entire frequency range of interest indicated that it may provide good closed-loop performance. On the other hand, a relatively large minimum condition number for the control scheme on the gas-tail currently in operation indicated a large system sensitivity to plant model mismatch, and hence poor closed-loop performance. A significantly large economic recovery in the penalty for back-off from the optimum was reported in the case the proposed optimising control scheme, compared to the control scheme on the gas-tail currently in operation.

Switching the gas-tail operation to the proposed optimising control policy, therefore, was shown to have strong economic justification. Closed-loop simulations on the entire gas-tail provided consistent results with these predictions.

The studies performed in this thesis thus provide a good basis for extending the concepts of integrated design and control for realistic processes.

7.2 RECOMMENDATIONS FOR FUTURE WORK

The proposed two-stage control system synthesis methodology uses a nonlinear process model. Set-points for the regulatory control system of the optimising controller are obtained through optimisation of the nonlinear process model subject to certain operational and design constraints. Optimisation studies on the process model over a range of operating conditions are necessary in identifying the active constraints for the process operation. Both stages of the proposed control system synthesis approach require, however, the process model to be linearised about the selected optimum steady-state.

The following are the three major "nonlinear effects " that need to be considered in future :

(1) Steady-state optimisation :

As discussed previously in Section 5. 3, steady-state optimisation of the nonlinear model is the primary requirement of optimising control. However, optimisation of a nonlinear model often gives rise to a situation , where the number of freed variables is not equal to the number of active constraints. Constraint control (as defined by Maarleveld and Rijnsdorp [1970]) for regulating the process about its optimum, therefore, is not generally not possible. No consistent framework is available to date to address the issue of optimising control in such a situation. In the gas-tail case-study , at the steady-state optimum, there was one less active constraints than the number of freed variables. The approach used in this thesis is based on regulating manually, one of the freed variables at it's optimum value, while the remaining freed variables are used to regulate all the active constraints, similar to a constraint control policy. Selection of which of the freed variables be chosen for a manual regulation, is done in the gas-tail case-study using plant experience and engineering judgement. However, this may not always be possible. An alternative approach would be by selecting an additional control objective (i.e. besides all the active constraints) based on some policy, thereby making use of all the available freed variables for regulating the control objectives. The key issue in this latter approach would be the policy used for selecting the additional

control objective (i.e. apart from all the active constraints). Further investigation on all the related issues would be required.

(2) Estimation of back-offs from the optimum :

A transfer function approach based on a linearised version of the process model is used to estimate the back-off from the optimum. The major deficiency of such an approach , however, is that the predicted estimates are valid only in the vicinity of the calculated optimum steady-state. It is quite possible that back-offs that are physically impossible to realise will be calculated using this approach. For example, in the gas-tail case-study, the open-loop back-offs estimated for the feed flowrate disturbance cannot be physically realised and indicate that nonlinear effects somehow need to be included all such estimations. This issue was not addressed in this thesis and needs further investigation.

(2) Controllability indicators:

The minimum condition number of a process, was the major open-loop indicator used to screen alternative control systems in this case-study. The **RGA** was used to resolve the issue of pairing, in some cases. It must be realised that all these controllability indicators are based on the linear models and may only provide a limited information. This issue related to obtaining a more reliable information on process controllability is crucial in the second stage of the proposed control system synthesis methodology and needs further investigation.

However, despite all the non-linear effects obviously being important in some cases, the linear analysis proposed in this thesis is simple, easy to use , adequate for first-pass calculations and has permitted us to develop a consistent economic methodology for developing optimising control schemes.

Being based on both the process and controller characteristics, there is no systematic approach available to date that would provide a reasonable estimate of the closed-loop back-off from the optimum operating conditions. A simple and easy to use heuristic method, however, was used as a first pass , in the the gas-tail case-study. However, what is ideally required is some form of index relating the closed-loop back-offs to both the process and controller characteristics. The method suggested for estimating both the fractional economic recovery in the open-loop penalty and the closed-loop back-offs, based on maximum singular values of both closed and open-loop transfer function matrices, is simple and easy to compute . However, further examination of the issues associated with this approach , is necessary.

APPENDIX A1

ESTIMATION OF (g_Z^{-1}) FOR THE UNIVERSAL COMPARTMENTAL MODEL (UCM)

In Section 2. 4. 3 it was shown that a nonlinear process can be expressed in state-space form by linearising the process model around a known steady-state. For the UCM approach , the term 'g_Z' of Equation (2. 4. 35) (which is the matrix of derivatives of all the algebraic equations with respect to each algebraic variable) is of the form;

$$g_Z = \begin{bmatrix} -(L+VK_1) & VK_2 & 0 & \cdot & 0 & 0 & 0 \\ L & -(L+VK_2) & VK_3 & \cdot & \cdot & \cdot & \cdot \\ 0 & L & -(L+VK_3) & \cdot & \cdot & \cdot & \cdot \\ \cdot & 0 & L & \cdot & \cdot & \cdot & \cdot \\ \cdot & \cdot & \cdot & \cdot & \cdot & \cdot & \cdot \\ 0 & 0 & 0 & 0 & L & -(L+VK_{N-1}) & VK_N \\ 0 & 0 & 0 & 0 & 0 & 0 & -1 \end{bmatrix}_{NXN} \qquad (A1.1)$$

For a physically realisable system the determinant of g_Z is non zero and hence g_Z can be inverted to give g_Z^{-1} which will be taken to have the following form ;

$$g_Z^{-1} = \begin{bmatrix} C_{11} & C_{21} & \cdot & \cdot & C_{N1} \\ C_{21} & C_{22} & \cdot & \cdot & C_{N2} \\ \cdot & \cdot & \cdot & \cdot & \cdot \\ \cdot & \cdot & \cdot & \cdot & \cdot \\ \cdot & \cdot & \cdot & \cdot & \cdot \\ C_{N1} & C_{N2} & \cdot & \cdot & C_{NN} \end{bmatrix} \qquad (A1.2)$$

Expressions for C_{11} , C_{1N}, C_{N1} and C_{NN} only are derived here, as the remaining elements of the matrix g_Z^{-1} will not be used in the model calculations (see Section 2. 4. 3).

Estimation of the inverse of a square matrix requires computation of its determinant and the adjoints of each of the matrix elements (see Appendix A10). From the definition of inverse of a matrix , the following transformation will be used to estimate the required elements of g_Z^{-1} ;

$$C_{ij}(g_Z^{-1}) = \frac{\text{Adjoint}(g_{Z(ij)})}{\det(g_Z)} \qquad \text{(A1. 3)}$$

where $C_{ij}(g_Z{}^{-1})$ = the element in i^{th} row and j^{th} column of inverse matrix $g_Z{}^{-1}$

Adjoint $(g_{Z(ij)})$ = adjoint of element in i^{th} row and j^{th} column of matrix g_Z

$\det(g_Z)$ = determinant of matrix g_Z.

$$\text{(i)}\ \det(g_Z) = -\det\begin{bmatrix} -(L+VK_1) & VK_2 & 0 & .\ 0 & 0 \\ L & -(L+VK_2) & VK_3 & . . & . \\ 0 & L & -(L+VK_3) & . . & . \\ . & . & . & . . & . \\ . & . & . & . . & VK_{N-1} \\ 0 & 0 & 0 & .\ L & -(L+VK_{N-1}) \end{bmatrix}_{(N-1)\,X\,(N-1)}$$

(A1. 4)

The matrix g_Z has a tri-diagonal form and hence the determinant can be shown to contain N terms;

$$\det(g_Z) = (-1)^N(\text{Term 1} + \text{Term 2} + \ldots\ldots\ldots + \text{Term N}) \qquad \text{(A1.5)}$$

where

$$\text{Term 1} = L^{N-1}$$

$$\text{Term 2} = L^{N-2}VK_1$$

$$\text{Term 3} = L^{N-3}V^2K_1K_2$$

.....

$$\text{Term N} = V^{N-1}(K_1K_2 \ldots K_N) \qquad \text{(A1. 6)}$$

For a physically realisable system, all the terms in the parentheses of Equation (A1. 5) are positive.

$$\therefore \det(g_Z) \quad > 0 \text{ for N even}$$

$$< 0 \text{ for N odd} \qquad \text{(A1.7)}$$

(ii) Adjoint of $g_{Z(11)}$ = Cofactor of $g_{Z(11)}$

Adjoint of $g_{Z(11)}$ =

$$\det \begin{bmatrix} -(L+VK_2) & VK_3 & 0 & . & 0 & 0 & 0 \\ L & -(L+VK_3) & VK_4 & . & . & . & . \\ . & . & . & . & . & . & . \\ . & . & . & . & L & -(L+VK_{N-1}) & VK_N \\ 0 & 0 & 0 & . & 0 & 0 & -1 \end{bmatrix}_{(N-1)\ X\ (N-1)} \qquad (A1.8)$$

The above matrix also has a tri-diagonal form and hence its determinant can be shown to contain N terms;

$$= (-1)^{N-1}(\text{Term } 1 + \text{Term } 2 + \ldots\ldots\ldots + \text{Term } N) \qquad (A1.9)$$

where

$$\text{Term } 1 = L^{N-1}$$

$$\text{Term } 2 = L^{N-2}VK_2$$

$$\text{Term } 3 = L^{N-3}V^2K_2K_3$$

.....

$$\text{Term } N = V^{N-1}(K_2K_3 \ldots K_N) \qquad (A1.10)$$

For a physically realisable system, all the terms in the parentheses of Equation (A1.9) are positive.

$$\text{Adjoint of } g_{Z(11)} \quad \begin{matrix} < \\ > \end{matrix} \quad \begin{matrix} 0 \\ 0 \end{matrix} \quad \begin{matrix} \text{if N is even} \\ \text{if N is odd} \end{matrix} \qquad (A1.11)$$

$$\therefore \quad C_{11} = \frac{\text{Adjoint of } g_{Z(11)}}{\det(g_Z)} \quad < 0 \quad \text{for all N} \qquad (A1.12)$$

(iii) Adjoint of $g_{Z(N1)}$ = Cofactor of $g_{Z(1N)}$ = 0

$$C_{N1} = \frac{\text{Adjoint of } g_{Z(N1)}}{\det(g_Z)} \quad = 0 \quad \text{for all N} \qquad (A1.13)$$

(iv) Adjoint of $g_{Z(1N)}$ = Cofactor of $g_{Z(N1)}$

Adjoint of $g_{Z(1N)}$ =

$$(-1)^{N+1} \det \begin{bmatrix} VK_2 & 0 & . & 0 & 0 & 0 \\ -(L+VK_2) & VK_3 & . & . & . & . \\ . & . & . & . & . & . \\ . & . & . & . & . & . \\ 0 & 0 & . & L & -(L+VK_{N-1}) & VK_N \end{bmatrix}_{(N-1) \times (N-1)} \quad \text{(A1. 14)}$$

$$= (-1)^{N+1} V^{N-1} (K_2 K_3 ..... K_N) \quad > 0 \quad \text{if N is odd}$$

$$< 0 \quad \text{if N is even} \quad \text{(A1. 15)}$$

$$\therefore \quad C_{1N} = \frac{\text{Adjoint of } g_{Z(1N)}}{\det(g_Z)} \quad < \quad 0 \text{ if N is even or odd} \quad \text{(A1 . 16)}$$

(v) Adjoint of $g_{Z(NN)}$ = Cofactor of $g_{Z(NN)}$

$$\text{determinant of} \begin{bmatrix} -(L+VK_1) & VK_2 & 0 & . & 0 & 0 \\ L & -(L+VK_2) & VK_3 & . & . & . \\ 0 & L & -(L+VK_3) & . & . & . \\ . & . & . & . & . & . \\ . & . & . & . & . & VK_{N-1} \\ 0 & 0 & 0 & . & L & -(L+VK_{N-1}) \end{bmatrix}_{(N-1) \times (N-1)}$$

(A1. 17)

This has the same form as for det (g_Z) in Equation (A1. 8) , except that the numerical value in this case is negative.

$$\therefore \quad C_{NN} = -1 \quad \text{(A1. 18)}$$

Thus, all the necessary elements of g_Z^{-1} matrix, estimated in this appendix for the universal compartmental model, will be used in Section 2. 4. 3.

APPENDIX A2

ESTIMATION OF (g_Z^{-1}) FOR THE AVERAGE NODE SECTION (ANS) MODEL

In Section 2. 4. 3 it was shown that a nonlinear process can be expressed in a state-space form by linearising the process model around a known steady-state. For the ANS approach , the term 'g_Z' of Equation (2. 4. 35) (which is the matrix of derivatives of all the algebraic equations with respect to each algebraic variable) is of the form ;

$$g_Z = \begin{bmatrix} -(L+VK_1) & VK_2 & 0 & . & 0 & 0 & 0 \\ L & -(L+VK_2) & VK_3 & . & . & . & . \\ . & . & . & . & . & . & . \\ . & . & . & . & . & . & . \\ 0 & 0 & 0 & . & L & -(L+VK_{N-1}) & VK_N \\ -1 & -1 & -1 & . & -1 & -1 & -1 \end{bmatrix}_{N \times N} \qquad \text{(A2. 1)}$$

For a physically realisable system the determinant of g_Z is not zero and hence g_Z can be inverted to give g_Z^{-1} which will be taken to have the following form.;

$$g_Z^{-1} = \begin{bmatrix} C_{11} & C_{21} & . & . & C_{N1} \\ C_{21} & C_{22} & . & . & C_{N2} \\ . & . & . & . & . \\ . & . & . & . & . \\ . & . & . & . & . \\ C_{N1} & C_{N2} & . & . & C_{NN} \end{bmatrix} \qquad \text{(A2. 2)}$$

Expressions for C_{11} , C_{1N}, C_{N1} and C_{NN} only are derived here, as the remaining elements of the matrix g_Z^{-1} will not be used in the model calculations (see Section 2. 4. 3).

The definition and transformations used in Appendix A1 to compute the elements of a inverse matrix will be used here also.

$$(i)\quad \det(g_Z) = (-1)\ \det\begin{bmatrix} -(L+VK_1) & VK_2 & 0 & . & 0 & 0 \\ L & -(L+VK_2) & VK_3 & . & . & . \\ 0 & . & . & . & . & . \\ . & . & . & . & . & VK_{N-1} \\ 0 & 0 & 0 & . & L & -(L+VK_{N-1}) \end{bmatrix}_{(N-1)\ X\ (N-1)}$$

$$(-1)^{2N-1}\ (VK_N)\ \det\begin{bmatrix} -(L+VK_1) & VK_2 & 0 & . & 0 & 0 & 0 \\ L & -(L+VK_2) & VK_3 & . & . & . & . \\ . & . & . & . & . & . & . \\ 0 & 0 & 0 & . & L & -(L+VK_{N-2}) & VK_{N-1} \\ -1 & -1 & -1 & . & -1 & -1 & -1 \end{bmatrix}_{(N-1)\ X\ (N-1)}$$

(A2. 3)

$$= D^{N-1}_{N-1,0} + (-1)^{2N-1} VK_N \left(D^{N-2}_{N-2,0} + (-1)^{2N-2} VK_{N-1} \left(D^{N-3}_{N-3,0} + (-1)^{2N-3} VK_{N-2} (\ldots\ldots) \right) \right)$$

(A2. 4)

$$= D^{N-1}_{N-1,0} + (-1)^{N-1} VK_N D^{N-2}_{N-2,0} + (-1)^{2N-2} V^2 K_N K_{N-1} D^{N-3}_{N-3,0} + (-1)^{3N-3} V^3 K_N K_{N-1} K_{N-2} D^{N-4}_{N-4,0} + \ldots\ldots\ldots$$

(A2. 5)

It must be realised that alternative terms of Equation A2. 5 have opposite sign. Using the results for the individual determinants (see Equation A2. 11) i.e. $D^{N-i}_{N-1,0}$ for all i = 1, N , it can be proved that

$$\begin{aligned} \det(g_Z) &< 0 \quad \text{for N is odd} \\ \det(g_Z) &> 0 \quad \text{for N is even} \end{aligned}$$

(A2. 6)

$$(ii)\quad D^{N-1}_{N-1,0} = (-1)\ \det\begin{bmatrix} -(L+VK_1) & VK_2 & 0 & . & 0 & 0 \\ L & -(L+VK_2) & VK_3 & . & . & . \\ 0 & . & . & . & . & . \\ . & . & . & . & . & VK_{N-1} \\ 0 & 0 & 0 & . & L & -(L+VK_{N-1}) \end{bmatrix}_{(N-1)\ X\ (N-1)}$$

(A2. 7)

The above matrix has a tri-diagonal form and hence, the determinant can be shown to contain N terms ,

$$= (-1)^N(\text{Term 1} + \text{Term 2} + \ldots\ldots\ldots + \text{Term N}) \quad \text{(A2.8)}$$

where

$$\text{Term 1} = L^{N-1}$$

$$\text{Term 2} = L^{N-2}VK_1$$

$$\text{Term 3} = L^{N-3}V^2K_1K_2$$

$$\ldots\ldots\ldots\ldots\ldots\ldots\ldots\ldots\ldots\ldots$$

$$\text{Term N} = V^{N-1}(K_1K_2 \ldots K_N) \quad \text{(A2.9)}$$

For a physically realisable system, all the terms in the parentheses of Equation (A2. 8) are positive.

$$\therefore \det(g_Z) \quad \begin{matrix} > 0 \text{ for } N \text{ even} \\ < 0 \text{ for } N \text{ odd} \end{matrix} \quad \text{(A2.10)}$$

The structure of determinant of $D^{N-i}_{N-i,0}$ for all i = 1, N has a form similar to the one shown in equation (A2. 7) and all such determinants can be proved have the following characteristics.

$$\begin{matrix} D^{N-i}_{N-i,0} > 0 \text{ for } N \text{ even and } i \text{ even} \\ < 0 \text{ for } N \text{ even and } i \text{ odd} \\ > 0 \text{ for } N \text{ odd and } i \text{ odd} \\ < 0 \text{ for } N \text{ odd and } i \text{ even} \end{matrix} \quad \text{(A2.11)}$$

$$\text{(iii) Adjoint}(g_{Z(11)}) = \det \begin{bmatrix} -(L+VK_2) & VK_3 & 0 & \ldots & 0 & 0 & 0 \\ L & -(L+VK_3) & VK_4 & \ldots & \ldots & \ldots & \ldots \\ \ldots & \ldots & \ldots & \ldots & \ldots & \ldots & \ldots \\ 0 & 0 & 0 & \ldots & L & -(L+VK_N) & VK_N \\ -1 & -1 & -1 & \ldots & -1 & -1 & -1 \end{bmatrix}_{(N-1)\times(N-1)} \quad \text{(A2.12)}$$

$$= D^{N-1}_{N,1^*} \quad \text{(A2.13)}$$

$$= D^{N-2}_{N-1,1^*} - VK_N D^{N-3}_{N-2,,1^*} + V^2K_NK_{N-1} D^{N-4}_{N-3,1^*} - V^3K_NK_{N-1}K_{N-2} D^{N-5}_{N-4,1^*} + \ldots\ldots \quad \text{(A2.14)}$$

The structure of determinant of $D^{N-i-1}_{N-i,1^*}$ for all i = 1, N has a form similar to the one shown in equation (A2. 11) and all such determinants can be proved have the following characteristics.

$$D^{N-i}_{N-1,0} \begin{cases} < 0 & \text{for N even and i even} \\ > 0 & \text{for N even and i odd} \\ < 0 & \text{for N odd and i odd} \\ > 0 & \text{for N odd and i even} \end{cases} \qquad \text{(A2.15)}$$

$$\therefore \quad C_{11} = \frac{\text{Adjoint } (g_{Z(11)})}{\det(g_Z)} < 0 \quad \text{for N is even or odd} \qquad \text{(A2. 16)}$$

(iv) Adjoint $(g_{Z(N1)})$ = Cofactor of $(g_{Z(1N)})$

$$\text{Adjoint } (g_{Z(N1)}) = (-1)^{N+1} \det \begin{bmatrix} L & -(L+VK_2) & VK_3 & 0 & . & 0 & 0 \\ 0 & L & -(L+VK_3) & VK_4 & . & . & . \\ . & . & . & . & . & . & VK_{N-1} \\ . & . & . & . & . & L & -(L+VK_{N-1}) \\ 1 & 1 & 1 & 1 & . & 1 & 1 \end{bmatrix}_{(N-1) \times (N-1)} \qquad \text{(A2. 17)}$$

$$= (-1)^{N+1} \left\{ (-1)^N D^{N-2}_{N-1,1} + (-1)^{N-1} L D^{N-3}_{N-1,2} + \ldots\ldots + L^{N-2} \right\} \qquad \text{(A2. 18)}$$

$$\therefore \quad C_{N1} = \frac{\text{Adjoint } (g_{Z(N1)})}{\det(g_Z)} > 0 \quad \text{for N odd or even} \qquad \text{(A2. 19)}$$

(v) Adjoint of $(g_{Z(1N)})$ = Cofactor of $(g_{Z(N1)})$

$$\text{Adjoint}(g_{Z(1N)}) = (-1)^{N+1} \det \begin{bmatrix} VK_2 & 0 & . & 0 & 0 & 0 \\ -(L+VK_2) & VK_3 & . & . & . & . \\ L & . & . & . & . & . \\ . & . & . & . & . & . \\ 0 & 0 & . & L & -(L+VK_{N-1}) & VK_N \end{bmatrix}_{(N-1) \times (N-1)}$$

(A2. 20)

$$= (-1)^{N+1} V^{N-1} (K_2 K_3 \ldots\ldots K_N) \qquad \text{(A2. 21)}$$

$$\begin{cases} > 0 & \text{for N odd} \\ < 0 & \text{for N even} \end{cases} \qquad \text{(A2.22)}$$

$$\therefore \quad C_{1N} = \frac{\text{Adjoint } (g_{Z(1N)})}{\det(g_Z)} < 0 \quad \text{if N is even or odd} \qquad \text{(A2. 23)}$$

$$(vi) \quad \text{Adjoint of } (g_{Z(NN)}) = D^{(N-1)}_{N-1,0} \begin{cases} > 0 & \text{for N odd} \\ < 0 & \text{for N even} \end{cases} \qquad \text{(A2. 24)}$$

$$\therefore \quad C_{NN} = \frac{\text{Adjoint } (g_{Z(NN)})}{\det(g_Z)} < 0 \text{ for N is even or odd} \qquad \text{(A2. 25)}$$

Thus all the necessary elements of g_Z^{-1} matrix, estimated in this appendix for the average node section model, will be used in Section 2. 4. 3.

APPENDIX A3

ESTIMATION OF (g_Z^{-1}) FOR THE BENALLOU'S MODEL

In section 2. 4. 3 it was shown that a nonlinear process can be expressed in a state-space form by linearising the process model around a known steady-state. For the Benallou's compartmental approach, the term g_Z of Equation (2. 4. 35) (which is the matrix of derivatives of all the algebraic equations with respect to each algebraic variable) is of the form ;

$$g_Z = \begin{bmatrix} -(L+VK_1) & VK_2 & 0 & . & 0 & . & 0 & 0 & 0 \\ L & -(L+VK_2) & VK_3 & . & . & . & . & . & . \\ . & . & . & . & . & . & . & . & . \\ . & . & . & . & . & . & L & -(L+VK_{N-1}) & VK_N \\ 0 & 0 & 0 & . & -1 & . & 0 & 0 & 0 \end{bmatrix} \qquad \text{(A3.1)}$$

where S^{th} column contains -1.

For a physically realisable system the determinant of g_Z is not zero and hence g_Z can be inverted as g_Z^{-1} which will be taken to have the following form ;

$$g_Z^{-1} = \begin{bmatrix} C_{11} & C_{21} & . & . & C_{N1} \\ C_{21} & C_{22} & . & . & C_{N2} \\ . & . & . & . & . \\ . & . & . & . & . \\ . & . & . & . & . \\ C_{N1} & C_{N2} & . & . & C_{NN} \end{bmatrix} \qquad \text{(A3. 2)}$$

Expressions for C_{11} , C_{1N}, C_{N1} and C_{NN} , only, are derived here as the remaining elements of the matrix g_Z^{-1} will not be used in the model calculations (see Section 2. 4. 3).

The definition and transformations used in Appendix A1 to compute the elements of an inverse matrix will be used here also.

(i) As the position of column containing ' - 1' in the matrix g_Z changes , the matrices used for computing the determinant also change accordingly. Three types of matrices are considered here.

(a) For S = 1

$$\det(g_Z) = (-1)^N \begin{bmatrix} VK_2 & 0 & . & 0 \\ -(L+VK_2) & VK_3 & . & . \\ L & -(L+VK_3) & . & . \\ . & . & . & . \\ 0 & 0 & . & VK_N \end{bmatrix} \qquad \text{(A3. 3)}$$

$$\det(g_Z) = (-1)^N V^{N-1} (K_2 K_3 \ldots K_N)$$

$$> 0 \quad \text{if } N \text{ is even}$$

$$< 0 \quad \text{if } N \text{ is odd} \qquad \text{(A3.4)}$$

(b) For S = N, $\det(g_Z)$ has a form similar to the one, in the case of UCM approach (see Appendix A1).

$$\det(g_Z) = -\det \begin{bmatrix} -(L+VK_1) & VK_2 & 0 & . & 0 & 0 \\ L & -(L+VK_2) & VK_3 & . & . & . \\ 0 & L & -(L+VK_3) & . & . & . \\ . & . & . & . & . & . \\ . & . & . & . & . & VK_{N-1} \\ 0 & 0 & 0 & . & L & -(L+VK_{N-1}) \end{bmatrix}_{(N-1)\,X\,(N-1)}$$

(A3. 5)

The matrix g_Z, now has a tri-diagonal form and hence the determinant can be shown to contain N terms,

$$\det(g_Z) = (-1)^N (\text{Term 1} + \text{Term 2} + \ldots\ldots\ldots + \text{Term N}) \qquad \text{(A3. 6)}$$

where

$$\text{Term 1} = L^{N-1}$$

$$\text{Term 2} = L^{N-2} VK_1$$

$$\text{Term 3} = L^{N-3} V^2 K_1 K_2$$

.....

$$\text{Term N} = V^{N-1} (K_1 K_2 \ldots K_N) \qquad \text{(A3.7)}$$

For a physically realisable system, all the terms in the parentheses of Equation (A3. 6) are positive.

$$\therefore \det(g_Z) \quad \begin{matrix} > 0 \text{ for } N \text{ even} \\ < 0 \text{ for } N \text{ odd} \end{matrix} \qquad \text{(A3.8)}$$

(c) For $S \neq N$, $\det(g_Z)$ will have the following form ;

$$\det(gZ) = (-1)^{N+S+1} \begin{bmatrix} -(L+VK_1) & VK_2 & . & . & . & . \\ L & -(L+VK_2) & . & . & . & . \\ 0 & L & . & VK_{S-1} & . & . \\ 0 & 0 & . & -(L+VK_{S-1}) & VK_{S+1} & . \\ . & . & . & L & . & . \\ . & . & . & . & . & . \\ 0 & 0 & . & 0 & 0 & VK_N \end{bmatrix}_{(N-1)\,X\,(N-1)}$$

(A3. 9)

The matrix g_Z has a tri-diagonal form and hence the determinant can be shown to contain N terms that are of the form,

$$= (-1)^N (V)^{N-S} (K_{S+1} \ldots K_N) (\text{Term } 1 + \text{Term } 2 + \ldots\ldots\ldots + \text{Term } S) \qquad \text{(A3. 10)}$$

where

$$\text{Term } 1 = L^{S-1}$$

$$\text{Term } 2 = L^{S-2} VK_1$$

$$\text{Term } 3 = L^{S-3} V^2 K_1 K_2$$

.....

$$\text{Term } S = V^{S-1} (K_1 K_2 \ldots K_{S-1}) \qquad \text{(A3.11)}$$

For a physically realisable system, all the terms in the parentheses of Equation (A3. 10) are positive.

Thus, from the above analysis it is clear that the determinant of g_Z is independent of the position of S.

$$\det(g_Z) \quad \begin{matrix} > 0 & \text{if } N \text{ is even for all } S \\ < 0 & \text{if } N \text{ is odd for all } S \end{matrix} \qquad \text{(A3. 12)}$$

(ii) Adjoint of $g_{Z(11)}$ = Cofactor of $g_{Z(11)}$

Again, depending on the position of the column containing '-1', the structure of the corresponding for computing the cofactor changes. Four types of matrices are considered here.

(a) S = 1

$$\text{Adjoint of } g_{Z(11)} = (-1)^N \begin{bmatrix} VK_3 & 0 & .0 \\ -(L+VK_3) & VK_4 & .. \\ L & -(L+VK_4) & .. \\ . & . & .. \\ 0 & 0 & .0 \end{bmatrix}_{(N-2)\,X\,(N-2)} \quad \text{(A3. 13)}$$

$$= 0 \qquad \text{if N is odd or even} \quad \text{(A3.14)}$$

(b) S = 2

$$\text{Adjoint of } g_{Z(11)} = (-1)^N \begin{bmatrix} VK_3 & 0 & . & 0 \\ -(L+VK_3) & VK_4 & . & . \\ L & -(L+VK_4) & . & . \\ . & . & . & . \\ 0 & 0 & . & VK_N \end{bmatrix}_{(N-2)\,X\,(N-2)} \quad \text{(A3. 15)}$$

$$\text{Adjoint}\,(g_{Z(11)}) = (-1)^{N-1} V^{N-2} (K_3 \ldots K_N)$$

$$> 0 \qquad \text{if N is odd}$$

$$< 0 \qquad \text{if N is even} \quad \text{(A3.16)}$$

(c) S = N

$$\text{Adjoint of } g_{Z(11)} =$$

$$\det \begin{bmatrix} -(L+VK_2) & VK_3 & 0 & . & 0 & 0 & 0 \\ L & -(L+VK_3) & VK_4 & . & . & . & . \\ . & . & . & . & . & . & . \\ . & . & . & . & L & -(L+VK_{N-1}) & VK_N \\ 0 & 0 & 0 & . & 0 & 0 & -1 \end{bmatrix}_{(N-1)\,X\,(N-1)} \quad \text{(A3. 17)}$$

The above matrix also has a tri-diagonal form and hence its determinant can be shown to contain N terms,

$$= (-1)^{N-1} (\text{Term 1} + \text{Term 2} + \ldots\ldots\ldots + \text{Term N}) \quad \text{(A3.18)}$$

where

$$\text{Term 1} = L^{N-1}$$

$$\text{Term 2} = L^{N-2} VK_2$$

$$\text{Term } 3 = L^{N-3}V^2K_2K_3$$

.....

$$\text{Term } N = V^{N-1}(K_2K_3 \ldots K_N) \qquad \text{(A3.19)}$$

For a physically realisable system, all the terms in the parentheses of Equation (A1. 18) are positive.

$$\text{Adjoint of } g_{Z(11)} \quad \begin{matrix} < & 0 & \text{if N is even} \\ > & 0 & \text{if N is odd} \end{matrix} \qquad \text{(A3.20)}$$

(d) For $S \neq N$, Adjoint of $g_{Z(11)}$ depends on the position of S as shown below ;

$$\text{Adjoint of } g_{Z(11)} = (-1)^{N+S+1}\begin{bmatrix} -(L+VK_2) & VK_3 & . & . & . & . & . \\ L & -(L+VK_3) & . & . & . & . & . \\ 0 & L & . & VK_{S-1} & . & . & . \\ . & . & . & -(L+VK_{S-1}) & . & . & . \\ . & . & . & L & VK_{S+1} & . & . \\ . & . & . & . & . & . & . \\ 0 & 0 & . & 0 & 0 & . & VK_N \end{bmatrix}_{(N-2)X(N-2)}$$

(A1. 21)

The matrix g_Z has a tri-diagonal form and hence the determinant can be shown to contain N terms that are of the form,

$$= (-1)^{N-1}(V)^{N-S}(K_{S+1} \ldots K_N)(\text{Term } 1 + \text{Term } 2 + \ldots\ldots + \text{Term } (S-1)) \qquad \text{(A3. 22)}$$

where,

$$\text{Term } 1 = L^{S-2}$$

$$\text{Term } 2 = L^{S-3}VK_2$$

$$\text{Term } 3 = L^{S-4}V^2K_2K_3$$

.....

$$\text{Term } S = V^{S-2}(K_2 \ldots K_{S-1}) \qquad \text{(A3. 23)}$$

For a physically realisable system, all the terms in the parentheses of Equation (A3. 10) are positive.

$$\text{Adjoint of } g_{Z(11)} \quad \begin{matrix} < & 0 & \text{if N is even} \\ > & 0 & \text{if N is odd} \end{matrix} \qquad \text{(A3.24)}$$

Again, it is clear from above analysis that the adjoint of $g_{Z(11)}$ is independent of S.

$$\therefore \quad C_{11} = \frac{\text{Adjoint}\,(g_{Z(11)})}{\det(g_Z)} \quad \begin{cases} < 0 & \text{for all N and S} \\ = 0 & \text{if S = 1} \end{cases} \qquad \text{(A3.25)}$$

(iii) Adjoint of $g_{Z(N1)}$ = Cofactor of $g_{Z(1N)}$

Again, depending on the position of the column containing '-1', the structure of the corresponding matrix for computing the cofactor, changes. Three types of matrices are considered here.

(a) S = 1

Adjoint of $g_{Z(N1)}$ =

$$(-1)^{N+1} \det \begin{bmatrix} L & -(L+VK_2) & VK_3 & . & 0 & . \\ 0 & L & -(L+VK_3) & . & . & . \\ . & . & L & . & . & . \\ . & . & . & . & . & -(L+VK_{N-1}) \\ -1 & 0 & 0 & . & 0 & 0 \end{bmatrix}_{(N-1)\,X\,(N-1)}$$

(A3. 26)

The above matrix has a tri-diagonal form and hence its determinant can be shown to contain N terms,

$$= (-1)^N (\text{Term 1} + \text{Term 2} + \ldots\ldots\ldots + \text{Term (N-S)}) \qquad \text{(A3. 27)}$$

where,

$$\text{Term 1} = L^{N-2}$$

$$\text{Term 2} = L^{N-3} V K_2$$

$$\text{Term 3} = L^{N-4} V^2 K_2 K_3$$

.....

$$\text{Term (N - S)} = V^{N-S-1} (K_2 K_3 \ldots K_N) \qquad \text{(A3. 28)}$$

For a physically realisable system, all the terms in the parentheses of Equation (A1. 18) are positive.

$$\text{Adjoint of } g_{Z(N1)} \quad \begin{cases} > 0 & \text{if N is even} \\ < 0 & \text{if N is odd} \end{cases} \qquad \text{(A3.29)}$$

(b) S = N-1

Adjoint of $g_{Z(N1)}$ =

$$(-1)^{N+1} \det \begin{bmatrix} L & -(L+VK_2) & VK_3 & . & 0 & . \\ 0 & L & -(L+VK_3) & . & . & . \\ . & . & L & . & . & . \\ . & . & . & . & -(L+VK_{N-1}) & \\ 0 & 0 & 0 & . & 0 & -1 \end{bmatrix}_{(N-1)\,X\,(N-1)} \quad \text{(A3. 30)}$$

Adjoint of $g_{Z(N1)} = (-1)^N L^{N-S-1}$

Adjoint of $g_{Z(N1)}$ > 0 if N is even

< 0 if N is odd (A3.31)

(c) $S \neq N-1$ or 1

Adjoint of $g_{Z(N1)}$ =

$$\det \begin{bmatrix} L & -(L+VK_2) & VK_3 & . & 0 & . \\ 0 & L & -(L+VK_3) & . & . & . \\ . & . & L & . & . & . \\ . & . & . & . & -(L+VK_{N-1}) & \\ . & 0 & 0 & . & -1 & 0 \end{bmatrix}_{(N-1)\,X\,(N-1)} \quad \text{(A3. 32)}$$

The above matrix has a tri-diagonal form and hence its determinant can be shown to contain N terms,

$$= (-1)^N L^{N-S-1}(\text{Term 1} + \text{Term 2} + \ldots\ldots\ldots + \text{Term } (N-S)) \quad \text{(A3. 33)}$$

where,

Term 1 = L^{N3}

Term 2 = $L^{N-4} V K_3$

Term 3 = $L^{N-5} V^2 K_3 K_4$

.....

Term (N - S) = $V^{N-S-1}(K_3 \ldots K_{S+1})$ (A3. 34)

Adjoint of $g_{Z(N1)}$ > 0 if N is even

< 0 if N is odd (A3.35)

$$\therefore \quad C_{N1} = \frac{\text{Adjoint of } (g_{Z(N1)})}{\det (g_Z)} \quad > 0 \text{ for all N and S} \quad \text{(A3. 36)}$$

(iv) Adjoint of $g_{Z(1N)} = (-1)^{N+1} V^{N-1} (K_2 K_3 ..... K_N)$ (A3. 37)

Adjoint of $g_{Z(1N)}$ < 0 if N is even

> 0 if N is odd

$$\therefore \quad C_{1N} = \frac{\text{Adjoint } (g_{Z(1N)})}{\det (g_Z)} \quad < 0 \text{ for all N and S} \qquad (A3.38)$$

(v) Adjoint $(g_{Z(NN)}) = - \det (g_Z)$ (A3.39)

$$\therefore \quad C_{NN} = \frac{\text{Adjoint of } (g_{Z(NN)})}{\det (g_Z)} \quad < \quad 0 \quad \text{for all N and S} \qquad (A3.40)$$

Thus all the necessary elements of g_Z^{-1} matrix , estimated in this appendix for the Benallou's model, will be used in Section 2. 4. 3.

APPENDIX A4

MODELLING OF AN AIR-COOLED OVERHEAD CONDENSER

The major function of an overhead condenser is to cool and condense the hot vapour from the top of the column. A part of the condensed liquid thus formed is returned to the column as reflux. The remaining part of the condensed liquid is collected as a distillate product. Heat removal is frequently achieved using water or air as the cooling medium.

Air-cooled condensers are generally in the form of fin-fans. Air flowrate is regulated both by the number of fins-fans in operation and by the pitch of the blades in the fin-fans. Given sufficiently large cooling, all the hot vapour entering the condenser will be condensed. If the hot vapour is cooled to below its bubble point temperature , then we have a *total condenser* . On the other hand, if adequate cooling is not available, then some of the hot vapour remains uncondensed and we have a *partial condenser*. The uncondensed vapour can alter the condenser vapour holdup and consequently the column pressure changes. Regulation of the column pressure is , sometimes, achieved by adjusting the uncondensed vapour collected from the top of the condenser as another product stream.

The following model equations (A4. 1 - A4. 14) describe a partial overhead condenser (see Figure A4. 1) and will be used in the gas-tail case-study. The following terminology will be used to in these model equations ;

$M_p^{(in)}$	=	Flowrate of the process fluid entering the condenser (Kg-moles/hr)
$M_p^{(out)}$	=	Flowrate of the process fluid leaving the condenser (Kg-moles/hr)
$M_A^{(in)}$	=	Flowrate of the air (Kg-moles/hr)
M_{cond}	=	Rate at which the vapour is condensed (Kg-moles/hr)
R	=	Reflux rate (Kg-moles/hr)
D	=	Distillate product rate (Kg-moles/hr)
D_{UC}	=	Flowrate of the uncondensed vapours (Kg-moles/hr)
H^V	=	Vapour holdup (Kg-moles)
H^L	=	Liquid holdup (Kg-moles)
$T_A^{(in)}$	=	Inlet air temperature (deg C)
$T_A^{(out)}$	=	Exit air temperature (deg C)
$T_P^{(in)}$	=	Inlet temperature of the vapour (deg C)
$T_P^{(out)}$	=	Exit temperature of the vapour (deg C)
T_{Dew}	=	Dew point temperature of the uncondensed vapour (deg C)
T_{Bub}	=	Bubble point temperature of the condensed process fluid (deg C)

Figure A4. 1
Modelling of an overhead condenser

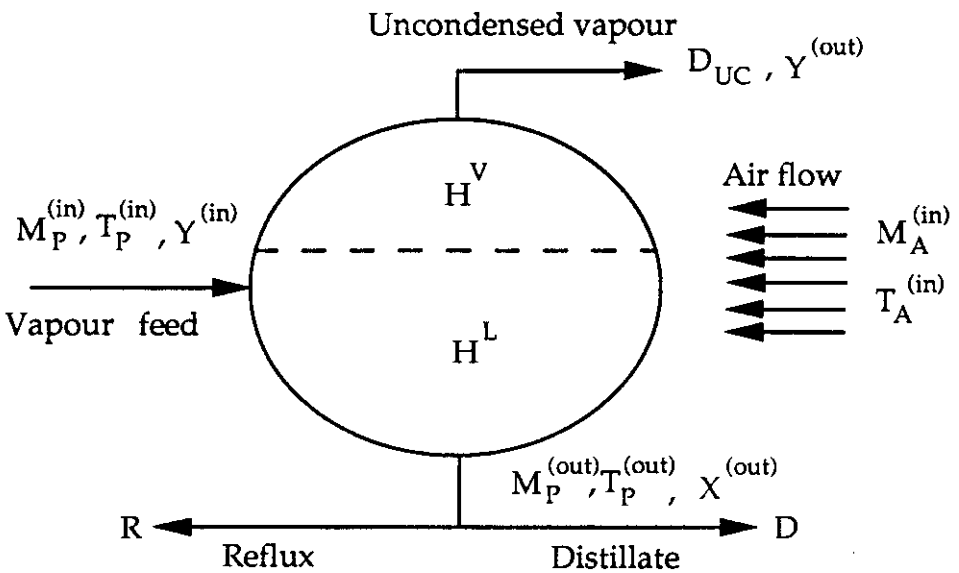

ΔT_{lmtd}	=	Log-mean temperature difference (deg C)
λ	=	Latent heat of condensation of the process fluid (Kcal/Kg-mole)
UA	=	Effective overall heat transfer coefficient (Kcal / deg C . hr)
ρ_L	=	Molar density of the process fluid (Kg-moles/ m^3)
V_{cond}	=	Volume of the condenser (m^3)
Q	=	Heat exchange duty of the condenser (Kcal/ hr)
P	=	Pressure in the condenser (Bar)
T_{pA}	=	Absolute temperature of the process fluid at the inlet (deg K)
R	=	Gas-constant (Bar . m^3 / Kg-moles . deg K)
α_i	=	Relative volatilities of the mixture components
$Y_i^{(in)}$	=	Component mole fractions in the inlet vapour (i = 1, .. , n)
$Y_i^{(out)}$	=	Component mole fractions in the uncondensed vapour (i =1, 2,.., n)
$X_i^{(out)}$	=	Component mole fractions in the condensed liquid (i =1, .., n)
n	=	Number of components in the separation mixture.

Model development is based performing mass and energy balances over the overhead condenser. The following assumptions have been used in modelling a partial over-head condenser ;

(a) Vapour and liquid phase changes take place at constant pressure.

(b) Enthalpy changes are significantly faster than composition changes and hence only the dynamics of the composition need to be modelled.

(c) Pressure dynamics of the column have been modelled entirely through the condenser.

Model Equations

Overall mass balance

$$\frac{dH^V}{dt} = M_P^{(in)} - M_{cond} - D_{UC} \qquad \text{(A4. 1)}$$

$$\frac{dH^L}{dt} = M_{cond} - M_P^{(out)} \qquad \text{(A4. 2)}$$

where $M_P^{(out)} = R + D$

Component mass balance

$$H^{L}\left(\frac{dX_i^{(out)}}{dt}\right) = M_P^{(in)}\,(Y_i^{(in)} - X_i^{(out)}) - D_{UC}\,(Y_i^{(out)} - X_i^{(out)}) \quad (\text{for all } i = 1,.., n) \qquad (A4.\ 3)$$

Pressure dynamics

$$V_{cond} = \frac{H^{V}}{(P * R^{*} T_{pA})} + \frac{H^{L}}{\rho_L} \qquad (A4.\ 4)$$

where $T_{pA} = T_P^{(in)} + 273.0$

Vapour-liquid equilibrium relationships

$$Y_i^{(out)} = f\{\alpha_i, X_i^{(out)}\} \qquad (A4.\ 5)$$

Steady-state heat exchange relationships

$$Q = UA.\Delta T_{lmtd} \qquad (A4.6)$$

$$Q = M_{cond}.\lambda_P + M_P^{(in)}\,C_P\,(T_P^{(in)} - T_P^{(out)}) \qquad (A4.\ 7)$$

$$Q = M_A^{(in)}\,C_A\,(T_A^{(out)} - T_A^{(in)}) \qquad (A4.\ 8)$$

$$\Delta T_{lmtd} = \frac{(\Delta T_1 - \Delta T_2)}{\ln\left(\frac{\Delta T_1}{\Delta T_2}\right)} \qquad (A4.\ 9)$$

$$\Delta T_1 = T_P^{(in)} - T_A^{(out)} \quad \text{and} \quad \Delta T_2 = T_P^{(out)} - T_A^{(in)} \qquad (A4.\ 10)$$

The effective overall heat transfer coefficient can be related to the air flowrate through a correlation such as

$$UA = f\{M_A^{(in)}\} \qquad (A4.\ 11)$$

The nature of correlations used in the gas-tail case-study for all the overhead condensers are discussed in Section 3. 1. 1 while Table 3. 1. 1 provides the actual values used.

For a total condenser,

$$T_P^{(out)} = T_{bub} \qquad (A4.\ 12)$$

For a partial condenser, condensed process fluid and uncondensed vapour are in equilibrium. In this case, the temperature of the vapour-liquid equilibrium mixture is obtained from the *inverse lever law* (see Equation 2. 5. 22) as

$$T_P^{(out)} = T_{bub} + \left(\frac{M_P^{(out)}}{M_P^{(out)} + D_{UC}} \right) (T_{dew} - T_{bub}) \qquad \text{(A4. 13)}$$

In the case of an overhead condenser, where the heat exchanging streams have a cross-flow arrangement (i.e. the hot and cold streams move in perpendicular directions), an additional correction factor in the effective log-mean temperature difference (LMTD) is necessary (Kern [1950]). All the overhead condensers in the gas-tail, for example, have a cross-flow type arrangement, and the corrected LMTD (in Equation A4. 6) has the following form ;

$$\Delta T_{lmtd}\ (\text{corrected}) = \Delta T_{lmtd} * C_f \qquad \text{(A4. 14)}$$

where C_f is the cross-flow correction factor.

Cross-flow correction factors often depend on the mechanical design of the condenser system , and several methods are available in the literature to estimate them . Thus, for all the gas-tail overhead condensers the corrected LMTD (see Equation A4. 14) should be used in all the model Equations (A4. 6) - (A4. 9). For all the gas-tail overhead condensers, C_f was estimated based on design specifications provided by Shell (see Table 3. 1. 2).

These model equations can be used for both performance and design problems. Therefore, given a set of results on an overhead condenser with the outlet air and process fluid temperatures measured (i.e. $T_A^{(out)}$, $T_P^{(out)}$, respectively) , it is possible to use the model to estimate both the latent heat of of condensation of the mixture and the overall effective heat transfer coefficient (i.e. λ , UA , respectively). Subsequently, these values (i.e. λ and UA) can be taken as constants in further simulations where the aim is to estimate the outlet temperatures of the air and the process fluid.

This approach was used for the all the overhead condensers throughout the the gas-tail case-study. Plant trial data on the gas-tail (see Section 3. 2. 2) were used used to estimate both λ and UA for all the overhead condensers. The SPEEDUP package was used to perform simulations.

APPENDIX A5

MODELLING OF A THERMOSYPHON REBOILER

A reboiler generally provides the heat necessary to generate an internal vapour stream in a distillation column. Some part of the liquid reaching the reboiler is returned to the column as vapour and is often referred to as the vapour reboil rate. The remaining part of the this liquid is collected as the bottoms product. The heat necessary to generate the required amount of reboil rate is obtained from a heat source, such as steam.

Vertical thermosyphon reboilers (see Figure A5. 1) will be discussed here, as they are used in all the gas-tail columns. In a steam heated thermosyphon reboiler the condensation of steam supplies the majority of the heat duty. The heat thus supplied converts the liquid mixture entering the reboiler into an equilibrium vapour-liquid mixture. This vapour mixture rises through the tubes of the thermosyphon reboiler. During this rise, more entrained liquid is converted into vapour. A disengager at the top of the reboiler separates this vapour-liquid mixture into vapour and liquid streams. The vapour stream re-enters the distillation column near the bottom. The liquid stream, on the other hand, returns to the reboiler. This liquid recycle flow is necessary both to maintain a continuous operation and to avoid the possibility of the reboiler running out of liquid. However, the recycle rate varies significantly with the reboiler operating conditions and is often difficult to estimate. Large recycle ratios (i.e. the ratio of the amount of liquid recycled to the amount of vapour produced) are quite common (typically of the order 10 : 1). Some part of this recycled liquid stream is collected as the bottoms product.

The following model Equations (A5. 1 - A5. 11) describe the operation of a thermosyphon reboiler (see Figure A5. 1). The following terminology will be used in deriving these model equations ;

$M_P^{(in)}$	=	Flowrate of the process fluid at its bubble-point entering the reboiler (Kg-moles/hr)
V	=	Vapour reboil rate (Kg-moles/hr)
R	=	Recycled liquid flowrate (Kg-moles/hr)
B	=	Bottoms product rate (Kg-moles/hr)
$M_S^{(in)}$	=	Flowrate of the steam (Kg-moles/hr)
H_R	=	Liquid holdup in the reboiler (Kg-moles)
$T_S^{(out)}$	=	Outlet temperature of the condensed steam (deg C)
$T_S^{(in)}$	=	Inlet temperature of the saturated steam (deg C)
$P_S^{(in)}$	=	Pressure of the saturated steam (Bar)
$T_P^{(in)}$	=	Inlet temperature of the process fluid (deg C)

Figure A5.1
Modelling of a thermosyphon reboiler

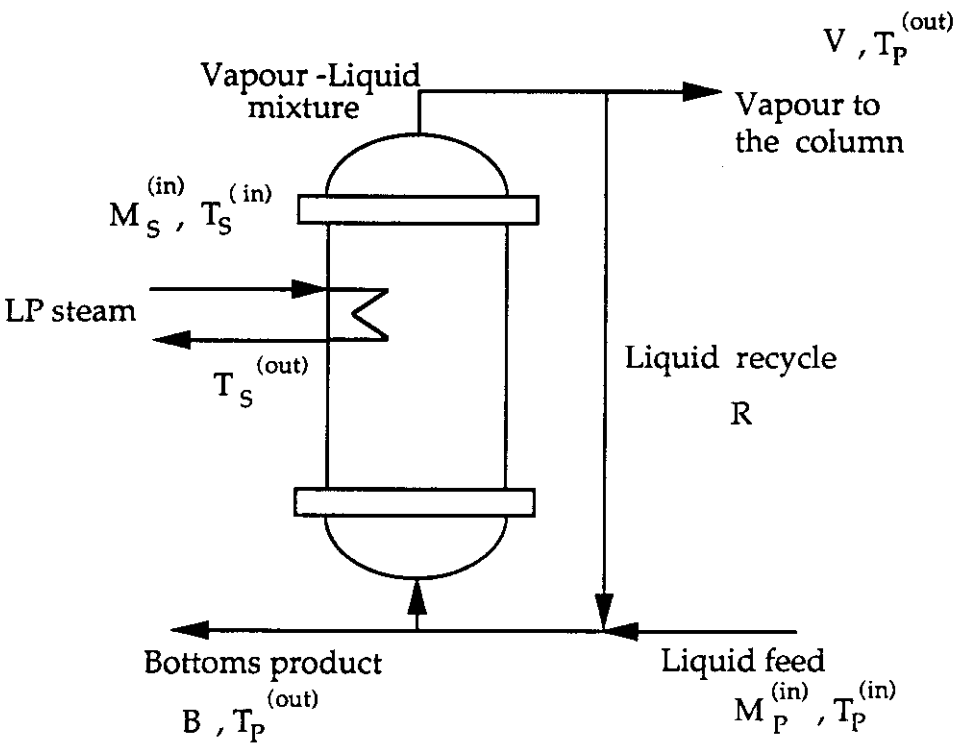

$T_P^{(out)}$	=	Exit temperature of the vapour mixture (deg C)
T_{Dew}	=	Dew-point temperature of the vapour-liquid mixture (deg C)
T_{Bub}	=	Bubble point temperature of the vapour-liquid mixture (deg C)
ΔT_{lmtd}	=	Log-mean temperature difference (deg C)
λ_P	=	Latent heat of vaporisation of the process fluid (Kcal/ Kg-mol)
λ_S	=	Latent heat of condensation of steam (Kcal/ Kg-mol)
UA	=	Effective overall heat transfer coefficient (Kcal / deg C . hr)
Q	=	Heat exchanger duty (Kcal / hr)
α_i	=	Relative volatilities of all components of the mixture (i =1, .., n)
$X_i^{(in)}$	=	Component mole fractions of the process fluid at the inlet conditions (i = 1, .. , n)
$Y_i^{(out)}$	=	Component mole fractions of the vapour product (i =1, .., n)
$X_i^{(out)}$	=	Component mole fractions of the bottoms liquid product (i =1, 2,.., n)
n	=	Number of components present in the separation mixture.

Model development is based performing mass and energy balances over the thermosyphon reboiler. The following assumptions were used in deriving the model equations ;

(a) Vapour and liquid phase changes take place at constant pressure.

(b) Enthalpy changes are significantly faster than composition changes and hence the dynamics of the composition and liquid holdups only need to be modelled. Steady-state balance is used for enthalpy balance.

(c) The temperature difference between process stream and steam (i.e the heat source) in the reboiler provides the necessary driving force for heat transfer , while the heat actually transferred is entirely due the latent heat of vaporisation of steam.

(d) The recycle rate (R) is sufficiently large and has little influence on both the mass and enthalpy balances. Therefore, no significant change in the recycled stream composition and temperature can be observed once a steady-state is established.

Model Equations

Overall mass balance

$$\frac{dH_R}{dt} = M_P^{lin)} - V - B \qquad \text{(A5. 1)}$$

Component mass balance

$$H_R\left(\frac{dX_i^{(out)}}{dt}\right) = M_P^{(in)}\left(X_i^{(in)} - X_i^{(out)}\right) - V\left(Y_i^{(out)} - X_i^{(out)}\right) \quad (\text{for all } i = 1,.., n) \qquad (A5.\ 2)$$

Vapour-liquid equilibrium relationships

$$Y_i^{(out)} = f\{\alpha_i, X_i^{(out)}\} \qquad (A5.\ 3)$$

Steady-state heat exchange relationships

$$Q = UA.\Delta T_{lmtd} \qquad (A5.4)$$

$$Q = M_P.\lambda_P \qquad (A5.\ 5)$$

$$Q = M_S\{\lambda_S + C_S(T_S^{(in)} - T_S^{(out)})\} \qquad (A5.\ 6)$$

where

$$\lambda_S = f(P_S) \qquad (A5.7)$$

$$\Delta T_{lmtd} = \frac{(\Delta T_1 - \Delta T_2)}{\ln\left(\frac{\Delta T_1}{\Delta T_2}\right)} \qquad (A5.\ 8)$$

$$\Delta T_1 = T_S^{(in)} - T_P^{(out)} \quad \text{and} \quad \Delta T_2 = T_S^{(out)} - T_P^{(in)} \qquad (A5.\ 9)$$

The temperature of the vapour-liquid equilibrium mixture is obtained from the *inverse lever law* (see Equation 2. 5. 22) as

$$T_P^{(out)} = T_{bub} + \left(\frac{V}{M_P^{(in)}}\right)(T_{dew} - T_{bub}) \qquad (A5.\ 10)$$

For all the gas-tail thermosyphon reboilers, the process side (which is a vapour-liquid mixture at equilibrium) seems to exert the most influence on the overall heat transfer coefficient, and hence a correlation of the following type was used.

$$UA = f\{M_P^{(in)}\} \qquad (A5.\ 11)$$

Again, the nature of correlations used in the gas-tail case-study are discussed in Section 3. 1. 1, while Table 3. 1. 1 provides the actual values used.

These model equations can be used for both performance and design problems. Therefore, given a set of results on a thermosyphon reboiler with the outlet steam and process fluid temperatures measured (i.e. $T_A^{(out)}$, $T_P^{(out)}$, respectively) , it is possible to use the model to estimate both the latent heat of of vaporisation of the mixture and the overall effective heat transfer coefficient (i.e. λ , UA , respectively). Subsequently, these

values (i.e. λ and UA) can be taken as constants in further simulations where the aim is to estimate the outlet temperatures of the air and the process fluid.

Plant trial data on the gas-tail (see Section 3. 2. 2) were used in each case to estimate both λ and UA. The SPEEDUP package was used to perform simulations.

APPENDIX A6

NON-IDEALITY COEFFICIENT FOR BUBBLE POINT ESTIMATION OF MULTICOMPONENT MIXTURES

The bubble point of a vapour mixture is defined as the temperature at which the first drop of liquid is formed and is related to the vapour pressure of the mixture. The non-ideal nature of components in a vapour-liquid mixture often alters the individual vapour pressures. A correction factor, therefore, is necessary to account for such variations in the vapour pressure, and to obtain a reliable bubble point estimation. A simple approach is proposed here for the estimation of a non-ideality coefficient (γ_{bub}) that is valid over a limited range of operating conditions of interest.

(a) Identify the components in the mixture.

(b) Identify the pressure range of operation.

(c) Identify the range of compositions of the major components in the mixture.

(d) Use an equilibrium flash model with a rigorous physical property package (e.g. PROCESS) to perform a series of bubble point estimations for various pressures and mixture compositions in line with (b) and (c).

(e) Identify the key component of the mixture (typically the least volatile is often chosen as the key component).

(f) Estimate the relative volatilities of the remaining components using the following equation (see Eqution 2. 5. 7) ;

$$\alpha_i = \frac{K_i}{K_k} \qquad \text{for all } i = 1, \ldots, n$$

where ' k ' is the key component.

(g) Use the following equation to estimate γ_{bub} for each bubble point estimation (i.e. performed in stage (d)) and using the relative volatilities estimated in (f).

$$\gamma_{bub} = \left\{ \frac{\sum_{i=1}^{n} (\alpha_{ik} X_i)}{P^{total}} \right\} e^{\left(A + \frac{B}{T_{bub} + C}\right)} \qquad \text{(A6. 1)}$$

where γ_{bub} = non-ideality coefficient for the bubble point temperature

T_{bub} = bubble point temperature of the mixture

α_{ik} = relative volatilities of components (for i = 1, 2, .., n)

Y_i = mole fraction of each component in the mixture (for i = 1, 2, ., n)

P^{total} = the operating pressure

The subscript k indicates key component while A, B and C are the Antoine coefficients for the key component.

(h) An arithmetic average of the γ_{bub} values thus estimated in all these cases can then be taken as a constant in further studies involving this mixture.

The approach proposed will be illustrated through the following example.

Example A6

Consider a six component mixture typical of that present in the de-propaniser's reboiler. The composition variation in the reboiler is essentially due to the variation in pentanes composition in the feed to the gas-tail. Below is the normal composition of the mixture at steady-state.

Component	Mole fraction
Propane	0.007
i-Butane	0.238
n-Butane	0.503
i-Pentane	0.096
n-Pentane	0.072
n-Hexane	0.084

(a) Range of pressure variation = 16 - 20 bar.

(b) Range of composition variation :

i-Butane	0.238 ± 0.05
n-Butane	0.503 ± 0.07
i-Pentane	0.096 ± 0.05
n-Pentane	0.072 ± 0.04
n-Hexane	0.084 ± 0.03

(c) A total of ten different mixtures spanning the entire pressure and composition ranges given in (b) were considered.

(d) n-pentane, the second least volatile component, was chosen as the key component. The following are the Antoine constants obtained from n-pentane (Chilton and Perry [1985]).

A = 9.31, B = -2510.78 and C = 39.47

(e) Given below are the relative volatilities (i.e. with respect to n-pentane) used throughout the gas-tail case-study.

Component	Relative volatility
Propane	3.744
i-Butane	2.241

n-Butane	1.888
i-Pentane	1.159
n-Hexane	0.536

(f) Given below are the bubble points of the ten mixtures (estimated using a rigorous flash model and the physical property data within PROCESS) and the corresponding non-ideality coefficients (γ_{bub}) estimated using Equation (A6. 1).

Bubble point	Non-ideality coefficient (γ_{bub})
111.69	0.782
111.37	0.793
111.06	0.774
112.01	0.762
112.57	0.768
112.34	0.779
108.30	0.789
114.31	0.805
116.84	0.762
118.98	0.786

(g) An average value of **0.78** was chosen as the representative value of γ_{bub} over these pressure and composition ranges. Using $\gamma_{bub} = 0.78$ the bubble point temperature was re-estimated for each of the ten mixtures and plotted against the actual bubble point temperature (see Figure A6.1). Points lying on the 45 degree line indicate that the estimated bubble point is the same as the actual bubble point temperature.

(h) Figure (A6. 1) indicates that a constant value of **0.78** for γ_{bub} provides a reasonably accurate estimation of the bubble point for the six component mixture over the entire range of operating conditions considered.

Figure A6.1
USE OF A NON-IDEALITY COEFFICIENT IN THE ESTIMATION OF THE BUBBLE POINT FOR A MULTICOMPONENT MIXTURE

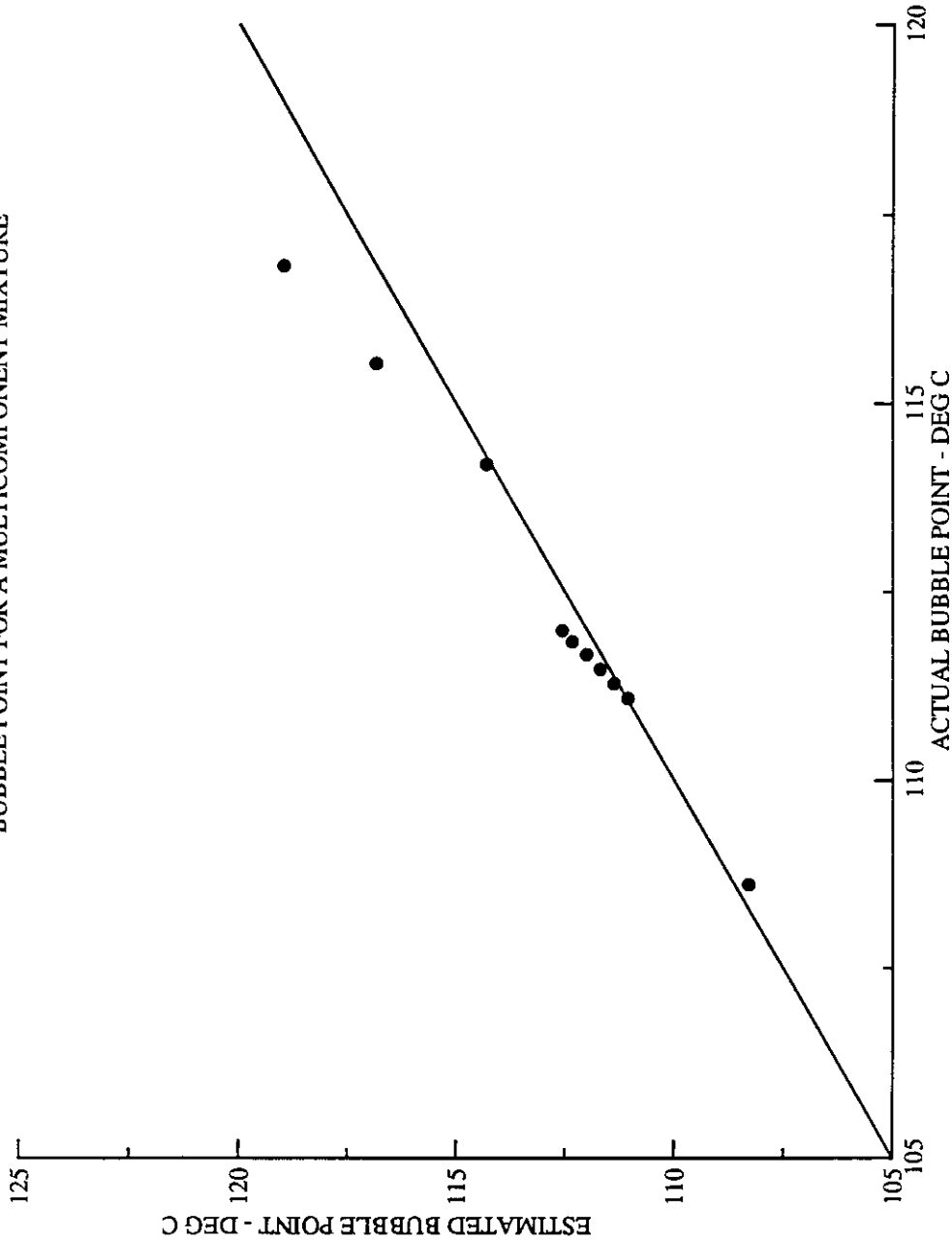

APPENDIX A7

NON-IDEALITY COEFFICIENT FOR DEW POINT ESTIMATION OF MULTICOMPONENT MIXTURES

The dew point of a vapour mixture is defined as the temperature at which the first drop of liquid is formed and is related to the vapour pressure of the mixture. For reasons, similar to those discussed in Appendix A6 , a correction factor for vapour pressure of a non-ideal mixture in vapour phase is necessary. A simple approach is proposed here for the estimation of a non-ideality coefficient (γ_{dew}) that is valid in a certain range of operating conditions of interest.

(a) Identify the components in the mixture.

(b) Identify the pressure range of operation.

(c) Identify the range of compositions of the major components in the mixture.

(d) Use an equilibrium flash model with a rigorous physical property package (e.g. PROCESS) to perform a series of dew point estimations , for various pressures and mixture compositions in line with (b) and (c).

(e) Identify the key component of the mixture (typically the least volatile one is often chosen as the key component).

(f) Estimate the relative volatilities of the remaining components , using the Equation 2.5.7 ;

(g) Use the following equation to estimate (γ_{dew}) for each dew point estimation (i.e. performed in stage (d)) and using the relative volatilities estimated in (f).

$$\gamma_{dew} = \left\{ \frac{1}{P^{total}\left(\sum_{i=1}^{n} \left(\frac{Y_i}{\alpha_{ik}} \right) \right)} \right\} e^{\left(A + \frac{B}{T_{bub} + C} \right)} \qquad \text{(A7. 1)}$$

where

γ_{dew} = non-ideality coefficient for the dew point temperature

T_{dew} = dew point temperature of the mixture

α_{ik} = relative volatilities of components (for i = 1, 2, ..., n)

Y_i = mole fraction of each component in the mixture (for i = 1, 2, ..., n)

P^{total} = the operating pressure

The subscript k indicates key component while A, B and C are the Antoine coefficients for the key component.

(h) An arithmetic average of the γ_{dew} values thus estimated in all these cases can then be taken as constant in further studies involving this mixture.

The approach proposed will be illustrated through the following example.

Example A7

Consider a five component mixture typical of that present in the de-propaniser's overhead condenser. The composition variation in the overhead condenser is essentially due to variation in the ethane and propane in the feed to the de-propaniser. Below is the nominal composition of that mixture at steady-state.

Component	Molefraction
Ethane	0.019
Propane	0.911
i-Butane	0.061
n-Butane	0.008
n-Pentane	0.001

(a) Range of pressure variation = 16 - 20 bar

(b) Range of composition variation :

Ethane	0.019 ± 0.015
Propane	0.911 ± 0.05
i-Butane	0.061 ± 0.03

(c) A total of ten different mixtures spanning the entire pressure and composition ranges given in (b) was considered.

(d) Here also, n-pentane , the second least volatile component , is chosen as the component. The following are the Antoine constants obtained from n-pentane (Chilton and Perry [1985]).

A = 9.31, B = - 2510.78 and C = 39.47

(e) Given below are the relative volatilities (i.e. with respect to n-pentane) used throughout the gas-tail case-study.

Component	Relative volatility
Ethane	13.491
Propane	5.352
i-Butane	2.817
n-Butane	2.268

(f) Given below are the dew points of the ten mixtures (estimated using a rigorous flash model and the physical property data of PROCESS) and the corresponding non-ideality coefficients (γ_{dew}) estimated using Equation (A7.1).

Dew point	Non-ideality coefficient (γ_{dew})
57.98	0.515
57.93	0.521
57.55	0.518
60.29	0.535
62.41	0.527
55.22	0.508
49.93	0.517
51.25	0.524
52.22	0.513
53.56	0.503

(vii) An average value of **0.52** was chosen as the representative value of γ_{dew}. Using $\gamma_{dew} = 0.52$ the dew point temperature was re-estimated for all the ten mixtures and plotted against the actual dew point temperature (see Figure A7.1). Points lying on the 45 degree line indicate that the estimated dew point is same as the actual dew temperature.

(ix) Figure (A7. 1) indicates that a constant value of **0.52** for γ_{dew} provides a reasonably accurate estimation of the dew point for the five component mixture over the entire range of operating conditions considered.

Figure A7.1
USE OF A NON-IDEALITY COEFFICIENT IN THE ESTIMATION OF THE DEW POINT FOR A MULTICOMPONENT MIXTURE

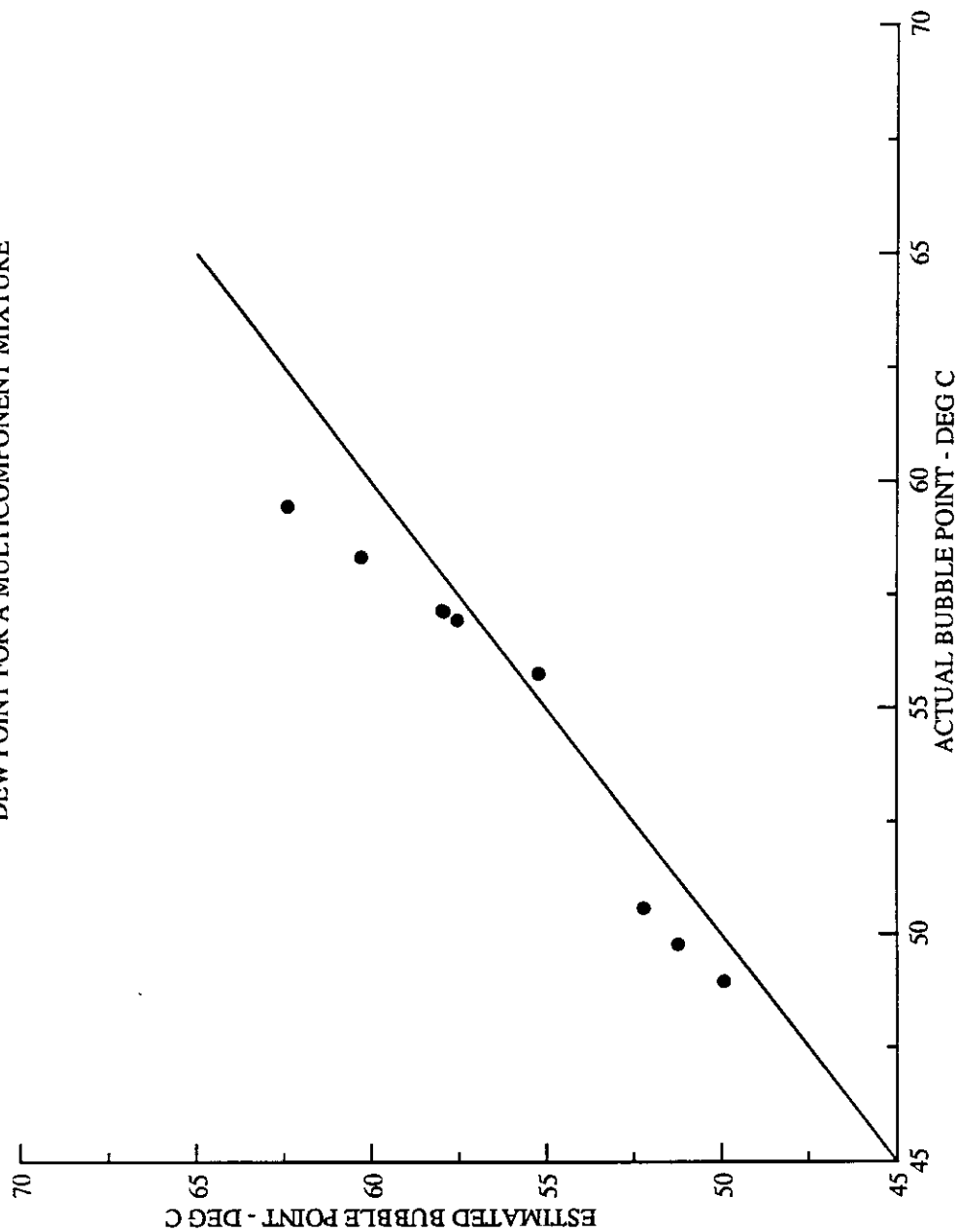

APPENDIX A8

THE SPEEDUP FLOWSHEETING PACKAGE

INTRODUCTION

SPEEDUP is an acronym for Simulation Package for Evaluation and Evolutionary Design of Unsteady Processes. It has been developed over the last two decades within the Department of Chemical Engineering at Imperial College , London and is currently being marketed through PROSYS Technology Ltd.

SPEEDUP is an equation-oriented flowsheeting package and hence all information about the process must be converted into a series of equations (Pantelides [1988]). The equations representing the entire problem are solved simultaneously. These equations can be a mixed set of differential and algebraic types. All the information about the process description can be stored on a database and can be readily retrieved and manipulated. Steady-state and dynamic simulations, as well as optimisation studies for a process, can each be performed using the same input file with little modification. Models for commonly used unit operations are available on the SPEEDUP Library database. The user can write his/her own models and use them in conjunction with the existing library models.

A problem description is presented as an input file to SPEEDUP. This input file consists of various SECTIONS, each of which supplies a specific type of information. Some of these sections are essential, while other are optional. Each of these SECTIONS is separated by a string '****' that denotes the end of the input for that section. Variables used in the various models must all be classified as belonging to a certain TYPE , e. g. mole fraction , temperature, flowrate etc.,. The rationale behind this becomes clearer later on. The mathematical description of the plant is formulated at two levels within SPEEDUP. At the higher level, the information flow is handled through a FLOWSHEET representing the connections between various process UNITS such as reactors , distillation columns etc.,. Each of these connections can either represent a real physical connection (i.e. such as a pipeline linking two units) or an information connection (i.e. a signal flow). This level ensures that the right information is being transferred between various UNITS at all stages of the simulation. Thus, the FLOWSHEET section of the input file contains the structural information for the complete process. The lower level involves the actual description of the process. Each UNIT used in the FLOWSHEET belongs to a specific MODEL that provides all the necessary mathematical descriptions for the corresponding unit operation. More than one UNIT can use the same MODEL. Thus, the FLOWSHEET, along with the various MODELs used , together set up the set of equations describing the

entire process. The numerical routine to solve this set of equations depends on the nature of the equation set and the problem requiring solution.
Given below is a brief description of the sections that must be present in any SPEEDUP input file, for a complete description of the problem.

(a) DECLARE

This section describes various TYPES of variables used in all the models forming the process description. Each type of variable is associated with certain physical units of measurement and has certain lower and upper bounds on the numerical values. These variable bounds mainly assist the simulation routines to search for a solution in the constrained space (i.e within the set bounds) , for all the corresponding variables.

(b) MODEL

Each model contains the mathematical description of a unit operation. Each set of equations can be a mixed set of differential and algebraic equations . Each SPEEDUP input file may contain more than one MODEL. Numerical values for certain physical constants and parameters can be specified here.

(c) UNIT

Each unit operation of a process flowsheet must be described by a single UNIT. However, more than one unit can use the same model.

(d) OPERATION

In this section numerical values for all the input variables , parameters (if not specified in the model) and the degrees of freedom will be specified. A steady-state simulation simply makes use of all these values and solves the equations representing the process description. Some of the specified variables may be freed during optimisation. The optimiser correspondingly varies this set of freed variables to identify a solution, satisfying all the constraints while minimising (or maximising) an objective function. If some variables are specified as functions of time (e.g. a step change at a specified time , or a ramp change), a solution for the problem incorporating these time dependent changes will be obtained at various time intervals during the dynamic simulation. In addition, first estimates of the unknown variables can be specified in the PRESET sub-section of OPERATION. In dynamic simulations the initial values of some of the variables can be specified under the INITIAL sub-section.

Each of these sections may have various sub-sections, each supplying various levels of information that is consistent with all the other sections. Apart from the above sections that are essential in an input file, the following are some of the sections that are optional :

(1) TITLE - specifies the title for the problem.
(2) OPTIONS - allows the user to supply and manipulate various levels of information processed during the simulation.
(3) GLOBAL - describes the objective function and contains the list of constraints. This section is essential for optimisation studies.
(4) REPORT - allows the user to extract information in a certain format.
(5) FUNCTIONS and PROCEDURES - allow the user to interface the input file to various Fortran based functions and subroutines performing specific tasks. When used they form a part of the MODEL.

The SPEEDUP input file for a simple illustrative example representing a blending tank (see Figure A8.1) will be discussed here.

EXAMPLE A8.1

Consider a CSTR with two feeds and one product stream. Here the CSTR acts like a blender. The amount of liquid present in the blender at any instant varies with both the feeds and product rates. The dynamics of liquid holdup can be described through an unsteady mass balance equation as follows :

$$\frac{dH}{dt} = F_1 + F_2 - F_3 \qquad (A8.1)$$

Holdup in the tank (H) is often regulated using the product rate. A square-root control valve , for example, uses the following relationship to perform the regulation ;

$$F_3 = K_C \sqrt{H} \qquad (A8.2)$$

where K_C is the valve constant.

In this problem we have five variables (i.e. F_1, F_2, F_3 , K_C and H) and two equations (i.e A8. 1 and A8. 2). Therefore the problem has three degrees of freedom (i.e. 5 - 2 = 3). Such a problem will have a unique solution when any of three variables are specified. SPEEDUP can be used to perform simulation.

The input file to the SPEEDUP is as follows; (The information enclosed between two ' # ' will be ignored by SPEEDUP compiler and hence can be used for indentation.)

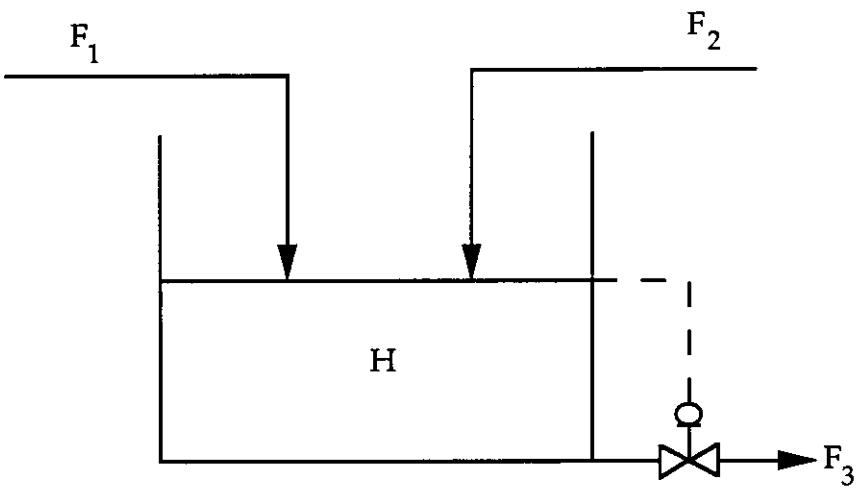

Figure A8.1
Schematic diagram of a blending tank

```
****
# The title of the problem is given in this section. This section is optional. #
TITLE " BLENDING  TANK  SIMULATION "
****
 DECLARE
# Three types of variables are defined in this section (i.e. flowrate type , holdup type #
# and notype ). The initial value , followed by the upper and lower bounds for each    #
# type are also given. This section is compulsory.                                     #
      TYPE
            FLOWRATE = 5.0 : 0.0 : 100          UNITS = " KG-MOLES/HR"
            HOLDUP   = 1.0 : 0.0 :  20          UNITS = " KG-MOLES"
            NOTYPE   = 0.1 : 1.0E-5 : 1.0E+5    UNITS = " NO UNITS"

      STREAM      FLOWSTREAM
            TYPE  FLOWRATE
****
MODEL  TANK
# All the model equations, as discussed previously ( i.e. Equations A8. 1 and A8.2 ),  #
# are supplied here. A delimiter ' ; ' at the end of each equation marks the end of    #
# each equation. A square function (i.e. SQRT) available in the SPEEDUP library is    #
# used here.          #
      TYPE
            F1 , F2, F3     AS    FLOWRATE
            H               AS    HOLDUP
            KC              AS    NOTYPE
      STREAM
            FEED            1     INPUT      1
            FEED            2     INPUT      2
            PRODUCT               OUTPUT
      EQUATION
      # Unsteady material balance equation is given here. '$' here indicates the #
      # differential variable with time.                                         #
            $ H   =    F1 +  F2  - F3      ;
      #  Equation for the square-root control valve is given here. #
            F3    =    KC  *  SQRT ( H )   ;

****
FLOWSHEET
# This section shows how various streams enter and leave the blender. The two input  #
# streams are given by FEED 1 and FEED 2 respectively, while PRODUCT stream          #
# represents output of the blender.                                                  #
      FEED        1     INPUT      1     BLENDER
      FEED        2     INPUT      2     BLENDER
      PRODUCT           OUTPUT           BLENDER
****
UNIT  BLENDER  IS  A  TANK
```

```
      PRODUCT          OUTPUT          BLENDER
****
UNIT  BLENDER   IS  A  TANK
****
OPERATION
      SET
       # Numerical values of 'known variables ' of blending tank have to be specified #
       # here.#
            WITHIN   BLENDER
                 F1      =       5.0    KC  =  10.0
                 F2      =      15.0

      PRESET
       # The starting values for the 'unknown variables ' can be given here. This sub- #
       # section is optional.                                                          #
            WITHIN   BLENDER
                 F3      =      18       ,   H  =  2.0
      INITIAL
      # For a dynamic simulation , the starting value of the differential variable can #
      # be   given here.                                                               #

            WITHIN   BLENDER
                 H       =      1.5

****
```

Thus the above example illustrates, how to convert the mathematical models into the SPEEDUP input files. As discussed previously, steady-state simulation, dynamic simulations and steady-state optimisation can be performed through SPEEDUP using the same input file. The entire case-study of the gas-tail is based on similar approach. The SPEEDUP files used for the gas-tail case-study , however, are not enclosed in this thesis to maintain confidentiality of Shell's regulations. They are available on request from the author/supervisor.

SPEECON

SPEECON is a controllability analysis programme that was originally written and interfaced to SPEEDUP by Wong [1984]. The interfacing routines used in this programme extract the necessary information from the SPEEDUP database after the simulation and estimate several controllability indicators for the process being simulated. Russell [1987] modified the original version of SPEECON , both to make use of the additional features in latest version of SPEEDUP and to widen its applications.

SPEECON runs in two separate stages. The first phase in simulation is concerned with obtaining a state-space form of the nonlinear model specified in the SPEEDUP input file. The following are some of the sub-tasks performed at this stage :

(i) Obtain the values of all variables in the system at a specified time (frequently this is at a steady-state) along with the occurrence matrix representing the equation set.

(ii) Sort out all these variables into different categories (such as , state , fixed , derivative and algebraic variables ; refer to Section 2. 4. 2 for details).

(iii) Allow the user to select the inputs and outputs , which will be used later to derive the state-space form of the system.

(iv) Calculate the Jacobian matrix of the differential-algebraic system of equations employing analytical partial derivatives provided by SPEEDUP wherever possible.

(v) Estimate the steady-state transfer function matrix G (0). Information about the state-space model and the steady-state transfer function matrix are stored in a file for communication to the second phase.

The second phase of SPEECON performs various controllability analyses on the available linear state-space or transfer function models. The following analyses are carried out during this phase.

(a) Calculation of the open-loop poles (i.e the eigenvalues of the system matrix, A).

(b) Calculation of the transmission zeros.

(c) Calculation of the relative gain array.

(d) Calculation of the transfer function matrix at various user specified frequencies.

(e) A singular value decomposition of the transfer function matrix can also be carried out at each frequency.

(f) Condition numbers subordinate to both the l_2 - norm and l_∞ - norm can also be calculated at each frequency. Various scaling policies are available at this point.

It must be realised that SPEECON is one example of a linear control system design/analysis package. SPEECON has been used in this thesis at various stages of controllability analysis in the gas-tail case-study.

SPEEDUP can now interface several other control analysis packages including CONSYD (Holt et al. [1987]) and MATLAB. Both these packages have a greater range of options compared to SPEECON.

PROCESS

Further information on PROCESS simulation package is available from :

Simulation Sciences Inc.
1051 W. Bastanchury
Fullerton, California 92633
USA.

APPENDIX A9

MULTILOOP CONTROLLER TUNING - THE BLT APPROACH

One of the major questions in multivariable control is how to tune a multiloop control system comprising a set of PI controllers, so as to obtain both system stability and acceptable closed-loop performance . In a multiloop system with N SISO loops all using PI controllers, there are 2N tuning parameters that must be specified (i.e. one controller gain and one reset time for each loop). Each SISO loop can be tuned independently using one of the standard methods available in the literature (Stephanopoulos [1984], Luyben [1990]). However, when two or more SISO loops (that have been tuned independently) are operated together to form a multiloop control system, the tuning parameters for each SISO loop often have to be detuned to to provide both stability and performance. Interactions existing amongst the various loops often induce unstable behaviour in a multiloop control system. A consistent and rational basis for tuning all the SISO loops together is therefore required.

Biggest log-modulus (usually referred to simply as BLT) tuning provides such a standard tuning approach. Although it may not provide the best results the method is easy to use , easily understandable by control engineers and leads to settings that compare very favourably with the empirical settings found by exhaustive trial-and-error methods (Luyben [1990]). BLT tuning involves the following steps ;

(1) Calculate the Ziegler-Nichols settings for each individual loop. These settings for each SISO loop are obtained in the standard way (Luyben [1990]). From the Bode plot for each diagonal transfer function element (i.e. the element corresponding to a specific controller pairing), both the ultimate frequency (ω_u) and ultimate gain (K_u) are obtained. A FORTRAN routine is provided later in this appendix to estimate these values given a square transfer function matrix. Zeigler-Nichols settings (K_c and τ_I) thus are obtained as follows;

$$K_{ci} = 0.45\ K_{ui} \quad \text{and} \quad \tau_{I\,i} = 2\pi / (1.2\ \omega_{ci}) \qquad \text{(A9.1)}$$

where

K_{ci} is the controller gain for the i^{th} loop (i= 1, 2, ..N).

$\tau_{I\,i}$ is the reset time for the i^{th} loop (i= 1, 2, ..N).

K_{ui} is the ultimate gain for the i^{th} loop (i= 1, 2, ..N).

ω_{ci} is the cross-over frequency for the i^{th} loop (i= 1, 2, ..., N).

If any of the control loops follows simple first-order dynamics, Ziegler-Nichols settings cannot be calculated. Controller tuning constants in such a case can be obtained using a method proposed in the latter part of this section.

(2) A detuning factor F is defined. F can be treated as a detuning factor that stabilises an otherwise unstable multiloop control system. The larger the value of the factor F , the more stable but sluggish is the overall control performance. The same value of F will be used for all N control loops.

$$K_{ci\,(final)} = \frac{K_{ci}}{F} \quad \text{and} \quad \tau_{Ii\,(final)} = F\ \tau_{Ii} \qquad \text{(A9.2)}$$

where K_{ci} (final) is the detuned controller gain for the i^{th} loop.

τ_{Ii} (final) is the detuned reset time for the i^{th} loop,

(3) Based on a guessed value of F and the resulting corrected controller parameter values, a scalar function W is defined as follows;

$$W = -1 + \det[I + G(s).B(s)] \qquad \text{(A9.3)}$$

where W is a scalar function.

det [ ] is the determinant of the matrix enclosed in the parentheses.

B(s) is a diagonal (N X N) matrix given by ;

$$B(s) = \begin{bmatrix} B_1(s) & 0 & . & 0 \\ 0 & B_2(s) & . & . \\ . & 0 & . & . \\ . & . & . & . \\ 0 & 0 & . & B_N(s) \end{bmatrix}$$

$$B_i(s) = K_{ci}\ (1 + 1 / \tau_I s) \text{ for all } i = 1, 2, .., N.$$

where s defines the Laplace domain and G (s) is the process transfer function matrix.

A closed-loop log-modulus (L_{cm}) can be defined next as follows;

$$L_{cm} = 20 \log \left| \frac{W}{1 + W} \right| \qquad \text{(A9.4)}$$

L_{cm} is plotted as a function of frequency and it is the size of any peak in such a plot that is used to determine the detuning parameter F .

(4) The factor F is varied until the biggest log-modulus (L_{cm}^{max}) just equals **2N**, where N is the number of SISO loops in the multivariable system. This is based on a criterion of +2 dB for one SISO loop. Therefore (2 X 2) and (3 X 3) systems will have (L_{cm}^{max}) values of 4 and 6 respectively. A FORTRAN program is also provided in this appendix to estimate F for both these systems.

This tuning approach can however be considered to provide only preliminary controller settings, although it does guarantee stability of the system when all the loops are in automatic, and that of each individual independent loops.

The BLT multiloop tuning approach is illustrated in the following example.

Example A9 . 1

Consider the de-propaniser column control system described in Section 5.4. The transfer function for Control System 4 (with the reflux rate controlling the distillate (LPG) composition, while steam flowrate to the reboiler regulates the column pressure) can be obtained from SPEECON. Figures A9. 3 and A9. 4 show the variation of both phase angle and amplitude ratio , respectively, as a function of frequency for both the control loops. It is clear from these results that only the reflux loop has high enough order dynamics (i.e. a phase angle of -180 degrees at some frequency), such that Ziegler-Nichols settings can be estimated. For the steam flowrate control loop, controller settings are obtained from the *quarter decay ratio method* presented in the following section.

Control loop of reflux flowrate and LPG composition in the distillate

ω_u = 23.8 hr^{-1}

Magnitude ratio (M) = - 6.475e-4

K_u = (1/M) = -1544.40

The Ziegler-Nichols controller settings for this loop are thus

K_c = 0.45 K_u = - 694.9

τ_I = 2 π /(1.2 ω_u) = 0.219 hrs.

Control loop of steam flowrate and column pressure

The controller settings based on the quarter-decay ratio method (see Example A9. 2) are

K_c = 0.16

τ_I = 0.518 hrs.

For the (2 X 2) control system considered, SPEECON was used to calculate the transfer function matrix elements at various desired frequencies :

$$\begin{array}{cc} P & X_d \\ \begin{bmatrix} G_{11} & G_{21} \\ G_{12} & G_{22} \end{bmatrix} & \begin{array}{l} \text{Reflux rate} \\ \\ \text{Steam flowrate} \end{array} \end{array}$$

where P and X_d are the column pressure and distillate composition, respectively.

The transfer function elements G_{11}, G_{21}, G_{12} and G_{22} thus estimated are listed in Table A9.1. In this table, the first element in parentheses shows the real part while the second element shows the imaginary part of corresponding transfer function element. G_{21} in this case corresponds to the gain between reflux flowrate and the distillate composition, while G_{12} corresponds to the gain between steam flowrate and the column pressure. These two transfer function elements are used for estimating the multiloop controller tuning parameters. However, information about all the transfer function elements (i.e. G_{11} and G_{22} as well) is necessary to estimate the de-tuning constant F as shown below.

The FORTRAN routine for BLT tuning of (2 X 2) control systems uses the information from Table A9.1 and the estimated values for the tuning parameters to predict the detuning factor F . The program stops when the log-modulus value equals a value of 4 .

An F value of 2.4 was found for this multiloop system. The corrected settings for both the control loops, are therefore :

Control loop of reflux flowrate and LPG composition in the distillate

K_c (final)	=	$K_c / 2.4$	=	- 289.58
τ_I (final)	=	$2.4\,\tau_I$	=	0.526 hrs.

Control loop of steam flowrate and column pressure

K_c (final)	=	$K_c / 2.4$	=	0.159
τ_I (final)	=	$2.4\,\tau_I$	=	0.518 hrs.

The value of detuning factor F (i.e F > 1) in this case indicates that a fair degree of interaction exists between the two control loops, and hence large detuning is required in the controller parameters to provide both stability and performance.

QUARTER-DECAY RATIO TUNING METHOD FOR A FIRST-ORDER LOOP WITH A PI CONTROLLER

Consider the response of a second-order underdamped system (Stephanopoulos [1984]) as shown in Figure A9.1. The size "a" in this figure shows the value by which the process response overshoots the final set-point value. A stable system will have a performance such that the response curve decreases in magnitude over a period of time. The ratio of the second peak " c " to that of the first peak " a " is called the " decay ratio" , and characterises the performance. A decay ratio of 25 % is called a "quarter-decay ratio response" and is generally taken as acceptable in the chemical industry.

Figure A9.2 shows a first-order system with a PI controller which has a closed-loop response that is similar to an underdamped second-order response (see Figure A9.1). The controller parameters can be calculated to obtain a quarter-decay response, as shown below.

The characteristic equation of the closed-loop system in Figure A9.2 is,

$$\left(\frac{\tau_I \tau_P}{A K_c}\right)s^2 + \frac{\tau_I (A K_c + 1)}{A K_c} s + 1 = 0 \qquad \text{(A9.5)}$$

where K_C is the controller gain

τ_I is the controller reset time

τ_P is the time constant of the first-order system

A is the steady-state gain of the process.

The characteristic equation of a second-order system (Stephanopoulos [1984]) is given by

$$\tau^2 s^2 + 2\xi\tau s + 1 \qquad \text{(A9. 6)}$$

Comparing Equation A9.5 and Equation A9.6 , we have,

$$\tau = \sqrt{\frac{\tau_I \tau_P}{A K_c}} \qquad \text{(A9.7)}$$

$$\xi = \frac{1}{2}\sqrt{\frac{A K_c \tau_I}{\tau_P}}\,(A K_c + 1) \qquad \text{(A9.8)}$$

where τ is the "time constant" of the controlled system

ξ is the damping ratio of the controlled system.

Another factor α can be defined as the ratio of the closed-loop time constant to that of the original open-loop time constant ,

$$\alpha = \frac{\tau}{\tau_p} \qquad \text{(A9.9)}$$

Physically α gives the ratio by which the original system response is attenuated. Typically the value of α varies from 0.75 -1.0. The response of the system for an ξ value of 0.5 is known as a "quarter-decay ratio response" and this is thus the value of ξ .

The procedure for estimating the controller parameters involves the following steps:

(1) Perform a step-change in the input variable and obtain the time dependent response curve for the corresponding output variable. Estimate the process time constant (τ_p) and the steady-state gain (A) as follows :

$$A = \frac{y_{final} - y_{initial}}{\Delta u} \qquad \text{(A9.10)}$$

(A9.11)

where $y_{initial}$ is the initial value of the output variable.

y_{final} is the final value of the output variable.

Δu is the magnitude of the step-change in the input variable.

τ_p is the time taken to reach 63.2% of the final set-point value

(2) Choose $\alpha = 0.75$ and $\xi = 0.5$ and estimate K_c from Equations A9.7 - A9.9 ;

$$K_c = (0.3333/A) \qquad \text{(A9.12)}$$

(3) Estimate τ_I from the definition of $\alpha$and Equations A9.7 and A9. 9 ,

$$\tau_I = (0.75)^2 (0.333)\ \tau_p \qquad \text{(A9.13)}$$

These controller parameters should thus provide the desired quarter-decay ratio performance. An application of this approach is illustrated through the following example.

Example A9 . 2:

Consider the same de-propaniser column control system of that given in Section 5.4. As shown in Figure A9.3 the control loop of Steam flowrate and column pressure does not have high order dynamics (i.e higher than first order) and cannot be tuned using Ziegler-Nichols settings. The quarter decay ratio method will be used to tune this control loop.

A step change in the steam flowrate to the de-propaniser reboiler (i.e. keeping the reflux flow constant) was performed to obtain the steady-state gain and tuning constants ;

Initial value of the output (pressure) variable = 16.651 Bars

Final value of the output (pressure) variable = 14.912 Bars

Change in the output (pressure) variable (Δy) = -1.739 Bars

Step change in the input (steam flowrate) variable (Δu) = - 2 Kg-moles/hr

Steady-state gain (A) = (Δy / Δu) = 0.87

The "First-order" process time constant (τ_p) was determined as the time taken to reach 63. 2 % of the final value. Using this definition a value of 1. 15 hr was obtained.

The controller settings , therefore, are given by ;

$$K_C = 0.333/A = 0.383$$

$$\tau_I = (0.75)^2 (0.3333)\tau_p = 0.216 \text{ hrs.}$$

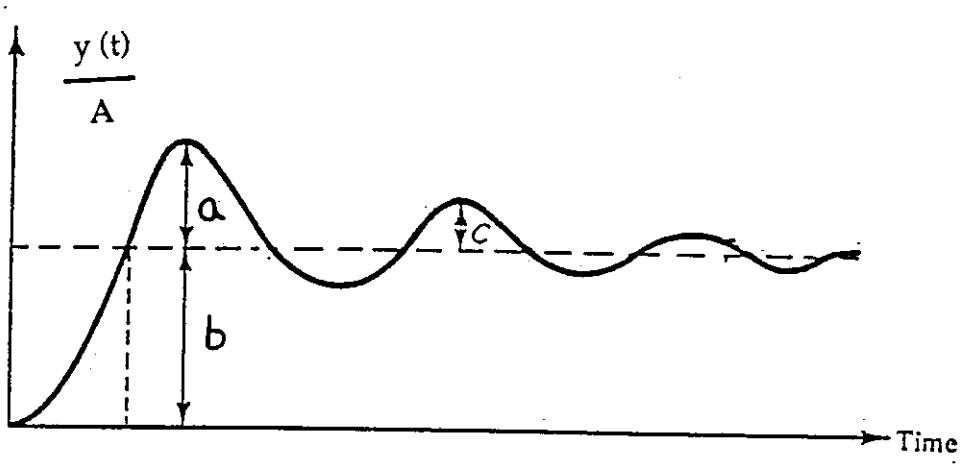

Figure A9. 1
Characteristics of an underdamped second-order response

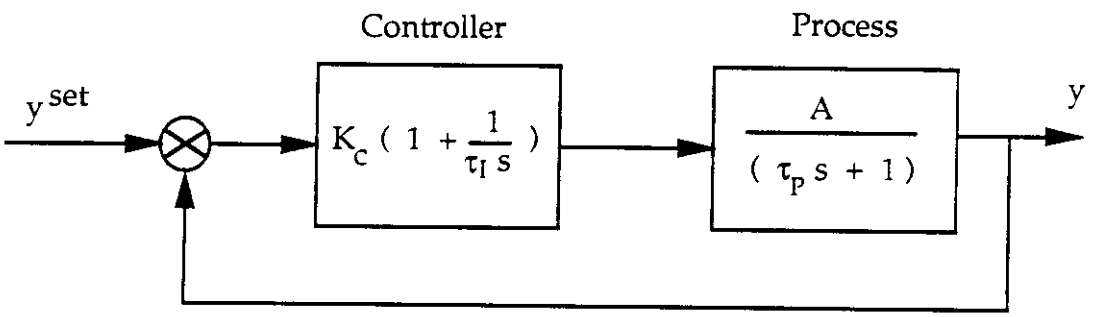

Figure A9. 2
Block diagram for a first-order process with a PI controller

Figure A9. 3
PHASE ANGLE FOR THE DE-PROPANISER CONTROL LOOPS

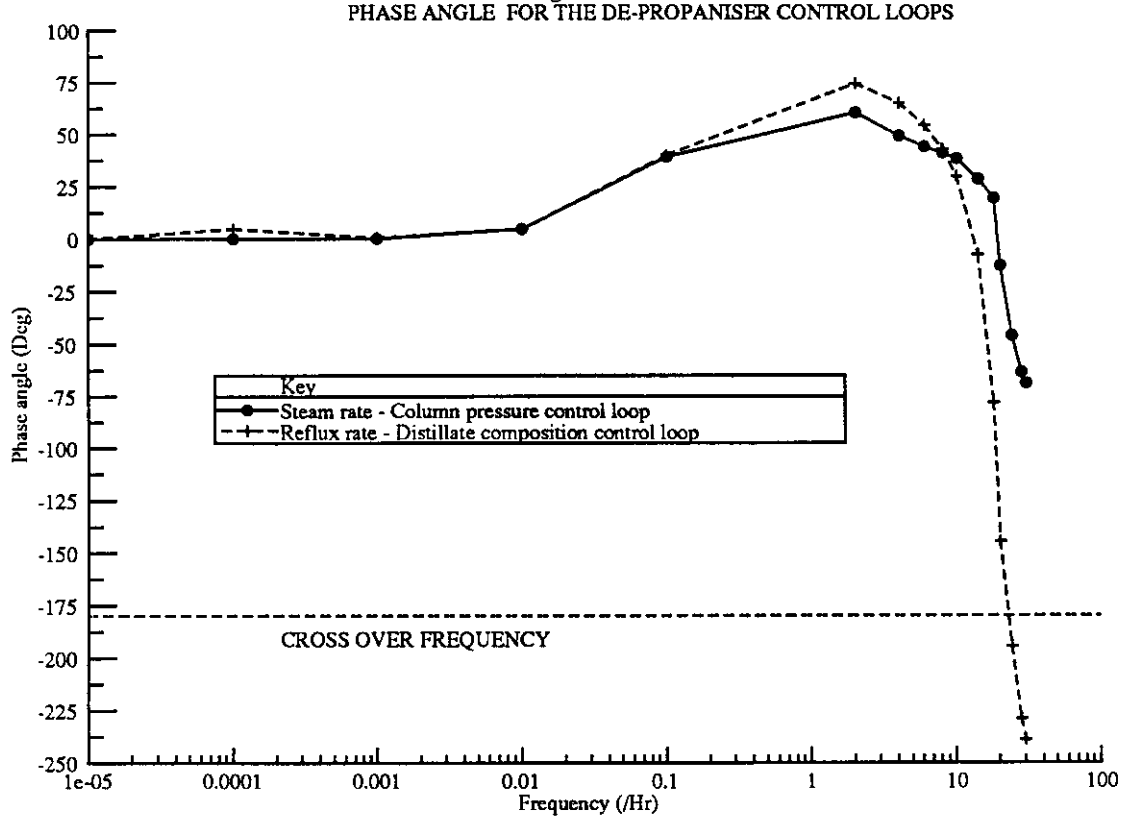

Figure A9.4
AMPLITUDE RATIO FOR THE DE-PROPANISER CONTROL LOOPS

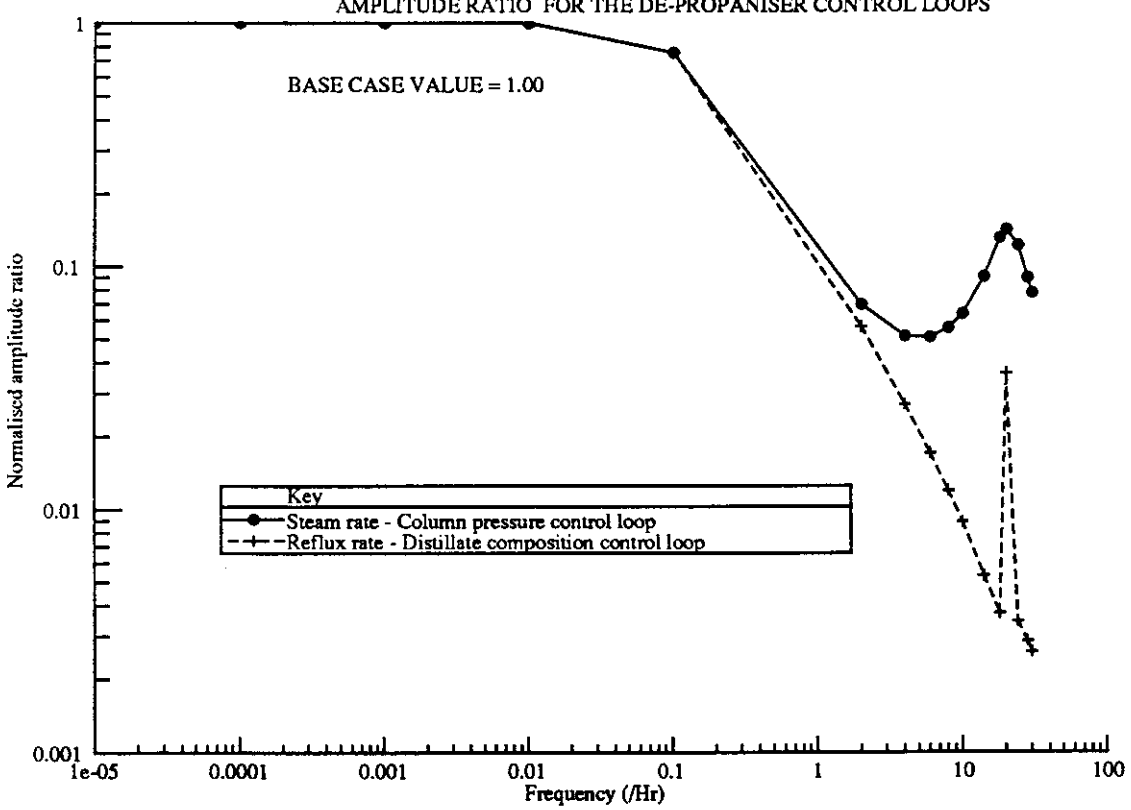

Table A9. 1
Transfer function matrix elements for the
de-propaniser control loops

Frequency	G_{11}	G_{12}
1.0e-5	(-1.79 , -1.55e-4)	(3.73, 3.15e-4)
1.0e-4	(-1.79, -1.55e-3)	(3.73, 3.15e-3)
1.0e-3	(-1.79, 1.55e-2)	(3.73, 3.15e-2)
1.0e-2	(-1.78, -0.154)	(3.70, 3.13e-1)
1.0e-1	(-1.02,-0.882)	(2.17, 1.79)
2	(-2.52, -0.113)	(0.126, 0.228)
4	(-2.38e-2,-7.46e-2)	(0.125,0.146)
6	(-2.82e-2,-6.99e-2)	(0.137,0.133)
8	(-3.59e-2,-7.59e-2)	(0.156,0.137)
10	(-4.80e-2,-8.34e-2)	(0.186,0.148)
14	(-9.69e-2,-0.104)	(0.231,0.159)
18	(-0.197, -7.51e-2)	(0.389,0.135)
20	(-0.233, -6.21e-3)	(0.519,-0.119)
24	(-0.167, 0.113)	(0.315,-0.329)
28	(-8.95e-2,0.120)	(0.146, -0.300)
30	(-6.72e-2,0.115)	(0.104, -0.271)
Frequency	G_{21}	G_{22}
1.0e-5	(-0.186, -1.59e-5)	(0.378, 3.25e-5)
1.0e-4	(-0.186, -1.59e-4)	(0.378, 3.25e-4)
1.0e-3	(-0.186, -1.59e-3)	(0.378, 3.25e-3)
1.0e-2	(-0.184, -1.59e-2)	(0.378, 3.23e-2)
1.0e-1	(-0.106,-9.09e-2)	(0.217,0.185)
2	(-2.64e-3,-1.01e-2)	(5.61e-3,2.05e-2)
4	(-2..10e-3,-4.59e-3)	(4.39e-3,9.21e-3)
6	(-1.85e-3,-2.60e-3)	(3.82e-3, 5.09e-3)
8	(-1.63e-3, -1.53e-3)	(3.31e-3,2.85e-3)
10	(-1.43e-3,-8.25e-4)	(2.81e-3,1.39e-3)
14	(-9.77e-3, 1.29e-4)	(1.63e-3,-5.12e-4)
18	(-1.37e-4, 6.78e-4)	(-2.99e-4,-1.30e-3)
20	(3.85e-4, 5.55e-4)	(-1.28e-3,-7.93e-4)
24	(6.22e-4, -1.62e-4)	(-1.33e-3,7.68e-4)
28	(3.47e-4, -4.05e-4)	(-6.15e-4,1.08e-3)
30	(2.44e-4,-4.15e-4)	(-3.92e-4,1.03e-3)

```
C   THE FOLLOWING  ROUTINE  PROPOSES A METHODOLOGY TO
C   ESTIMATE A LUYBEN'S DE-TUNING FACTOR FOR A ( 2 X 2 ) CONTROL SCHEME
C   THAT WOULD PROVIDE A REASONABLE CLOSED LOOP PERFORMANCE.
C
      PARAMETER (MAXM=2,MAXF=20,NDTMAX=20,LWORK=100)
      IMPLICIT DOUBLE PRECISION (A-H,O-Z)
      INTEGER OPT
      COMPLEX*16 GG(MAXF,MAXM,MAXM),B1,B2,C1,C2,C3,C4,WCL,RATIO
      REAL LC,LCMAX,KC1,KC2,TI1,TI2,KZN1,KZN2,TZN1,TZN2,A1,A2,
     + ARATIO,IRATIO,RRATIO,GG_O(MAXF,MAXM,MAXM)
      DIMENSION F(MAXM,NDTMAX),W(MAXF)
C
C     TERMINOLOGY USED
C     ****************
C     GG          IS THE REARRANGED TRANSFER FUNCTION MATRIX
C     GG_O        IS THE ORIGINAL TRANSFER FUNCTION MATRIX -OBTAINED FROM
C                 SPEECON
C     MAXF        IS THE MAXIMUM FREQUENCY RANGE OF INTEREST
C     MAXM        IS THE NUMBER OF INPUTS/OUTPUTS OF CONTROL SYSTEM
C     KC1,KC2     ARE FINAL CONTROLLER GAINS FOR 1,2 LOOPS RESPECTIVELY
C     KZN1,KZN2   ARE THE (ZEIGLER-NICOLS) INITIAL CONTROLLER GAINS FOR
C                 1,2 LOOPS RESPECTIVELY.
C     TI1,TI2     ARE FINAL RESET TIMES GAINS FOR 1,2 LOOPS RESPECTIVELY
C     TZN1,TZN2   ARE THE (ZEIGLER-NICOLS) INITIAL RESET TIMES FOR
C                 1,2 LOOPS RESPECTIVELY.
C     NDT         NUMBER OF ITERATIONS REQUIRED TO ESTIMATE DE-TUNING FACTOR
C     F(I, I)     DE-TUNING FACTOR FOR Ith LOOP AT THE Ith ITERATION.
C
C     NOTE :  VARIOUS OTHER CONSTANTS USED, ARE DEFINED WHEN NEEDED.
C
C   READ THE DATA FROM THE FOLLOWING FILE:
C        OPEN(UNIT=13,FILE='BLT1_CON1.LIS',STATUS='OLD')
C        OPEN(UNIT=13,FILE='BLT1_CON4.LIS',STATUS='OLD')
C
C
C   INITIALISE THE DE-TUNING CONSTANTS
      F(1,1) = 2.0
      F(2,1) = 2.0
C    THE FOLLOWING ARE THE CONTROL ZEIGLER-NICHOL'S TUNING CONSTANTS FOR
C    BOTH THE CONTROL LOOPS OF CONTROL SYSTEM - 1
C
C        KZN1 =-25.062
C        KZN2 = 0.2835
C        TZN1 = 0.09
C        TZN2 = 22.0e-3
C
C    THE FOLLOWING ARE THE CONTROL ZEIGLER-NICHOL'S TUNING CONSTANTS FOR
C    BOTH THE CONTROL LOOPS OF CONTROL SYSTEM - 4
C
      KZN1 =-694.98
      KZN2 = 0.3831
      TZN1 = 0.219
      TZN2 = 0.216
C   READ STATE FREQUENCY AND THE TRANSFER FUNCTION MATRIX
      DO 5 K=1,MAXF
      READ(13,*) W(K)
      DO 6 I=1,MAXM
      DO 6 J=1,MAXM
      READ(13,*) A1,A2
      GG_O(K,I,J)= DCMPLX(A1,A2)
6     CONTINUE
5     CONTINUE
      DO 100 NDT=1,NDTMAX
      PRINT*, 'MAXIMUM - LC          LC          FREQUENCY'
      PRINT*,'***********************************************'
      DO 50 K =1,MAXF
C    CORRECTED CONTROL PARAMETERS FOR EACH LOOP
      KC1 = KZN1/F(1,NDT)
      TI1 = TZN1*F(1,NDT)
      KC2 = KZN2/F(2,NDT)
      TI2 = TZN2*F(2,NDT)
C   THE FOLLOWING RE-ARRANGEMENT WAS NECESSARY FOR CONTROL SYSTEM 4 OF THE
```

```
C    DE-PROPANISER AS THE SPEECON- ESTIMATED TRANSFER FUNCTION MATRIX ELEMENTS
C    ARE OF THE RIGHT ORDER.
           GG(K,1,1) = GG_O(K,1,1)
           GG(K,2,2) = GG_O(K,2,2)
           GG(K,1,2) = GG_O(K,1,2)
           GG(K,2,1) = GG_O(K,2,1)
C
C     ESTIMATION OF PARAMATERS OF EQUATION
C
           B1=KC1*(1.0 + 1.0/(TI1*W(K)))
           B2=KC2*(1.0 + 1.0/(TI2*W(K)))
           C1 = B1*GG(K,1,1)
           C2 = B2*GG(K,2,2)
           C3 = B1 * B2
           C4 = (GG(K,1,1)*GG(K,2,2) - GG(K,1,2)*GG(K,2,1))
           WCL = C1 + C2 + C3 - C4
           RATIO = WCL/(1.0D0+WCL)
           RRATIO = DREAL(RATIO)
           IRATIO = DIMAG(RATIO)
           ARATIO = SQRT( RRATIO *RRATIO + IRATIO*IRATIO)
C    ESTIMATE THE LOG-MODULUS OF 'RATIO'
C
           LC = 20.0*LOG10(ARATIO)
C    IDENTIFY THE MAXIMUM VALUE OF 'LC'
C
           IF(K.EQ.1) THEN
            LCMAX = LC
           ELSE
            LCMAX = MAX(LCMAX, LC)
           ENDIF
           PRINT*, LCMAX, LC , W(K)
50         CONTINUE
           PRINT*, 'THE DE-TUNING FACTOR IS =', F(1,NDT),F(2,NDT),NDT
           IF (LCMAX.GE.4.0) GO TO 150
C
C   UPDATE THE DE-TUNING FACTOR
C
           F(1,NDT +1)= F(1,NDT) - 0.1
           F(2,NDT +1)= F(2,NDT) - 0.1
100        CONTINUE
150        CONTINUE
           STOP
           END
```

```
C
C   THE FOLLOWING  ROUTINE  PROPOSES A METHODOLOGY TO
C   ESTIMATE A LUYBEN'S DE-TUNING FACTOR FOR A ( 3 X 3 ) CONTROL SCHEME
C   THAT WOULD PROVIDE A REASONABLE CLOSED LOOP PERFORMANCE.
C
      PARAMETER (MAXM=3,MAXF=20,NDTMAX=20,LWORK=100)
      IMPLICIT DOUBLE PRECISION (A-H,O-Z)
      INTEGER OPT
      COMPLEX*16 GG(MAXF,MAXM,MAXM),B1,B2,B3,C1,C2,C3,C4,C5,C6,C7,
     +  C8,C9,C10,WCL,RATIO
      REAL LC,LCMAX,KC1,KC2,KC3,TI1,TI2,TI3,KZN1,KZN2,KZN3,
     +  TZN1,TZN2,TZN3,A1,A2,ARATIO,IRATIO,RRATIO
      DIMENSION F(MAXM,NDTMAX),W(MAXF)
C
C   TERMINOLOGY USED
C   ****************
C   GG               IS THE RE-ARRANGED TRANFER FUNCTION MATRIX
C   MAXF             IS THE MAXIMUM FREQUENCY RANGE OF INTEREST
C   MAXM             IS THE NUMBER OF INPUTS/OUTPUTS OF CONTROL SYSTEM
C   KC1,KC2          ARE FINAL CONTROLLER GAINS FOR 1,2 LOOPS RESPECTIVELY
C   KZN1,KZN2,KZN3 ARE THE (ZEIGLER-NICOLS) INITIAL CONTROLLER GAINS FOR
C                    1,2 LOOPS RESPECTIVELY.
C   TI1,TI2,TI3      ARE FINAL RESET TIMES GAINS FOR 1,2 LOOPS RESPECTIVELY
C   TZN1,TZN2,TZN3 ARE THE (ZEIGLER-NICOLS) INITIAL RESET TIMES FOR
C                    1,2 LOOPS RESPECTIVELY.
C   NDT              NUMBER OF ITERATIONS REQUIRED TO ESTIMATE DE-TUNING FACTOR
C   F(I, I)          DE-TUNING FACTOR FOR Ith LOOP AT THE Ith ITERATION.
C
C   NOTE :  VARIOUS OTHER CONSTANTS USED, ARE DEFINED WHEN NEEDED.
C
C   READ THE DATA FROM THE FOLLOWING FILE:
      OPEN(UNIT=13,FILE='BLT_DEBUT_CON1.LIS',STATUS='OLD')
C
C   INITIALISE THE DE-TUNING CONSTANTS
      F(1,1) = 1.505
      F(2,1) = 1.505
      F(3,1) = 1.505
C    THE FOLLOWING ARE THE CONTROL ZEIGLER-NICHOL'S TUNING CONSTANTS FOR
C    BOTH THE CONTROL LOOPS OF CONTROL SYSTEM - 1
      KZN1=32.676
      KZN2=-1.397
      KZN3=213.654
      TZN1 =3.9563
      TZN2=0.01406
      TZN3 =0.1688
C   READ STATE FREQUENCY AND THE TRANSFER FUNCTION MATRIX
      DO 5 K=1,MAXF
      DO 6 I=1,MAXM
      DO 6 J=1,MAXM
      READ(13,*) A1,A2
      GG(K,I,J)= DCMPLX(A1,A2)
 6    CONTINUE
      READ(13,*) W(K)
 5    CONTINUE
      DO 100 NDT=1,NDTMAX
      PRINT*, 'MAXIMUM - LC          LC          FREQUENCY'
      PRINT*,'*********************************************'
      DO 50 K =1,MAXF
C    CORRECTED CONTROL PARAMETERS FOR EACH LOOP
      KC1 = KZN1/F(1,NDT)
      TI1 = TZN1*F(1,NDT)
      KC2 = KZN2/F(2,NDT)
      TI2 = TZN2*F(2,NDT)
      KC3 = KZN3/F(3,NDT)
      TI3 = TZN3*F(3,NDT)
C
C   ESTIMATION OF PARAMATERS
C

      B1=KC1*(1.0 + 1.0/(TI1*W(K)))
      B2=KC2*(1.0 + 1.0/(TI2*W(K)))
      B3=KC3*(1.0 + 1.0/(TI3*W(K)))
      C1 = B1*GG(K,1,1)
```

```
      C2 = B2*GG(K,2,2)
      C3 = B3*GG(K,3,3)
      C4 = B1 * B2
      C5 = B2 * B3
      C6 = B1 * B3
      C7 = (GG(K,1,1)*GG(K,2,2) - GG(K,1,2)*GG(K,2,1))
      C8 = (GG(K,2,2)*GG(K,3,3) - GG(K,2,3)*GG(K,3,2))
      C9 = (GG(K,1,1)*GG(K,3,3) - GG(K,1,3)*GG(K,3,1))
      C10 = B1 * B2 * B3
      WCL = C1 + C2 + C3 + C4*C7 + C5*C8 + C6*C9 +
     +       C10 * (GG(K,1,1)*C8 + GG(K,1,2)*(GG(K,2,3)*GG(K,3,1) -
     +              GG(K,2,1)*GG(K,3,3)) +  GG(K,1,3) *(GG(K,2,1)*
     +              GG(K,3,2) -  GG(K,2,2)*GG(K,3,1)))
      RATIO  = WCL/(1.0D0+WCL)
      RRATIO = DREAL(RATIO)
      IRATIO = DIMAG(RATIO)
      ARATIO = SQRT( RRATIO *RRATIO + IRATIO*IRATIO)

C   ESTIMATE THE LOG-MODULUS OF 'RATIO'
C
      LC = 20.0*LOG10(ARATIO)
C   IDENTIFY THE MAXIMUM VALUE OF 'LC'
C
      IF(K.EQ.1) THEN
       LCMAX = LC
      ELSE
       LCMAX = MAX(LCMAX, LC)
      ENDIF
      PRINT*, LCMAX, LC , W(K)
50    CONTINUE
      PRINT*, 'THE DE-TUNING FACTOR IS =', F(1,NDT),F(2,NDT),F(3,NDT),
     + NDT
      IF (LCMAX.GE.6.0) GO TO 150
C
C  UPDATE THE DE-TUNING FACTOR
C
      F(1,NDT +1)= F(1,NDT) + 0.1
      F(2,NDT +1)= F(2,NDT) + 0.1
      F(3,NDT +1)= F(3,NDT) + 0.1
100   CONTINUE
150   CONTINUE
      STOP
      END
```

APPENDIX A10

BASICS OF MATRICES

A matrix is an array of elements. An (N X N) matrix A is represented as

$$A = \begin{bmatrix} a_{11} & a_{12} & \cdot & a_{1N} \\ a_{21} & a_{22} & \cdot & a_{2N} \\ \cdot & \cdot & \cdot & \cdot \\ \cdot & \cdot & \cdot & \cdot \\ a_{N1} & a_{N2} & \cdot & a_{NN} \end{bmatrix}_{(NX\ N)} \qquad \text{(A10. 1)}$$

where element a_{ij} represents the element in the i^{th} row and j^{th} column.

Transpose of a matrix **A** (usually denoted by A^T) is obtained by interchaning each row and each column of matrix **A** (Stewart [1973]). Therefore

$$A^T = \begin{bmatrix} a_{11} & a_{21} & \cdot & a_{N1} \\ a_{12} & a_{22} & \cdot & a_{N2} \\ \cdot & \cdot & \cdot & \cdot \\ \cdot & \cdot & \cdot & \cdot \\ a_{1N} & a_{2N} & \cdot & a_{NN} \end{bmatrix}_{(NX\ N)} \qquad \text{(A10. 2)}$$

such that a_{ji} of matrix A^T = a_{ij} of matrix **A** (for $i = 1,..., N$; $j = 1,..., N$).

The determinant of a matrix is an important property and is used extensively in matrix theory. If the elements of a matrix **A** , i.e. a_{ij} (i=1,.., N ; j = 1,..., N) are thought of as variables, the determinant of the matrix **A** (often denoted as **D** or **det**) is said to be the function of these variables given by

$$D = \begin{bmatrix} a_{11} & a_{12} & \cdot & a_{1N} \\ a_{21} & a_{22} & \cdot & a_{2N} \\ \cdot & \cdot & \cdot & \cdot \\ \cdot & \cdot & \cdot & \cdot \\ a_{N1} & a_{N2} & \cdot & a_{NN} \end{bmatrix} \qquad \text{(A10. 3)}$$

or alternatively $$D = \Sigma \pm (a_{1 j_1}\ a_{1 j_2} \cdots\ a_{1 j_N}) \qquad \text{(A10. 4)}$$

where Σ indicates that the terms are to be summed over all permutations (j_1, j_2 ...., j_N) and the + or - is selected in each term according to whether the permutation is even or odd.

For example , when N = 3,

$$D = \begin{bmatrix} a_{11} & a_{12} & a_{13} \\ a_{21} & a_{22} & a_{23} \\ a_{31} & a_{32} & a_{33} \end{bmatrix} = a_{11} \cdot \begin{bmatrix} a_{22} & a_{23} \\ a_{32} & a_{33} \end{bmatrix} - a_{12} \cdot \begin{bmatrix} a_{21} & a_{23} \\ a_{31} & a_{33} \end{bmatrix} + a_{13} \cdot \begin{bmatrix} a_{21} & a_{22} \\ a_{31} & a_{32} \end{bmatrix} \qquad \text{(A10.5)}$$

$$= a_{11}.a_{22}.a_{33} + a_{12}.a_{23}.a_{31} + a_{13}.a_{21}.a_{32} - a_{11}.a_{23}.a_{32} - a_{13}.a_{22}.a_{31} - a_{12}.a_{21}.a_{33} \qquad \text{(A10.6)}$$

One of the important uses of determiants is in the definition of inversion of a matrix (for further discussion on the properties of determinants see Stewart [1973]).

It must be realised that in Equation (A10. 5) a determinant of size three was expressed as a function of three determinants of size two (i.e 3 - 1 = 2). Each of these smaller determinants are obtained by selectively removing a row and a column from the large determinant. The subscripts of the coefficient elements (i.e. i and j of element a_{ij}) provide the details of which row and which column have to be removed. Each of these smaller determinants are called minors (usually denoted by M).

Therefore M_{ij} represents the minor of element a_{ij} of matrix A which is obtained by removing the ith row and jth column from the determinant of A. Another important property is due to cofactors (usually determined by C). If M_{ij} is the minor of a_{ij} then cofactor of a_{ij} is given by ,

$$C_{ij} = (-1)^{i+j} . M_{ij} \qquad \text{(A10.7)}$$

It may be noticed that the minors and the cofactors differ only in sign , i.e. $C_{ij} = \pm M_{ij}$.

The adjoint of a matrix A (usually denoted as adj) is given by,

$$adj = \begin{bmatrix} C_{11} & C_{12} & . & C_{1N} \\ C_{21} & C_{22} & . & C_{2N} \\ . & . & . & . \\ . & . & . & . \\ C_{N1} & C_{N2} & . & C_{NN} \end{bmatrix}^T \qquad \text{(A10.8)}$$

The superscript T indicates transpose of matrix. Therefore the element in the i^{th} row and j^{th} column of the adjoint matrix is given by

$$adj_{ij} = C_{ji} \qquad \text{(A10.9)}$$

The adjoint matrix will be used to define the inverse of a matrix (usually denoted by A^{-1}) as,

$$A^{-1} = \frac{adj}{D} \qquad (A10.10)$$

The approach used in this thesis for the estimation of an element of inverse matrix is as follows ;

$$A^{-1}_{ij} = \frac{adj_{ij}}{D} \qquad (A10.11)$$

where $A^{-1}{}_{ij}$ is the (i, j) th element of the inverse matrix of A ,

adj_{ij} is the (i, j) th element of the adjoint matrix of A ,

D is the determinant of A.

A matrix A is said to be tri-diagonal if it has the following form ;

$$A = \begin{bmatrix} a_{11} & a_{12} & 0 & \cdot & 0 \\ a_{21} & a_{22} & a_{23} & \cdot & \cdot \\ 0 & a_{32} & a_{33} & \cdot & \cdot \\ \cdot & 0 & \cdot & \cdot & \cdot \\ \cdot & \cdot & \cdot & \cdot & a_{(N-1)\,N} \\ 0 & 0 & 0 & \cdot & a_{NN} \end{bmatrix} \qquad (A10.12)$$

with all the elements except those forming the three diagonals shown, have zero elements.

Many of the staged separation systems in Chemical Engineering can be represented through tri-diagonal matrices. They have some special properties with respet to their determinants, as was discussed in Appendices A1 , A2 and A3.

BIBLIOGRAPHY

Adby, P. R. and M. A. H. Dempster, " Introduction to Optimization Methods ", Chapman and Hall , London, 1974.

Anderson, J. S., "A Practical Problem in Dynamic Heat Transfer ", The Chem. Engineer, pp. 97 - 103, 1966.

Arkun, Y., " Design of Steady-State Optimising Control Structures for Chemical Processes", Ph. D. Thesis, Univ. of Minnesota , 1979.

Arkun, Y., "Dynamic Process Operability. Important Problems, Recent Results and New Challenges", CPC III , Asilomar , California, USA, Jan. 1986.

Arkun, Y. and G. Stephanopoulos, "Studies in the Synthesis of Control Structures for Chemical Processes: Part IV. Design of Steady-State Optimizing Control Structures for Chemical Process Units ", AIChE Journal, vol. 26 (6), pp. 975-991, 1980.

Arkun, Y. and G. Stephanopoulos, "Studies in the Synthesis of Control Structures for Chemical Processes. Part V. Design of Steady-State Optimizing Control Structures for Integrated Chemical Plants", AIChE Journal, vol. 27 (5), pp. 779-793, 1981.

Barton, G. W. and J. D. Perkins, "Theory and Tools for Overall Process Control System Design", 10th IFAC World Congress, vol. 2, pp. 232-237, Munich , July 1987.

Bauer, F. L., " Optimally Scaled Matrices ", Numer. Math., vol. 5, pp. 73-87 , 1963.

Benallou, A., Seborg, D. E. and D. A. Mellichamp, "Dynamic Compartmental Models for Separation Processes", AIChE Journal, vol. 32 (7), pp. 1067-1078, 1986.

Bristol, E. H., "On a New Measure of Interaction for Multivariable Process Control", IEEE Trans. Aut. Control , pp. 133-134, 1966.

Bristol, E. H., "Recent Results on Interaction in Multivariable Process Control ", 71 st AIChE Conference, Miami, USA , Nov. 1978.

Brockett, R. W. and M. D. Mesarovic, "The Reproducibility of Multivariable System ", J. Math. Analysis, vol. 11 , p. 458 , 1965.

Browne, D. W., Ishii, Y., and Otto, F. D., " Solving Multicolumn Equilibrium Stage Operations by Total Linearisation", Can. J. Chem. Eng., vol. 55, pp. 307-312 , 1977.

Buckley, P. S., "Techniques of Process Control " , Wiley & Sons, New York , 1964.

Businger, P. A., "Matrices Which Can be Optimally Scaled ", Numer. Math., vol. 12, pp. 346 - 348, 1968.

Celebi, C. and H. Chimowitz, "Analytic Reduced-Order Dynamic Models for Large Equilibrium Staged Cascades", AIChE Journal, vol. 31 (12), pp. 2039-2051, 1985.

Chan, W-K., Barton, G. W. , Perkins, J. D. and R. G. H. Prince, "Controllability Analysis of Alternative Process Designs", Chemeca'86, Adelaide , Australia, 1986.

Chan, W-K., " Computer-Aided Synthesis of Chemical Process Flowsheets ", Ph. D. Thesis, University of Sydney, Australia, 1987.

Chang., T. N. and E. J. Davison, " Steady-state Interaction Indices for Decentralised Unknown", Proc. of 25th Conference on Decision and Control, Athens, Greece, Dec.1986.

Chilton, C. H. and R. J. Perry , "Chemical Engineers' Handbook", 5th ed. , McGraw-Hill, New York, 1985.

Cho, Y. S. and B. Joseph, "Reduced-Order Steady-State and Dynamic Models for Separation Processes. Part 1. Development of the Model Reduction Procedure", AIChE Journal, vol. 29 (2), pp. 261-276, 1983.

Coulson, J. M. and J. F. Richardson , " Chemical Engineering Volume II - Unit Operations ", Pergamon Press, England, 1983.

Cutler, C. R. and B. L. Ramaker , "Dynamic Matrix Control - A Computer Control Algorithm ", AIChE 86th National Meeting, Houston, Texas, USA, 1979.

Dalhquist, S. A., " Control of the Top and Bottom Composition in a Pilot Distillation Column ", I.Chem.Eng. Symp. Ser., vol. 56 , pp. 25 , 1980.

Davison, E. J. and S. G. Chow, " Perfect Control in Linear Time-Invariant Multivariable Systems : The Control Inequality Principle ", 8th Annual Princeton Conference on Information Sciences and Systems ", 1974.

Published in :
Falliside, F. (ed.), " Control system design by pole-zero assignment ", Academic Press, New York, 1977.

Doherty, M. F. and J. D. Perkins, "On the Dynamics of Distillation Processes-IV. Uniqueness and Stability of the Steady-State in Homogeneous Continuous Distillations", Chem. Eng. Sci., vol. 37 (3), pp. 381-392, 1982.

Douglas, J. M., "A Preliminary Procedure for Control Systems for Complete Plants", 73rd Annual AIChE Meeting, Chicago, USA, 1980.

Douglas, J. M., "Process Operability and Control of Preliminary Design. " Chemical Process Control 2 , Seborg, D. E. and T. F. Edgar, (eds.), Proc. Eng. Found. Conf. on CPC, Sea Island, Georgia, USA, pp. 497 - 524 , 1981.

Doyle, J. C. and G. Stein, "Multivariable Feedback Design: Concepts for a Classical/Modern Synthesis", IEEE Trans. Aut. Control, vol. 26 (1), pp. 4-16, 1981.

Edgar, T. F. and D. M. Himmelblau, "Optimization of Chemical Processes", McGraw-Hill, Singapore, 1989.

Engineering Data Book , (SI , Edition) by the Gas Processors Suppliers Association, 1980.

Espana, M. and I. D. Landau, "Reduced Order Bilinear Models for Distillation Columns", Automatica, vol. 14, pp. 345-355, 1978.

Fiacco, A. V., "Sensitivity Analysis for Nonlinear Programming Using Penalty Methods", Mathematical Programming, vol. 10, pp. 287-311, 1976.

Finco, M. V., Luyben,W. L. and R. E. Polleck, "Control of Distillation Columns with Low Relative Volatilities", Ind. Eng. Chem. Res., vol. 28 (1), pp. 75-83, 1989.

Forsythe, G. E., and C. B. Moler, " Computer Solution of Linear Algebraic Systems. ", Prentice-Hall Inc., Englewood Cliffs, New Jersey, 1967.

Forsythe, G. E., Malcom, M. A. and C. B. Moler, " Computer Methods for Mathematical Computations ", Prentice-Hall Inc., Englewood Cliffs, New Jersey, 1977.

Foss, A. S., "Critique of chemical process control theory ", AIChE J, vol. 19 (2) , pp 209 - 214 , 1973.

Furzer, I., " Distillation for University Students", Star Printery Pty Limited, Erskenville, NSW, Australia, 1986.

Gagnepain, J. P., and D. E. Seborg, " Analysis of Process Interactions with Applications to Multiloop Control System Design", 72nd Annual Meeting, AIChE , San Francisco, USA, 1979.

Gani, R., Ruiz, C. A. and I. T. Cameron, " A General Model for Distillation Columns I - Model Description and Applications ", Comp. Chem. Eng., vol. 10 (3), pp. 181-198, 1986.

Gannavarapu, C., Barton, G.W. and J.D.Perkins, "Simulation , Optimisation, and Control system Design for an Industrial Process " , I.Chem.E. Symposium Series No., 114, Leeds, England, pp. 141 - 156, 1989.

Gannavarapu, C., Barton, G.W., Perkins, J.D. and J.B. Lear , "Economic Choice of Control Structures for Continuous Processes", The Fourth Conference on Control Engineering, GoldCoast, Australia, 1990.

Garcia, C. E. and M. Morari, "Internal Model Control. 1. A unifying review and some new results", Ind. Eng. Chem. Proc. Des. Dev., vol. 21 (2), pp. 308-323 , 1982.

Gill, P. E., Murray, W. and M. W. Wright, " Practical Optimisation ", Academic Press , New York , 1981.

Glover, K. and L. M. Silverman, " Characterisation of Structural Controllability ", IEEE Trans. Auto. Cont., vol. AC-21 (4), pp 534 - 537, 1976.

Golub, G. H. and J. M. Varah, " On a Characterisation of the Best l_2 - Scaling of a Matrix ", SIAM J , Numer. Analysis, vol. 11 , pp. 472 - 479, 1974.

Govind, R. and G. J. Powers, "Control System Synthesis Strategies", AIChE Journal, vol. 28 (1), pp. 60-73, 1982.

Grosdidier, P., Morari, M., and B. R. Holt, "Closed-Loop Properties from Steady-State Gain Information", Ind. Eng. Chem. Fundam., vol. 24 (2), pp. 221-235, 1985.

Grossmann, I. E. and M. Morari, "Operability, Resiliency and Flexibility - Process Design Objectives for a Changing World", 2nd Int. Conf. on Foundations of Computer-Aided Process Design , Snowmass, Colorado, USA, 1983.

Holland, C. D., " Fundamentals and Modelling of Separation Processes" , Prentice-Hall Inc., Englewood Cliffs, New Jersey, 1975.

Holt, B. R., Jerome, N. F. and U. Buck et. al., "CONSYD - Integrated Software for Computer Aided Control System Design and Analysis", Comp. Chem. Eng., vol. 11 (2), pp. 187-203, 1987.

Holt, B. R., and M. Morari, " Design of Resilient Processing Plants VI - The effect of Right-half-Plane Zeros on Dynamic Resilience " , Chem. Eng. Sci. , vol 40 (1), pp 59-74 , 1985.

Howell, J. M., " The Effect of Energy Integration on the Switchability of Chemical Processes ", Ph. D., Thesis, Dept. of Chem. Eng., Imperial College, London, U. K., 1984.

Iinoya, K. and R. J. Altpeter, " Inverse Response in Process Control ", Ind. Eng. Chem. , vol. 54 (7), pp. 39 - 43 , 1962.

Ishida, C., "An Approach to Optimal Process Plant Operation ", Japan - US Joint Seminar, Kyoto, Japan, Jun. , 1975.

Jensen, N., Fisher, D. G. and S. L. Shah, "Interaction Analysis in Multivariable Control Systems", AIChE Journal, vol. 32 (6), pp. 959-970, 1986.

Johnston, R. D. , Barton, G. W. and M. L. Brisk, " The Synthesis of Process Control Systems ", Chemeca'83 - 11th Australian Conference on Chem. Eng., Brisbane , Australia, 1983.

Johnston, R. D., "The Synthesis and Evaluation of Control Systems for Chemical Plants", Ph. D., Thesis , University of Sydney, Australia, 1985.

Johnston, R. D. and G. W. Barton, "Single-Input-Single-Output Control System Synthesis. Part 1 : Structural Analysis and the Development of Feedback Control Schemes ", Comp. Chem. Eng., vol. 9 (6), pp. 547 - 556, 1985a.

Johnston, R. D. and G. W. Barton, "Single-Input-Single-Output Control System Synthesis. Part 2 : Application of the Synthesis Algorithm to an Integrated Plant ", Comp. Chem. Eng., vol. 9 (6), pp. 557 - 566, 1985b.

Kalman, R. E., " Contributions to the Theory of Optimal Control ", Bol Soc Mat Mexicana, vol. 5, p. 102, 1960.

Kern, D. Q., " Process Heat Transfer ", McGraw-Hill , New York , 1950.

Kestenbaum, A., Shinnar, R. and R. E. Thau, " Design concepts for Process Control " Ind. Eng. Chem. Proc. Des. Dev., vol. 15 (2) , pp. 2-13, 1976.

Kim, H. S., Lee, K. S. , Yoo, K. P., Lee, W. H. and H. S. Park, "Two-Part Modular Reduced-Order Model for Multicomponent Multistage Distillation Columns", Journal of Chem. Eng. Japan, vol. 22 (1), pp. 41-47, 1989.

Kisakurek, B., " A Predictive Model for Dynamic Simulation ", Chem. Eng. Commun., vol. 20, pp 63- 79, 1983.

Klema, V. C. and A. J. Laub, "The Singular Value Decomposition: Its Computation and Some Applications", IEEE Trans. Aut. Control, vol. 25 (2), pp. 164-176, 1980.

Krishnan, S., " Parameter Estimation in on-line Optimisation ", Ph. D. Thesis, University of Sydney, Australia, 1990.

Kuhn, H. W. and A. W. Tucker, " Nonlinear Programming " , Proceedings of the Second Berkley Symposium on Mathematical Statistics and Probability, Neyman, J. (ed.)Uni. of California Press : Berkley , California, pp 481 - 492, 1951.

Kwakernaak, H. and R. Sivan , " Linear Optimal Control Systems ", Wiley-Interscience, New York, 1972.

Landau, I. D., "Adaptive Control - The Model Reference Approach ", Marcel Dekker Inc., New York, 1979.

Lau, H. and K. F. Jensen, "Evaluation of Changeover Control Policies by Singular Value Analysis - Effects of Scaling", AIChE Journal, vol. 31 (1), pp. 135-146, 1985.

Lear, J. B., Barton, G. W. and J. D. Perkins, "Optimising Control for an Industrial Distillation Column Using a Simplified Model", Modelling and Simulation of Systems, P. Beedveld et. al (Editors), J. C. Baltzer AG, Scientific Publishing Co. IMACS, pp. 341-345, 1989.

Lee, P. L. and G. R. Sullivan, "Generic Model Control - Theory and Applications", IFAC Workshop on Model Based Process Control, Atlanta, Georgia, USA, June 1988.

Levy, R. E., Foss, A. S. and E. A. Grens , "Response Modes of a Binary Distillation Column", Ind. Eng. Chem. Fund., vol. 8 (4), pp. 765-776, 1969.

Lin, C. T., "Structural Controllability ", IEEE Trans. Auto. Cont. vol. AC-19 (3), pp 201-208, 1974.

Linhoff, B. and J. A. T. Turner, " Simple Concepts in Process Synthesis Give Energy Savings and Element Designs ", The Chem. Engineer, p. 742, Dec. 1980.

Luyben, W. L., "The Impact of Process Diversity on Distillation Column Control", DYCORD+89, Maastricht, Netherlands, pp. 3-9, 1989.

Luyben, W. L., "Process Modelling, Simulation and Control for Chemical Processes", McGraw-Hill , Japan, 1990.

Maarleveld, A. and J. E. Rijnsdorp, "Constraint Control on Distillation Columns", Automatica, vol. 6, pp. 51-58, 1970.

MacFarlane, A. G. J. and N. Karcanias, "Poles and Zeros of Linear Multivariable Systems: A Survey of the Algebraic, Geometric and Complex-Variable Theory", Int. J. Control, vol. 24 (1), pp. 33-74, 1976.

McDonald, K., " Performance Comparisons of Methods for On-line Updating of Process Models for High Purity Distillation Control", AIChE Spring National Meeting, Houston, 1987.

Mesarovic, M. D., Macko, D., and Y. Takahara, " Theory of Hierarchical Multilevel systems ", Academic Press, New York, 1970.

Moczek, J. S., Otto, R. E. and T. J. Williams, "Approximation Models for the Dynamic Response of Large Distillation Columns", Process Control and Applied Mathematics, Chem Eng. Prog. Symp. Sp. Ser., vol. 61 (55), pp. 136-146, 196?

Morari, M., Arkun, Y. and G. Stephanopoulos, "An Integrated Approach to the Synthesis of Process Control Structures ", JACC Proc., Philadelphia, USA, 1978 .

Morari, M., Arkun, Y. and G. Stephanopoulos, "Studies in the Synthesis of Control Structures for Chemical Processes. Part I. Formulation of the Problem , Process Decomposition and the Classification of the Control Tasks. Analysis of the Optimizing Control Structures", AIChE Journal, vol. 26 (2), pp. 220-232, 1980.

Morari, M. and G. Stephanopoulos, "Studies in the Synthesis of Control Structures for Chemical Processes. Part II: Structural Aspects and the Synthesis of Alternative Feasible Control Schemes", AIChE Journal, vol. 26(2), pp. 232-246, 1980.

Morari, M., "Integrated Plant Control : A Solution at Hand or a Research Topic for the Next Decade ", CPC II, Sea Island, Georgia, USA, pp. 467-495, Jan. 1982.

Morari, M., "Design of Resilient Processing Plants - III. A General Framework for the Assessment of Dynamic Resilience", Chem. Eng. Sci., vol. 38 (11), pp. 1881-1891, 1983.

Morari, M. and S. Skogestad, " Effect of Model Uncertainty on Dynamic Resilience ", I. Chem. E. Symp. Ser. No. 92, pp. 493-504, 1985.

Narendra, K. S. and R. V. Monopoli (eds.), "Applications of Adaptive Control", Academic Press, New York, 1980.

Nguyen , T. C., Barton, G. W., Johnston, R. D. and J. D. Perkins, " A Condition Number Scaling Policy for Stability Robustness Analysis ", AIChE J , vol. 34 (7), pp. 1200-1206 , 1988.

Nishida, N. G., Stephanopoulos, G. and A. W. Westerberg, " A Review of Process Synthesis ", AIChE J., vol. 27, pp 321-351, 1981.

Osborne, W. G., Jr. and R. N. Maddox , " Control of Distillation Columns Using a Simplified Dynamic Model " , Chem. Eng. Prog. Technical manual on System and Process Control, AIChE J, New York , 1965.

Pantelides, C. C., " SPEEDUP - Recent Advances in Process Simulation ", Comp. Chem. Eng., vol. 12 (7), pp 745 - 755, 1988.

Peiser, A. M. and S. S. Grover, "Dynamic Simulation of a Distillation Tower", Chem. Eng. Prog., vol. 58 (9), pp. 65-70, 1962.

Perkins, J. D. and M. P. F. Wong, "Assessing Controllability of Chemical Plants", I.Chem.E. Symposium Series No. 92, pp. 481-492, (PSE'85), 1985.

Perkins, J. D., Howell, J. M. and M. P. F. Wong, "The Significance of Modeling and Simulation in Process Design", Modelling, Identification and Control, vol. 7 (2), pp. 57-70, 1986.

Perkins, J. D., "Interaction Between Process Design and Process Control", DYCORD+89, Maastricht, Netherlands, 1989.

Powell, M. J. D., " A Fast Algorithm for Nonlinear Constrained Optimization Calculations ", in Lecture Notes in Mathematics vol. 630 , G. A. Watson (ed.,), Spinger-Verlag, pp. 144-157, 1978.

Prett, D. M. and R. D. Gillette, " Optimization and Constrained Multivariable Control of a Catalytic Cracking Unit ", 86th National AIChE Meeting, April 1979.

Ray, W. H., "Advanced Process Control" , McGraw-Hill, New York , 1981.

Rijnsdorp, J. E., " Interaction in Two-variable Control Systems for Distillation Columns I ", Automatica, vol. 1, p. 15, 1965.

Rijnsdorp, J. E., " Chemical Process Systems and Automatic Control ", Chem. Eng. Prog., Vol. 63 (7), pp 97-116, 1967.

Roffel, B. and H. J. Fontein, "Constraint Control of Distillation Processes", Chem. Eng. Sci., vol. 34, pp. 1007-1018, 1979.

Rosenbrock, H. H., "Distinctive Problems of Process Control", Chem. Eng. Prog., vol. 58 (9), pp. 43-50, 1962a.

Rosenbrock, H. H., "The Control of Distillation Columns", Trans. Inst. Chem. Eng., vol. 40, pp. 35-53, 1962b.

Rosenbrock, H. H., " The Transient Behaviour of Distillation Columns and Heat Exchangers. An Historical and Critical Review", Trans. I. Chem, Eng. , vol. 40 , pp. 376 - 384, 1962c.

Rosenbrock, H. H., "State-Space and Multivariable Theory", Thomas Nelson, London , 1970.

Rouhani, R. and R. K. Mehra, " Model Algorithmic Control (MAC) ; Basic Theoretical Properties ", Automatica, vol. 18 , p 401-414 , 1982

Russell, L. W., " Control System Synthesis for Plants with Time delays ", Ph. D. Thesis, Dept. of Chem. Eng., Imperial College, London, U. K., 1987.

Shields, R. W. and J. B. Pearson, " Structural Controllability of multi-input linear systems ", IEEE Trans. , vol. AC-21 (2), pp 203-212, 1976.

Shimizu, K. and M. Matsubara, "Directions of Disturbances and Modeling Errors on the Control Quality in Distillation Systems", Chem. Eng. Commun., vol. 37, pp. 67-91, 1985.

Shinskey, F. G., "The Stability of Interacting Control Loops With and Without Decoupling", Proc. IFAC Multivariable Technological Systems Conference, University of New Brunswick, pp. 21-30 , 1977.

Shinskey, F. G., " Uncontrollable Processes and What to Do About Them ", Hydrocarbon Processing, vol. 62 (11), pp. 179-182 , 1983.

Shinskey, F. G., "Distillation Control", McGraw-Hill , New York, 1984.

Shinskey, F. G., "Process Control Systems", 3rd Ed., McGraw-Hill , New York, 1988.

Simon, J. D. and S. K. Mitter, " A Theory of Modal Control ", Information and Control, vol. 13, p. 316, 1968.

Skogestad, S. and M. Morari, "Implications of Large RGA-Elements on Control Performance", AIChE Annual Meeting, Miami Beach, Florida, vol. Paper 6d, 1986.

Skogestad, S. and M. Morari, "Control Configuration Selection for Distillation Columns", AIChE Journal, vol. 33 (10), pp. 1620-1635, 1987a.

Skogestad, S. and M. Morari, "Design of Resilient Processing Plants-IX. Effect of Model Uncertainty on Dynamic Resilience", Chem. Eng. Sci., vol. 42 (7), pp. 1765-1780, 1987b.

Skogestad, S. and M. Morari, "Effect of Disturbance Directions on Closed-Loop Performance", Ind. Eng. Chem. Res., vol. 26 (10), pp. 2029-2035, 1987c.

Skogestad, S. and M. Morari, "LV-Control of a High-Purity Distillation Column", Chem. Eng. Sci., vol. 43 (1), pp. 33-48, 1988a.

Skogestad, S. and M. Morari, "Understanding the Dynamic Behaviour of Distillation Columns", Ind. Eng. Chem. Res., vol. 27, pp. 1848-1862, 1988b.

Skogestad, S., Jacobsen, E. W. and P. Lundstrom, "Selecting the Best Distillation Control Structure", DYCORD+89, pp. 295- 302, Maastricht, Netherlands, 1989.

Smith, J. M. , and H. C. Van Ness , "Introduction to Chemical Engineering Thermodynamics ", 3rd ed., McGraw-Hill, New York , 1975.

Smith, O. J. M., " Close Control of Loops with Dead Time ", Chem. Eng. Prog. , vol. 53 (5), pp. 217-219, 1957.

Stathaki, A., Mellichamp, D. A. and D. E. Seborg, "Dynamic Simulation of a Multicomponent Distillation Column with Asymmetric Dynamics", Canadian Journal of Chem. Eng., vol. 63, pp. 510-518, 1985.

Stephanopoulos, G., "Synthesis of Process flowsheets : An adventure in Heuristic Design or a Utopia of Mathematical Programming ? ", paper presented to the Conf. of Found. of Computer-aided Chem. Pro. Design, Henniker, New Hampshire, USA, 1980.

Stephanopoulos, G., "Synthesis of Control Systems for Chemical Plants - A Challenge for Creativity", Comp. Chem. Eng., vol. 7 (4), pp. 331-365, 1983.

Stephanopoulos, G., " Chemical Process Control - An Introduction to Theory and Practice ", McGraw-Hill, New York , 1984.

Stewart, G. W., " Introduction to Matrix Computation ", Academic Press , New York, 1973.

Stewart, W. E., Levien, K. L. and M. Morari, " A New Model Reduction Technique for Staged Separation Operation ", 74th Annual AIChE Meet., New Orleans, USA, 1981.

Stewart, W. E., Levien, K. L. and M. Morari, " Collocation Methods in Distillation" , Proc. Second Int. Conf. on Found. of Comp. Aided Process Design, Snowmass, Colorado, June 1983.

Trebal, R. E., " Mass Transfer Operations " , McGraw-Hill, New York , 1980.

Tung, L. S. and T. F. Edgar, " Analysis of Control-Output Interactions in Dynamic Systems", AIChE J, vol. 27 (4), pp 690-693, 1981.

Umeda, T., Kuriyama, T. and A. Ichikawa, " A Logical Structure for Process Control System Synthesis", Proc. IFAC Congress, Helsinki, vol. 1, p. 271, 1978.

Villadsen, J. and M. L. Michelsen , "Solution of Differential Equation Models by Polynomial Approaximation", Prentice-Hall, Englewood Cliffs, New Jersey, 1978.

Wahl, E. F. and P. Harriott, "Understanding and Prediction of the Dynamic Behaviour of Distillation Columns", Ind. Eng. Chem. Proc. Des. Dev., vol. 9 (3), pp. 396-406, 1970.

Waller, K. V. T., and C. G. Nygardas, " On Inverse Response in Process Control ", Ind. Eng. Chem. Fundam., vol. 14 (3), pp. 221 - 223 , 1975.

Williams, T. J. and R. E. Otto, " A Generalised Chemical Processing Model for the investigation of Computer Control", AIEE Trans. Part- 1, vol. 79, p. 758 , 1963.

Witcher, M. F. and T. J. McAvoy, " Interacting Control Systems - Steady State and Dynamic Measurement of Interaction", ISA Trans., vol. 16 (3), p. 35 , 1977.

Wong, K. T. and R. Luss, " Model Reduction of High-Order Multistage Systems by the Method of Orthogonal Collocation ", Can. J. Chem. Eng., vol. 58, pp. 382-388 , 1980.

Wong, M. P. F., "The Assessment of Controllability of Heat-integrated Chemical Processes ", Ph. D. Thesis, Dept. of Chem. Eng ., Imperial College, London, U. K., 1984.

Wonham, "On Pole Assignment in Multi-input Controllable Linear Systems, " IEEE Trans. Auto. Control, AC-12, pp 660-665, 1967.

Zakrzewski, A. M., "Cost Effective Computer Control - Some Examples ", I. Chem. E. Symp. Series , No. 79, pp. 226-242, 1983.